

AWARD NUMBER: W81XWH-14-1-0302

TITLE: A translational pathway toward a clinical trial using the second-generation AAV micro-dystrophin vector

PRINCIPAL INVESTIGATOR: Dongsheng Duan

CONTRACTING ORGANIZATION: University of Missouri System; 316 University Hall; Columbia, MO 65211-3020

REPORT DATE: March 2018

TYPE OF REPORT: Final

PREPARED FOR: U.S. Army Medical Research and Materiel Command  
Fort Detrick, Maryland 21702-5012

DISTRIBUTION STATEMENT: Approved for Public Release;  
Distribution Unlimited

The views, opinions and/or findings contained in this report are those of the author(s) and should not be construed as an official Department of the Army position, policy or decision unless so designated by other documentation.

# REPORT DOCUMENTATION PAGE

*Form Approved*  
OMB No. 0704-0188

Public reporting burden for this collection of information is estimated to average 1 hour per response, including the time for reviewing instructions, searching existing data sources, gathering and maintaining the data needed, and completing and reviewing this collection of information. Send comments regarding this burden estimate or any other aspect of this collection of information, including suggestions for reducing this burden to Department of Defense, Washington Headquarters Services, Directorate for Information Operations and Reports (0704-0188), 1215 Jefferson Davis Highway, Suite 1204, Arlington, VA 22202-4302. Respondents should be aware that notwithstanding any other provision of law, no person shall be subject to any penalty for failing to comply with a collection of information if it does not display a currently valid OMB control number. **PLEASE DO NOT RETURN YOUR FORM TO THE ABOVE ADDRESS.**

<b>1. REPORT DATE</b> March 2018		<b>2. REPORT TYPE</b> Final		<b>3. DATES COVERED</b> 1 Sept 2014 - 31 Dec 2017	
<b>4. TITLE AND SUBTITLE</b> A Translational Pathway Toward a Clinical Trial Using the Second-Generation AAV Micro-Dystrophin Vector				<b>5a. CONTRACT NUMBER</b>	
				<b>5b. GRANT NUMBER</b> W81XWH-14-1-0302	
				<b>5c. PROGRAM ELEMENT NUMBER</b>	
<b>6. AUTHOR(S)</b> Dongsheng Duan, Craig Emter, Yi Lai, Hsiao Tung Yang; Yongping Yue, Aihua Dai  E-Mail: duand@missouri.edu				<b>5d. PROJECT NUMBER</b>	
				<b>5e. TASK NUMBER</b>	
				<b>5f. WORK UNIT NUMBER</b>	
<b>7. PERFORMING ORGANIZATION NAME(S) AND ADDRESS(ES)</b>  University of Missouri System; 316 University Hall; Columbia, MO 65211-3020				<b>8. PERFORMING ORGANIZATION REPORT NUMBER</b>	
<b>9. SPONSORING / MONITORING AGENCY NAME(S) AND ADDRESS(ES)</b>  U.S. Army Medical Research and Materiel Command Fort Detrick, Maryland 21702-5012				<b>10. SPONSOR/MONITOR'S ACRONYM(S)</b>	
				<b>11. SPONSOR/MONITOR'S REPORT NUMBER(S)</b>	
<b>12. DISTRIBUTION / AVAILABILITY STATEMENT</b>  Approved for Public Release; Distribution Unlimited					
<b>13. SUPPLEMENTARY NOTES</b>					
<b>14. ABSTRACT</b>  Duchenne muscular dystrophy (DMD) can be caused by thousands of different mutations in the dystrophin gene. Replacing the mutated gene with a functional microgene offers a one-size-fits-all therapy. Several dozens of first-generation microgenes have been shown to reduce muscle disease in mdx mice. However, early attempts in DMD dogs and human patients have failed to reproduce the success in mice. We have recently discovered the dystrophin domain responsible for restoring neuronal nitric oxide synthase (nNOS). Failure to restore nNOS significantly contributes to the initiation and progression of DMD. DMD affects all muscles in the body. An effective therapy for DMD requires bodywide therapy. While studies performed in the mouse models have been encouraging, they are poorly translated to patients. Testing systemic microgene therapy in the symptomatic dystrophic dog model is absolutely required to establish the premise for a clinical trial. In this study, we demonstrated effective bodywide systemic AAV microgene therapy in the canine DMD model. Our findings have provided the foundation for the recent initiation of human trials.					
<b>15. SUBJECT TERMS</b> Duchenne muscular dystrophy, DMD, dystrophin, micro-dystrophin, adeno-associated virus, AAV, muscle, gene therapy, systemic gene delivery, canine model					
<b>16. SECURITY CLASSIFICATION OF:</b>			<b>17. LIMITATION OF ABSTRACT</b>  UU Unclassified	<b>18. NUMBER OF PAGES</b>  328	<b>19a. NAME OF RESPONSIBLE PERSON</b> USAMRMC
<b>a. REPORT</b> U Unclassified	<b>b. ABSTRACT</b> U Unclassified	<b>c. THIS PAGE</b> U Unclassified			<b>19b. TELEPHONE NUMBER</b> (include area code)

## Table of Contents

	<u>Page</u>
1. Introduction.....	4
2. Keywords .....	4
3. Accomplishments .....	4
4. Impact .....	33
5. Changes/Problems.....	33
6. Products .....	33
7. Participants & Other Collaborating Organizations .....	37
8. Special Reporting Requirements .....	44
9. Appendices.....	45

Peer-reviewed publications

## 1. Introduction

Duchenne muscular dystrophy (DMD) is a life threatening disease affecting approximately one in 5,000 newborn boys. It is caused by dystrophin deficiency. Adeno-associated virus (AAV)-mediated micro-dystrophin gene therapy has resulted in unprecedented successful in mouse models of DMD. We propose to develop systemic AAV micro-dystrophin gene therapy in the canine model.

## 2. Keywords

Duchenne muscular dystrophy, DMD, dystrophin, micro-dystrophin, adeno-associated virus, AAV, muscle, gene therapy, systemic gene delivery, canine model

## 3. Accomplishments

**Major goal.** The major goals of our study is to engineer the AAV micro-dystrophin vector and test the vector by systemic delivery in young adult DMD dogs.

**Accomplishment 1.** We have developed a novel micro-dystrophin vector for systemic AAV therapy.

We started with a vector that we have published before called SJ13. To further enhance the function of the micro-dystrophin gene, we first engineered the dystrophin syntrophin/dystrobrevin binding site (syn/dbr) into SJ46 and the resulting construct was termed YL391. Next, we added the proposed hematopoietic lineage specific microRNA 142-3 binding site (mirT) into YL391. The resulting vector YL396 has a size of 5,124bp. Next we replaced the CMV promoter with the muscle specific Spc5-12 promoter and generated the vector YL398. Since YL398 has a size (4,971bp) close to that of AAV packing limit (5,000bp). So we generated another vector called YL397 (4,849bp).

**Figure 1** showed cloning steps of these vectors.

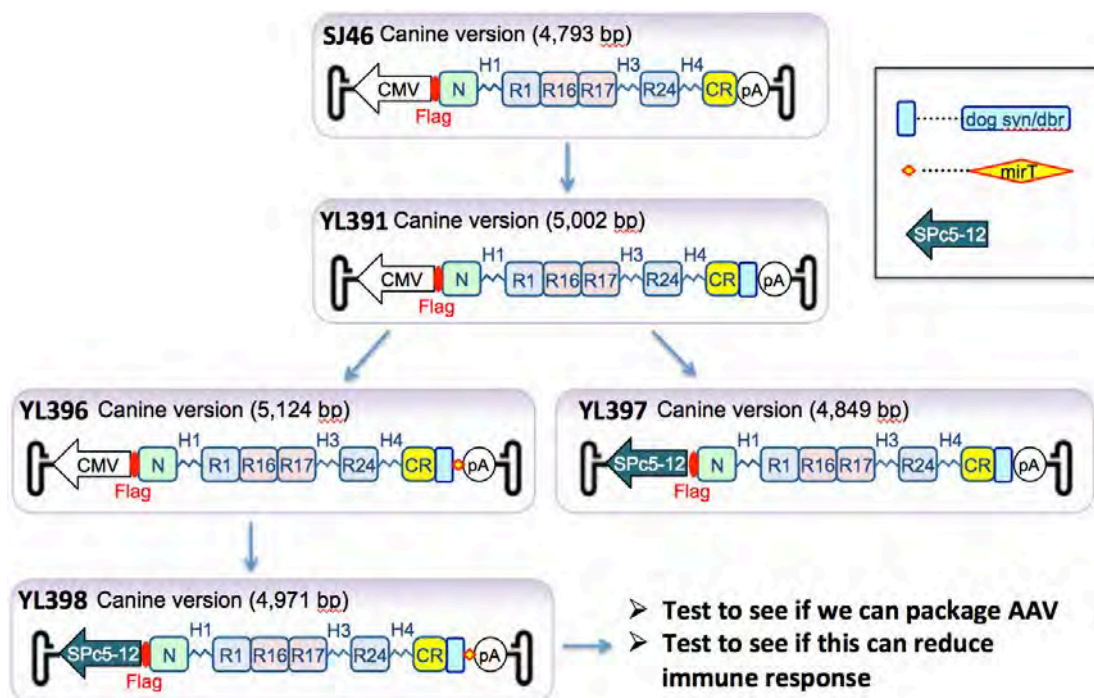
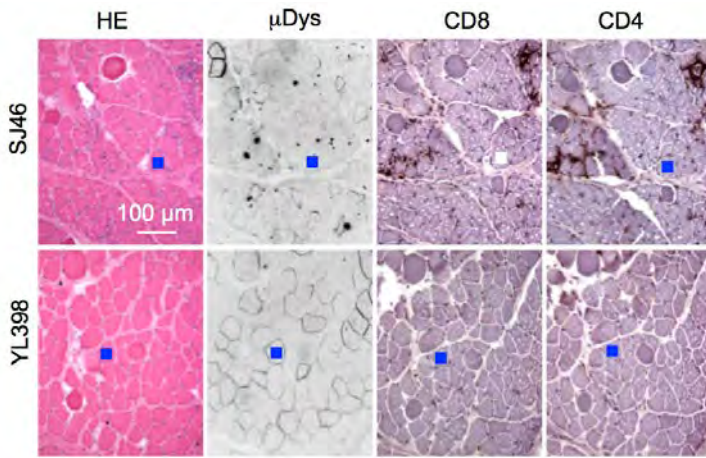


Figure 1. Engineering of the original canine microgene vector SJ46 to test the concept of reduced immunogenicity by the muscle specific promoter and miR142-3p binding site.

Next, we tested whether we can successfully package YL398 into a functional AAV vector and whether the presumed low-immunogenic property of YL398 can indeed reduce immunogenicity. We



successfully achieved high titer YL398 AAV virus. Injection in one adult affected dog revealed great reduction of CD4+ and CD8+ T cell infiltration (Figure 2).

Figure 2. The use of muscle specific promoter and inclusion of hematopoietic lineage microRNA 142-3p target site in the AAV vector greatly reduced T cell infiltration. This preliminary data confirmed our original hypothesis and provided a strong rationale to engineer novel human microgene vector.

Together, we have successfully

demonstrated that our originally proposed strategy is a valid approach to reduce immunogenicity of the AAV vector in dystrophic dogs.

To engineer the human version of the low-immunogenic AAV micro-dystrophin vector, we first replaced the dog microgene with a codon-optimized human microgene and generated construct XP8. This packaging plasmid of this construct has a backbone of ~3.6kb. This is smaller than the AAV packaging limit. Hence, there is a high possibility that the backbone can be packaged during vector production. Since the backbone is composed of the bacterial replication origin and the bacterial ampicillin resistant gene, there will be highly immunogenic in human patients. Thus, we further modified XP8 with enlarged backbone. We made two different versions of backbone enlarged XP8 and named them as XP9 and XP11 (Figure 3).

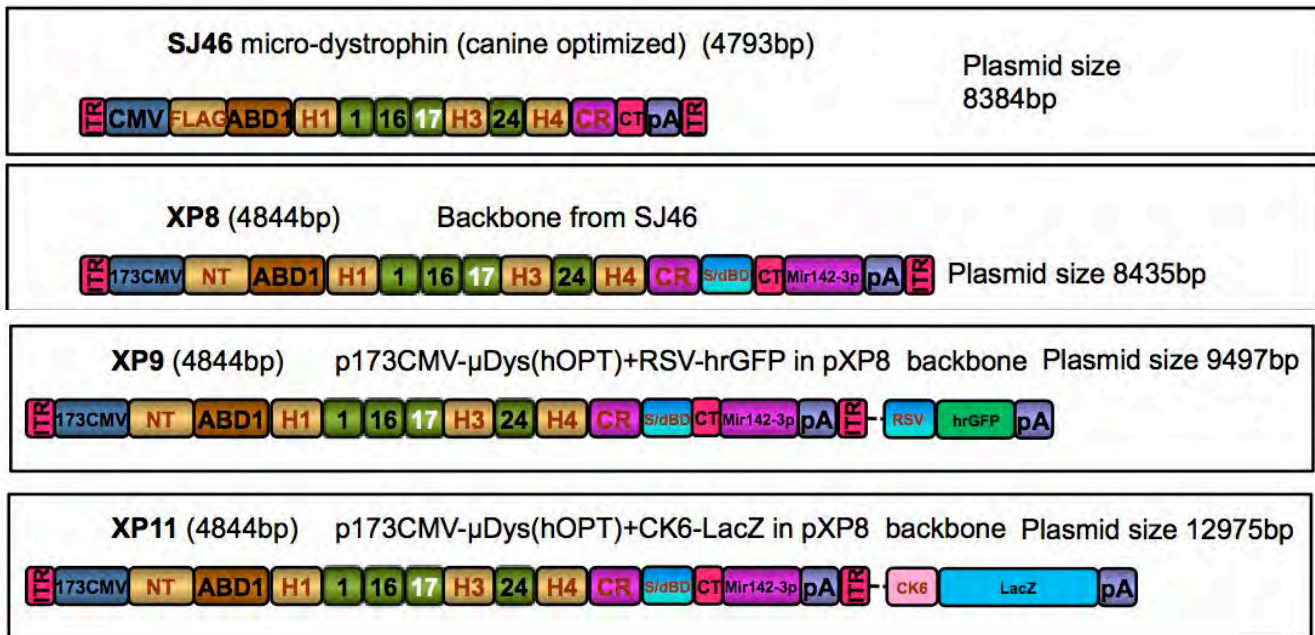
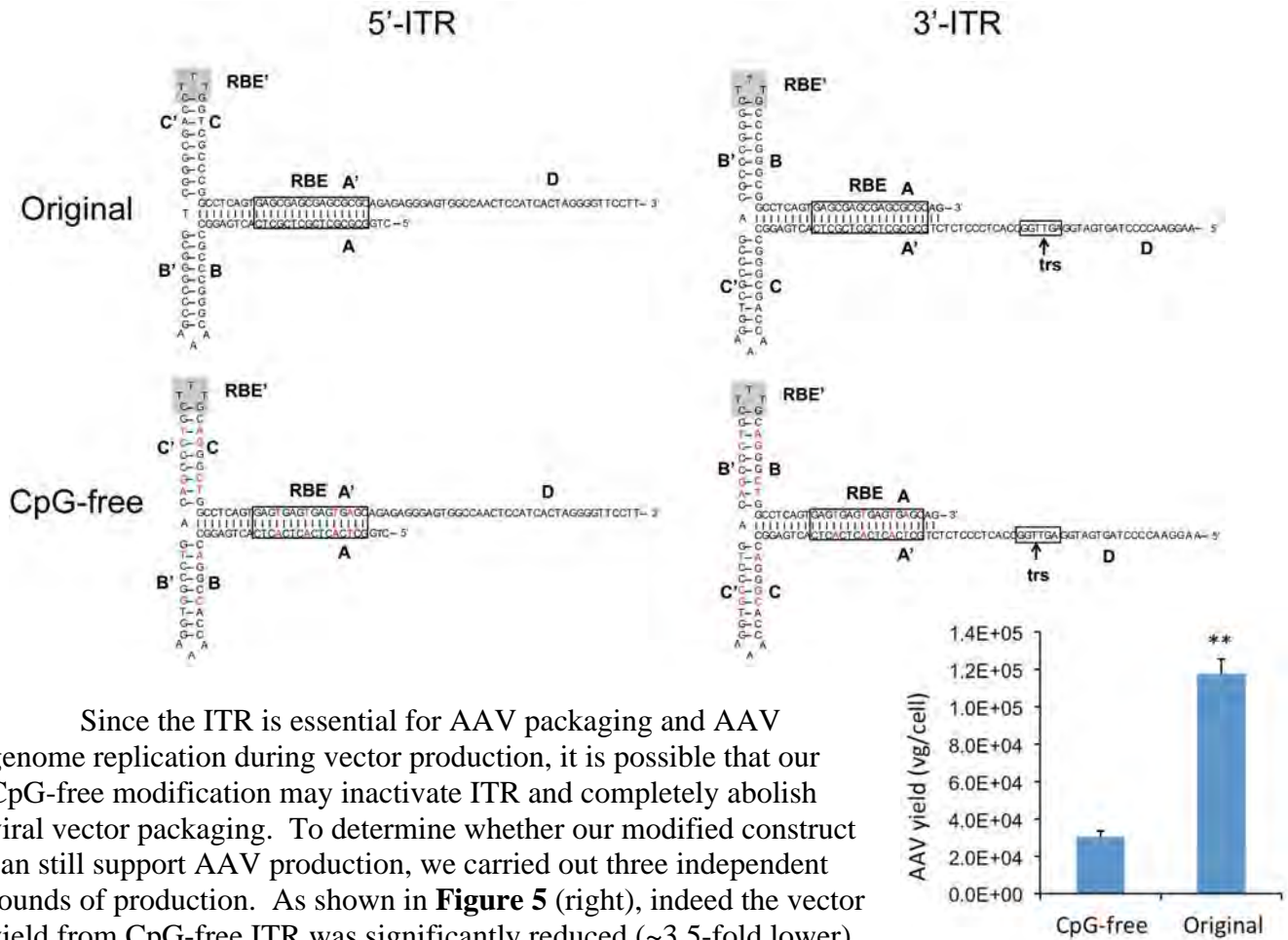


Figure 3. Cartoon outline of the construct SJ46 (the original canine microgene vector) and three human microgene vectors including XP8, XP9 and XP11.

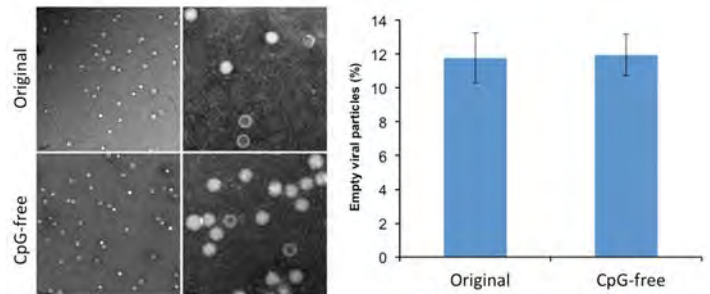
During our engineering of the new canine and human gene vectors, a new study was published suggesting that the CpG motif is another critical determining factor for AAV-induced immune response (Faust et al., 2013). In light of this new finding, we decide to upgrade our newly generated human microgene vector by removing the CpG motif

Each AAV vector has two ITRs. **Figure 4** (below) shows the sequence structure of the original 5' and 3'-ITRs and our modified CpG-free 5' and 3'-ITRs. The capital letters A, B, C and D mark different region of the ITR. RBE stands for the Rep-binding element and trs stands for the terminal resolution site. CpG changes are marked in red.

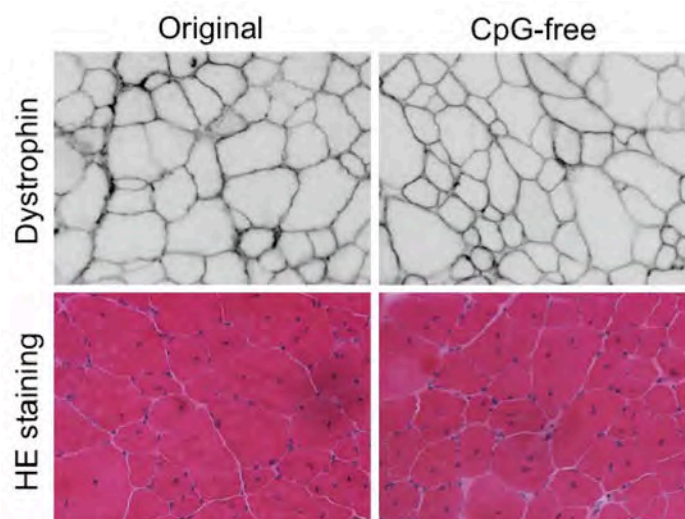


Since the ITR is essential for AAV packaging and AAV genome replication during vector production, it is possible that our CpG-free modification may inactivate ITR and completely abolish viral vector packaging. To determine whether our modified construct can still support AAV production, we carried out three independent rounds of production. As shown in **Figure 5** (right), indeed the vector yield from CpG-free ITR was significantly reduced (~3.5-fold lower). Nevertheless, our modification did not eliminate AAV production.

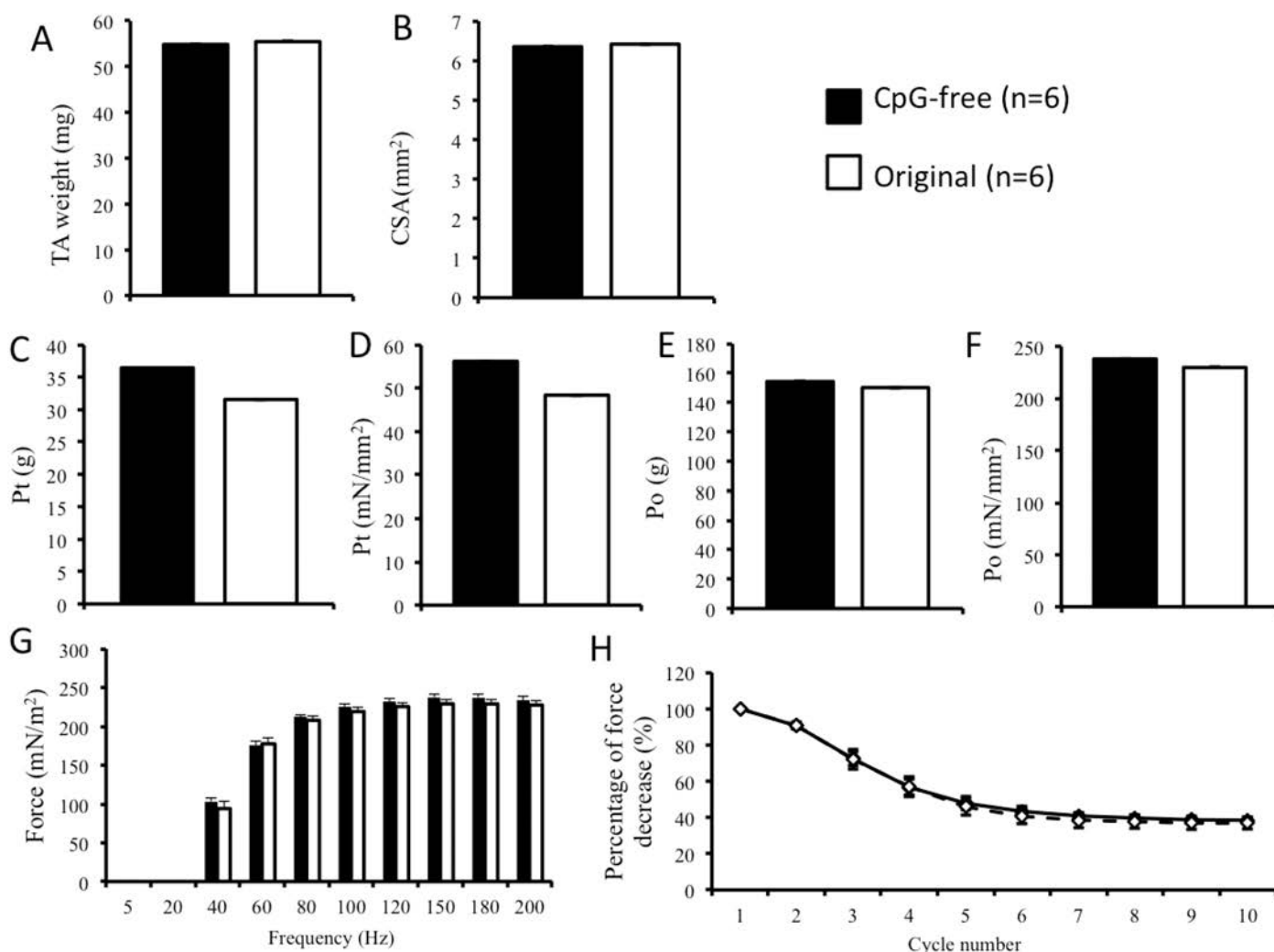
Next we examined the CpG-free AAV vector by transmission electron microscopy. The ITR CpG-free AAV particles showed similar structure as that of the original un-modified AAV particle (**Figure 6** right panel). In light of inefficient packaging (as reflected by the low yield), we thought that we might see more empty particles in the ITR CpG-free vector preparation. Surprisingly, there was no difference compared to that of the un-modified vector (**Figure 3**).



To determine the functionality of the ITR CpG-free vector, we performed local injection at the tibialis anterior muscle in 10-m-old mdx mice. One side of the muscle received the ITR CpG-free vector and the contralateral side received the un-modified vector. Two months after injection, we examined muscle histology and muscle function. On immunostaining and histology, we did not see much difference between two vectors (**Figure 7**, right). Both showed saturated sarcolemmal expression of micro-dystrophin. Since the treatment was performed in 10-m-old mice, we expected no change in centronucleation. This is confirmed by HE staining (**Figure 7**, right).



To further compare the two vectors, we evaluated TA muscle weight, cross-sectional area (CSA), absolute twitch force (Pt in g), specific twitch force (Pt in mN/mm<sup>2</sup>), absolute tetanic force (Po in g), specific tetanic force (Po in mN/mm<sup>2</sup>),



force-frequency relationship and percentage of the force drop follow 10 cycles of eccentric contraction

(**Figure 8**, the bottom of previous page). No difference was noticed between the modified ITR CpG-free vector and the original unmodified vector. Our data suggests that elimination of the CpG islands from the ITR does not affect the therapeutic efficacy of the vector.

In our original DOD application, we proposed to generate a human version of our published canine  $\Delta R2-15/\Delta R18-19/\Delta R20-23/\Delta C$  microgene (**Figure 9**, right) (Shin et al., 2013). In this proposed construct, we will express the codon-optimized human  $\Delta R2-15/\Delta R18-19/\Delta R20-23/\Delta C$  microgene from the muscle-specific SpC5-12 promoter. As stated above, we have decided to further improve our vector by making it CpG-free in the year 2 of the project. During this genetic engineering process, we realized that we could further enhance our construct by making additional changes. (1) We decided to add a Dys-2 epitop at the end of the microgene. In our original plan, the microgene was ended at the syntrophin/dystrobrevin binding site. A drawback of this design is that there is no antibody that can recognize the syntrophin/dystrobrevin binding site. This makes it challenging to determining whether we have a full-length micro-dystrophin protein. Dys-2 is a short peptide in the wide-type full-length dystrophin. It can be recognized by the Dys-2 monoclonal antibody. Addition of Dys-2 epitope will now allow us to definitively confirm that our micro-dystrophin is intact when expressed in muscle. (2) We decided to remove all CpG islands from the codon-optimized human microgene to reduce the immunity of the vector. (3) A new paper published by Liang et al caught our attention (Liang et al., 2015). In this study, the authors found that patients who have hinge 3 missing in their dystrophin show less severe disease. In reviewing the literature, we found another clinical study by Carsana et al (Carsana et al., 2005). The authors also found that in-frame deletion of hinge 3 is associated with milder clinical presentation. Unfortunately, no study has directly compared the pros and cons of hinge 3 in experimental animals. To generate the most functional microgene, we decided to compare the therapeutic efficacy of micro-dystrophins with or without hinge 3. To this end, we engineered two different CpG-free codon-optimized human microgenes. We named them XP16 (with hinge 3) and XP23 (without hinge 3) (**Figure 10**, below).

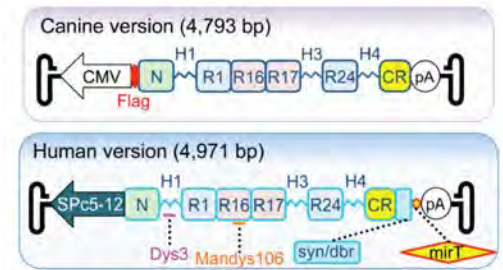
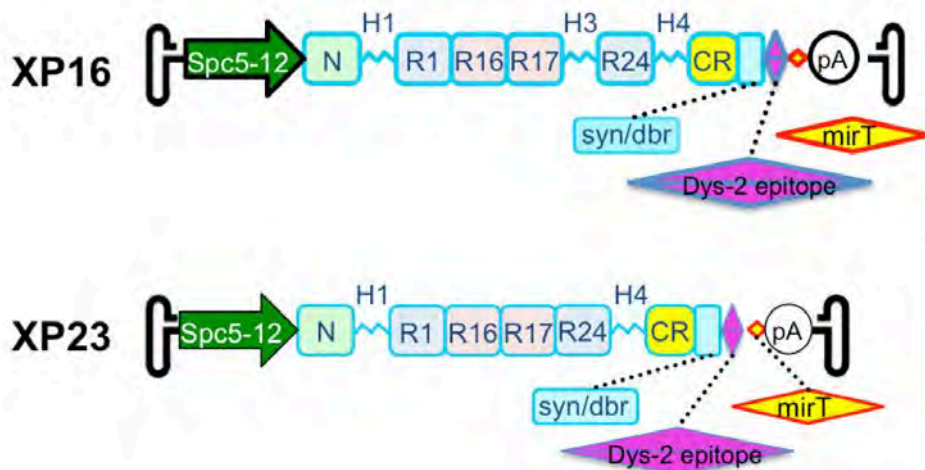
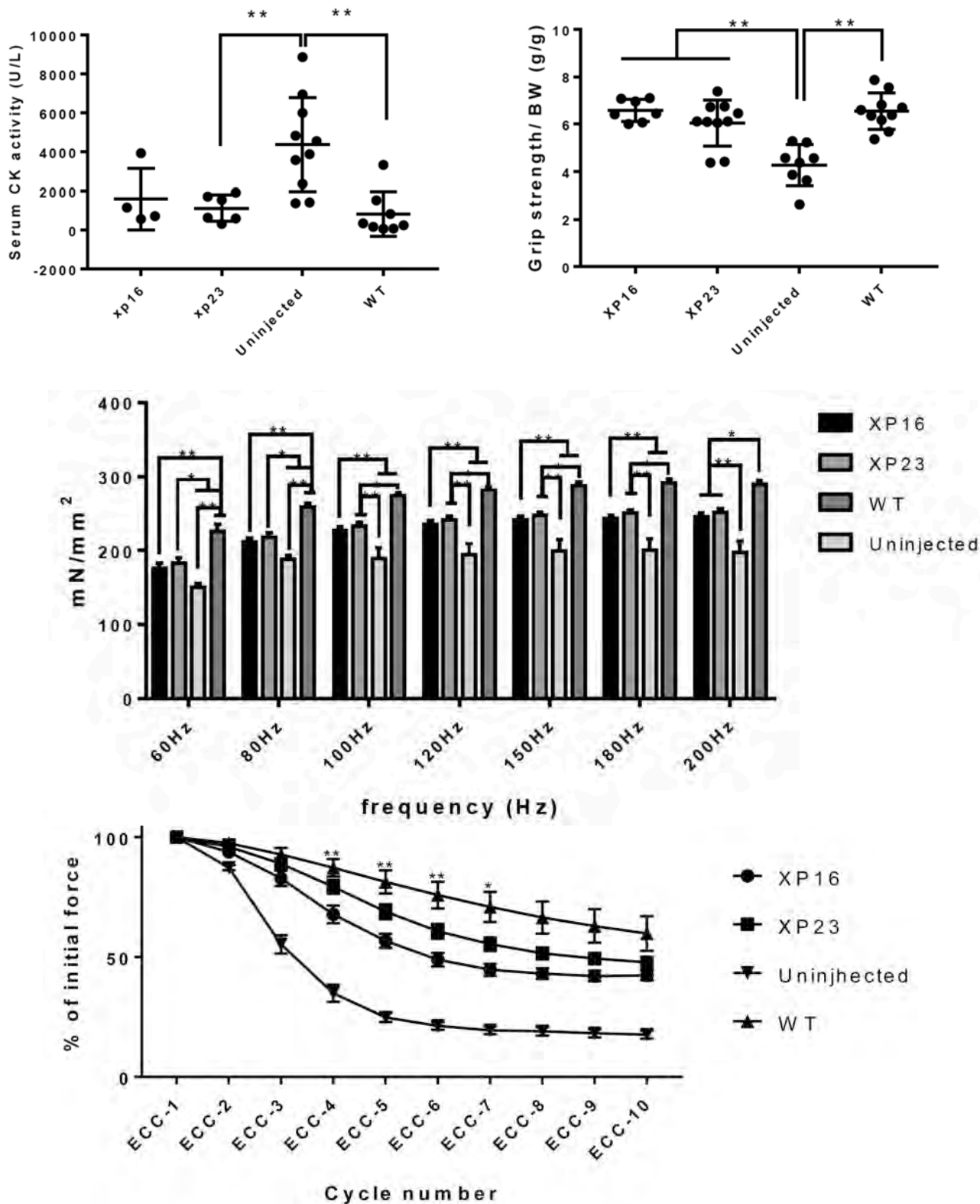


**Figure 6.** Schematic outline of the canine (top) and human (bottom) version microgene cassette. mirT, mir142-3p target sequence; syn/dbr, syntrophin and dystrobrevin binding site.

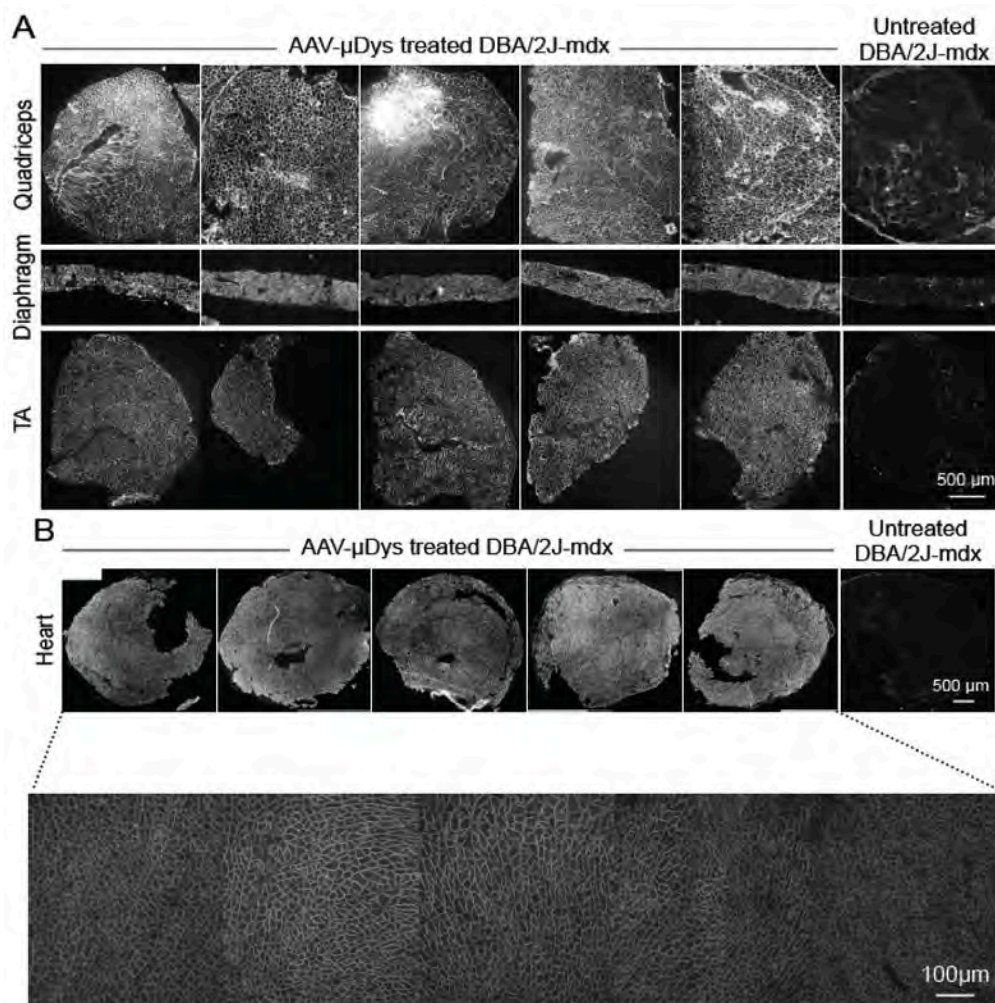


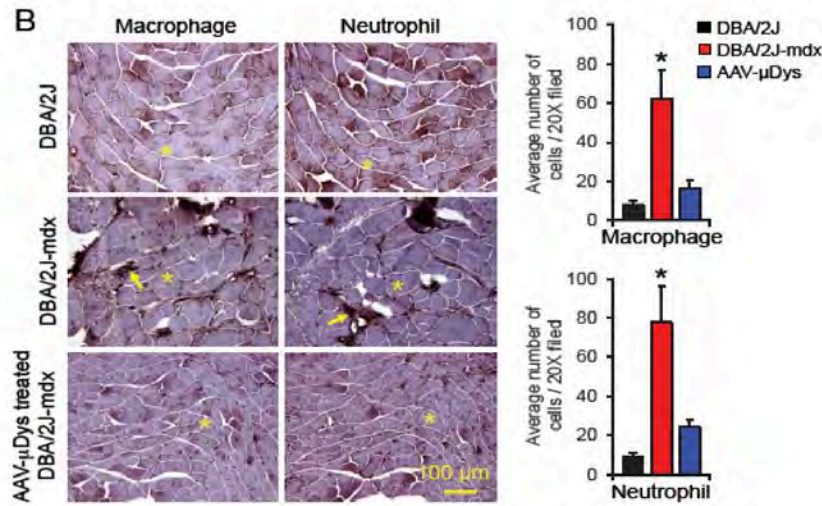
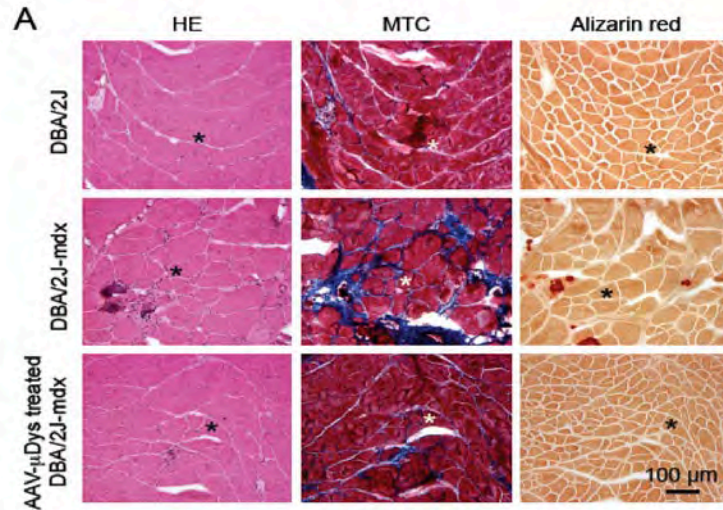
To compare the therapeutic efficacy of XP16 and XP23, we performed systemic delivery in 10-week-old mdx mice. Seven mice received XP16. Ten mice received XP23. We also included 9 untreated mdx mice and 7 wild type BL10 mice as controls. At 24 weeks after gene transfer, we measured the serum creatine kinase (CK) level, grip strength, force-frequency relationship and eccentric contraction profile (Figure 11, below).



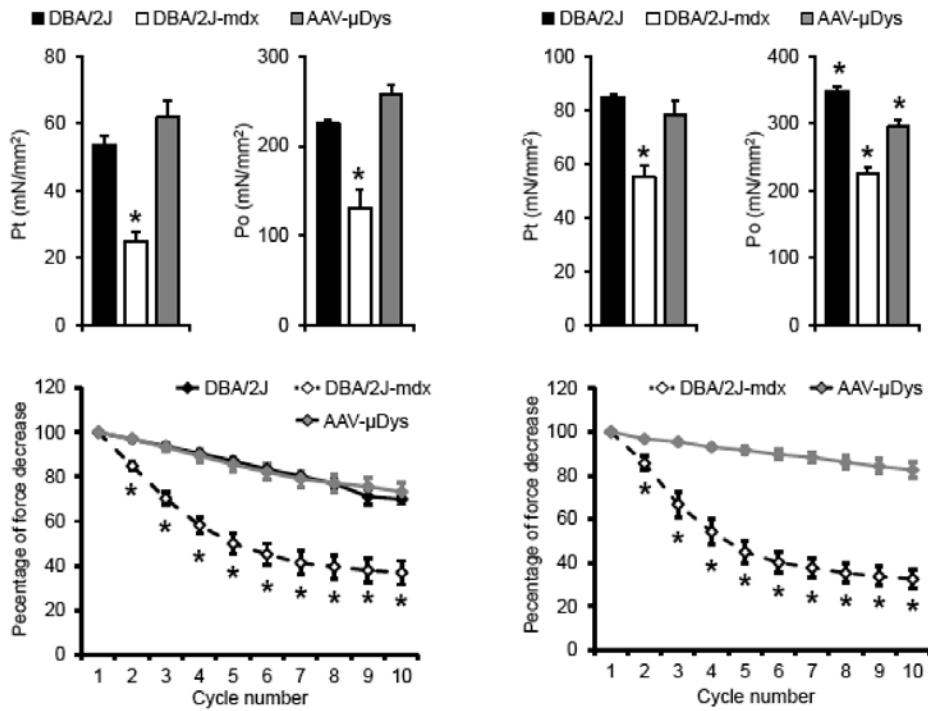
We found that both XP16 and XP23 were equally effective in improving grip strength and tetanic force (at the frequency of 60, 80, 100, 120, 150, 180 and 200 Hz). While both constructs reduced the serum CK level, the statistical significance was only achieved with XP23. In eccentric contraction, both constructs protected against muscle damage. However, XP23 consistently outperformed XP16. In summary, our results are in line with clinical observations suggesting that a hing3-free micro-dystrophin is more effective in protecting dystrophic muscle in adult mdx mice.

We originally proposed to use the synthetic SPc5-12 promoter (Li et al., 1999). However, this promoter has many CpG and further it difficult to work in AAV cloning (likely due to its GC-rich nature). Recently, a superior muscle-specific promoter called CK8 promoter became available from Hauschka lab. This lab has focused on developing muscle-specific promoter for more than three decades and has generated the best muscle-specific promoter for the field (Bengtsson et al., 2016; Himeda et al., 2011). For this reason, we tested the CK8 promoter. Following systemic delivery of a CK8 driven micro-dystrophin AAV vector in a much severe DBA2/J-mdx model (Coley et al., 2016; Fukada et al., 2010), we observed super-strong expression in all muscles and the heart (**Figure 12**, below). Treatment significantly improved muscle histology (HE staining), minimized fibrosis (MTC staining), eliminated calcification (Alizarin red staining), and diminished inflammation (macrophage and neutrophil immunostaining) (**Figure 13** next page top panels). Importantly, muscle function was nearly normalized (**Figure 14**, next page bottom panels).





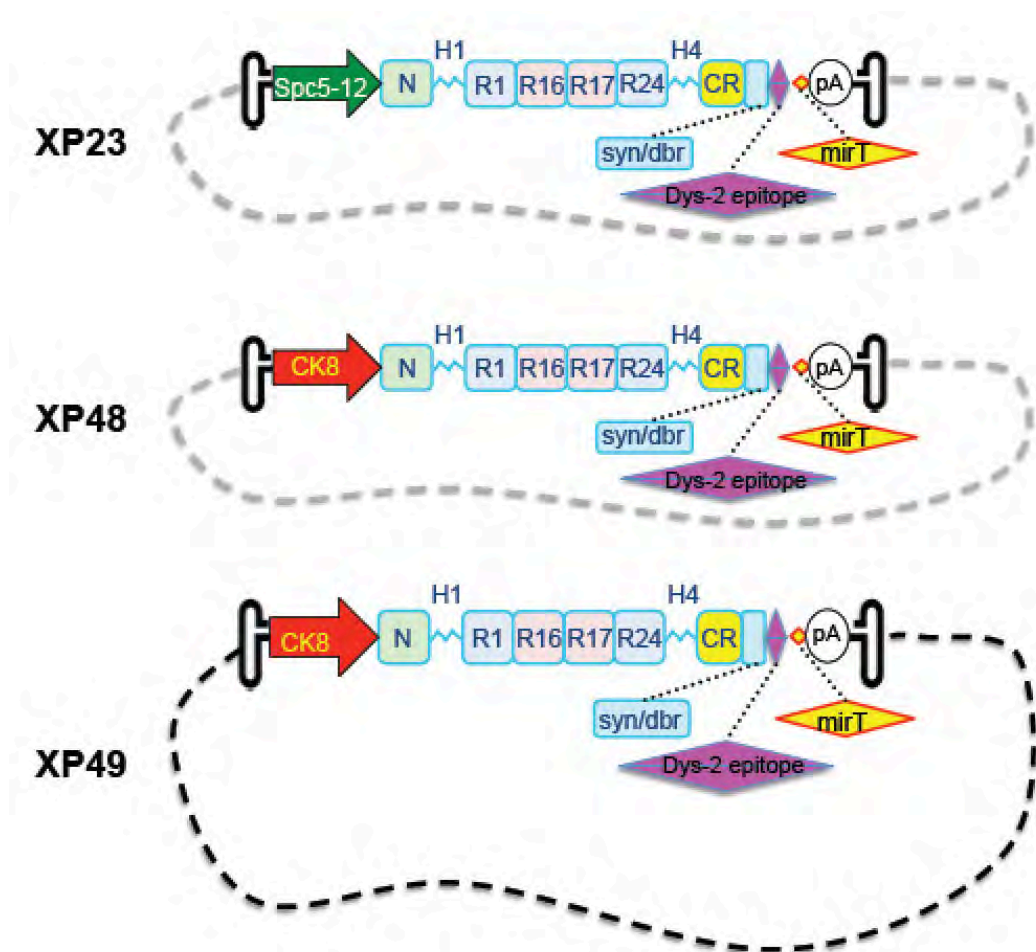
**A**



Based on the results of XP16 and XP23 comparison study, we decided to remove hinge 3 from our originally proposed design.

Based on the evaluation on the CK8 promoter, we decided to use the CK8 promoter, instead of the SpC5-12 promoter. With this in mind, we generated XP48 (**Figure 12**, below).

The AAV packaging plasmids described above (XP16, XP23 and XP48) all have a relatively small backbone (<4kb). On evaluating the stocks using a highly sensitive TaqMan PCR protocol, we noticed a very low level (<1%) of contamination of the backbone DNA in the viral stock. This is thought to be caused by so-called “reverse packaging”. For the mouse study, <1% contamination may not be a big problem. However, when we inject up to  $10^{15}$  to  $10^{16}$  vg particles per subject in large mammals, the amount of contaminating backbone becomes a safety concern. Increasing the size of the backbone to >5kb will prevent “reverse packaging” because this will make the backbone exceed AAV packaging capacity. To this end, we further modified XP48 and generated XP49 that is on a much larger (6kb) backbone (**Figure 15**, below).



In summary, we have made great progress in Aim1. Specifically, (1) we have obtained all regulatory approval for our animal studies, (2) we have prepared vectors for mouse studies, (3) we have tested human micro-dystrophin AAV vector in two independent studies in mdx mice including (a) comparison of CpG-free ITR and wild type ITR, and (b) comparison of hinge3-free and hinge3-containing micro-dystrophin, (4) we have tested the CK8 micro-dystrophin AAV vector in the much severe DBA/2J-mdx mice, (5) we have generated AAV vector for local injection in affected dogs, (6) we have generated affected dogs and demonstrated in these dogs that inclusion of muscle-specific

promoter and miR142-3p target site significantly attenuated immune response associated with AAV micro-dystrophin injection in dystrophic dog muscle (described in the last progress report), and (7) most importantly, we have developed a AAV vector much superior than we originally proposed. We will now use this improved vector (XP49) for systemic injection in affected dogs. We envision to carry this vector forward to a phase I human trial in the future.

***Accomplishment 2. We have demonstrated that AAV-8 is more effective than AAV-9 in transducing dog heart for systemic AAV therapy.***

Our eventual goal is to test systemic AAV-8 delivery in young adult dogs with our low-immunogenic vector. As a first step toward this goal, we tested if AAV-8 can efficiently transduce

TABLE 1. SUMMARY OF EXPERIMENTAL PROTOCOL AND DOGS

	<i>Christa</i>	<i>Barbara</i>	<i>Artemis</i> <sup>a</sup>	<i>Dojo</i> <sup>a</sup>	<i>Generic</i>
Gender	Female	Female	Female	Male	Female
Genotype	Carrier	Carrier	Carrier	Normal	Carrier
Age at the time of injection (day)	2	2	2	2	N/A
BW at the time of injection (g)	380	380	412	520	N/A
AAV serotype	AAV-9	AAV-9	AAV-8	AAV-9	N/A
Injection volume (ml/kg BW)	9.21	14.47	14.56	8	N/A
AAV dosage (vg particle/kg BW)	$6.14 \times 10^{14}$	$9.65 \times 10^{14}$	$9.06 \times 10^{14}$	$2 \times 10^{14}$	N/A
BW at 2.5 months of age (kg)	5.40	5.44	6.02	—	5.8
Age at necropsy (month)	2.5	2.5	2.5	6	2.5

AAV, adeno-associated virus; BW, body weight; N/A, not applicable; —, not available.

<sup>a</sup>Dogs used in previous published experiment.

TABLE 2. BLOOD EXAMINATION RESULTS

	Age (2.5 months)			Age (1.5–3.5 months) (n=20)	
	<i>Christa</i>	<i>Barbara</i>	<i>Artemis</i>	Uninjected control, mean ± SEM	Uninjected control, range
Calcium (mg/dl)	11.8	11.8	10.8	11.2 ± 0.1	10.5–11.9
Chloride (mEq/liter)	109	<b>113</b> <sup>a</sup>	109	106.6 ± 0.6	99–111
Phosphorus (mg/dl)	9.4	9.2	9.2	8.5 ± 0.2	7.0–10.1
Potassium (mEq/liter)	<b>7</b>	5.1	5	5.8 ± 0.1	5.2–7.1
Sodium (mEq/liter)	142	145	148	141.5 ± 0.8	133–148
Albumin (g/dl)	2.5	2.6	2.3	2.7 ± 0.1	2.1–3.6
Alkaline phosphatase (ALP) (U/liter)	<b>209</b>	<b>310</b>	<b>239</b>	147.9 ± 5.4	111–200
Alanine aminotransferase (ALT) (U/liter)	70	52	42	25.7 ± 4.4	9–97
ALP/ALT ratio	2.9	5.9	5.7	8.1 ± 1.1	1.3–22
Anion gap (mEq/liter)	20	<b>17</b>	25	22.2 ± 0.5	19–28
Cholesterol (mg/dl)	236	194	186	254.2 ± 14.7	173–427
Creatinine (mg/dl)	0.5	0.4	0.5	0.4 ± 0.0	0.2–0.7
Gamma-glutamyl transpeptidase (GGT) (U/liter)	<3	2	<3	0.9 ± 0.4	0–6
Globulin (g/dl)	2.2	2.2	1.9	2.2 ± 0.1	1.7–2.7
Glucose (mg/dl)	<b>197</b>	110	<b>88</b>	105.3 ± 2.4	89–126
Total bilirubin (mg/dl)	0.2	0.2	0.3	0.2 ± 0.0	0.1–0.4
Total CO <sub>2</sub> (mEq/liter)	20	20	19	18.6 ± 0.9	7–24
Total protein (g/dl)	4.7	4.8	4.2	4.9 ± 0.1	4.1–6.3
Urea nitrogen (mg/dl)	10	14	19	11.8 ± 1.4	4–22

<sup>a</sup>Bold font indicates the value is not within the range of uninjected control.

newborn dogs after systemic delivery (Pan et al., 2015). We used newborn dogs because they are minimally immunogenic so that we can test if AAV-8 can efficiently transduce dog muscles before we clone our new CpG-free vector. The experimental protocol and dogs are summarized in **Table 1**.

As safety is the most important concern, we first looked at the blood panel in treated dogs. Although a few values are slightly over the range of our un-injected controls, they either reflect transgene expression (alkaline phosphatase) or are not clinically meaningful (**Table 2**).

In our previous study, we demonstrated bodywide skeletal muscle transduction after intravenous injection of  $2 \times 10^{14}$  vg/kg of AAV-9 in newborn puppies. However, gene transfer in many muscles (such as RF, CS, and AR) remains sub-optimal (50-80%) (**Figure 16A**). A 3-fold increase in the vector dose (to  $6.14 \times 10^{14}$  vg/kg) resulted in complete (~100%) transduction of every limb muscle in Christa (**Figure 16A**). Boosting the dose further to  $9.65 \times 10^{14}$  vg/kg in Barbara (~5-fold higher than the dose used in Dojo) increased the vector genome copy number in most muscles but it did not yield dramatically much higher AP activity in muscle lysate suggesting a saturation effect in skeletal muscle (**Figure 16C, D**).

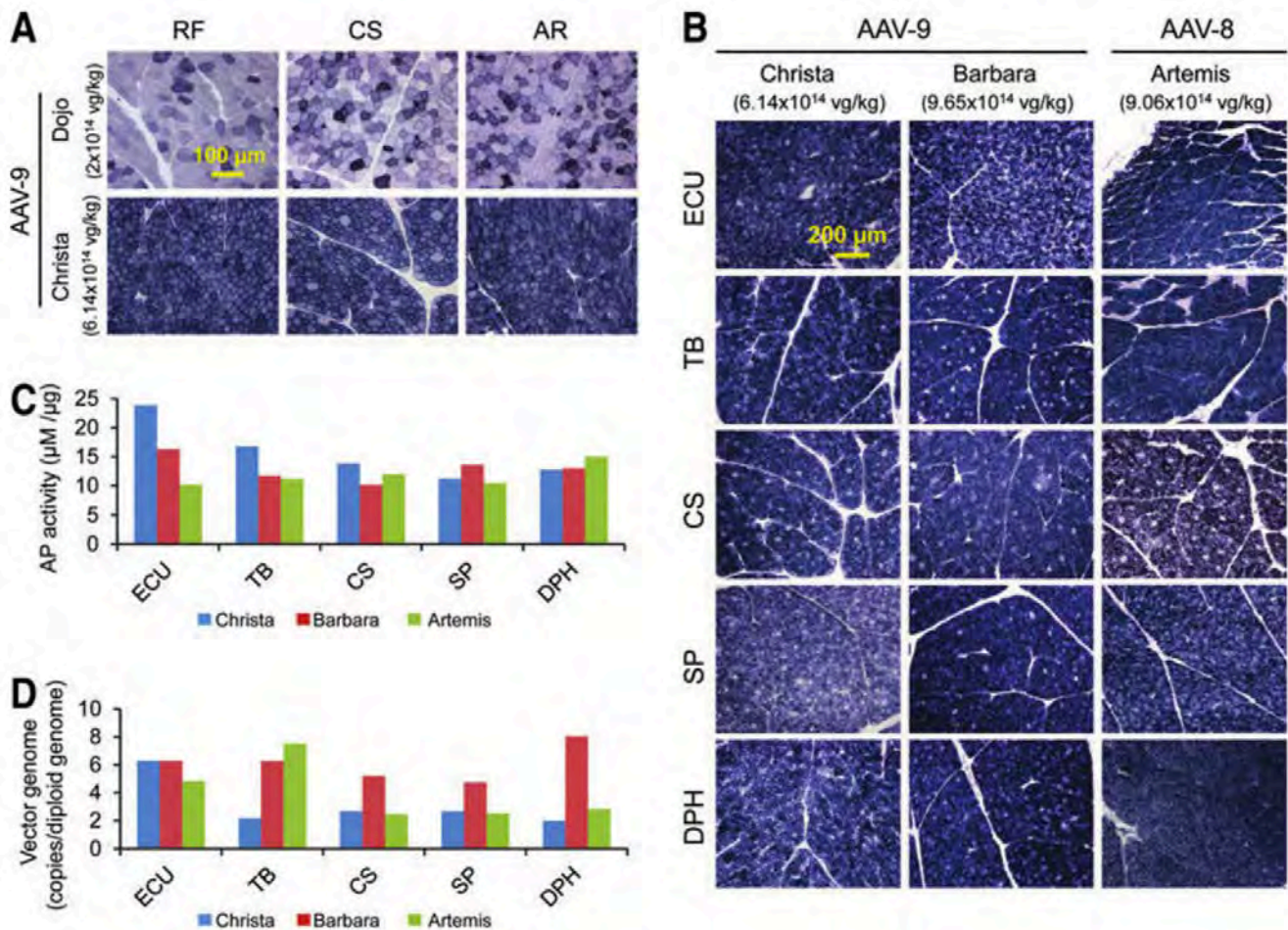
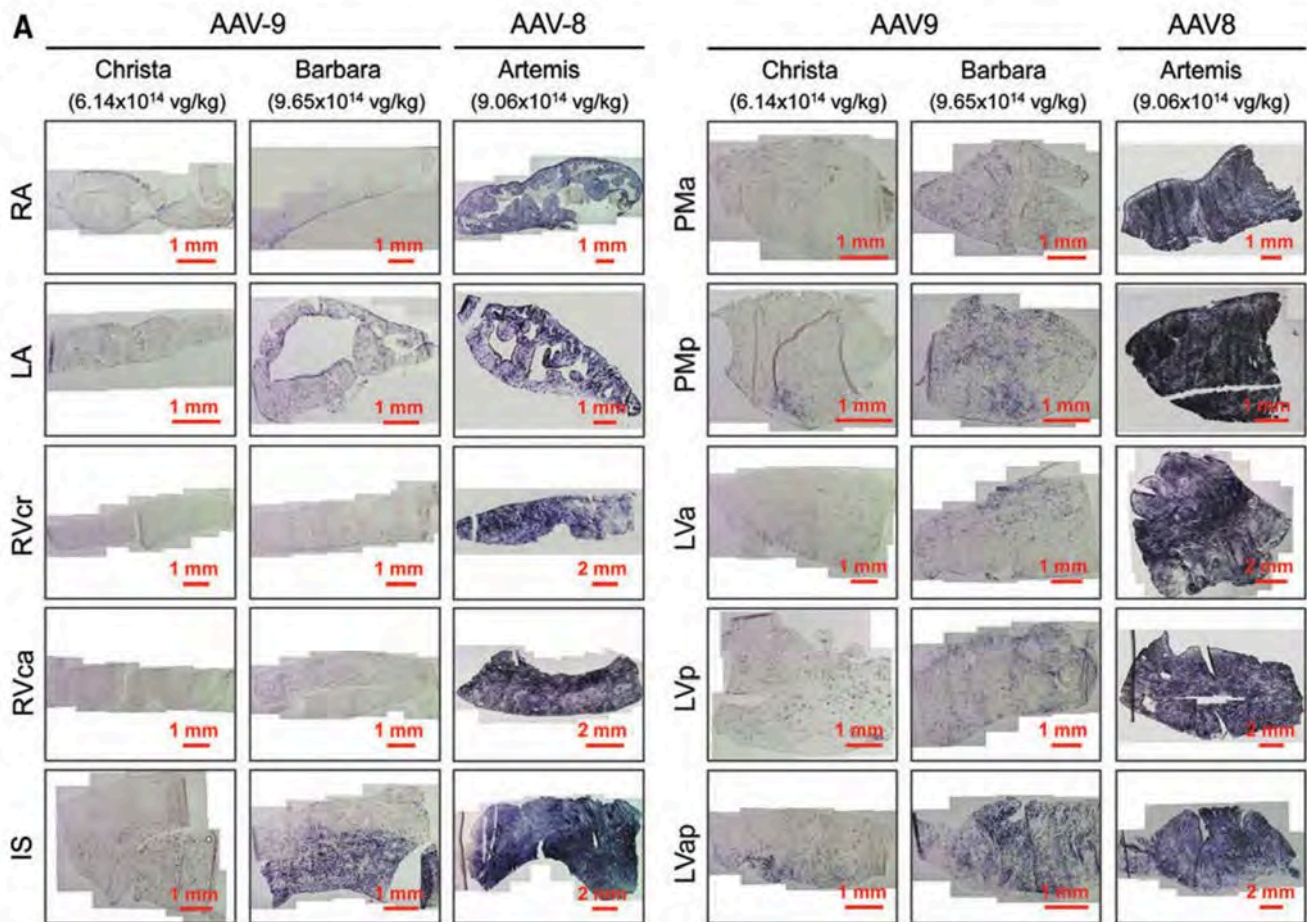


Figure 13. Intravenous injection of high dose AAV-9 results in improved skeletal muscle transduction in neonatal dogs. A, Representatively photomicrographs of AP histochemical staining from muscles that were injected with low (Dojo,  $2 \times 10^{14}$  vg/kg) and medium (Christa,  $6.14 \times 10^{14}$  vg/kg) doses of the AAV-9 AP reporter vector. RF, rectus femoris; CS, cranial sartorius; AR, abdominal rectus. B,

Representatively photomicrographs of skeletal muscle AP histochemical staining from AAV-9 injected dog Christa and Barbara as well as AAV-8 injected dog Artemis. ECU, extensor carpi ulnaris; TB, triceps brachii; CS, cranial sartorius; SP, superficial pectoralis; DPH, diaphragm. C, Quantitative examination of AP activity in muscle lysate. D, Comparison of the AAV vector genome copy number in different skeletal muscles.

Next, we examined AAV transduction in the heart. In our published studies with AAV-9 (1 to  $2.5 \times 10^{14}$  vg/kg), hardly any expression was detected in the heart. In Christa ( $6.14 \times 10^{14}$  vg/kg), AP positive cells became readily detectable by histochemical staining in the interventricular septum, left ventricle and papillary muscle (**Figure 17A**). A dose-dependent increase in AP expression was observed in almost every region of the heart in Barbara ( $9.65 \times 10^{14}$  vg/kg). Widespread AP positive cells were seen in the left atrium, interventricular septum, papillary muscle and left ventricle (**Figure 17A**). However, it never reached the level seen in Artemis, a puppy injected with  $9.06 \times 10^{14}$  vg/kg of AAV-8 (**Figure 17A, B**). Interestingly, on histochemical staining, the right heart (RA and RV) was efficiently transduced by AAV-8 but barely transduced by AAV-9 (**Figure 17A**).

AAV copy number quantification revealed an interesting pattern. In the right ventricle and interventricular septum, we detected more vector genome in AAV-8 injected Artemis, consistent with high transduction. But in the right atrium, similar number of the AAV genome copy was found despite a substantially much more robust expression in the AAV-8 injected puppy (**Figure 17**). Most



surprisingly, in the left atrium, papillary muscle and left ventricle, AAV copy number in Barbara ( $9.65 \times 10^{14}$  vg/kg of AAV-9) was 3 to 5-fold higher than that of Artemis ( $9.06 \times 10^{14}$  vg/kg of AAV-8).

However, the high copy number did not result in high expression suggesting that a significant portion of the AAV-9 genome may have been trapped in a yet to be defined dead compartment and/or not converted to the transcription-competent form in cardiomyocytes and cannot express the transgene.

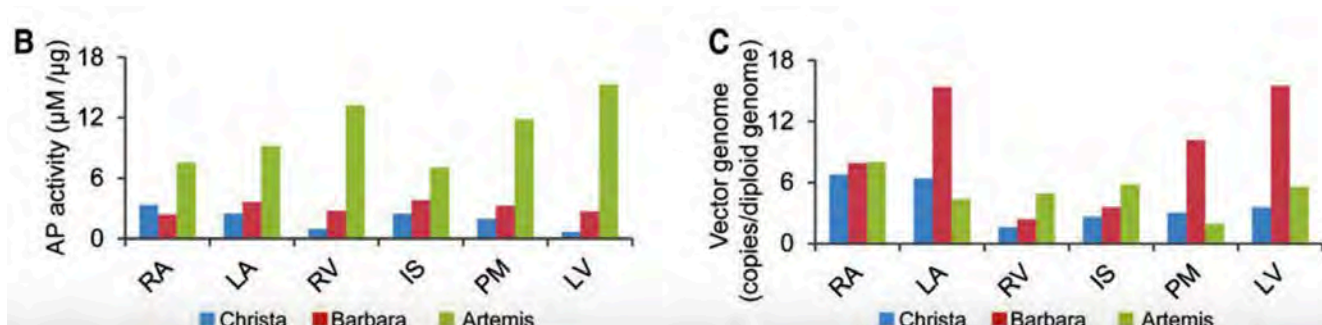


**Figure 17.** AAV-8 is more efficient than AAV-9 in transducing neonatal dog heart. A, Representative lower magnification microphotographs of AP staining in different parts of the heart including from right atrium (RA), left atrium (LA), right ventricular cranial wall (RVcr), right ventricular caudal wall (RVca), interventricular septum (IS), anterior papillary muscle (PMa), posterior papillary muscle (PMp), left ventricular anterior wall (LVa), left ventricular posterior wall (LVp) and left ventricular apex (LVap). B, Quantitative examination of AP activity in muscle lysate from different parts of the heart. C, AAV genome copy quantification in different parts of the heart. RA, right atrium; LA, left atrium; RV, right ventricle; IS, interventricular septum; PM, papillary muscle; LV, left ventricle.

In summary, our data suggests that AAV-8 can lead to bodywide muscle transduction (Pan et al., 2015). Importantly, we found AAV-8 can transduce newborn dog heart at high efficiency independent of the vector dose (Pan et al., 2015). Because cardiomyopathy is a major cause of death in DMD patients, this piece of new data provides further support to develop AAV-8 microgene therapy in the canine model.

***Accomplishment 3. We have demonstrated for the first time successful systemic AAV vector (reporter and micro-dystrophin delivery in young adult dystrophic dogs.***

A previous study suggests that systemic AAV delivery in affected dogs

Dog name	Bouchelle	Stephan	Brooke
Dystrophin gene mutation	Intron 19 insertion	Intron 6 point mutation	Intron 13 insertion
Gender	Male	Female	Male
Body weight at injection (kg)	3.7	3.5	3.2
Body weight at necropsy (kg)	10.6	10.6	11.3
Promoter	RSV	CMV	CMV
Transgene	Human AP reporter gene	Canine $\mu$ -dystrophin	Canine $\mu$ -dystrophin
Total AAV injected (vg particles)	$7.09 \times 10^{14}$	$1.77 \times 10^{15}$	$2.0 \times 10^{15}$
Vector dose (vg particles/kg BW)	$1.92 \times 10^{14}$	$5.04 \times 10^{14}$	$6.24 \times 10^{14}$
Vector volume (ml/kg BW)	4.9	5.7	6.2
Age at AAV injection (month)	2.0	1.8	1.8
Age at biopsy (month)	3.0	2.8	2.8
Age at necropsy (month)	5.5	5.3	5.8

may induce an inflammatory response and further worsen the disease (Kornegay et al., 2010). To probe the feasibility and safety of systemic AAV gene therapy in young adult DMD dogs, we performed a study using our previously published AAV vectors including a alkaline phosphatase reporter gene vector and a micro-dystrophin gene vector (Yue et al., 2015). Experimental dogs are listed in **Table 3** in the previous page.

Dog Bouchelle was injected with  $1.92 \times 10^{14}$  vg particles/kg ( $7.09 \times 10^{14}$  vg particles total) of a Rous sarcoma virus (RSV) promoter driven alkaline phosphatase (AP) reporter AAV vector (Table 3). This dog also received five-week transient immune suppression. We also delivered a micro-dystrophin AAV vector to affected dogs Stephan ( $5.04 \times 10^{14}$  vg particles/kg,  $1.77 \times 10^{15}$  vg particles total) and Brooke ( $6.24 \times 10^{14}$  vg particles/kg,  $2.00 \times 10^{15}$  vg particles total) (**Table 3**).

We first examined the potential toxicity. We found that the body weights of all these three injected dogs were within the range of untreated affected dogs in our colony (**Figure 18**, right). On the blood chemistry panel, we did not find any abnormality (**Figure 19**, Below).

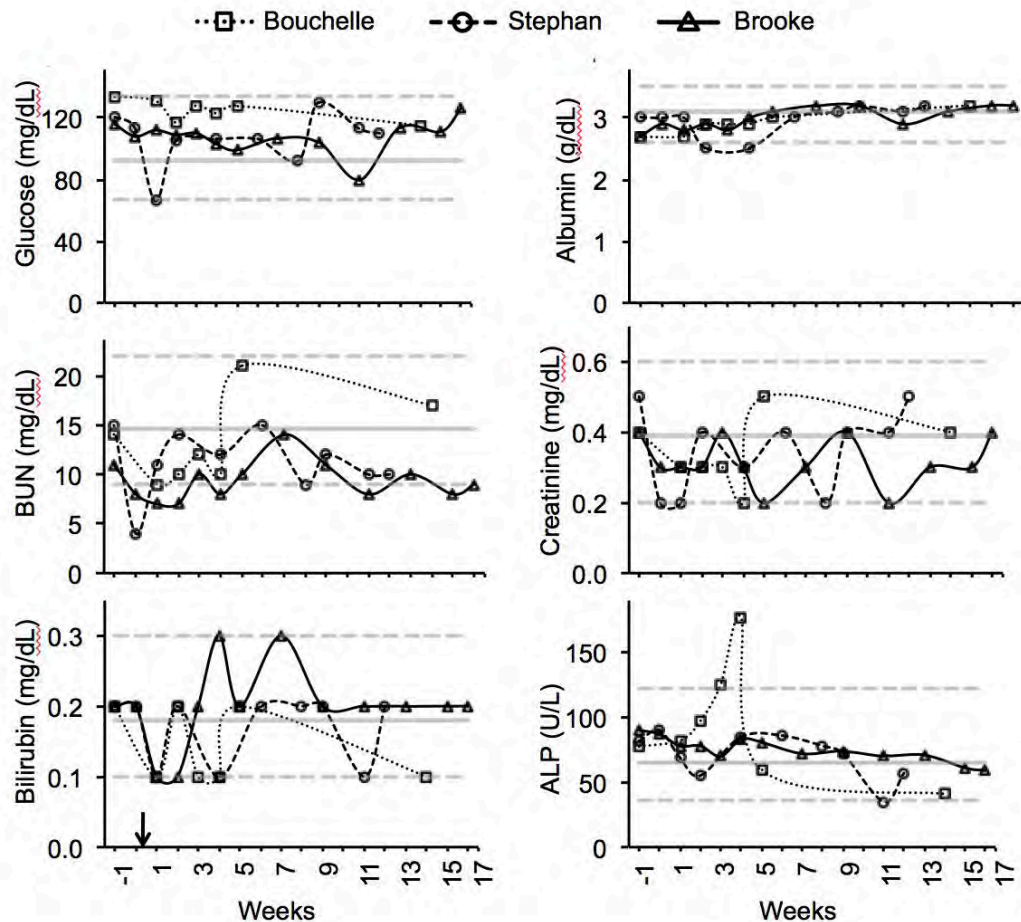
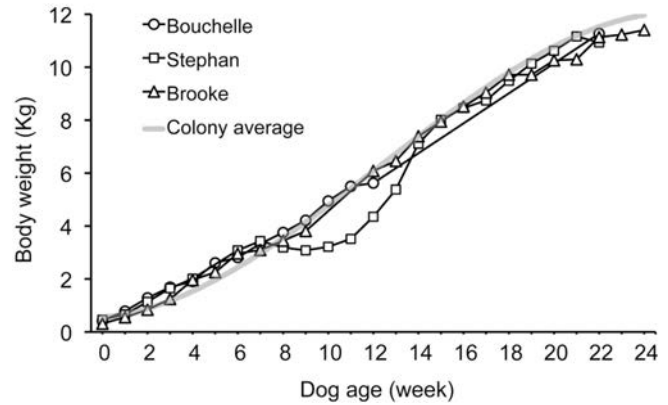


Figure 16. Blood biochemistry in experimental dogs. Dotted gray lines, the maximal and minimal values for age-matched untreated DMD dogs in our colony (N = 31). Solid gray line, the average value of age-matched untreated DMD dogs in our colony (N = 31).

Since our ultimate goal is to see if we can achieve bodywide systemic delivery to all muscles in the affected dog. We evaluated transgene expression and vector genome copy number. **Figure 20** shows the results from the dog Bouchelle. **Figure 21** shows the results from dogs Stephan and Brooke.

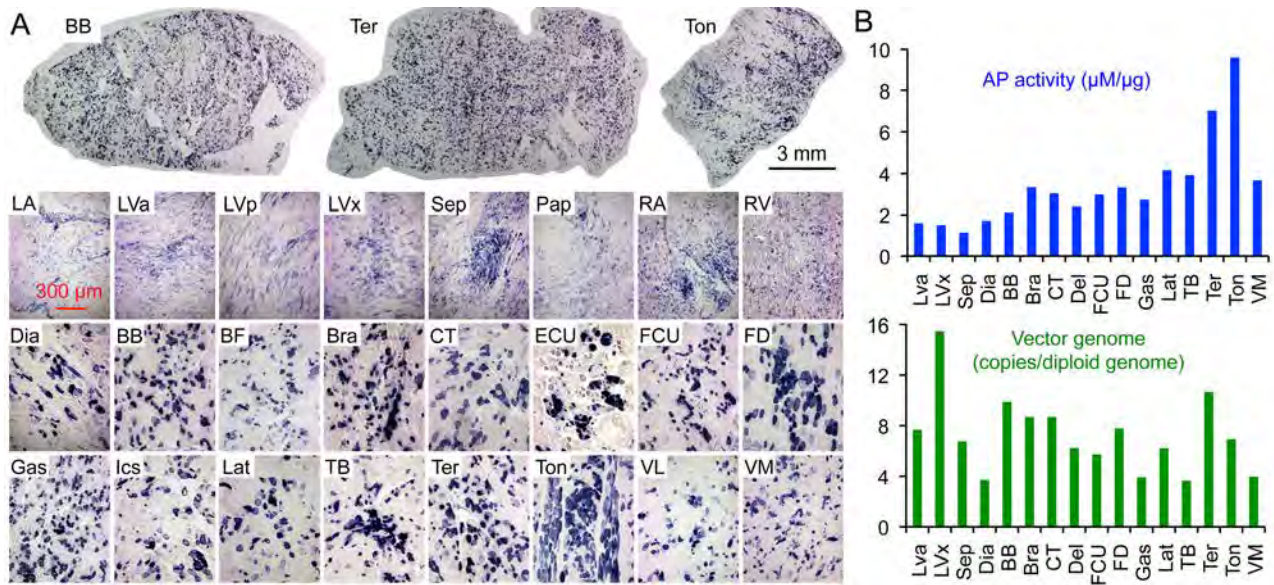


Figure 17. A single intravenous injection resulted in robust bodywide transduction with a reporter AAV vector.

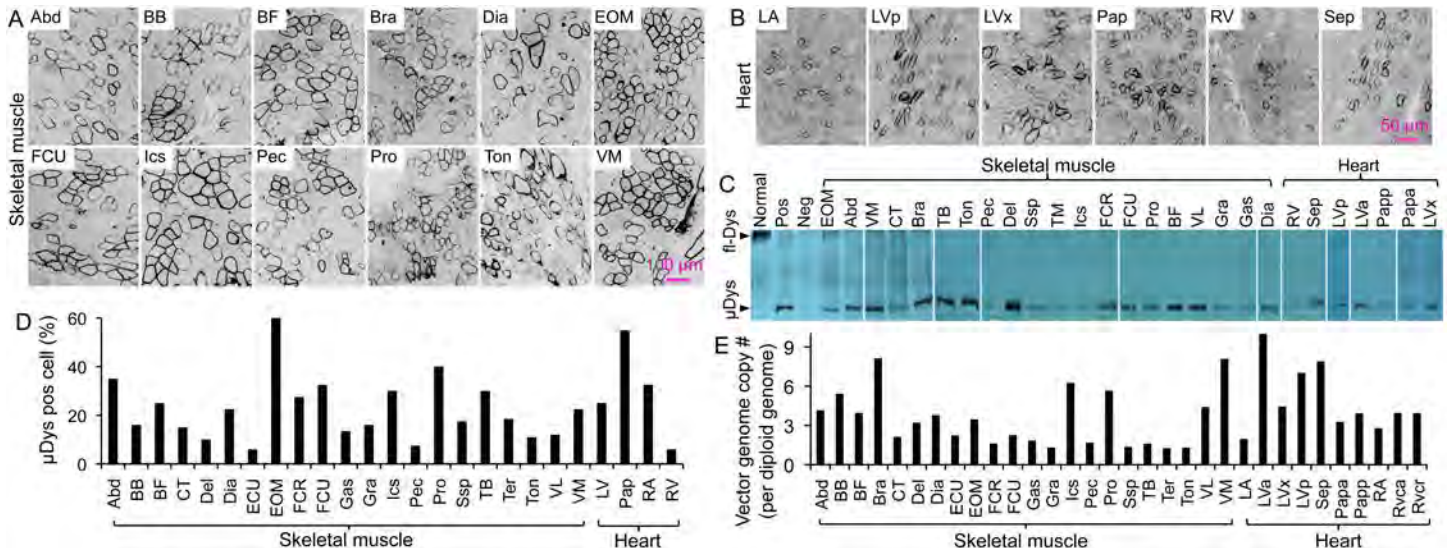
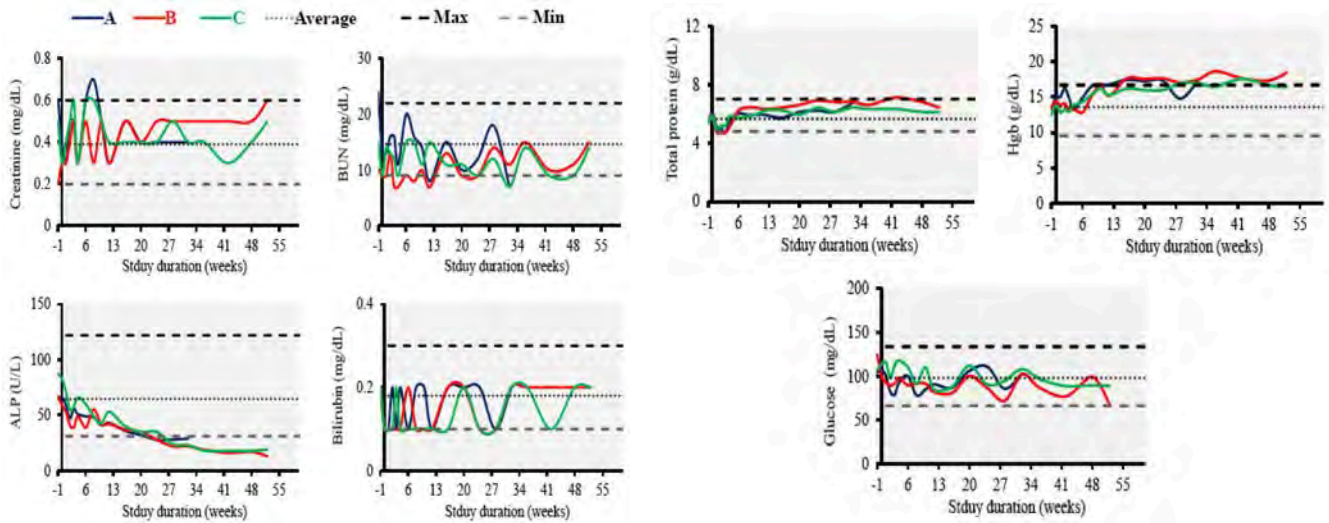


Figure 18. A single intravenous injection resulted in robust bodywide transduction with a micro-dystrophin AAV vector

In summary, our results suggest that systemic AAV gene transfer is safe and efficient in dystrophic large mammals (Yue et al., 2015). Our data established a strong foundation to test systemic AAV gene therapy in the canine model using the CpG-free human microgene vector.

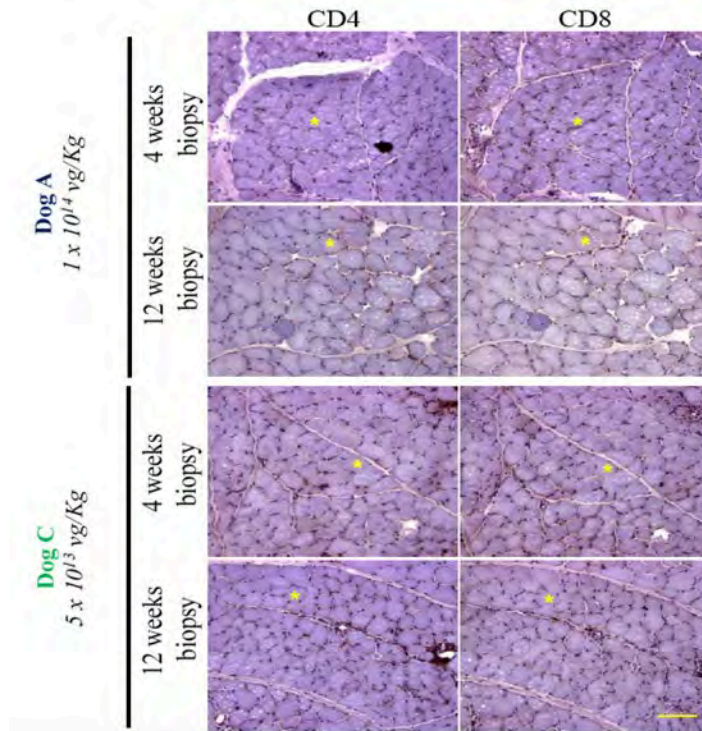
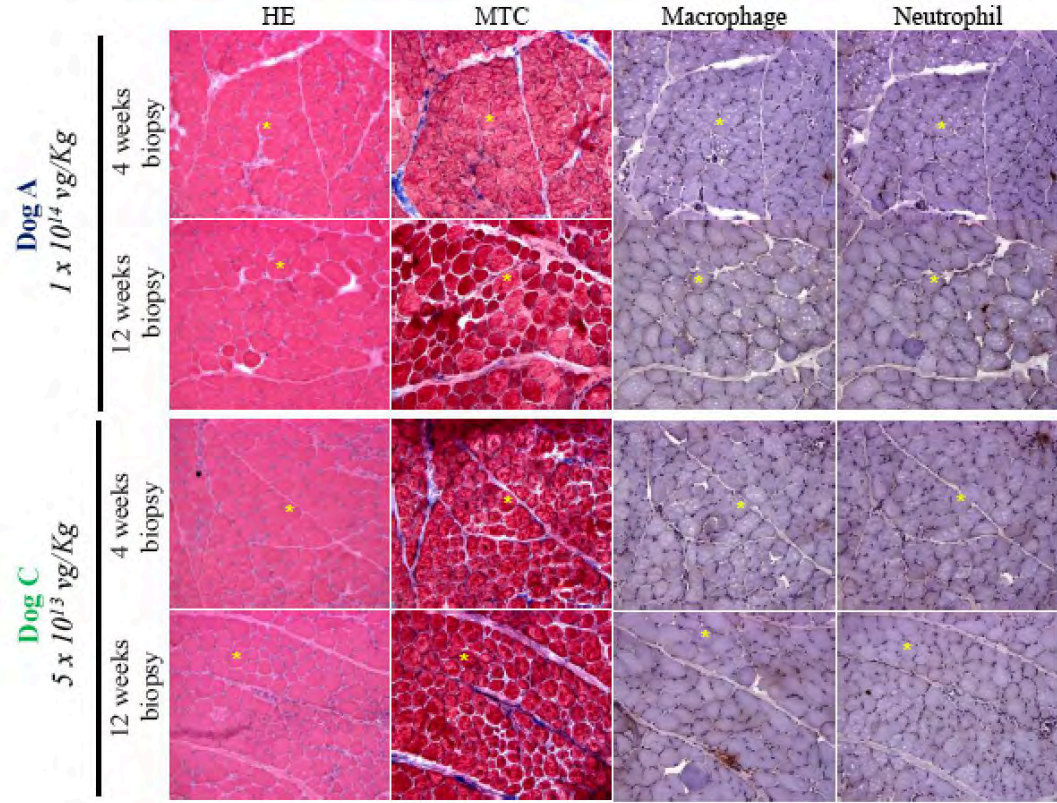
**Accomplishment 4. We have demonstrated for the first time long-term successful systemic AAV micro-dystrophin gene therapy in young adult dystrophic dogs.**

In t **Accomplishment 3t**, we described our initial test of systemic AAV micro-dystrophin delivery in affected dogs (Yue et al., 2015). Our report is the first convincing demonstration that systemic gene therapy is feasible in a young adult large mammal that suffers from Duchenne muscular dystrophy. As the first report, we only followed AAV injected dogs for four months. Since DMD is a lifelong disease, it is important to determine whether we can achieve long-term micro-dystrophin expression. To this end, we performed additional study in three more dogs (named dog A, B and C in Figures 16 to 19). Consistent with our report in 2015 (Yue et al., 2015), the blood profiles of all three treated dogs were within the normal range suggesting there is no major safety concern (**Figure 22**, below).

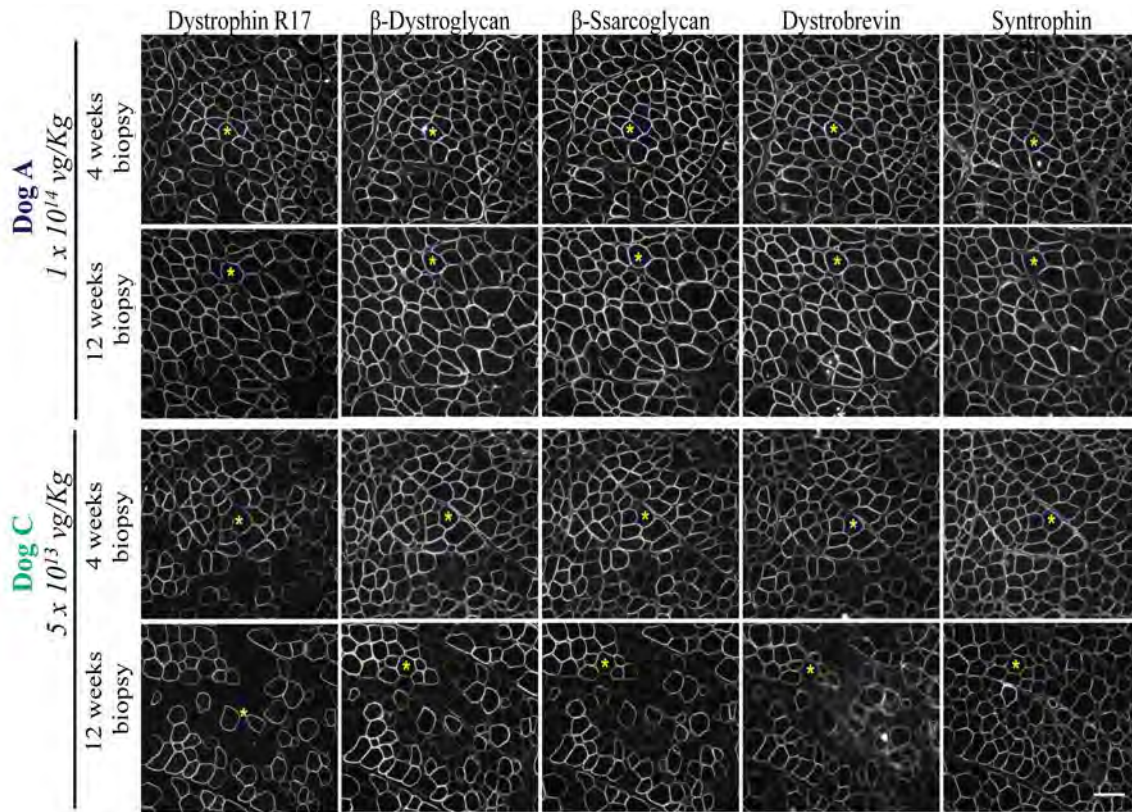


Next we examined muscle histology on the biopsied tissues (**Figure 23** next page top panel). On HE staining, muscle appeared normal although we indeed noticed a few infiltrating mononuclear cells in the interstitial region. Nevertheless, mononuclear cell infiltration was limited to small areas. We suspect that they may come from muscle damage that already happened before our AAV gene therapy. On Masson trichrome staining, we did not see apparent fibrosis. A little bit of fiber tissue was seen in the interstitial region where we expect to see the fascia. Immunohistochemistry staining for macrophage and neutrophil revealed minimal inflammation.

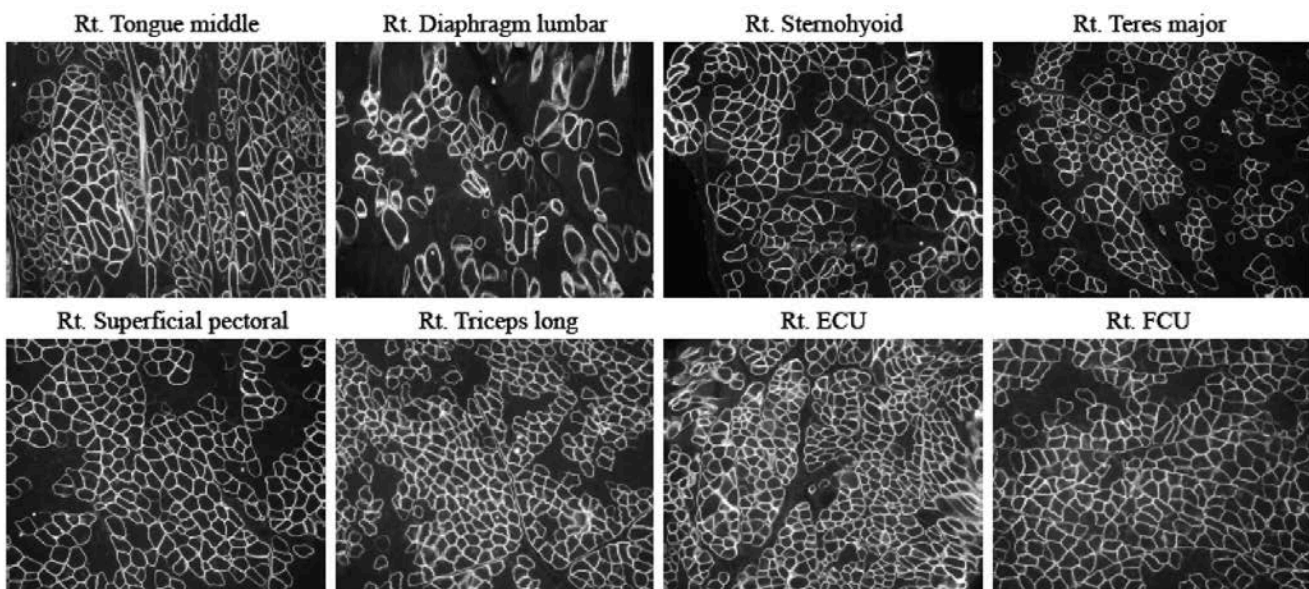
Since the T cell response is a major barrier for AAV micro-dystrophin gene therapy, we next evaluated CD4+ and CD8+ T cells by immunohistochemistry staining (**Figure 24**, next page bottom panel). We did not detect massive infiltration of CD4+ and CD8+ T cells suggesting there was minimal immune reaction.

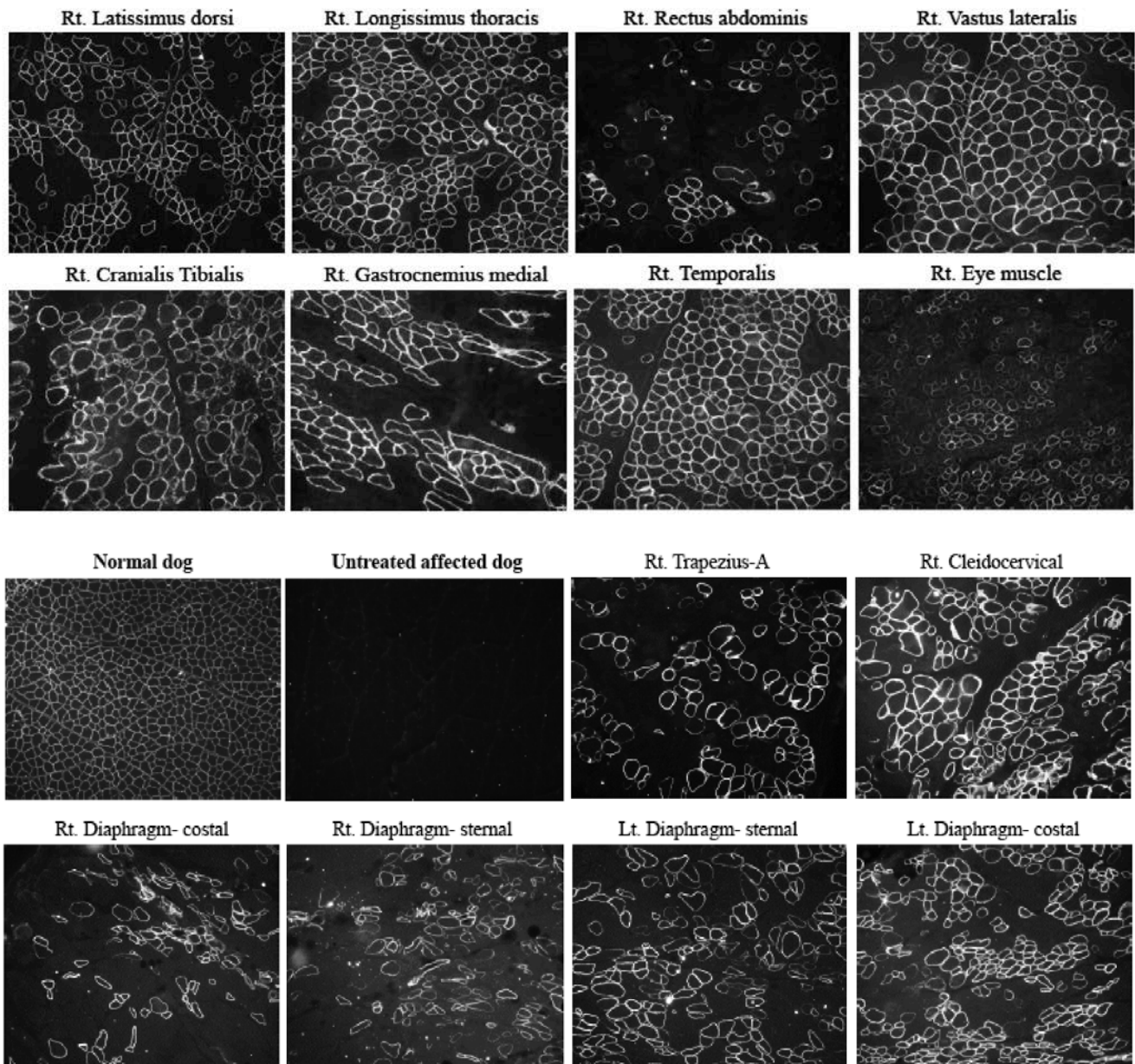


Next, we examined the dystrophin-associated glycoprotein complex by immunostaining (**Figure 25**, below). Micro-dystrophin expression (detected by an antibody against dystrophin spectrin-like repeat 17, R17) successfully restored  $\beta$ -dystroglycan,  $\beta$ -sarcoglycan, dystrobrevin and syntrophin.



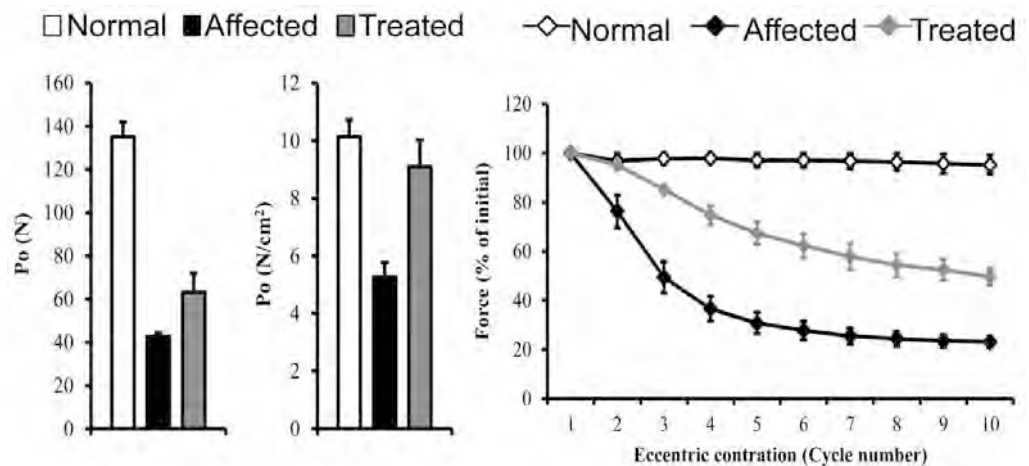
To confirm bodywide transduction, we euthanized one dog at 8 months after AAV injection. Dystrophin immunostaining photos from various muscles are shown in **Figure 26** (below and next page). We indeed achieved efficient whole body muscle micro-dystrophin expression.





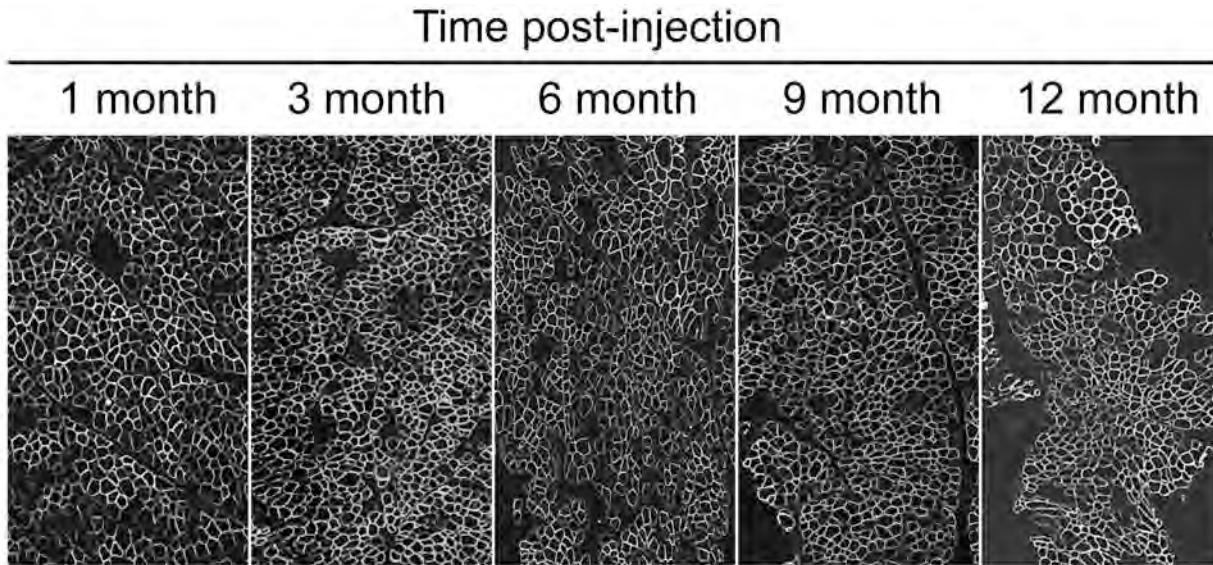
At the time of necropsy, we also performed in situ muscle force assay on the ECU muscle (both left and right side) (**Figure 27**, right).

Although we only have N=2 treated muscles, the absolute muscle force ( $P_o$  in N) was clearly improved. Muscle cross-sectional area normalized specific force ( $P_o$  in  $N/cm^2$ ) almost reached the level of normal dogs.



On eccentric contraction, we also detected clear improvement. The force drop following cycles of eccentric contraction was greatly attenuated in the treated dog.

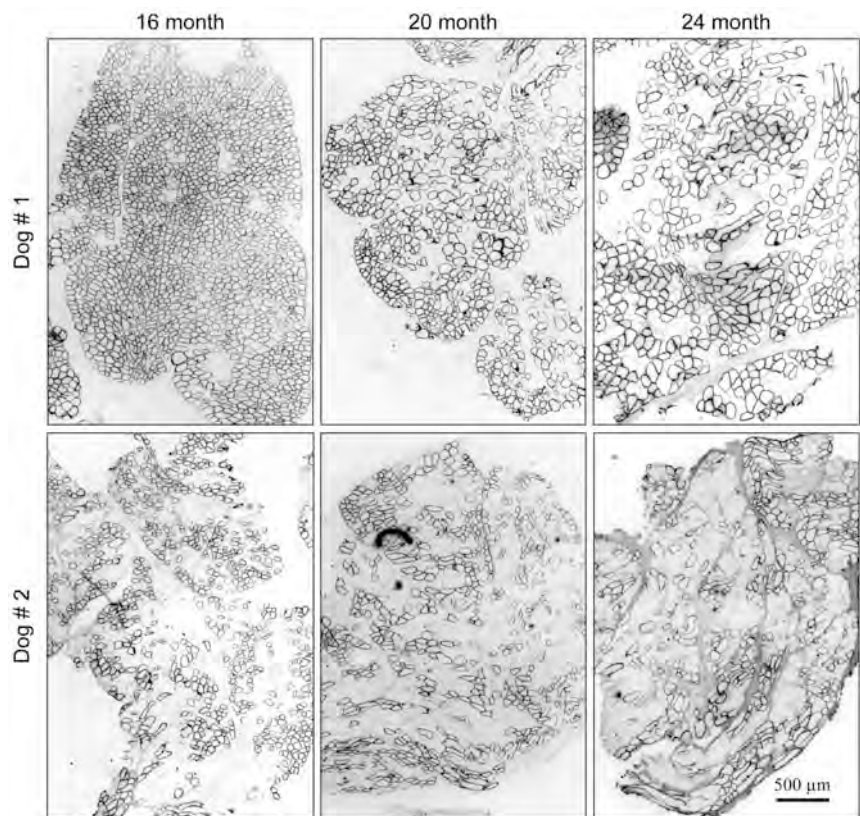
We have now kept these dogs for 12 months. Periodic biopsy revealed persistent robust micro-dystrophin expression for at least 12 months (**Figure 28**, below). We will continually monitor treated dogs till the end of the study.

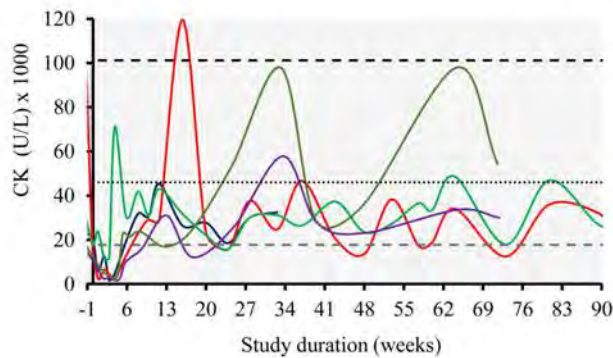
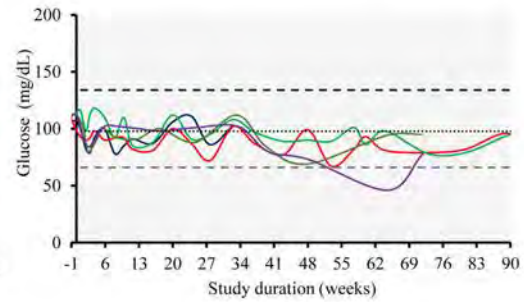
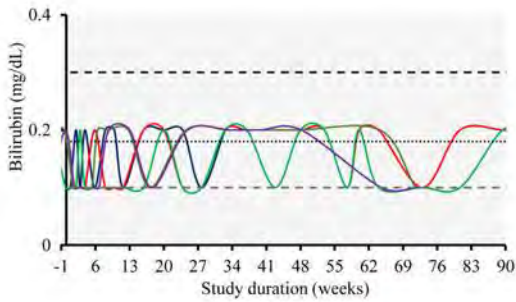
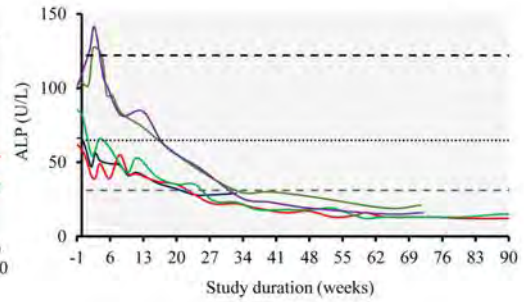
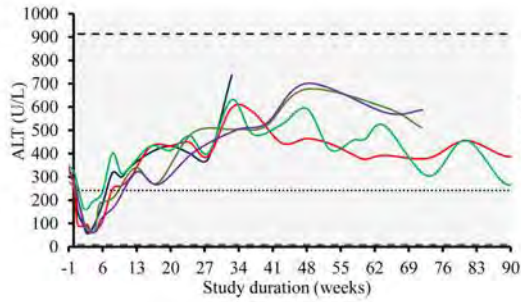
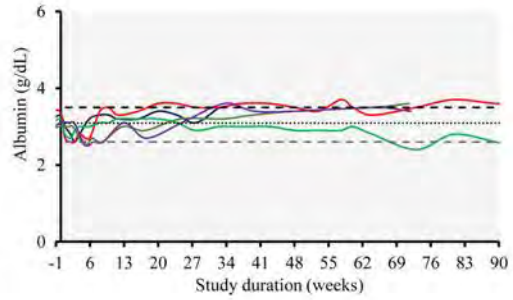
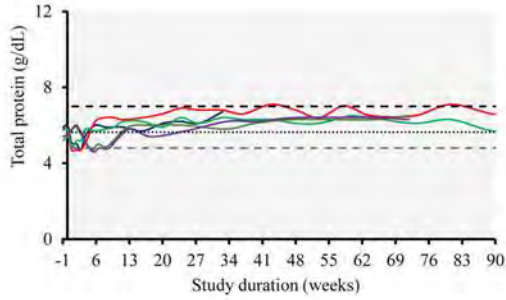
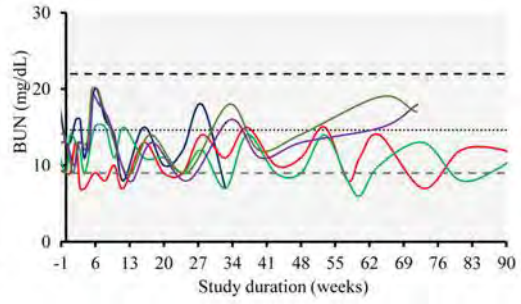
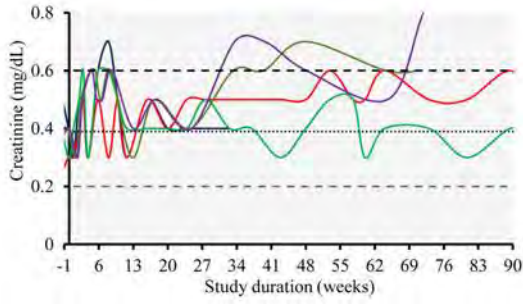


We have now accumulated additional data demonstrating persistent micro-dystrophin expression up to 48 weeks post-injection demonstrating lack of toxic or side effect. Below we show biopsy data up to 24 months after injection (**Figure 29** right).

We have now had additional safety data on blood profiles up to 90 weeks after injection (**Figure 30** next page).

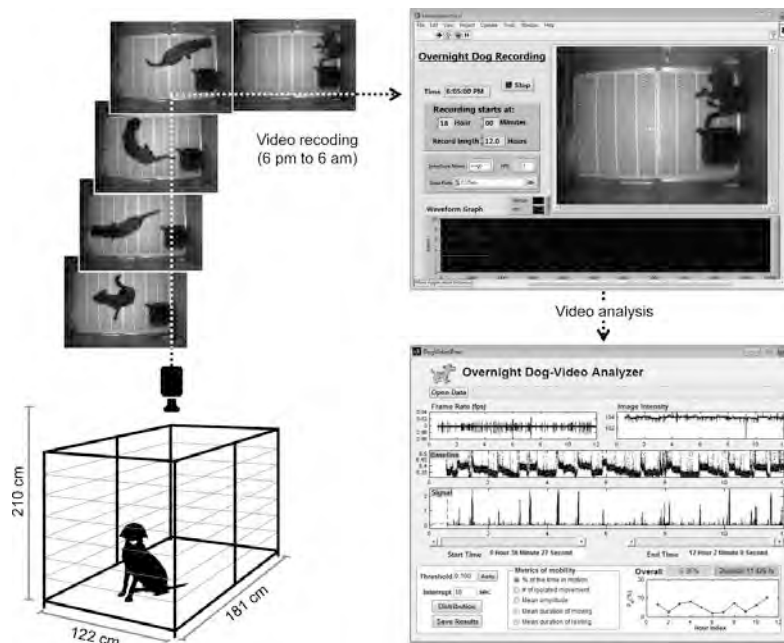
**Our data suggest that a one-time therapy in young adult dystrophic dogs resulted in persistent micro-dystrophin expression for two years and importantly, the blood profiles were all within the expected ranges and there is no adverse reaction.**





***Accomplishment 5. We have developed a novel non-invasive method to evaluate the overall activity of dogs.***

Issues related to the outcome measurement have greatly and negatively impacted drug development in the field of DMD. This has caught significant attention in recent FDA review of read-through drug Ataluren and exon-skipping drugs (Eteplirsen and Drisapersen). The situation is even worse in regards to the dog model. So far, there is no effective method to objectively evaluate whole-body mobility in a dog. Since a robust outcome measurement is essential to the success of our project, we decided to explore new non-invasive approaches that can objectively quantify dog mobility. Specifically, we developed a robust automatic video capturing/processing system to quantify dog mobility at night (**Figure 31**, below).



Using this system, we captured and analyzed dog movement at night. **Figure 32** (below) shows representative data from a normal and an affected dog.

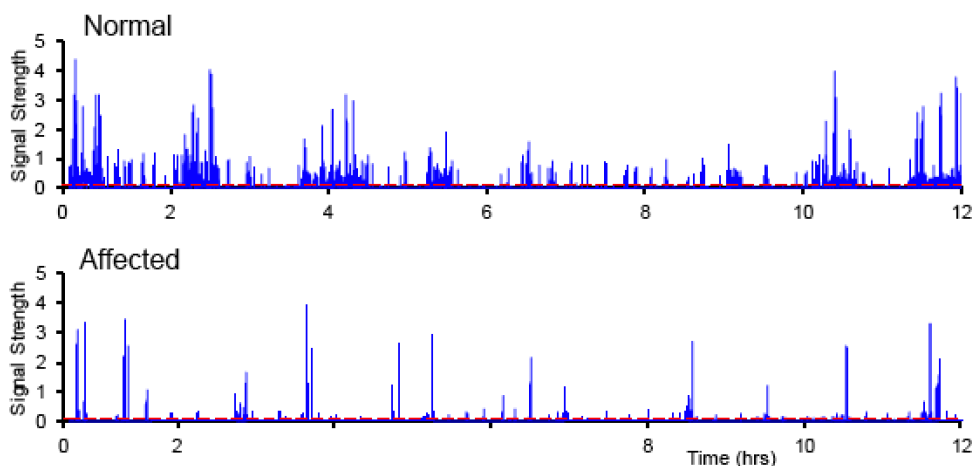
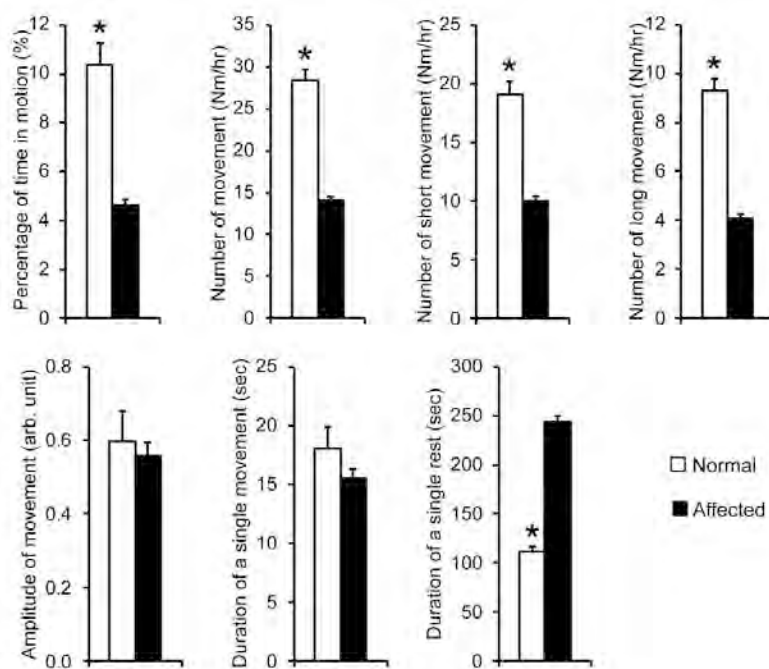


**Figure 33** (below) shows population data from 12 normal (age  $14.7 \pm 1.9$  months) and 22 affected dogs (age  $15.4 \pm 1.24$  months). Throughout the night, normal dogs were in motion  $10.4 \pm 0.9\%$  of the time while affected dogs were in motion  $4.6 \pm 0.2\%$  of the time ( $p < 0.0001$ ). In other words, normal dogs moved approximately 75 min and affected dogs moved approximately 33 min during 12-hr recording. On average, normal dogs moved  $28.3 \pm 1.3$  times per hour while affected dogs only moved  $14.1 \pm 0.4$  times per hour ( $p < 0.00001$ ). Additional analysis showed that normal dogs not only made significantly more short movements but also made significantly more long movements ( $p < 0.00001$ ). Interestingly, the average amplitude of movement was similar between normal ( $0.60 \pm 0.08$ ) and affected ( $0.56 \pm 0.04$ ) dogs ( $p = 0.68$ ). Further, there was no significant difference in the average duration of movement between normal and affected dogs. In contrast to the duration of movement, the average duration of rest in affected dogs ( $243.1 \pm 0.6$  sec) was significantly longer than that of normal dogs ( $111.5 \pm 4.5$  sec) ( $p < 0.00001$ ). Collectively, we have established this overnight activity monitoring as an excellent outcome measurement for studying whole body activity in adult dogs. We expect this assay to greatly enhance our ability to study the functional outcome of systemic AAV micro-dystrophin gene therapy in affected dogs. We will include this assay in our future studies.



***Accomplishment 6. We have developed a new physiological assays to study sympatholysis and functional ischemia in dogs.***

Functional ischemia is an important pathogenic factor in the initiation and progression of muscle disease in Duchenne muscular dystrophy. This is mainly due to failure to anchor nNOS to the sarcolemma. Unfortunately, the first generation micro-dystrophin gene cannot restore nNOS to the sarcolemma. We discovered R16/17 as the critical nNOS-binding domain in dystrophin. Hence, we engineered the second-generation R16/17-containing micro-dystrophin gene. We showed in mouse models that R16/17-containing microgene can effectively counteract functional ischemia and improve therapeutic efficacy. The canine DMD model has been established since 1988 and DMD dogs have been used in numerous studies to evaluate pharmacological and genetic therapies for DMD. Yet, there

has been no study on functional ischemia in DMD dogs. To fill this knowledge gap, we developed a novel assay to quantify limb muscle blood flow in resting and contracting dog muscle during this funding period. This assay will allow us to test whether R16/17-containing micro-dystrophin vector can effectively prevent functional ischemia in the canine DMD model.

The protocol was developed on our previously published in situ ECU muscle force assay (**Figure 34**). A similar set-up was used except the placement of a flow probe inside the brachial arterial for quantifying blood flow changes at rest and during contraction in the absence and presence of NE administration. **Figure 35** illustrates the step-by-step protocol.

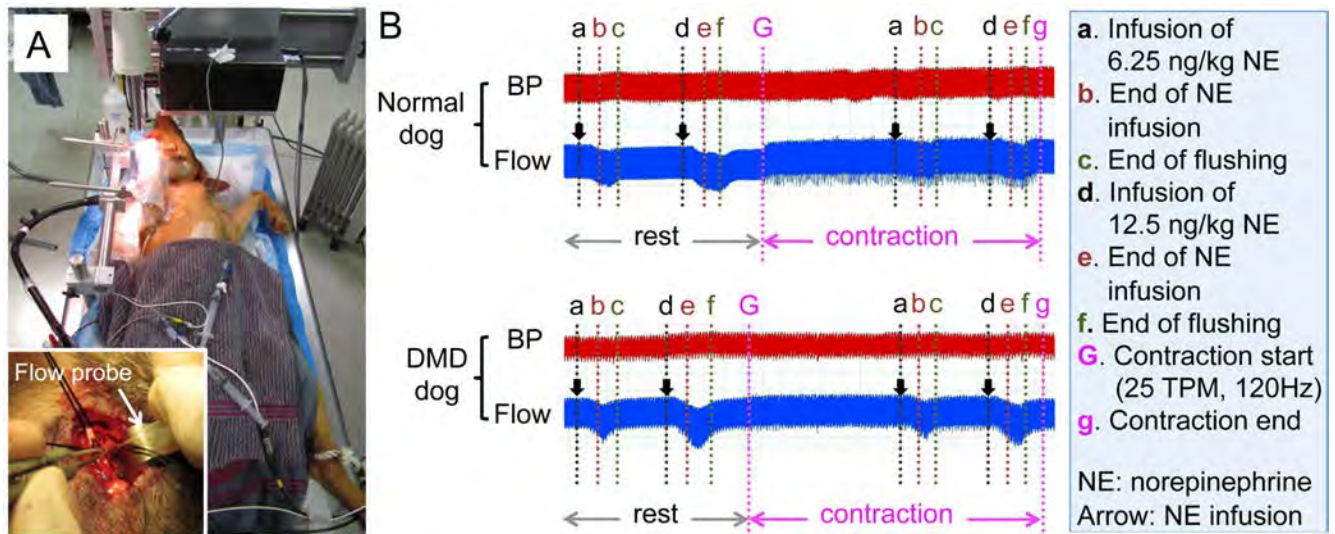


**Figure 34.** Development of a novel physiological assay to study functional ischemia in dogs. **A**, Dog hemodynamic assay set-up. **B**, Representative tracing from a normal (top panel) and an affected (bottom panel) dogs. During contraction, NE-induced reduction of the blood flow is blunted in normal dogs but not in affected dogs.

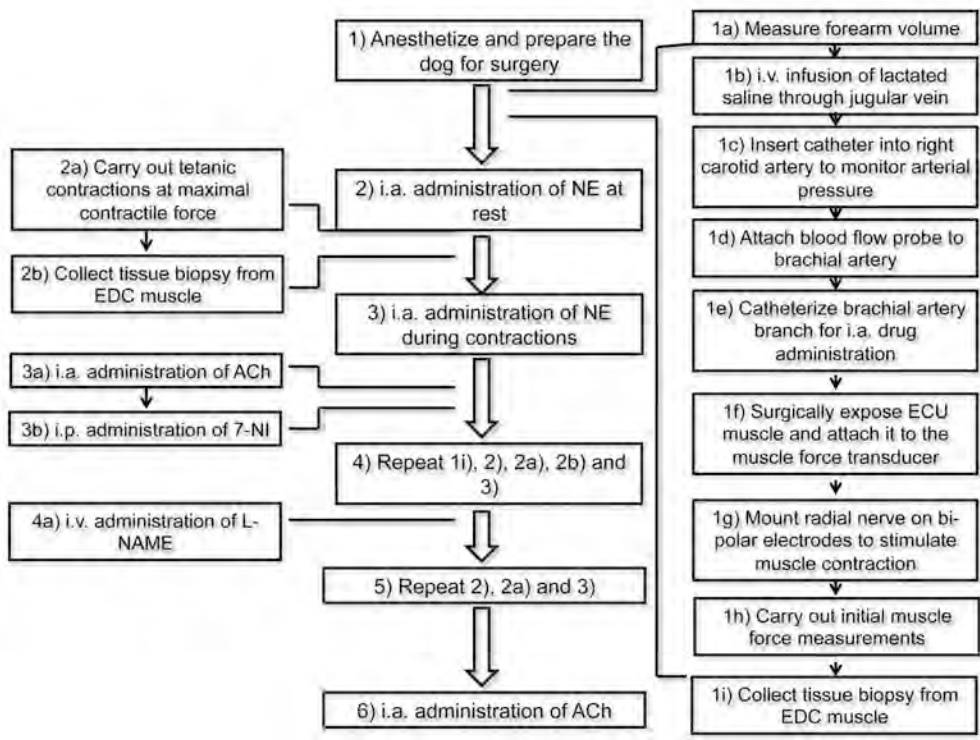


**Figure 35.** Step-by-step illustration of the protocol used for studying the dog muscle perfusion at rest and during contraction. Following surgery preparation, we first quantified the blood flow at rest and contraction in the absence of non-epinephrine (NE). Then we quantified blood flow in the presence of NE and various chemicals.

Normal and DMD dogs had a similar mean arterial pressure (MAP) at the baseline (**Table 1**). The baseline mean artery blood flow in the brachial artery (MABF) of DMD dogs only reached ~50% of that of normal dogs (**Table 4**). Nevertheless, the forearm volume normalized mean vascular conductance (MVC) was also similar between normal and DMD dogs at the baseline. Forelimb contraction at the maximal contractile force significantly increased MABF and MVC in both normal and DMD dogs (**Table 4**).

Drug condition	Muscle contractile status	Group	MAP (Hgmm)	MABF (mL/min)	MVC (mL/min/Hgmm/100mL)
Baseline					
	Rest	Normal	70.82 ± 3.27	102.00 ± 18.78	0.44 ± 0.06
		DMD	70.29 ± 3.95	57.93 ± 7.56 <sup>a</sup>	0.42 ± 0.04
	Contraction	Normal	69.50 ± 4.06	123.00 ± 24.97 <sup>b</sup>	0.52 ± 0.07 <sup>b</sup>
		DMD	69.93 ± 3.33	66.43 ± 7.70 <sup>a,b</sup>	0.50 ± 0.05 <sup>b</sup>
After 7-NI					
	Rest	Normal	70.10 ± 3.33	100.60 ± 16.12	0.46 ± 0.06
		DMD	67.14 ± 3.58	51.00 ± 5.43 <sup>a</sup>	0.41 ± 0.04
	Contraction	Normal	69.00 ± 3.19	126.56 ± 22.21 <sup>b</sup>	0.56 ± 0.06 <sup>b</sup>
		DMD	66.86 ± 3.25	62.57 ± 6.07 <sup>a,b</sup>	0.51 ± 0.05 <sup>b</sup>
After L-NAME					
	Rest	Normal	84.20 ± 3.83 <sup>c</sup>	132.10 ± 19.43 <sup>c</sup>	0.50 ± 0.06
		DMD	80.21 ± 3.49 <sup>c</sup>	62.79 ± 6.40 <sup>a,c</sup>	0.42 ± 0.04
	Contraction	Normal	84.90 ± 3.70 <sup>c</sup>	152.40 ± 21.90 <sup>b,c</sup>	0.58 ± 0.07 <sup>b</sup>
		DMD	81.93 ± 3.38 <sup>c</sup>	75.07 ± 6.81 <sup>a,b,c</sup>	0.50 ± 0.05 <sup>b</sup>

Abbreviations: MAP, mean arterial pressure; MABF, mean arterial blood flow; MVC, mean vascular conductance; DMD, Duchenne muscular dystrophy.

a, Significantly different from that of normal.

b, Significantly different from that of at rest.

c, Significantly different from that of at baseline and after 7-NI.

c, Significantly different from that of at baseline and after 7-NI.

To assess sympatholysis, we administrated NE to induce sympathetic vasoconstriction at rest and during muscle contraction (**Figure 36, Tables 5 and 6**) (next two pages). In normal dogs, NE administration resulted in 63.76 ± 5.62% reduction of MVC at rest but only 29.46 ± 4.68% during contraction ( $P < 0.05$ , **Figure 36C, Table 5**). Sympatholysis efficiency reached 56.34 ± 5.07% ( $P < 0.05$ , rest vs contraction; **Figure 36E, Table 5**). In DMD dogs, NE administration resulted in 76.89 ± 2.51% reduction of MVC at rest and 56.82 ± 3.15% reduction during contraction ( $P < 0.05$ , rest vs contraction; **Figure 36D, Table 5**). Interestingly, the sympatholytic efficiency between rest and contraction also reached statistical significance for DMD dogs. Nevertheless, the sympatholytic efficiency in DMD dogs (25.72 ± 3.77%) was significantly lower than that of normal dogs ( $P < 0.05$ , normal vs DMD; **Figure 36E, Table 5**).

Our protocol reliably portrayed a hemodynamic profile consistent with classic reflex sympathetic vasoconstriction during exercise. In normal dogs, administration of NE significantly reduced the artery conductance in resting muscle (**Figure 36A and C, Table 6**). This vasoconstriction effect is significantly blunted in contracting muscle (**Figure 36A and C, Table 6**). Establishment of

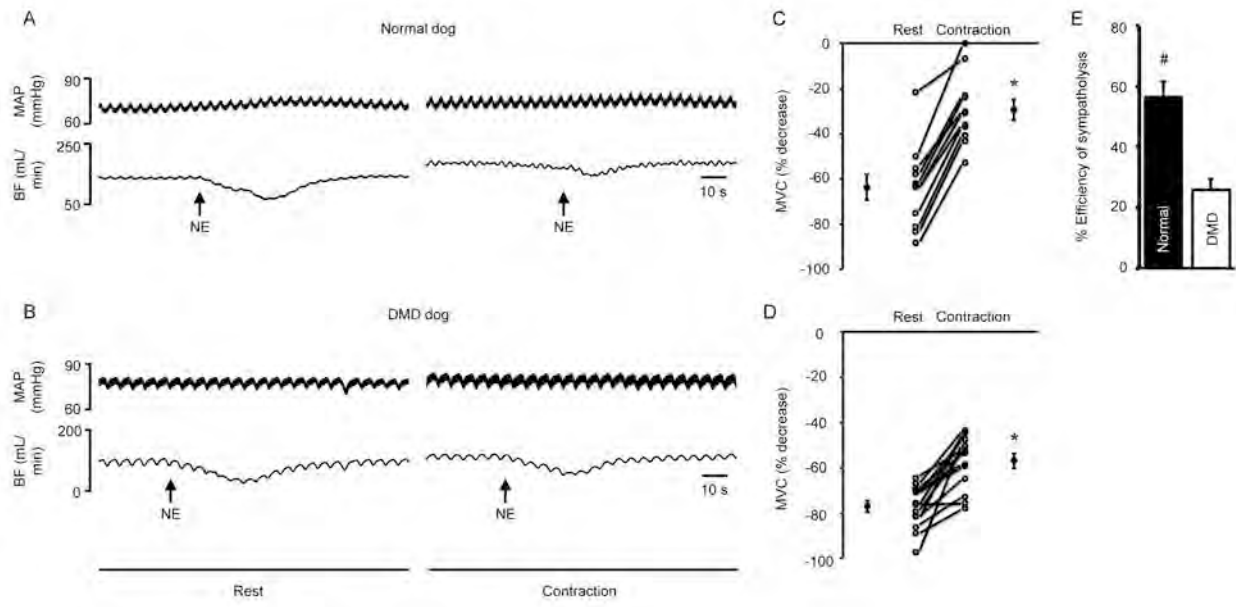


**Figure 36. Attenuation of sympathetic vasoconstriction in contracting skeletal muscle is impaired in DMD dogs. (A and B)** Representative tracing from a normal and a DMD dog. MAP, mean arterial pressure; BF, blood flow; NE, norepinephrine (NE). **(C and D)** MVC (mean vascular conductance) changes in normal ( $n = 11$ ) and DMD dogs ( $n = 14$ ). **(E)** Efficiency of functional sympatholysis in normal and DMD dogs. \* significantly different from rest. # significantly different from DMD.

**Table 5 Change in hemodynamic responses to NE induced sympathetic vasoconstriction**

Drug condition	Muscle contractile status	Group	$\Delta$ MAP (Hgmm)	$\Delta$ MABF (mL/min)	$\Delta$ MVC
Baseline	Rest	Normal	$2.43 \pm 1.10$	$-58.20 \pm 10.76$	$-0.27 \pm 0.03$
		DMD	$-0.74 \pm 0.87$	$-40.64 \pm 5.64$	$-0.29 \pm 0.03$
	Contraction	Normal	$0.67 \pm 0.75$	$-34.85 \pm 8.97^a$	$-0.16 \pm 0.03^a$
		DMD	$0.23 \pm 0.77$	$-36.56 \pm 4.85$	$-0.27 \pm 0.03$
After 7-NI	Rest	Normal	$0.39 \pm 4.05$	$-51.43 \pm 9.76$	$-0.24 \pm 0.02$
		DMD	$0.02 \pm 1.22$	$-39.83 \pm 4.27$	$-0.32 \pm 0.03$
	Contraction	Normal	$1.07 \pm 1.54$	$-48.71 \pm 8.48$	$-0.24 \pm 0.03$
		DMD	$-0.51 \pm 1.47$	$-36.70 \pm 4.49$	$-0.29 \pm 0.03$
After L-NAME	Rest	Normal	$0.52 \pm 1.13$	$-68.32 \pm 9.73$	$-0.27 \pm 0.03$
		DMD	$1.15 \pm 1.20$	$-46.56 \pm 5.29$	$-0.30 \pm 0.03$
	Contraction	Normal	$0.87 \pm 0.95$	$-67.17 \pm 12.47^b$	$-0.26 \pm 0.03$
		DMD	$0.35 \pm 1.16$	$-43.66 \pm 5.47$	$-0.27 \pm 0.03$

Abbreviations: MAP, mean arterial pressure; MABF, mean arterial blood flow; MVC, mean vascular conductance; DMD, Duchenne muscular dystrophy.

- a, Significantly different from that of normal at rest.
- b, Significantly different from that of normal at baseline and after 7-NI.

interventions aimed at improving sympatholysis in large animal models.

**Table 6** Hemodynamic responses to NE induced sympathetic vasoconstriction

Drug condition	Muscle contractile status	Group	Before NE			After NE		
			MAP (Hgmm)	MABF (mL/min)	MVC (mL/min/Hgmm/100)	MAP (Hgmm)	MABF (mL/min)	MVC (mL/min/Hgmm/100)
Baseline	Rest	Normal	66.76 ± 3.86	99.87 ± 19.00	0.46 ± 0.05	69.19 ± 3.28	41.67 ± 13.00 <sup>a</sup>	0.19 ± 0.05 <sup>a</sup>
		DMD	72.14 ± 4.21	52.60 ± 7.14 <sup>b</sup>	0.38 ± 0.04	71.40 ± 3.75	11.96 ± 2.12 <sup>a,b</sup>	0.08 ± 0.01 <sup>a,b</sup>
	Contraction	Normal	67.17 ± 4.86	123.18 ± 26.55	0.54 ± 0.07	67.84 ± 4.60	88.33 ± 21.72 <sup>a</sup>	0.37 ± 0.06 <sup>a</sup>
		DMD	71.66 ± 4.04	63.99 ± 7.05 <sup>b</sup>	0.48 ± 0.05	71.89 ± 3.90	27.44 ± 3.51 <sup>a,b</sup>	0.21 ± 0.03 <sup>a,b</sup>
After 7-NI	Rest	Normal	66.19 ± 4.66	95.76 ± 16.44	0.46 ± 0.05	66.58 ± 4.05	44.32 ± 10.79 <sup>a</sup>	0.22 ± 0.05 <sup>a</sup>
		DMD	64.96 ± 3.33	48.66 ± 5.13 <sup>b</sup>	0.40 ± 0.04	64.99 ± 3.30	8.84 ± 1.41 <sup>a,b</sup>	0.08 ± 0.01 <sup>a,b</sup>
	Contraction	Normal	64.46 ± 3.28	119.83 ± 20.49	0.58 ± 0.06	65.52 ± 3.85	71.12 ± 13.65 <sup>a</sup>	0.34 ± 0.05 <sup>a</sup>
		DMD	64.93 ± 3.48	59.29 ± 5.77 <sup>b</sup>	0.50 ± 0.05	64.42 ± 3.27	22.59 ± 2.76 <sup>a,b</sup>	0.20 ± 0.04 <sup>a,b</sup>
After L-NAME	Rest	Normal	83.74 ± 3.31	126.98 ± 16.82	0.50 ± 0.06	84.26 ± 3.86	58.66 ± 12.10 <sup>a</sup>	0.23 ± 0.05 <sup>a</sup>
		DMD	80.26 ± 4.17	59.99 ± 5.89 <sup>b</sup>	0.40 ± 0.04	81.41 ± 3.69	13.43 ± 1.75 <sup>a,b</sup>	0.10 ± 0.02 <sup>a,b</sup>
	Contraction	Normal	81.57 ± 3.72	158.43 ± 24.15	0.61 ± 0.08	82.43 ± 3.50	91.27 ± 15.04 <sup>a</sup>	0.35 ± 0.06 <sup>a</sup>
		DMD	83.05 ± 3.75	73.13 ± 6.10 <sup>b</sup>	0.48 ± 0.05	83.40 ± 3.60	29.47 ± 2.90 <sup>a,b</sup>	0.21 ± 0.04 <sup>a,b</sup>

Abbreviations: NE, norepinephrine; MAP, mean arterial pressure; MABF, mean arterial blood flow; MVC, mean vascular conductance; DMD, Duchenne muscular dystrophy.

a, Significantly different from that of before NE.

b, Significantly different from that of normal.

***Additional accomplishments that have benefited from this grant support.***

***Accomplishment benefit from this grant 1.*** We provided a comprehensive perspective on AAV capsid modification for DMD gene therapy (Nance and Duan, 2015).

***Accomplishment benefit from this grant 2.*** We provided a comprehensive review on gene therapy for muscular dystrophy associated cardiomyopathy (Yue et al., 2016a).

***Accomplishment benefit from this grant 3.*** We provided a comprehensive review on the current status of DMD gene therapy (Duan, 2016).

***Accomplishment benefited from this grant 4.*** In this study, we have proposed to use AAV vectors as the delivery tool. AAV is a bio-nanoparticle. We published a review article on the current state-of-art on nanotherapy (both viral and noviral) for DMD (Nance et al, 2017).

***Accomplishment benefited from this grant 5.*** The ultimate goal of this project is to develop the best micro-dystrophin AAV gene therapy. A better understanding of dystrophin biology is essential to decide which part(s) of the dystrophin coding sequence should be included in the synthetic micro-dystrophin gene. To this end, we identified 3 new membrane-binding domains in full-length

dystrophin. This information will be used to engineer future more functional micro-dystrophin genes (Zhao et al 2016).

***Accomplishment benefited from this grant 6.*** Repeated biopsy is a burden to patients following AAV micro-dystrophin gene therapy. Electrical impedance myography is a recently developed technology that will allow investigators to study muscle architecture without performing biopsy. We established the protocol for using electrical impedance myography to evaluate normal and dystrophic dog muscles (Hakim et al 2017 PLoS One).

***Accomplishment benefited from this grant 7.*** We quantified the loss of ambulation by 6 months of age in our colony and several other colonies. This study suggests that the early loss of ambulation is not a typical clinical presentation in affected dogs (**Table 7**).

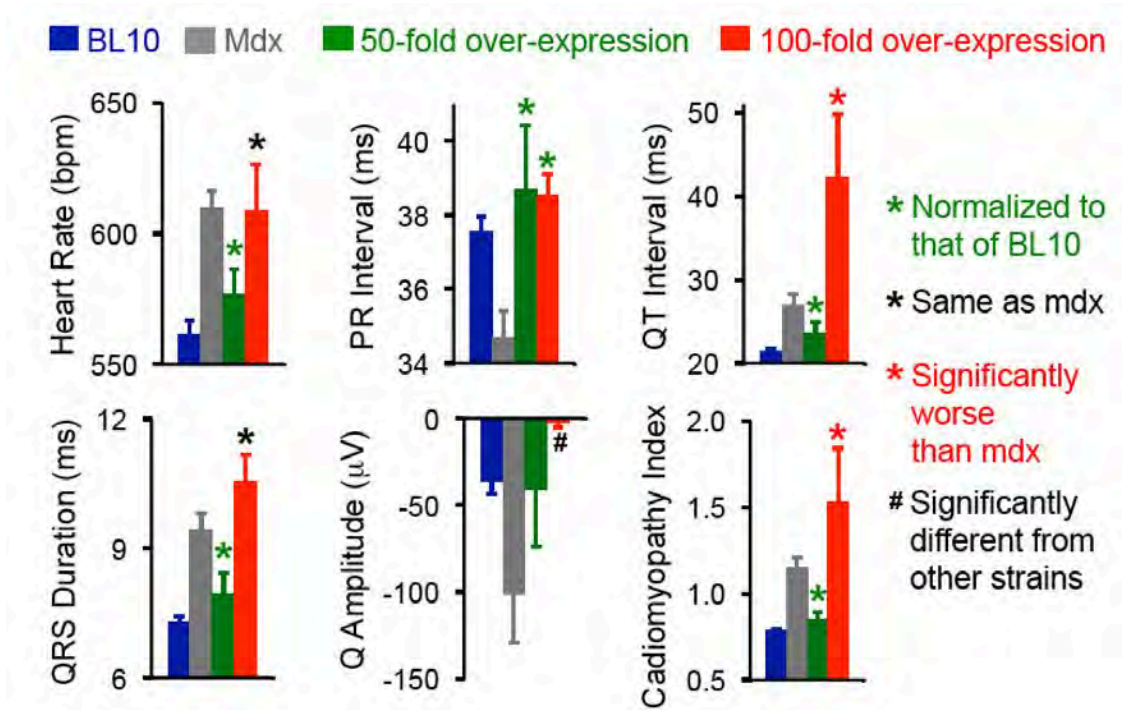
Table 7. Complete loss of ambulation is not a clinical feature in young adult DMD dogs.

Investigator (or reference paper)	Colony location	Strain background	Mutation	Sample size	Loss of ambulation by 6 months	
					Number	Percentage (%)
Carlos Ambrosio	Brazil	Golden retriever	Intron 6 point mutation (GRMD)	160	1	0.63
Dongsheng Duan	Columbia, MO	Golden retriever	Intron 6 point mutation (GRMD)	130	0	0.00
		Corgi	Intron 13 insertion			
		Labrador	Intron 19 insertion			
		Hybrid	Mixed			
Bruce Smith	Auburn, AL	Corgi	Intron 13 insertion	30	0	0.00
		Labrador	Intron 19 insertion			
		Labradoodle	Unknown			
		Springer	Unknown			
Lee Sweeney	Philadelphia, PA	Golden retriever	Intron 6 point mutation (GRMD)	35	0	0.00
Valentine et al., 1988	Ithaca, NY	Golden retriever	Intron 6 point mutation (GRMD)	25	0	0.00
		Golden retriever/ Beagle hybrid	Intron 6 point mutation (GRMD)			
<b>Total</b>				<b>380</b>	<b>1</b>	<b>0.26</b>

***Accomplishment benefited from this grant 8.*** A major concern of AAV micro-dystrophin therapy is that the therapeutic microgene may lose over time. A previous study from Dickson lab suggests that such loss may not compromise therapeutic benefits. In other words, there is no need for re-administration. We now took a more stringent genomic approach and revisited this question. Our results suggest that a loss of therapeutic mini-dystrophin is accompanied with the loss of protection in both skeletal muscle and the heart. Our study corrected an important misconception in the field of AAV dystrophin replacement therapy (Wasala et al 2016).

***Accomplishment benefited from this grant 9.*** In our initial study on systemic AAV micro-dystrophin delivery in young adult dystrophic dogs (these data were presented in previous progress reports), we found robust transduction in skeletal muscle but gene transfer in the heart is limited with AAV-9. To address whether low-level dystrophin expression in the heart can still offer some protection, we studied mdx3cv mice which expressed ~3.8% of dystrophin in the heart. We found that this low-level dystrophin expression resulted in slight, but significantly better functional rescue in aged mice than mdx4cv mice which have no dystrophin in the heart. This result suggests that some dystrophin is better than no dystrophin. It support our continued pursuing of AAV micro-dystrophin therapy (Wasala et al 2017)

**Accomplishment benefited from this grant 8.** A potential outcome of systemic AAV gene therapy is supra-physiological expression of the therapeutic micro-dystrophin gene. While it has been accepted that dystrophin over-expression is not toxic. We now found that 50-fold over-expression was tolerated and effectively ameliorated electrophysiological deficiency in mdx mice. However, 100-fold over-expression of dystrophin causes cardiac toxicity (Yue et al., 2016b). Specifically, 100-fold over-expression did not mitigate tachycardia neither did it correct QRS prolongation. Importantly, 100-fold over-expression significantly worsened QT interval and cardiomyopathy index (**Figure 37**, below).



*Training and professional development opportunities.* Nothing to report.

*Dissemination of the results.* Above mentioned studies and review articles have been either published in peer-reviewed scientific journals or presented in academic conferences.

*Plan for future.* Nothing to report.

**4. Impact.** Nothing to report.

**5. Changes/Problems.** Nothing to report.

## **6. Products**

### **6.1. Peer-reviewed publications**

1. McGreevy JW, Hakim CH, McIntosh M, **Duan D.** *Animal models for Duchenne muscular dystrophy: from basic mechanisms to gene therapy.* **Disease Model and Mechanism** 8(3):195-213, **2015.**
2. Pan X, Yue Y, Zhang K, Hakim CH, Kodippili K, McDonald T, **Duan D.** *AAV-8 is more efficient than AAV-9 in transducing neonatal dog heart.* **Human Gene Therapy Methods.** 26(4):54-61, **2015.**
3. **Duan D.** *Duchenne muscular dystrophy gene therapy in the canine model.* **Human Gene Therapy Clinical Development.** 26(3):157-169, **2015.**
4. **Duan D,** Hakim CH, Ambrosio C, Smith B, Sweeney L. *Early loss of ambulation is not a representative clinical feature in Duchenne muscular dystrophy dogs.* **Disease Model and Mechanism** 8(3):193-194, **2015.**
5. Yue Y, Pan X, Hakim CH, Kodippili K, Zhang K, Shin J-H, Yang HS, McDonald T, **Duan D.** *Safe and bodywide muscle transduction in young adult Duchenne muscular dystrophy dogs with adeno-associated virus.* **Human Molecular Genetics.** 24(20):5880-5890, **2015.** (highlighted in [Human Gene Therapy Clinical Development](#) 26(4):213-214, 2015)
6. Hakim CH, Peters AA, Feng F, Yao G, **Duan D.** *Night activity reduction is a signature physiological biomarker for Duchenne muscular dystrophy dogs.* **Journal of Neuromuscular Diseases.** 2(4):397-407, **2015.**
7. Nance ME and **Duan D.** *Perspective on adeno-associated virus (AAV) capsid modification for Duchenne muscular dystrophy gene therapy.* **Human Gene Therapy** 26(12):786-800, **2015.**
8. Yue Y, Binalsheikh IM, Leach SB, Domeier TL, **Duan D.** *Prospect of gene therapy for cardiomyopathy in hereditary muscular dystrophy.* **Expert Opinion on Orphan Drugs** 4(2):169-183, **2016.**

9. **Duan D.** *Dystrophin gene replacement and gene repair therapy for Duchenne muscular dystrophy in 2016.* **Human Gene Therapy Clinical Development.** 27(1):9-18, **2016.**
10. Yue Y, Wasala NB, Bostick B, **Duan D.** *100-fold but not 50-fold dystrophin overexpression aggravates electrocardiographic defects in the mdx model of Duchenne muscular dystrophy.* **Molecular Therapy-Methods & Clinical Development.** 3:16045, **2016**
11. **Duan D.** *Systemic delivery of adeno-associated viral vectors.* **Current Opinion in Virology** 21:16-25, **2016**
12. Zhao J, Kodippili K, Yue Y, Hakim CH, Wasala L, Pan X, Zhang K, Yang NN, **Duan D**, Lai Y. *Dystrophin contains multiple independent membrane-binding domains.* **Human Molecular Genetics** 25(10):3647-3653, **2016** (DD and YL as co-corresponding authors).
  - a. “This work was supported in part by the Department of Defense, Duchenne Muscular
13. Wasala NB, Lai Y, Shin J-H, Zhao J, Yue Y, **Duan D.** *Genomic removal of a therapeutic mini-dystrophin gene from adult mice elicits a Duchenne muscular dystrophy-like phenotype.* **Human Molecular Genetics** 25(13):2633-2644, **2016**
14. Wasala NB, Yue Y, Jenna Vance, **Duan D.** *Uniform low-level dystrophin expression in the heart partially preserved cardiac function in an aged mouse model of Duchenne cardiomyopathy.* **Journal of Molecular and Cellular Cardiology** 102:45-52, **2017**
15. Nance ME, Hakim CH, Yang NN and **Duan D.** *Nanotherapy for Duchenne muscular dystrophy.* **WIREs Nanomedicine and Nanobiotechnology** e1472, **2017**
16. Hakim CH, Mijailovic A, Lessa TB, Coates JR, Rutkove SB, **Duan D.** *Non-invasive evaluation of muscle disease in the canine model of Duchenne muscular dystrophy by electrical impedance myography.* **PLoS One** 12(3):e0173557, **2017**
17. Hakim CH, Wasala NB, Pan X, Kodippili K, Yue Y, Zhang K, Yao G, Haffner B, Duan XS, Schneider JS, Yang NN, Chamberlain JS, **Duan D.** *A five-repeat micro-dystrophin gene ameliorated dystrophic phenotype in the severe DBA/2J-mdx model of Duchenne muscular dystrophy.* **Molecular Therapy-Methods & Clinical Development** 6:216-230, **2017**
18. **Duan D.** *Micro-dystrophin gene therapy goes systemic in Duchenne muscular dystrophy patients.* **Human Gene Therapy** In-press, **2018**

## 6.2. Conference presentations

- 1) Chady Hakim, Xiufang Pan, Kasun Kodippili, Thais Blessa, Hsiao T Yang, Gary Yao, Stacey Leach, Craig Emter, Yongping Yue, Keqing Zhang, Sean X Duan, Nalinda Wasala, Gregory Jenkins, Charles R. Legg, Joel S. Schneider, Jeffrey S Chamberlain, and Dongsheng Duan. **Intravenous delivery of a novel micro-dystrophin vector prevented muscle deterioration in young adult canine Duchenne muscular dystrophy dogs** 2016 *19th Annual Meeting of the American Society of Gene & Cell Therapy.* Washington, DC May 4-7, 2016 (**selected for oral presentation**)

- 2) Chady Hakim, Xiufang Pan, Kasun Kodippili, Thais Blessa, Hsiao T Yang, Gary Yao, Stacey Leach, Craig Emter, Yongping Yue, Keqing Zhang, Sean X Duan, Nalinda Wasala, Gregory Jenkins, Charles R. Legg, Joel S. Schneider, Nora Yang, Jeffrey S Chamberlain, and Dongsheng Duan. **A single intravenous injection of a novel AAV micro-dystrophin vector resulted in extended amelioration of muscle disease in the canine model of Duchenne muscular dystrophy.** 2016 *16th International Workshop on Parvoviruses*. Ajaccio, Corsica, June 19-June 23, 2016 (selected for oral presentation)
- 3) Chady H Hakim, Nalinda B. Wasala, Xiufang Pan, Kasun Kodippili, Yongping Yue, Keqing Zhang, Gang Yao, Joel S. Schneider, Nora Yang, Jeffrey Chamberlain, Dongsheng Duan. **A 5-repeat micro-dystrophin gene ameliorated dystrophic phenotype in the severe DBA/mdx model of Duchenne muscular dystrophy** 2016 *16th International Workshop on Parvoviruses*. Ajaccio, Corsica, June 19-June 23, 2016.
- 4) Xiufang Pan, Nalinda B Wasala, Chady H Hakim, Yongping Yue, Keqing Zhang, John Hu, Dongsheng Duan. **Comparison of 4-repeat and 5-repeat micro-dystrophins in dystrophin deficient mice.** 2016 *New Directions in Biology and Disease of Skeletal Muscle Conference*. Orlando, Florida, June 29-July 2, 2016.
- 5) Nalinda B. Wasala, Yi Lai, Jinhong Shin, Junling Zhao, Yongping Yue, Dongsheng Duan. **Genomic removal of a therapeutic mini-dystrophin gene from adult mice elicits a Duchenne muscular dystrophy-like phenotype.** 2016 *New Directions in Biology and Disease of Skeletal Muscle Conference*. Orlando, Florida, June 29-July 2, 2016.
- 6) Chady H Hakim, Nalinda B. Wasala, Xiufang Pan, Kasun Kodippili, Yongping Yue, Keqing Zhang, Gang Yao, Joel S. Schneider, Nora Yang, Jeffrey Chamberlain, Dongsheng Duan. **A 5-repeat micro-dystrophin gene ameliorated dystrophic phenotype in the severe DBA/mdx model of Duchenne muscular dystrophy.** 2016 *New Directions in Biology and Disease of Skeletal Muscle Conference*. Orlando, Florida, June 29-July 2, 2016.
- 7) Michael Nance, Yongping Yue, Dennis Discher, Dongsheng Duan. **Development of novel adeno-associated virus that are resistant to macrophage phagocytosis.** 2016 *New Directions in Biology and Disease of Skeletal Muscle Conference*. Orlando, Florida, June 29-July 2, 2016.
- 8) Chady Hakim, Xiufang Pan, Kasun Kodippili, Thais Blessa, Hsiao T Yang, Gary Yao, Stacey Leach, Craig Emter, Yongping Yue, Keqing Zhang, Sean X Duan, Nalinda Wasala, Gregory Jenkins, Charles R. Legg, Joel S. Schneider, Nora Yang, Jeffrey S Chamberlain, and Dongsheng Duan. **A single intravenous injection of a novel AAV micro-dystrophin vector resulted in extended amelioration of muscle disease in the canine model of Duchenne muscular dystrophy.** 2016 *New Directions in Biology and Disease of Skeletal Muscle Conference*. Orlando, Florida, June 29-July 2, 2016. (selected for oral presentation)
- 9) Dongsheng Duan. **Duchenne muscular dystrophy gene therapy.** *Clinical and Translational Medicine* 2016, 5(Supp 1):A16. *A One Health overview, facilitating advances in comparative medicine and translational research.* Kansas City, MO August 28-29, 2016.

- 10) Angus Lindsay, Dawn A. Lowe, **Dongsheng Duan**, Luke M. Judge, Jeffery S. Chamberlain and James M. Ervasti. *Deletion of sequences encoding spectrin repeat 2 through hinge 2 from microdystrophin compromises protection from eccentric contraction-induced force drop in mdx mice*. Advances in Skeletal Muscle Biology in Health and Disease. University of Florida, Gainesville, FL. March 8-10, 2017
- 11) Chady H. Hakim, Kasun Kodippili, Gregory Jenkins, Hsiao T. Yang, Xiufang Pan, Thais B. Lessa, Stacey B. Leach, Craig Emter, Yongping Yue, Keqing Zhang, Sean X. Duan, Gang Yao, Joel S. Schneider, Nora N. Yang, Jeffrey S. Chamberlain, **Dongsheng Duan**. *Single systemic AAV microdystrophin therapy ameliorates muscular dystrophy in young adult Duchenne muscular dystrophy dogs for up to two years*. 2017 Inaugural Musculoskeletal Regenerative Medicine and Biology Meeting. Saint louis, MO. May 4-6, 2017. **(selected for oral presentation)**
- 12) Chady H. Hakim, Kasun Kodippili, Gregory Jenkins, Hsiao T. Yang, Xiufang Pan, Thais B. Lessa, Stacey B. Leach, Craig Emter, Yongping Yue, Keqing Zhang, Sean X. Duan, Gang Yao, Joel S. Schneider, Nora N. Yang, Jeffrey S. Chamberlain, **Dongsheng Duan**. *Single systemic AAV microdystrophin therapy ameliorates muscular dystrophy in young adult Duchenne muscular dystrophy dogs for up to two years*. 2017 20th Annual Meeting of the American Society of Gene & Cell Therapy. Washington, DC May 10-13, 2017
- 13) Chady H. Hakim, Kasun Kodippili, Gregory Jenkins, Hsiao T. Yang, Xiufang Pan, Thais B. Lessa, Stacey B. Leach, Craig Emter, Yongping Yue, Keqing Zhang, Sean X. Duan, Gang Yao, Joel S. Schneider, Nora N. Yang, Jeffrey S. Chamberlain, **Dongsheng Duan**. *Single systemic AAV microdystrophin therapy ameliorates muscular dystrophy in young adult Duchenne muscular dystrophy dogs for up to two years*. 2017 4th Ottawa International Conference on Neuromuscular Disease and Biology. Ottawa, Ontario, Canada Sep 7-9, 2017
- 14) Hakim CH, Wasala NB, Pan X, Kodippili K, Yue Y, Zhang K, Yao G, Haffner B, Duan XS, Schneider JS, Yang NN, Chamberlain JS, **Dongsheng Duan**. *A five-repeat micro-dystrophin gene ameliorated dystrophic phenotype in the severe DBA/2J-mdx model of Duchenne muscular dystrophy*. 2017 4th Ottawa International Conference on Neuromuscular Disease and Biology. Ottawa, Ontario, Canada Sep 7-9, 2017
- 15) Chady H. Hakim, Nathalie Clement, Lakmini P. Wasala, Hsiao T. Yang, Yongping Yue, Keqing Zhang, Kasun Kodippili, Joel S. Schneider, Nora N. Yang, Jeffrey S. Chamberlain, Barry J. Byrne, **Dongsheng Duan** *In vivo comparison of the biological potency of rAAV9-microdystrophin made by transient transfection and a scalable herpesvirus system* 2017 4th Ottawa International Conference on Neuromuscular Disease and Biology. Ottawa, Ontario, Canada Sep 7-9, 2017
- 16) Nalinda B. Wasala, Jinhong Shin, Yi Lai, Yongping Yue, Federica Montanaro, **Dongsheng Duan**. *R16-19 is a putative heart protection domain in dystrophin* 2017 4th Ottawa International Conference on Neuromuscular Disease and Biology. Ottawa, Ontario, Canada Sep 7-9, 2017
- 17) D. M. Nelson, **Dongsheng Duan**, L. M. Judge, J. S. Chamberlain and J.M. Ervasti *Variable rescue of microtubule defects in mdx skeletal muscle expressing miniaturized dystrophins* 2017 ASCB-EMBO Annual Meeting. Philadelphia, PA, Dec 2-6, 2017.

## **7. Participants/collaborating organizations:**

### ***What individuals have worked on the project?***

Name: Dongsheng Duan – “No change”

Name: Craig Emter – “No change”

Name: Yi Lai – “No change”

Name: Hsiao Tung “Steve” Yang – “No change”

Name: Yongping Yue – “No change”

Name: Aihua Dai – “No change”

### ***Changes in the active other support of the PI and key personnel since the last reporting period.***

#### **Dongsheng Duan, PI**

#### **Previous/active grants that have closed:**

##### R16/17-independent nNOS anchoring mechanism

8% effort, PI

NIH/NIAMS (R21 AR067985-01A1)

National Institutes of Health; 6701 Rockledge Drive, Suite 1040, MSC 7710; Bethesda, MD 20817

04/01/2016-03/31/2018

The goal is to identify the dog nNOS-binding domain and develop relevant gene delivery vectors.

The specific aims are (1) to identify the canine specific nNOS-binding domain in dog dystrophin and (2) to develop the nNOS-binding canine dystrophin adeno-associated virus (AAV) vector.

(There is no scientific/budget overlap with the current proposal)

##### Evaluation of the human version second-generation AAV micro-dystrophin vector in adult dystrophic dogs

5% effort, PI

Jesse's Journey; The Foundation for Gene & Cell Therapy

Rick Moss; Managing Director; 195 Dufferin Avenue; Suite #605; London, ON N6A 1K7 CANADA

7/1/14-12/31/2017 (extension)

Goal: We propose to generate the human version microgene vector and confirm its function in adult DMD dogs.

The specific aims are: (1) to engineer a codon-optimized second-generation human dystrophin microgene in a customer-optimized expression cassette and package it in an AAV-8 vector; (2) to validate the efficacy of the human version vector in dystrophin deficient mdx mice by systemic gene transfer; (3) to validate the efficacy of the human version vector in adult dystrophic dogs by local gene transfer; (4) to explore systemic gene therapy in young adult dystrophic dogs.

(This is a supplementary grant to the DOD grant awarded September 2014 that has been approved for extension to 12/31/2017).

(There is no scientific/budget overlap with the current proposal)

Evaluation of osteoprotegerin (OPG) in the mdx model of Duchenne muscular dystrophy

10% effort, Duan, PI

Ryan's Quest

David Schultz; PO Box 2544; Hamilton, NJ 08690-0044

10/15/2017-04/15/2018

To validate muscle protection effect of osteoprotegerin (OPG) in 25-day-old mdx mice.

(There is no scientific/budget overlap with the current proposal)

Polyethylenimine (PEI)-GFP and micro-dystrophin injection in mdx mice

2.5% effort, Co-I; Yi Lai, PI

Solid Biosciences

161 1<sup>st</sup> Street; Cambridge, MA 02142-1211

12/01/2017-03/31/2018

The goal is to assess expression of dsDNA in mdx male mice following a single intramuscular (IM) dose administration.

(There is no scientific/budget overlap with the current proposal)

**Current research support:**

CRISPR/Cas9-based gene editing for the correction of Duchenne muscular dystrophy

8% effort, Co-PI (PI: Charles Gersbach)

Duke University, NIH (R01 AR069085-01A1)

Charles Gersbach, Ph.D.; Duke University, 2353C CIEMAS Box 90281; Durham, NC 27708-0281

04/01/2016-03/31/2021

The Duan lab will perform in vivo gene delivery and functional outcome measurements in mice treated by AAV-CRISPR gene repair vectors and if needed will also assist with the production of recombinant AAV vectors.

Specific aim: To test CRISPR/Cas9 gene therapy to treat muscle disease in mdx mice and hDMD mice.

(There is no scientific/budget overlap with the current proposal)

A pilot study to evaluate long-term safety and efficacy of AAV-9 5Rc micro-dystrophin therapy

5% effort, PI

Solid Biosciences

Joel Schneider, Ph.D.; 101 Main Street; Cambridge, MA 02142

06/01/2016-05/31/2019

The overarching goal of this project is to determine whether systemic AAV-9 5Rc micro-dystrophin gene therapy can yield long-term (up to 4 years after injection) microgene expression without causing serious adverse events (SAEs).

(There is no scientific/budget overlap with the current proposal)

Treatment of Duchenne muscular dystrophy with the muscle calcium pump

17% effort, PI

NIH/NIAMS (R01 AR070517-01)

National Institutes of Health; 6701 Rockledge Drive, Suite 1040, MSC 7710; Bethesda, MD 20817  
07/01/2016-08/31/2021

Goal: Elevation of cytosolic calcium is a pivotal pathogenic event in Duchenne muscular dystrophy (DMD). We found that sarco/endoplasmic reticulum calcium ATPase 2a (SERCA2a) therapy can reduce muscle disease and improve muscle function in the mouse DMD model. In the proposed study, we will test whether this therapy can treat symptomatic DMD dogs and our results will lay the foundation for a future clinical trial.

The specific aims are: (1) to test whether regional AAV SERCA2a therapy can ameliorate limb muscle disease and improve function and (2) to test whether systemic AAV SERCA2a therapy can lead to bodywide improvement in affected dogs.

(There is no scientific/budget overlap with the current proposal)

Treating Duchenne cardiomyopathy in the mouse model by gene repair

10% effort, Duan, PI

Department of Defense W81XWH-16-1-0221

USA Med Research Mat CMD; 1077 Patchel Street; Bldg 1056; Fort Detrick, MD 21702  
08/01/2016-07/31/2019

We propose to test this "permanent exon skipping" therapy to the treatment of Duchenne cardiomyopathy in an authentic mouse model. Our study will open the door to the eventual application of CRISPR/Cas9 therapy in human patients in the future.

(There is no scientific/budget overlap with the current proposal)

Whole body single AAV microgene therapy in canine DMD

17% effort, PI

NIH, NINDS R01 NS090634

National Institutes of Health; 6701 Rockledge Drive; Suite 1040, MSC 7710; Bethesda, MD 20817  
09/01/2015-07/31/2020

In this study, we will test whether a newly developed canine Y731F AAV-9 micro-dystrophin vector gene therapy can lead to clinically meaningful improvement in dystrophic dogs.

Specific aim 1 is to test regional therapy in the hope of applying it to improve life quality in late-stage patients and aim 2 is to test systemic therapy in the hope of achieving bodywide improvement in young patients.

(There is no scientific/budget overlap with the current proposal)

Fine-needle microscopic tractography for in vivo high-resolution imaging of muscle damage

2% effort, Co-PI (PI: Gang Yao)

University of Missouri, Interdisciplinary Pilot Studies in Translational Science and Biomedical Innovations

Debbie Taylor, MA204 Medical Sciences Building, University of Missouri

07/01/2017 to 06/30/2018

The goal and aim of this project is to develop a new microscopic imaging method for minimal invasive imaging of muscle damage.

(There is no scientific/budget overlap with the current proposal)

Evaluation of Montelukast as a potential therapy for Duchenne muscular dystrophy in the murine model

3% effort, PI

Duchenne UK

David R. Bull; 56 Wood Lane; London, W12 7SB; GBR United Kingdom

03/01/2017-02/28/2020

We propose to evaluate safety and therapeutic efficacy of Montelukast in mdx mice, the most commonly used mouse model for DMD.

(There is no scientific/budget overlap with the current proposal)

Evaluation of Montelukast as a potential therapy for Duchenne muscular dystrophy in the murine model

0% effort, PI

Michael's Cause

Robert Capolongo; PO Box 120323; Staten Island, NY 10312

03/01/2017-02/28/2020

We propose to evaluate safety and therapeutic efficacy of Montelukast in mdx mice, the most commonly used mouse model for DMD. This is a supplementary grant to the Duchenne UK grant.

(There is no scientific/budget overlap with the current proposal)

Evaluation of Montelukast as a potential therapy for Duchenne muscular dystrophy in the murine model

0% effort, PI

Ryan's Quest

David Shultz; PO Box 2544; Hamilton, NJ 08690

03/01/2017-02/28/2020

We propose to evaluate safety and therapeutic efficacy of Montelukast in mdx mice, the most commonly used mouse model for DMD. This is a supplementary grant to the Duchenne UK grant.

(There is no scientific/budget overlap with the current proposal)

Evaluation of Montelukast as a potential therapy for Duchenne muscular dystrophy in the murine model

0% effort, PI

Rally for Ryan

Marty Karlin; 2623 Evercrest Court; Naperville, IL 60564

03/01/2017-02/28/2020

We propose to evaluate safety and therapeutic efficacy of Montelukast in mdx mice, the most commonly used mouse model for DMD. This is a supplementary grant to the Duchenne UK grant.

(There is no scientific/budget overlap with the current proposal)

DMD gene therapy in the canine model by intramuscular sarcolipin knockdown

5% effort, PI

Jesse's Journey: The Foundation for Gene & Cell Therapy

Lisa Hoffman ; PO Box 51 Station B; London, ON NGA 4V3; CANADA

08/01/2017-07/31/2020

The major goal of this study is to demonstrate that sarcolipin (SLN) knockdown improves the sarco/endoplasmic reticulum calcium ATPase (SERCA) function and ameliorate the muscle disease in a dog model of Duchenne muscular dystrophy.

(There is no scientific/budget overlap with the current proposal)

Pilot study to evaluate protein CRISPR therapy in the DMD mouse model

0% effort, PI

Hubrecht Institute, Utrecht University, Netherlands

10/01/2017-09/30/2019

In this pilot study, the Geijsen lab and the Duan lab will analyze the functional improvement of a mouse model of Duchenne muscular dystrophy upon Dystrophin gene repair by the iTOP-mediated introduction of Cas9 and sgRNA to skeletal muscle fibers and satellite cells of (DMD) to test DMD CRISPR therapy.

(There is no scientific/budget overlap with the current proposal)

**New/active grants:**

Solid micro-dystrophin optimization

5% effort, Co-I; Yi Lai, PI

Solid Biosciences

161 First Street, 3<sup>rd</sup> Floor

Cambridge, MA 02142

12/07/2017-07/31/2018

(1) To engineer new adeno-associated virus (AAV) micro-dystrophin vectors by incorporating our recently discovered membrane-binding domains (MBD)s, and (2) to identify the best vector by examining therapeutic efficacy of new AAV micro-dystrophin vectors in mouse models of Duchenne muscular dystrophy (DMD).

(There is no scientific/budget overlap with the current proposal)

Cardiac and skeletal muscle function evaluation and tissue banking of aged carrier DMD dogs 0.50% effort, PI

Parent Project Muscular Dystrophy

401 Hackensack Avenue, 9<sup>th</sup> Floor; Hackensack, NJ 07601

04/01/2018-03/31/2019

We propose to conduct a function-histology correlation study in aged carrier dogs.

(There is no scientific/budget overlap with the current proposal)

Pilot study of OPG analog 6 (OPG-6) in the mdx model of Duchenne muscular dystrophy

5% effort, PI  
Ryan's Quest  
PO Box 2544; Hamilton, NJ 08690-0044  
03/01/2018-05/31/2018

To study muscle function rescue in the diaphragm and EDL muscle following OPG-6 therapy.  
(There is no scientific/budget overlap with the current proposal)

**Craig Emter, Co-PI**

**Previous/active grants that have closed:**

Mechanisms of sympathetic-mediated cerebrovascular vasoconstriction in heart failure with preserved ejection fraction

AHA Postdoctoral Fellowship (Olver, PI)

0% effort, Emter, Supervising PI

American Heart Association

1/1/2016-12/31/2017

Major goals: Salary support for research career development.

**Current research support:**

Coronary Dysfunction, BK Channels, & Exercise in Heart Failure

33% effort, Emter, PI

NIH/NHLBI, R01 HL112998

5/1/14-4/30/2019

Major Goals: The goal of this project is to determine the role of the coronary vascular BK<sub>Ca</sub> channel in the development of heart failure with preserved ejection fraction.

Pathological Mechanisms of Sympathetic-mediated Cerebrovascular Vasoconstriction as a Function of Menopause in Heart Failure with Preserved Ejection Fraction

Olver, PI

0% effort, Emter, Supervising PI

University of Missouri, Internal

MU Interdisciplinary Center on Aging - Research Enrichment and Dissemination (READ) Small Grants Program

1/22/16-12/31/18

Major goals: Pilot clinical and translational studies for examining sympathetic nervous system contributions to developing heart failure in a mini-swine model of HFpEF

**New/active grants:**

RSK3-mAKAP Targeting as a New Therapeutic Strategy for Heart Failure with Preserved Ejection Fraction in Women

25% effort, Emter, PI (Emter/Kapiloff, MPI)

Department of Defense (DOD) PR170699  
4/1/18-9/30/2023

Major Goals: The goal of this project is to investigate novel gene therapies for treating HFpEF in women.

Role of endothelial NO on sympathetic-activated NPY-mediated pial artery vasoconstriction along the pial vascular tree

5% effort, Emter/Olver, Co-PI's

University of Missouri; Internal

College of Veterinary Medicine COR Faculty Research Program

1/1/18-12/31/18

Major goals: To elucidate the role of impaired NO signaling in facilitating sympathetic-activated NPY-Y1R-mediated vasoconstriction along the arterial tree to improve brain blood flow control in a setting of heart failure.

**Yi Lai, Associate Research Professor**

**Previous/active grants that have closed:**

R16/17-independent nNOS anchoring mechanism

10% effort, Co-I (Dongsheng Duan, PI)

NIH/NIAMS (R21 AR067985-01A1)

04/01/2016-03/31/2018

National Institutes of Health; 6701 Rockledge Drive, Suite 1040, MSC 7710; Bethesda, MD 20817

The goal is to identify the dog nNOS-binding domain and develop relevant gene delivery vectors. The specific aims are (1) to identify the canine specific nNOS-binding domain in dog dystrophin and

(2) to develop the nNOS-binding canine dystrophin adeno-associated virus (AAV) vector.

(There is no scientific/budget overlap with the current proposal.)

Polyethylenimine (PEI)-GFP and micro-dystrophin injection in mdx mice

20% effort, PI

Solid Biosciences

161 1<sup>st</sup> Street; Cambridge, MA 02142-1211

12/01/2017-03/31/2018

The goal is to assess expression of dsDNA in mdx male mice following a single intramuscular (IM) dose administration.

(There is no scientific/budget overlap with the current proposal.)

**Current research support:**

**New/active grants:**

Solid micro-dystrophin optimization

50% effort, PI

Solid Biosciences  
161 First Street, 3<sup>rd</sup> Floor  
Cambridge, MA 02142  
12/07/2017-07/31/2018

(1) To engineer new adeno-associated virus (AAV) micro-dystrophin vectors by incorporating our recently discovered membrane-binding domains (MBD)s, and (2) to identify the best vector by examining therapeutic efficacy of new AAV micro-dystrophin vectors in mouse models of Duchenne muscular dystrophy (DMD).

(There is no scientific/budget overlap with the current proposal.)

**Hsiao Tung Yang, Research Professor**

**Previous/active grants that have closed:**

None

**Current research support:**

None

**New/active grants:**

None

**8. Special reporting requirements:** None

**9. Appendices:**

Peer-reviewed publications

## REVIEW

# Animal models of Duchenne muscular dystrophy: from basic mechanisms to gene therapy

Joe W. McGreevy<sup>1</sup>, Chady H. Hakim<sup>1</sup>, Mark A. McIntosh<sup>1</sup> and Dongsheng Duan<sup>1,2,\*</sup>

## ABSTRACT

Duchenne muscular dystrophy (DMD) is a progressive muscle-wasting disorder. It is caused by loss-of-function mutations in the dystrophin gene. Currently, there is no cure. A highly promising therapeutic strategy is to replace or repair the defective dystrophin gene by gene therapy. Numerous animal models of DMD have been developed over the last 30 years, ranging from invertebrate to large mammalian models. *mdx* mice are the most commonly employed models in DMD research and have been used to lay the groundwork for DMD gene therapy. After ~30 years of development, the field has reached the stage at which the results in *mdx* mice can be validated and scaled-up in symptomatic large animals. The canine DMD (cDMD) model will be excellent for these studies. In this article, we review the animal models for DMD, the pros and cons of each model system, and the history and progress of preclinical DMD gene therapy research in the animal models. We also discuss the current and emerging challenges in this field and ways to address these challenges using animal models, in particular cDMD dogs.

**KEY WORDS:** Duchenne muscular dystrophy, Dystrophin, Animal model, Canine DMD, Gene therapy

## Introduction

Duchenne muscular dystrophy (DMD) is the most common muscular dystrophy, with a worldwide incidence of one in 5000 live male births according to newborn screening (Emery and Muntoni, 2003; Mendell and Lloyd-Puryear, 2013). It is caused by the lack of dystrophin, a critical muscle protein that connects the cytoskeleton and the extracellular matrix (ECM) (Bonilla et al., 1988; Hoffman et al., 1987). The 2.4-Mb dystrophin gene was discovered in 1986 (Kunkel, 2005; Monaco et al., 1986). It contains 79 exons and encodes a ~14-kb cDNA (Koenig et al., 1987). The full-length protein has four functional domains: the N-terminal (NT), rod, cysteine-rich (CR) and C-terminal (CT) domains. Dystrophin assembles several transmembrane (dystroglycan, sarcoglycan, sarcospan) and cytosolic [syntrophin, dystrobrevin and neuronal nitric oxide synthase (nNOS)] proteins into a dystrophin-associated glycoprotein complex (DAGC) at the sarcolemma (Fig. 1; Box 1 for a glossary of terms) (Ervasti, 2007). Frame-shift mutations of the dystrophin gene abolish protein expression and lead to DMD (Box 1). In-frame deletions often generate truncated dystrophin and result in the milder Becker muscular dystrophy (BMD) (Fig. 2A) (Beggs et al., 1991; Hoffman and Kunkel, 1989; Monaco et al., 1988).

<sup>1</sup>Department of Molecular Microbiology and Immunology, School of Medicine, University of Missouri, Columbia, MO 65212, USA. <sup>2</sup>Department of Neurology, School of Medicine, University of Missouri, Columbia, MO 65212, USA.

\*Author for correspondence (duand@missouri.edu)

This is an Open Access article distributed under the terms of the Creative Commons Attribution License (<http://creativecommons.org/licenses/by/3.0/>), which permits unrestricted use, distribution and reproduction in any medium provided that the original work is properly attributed.

The identification of the disease-causing gene and the molecular basis for the DMD and BMD phenotypes establishes the foundation for DMD gene therapy (Fig. 2A). To mitigate muscle disease, one can either restore the full-length transcript or express a truncated but in-frame dystrophin gene (Duan, 2011; Goyenvalle et al., 2011; Konieczny et al., 2013; Mendell et al., 2012; Verhaart and Aartsma-Rus, 2012). Several gene therapy strategies are currently under development. They include replacing the mutated gene with a functional candidate gene (gene replacement) or repairing the defective gene by targeted correction and exon skipping (gene repair). Currently, adeno-associated virus (AAV)-mediated gene replacement and antisense oligonucleotide (AON)-mediated exon skipping are at the forefront (see Box 1).

In this Review, we discuss existing DMD animal models and their application in preclinical gene therapy research. We also discuss how to use these models to address the current and emerging challenges in DMD gene therapy.

## Animal modeling of dystrophin deficiency

Both naturally occurring and laboratory-generated animal models are available to study the pathobiology of dystrophin deficiency and to develop innovative therapies for treating DMD. Currently, there are nearly 60 different animal models for DMD, and the list keeps growing (supplementary material Table S1). Non-mammalian (such as *Caenorhabditis elegans*, *Drosophila melanogaster* and zebrafish) and the feline (either hypertrophic or non-hypertrophic) DMD models are rarely used in gene therapy studies (Berger and Currie, 2012; Chamberlain and Benian, 2000; Kunkel et al., 2006; Lloyd and Taylor, 2010; Shelton and Engvall, 2005; Smith, 2011; Winand et al., 1994a), and the newly developed rat and pig DMD models have yet to be used in such research (Hollinger et al., 2014; Klymiuk et al., 2013; Nakamura et al., 2014; Nonneman et al., 2012). As such, we focus this Review on the mouse and dog models (Fig. 2B). We discuss the pros and cons of each system and their use in gene therapy (Table 1).

## Dystrophin-deficient mice

The most widely used animal model for DMD research is the *mdx* mouse. It was discovered in the early 1980s in a colony of C57BL/10ScSn mice due to elevated serum creatine kinase (CK) and histological evidence of myopathy (Bulfield et al., 1984). The mutation in the *mdx* mouse is a nonsense point mutation (C-to-T transition) in exon 23 that aborted full-length dystrophin expression (Fig. 2B) (Sicinski et al., 1989).

Despite being deficient for dystrophin, *mdx* mice have minimal clinical symptoms and their lifespan is only reduced by ~25% (Fig. 3; Table 1) (Chamberlain et al., 2007; Li et al., 2009). In contrast, the lifespan of individuals with DMD is reduced by ~75% (Box 2; Fig. 3B). *mdx* skeletal muscle disease has several distinctive phases. In the first 2 weeks, *mdx* muscle is indistinguishable from that of normal mice. Between 3 to 6 weeks, it undergoes startling

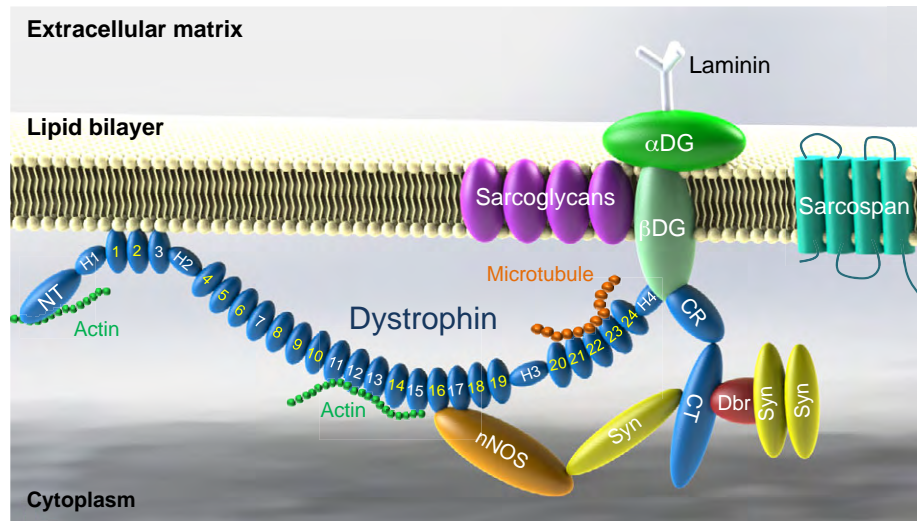


**Fig. 1. Schematic outline of dystrophin and the dystrophin-associated glycoprotein complex (DAGC).** Dystrophin contains N-terminal (NT), middle rod, cysteine-rich (CR) and C-terminal (CT) domains. The middle rod domain is composed of 24 spectrin-like repeats (numerical numbers in the cartoon, positively charged repeats are marked in white color) and four hinges (H1, H2, H3 and H4). Dystrophin has two actin-binding domains located at NT and repeats 11-15, respectively. Repeats 1-3 interact with the negatively charged lipid bilayer. Repeats 16 and 17 form the neuronal nitric oxide synthase (nNOS)-binding domain. Dystrophin interacts with microtubule through repeats 20-23. Part of H4 and the CR domain bind to the  $\beta$ -subunit of dystroglycan ( $\beta$ DG). The CT domain of dystrophin interacts with syntrophin (Syn) and dystrobrevin (Dbr). Dystrophin links components of the cytoskeleton (actin and microtubule) to laminin in the extracellular matrix. Sarcoglycans and sarcospan do not interact with dystrophin directly but they strengthen the entire DAGC, which consists of dystrophin, DG, sarcoglycans, sarcospan, Syn, Dbr and nNOS.

necrosis. Subsequently, the majority of skeletal muscle enters a relatively stable phase owing to robust regeneration. *mdx* limb muscles often become hypertrophic during this phase. The only exception is the diaphragm, which shows progressive deterioration, as is also seen in affected humans (Box 2) (Stedman et al., 1991). Severe dystrophic phenotypes, such as muscle wasting, scoliosis and heart failure, do not occur until mice are 15 months or older (Bostick et al., 2008b; Bostick et al., 2009; Hakim et al., 2011; Lefaucheur et al., 1995; Lynch et al., 2001; Pastoret and Sebillé, 1995). A significant portion of aged *mdx* mice also develops spontaneous sarcoma (Fig. 3A) (Chamberlain et al., 2007; Schmidt et al., 2011; Wang et al., 2014).

The *mdx* mouse has been crossed to several different genetic backgrounds, including the albino, BALB/c, C3H, C57BL/6, DBA/2 and FVB strains, and several immune-deficient strains. Phenotypic variation has been observed in different backgrounds (supplementary material Table S1). For example, albino-*mdx* mice show more severe neurological dysfunction and higher circulating cytokines (Stenina et al., 2013). BALB/c-*mdx* and C3H-*mdx* mice are less susceptible to sarcoma (Krivov et al., 2009; Schmidt et al., 2011; Stenina et al., 2013). Immune-deficient nude-*mdx* and *scid-mdx* mice show less fibrosis (Farini et al., 2007; Morrison et al., 2000). The DBA/2-*mdx* mice are thought to better represent human disease because they display more fibrosis and less regeneration (Fukada et al., 2010). However, according to The Jackson Laboratory, the DBA/2 strain is a challenging breeder and it also carries mutations in a variety of genes that cause hearing loss and eye abnormalities (<http://jaxmice.jax.org/strain/000671.html>).

In 1989, four chemical variant (cv) *mdx* strains were published (Chapman et al., 1989). These mice were generated on the C57BL/6 background using the mutagen N-ethyl-N-nitrosourea (ENU) and they are named as *mdx*<sup>2cv</sup>, *mdx*<sup>3cv</sup>, *mdx*<sup>4cv</sup> and *mdx*<sup>5cv</sup>. Each of these strains carries a different point mutation (Fig. 2B; supplementary material Table S1) (Cox et al., 1993b; Im et al., 1996). Although the overall clinical presentation of these mice differs very little from that

of *mdx* mice, each line has unique features. Specifically, *mdx*<sup>3cv</sup> mice still express ~5% of a near-full-length dystrophin protein (Cox et al., 1993b; Li et al., 2008). *mdx*<sup>5cv</sup> mice have a more severe skeletal muscle phenotype (Beastrom et al., 2011). Revertant fibers (see Box 1) are rarely seen in *mdx*<sup>4cv</sup> and *mdx*<sup>5cv</sup> mice (Danko et al., 1992; Partridge and Lu, 2008). In addition to these four strains, several new ENU-induced dystrophin-null lines have been recently generated (supplementary material Table S1) (Aigner et al., 2009).

In addition to the above-mentioned strains, several other dystrophin-deficient lines (*Dup2*, *MD-null*, *Dp71-null*, *mdx52* and *mdx  $\beta$ geo*) have been created using various genetic engineering techniques (see supplementary material Table S1 for details).

Immune-deficient *mdx* strains are dystrophin-null mice that have been crossed to the immune-deficient background. These mice can be used to study cell or gene therapy without the compounding effects of the host immune response. Besides the commonly used nude-*mdx* and *scid-mdx* mice (Farini et al., 2007; Morrison et al., 2000), several new lines (*NSG-mdx*<sup>4cv</sup>, *Rag2-IL2rb-Dmd*<sup>-</sup> and *W41 mdx*) have recently been developed (supplementary material Table S1) (Arpke et al., 2013; Bencze et al., 2012; Vallese et al., 2013; Walsh et al., 2011). These new lines carry additional mutations that further compromise the immune system.

#### Mouse models that recapitulate the DMD phenotype

Dystrophin-deficient mice show minimal clinical disease. This could be due to the upregulation of compensatory mechanisms or to a species-specific property of the muscle. Elimination of compensatory mechanisms or humanization of *mdx* mice results in mouse models that recapitulate the dystrophic phenotype of human with DMD. A major function of dystrophin is to strengthen the sarcolemma by cross-linking the ECM with the cytoskeleton. Two other proteins, utrophin and  $\alpha$ 7 $\beta$ 1-integrin fulfil the same function and their expression is upregulated in *mdx* mice. The genetic elimination of utrophin and  $\alpha$ 7-integrin in *mdx* mice creates utrophin/dystrophin and integrin/dystrophin double-knockout (*dko*) mice, respectively

## Box 1. Glossary

**Adeno-associated virus (AAV):** a single-stranded DNA virus identified in 1965. AAV has a ~4.7-kb genome and encodes at least three open reading frames (ORFs), one for viral capsid proteins, one for replication proteins and a third one for the assembly-activating protein. In recombinant AAV vectors, viral ORFs are replaced by a reporter or therapeutic expression cassette. An up to 5-kb vector genome can be packaged in an AAV vector. At least 13 different AAV serotypes have been reported. Hundreds of genetically modified AAV capsids have also been developed. AAV can efficiently transduce post-mitotic tissues and wild-type AAV does not cause human disease. Because of these features, AAV has been used in numerous clinical trials.

**Dual and tri-AAV vectors:** engineered AAV vector systems that can deliver a 10-kb (dual vector) or 15-kb (tri-vector) expression cassette. Specifically, a large expression cassette is divided into two pieces (dual vectors) or three pieces (tri-vector). An individual piece contains either a region that overlaps with another piece and/or is engineered with splicing signals. Each piece is packaged in a single viral particle. Co-delivery of vectors containing different pieces of the expression cassette results in reconstitution of the original expression cassette *in vivo* by cellular recombination mechanisms.

**Exon skipping:** a phenomenon in which one or multiple exons are spliced out and eliminated from the mature mRNA.

**Frame-shift mutation:** a mutation that disrupts the open reading frame of an mRNA transcript.

**Freezing response:** a reflex defense mechanism observed in prey animals where they freeze or completely stop moving when scared.

**Hydrodynamic intravascular delivery:** a technique used for gene delivery where the hydrostatic pressure is applied to increase the permeability of the vascular wall. This allows efficient penetration of gene therapy plasmids into the tissue parenchyma.

**Liposome:** an artificially created lipid-bilayer sphere. A DNA plasmid can be incorporated inside the lipid sphere. The fusion of the lipid bilayer with cell membrane allows delivery of the DNA plasmid into a cell.

**Microspheres:** generic name given to a nanoscale spherical object that can be made out of a variety of materials, including lipids, polymers and metal oxides. They can be used to deliver a DNA plasmid to the cell.

**Nuclease-based gene editing:** DNA gene editing technique that uses endonucleases to make double-stranded breaks in the DNA at a user-specified location to initiate error-prone DNA repair. As a consequence, the DNA sequence at the site of break is altered. These endonucleases are often linked to sequence-specific targeting proteins, such as zinc fingers.

**Phosphorodiamidate morpholino oligomer (PMO):** a synthetic oligonucleotide in which the ribose or deoxyribose backbone is replaced by a morpholine ring and the phosphate replaced by phosphorodiamidate. Any one of the four nucleobases can be attached to the morpholine ring. Because of the unnatural backbone, PMO is more resistant than the ordinary antisense oligonucleotide (AON) to nuclease digestion.

**Revertant fibers:** rarely occurring dystrophin-positive myofibers found in animals that carry a null mutation in the dystrophin gene. The molecular mechanisms underlying the formation of revertant fibers are not completely clear. They might arise from sporadic alternative splicing that eliminates the mutation from the dystrophin transcript and/or a second mutation that corrects the original mutation on the DNA.

**Sarcolemma:** muscle-cell plasma membrane.

**Vivo-morpholino:** a morpholino oligomer that has been covalently linked to an octa-guanidine dendrimer moiety. Conjugation with octa-guanidine increases cell penetration.

**WW domain:** a protein module of approximately 40 amino acids. It contains two preserved tryptophan (W) residues that are spaced 20 to 22 amino acids apart. The WW domain folds into a stable, triple-stranded  $\beta$ -sheet and mediates protein-protein interaction.

However, they are difficult to generate and care for, and they often die prematurely (compared with the single knockouts; Fig. 3B). Recent studies suggest that utrophin heterozygous *mdx* mice might represent an intermediate model between the extreme *dko* mice and mildly affected *mdx* mice (Rafael-Fortney et al., 2011; van Putten et al., 2012b; Zhou et al., 2008).

Robust skeletal muscle regeneration also explains the slowly progressive phenotype of *mdx* mice. Two different approaches have been used to reduce muscle regeneration in *mdx* mice. Megeney et al. eliminated MyoD, a master myogenic regulator, from *mdx* mice (Megeney et al., 1996). The resulting MyoD/dystrophin double-mutant mouse shows marked myopathy, dilated cardiomyopathy and premature death (Fig. 3B) (Megeney et al., 1996; Megeney et al., 1999). Compared with normal muscle, the length of telomere is reduced in DMD muscle (Decary et al., 2000). Sacco et al. hypothesized that the long telomere length in mouse myogenic stem cells contributes to the high regenerative capacity of mouse muscle (Mourkioti et al., 2013; Sacco et al., 2010). Telomerase RNA (*mTR*) is required for the maintenance of the telomere length. To reduce telomere length in dystrophin-null mice, Sacco et al. crossed *mdx<sup>4cv</sup>* mice with *mTR*-null mice. These *mTR/mdx* double-mutant mice show more severe muscle wasting and cardiac defects (Mourkioti et al., 2013; Sacco et al., 2010). Their lifespan is reduced to ~12 months (Fig. 3B).

Other symptomatic *dko* strains (supplementary material Table S1) have also been generated by mutating genes involved in: (1) cytoskeleton-ECM interactions (such as desmin, laminin and like-glycosyltransferase) (Banks et al., 2014; Gawlik et al., 2014; Martins et al., 2013), (2) the DAGC (such as dystrobrevin and  $\delta$ -sarcoglycan) (Grady et al., 1999; Li et al., 2009), (3) muscle repair (such as dysferlin) (Grady et al., 1999; Han et al., 2011; Hosur et al., 2012; Li et al., 2009) and (4) inflammation and fibrosis [such as interleukin-10, a disintegrin and metalloproteinase protein (ADAM)-8, and plasminogen activator inhibitor-1] (Ardite et al., 2012; Nishimura et al., 2015; Nitahara-Kasahara et al., 2014).

Humanization is another method of increasing *mdx* disease severity. The gene encoding cytidine monophosphate sialic acid hydroxylase (*Cmah*) is naturally inactivated in humans but not in mice (Varki, 2010). *Cmah* converts cell-surface sialic acid N-acetylneuraminic acid (Neu5Ac) to N-glycolylneuraminic acid (Neu5Gc). Hence, human cells only have Neu5Ac but no Neu5Gc. Genetic elimination of *Cmah* humanizes the cell-surface glycan profile in mice (Hedlund et al., 2007). Interestingly, *Cmah*-deficient *mdx* mice show a more severe phenotype (Fig. 3B). This humanization process renders *Cmah/mdx* mice a better model because they more closely recapitulate human disease (Chandrasekharan et al., 2010).

In summary, the large collection of symptomatic double-mutant mouse lines has greatly expanded the armory of potential mouse models for preclinical studies. Accelerated disease progression in these *dko* mice provides an excellent opportunity not only to obtain results from experimental therapies more rapidly but also to confirm whether a therapy can indeed ameliorate clinically relevant manifestations and increase lifespan. Nevertheless, there are also important limitations. For example, most *dko* mice are difficult to breed and are often not commercially available. Importantly, unlike in humans with DMD, all *dko* mice carry a mutation not only in the dystrophin gene but also in another gene (although because the gene encoding *Cmah* is inactivated in humans this is not an issue for *Cmah/mdx* mice). This is not the case in affected humans. How this additional mutation influences data interpretation remains incompletely understood.

(Deconinck et al., 1997a; Grady et al., 1997; Guo et al., 2006; Rooney et al., 2006). These *dko* mice are significantly smaller than their single-gene null parents and show much more severe muscle disease (similar to or even worse than that of humans with DMD) (Fig. 3A).



**Table 1. Comparison of disease severity and gene therapy status in dystrophin-null mice, dogs and humans**

	Mice	Dogs	Humans
<b>Clinical manifestations</b>			
Birth body weight	= normal	= normal	= normal
Grown-up body weight	≥ normal	< normal	< normal
Clinical course	Mild, non-progressive	Severe, progressive	Severe, progressive
Lifespan	= 75% of normal	= 25% of normal	= 25% of normal
Neonatal death	Rare	~ 25% of affected dogs	Rare
Age at first symptom	≥ 15 months	Birth to 3 months	2 to 4 years
Loss of ambulation	Rare	Uncommon	Common at early teenage
Muscle wasting	Minimal until ≥ 15 months	Progressive	Progressive
ECG abnormality	Frequent	Frequent	Frequent
Cardiomyopathy	≥ 20 months; dilated (female) and hypertrophic (male)	Detectable at 6 months by echocardiography	Evident at 16 years
Cognitive and CNS defects	Mild	No information available	One-third of affected individuals
<b>Histopathology</b>			
At birth	Minimal	Minimal	Minimal
Acute necrosis	2 to 6 weeks	None	None
Limb muscle fibrosis	Minimum in adult	Extensive and progressive	Extensive and progressive
Muscle regeneration	Robust	Poor	Poor
<b>Gene therapy status</b>			
Vectors tested	Nonviral (plasmid and oligonucleotides), retrovirus, herpes simplex virus, adenovirus, AAV	Nonviral (plasmid and oligonucleotides), adenovirus, AAV	Nonviral (plasmid and oligonucleotides), AAV
Dystrophin genes tested	Microgene, minigene, and full-length cDNA	Microgene, minigene, and full-length cDNA	Microgene and full-length gene
Strategies tested	Micro/mini/full-length gene replacement, RNA- and DNA-level gene repair, dystrophin-independent gene therapy	Micro/mini-gene replacement, RNA- and DNA-level gene repair, dystrophin-independent gene therapy	AAV-mediated microgene replacement, RNA-level gene repair by exon-skipping, AAV-mediated follistatin expression
Current focus	Optimization of existing approaches, exploration of new technology	AAV microgene; AAV exon skipping	Exon skipping

AAV, adeno-associated virus; ECG, electrocardiography.

2001; Kornegay et al., 1988; Lanfossi et al., 1999; McCully et al., 1991; Moise et al., 1991; Nguyen et al., 2002; Sharp et al., 1992; Valentine et al., 1989a; Valentine et al., 1990a; Valentine et al., 1991; Valentine and Cooper, 1991; Valentine et al., 1990b; Valentine et al., 1986; Valentine et al., 1988; Valentine et al., 1989b; Valentine et al., 1989c; Valentine et al., 1989d; Valentine et al., 1992). Currently, GRMD dogs are maintained in several colonies throughout the USA (including the University of Missouri and Texas A&M University, among others), and in France, Brazil and Australia. The GRMD mutation has also been crossed to the Beagle background and a colony is now maintained in Japan; these dogs are called canine X-linked muscular dystrophy in Japan or CXMD<sub>J</sub> (Shimatsu et al., 2003; Valentine et al., 1988). Recently, we and others have created hybrid strains that are on mixed genetic backgrounds and/or contain mutations of different breeds (Cotten et al., 2013; Fine et al., 2011; Miyazato et al., 2011; Shin et al., 2013a; Yang et al., 2012). Besides GRMD-based colonies, research colonies have also been generated from affected Pembroke Welsh corgis and Labrador retrievers (Auburn University and University of Missouri), and CKCS-MD (Royal Veterinary College, UK) (Smith et al., 2007; Smith et al., 2011; Walmsley et al., 2010). The CKCS-MD model is especially interesting because the mutation in this breed corresponds to a major deletion hot spot (exons 45-53) in humans with DMD (Aartsma-Rus et al., 2006; Flanigan et al., 2009b; Tuffery-Giraud et al., 2009).

Affected dogs share a remarkably similar clinical course to that of DMD boys (Box 2; Fig. 3; Table 1) (Shimatsu et al., 2005; Smith et al., 2011; Valentine et al., 1988). Limb weakness and exercise intolerance start around 2 to 3 months of age (analogous to ~3 years of age in humans) (Valentine et al., 1988). Muscle atrophy, joint contracture, hypersalivation, dysphagia, abnormal gait and signs of cardiac involvement become apparent at ~6 months (Fig. 3A; Table

1) (Fan et al., 2014; Fine et al., 2011; Valentine et al., 1988; Valentine et al., 1989c; Yugeta et al., 2006). At around 6 to 10 months, disease progression enters a relatively stable 'honeymoon' period (Fan et al., 2014; Shimatsu et al., 2005; Valentine et al., 1988). Death often occurs around 3 years of age (a ~75% reduction of the lifespan) (Fig. 3B). Humans with DMD show heterogeneity in their clinical manifestation (Box 2) (Ashwath et al., 2014; Desguerre et al., 2009; Siffringer et al., 2004). cDMD dogs also show variation in their symptoms. In extreme cases, affected subjects are essentially asymptomatic despite the lack of dystrophin in their muscles (Ambrósio et al., 2008; Dubowitz, 2006; Hattori et al., 1999; Wakefield et al., 2009; Zatz et al., 2014; Zucconi et al., 2010).

Besides clinical resemblance, cDMD dogs also have histological lesions similar to affected humans. For example, limb muscle fibrosis is a salient disease feature in humans with DMD and in affected dogs but not in *mdx* mice (C.H.H. and D.D., unpublished observations). Vigorous regeneration in mouse muscle contributes substantially to the mild phenotype of *mdx* mice. This regeneration is evident by high proportions of centrally nucleated myofibers in *mdx* mice. Similar to humans with DMD, cDMD dogs have much fewer myofibers containing central nucleation (Cozzi et al., 2001; Shin et al., 2013b; Smith et al., 2011; Yang et al., 2012).

It should be noted that the clinical presentation of cDMD dogs is not identical to that of humans with DMD (Table 1). About 20-30% of cDMD puppies die within 2 weeks of birth likely due to diaphragm failure (Ambrósio et al., 2008; Nakamura et al., 2013; Shimatsu et al., 2005; Valentine et al., 1988). However, this neonatal death is not seen in newborn DMD boys. Growth retardation is another canine-specific symptom (West et al., 2013). Body weight at birth is similar between normal and affected cDMD puppies (Smith et al., 2011). However, at 1 and 6 months of age, the body

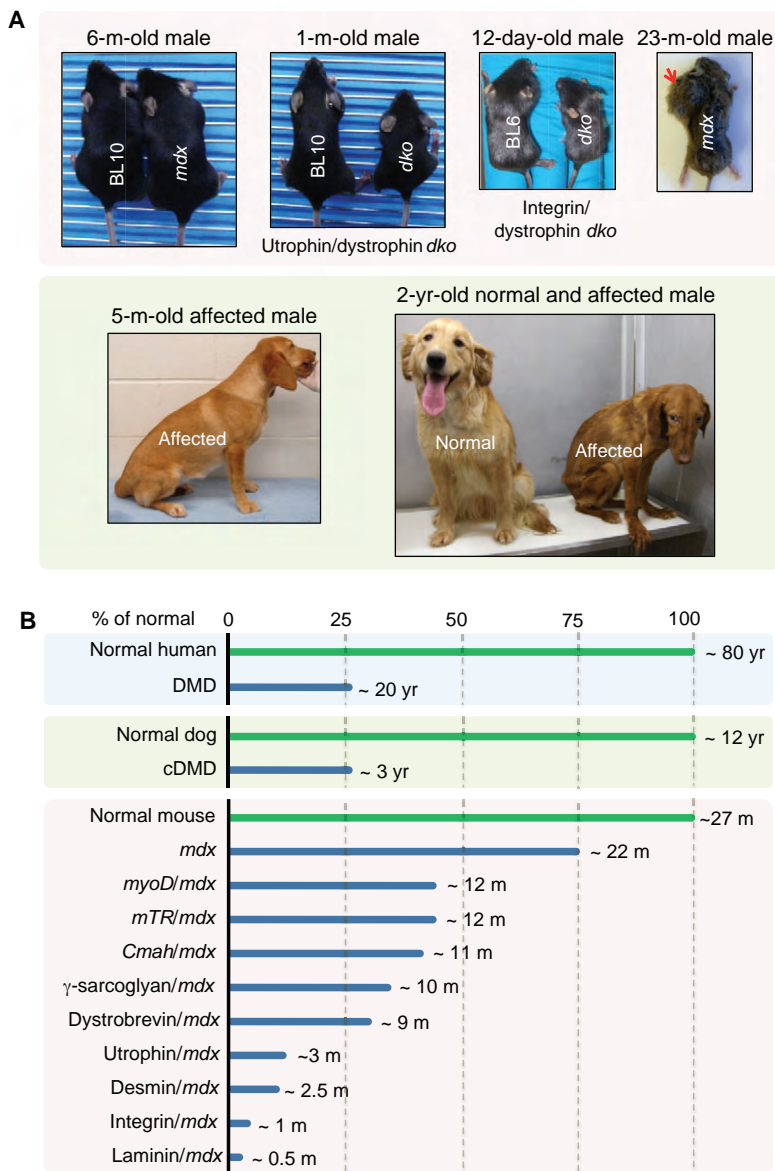


**Fig. 3. Representative animal models for DMD.**

(A) Representative pictures of selected DMD mouse and dog models. *mdx* mice do not show symptoms (see 6-month-old photo) until very old (see 23-month-old photo). Aged *mdx* mice are also prone to rhabdomyosarcoma (a tumor of muscle origin; red arrow). Utrophin/dystrophin and integrin/dystrophin double-knockout (*dko*) mice are much smaller than the age-matched wild-type (BL10 and BL6) mice. A 5-month-old affected dog shows limb muscle atrophy and is reluctant to exercise. At the age of 2 years old, the affected dog displays severe clinical disease, whereas its normal sibling remains healthy. (B) Lifespan comparison among affected humans, affected dogs and various mouse models.

weight of affected puppies reaches only ~80% and ~60% of normal, respectively (C.H.H. and D.D., unpublished observation from  $n > 50$  dogs). Finally, untreated humans with DMD usually lose ambulation during the early teenage years. However, complete loss of ambulation is not a clinical feature in young cDMD dogs (Duan et al., 2015; Valentine et al., 1988).

Overall, cDMD dogs share many features with that of humans with DMD. These features make cDMD dogs an excellent model to conduct preclinical gene therapy studies (Duan, 2011; Duan, 2015). Nevertheless, *mdx* mice remain the most commonly used model in DMD gene therapy studies owing to the low cost and easy access. Any discussion of DMD models in gene therapy that lacked mention of *mdx* mice would not be complete.

Establishing the foundations of gene therapy: transgenic *mdx* mice

The successful development of a gene therapy requires research to identify the therapeutic candidate gene, the level of expression needed to produce a therapeutic effect and the tissue that should be targeted (Chamberlain, 2002; Duan, 2006). As we discuss in this

section, for DMD gene therapy research, these fundamental questions have been addressed using transgenic *mdx* mice.

**Therapeutic potential of truncated dystrophin genes**

Naturally occurring small dystrophin isoforms

The enormous size of the full-length dystrophin gene poses one of the biggest challenges for gene therapy because it exceeds the packaging limit of most viral vectors. For this reason, identifying a smaller but functional gene has been an ongoing goal in the development of a dystrophin gene-replacement therapy. Early studies showed that, besides the 427-kDa full-length protein, the dystrophin gene also encodes a number of smaller N-terminal-truncated non-muscle isoforms (Ahn and Kunkel, 1993; Blake et al., 2002; Ervasti, 2007). These include Dp260, Dp140, Dp116, Dp71 and Dp40 (numbers refer to the molecular weight) (Fig. 4A). With the exception of Dp40 (Fujimoto et al., 2014), they all contain the CT and CR domains but are missing the NT actin-binding domain. To determine whether these miniature isoforms are therapeutically relevant, the Chamberlain lab, as well as others, made transgenic *mdx* mice for Dp260, Dp116 and Dp71 (see supplementary material

**Box 2. Clinical features of DMD**

Large-scale population studies have outlined the natural disease progression in affected humans (Table 1) (Bushby and Connor, 2011; Henricson et al., 2013; Magri et al., 2011; McDonald et al., 2013a; McDonald et al., 2013b; Spurney et al., 2014). The first clinical sign usually appears around age 3. Between ages 5 and 8, symptoms are often stabilized or even slightly improved (known as the 'honeymoon' period) in the absence of any treatment (Bushby and Connor, 2011; McDonald et al., 2013a; McDonald et al., 2010). Rapid clinical deterioration starts around 7 to 8 years of age (Mercuri and Muntoni, 2013). Individuals with DMD lose their ambulation at approximately age 10, develop cardiomyopathy at about age 16 and die around age 20 (life expectancy is reduced by ~75%). With the use of steroids, symptom management and multidisciplinary care (especially nocturnal ventilation), the lifespan of an affected individual is now extended to 30 to 40 years of age. In these individuals, cardiac complications (cardiomyopathy and/or cardiac arrhythmia) have emerged as a major source of morbidity and mortality. Despite the overall trend of disease progression throughout life, affected individuals actually show heterogeneity in clinical manifestations. One retrospective study of 75 drug-naïve affected individuals classified DMD into four distinctive groups (infantile, classical, moderate pure motor and severe pure motor) based on the intellectual and motor outcome (Desguerre et al., 2009).

Table S1 for details) (Cox et al., 1994; Gaedigk et al., 2006; Greenberg et al., 1994; Judge et al., 2011; Judge et al., 2006; Warner et al., 2002).

Dp71 is the most abundant non-muscle dystrophin isoform. It contains only the CR and CT domains (Fig. 4A). Because the CT domain carries the binding sites for syntrophin and dystrobrevin, it was initially thought that Dp71 might restore some of the signaling functions of dystrophin. Surprisingly, however, transgenic overexpression of Dp71 results in more severe muscle disease in *mdx* mice (Cox et al., 1994; Greenberg et al., 1994) and myopathy in normal mice (Leibovitz et al., 2002). The WW domain of hinge 4 (H4; see Fig. 1A and Box 1), which is partially truncated in Dp71, participates in dystrophin-dystroglycan interaction (Huang et al., 2000). To fully appreciate the contribution of dystroglycan binding and dystrophin signaling in DMD pathogenesis, Judge et al. generated Dp116 transgenic *mdx* mice. Dp116 is a Schwann-cell-specific dystrophin isoform. It contains the last three spectrin-like repeats, H4, and the CR and CT domains (Fig. 4A). Dp116 expression does not improve muscle disease in *mdx*<sup>3cv</sup> mice nor does it reduce the histopathology in utrophin/dystrophin *dko* mice (Judge et al., 2011; Judge et al., 2006). Interestingly, the lifespan of utrophin/dystrophin *dko* mice was significantly increased by transgenic *Dp116* expression (Judge et al., 2011).

Two independent strains of Dp260 transgenic mice have been studied (Gaedigk et al., 2006; Warner et al., 2002). Although Dp260 (also known as the retinal isoform of dystrophin) does not carry the NT domain, it contains the ABD2 domain (Fig. 2B; Fig. 4A). Its overexpression significantly reduces the dystrophic phenotype of *mdx* and utrophin/dystrophin *dko* mice but does not completely prevent muscle degeneration, inflammation and fibrosis (Gaedigk et al., 2006; Warner et al., 2002). In summary, transgenic analyses of naturally occurring dystrophin isoforms suggest that the N-terminal domain is required for maximum muscle protection and that a complete dystroglycan-binding domain (including the WW domain in H4 and the CR domain) is important.

**Synthetic mini- and micro-dystrophin genes**

An alternative approach to developing a smaller but functional dystrophin gene is through genetic engineering. To achieve this, one needs to know which regions of the dystrophin gene are dispensable

for its normal functions. The first clue about this came from a mildly affected individual, who was ambulant at age 61 (England et al., 1990). This person carries a large in-frame deletion ( $\Delta$ 17-48) in the rod domain, which eliminates 46% of the coding sequence. Transgenic expression of the  $\Delta$ 17-48 minigene in *mdx* mice significantly reduced skeletal muscle pathology and increased specific muscle force (Phelps et al., 1995; Wells et al., 1995). Subsequent optimization by removing residue repeat 19 in the  $\Delta$ 17-48 minigene resulted in a more protective  $\Delta$ H2-R19 minigene (Fig. 4B) (Harper et al., 2002).

An important function of dystrophin is to recruit nNOS to the sarcolemma. Failure to do so results in functional ischemia and aggravates muscle disease (Thomas, 2013). We recently identified the dystrophin nNOS-binding site at R16/17 of the rod domain (Fig. 1; Fig. 2B) (Lai et al., 2009; Lai et al., 2013). Inclusion of this binding site in synthetic dystrophins (Fig. 4B) significantly enhances muscle protection and exercise capacity (Lai et al., 2009; Zhang et al., 2013).

The mini-dystrophin gene is ~6 to 8 kb. One drawback is that it cannot fit into the 5-kb packaging limit of AAV, the most efficient muscle gene-transfer vector. A pivotal transgenic study from the Chamberlain lab opened the door to further reducing the size of the dystrophin gene by deleting the entire CT domain (Crawford et al., 2000). Specifically, Chamberlain and colleagues showed that a C-terminal-truncated dystrophin gene successfully restored syntrophin and dystrobrevin to the sarcolemma and completely protected young adult *mdx* mice (Crawford et al., 2000). Consistent with this transgenic study, a subset of affected individuals who have partial or complete CT-domain deletion also show mild disease (Aartsma-Rus et al., 2006; McCabe et al., 1989; Patria et al., 1996; Tuffery-Giraud et al., 2009). Collectively, the existing data suggest that the majority of the rod domain (except for R16/17) and the entire C-terminal domain are not essential for dystrophin function. Based on this understanding, several versions of highly abbreviated synthetic micro-dystrophin genes (<4 kb) have been engineered (Fig. 4B) (Harper et al., 2002; Lai et al., 2009; Wang et al., 2000). These microgenes greatly prevent muscle damage in transgenic *mdx* mice (Hakim and Duan, 2013; Harper et al., 2002; Li et al., 2011).

**Level of expression**

Two essential questions in DMD gene therapy are: (1) how much dystrophin is too much, and (2) how much dystrophin is enough to ameliorate disease? In transgenic *mdx* mice, Chamberlain and colleagues found that 50-fold overexpression of full-length dystrophin was not toxic to skeletal muscle, thus providing a high safety margin (Cox et al., 1993a). Studies in transgenic *mdx* mice have also revealed the threshold for histological and physiological protection (Phelps et al., 1995; Wells et al., 1995). Dystrophin expression at ~20% of the wild-type level significantly mitigated muscle pathology and enhanced muscle contractility (Phelps et al., 1995; Wells et al., 1995). *mdx*<sup>3cv</sup> mice express ~5% of a near-full-length dystrophin protein and *mdx-Xist*<sup>Δhs</sup> mice express variable low levels of dystrophin (supplementary material Table S1) (Cox et al., 1993b; van Putten et al., 2012a). Recent studies in *mdx*<sup>3cv</sup> and *mdx-Xist*<sup>Δhs</sup> mice suggest that dystrophin expression at a 5% level still preserves some muscle function in *mdx* mice and extends the lifespan of utrophin/dystrophin *dko* mice (Li et al., 2008; Li et al., 2010; van Putten et al., 2012a; van Putten et al., 2013). A clear correlation between the dystrophin level and clinical manifestation has also been noticed in humans with DMD (Nicholson et al., 1993a; Nicholson et al., 1993b). Affected individuals with ≥20% wild-type dystrophin protein expression are often ambulant beyond

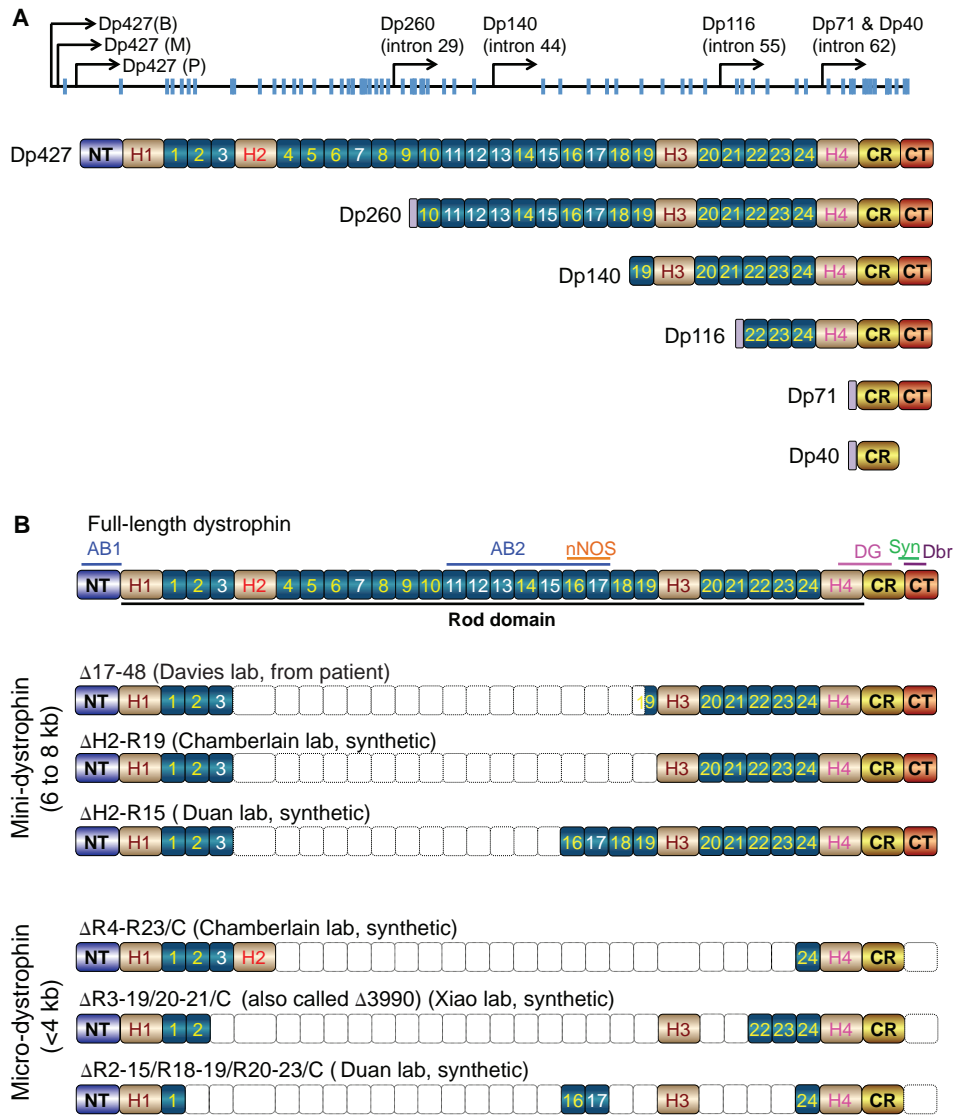


**Fig. 4. Structure of abbreviated dystrophins.** (A) Naturally occurring dystrophin isoforms. In the topmost schematic, blue boxes denote exons. The full-length dystrophin (Dp427) transcripts have three isoforms, including brain Dp427 (B), muscle Dp427 (M) and Purkinje cell Dp427 (P). Smaller dystrophin isoforms are produced from promoters located in different introns (intron positions are marked for each isoform). Dp260 is expressed in the retina, Dp140 in the brain and kidney, Dp116 in Schwann cells, and Dp71 and Dp40 are expressed from the same promoter except Dp71 is ubiquitously expressed whereas Dp40 only exists in the brain. Except for Dp140, all other dystrophin isoforms have unique N-terminal sequences not present in the full-length protein. (B) Structure of representative mini- and micro-dystrophins. The full-length dystrophin protein is shown uppermost, and features the same terminology as that used in Fig. 1.

age 20 (Bulman et al., 1991; Byers et al., 1992; Hoffman et al., 1989). An affected individual with 30% dystrophin protein expression, measured through western blot, was even free of skeletal muscle disease at age 23 (Neri et al., 2007). Where gene therapy is concerned, there is no doubt that restoring  $\geq 20\%$  protein expression will be needed to achieve clinically meaningful improvement. Nonetheless, mouse data suggest that even a low level of expression ( $\sim 5\%$ ) might still be beneficial.

**Target tissue: skeletal muscle versus heart**

Humans with DMD suffer from both skeletal muscle disease and cardiomyopathy. It thus seems obvious that both skeletal and heart muscle should be treated. However, many existing gene therapy approaches (such as some AONs used for exon skipping and AAV serotype-9-mediated systemic gene transfer in newborn dogs) cannot efficiently reach the heart (Alter et al., 2006; Hakim et al., 2014; Yokota et al., 2009; Yue et al., 2008). Will skeletal-muscle-centered therapy benefit individuals with DMD? An early study in young (4- to 5-month-old) transgenic *mdx*<sup>4cv</sup> mice suggests that targeted repair of skeletal muscle accelerates heart disease (Townsend et al., 2008). However, the interpretation of the heart function data in this study has been questioned (Wasala et al.,

2013). Using a different approach, Crisp et al. reached a completely opposite conclusion in adult (6- to 9-month-old) *mdx* mice and neonatal (10-day-old) utrophin/dystrophin *dco* mice (Crisp et al., 2011). They concluded that skeletal muscle rescue can prevent cardiomyopathy (Crisp et al., 2011). Because *mdx* mice do not develop clinically evident cardiomyopathy until they are 21-months old (Bostick et al., 2008b; Bostick et al., 2009), we recently re-evaluated this issue in a similar transgenic strain used by Townsend et al. (Townsend et al., 2008; Wasala et al., 2013). Surprisingly, skeletal-muscle-rescued *mdx* mice showed the identical heart disease as that of non-transgenic *mdx* mice at the age of 23 months (Wasala et al., 2013). In summary, skeletal muscle rescue might neither aggravate nor completely alleviate cardiomyopathy. As such, we believe that gene therapy should treat both skeletal and cardiac muscles.

**Gene replacement therapy**

A straightforward approach to treating DMD is to add back a functional dystrophin gene. This can be achieved using a variety of gene-transfer vectors, including nonviral, retroviral, adenoviral, herpes simplex viral and AAV vectors. The candidate gene can be the full-length cDNA or an abbreviated synthetic gene.

### Replacement with the full-length dystrophin coding sequence

Several strategies have been explored to deliver the 14-kb, full-length dystrophin cDNA. Direct plasmid injection was tested in *mdx* mice soon after the discovery of the dystrophin gene (Acsadi et al., 1991). A number of different nonviral delivery approaches have since been evaluated in *mdx* mice. These include the use of liposomes, microspheres, electroporation and hydrodynamic intravascular delivery (see Box 1). Direct plasmid injection has also been tested in the GRMD model and in a Phase 1 human trial (Braun, 2004; Duan, 2008). However, poor transduction and transient expression have limited further development of these plasmid-based therapeutic strategies.

The gutted adenoviral vector does not carry any viral genes and can package a 35-kb genome. It has been used to express the full-length dystrophin cDNA (Haecker et al., 1996; Kochanek et al., 1996; Kumar-Singh and Chamberlain, 1996). Tests conducted in *mdx* and utrophin/dystrophin *dko* mice have yielded promising results (Clemens et al., 1996; DelloRusso et al., 2002; Ishizaki et al., 2011; Kawano et al., 2008). The current challenges are the host immune response to the adenoviral capsid and the contaminating wild-type adenovirus. Herpes simplex virus also has an extremely large capacity (~150 kb) and has been used to package the full-length dystrophin cDNA (Akkaraju et al., 1999; Liu et al., 2006). However, there have been very few animal studies performed with it due to the toxicity of the virus.

Recently, tri-AAV vectors were used to deliver the full-length dystrophin cDNA (see Box 1) (Koo et al., 2014; Lostal et al., 2014). In this system, the full-length cDNA expression cassette is split into three fragments and separately packaged in an AAV vector. Co-infection with all three AAV vectors results in the production of a full-length dystrophin protein. This approach has been tested in *mdx* and *mdx<sup>4ev</sup>* mice by direct muscle injection. The therapeutic benefits of this system await substantial improvement in transduction efficiency.

### Replacement with small synthetic dystrophin genes

The 6- to 8-kb minigenes discussed earlier in the Review have been tested with plasmid, retrovirus, adenovirus and AAV. Retroviral delivery is very inefficient because the virus does not transduce post-mitotic muscle cells (Dunckley et al., 1993). The first-generation E1-deleted adenovirus was used to deliver the  $\Delta 17-48$  minigene to *mdx* mice and GRMD dogs (Howell et al., 1998; Ragot et al., 1993). Although this vector is more efficient than a retroviral vector, it induces a strong cellular immune response in *mdx* mice (Howell et al., 1998; Ragot et al., 1993). The Chamberlain and Duan labs have tested dual-AAV-vector-mediated mini-dystrophin therapy in *mdx* mice using local and systemic gene transfer (see Box 1) (Ghosh et al., 2008; Lai et al., 2005; Odom et al., 2011; Zhang and Duan, 2012; Zhang et al., 2013). In the dual AAV vector system, mini-dystrophin expression is achieved with a pair of AAV vectors, each carrying half of the minigene. These studies have shown a significant improvement of histology and function in treated *mdx* mice. Noticeably, the use of the R16/17-containing mini-dystrophin dual AAV vectors has successfully restored sarcolemmal nNOS expression and ameliorated functional ischemia (Zhang and Duan, 2012; Zhang et al., 2013).

AAV-mediated, micro-dystrophin gene therapy is currently at the cutting edge of DMD gene-replacement therapy. Local injection studies performed in the Chamberlain, Dickson, Duan, Takeda and Xiao laboratories suggest that a rationally designed dystrophin microgene can protect limb muscles and the heart in *mdx* mice despite the absence of ~70% of the coding sequence (Harper et al.,

2002; Wang et al., 2000; Yoshimura et al., 2004; Yue et al., 2003). Using the newly developed AAV serotype-6 and -8 vectors (Gao et al., 2002; Rutledge et al., 1998), the Chamberlain and Xiao labs achieved widespread whole-body muscle gene transfer in the rodent models of muscular dystrophies (Gregorevic et al., 2004; Wang et al., 2005). Later, it was found that AAV serotype-9 can also provide efficient systemic muscle delivery (Bostick et al., 2007; Pacak et al., 2006). More recent studies suggest that AAV-8 and AAV-9 can also produce robust body-wide muscle gene transfer in neonatal dogs (Hakim et al., 2014; Kornegay et al., 2010; Pan et al., 2013; Yue et al., 2008).

The first systemic gene therapy test was performed in *mdx* mice by Gregorevic et al. (Gregorevic et al., 2004) and subsequently in utrophin/dystrophin and myoD/dystrophin *dko* mice (Gregorevic et al., 2006; Lai et al., 2009). In these studies, micro-dystrophin gene therapy significantly ameliorated the histological and physiological signs of muscular dystrophy, reduced CK levels and extended lifespan. To further improve therapeutic efficacy, several labs made additional changes to the existing micro-dystrophin constructs. Dickson and colleagues found that codon-optimization and inclusion of the syntrophin/dystrobrevin-binding site resulted in better rescue (Foster et al., 2008; Koo et al., 2011a). The Chamberlain lab found that the rigid poly-proline site in hinge 2 compromised micro-dystrophin function (Banks et al., 2010). Our studies have suggested that R16/17 should be incorporated in the microgene design to normalize nNOS expression (Harper, 2013; Lai et al., 2009; Lai et al., 2013; Li et al., 2011; Shin et al., 2013b).

In an effort to translate AAV microgene therapy to large mammals, several groups have extended research into cDMD models (Koo et al., 2011b; Kornegay et al., 2010; Shin et al., 2012a; Shin et al., 2012b; Wang et al., 2007). These studies uncovered two important issues that were not encountered during mouse studies. First, intramuscular injection results in a strong cellular immune response (Ohshima et al., 2009; Wang et al., 2007; Yuasa et al., 2007; Yue et al., 2008). As a result, transient immune suppression is necessary for persistent transduction in dog muscle (Shin et al., 2012b; Wang et al., 2007). Second, a microgene that reduces muscle disease in mice might not work effectively in dogs (Kornegay et al., 2010; Sampaolesi et al., 2006). Specifically, the  $\Delta R4-23/C$  dystrophin microgene did not improve muscle histology when tested in a cell therapy study (Sampaolesi et al., 2006). Newborn GRMD dogs developed more severe disease after treatment with the  $\Delta R3-19/20-21/C$  (also called  $\Delta 3990$ ) microgene (Kornegay et al., 2010). Currently, convincing physiological improvement has only been demonstrated in the  $\Delta R2-15/R18-19/R20-23/C$  microgene-treated dogs (Shin et al., 2013b).

### Gene repair therapy

Therapeutic approaches that aim to repair or correct a DMD gene mutation have been conducted at both the RNA and DNA level using oligonucleotides or engineered endonucleases (Aartsma-Rus, 2012; Bertoni, 2014). Although AON-mediated exon skipping has already reached Phase 3 human trials, endonuclease-based gene repair has just begun to emerge (Koo and Wood, 2013; Lu et al., 2011).

### Repairing the dystrophin transcript

Therapeutic RNA targeting using exon skipping is by far the most advanced DMD gene therapy technology developed to date. In exon skipping, AONs are used to modulate the splicing of the RNA transcript such that one or several exons are excluded. As a result, an out-of-frame mRNA is converted into an in-frame transcript or

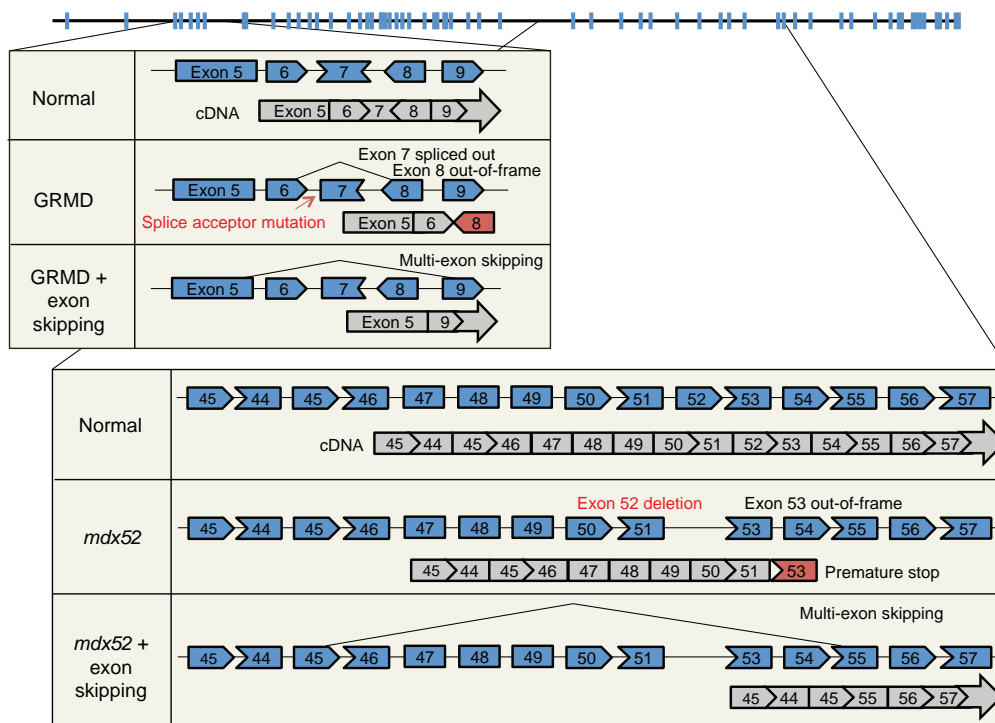


**Fig. 5. Multiple-exon skipping.** The uppermost diagram is the intron/exon structure of the dystrophin gene. Blue boxes denote exons. The top box shows the golden retriever muscular dystrophy dog (GRMD) mutation and exon skipping for GRMD. A point mutation in intron 6 alters normal splicing, and the resulting transcript (gray) is out-of-frame. Skipping exons 6, 7 and 8 yields an in-frame transcript. The bottom box shows the *mdx52* mutation and exon skipping in *mdx52*. Deletion of exon 52 disrupts the reading frame and results in a premature stop. Removing exons 45 to 55 from the mutated transcript generates an in-frame transcript.

an exon that contains a premature stop codon is removed from the transcript (Spitali and Aartsma-Rus, 2012). An internally deleted but partially functional dystrophin produced from exon skipping is expected to convert severe DMD to the milder Becker phenotype. This approach represents an excellent example of how a rationally designed strategy can rapidly move from bench to bedside.

The initial proof-of-principle study for exon skipping was conducted in cultured *mdx* mouse muscle cells (Dunckley et al., 1998). Subsequent *in vivo* tests in *mdx* mice showed that this approach produced a highly efficient restoration of dystrophin expression and improved muscle function, following local or systemic injection (Alter et al., 2006; Gebiski et al., 2003; Lu et al., 2003; Lu et al., 2005; Mann et al., 2001). Similarly, exon skipping (Fig. 5) has been achieved in cultured cDMD muscle cells and in CXMD<sub>1</sub> dogs by local and systemic delivery (McCloy et al., 2006; Walmsley et al., 2010; Yokota et al., 2009). Several clinical trials have been initiated based on the results of animal studies (Koo and Wood, 2013; Opar, 2012). Data from the Phase 1 and 2 trials are highly promising (Cirak et al., 2011; Goemans et al., 2011; Kinali et al., 2009; Mendell et al., 2013; van Deutekom et al., 2007). However, the expected efficacy remains to be confirmed in a Phase 3 study (Hoffman and McNally, 2014; Wood, 2013).

Early exon-skipping studies used AONs based on 2'-O-methylated phosphorothioate (2OMe-PS) or phosphorodiamidate morpholino oligomers (PMOs) (Box 1). An important limitation of these AONs is that they cannot reach the heart. To overcome this hurdle, a variety of conjugated PMOs have been developed (Aoki et al., 2012; Jearawiriyapaisarn et al., 2008; Wu et al., 2009; Wu et al., 2008; Yin et al., 2008; Yin et al., 2011). In these PMOs, oligonucleotides are covalently linked to a cell-penetrating peptide or an octa-guanidine dendrimer, which can enhance cell penetration (the octa-guanidine-modified PMO is called vivo-morpholino; see Box 1). Systemic delivery of conjugated AONs in *mdx* mice produced robust exon skipping in the heart and the restoration of cardiac function (Wu et al., 2008; Wu et al., 2011). Another drawback of AON therapy is the rapid turnover of the therapeutic

oligonucleotides. To solve this problem, investigators have begun to use the AAV vector to achieve persistent AON delivery *in vivo* in *mdx* mice (Denti et al., 2006; Goyenvalle et al., 2004). Recently, AAV-based exon skipping has been shown to significantly improve the dystrophic phenotype in utrophin/dystrophin *dco* mice and in GRMD dogs (Barbash et al., 2013; Bish et al., 2012; Goyenvalle et al., 2012; Le Guiner et al., 2014; Vulin et al., 2012).

*mdx* mice and GRMD dogs carry point mutations in the dystrophin gene. However, ~ 60% of DMD is due to deletions in exons 45-53 or duplications in exon 2 (Flanigan et al., 2009b). *mdx52* and *dup2* mice carry mutations that resemble the deletions and duplications in affected humans, respectively. Hence, they are excellent models for preclinical testing. Aoki et al. delivered a cocktail of ten *in vivo*-morpholino AONs to *mdx52* mice and achieved efficient multiple-exon skipping (exons 45-55) (Fig. 5) (Aoki et al., 2012). The resulting  $\Delta 45-55$  dystrophin transcript is highly protective and significantly improves muscle strength and histology without causing any toxicity (Aoki et al., 2012). The duplication of exon 2 is a more challenging error to correct because a complete skipping of exon 2 leads to an out-of-frame transcript. Wein et al. recently tested exon 2 skipping in the *dup2* model using an AAV-based exon-skipping system (Wein et al., 2014). The treatment generated a  $\Delta 2$  transcript with a premature stop codon in exon 3. Surprisingly, however, the dystrophic phenotype was significantly ameliorated. Further investigation suggests that the removal of exon 2 activates a downstream internal ribosome entry site in exon 5. Translation from this site yields a highly functional protein (Wein et al., 2014). The results of the Aoki et al. and Wein et al. studies are especially appealing because humans who carry similar transcripts are often asymptomatic (Ferreiro et al., 2009; Flanigan et al., 2009a; Nakamura et al., 2008). Therapies based on the same principle might therefore yield dramatic clinical improvement in boys with DMD.

#### Repair at the DNA level

Compared to exon skipping, approaches to correct the mutated dystrophin gene are less developed (Bertoni, 2014). Initial DNA-

repair strategies used oligonucleotides that are homologous to the target DNA. This approach has resulted in gene correction in *mdx* and *mdx<sup>scv</sup>* mice, and in one GRMD dog, but the efficiency was too low for clinical application (Bartlett et al., 2000; Kayali et al., 2010; Rando et al., 2000). Nuclease-based gene editing is a powerful technology to correct DNA defects (Box 1). Briefly, a nuclease is used as a pair of molecular scissors to cut DNA at the target site. When a double-strand DNA break is repaired by cellular mechanisms, insertions and/or deletions are introduced at the break point. Some of these modifications yield the wild-type sequence, hence gene correction. Four families of engineered nucleases have been recently developed, including meganuclease, zinc-finger nuclease, TALEN (transcription activator-like effector nuclease) and the CRISPR/Cas (clustered regularly interspaced short palindromic repeat/CRISPR-associated nuclease/helicase) system. These have all been explored for use in DMD therapy; however, the majority of the studies are currently limited to cultured cells (Chapdelaine et al., 2010; Long et al., 2014; Ousterout et al., 2014; Ousterout et al., 2013; Rousseau et al., 2011). Future studies are needed to validate these highly promising gene-editing strategies in animal models of DMD.

#### Gene therapy for cardiomyopathy and neuronal defects

Cardiomyopathy and neuronal defects are two other prominent clinical features of DMD. Gene therapy for the heart and central nervous system (CNS) requires special consideration (Anderson et al., 2002; Duan, 2006; Lai and Duan, 2012; Nardes et al., 2012; Ricotti et al., 2011; Shin et al., 2010; Snow et al., 2013) because these organs differ from skeletal muscle in their anatomy and physiology. Importantly, dystrophin deficiency produces a unique disease profile in the heart and CNS.

#### Duchenne cardiomyopathy gene therapy

The characteristic cardiac manifestation of DMD is dilated cardiomyopathy (Duan, 2006; Finsterer and Cripe, 2014). Heart damage is also a prominent phenotype in various strains of *dko* mice, including the utrophin/dystrophin *dko*,  $\alpha$ 7-integrin/dystrophin *dko*, myoD/dystrophin *dko* and mTR/dystrophin *dko* mice (Grady et al., 1997; Guo et al., 2006; Megency et al., 1999; Mourkioti et al., 2013) (supplementary material Table S1). However, aged female *mdx* mice are by far the best mouse models for studying Duchenne dilated cardiomyopathy because they are genetically and phenotypically identical to affected humans (Bostick et al., 2010; Bostick et al., 2008b).

Most Duchenne cardiomyopathy gene therapy studies have been conducted in the *mdx* model. Using dystrophin heterozygous mice, Duan and colleagues demonstrated that dystrophin expression in 50% of cardiomyocytes was sufficient to mitigate heart injury in *mdx* mice (Bostick et al., 2008b; Yue et al., 2004). The first cardiac gene therapy study was performed in neonatal *mdx* mice using an AAV-5  $\Delta$ R4-23/ $\Delta$ C microgene vector in our laboratory (Fig. 4B). This micro-dystrophin gene therapy restores the DAGC and increases the strength of the cardiomyocyte membrane (Yue et al., 2003). Subsequent studies using the same microgene normalized the electrocardiography (ECG) defects and improved cardiac hemodynamics in young and adult *mdx* mice (Bostick et al., 2008a; Schinkel et al., 2012; Shin et al., 2011b; Townsend et al., 2007). To further explore the therapeutic potential, Bostick et al. treated aged female *mdx* mice with an AAV-9  $\Delta$ R4-23/ $\Delta$ C microgene vector (Bostick et al., 2011; Bostick et al., 2012). They achieved efficient whole-heart gene transfer despite the presence of extensive myocardial fibrosis. In near-terminal-age mice (16-

20 months old), fibrosis was significantly reduced and hemodynamic performance significantly enhanced (Bostick et al., 2011). However, such improvements were not observed in terminal-age mice (>21 months old) (Bostick et al., 2012). The cardiac protection of the mini-dystrophin gene has only been examined using the 6-kb  $\Delta$ H2-R19 minigene in transgenic *mdx* mice (Fig. 4B) (Bostick et al., 2009). This minigene completely normalizes skeletal muscle force in transgenic *mdx* mice (Harper et al., 2002). However, it does not lead to a full recovery of heart function (Bostick et al., 2009).

Exon skipping has also been explored for treating *mdx* heart disease. The original 2OMe-PS and PMO AONs cannot reach the heart (Alter et al., 2006). However, conjugated PMOs developed in the Lu and Wood labs have significantly increased cardiac exon skipping and heart contractility in *mdx* mice (Wu et al., 2009; Wu et al., 2008; Wu et al., 2011; Yin et al., 2008; Yin et al., 2011). Recently, two groups tested AAV-based exon skipping in GRMD dogs. Sweeney and colleagues delivered the vector to the heart via fluoroscopy-guided trans-endocardial injection (Bish et al., 2012). This treatment restored dystrophin expression in the heart, reduced fibrosis and improved left ventricular function (Bish et al., 2012). Using X-ray-fused magnetic resonance, Barbash et al. have further improved the transendocardial gene-delivery method and achieved dystrophin expression in the GRMD heart (Barbash et al., 2013).

#### Correcting neuronal defects with gene therapy

About one-third of individuals with DMD display cognitive deficiency and other CNS symptoms (Anderson et al., 2002; D'Angelo and Bresolin, 2006; Nardes et al., 2012; Ricotti et al., 2011; Snow et al., 2013). Although all dystrophin isoforms have been detected in the nervous system (Lidov, 1996; Tozawa et al., 2012), only Dp140 and Dp71 have been implicated in neuronal abnormalities in humans with DMD (Bardoni et al., 2000; Bardoni et al., 1999; Daoud et al., 2009a; Daoud et al., 2009b; Felisari et al., 2000; Moizard et al., 1998; Moizard et al., 2000; Pane et al., 2012; Taylor et al., 2010). Among all DMD models, only *mdx<sup>scv</sup>* and *mdx  $\beta$ geo* mice do not express Dp140 and Dp70. Surprisingly, neurocognitive behaviors of *mdx<sup>scv</sup>* mice are only slightly different from those of *mdx* mice (Muntoni et al., 1991; Vaillend et al., 1998; Vaillend et al., 2004; Vaillend et al., 1995; Vaillend and Ungerer, 1999; Yamamoto et al., 2010). Dp71-specific knockout mice have also been generated and, interestingly, they show more severe learning impairment than *mdx* mice (Daoud et al., 2009b; Sarig et al., 1999). It is very likely that none of the existing mouse models can fully recapitulate the neurocognitive impairments of humans with DMD (D'Angelo and Bresolin, 2006). Nevertheless, most investigators have used *mdx* mice to dissect the molecular and cellular consequences of dystrophin deficiency in the brain. Collectively, these studies have revealed abnormalities in the hippocampus and in several other regions of the brain (Ghedini et al., 2012; Graciotti et al., 2008; Miranda et al., 2011; Miranda et al., 2009; Parames et al., 2014; Vaillend et al., 2004; Vaillend et al., 1999). So far, only exon skipping has been explored to treat CNS defects. Vaillend and colleagues injected an AAV exon-skipping vector to the *mdx* brain and found improvement of hippocampus function (Dall rac et al., 2011; Vaillend et al., 2010). Sekiguchi et al. ameliorated the abnormal freezing response (see Box 1) seen in *mdx* mice by injecting PMO AON to the ventricles of the brain (Sekiguchi et al., 2009). Utrophin has been considered as a highly promising replacement for dystrophin (see next section for details). Interestingly, a recent study suggested that utrophin upregulation in the brain might not rescue behavioral deficiency in *mdx* mice (Perronet et al., 2012).

Dystrophin-independent gene therapy for DMD: lessons from animal models

The striking phenotypic differences between dystrophin-deficient mice and affected humans have stimulated much interest in identifying the genes that modify DMD phenotypes. Compared with dystrophin-based therapy, the modulation of genes that already exist in the body has clear immunological advantages; the therapeutic expression of these genes is unlikely to induce immune rejection because they are considered as self (Ebihara et al., 2000).

Utrophin and  $\alpha 7\beta 1$ -integrin are among the most obvious candidates to consider because: (1) similarly to dystrophin, they strengthen the sarcolemma by cross-linking the ECM and the cytoskeleton; (2) their expression is upregulated in *mdx* mice; (3) genetic elimination of either gene aggravates dystrophic manifestations in *mdx* mice; and (4) overexpression of either gene ameliorates muscle disease in *mdx* mice (Burkin et al., 2005; Burkin et al., 2001; Deconinck et al., 1997a; Deconinck et al., 1997b; Grady et al., 1997; Guo et al., 2006; Rafael et al., 1998; Rooney et al., 2006; Tinsley et al., 1998; Tinsley et al., 1996). As a result, gene therapy studies have been conducted in dystrophic mice (and some dogs) using full-length utrophin (Deol et al., 2007), mini-utrophin (Cerletti et al., 2003; Gilbert et al., 1999; Wakefield et al., 2000), micro-utrophin (Odom et al., 2008) and  $\alpha 7$ -integrin (Heller et al., 2013). As predicted from knockout and transgenic experiments, the dystrophic phenotype was significantly reduced by utrophin or integrin gene therapy.

Myostatin inhibition is another example of dystrophin-independent therapy for DMD. Myostatin is an endogenous muscle-growth inhibitor (Lee, 2004; McPherron et al., 1997). Mutations in the myostatin gene cause hypermuscularity in mouse, cattle, sheep, dog and humans (Stinckens et al., 2011). Elimination of the myostatin gene protects *mdx* mice by reducing fibrosis and increasing muscle strength (Wagner et al., 2002). These observations provide compelling justification to explore myostatin inhibition gene therapy in animal models and, more recently, in BMD patients (Mendell et al., 2015; Rodino-Klapac et al., 2009).

Evidence from preclinical studies is opening up new lines of investigation concerning how other endogenous genes could be used in DMD gene therapy. These include genes encoding cytotoxic T-cell GalNAc transferase (Xu et al., 2007), nNOS (Lai et al., 2014), sarcoplasmic reticulum calcium ATPase 2a (Shin et al., 2011a), peroxisome proliferator-activated receptor gamma coactivator 1-alpha (Selsby et al., 2012) and sarcospan (Marshall et al., 2013).

#### Conclusions and perspective

Animal models have greatly enriched our understanding of the biological function of dystrophin and the pathology of DMD, providing excellent platforms for investigating the efficacy and toxicity of experimental gene therapies. Considerable progress has been made in model development in the last three decades. We now have a large (and still expanding) collection of animal models (supplementary material Table S1). Although this offers an unprecedented opportunity for cross-species comparison and translation (Poussin et al., 2014), it also adds complexity and difficulty in model selection for preclinical studies. The advantages and limitations of each model system can vary depending on the study question. Some aspects of the DMD pathology (such as neurocognitive deficiency) remain difficult to model. Furthermore, animals are not humans. The findings from animal studies may guide but not completely predict the outcome of clinical studies. Nevertheless, the value of animal models should never be underestimated. The development of an effective gene therapy for

DMD has relied heavily, and will continue to rely, on animal models (Duan, 2011). Animal studies not only establish the proof-of-principle, they are also crucial for protocol optimization before and during human tests. Certain studies that cannot be performed in affected individuals (such as necropsy, *in situ* and *ex vivo* single-muscle force measurement) will have to be carried out in animal models. The field has surmounted many obstacles in the development of DMD models. The mild *mdx* mice are now complemented by numerous background and mutation variants that can better mimic affected humans. However, as therapies that have been in development for the last decade enter clinical trials, new questions are emerging. Many of these new questions (such as the immune response to the AAV vector and scaling-up of systemic gene transfer) might be better answered with cDMD dogs, a model that remains to be fully characterized (Duan, 2011; Duan, 2015).

#### Acknowledgements

We thank Mitchell C. Tarka for help with the Fig. 1 illustration.

#### Competing interests

D.D. is a member of the scientific advisory board for Solid GT, a subsidiary of Solid Ventures.

#### Funding

DMD research in the Duan lab is supported by the National Institutes of Health (AR-49419, HL-91883), Department of Defense (MD-13), Muscular Dystrophy Association, Parent Project Muscular Dystrophy, Jesse's Journey-The Foundation for Gene and Cell Therapy, Hope for Javier, Kansas City Area Life Sciences Institute and the University of Missouri.

#### Supplementary material

Supplementary material available online at <http://dmm.biologists.org/lookup/suppl/doi:10.1242/dmm.018424/-DC1>

#### References

- Aartsma-Rus, A. (2012). Overview on DMD exon skipping. *Methods Mol. Biol.* **867**, 97-116.
- Aartsma-Rus, A., Van Deutekom, J. C., Fokkema, I. F., Van Ommen, G. J. and Den Dunnen, J. T. (2006). Entries in the Leiden Duchenne muscular dystrophy mutation database: an overview of mutation types and paradoxical cases that confirm the reading-frame rule. *Muscle Nerve* **34**, 135-144.
- AcSaudi, G., Dickson, G., Love, D. R., Jani, A., Walsh, F. S., Gurusinghe, A., Wolff, J. A. and Davies, K. E. (1991). Human dystrophin expression in *mdx* mice after intramuscular injection of DNA constructs. *Nature* **352**, 815-818.
- Ahn, A. H. and Kunkel, L. M. (1993). The structural and functional diversity of dystrophin. *Nat. Genet.* **3**, 283-291.
- Aigner, B., Rathkolb, B., Klafoten, M., Sedlmeier, R., Klempt, M., Wagner, S., Michel, D., Mayer, U., Klopstock, T., de Angelis, M. H. et al. (2009). Generation of N-ethyl-N-nitrosourea-induced mouse mutants with deviations in plasma enzyme activities as novel organ-specific disease models. *Exp. Physiol.* **94**, 412-421.
- Akkaraju, G. R., Huard, J., Hoffman, E. P., Goins, W. F., Pruchnic, R., Watkins, S. C., Cohen, J. B. and Glorioso, J. C. (1999). Herpes simplex virus vector-mediated dystrophin gene transfer and expression in *mdx* mouse skeletal muscle. *J. Gene Med.* **1**, 280-289.
- Alter, J., Lou, F., Rabinowitz, A., Yin, H., Rosenfeld, J., Wilton, S. D., Partridge, T. A. and Lu, Q. L. (2006). Systemic delivery of morpholino oligonucleotide restores dystrophin expression bodywide and improves dystrophic pathology. *Nat. Med.* **12**, 175-177.
- Ambrósio, C. E., Valadares, M. C., Zucconi, E., Cabral, R., Pearson, P. L., Gaiad, T. P., Canovas, M., Vainzof, M., Miglino, M. A. and Zatz, M. (2008). Ringo, a Golden Retriever Muscular Dystrophy (GRMD) dog with absent dystrophin but normal strength. *Neuromuscul. Disord.* **18**, 892-893.
- Anderson, J. L., Head, S. I., Rae, C. and Morley, J. W. (2002). Brain function in Duchenne muscular dystrophy. *Brain* **125**, 4-13.
- Aoki, Y., Yokota, T., Nagata, T., Nakamura, A., Tanihata, J., Saito, T., Duguez, S. M., Nagaraju, K., Hoffman, E. P., Partridge, T. et al. (2012). Bodywide skipping of exons 45-55 in dystrophic *mdx52* mice by systemic antisense delivery. *Proc. Natl. Acad. Sci. USA* **109**, 13763-13768.
- Ardite, E., Perdiguero, E., Vidal, B., Gutarra, S., Serrano, A. L. and Muñoz-Cánoves, P. (2012). PAI-1-regulated miR-21 defines a novel age-associated fibrogenic pathway in muscular dystrophy. *J. Cell Biol.* **196**, 163-175.
- Arpke, R. W., Darabi, R., Mader, T. L., Zhang, Y., Toyama, A., Lonetree, C. L., Nash, N., Lowe, D. A., Perlingeiro, R. C. and Kyba, M. (2013). A new immuno-, dystrophin-deficient model, the NSG-*mdx4cv* mouse, provides evidence for functional improvement following allogeneic satellite cell transplantation. *Stem Cells* **31**, 1611-1620.

- Ashwath, M. L., Jacobs, I. B., Crowe, C. A., Ashwath, R. C., Super, D. M. and Bahler, R. C. (2014). Left ventricular dysfunction in Duchenne muscular dystrophy and genotype. *Am. J. Cardiol.* **114**, 284-289.
- Atencia-Fernandez, S., Shiel, R. E., Mooney, C. T. and Nolan, C. M. (2015). Muscular dystrophy in the Japanese Spitz: an inversion disrupts the *DMD* and *RPGR* genes. *Anim. Genet.* [Epub ahead of print] doi: 10.1111/age.12266.
- Banks, G. B., Judge, L. M., Allen, J. M. and Chamberlain, J. S. (2010). The polyproline site in hinge 2 influences the functional capacity of truncated dystrophins. *PLoS Genet.* **6**, e1000958.
- Banks, G. B., Combs, A. C., Odum, G. L., Bloch, R. J. and Chamberlain, J. S. (2014). Muscle structure influences utrophin expression in mdx mice. *PLoS Genet.* **10**, e1004431.
- Barbash, I. M., Cecchini, S., Faranesh, A. Z., Virag, T., Li, L., Yang, Y., Hoyt, R. F., Kornegay, J. N., Bogan, J. R., Garcia, L. et al. (2013). MRI roadmap-guided transendocardial delivery of exon-skipping recombinant adeno-associated virus restores dystrophin expression in a canine model of Duchenne muscular dystrophy. *Gene Ther.* **20**, 274-282.
- Bardoni, A., Sironi, M., Felisari, G., Comi, G. P. and Bresolin, N. (1999). Absence of brain Dp140 isoform and cognitive impairment in Becker muscular dystrophy. *Lancet* **353**, 897-898.
- Bardoni, A., Felisari, G., Sironi, M., Comi, G., Lai, M., Robotti, M. and Bresolin, N. (2000). Loss of Dp140 regulatory sequences is associated with cognitive impairment in dystrophinopathies. *Neuromuscul. Disord.* **10**, 194-199.
- Bartlett, R. J., Stockinger, S., Denis, M. M., Bartlett, W. T., Inverardi, L., Le, T. T., thi Man, N., Morris, G. E., Bogan, D. J., Metcalf-Bogan, J. et al. (2000). In vivo targeted repair of a point mutation in the canine dystrophin gene by a chimeric RNA/DNA oligonucleotide. *Nat. Biotechnol.* **18**, 615-622.
- Beastrom, N., Lu, H., Macke, A., Canan, B. D., Johnson, E. K., Penton, C. M., Kaspar, B. K., Rodino-Klapac, L. R., Zhou, L., Janssen, P. M. et al. (2011). Mdx5cv mice manifest more severe muscle dysfunction and diaphragm force deficits than do mdx Mice. *Am. J. Pathol.* **179**, 2464-2474.
- Beggs, A. H., Hoffman, E. P., Snyder, J. R., Arahata, K., Specht, L., Shapiro, F., Angelini, C., Sugita, H. and Kunkel, L. M. (1991). Exploring the molecular basis for variability among patients with Becker muscular dystrophy: dystrophin gene and protein studies. *Am. J. Hum. Genet.* **49**, 54-67.
- Benzein, M., Negroni, E., Vallese, D., Yacoub-Youssef, H., Chaouch, S., Wolff, A., Aamiri, A., Di Santo, J. P., Chazaud, B., Butler-Browne, G. et al. (2012). Proinflammatory macrophages enhance the regenerative capacity of human myoblasts by modifying their kinetics of proliferation and differentiation. *Mol. Ther.* **20**, 2168-2179.
- Berger, J. and Currie, P. D. (2012). Zebrafish models flex their muscles to shed light on muscular dystrophies. *Dis. Model. Mech.* **5**, 726-732.
- Bertoni, C. (2014). Emerging gene editing strategies for Duchenne muscular dystrophy targeting stem cells. *Front. Physiol.* **5**, 148.
- Bish, L. T., Sleeper, M. M., Forbes, S. C., Wang, B., Reynolds, C., Singletary, G. E., Trafny, D., Morine, K. J., Sanmiguel, J., Cecchini, S. et al. (2012). Long-term restoration of cardiac dystrophin expression in golden retriever muscular dystrophy following rAAV6-mediated exon skipping. *Mol. Ther.* **20**, 580-589.
- Blake, D. J., Weir, A., Newey, S. E. and Davies, K. E. (2002). Function and genetics of dystrophin and dystrophin-related proteins in muscle. *Physiol. Rev.* **82**, 291-329.
- Bonilla, E., Samitt, C. E., Miranda, A. F., Hays, A. P., Salviati, G., DiMauro, S., Kunkel, L. M., Hoffman, E. P. and Rowland, L. P. (1988). Duchenne muscular dystrophy: deficiency of dystrophin at the muscle cell surface. *Cell* **54**, 447-452.
- Bostick, B., Ghosh, A., Yue, Y., Long, C. and Duan, D. (2007). Systemic AAV-9 transduction in mice is influenced by animal age but not by the route of administration. *Gene Ther.* **14**, 1605-1609.
- Bostick, B., Yue, Y., Lai, Y., Long, C., Li, D. and Duan, D. (2008a). Adeno-associated virus serotype-9 microdystrophin gene therapy ameliorates electrocardiographic abnormalities in mdx mice. *Hum. Gene Ther.* **19**, 851-856.
- Bostick, B., Yue, Y., Long, C. and Duan, D. (2008b). Prevention of dystrophin-deficient cardiomyopathy in twenty-one-month-old carrier mice by mosaic dystrophin expression or complementary dystrophin/utrophin expression. *Circ. Res.* **102**, 121-130.
- Bostick, B., Yue, Y., Long, C., Marschalk, N., Fine, D. M., Chen, J. and Duan, D. (2009). Cardiac expression of a mini-dystrophin that normalizes skeletal muscle force only partially restores heart function in aged mdx mice. *Mol. Ther.* **17**, 253-261.
- Bostick, B., Yue, Y. and Duan, D. (2010). Gender influences cardiac function in the mdx model of Duchenne cardiomyopathy. *Muscle Nerve* **42**, 600-603.
- Bostick, B., Shin, J.-H., Yue, Y. and Duan, D. (2011). AAV-microdystrophin therapy improves cardiac performance in aged female mdx mice. *Mol. Ther.* **19**, 1826-1832.
- Bostick, B., Shin, J. H., Yue, Y., Wasala, N. B., Lai, Y. and Duan, D. (2012). AAV micro-dystrophin gene therapy alleviates stress-induced cardiac death but not myocardial fibrosis in >21-m-old mdx mice, an end-stage model of Duchenne muscular dystrophy cardiomyopathy. *J. Mol. Cell. Cardiol.* **53**, 217-222.
- Braun, S. (2004). Naked plasmid DNA for the treatment of muscular dystrophy. *Curr. Opin. Mol. Ther.* **6**, 499-505.
- Bulfield, G., Siller, W. G., Wight, P. A. and Moore, K. J. (1984). X chromosome-linked muscular dystrophy (mdx) in the mouse. *Proc. Natl. Acad. Sci. USA* **81**, 1189-1192.
- Bulman, D. E., Murphy, E. G., Zubrzycka-Gaarn, E. E., Worton, R. G. and Ray, P. N. (1991). Differentiation of Duchenne and Becker muscular dystrophy phenotypes with amino- and carboxy-terminal antisera specific for dystrophin. *Am. J. Hum. Genet.* **48**, 295-304.
- Burkin, D. J., Wallace, G. Q., Nicol, K. J., Kaufman, D. J. and Kaufman, S. J. (2001). Enhanced expression of the alpha 7 beta 1 integrin reduces muscular dystrophy and restores viability in dystrophic mice. *J. Cell Biol.* **152**, 1207-1218.
- Burkin, D. J., Wallace, G. Q., Milner, D. J., Chaney, E. J., Mulligan, J. A. and Kaufman, S. J. (2005). Transgenic expression of alpha7beta1 integrin maintains muscle integrity, increases regenerative capacity, promotes hypertrophy, and reduces cardiomyopathy in dystrophic mice. *Am. J. Pathol.* **166**, 253-263.
- Bushby, K. and Connor, E. (2011). Clinical outcome measures for trials in Duchenne muscular dystrophy: report from International Working Group meetings. *Clin. Investig. (Lond)* **1**, 1217-1235.
- Byers, T. J., Neumann, P. E., Beggs, A. H. and Kunkel, L. M. (1992). ELISA quantitation of dystrophin for the diagnosis of Duchenne and Becker muscular dystrophies. *Neurology* **42**, 570-576.
- Cerletti, M., Negri, T., Cozzi, F., Colpo, R., Andreatta, F., Croci, D., Davies, K. E., Cornelio, F., Pozza, O., Karpati, G. et al. (2003). Dystrophic phenotype of canine X-linked muscular dystrophy is mitigated by adenovirus-mediated utrophin gene transfer. *Gene Ther.* **10**, 750-757.
- Chamberlain, J. S. (2002). Gene therapy of muscular dystrophy. *Hum. Mol. Genet.* **11**, 2355-2362.
- Chamberlain, J. S. and Benian, G. M. (2000). Muscular dystrophy: the worm turns to genetic disease. *Curr. Biol.* **10**, R795-R797.
- Chamberlain, J. S., Metzger, J., Reyes, M., Townsend, D. and Faulkner, J. A. (2007). Dystrophin-deficient mdx mice display a reduced life span and are susceptible to spontaneous rhabdomyosarcoma. *FASEB J.* **21**, 2195-2204.
- Chandrasekharan, K., Yoon, J. H., Xu, Y., deVries, S., Camboni, M., Janssen, P. M., Varki, A. and Martin, P. T. (2010). A human-specific deletion in mouse Cmah increases disease severity in the mdx model of Duchenne muscular dystrophy. *Sci. Transl. Med.* **2**, 42ra54.
- Chapdelaine, P., Pichavant, C., Rousseau, J., Pâques, F. and Tremblay, J. P. (2010). Meganucleases can restore the reading frame of a mutated dystrophin. *Gene Ther.* **17**, 846-858.
- Chapman, V. M., Miller, D. R., Armstrong, D. and Caskey, C. T. (1989). Recovery of induced mutations for X chromosome-linked muscular dystrophy in mice. *Proc. Natl. Acad. Sci. USA* **86**, 1292-1296.
- Cirak, S., Arechavala-Gomez, V., Guglieri, M., Feng, L., Torelli, S., Anthony, K., Abbs, S., Garralda, M. E., Bourke, J., Wells, D. J. et al. (2011). Exon skipping and dystrophin restoration in patients with Duchenne muscular dystrophy after systemic phosphorodiamidate morpholino oligomer treatment: an open-label, phase 2, dose-escalation study. *Lancet* **378**, 595-605.
- Clemens, P. R., Kochanek, S., Sunada, Y., Chan, S., Chen, H. H., Campbell, K. P. and Caskey, C. T. (1996). In vivo muscle gene transfer of full-length dystrophin using an adenoviral vector that lacks all viral genes. *Gene Ther.* **3**, 965-972.
- Cooper, B. J., Valentine, B. A., Wilson, S., Patterson, D. F. and Concannon, P. W. (1988a). Canine muscular dystrophy: confirmation of X-linked inheritance. *J. Hered.* **79**, 405-408.
- Cooper, B. J., Winand, N. J., Stedman, H., Valentine, B. A., Hoffman, E. P., Kunkel, L. M., Scott, M. O., Fischbeck, K. H., Kornegay, J. N., Avery, R. J. et al. (1988b). The homologue of the Duchenne locus is defective in X-linked muscular dystrophy of dogs. *Nature* **334**, 154-156.
- Cooper, B. J., Gallagher, E. A., Smith, C. A., Valentine, B. A. and Winand, N. J. (1990). Mosaic expression of dystrophin in carriers of canine X-linked muscular dystrophy. *Lab. Invest.* **62**, 171-178.
- Cotten, S. W., Kornegay, J. N., Bogan, D. J., Wadosky, K. M., Patterson, C. and Willis, M. S. (2013). Genetic myostatin decrease in the golden retriever muscular dystrophy model does not significantly affect the ubiquitin proteasome system despite enhancing the severity of disease. *Am. J. Transl. Res.* **6**, 43-53.
- Cox, G. A., Cole, N. M., Matsumura, K., Phelps, S. F., Hauschka, S. D., Campbell, K. P., Faulkner, J. A. and Chamberlain, J. S. (1993a). Overexpression of dystrophin in transgenic mdx mice eliminates dystrophic symptoms without toxicity. *Nature* **364**, 725-729.
- Cox, G. A., Phelps, S. F., Chapman, V. M. and Chamberlain, J. S. (1993b). New mdx mutation disrupts expression of muscle and nonmuscle isoforms of dystrophin. *Nat. Genet.* **4**, 87-93.
- Cox, G. A., Sunada, Y., Campbell, K. P. and Chamberlain, J. S. (1994). Dp71 can restore the dystrophin-associated glycoprotein complex in muscle but fails to prevent dystrophy. *Nat. Genet.* **8**, 333-339.
- Cozzi, F., Cerletti, M., Luvoni, G. C., Lombardo, R., Brambilla, P. G., Faverzani, S., Blasevich, F., Cornelio, F., Pozza, O. and Mora, M. (2001). Development of muscle pathology in canine X-linked muscular dystrophy. II. Quantitative characterization of histopathological progression during postnatal skeletal muscle development. *Acta Neuropathol.* **101**, 469-478.
- Crawford, G. E., Faulkner, J. A., Crosbie, R. H., Campbell, K. P., Froehner, S. C. and Chamberlain, J. S. (2000). Assembly of the dystrophin-associated protein complex does not require the dystrophin COOH-terminal domain. *J. Cell Biol.* **150**, 1399-1410.
- Crisp, A., Yin, H., Goyenville, A., Betts, C., Moulton, H. M., Seow, Y., Babbs, A., Merritt, T., Saleh, A. F., Gait, M. J. et al. (2011). Diaphragm rescue alone prevents heart dysfunction in dystrophic mice. *Hum. Mol. Genet.* **20**, 413-421.
- D'Angelo, M. G. and Bresolin, N. (2006). Cognitive impairment in neuromuscular disorders. *Muscle Nerve* **34**, 16-33.
- Dall'érac, G., Perronnet, C., Chagneau, C., Leblanc-Veyrac, P., Samson-Desvignes, N., Peltekian, E., Danos, O., Garcia, L., Laroche, S., Billard, J. M. et al. (2011). Rescue of a dystrophin-like protein by exon skipping normalizes synaptic plasticity in the hippocampus of the mdx mouse. *Neurobiol. Dis.* **43**, 635-641.
- Danko, I., Chapman, V. and Wolff, J. A. (1992). The frequency of revertants in mdx mouse genetic models for Duchenne muscular dystrophy. *Pediatr. Res.* **32**, 128-131.
- Daoud, F., Angeard, N., Demerre, B., Martie, I., Benyau, R., Leturcq, F., Cossée, M., Deburgrave, N., Saillour, Y., Tuffery, S. et al. (2009a). Analysis of Dp71

- contribution in the severity of mental retardation through comparison of Duchenne and Becker patients differing by mutation consequences on Dp71 expression. *Hum. Mol. Genet.* **18**, 3779-3794.
- Daoud, F., Candelario-Martínez, A., Billard, J. M., Avital, A., Khelifaoui, M., Rozenvald, Y., Guegan, M., Mornet, D., Jaillard, D., Nudel, U. et al. (2009b). Role of mental retardation-associated dystrophin-gene product Dp71 in excitatory synapse organization, synaptic plasticity and behavioral functions. *PLoS ONE* **4**, e6574.
- Decary, S., Hamida, C. B., Mouly, V., Barbet, J. P., Hentati, F. and Butler-Browne, G. S. (2000). Shorter telomeres in dystrophic muscle consistent with extensive regeneration in young children. *Neuromuscul. Disord.* **10**, 113-120.
- Deconinck, A. E., Rafael, J. A., Skinner, J. A., Brown, S. C., Potter, A. C., Metzinger, L., Watt, D. J., Dickson, J. G., Tinsley, J. M. and Davies, K. E. (1997a). Utrophin-dystrophin-deficient mice as a model for Duchenne muscular dystrophy. *Cell* **90**, 717-727.
- Deconinck, N., Tinsley, J., De Backer, F., Fisher, R., Kahn, D., Phelps, S., Davies, K. and Gillis, J. M. (1997b). Expression of truncated utrophin leads to major functional improvements in dystrophin-deficient muscles of mice. *Nat. Med.* **3**, 1216-1221.
- DelloRusso, C., Scott, J. M., Hartigan-O'Connor, D., Salvatori, G., Barjot, C., Robinson, A. S., Crawford, R. W., Brooks, S. V. and Chamberlain, J. S. (2002). Functional correction of adult mdx mouse muscle using gutted adenoviral vectors expressing full-length dystrophin. *Proc. Natl. Acad. Sci. USA* **99**, 12979-12984.
- Denti, M. A., Rosa, A., D'Antona, G., Sthandier, O., De Angelis, F. G., Nicoletti, C., Allocca, M., Pansarasa, O., Parente, V., Musaro, A. et al. (2006). Body-wide gene therapy of Duchenne muscular dystrophy in the mdx mouse model. *Proc. Natl. Acad. Sci. USA* **103**, 3758-3763.
- Deol, J. R., Danialou, G., Laroche, N., Bourget, M., Moon, J. S., Liu, A. B., Gilbert, R., Petrof, B. J., Nalbantoglu, J. and Karpati, G. (2007). Successful compensation for dystrophin deficiency by a helper-dependent adenovirus expressing full-length utrophin. *Mol. Ther.* **15**, 1767-1774.
- Desguerre, I., Christov, C., Mayer, M., Zeller, R., Becane, H. M., Bastuji-Garin, S., Leturcq, F., Chiron, C., Chelly, J. and Gherardi, R. K. (2009). Clinical heterogeneity of duchenne muscular dystrophy (DMD): definition of sub-phenotypes and predictive criteria by long-term follow-up. *PLoS ONE* **4**, e4347.
- Duan, D. (2006). Challenges and opportunities in dystrophin-deficient cardiomyopathy gene therapy. *Hum. Mol. Genet.* **15**, R253-R261.
- Duan, D. (2008). Myodys, a full-length dystrophin plasmid vector for Duchenne and Becker muscular dystrophy gene therapy. *Curr. Opin. Mol. Ther.* **10**, 86-94.
- Duan, D. (2011). Duchenne muscular dystrophy gene therapy: lost in translation? *Res. Rep. Biol.* **2011**, 31-42.
- Duan, D. (2015). Duchenne muscular dystrophy gene therapy in the canine model. *Hum. Gene Ther. Clin. Dev.* [Epub ahead of print] doi:10.1089/hum.2015.006.
- Duan, D., Hakim, C. H., Ambrosio, C. E., Smith, B. F. and Sweeney, H. L. (2015). Early loss of ambulation is not a representative clinical feature in Duchenne muscular dystrophy dogs: remarks on the article of Barthélémy et al. *Dis. Model. Mech.* **8**, 193-194.
- Dubowitz, V. (2006). Enigmatic conflict of clinical and molecular diagnosis in Duchenne/Becker muscular dystrophy. *Neuromuscul. Disord.* **16**, 865-866.
- Dunckley, M. G., Wells, D. J., Walsh, F. S. and Dickson, G. (1993). Direct retroviral-mediated transfer of a dystrophin minigene into mdx mouse muscle in vivo. *Hum. Mol. Genet.* **2**, 717-723.
- Dunckley, M. G., Manoharan, M., Villiet, P., Eperon, I. C. and Dickson, G. (1998). Modification of splicing in the dystrophin gene in cultured mdx muscle cells by antisense oligonucleotides. *Hum. Mol. Genet.* **7**, 1083-1090.
- Ebihara, S., Guibinga, G. H., Gilbert, R., Nalbantoglu, J., Massie, B., Karpati, G. and Petrof, B. J. (2000). Differential effects of dystrophin and utrophin gene transfer in immunocompetent muscular dystrophy (mdx) mice. *Physiol. Genomics* **3**, 133-144.
- Emery, A. E. H. and Muntoni, F. (2003). Duchenne muscular dystrophy. Oxford; New York, NY: Oxford University Press.
- England, S. B., Nicholson, L. V., Johnson, M. A., Forrest, S. M., Love, D. R., Zubrzycka-Gaarn, E. E., Bulman, D. E., Harris, J. B. and Davies, K. E. (1990). Very mild muscular dystrophy associated with the deletion of 46% of dystrophin. *Nature* **343**, 180-182.
- Ervasti, J. M. (2007). Dystrophin, its interactions with other proteins, and implications for muscular dystrophy. *Biochim. Biophys. Acta* **1772**, 108-117.
- Fan, Z., Wang, J., Ahn, M., Shiloh-Malawsky, Y., Chahin, N., Elmore, S., Bagnell, C. R., Jr, Wilber, K., An, H., Lin, W. et al. (2014). Characteristics of magnetic resonance imaging biomarkers in a natural history study of golden retriever muscular dystrophy. *Neuromuscul. Disord.* **24**, 178-191.
- Farini, A., Meregalli, M., Belicchi, M., Battistelli, M., Parolini, D., D'Antona, G., Gavina, M., Ottoboni, L., Constantin, G., Bottinelli, R. et al. (2007). T and B lymphocyte depletion has a marked effect on the fibrosis of dystrophic skeletal muscles in the scid/mdx mouse. *J. Pathol.* **213**, 229-238.
- Felisari, G., Martinelli Boneschi, F., Bardoni, A., Sironi, M., Comi, G. P., Robotti, M., Turconi, A. C., Lai, M., Corrao, G. and Bresolin, N. (2000). Loss of Dp140 dystrophin isoform and intellectual impairment in Duchenne dystrophy. *Neurology* **55**, 559-564.
- Ferreiro, V., Gilbert, F., Muñoz, G. M., Francipane, L., Marzese, D. M., Mampel, A., Roqué, M., Frechtel, G. D. and Szijan, I. (2009). Asymptomatic Becker muscular dystrophy in a family with a multiexon deletion. *Muscle Nerve* **39**, 239-243.
- Fine, D. M., Shin, J. H., Yue, Y., Volkman, D., Leach, S. B., Smith, B. F., McIntosh, M. and Duan, D. (2011). Age-matched comparison reveals early electrocardiography and echocardiography changes in dystrophin-deficient dogs. *Neuromuscul. Disord.* **21**, 453-461.
- Finsterer, J. and Cripe, L. (2014). Treatment of dystrophin cardiomyopathies. *Nat. Rev. Cardiol.* **11**, 168-179.
- Flanigan, K. M., Dunn, D. M., von Niederhausern, A., Howard, M. T., Mendell, J., Connolly, A., Saunders, C., Modrcin, A., Dasouki, M., Comi, G. P. et al. (2009a). DMD Trp3X nonsense mutation associated with a founder effect in North American families with mild Becker muscular dystrophy. *Neuromuscul. Disord.* **19**, 743-748.
- Flanigan, K. M., Dunn, D. M., von Niederhausern, A., Soltanzadeh, P., Gappmaier, E., Howard, M. T., Sampson, J. B., Mendell, J. R., Wall, C., King, W. M. et al.; United Dystrophinopathy Project Consortium (2009b). Mutational spectrum of DMD mutations in dystrophinopathy patients: application of modern diagnostic techniques to a large cohort. *Hum. Mutat.* **30**, 1657-1666.
- Foster, H., Sharp, P. S., Athanasopoulos, T., Trollet, C., Graham, I. R., Foster, K., Wells, D. J. and Dickson, G. (2008). Codon and mRNA sequence optimization of microdystrophin transgenes improves expression and physiological outcome in dystrophic mdx mice following AAV2/8 gene transfer. *Mol. Ther.* **16**, 1825-1832.
- Fujimoto, T., Itoh, K., Yaoi, T. and Fushiki, S. (2014). Somatodendritic and excitatory postsynaptic distribution of neuron-type dystrophin isoform, Dp40, in hippocampal neurons. *Biochem. Biophys. Res. Commun.* **452**, 79-84.
- Fukada, S., Morikawa, D., Yamamoto, Y., Yoshida, T., Sumie, N., Yamaguchi, M., Ito, T., Miyagoe-Suzuki, Y., Takeda, S., Tsujikawa, K. et al. (2010). Genetic background affects properties of satellite cells and mdx phenotypes. *Am. J. Pathol.* **176**, 2414-2424.
- Funkquist, B., Haraldsson, I. and Stahre, L. (1980). Primary progressive muscular dystrophy in the dog. *Vet. Rec.* **106**, 341-343.
- Gaedigk, R., Law, D. J., Fitzgerald-Gustafson, K. M., McNulty, S. G., Nsumu, N. N., Modrcin, A. C., Rinaldi, R. J., Pinson, D., Fowler, S. C., Bilgen, M. et al. (2006). Improvement in survival and muscle function in an mdx/utrn(-/-) double mutant mouse using a human retinal dystrophin transgene. *Neuromuscul. Disord.* **16**, 192-203.
- Gao, G. P., Alvira, M. R., Wang, L., Calcedo, R., Johnston, J. and Wilson, J. M. (2002). Novel adeno-associated viruses from rhesus monkeys as vectors for human gene therapy. *Proc. Natl. Acad. Sci. USA* **99**, 11854-11859.
- Gawlik, K. I., Holmberg, J. and Durbeej, M. (2014). Loss of dystrophin and  $\beta$ -sarcoglycan significantly exacerbates the phenotype of laminin  $\alpha$ 2 chain-deficient animals. *Am. J. Pathol.* **184**, 740-752.
- Gebski, B. L., Mann, C. J., Fletcher, S. and Wilton, S. D. (2003). Morpholino antisense oligonucleotide induced dystrophin exon 23 skipping in mdx mouse muscle. *Hum. Mol. Genet.* **12**, 1801-1811.
- Ghedini, P. C., Avellar, M. C., De Lima, T. C., Lima-Landman, M. T., Lapa, A. J. and Souccar, C. (2012). Quantitative changes of nicotinic receptors in the hippocampus of dystrophin-deficient mice. *Brain Res.* **1483**, 96-104.
- Ghosh, A., Yue, Y., Lai, Y. and Duan, D. (2008). A hybrid vector system expands adeno-associated viral vector packaging capacity in a transgene-independent manner. *Mol. Ther.* **16**, 124-130.
- Gilbert, R., Nalbantoglu, J., Petrof, B. J., Ebihara, S., Guibinga, G. H., Tinsley, J. M., Kamen, A., Massie, B., Davies, K. E. and Karpati, G. (1999). Adenovirus-mediated utrophin gene transfer mitigates the dystrophic phenotype of mdx mouse muscles. *Hum. Gene Ther.* **10**, 1299-1310.
- Goemans, N. M., Tulinus, M., van den Akker, J. T., Burm, B. E., Ekhardt, P. F., Heuvelmans, N., Holling, T., Janson, A. A., Platenburg, G. J., Sipkens, J. A. et al. (2011). Systemic administration of PRO051 in Duchenne's muscular dystrophy. *N. Engl. J. Med.* **364**, 1513-1522.
- Goyenvalle, A., Vulin, A., Fougereuse, F., Leturcq, F., Kaplan, J. C., Garcia, L. and Danos, O. (2004). Rescue of dystrophic muscle through U7 snRNA-mediated exon skipping. *Science* **306**, 1796-1799.
- Goyenvalle, A., Seto, J. T., Davies, K. E. and Chamberlain, J. (2011). Therapeutic approaches to muscular dystrophy. *Hum. Mol. Genet.* **20**, R69-R78.
- Goyenvalle, A., Babbs, A., Wright, J., Wilkins, V., Powell, D., Garcia, L. and Davies, K. E. (2012). Rescue of severely affected dystrophin/utrophin-deficient mice through scAAV-U7snRNA-mediated exon skipping. *Hum. Mol. Genet.* **21**, 2559-2571.
- Graciotti, L., Minelli, A., Minciacchi, D., Procopio, A. and Fulgenzi, G. (2008). GABAergic miniature spontaneous activity is increased in the CA1 hippocampal region of dystrophic mdx mice. *Neuromuscul. Disord.* **18**, 220-226.
- Grady, R. M., Teng, H., Nichol, M. C., Cunningham, J. C., Wilkinson, R. S. and Sanes, J. R. (1997). Skeletal and cardiac myopathies in mice lacking utrophin and dystrophin: a model for Duchenne muscular dystrophy. *Cell* **90**, 729-738.
- Grady, R. M., Grange, R. W., Lau, K. S., Maimone, M. M., Nichol, M. C., Stull, J. T. and Sanes, J. R. (1999). Role for alpha-dystrobrevin in the pathogenesis of dystrophin-dependent muscular dystrophies. *Nat. Cell Biol.* **1**, 215-220.
- Greenberg, D. S., Sunada, Y., Campbell, K. P., Yaffe, D. and Nudel, U. (1994). Exogenous Dp71 restores the levels of dystrophin associated proteins but does not alleviate muscle damage in mdx mice. *Nat. Genet.* **8**, 340-344.
- Gregorevic, P., Blankinship, M. J., Allen, J. M., Crawford, R. W., Meuse, L., Miller, D. G., Russell, D. W. and Chamberlain, J. S. (2004). Systemic delivery of genes to striated muscles using adeno-associated viral vectors. *Mol. Med.* **10**, 828-834.
- Gregorevic, P., Allen, J. M., Minami, E., Blankinship, M. J., Haraguchi, M., Meuse, L., Finn, E., Adams, M. E., Froehner, S. C., Murry, C. E. et al. (2006). rAAV6-microdystrophin preserves muscle function and extends lifespan in severely dystrophic mice. *Nat. Med.* **12**, 787-789.
- Guo, C., Willem, M., Werner, A., Raivich, G., Emerson, M., Neyses, L. and Mayer, U. (2006). Absence of alpha 7 integrin in dystrophin-deficient mice causes a myopathy similar to Duchenne muscular dystrophy. *Hum. Mol. Genet.* **15**, 989-998.

- Haecker, S. E., Stedman, H. H., Balice-Gordon, R. J., Smith, D. B., Grellish, J. P., Mitchell, M. A., Wells, A., Sweeney, H. L. and Wilson, J. M. (1996). In vivo expression of full-length human dystrophin from adenoviral vectors deleted of all viral genes. *Hum. Gene Ther.* **7**, 1907-1914.
- Hakim, C. H. and Duan, D. (2013). Truncated dystrophins reduce muscle stiffness in the extensor digitorum longus muscle of mdx mice. *J. Appl. Physiol.* **114**, 482-489.
- Hakim, C. H., Grange, R. W. and Duan, D. (2011). The passive mechanical properties of the extensor digitorum longus muscle are compromised in 2- to 20-month-old mdx mice. *J. Appl. Physiol.* **110**, 1656-1663.
- Hakim, C. H., Yue, Y., Shin, J. H., Williams, R. R., Zhang, K., Smith, B. F. and Duan, D. (2014). Systemic gene transfer reveals distinctive muscle transduction profile of tyrosine mutant AAV-1, -6, and -9 in neonatal dogs. *Mol. Ther. Methods Clin. Dev.* **1**, 14002.
- Han, R., Rader, E. P., Levy, J. R., Bansal, D. and Campbell, K. P. (2011). Dystrophin deficiency exacerbates skeletal muscle pathology in dysferlin-null mice. *Skelet. Muscle* **1**, 35.
- Harper, S. Q. (2013). Molecular dissection of dystrophin identifies the docking site for nNOS. *Proc. Natl. Acad. Sci. USA* **110**, 387-388.
- Harper, S. Q., Hauser, M. A., DelloRusso, C., Duan, D., Crawford, R. W., Phelps, S. F., Harper, H. A., Robinson, A. S., Engelhardt, J. F., Brooks, S. V. et al. (2002). Modular flexibility of dystrophin: implications for gene therapy of Duchenne muscular dystrophy. *Nat. Med.* **8**, 253-261.
- Hattori, N., Kaido, M., Nishigaki, T., Inui, K., Fujimura, H., Nishimura, T., Naka, T. and Hazama, T. (1999). Undetectable dystrophin can still result in a relatively benign phenotype of dystrophinopathy. *Neuromuscul. Disord.* **9**, 220-226.
- Hedlund, M., Tangvoranuntakul, P., Takematsu, H., Long, J. M., Housley, G. D., Kozutsumi, Y., Suzuki, A., Wynshaw-Boris, A., Ryan, A. F., Gallo, R. L. et al. (2007). N-glycolylneuraminic acid deficiency in mice: implications for human biology and evolution. *Mol. Cell. Biol.* **27**, 4340-4346.
- Heller, K. N., Montgomery, C. L., Janssen, P. M., Clark, K. R., Mendell, J. R. and Rodino-Klapac, L. R. (2013). AAV-mediated overexpression of human  $\alpha 7$  integrin leads to histological and functional improvement in dystrophic mice. *Mol. Ther.* **21**, 520-525.
- Henricson, E. K., Abresch, R. T., Cnaan, A., Hu, F., Duong, T., Arrieta, A., Han, J., Escobar, D. M., Florence, J. M., Clemens, P. R. et al.; CINRG Investigators (2013). The cooperative international neuromuscular research group Duchenne natural history study: glucocorticoid treatment preserves clinically meaningful functional milestones and reduces rate of disease progression as measured by manual muscle testing and other commonly used clinical trial outcome measures. *Muscle Nerve* **48**, 55-67.
- Hoffman, E. P. and Gorospe, J. R. M. (1991). The animal models of Duchenne muscular dystrophy: windows on the pathophysiological consequences of dystrophin deficiency. *Curr. Top. Membr.* **38**, 113-154.
- Hoffman, E. P. and Kunkel, L. M. (1989). Dystrophin abnormalities in Duchenne/Becker muscular dystrophy. *Neuron* **2**, 1019-1029.
- Hoffman, E. P. and McNally, E. M. (2014). Exon-skipping therapy: a roadblock, detour, or bump in the road? *Sci. Transl. Med.* **6**, 230fs14.
- Hoffman, E. P., Brown, R. H., Jr and Kunkel, L. M. (1987). Dystrophin: the protein product of the Duchenne muscular dystrophy locus. *Cell* **51**, 919-928.
- Hoffman, E. P., Kunkel, L. M., Angelini, C., Clarke, A., Johnson, M. and Harris, J. B. (1989). Improved diagnosis of Becker muscular dystrophy by dystrophin testing. *Neurology* **39**, 1011-1017.
- Hollinger, K., Yang, C. X., Montz, R. E., Nonneman, D., Ross, J. W. and Selsby, J. T. (2014). Dystrophin insufficiency causes selective muscle histopathology and loss of dystrophin-glycoprotein complex assembly in pig skeletal muscle. *FASEB J.* **28**, 1600-1609.
- Hosur, V., Kavirayani, A., Riefler, J., Carney, L. M., Lyons, B., Gott, B., Cox, G. A. and Shultz, L. D. (2012). Dystrophin and dysferlin double mutant mice: a novel model for rhabdomyosarcoma. *Cancer Genet* **205**, 232-241.
- Howell, J. M., Lochmüller, H., O'Hara, A., Fletcher, S., Kakulas, B. A., Massie, B., Nalbantoglu, J. and Karpati, G. (1998). High-level dystrophin expression after adenovirus-mediated dystrophin minigene transfer to skeletal muscle of dystrophic dogs: prolongation of expression with immunosuppression. *Hum. Gene Ther.* **9**, 629-634.
- Huang, X., Poy, F., Zhang, R., Joachimiak, A., Sudol, M. and Eck, M. J. (2000). Structure of a WW domain containing fragment of dystrophin in complex with beta-dystroglycan. *Nat. Struct. Biol.* **7**, 634-638.
- Im, W. B., Phelps, S. F., Copen, E. H., Adams, E. G., Slightom, J. L. and Chamberlain, J. S. (1996). Differential expression of dystrophin isoforms in strains of mdx mice with different mutations. *Hum. Mol. Genet.* **5**, 1149-1153.
- Innes, J. R. (1951). Myopathies in animals; a record of some cases including progressive muscular dystrophy (pseudo-hypertrophic) (dog), "weisses Fleisch" (lamb), neuropathic muscular atrophy (sheep) and lymphocytic/histiocytic myositis, neuritis, radiculitis (dog). *Br. Vet. J.* **107**, 131-143.
- Ishizaki, M., Maeda, Y., Kawano, R., Suga, T., Uchida, Y., Uchino, K., Yamashita, S., Kimura, E. and Uchino, M. (2011). Rescue from respiratory dysfunction by transduction of full-length dystrophin to diaphragm via the peritoneal cavity in utrophin/dystrophin double knockout mice. *Mol. Ther.* **19**, 1230-1235.
- Jearawiriyapaisarn, N., Moulton, H. M., Buckley, B., Roberts, J., Sazani, P., Fucharoen, S., Iversen, P. L. and Kole, R. (2008). Sustained dystrophin expression induced by peptide-conjugated morpholino oligomers in the muscles of mdx mice. *Mol. Ther.* **16**, 1624-1629.
- Judge, L. M., Haraguchin, M. and Chamberlain, J. S. (2006). Dissecting the signaling and mechanical functions of the dystrophin-glycoprotein complex. *J. Cell Sci.* **119**, 1537-1546.
- Judge, L. M., Arnett, A. L., Banks, G. B. and Chamberlain, J. S. (2011). Expression of the dystrophin isoform Dp116 preserves functional muscle mass and extends lifespan without preventing dystrophy in severely dystrophic mice. *Hum. Mol. Genet.* **20**, 4978-4990.
- Kawano, R., Ishizaki, M., Maeda, Y., Uchida, Y., Kimura, E. and Uchino, M. (2008). Transduction of full-length dystrophin to multiple skeletal muscles improves motor performance and life span in utrophin/dystrophin double knockout mice. *Mol. Ther.* **16**, 825-831.
- Kayali, R., Bury, F., Ballard, M. and Bertoni, C. (2010). Site-directed gene repair of the dystrophin gene mediated by PNA-ssODNs. *Hum. Mol. Genet.* **19**, 3266-3281.
- Kindall, M., Arechavala-Gomez, V., Feng, L., Cirak, S., Hunt, D., Adkin, C., Guglieri, M., Ashton, E., Abbs, S., Nihoyannopoulos, P. et al. (2009). Local restoration of dystrophin expression with the morpholino oligomer AVI-4658 in Duchenne muscular dystrophy: a single-blind, placebo-controlled, dose-escalation, proof-of-concept study. *Lancet Neurol.* **8**, 918-928.
- Klymiuk, N., Blutke, A., Graf, A., Krause, S., Burkhardt, K., Wuensch, A., Krebs, S., Kessler, B., Zakhartchenko, V., Kurome, M. et al. (2013). Dystrophin-deficient pigs provide new insights into the hierarchy of physiological derangements of dystrophic muscle. *Hum. Mol. Genet.* **22**, 4368-4382.
- Kochanek, S., Clemens, P. R., Mitani, K., Chen, H. H., Chan, S. and Caskey, C. T. (1996). A new adenoviral vector: Replacement of all viral coding sequences with 28 kb of DNA independently expressing both full-length dystrophin and beta-galactosidase. *Proc. Natl. Acad. Sci. USA* **93**, 5731-5736.
- Koenig, M., Hoffman, E. P., Bertelson, C. J., Monaco, A. P., Feener, C. and Kunkel, L. M. (1987). Complete cloning of the Duchenne muscular dystrophy (DMD) cDNA and preliminary genomic organization of the DMD gene in normal and affected individuals. *Cell* **50**, 509-517.
- Konieczny, P., Swiderski, K. and Chamberlain, J. S. (2013). Gene and cell-mediated therapies for muscular dystrophy. *Muscle Nerve* **47**, 649-663.
- Koo, T. and Wood, M. J. (2013). Clinical trials using antisense oligonucleotides in Duchenne muscular dystrophy. *Hum. Gene Ther.* **24**, 479-488.
- Koo, T., Malerba, A., Athanasopoulos, T., Trollet, C., Boldrin, L., Ferry, A., Popplewell, L., Foster, H., Foster, K. and Dickson, G. (2011a). Delivery of AAV2/9-microdystrophin genes incorporating helix 1 of the coiled-coil motif in the C-terminal domain of dystrophin improves muscle pathology and restores the level of  $\alpha 1$ -syntrophin and  $\alpha$ -dystrobrevin in skeletal muscles of mdx mice. *Hum. Gene Ther.* **22**, 1379-1388.
- Koo, T., Okada, T., Athanasopoulos, T., Foster, H., Takeda, S. and Dickson, G. (2011b). Long-term functional adeno-associated virus-microdystrophin expression in the dystrophic CXMDJ dog. *J. Gene Med.* **13**, 497-506.
- Koo, T., Popplewell, L., Athanasopoulos, T. and Dickson, G. (2014). Triple trans-splicing adeno-associated virus vectors capable of transferring the coding sequence for full-length dystrophin protein into dystrophic mice. *Hum. Gene Ther.* **25**, 98-108.
- Kornegay, J. N., Tuler, S. M., Miller, D. M. and Levesque, D. C. (1988). Muscular dystrophy in a litter of golden retriever dogs. *Muscle Nerve* **11**, 1056-1064.
- Kornegay, J. N., Li, J., Bogan, J. R., Bogan, D. J., Chen, C., Zheng, H., Wang, B., Qiao, C., Howard, J. F., Jr and Xiao, X. (2010). Widespread muscle expression of an AAV9 human mini-dystrophin vector after intravenous injection in neonatal dystrophin-deficient dogs. *Mol. Ther.* **18**, 1501-1508.
- Kornegay, J. N., Bogan, J. R., Bogan, D. J., Childers, M. K., Li, J., Nghiem, P., Detwiler, D. A., Larsen, C. A., Grange, R. W., Bhavaraju-Sanka, R. K. et al. (2012). Canine models of Duchenne muscular dystrophy and their use in therapeutic strategies. *Mamm. Genome* **23**, 85-108.
- Krivov, L. I., Stenina, M. A., Yarygin, V. N., Polyakov, A. V., Savchuk, V. I., Oubrov, S. A. and Komarova, N. V. (2009). A new genetic variant of mdx mice: study of the phenotype. *Bull. Exp. Biol. Med.* **147**, 625-629.
- Kumar-Singh, R. and Chamberlain, J. S. (1996). Encapsidated adenovirus minichromosomes allow delivery and expression of a 14 kb dystrophin cDNA to muscle cells. *Hum. Mol. Genet.* **5**, 913-921.
- Kunkel, L. M. (2005). 2004 William Allan award address. cloning of the DMD gene. *Am. J. Hum. Genet.* **76**, 205-214.
- Kunkel, L. M., Bachrach, E., Bennett, R. R., Guyon, J. and Steffen, L. (2006). Diagnosis and cell-based therapy for Duchenne muscular dystrophy in humans, mice, and zebrafish. *J. Hum. Genet.* **51**, 397-406.
- Lai, Y. and Duan, D. (2012). Progress in gene therapy of dystrophic heart disease. *Gene Ther.* **19**, 678-685.
- Lai, Y., Yue, Y., Liu, M., Ghosh, A., Engelhardt, J. F., Chamberlain, J. S. and Duan, D. (2005). Efficient in vivo gene expression by trans-splicing adeno-associated viral vectors. *Nat. Biotechnol.* **23**, 1435-1439.
- Lai, Y., Thomas, G. D., Yue, Y., Yang, H. T., Li, D., Long, C., Judge, L., Bostick, B., Chamberlain, J. S., Terjung, R. L. et al. (2009). Dystrophins carrying spectrin-like repeats 16 and 17 anchor nNOS to the sarcolemma and enhance exercise performance in a mouse model of muscular dystrophy. *J. Clin. Invest.* **119**, 624-635.
- Lai, Y., Zhao, J., Yue, Y. and Duan, D. (2013).  $\alpha 2$  and  $\alpha 3$  helices of dystrophin R16 and R17 frame a microdomain in the  $\alpha 1$  helix of dystrophin R17 for neuronal NOS binding. *Proc. Natl. Acad. Sci. USA* **110**, 525-530.
- Lai, Y., Zhao, J., Yue, Y., Wasala, N. B. and Duan, D. (2014). Partial restoration of cardiac function with  $\Delta$ PDZ nNOS in aged mdx model of Duchenne cardiomyopathy. *Hum. Mol. Genet.* **23**, 3189-3199.
- Lanfoss, M., Cozzi, F., Bugini, D., Colombo, S., Scarpa, P., Morandi, L., Galbiati, S., Cornelio, F., Pozza, O. and Mora, M. (1999). Development of muscle pathology in canine X-linked muscular dystrophy. I. Delayed postnatal maturation of affected and normal muscle as revealed by myosin isoform analysis and utrophin expression. *Acta Neuropathol.* **97**, 127-138.

- Le Guiner, C., Montus, M., Servais, L., Cherel, Y., Francois, V., Thibaud, J. L., Wary, C., Matot, B., Larcher, T., Guigand, L. et al. (2014). Forelimb treatment in a large cohort of dystrophic dogs supports delivery of a recombinant AAV for exon skipping in Duchenne patients. *Mol. Ther.* **22**, 1923-1935.
- Lee, S. J. (2004). Regulation of muscle mass by myostatin. *Annu. Rev. Cell Dev. Biol.* **20**, 61-86.
- Lefaucheur, J. P., Pastoret, C. and Sebille, A. (1995). Phenotype of dystrophinopathy in old mdx mice. *Anat. Rec.* **242**, 70-76.
- Leibovitz, S., Meshorer, A., Fridman, Y., Wieneke, S., Jockusch, H., Yaffe, D. and Nudel, U. (2002). Exogenous Dp71 is a dominant negative competitor of dystrophin in skeletal muscle. *Neuromuscul. Disord.* **12**, 836-844.
- Li, D., Yue, Y. and Duan, D. (2008). Preservation of muscle force in Mdx3cv mice correlates with low-level expression of a near full-length dystrophin protein. *Am. J. Pathol.* **172**, 1332-1341.
- Li, D., Long, C., Yue, Y. and Duan, D. (2009). Sub-physiological sarcoglycan expression contributes to compensatory muscle protection in mdx mice. *Hum. Mol. Genet.* **18**, 1209-1220.
- Li, D., Yue, Y. and Duan, D. (2010). Marginal level dystrophin expression improves clinical outcome in a strain of dystrophin/utrophin double knockout mice. *PLoS ONE* **5**, e15286.
- Li, D., Yue, Y., Lai, Y., Hakim, C. H. and Duan, D. (2011). Nitrosative stress elicited by nNOS $\mu$  delocalization inhibits muscle force in dystrophin-null mice. *J. Pathol.* **223**, 88-98.
- Lidov, H. G. (1996). Dystrophin in the nervous system. *Brain Pathol.* **6**, 63-77.
- Liu, Q., Perez, C. F. and Wang, Y. (2006). Efficient site-specific integration of large transgenes by an enhanced herpes simplex virus/adeno-associated virus hybrid amplicon vector. *J. Virol.* **80**, 1672-1679.
- Lloyd, T. E. and Taylor, J. P. (2010). Flightless flies: Drosophila models of neuromuscular disease. *Ann. N. Y. Acad. Sci.* **1184**, e1-e20.
- Long, C., McAnally, J. R., Shelton, J. M., Mireault, A. A., Bassel-Duby, R. and Olson, E. N. (2014). Prevention of muscular dystrophy in mice by CRISPR/Cas9-mediated editing of germline DNA. *Science* **345**, 1184-1188.
- Lostal, W., Kodippili, K., Yue, Y. and Duan, D. (2014). Full-length dystrophin reconstitution with adeno-associated viral vectors. *Hum. Gene Ther.* **25**, 552-562.
- Lu, Q. L., Mann, C. J., Lou, F., Bou-Gharios, G., Morris, G. E., Xue, S. A., Fletcher, S., Partridge, T. A. and Wilton, S. D. (2003). Functional amounts of dystrophin produced by skipping the mutated exon in the mdx dystrophic mouse. *Nat. Med.* **9**, 1009-1014.
- Lu, Q. L., Rabinowitz, A., Chen, Y. C., Yokota, T., Yin, H., Alter, J., Jadoon, A., Bou-Gharios, G. and Partridge, T. (2005). Systemic delivery of antisense oligoribonucleotide restores dystrophin expression in body-wide skeletal muscles. *Proc. Natl. Acad. Sci. USA* **102**, 198-203.
- Lu, Q. L., Yokota, T., Takeda, S., Garcia, L., Muntoni, F. and Partridge, T. (2011). The status of exon skipping as a therapeutic approach to duchenne muscular dystrophy. *Mol. Ther.* **19**, 9-15.
- Lynch, G. S., Hinkle, R. T., Chamberlain, J. S., Brooks, S. V. and Faulkner, J. A. (2001). Force and power output of fast and slow skeletal muscles from mdx mice 6-28 months old. *J. Physiol.* **535**, 591-600.
- Magri, F., Govoni, A., D'Angelo, M. G., Del Bo, R., Ghezzi, S., Sandra, G., Turconi, A. C., Sciacco, M., Ciscato, P., Bordini, A. et al. (2011). Genotype and phenotype characterization in a large dystrophinopathic cohort with extended follow-up. *J. Neurol.* **258**, 1610-1623.
- Mann, C. J., Honeyman, K., Cheng, A. J., Ly, T., Lloyd, F., Fletcher, S., Morgan, J. E., Partridge, T. A. and Wilton, S. D. (2001). Antisense-induced exon skipping and synthesis of dystrophin in the mdx mouse. *Proc. Natl. Acad. Sci. USA* **98**, 42-47.
- Marshall, J. L., Kwok, Y., McMorran, B. J., Baum, L. G. and Crosbie-Watson, R. H. (2013). The potential of sarcospan in adhesion complex replacement therapeutics for the treatment of muscular dystrophy. *FEBS J.* **280**, 4210-4229.
- Martins, P. C., Ayub-Guerrieri, D., Martins-Bach, A. B., Onofre-Oliveira, P., Malheiros, J. M., Tannus, A., de Sousa, P. L., Carlier, P. G. and Vainzof, M. (2013). Dmd<sup>mdx</sup>/Large<sup>myd</sup>: a new mouse model of neuromuscular diseases useful for studying physiopathological mechanisms and testing therapies. *Dis. Model. Mech.* **6**, 1167-1174.
- McCabe, E. R., Towbin, J., Chamberlain, J., Baumbach, L., Witkowski, J., van Ommen, G. J., Koenig, M., Kunkel, L. M. and Seltzer, W. K. (1989). Complementary DNA probes for the Duchenne muscular dystrophy locus demonstrate a previously undetectable deletion in a patient with dystrophic myopathy, glycerol kinase deficiency, and congenital adrenal hypoplasia. *J. Clin. Invest.* **83**, 95-99.
- McCloy, G., Moulton, H. M., Iversen, P. L., Fletcher, S. and Wilton, S. D. (2006). Antisense oligonucleotide-induced exon skipping restores dystrophin expression in vitro in a canine model of DMD. *Gene Ther.* **13**, 1373-1381.
- McCully, K., Giger, U., Argov, Z., Valentine, B., Cooper, B., Chance, B. and Bank, W. (1991). Canine X-linked muscular dystrophy studied with in vivo phosphorus magnetic resonance spectroscopy. *Muscle Nerve* **14**, 1091-1098.
- McDonald, C. M., Henricson, E. K., Han, J. J., Abresch, R. T., Nicorici, A., Atkinson, L., Elfving, G. L., Reha, A. and Miller, L. L. (2010). The 6-minute walk test in Duchenne/Becker muscular dystrophy: longitudinal observations. *Muscle Nerve* **42**, 966-974.
- McDonald, C. M., Henricson, E. K., Abresch, R. T., Florence, J. M., Eagle, M., Gappmaier, E., Glanzman, A. M., Spiegel, R., Barth, J., Elfving, G. et al.; PTC124-GD-007-DMD Study Group (2013a). The 6-minute walk test and other endpoints in Duchenne muscular dystrophy: longitudinal natural history observations over 48 weeks from a multicenter study. *Muscle Nerve* **48**, 343-356.
- McDonald, C. M., Henricson, E. K., Abresch, R. T., Han, J. J., Escolar, D. M., Florence, J. M., Duong, T., Arrieta, A., Clemens, P. R., Hoffman, E. P. et al.; Cingr Investigators (2013b). The cooperative international neuromuscular research group Duchenne natural history study—a longitudinal investigation in the era of glucocorticoid therapy: design of protocol and the methods used. *Muscle Nerve* **48**, 32-54.
- McPherron, A. C., Lawler, A. M. and Lee, S. J. (1997). Regulation of skeletal muscle mass in mice by a new TGF-beta superfamily member. *Nature* **387**, 83-90.
- Megene, L. A., Kablar, B., Garrett, K., Anderson, J. E. and Rudnicki, M. A. (1996). MyoD is required for myogenic stem cell function in adult skeletal muscle. *Genes Dev.* **10**, 1173-1183.
- Megene, L. A., Kablar, B., Perry, R. L., Ying, C., May, L. and Rudnicki, M. A. (1999). Severe cardiomyopathy in mice lacking dystrophin and MyoD. *Proc. Natl. Acad. Sci. USA* **96**, 220-225.
- Mendell, J. R. and Lloyd-Puryear, M. (2013). Report of MDA muscle disease symposium on newborn screening for Duchenne muscular dystrophy. *Muscle Nerve* **48**, 21-26.
- Mendell, J. R., Rodino-Klapac, L., Sahenk, Z., Malik, V., Kaspar, B. K., Walker, C. M. and Clark, K. R. (2012). Gene therapy for muscular dystrophy: lessons learned and path forward. *Neurosci. Lett.* **527**, 90-99.
- Mendell, J. R., Rodino-Klapac, L. R., Sahenk, Z., Roush, K., Bird, L., Lowes, L. P., Alfano, L., Gomez, A. M., Lewis, S., Kota, J. et al.; Eteplirsen Study Group (2013). Eteplirsen for the treatment of Duchenne muscular dystrophy. *Ann. Neurol.* **74**, 637-647.
- Mendell, J. R., Sahenk, Z., Malik, V., Gomez, A. M., Flanigan, K. M., Lowes, L. P., Alfano, L. N., Berry, K., Meadows, E., Lewis, S. et al. (2015). A phase 1/2a follistatin gene therapy trial for Becker muscular dystrophy. *Mol. Ther.* **23**, 192-201.
- Mercuri, E. and Muntoni, F. (2013). Muscular dystrophy: new challenges and review of the current clinical trials. *Curr. Opin. Pediatr.* **25**, 701-707.
- Miranda, R., Sébrié, C., Degrouard, J., Gillet, B., Jaillard, D., Laroche, S. and Vaillend, C. (2009). Reorganization of inhibitory synapses and increased PSD length of perforated excitatory synapses in hippocampal area CA1 of dystrophin-deficient mdx mice. *Cereb. Cortex* **19**, 876-888.
- Miranda, R., Nudel, U., Laroche, S. and Vaillend, C. (2011). Altered presynaptic ultrastructure in excitatory hippocampal synapses of mice lacking dystrophins Dp427 or Dp71. *Neurobiol. Dis.* **43**, 134-141.
- Miyazato, L. G., Moraes, J. R., Beretta, D. C. and Kornegay, J. N. (2011). Muscular dystrophy in dogs: does the crossing of breeds influence disease phenotype? *Vet. Pathol.* **48**, 655-662.
- Moise, N. S., Valentine, B. A., Brown, C. A., Erb, H. N., Beck, K. A., Cooper, B. J. and Gilmour, R. F. (1991). Duchenne's cardiomyopathy in a canine model: electrocardiographic and echocardiographic studies. *J. Am. Coll. Cardiol.* **17**, 812-820.
- Moizard, M. P., Billard, C., Toutain, A., Berret, F., Marmin, N. and Moraine, C. (1998). Are Dp71 and Dp140 brain dystrophin isoforms related to cognitive impairment in Duchenne muscular dystrophy? *Am. J. Med. Genet.* **80**, 32-41.
- Moizard, M. P., Toutain, A., Fournier, D., Berret, F., Raynaud, M., Billard, C., Andres, C. and Moraine, C. (2000). Severe cognitive impairment in DMD: obvious clinical indication for Dp71 isoform point mutation screening. *Eur. J. Hum. Genet.* **8**, 552-556.
- Monaco, A. P., Neve, R. L., Colletti-Feener, C., Bertelson, C. J., Kurnit, D. M. and Kunkel, L. M. (1986). Isolation of candidate cDNAs for portions of the Duchenne muscular dystrophy gene. *Nature* **323**, 646-650.
- Monaco, A. P., Bertelson, C. J., Liechti-Gallati, S., Moser, H. and Kunkel, L. M. (1988). An explanation for the phenotypic differences between patients bearing partial deletions of the DMD locus. *Genomics* **2**, 90-95.
- Morrison, J., Lu, Q. L., Pastoret, C., Partridge, T. and Bou-Gharios, G. (2000). T-cell-dependent fibrosis in the mdx dystrophic mouse. *Lab. Invest.* **80**, 881-891.
- Mourikioti, F., Kustan, J., Kraft, P., Day, J. W., Zhao, M. M., Kost-Alimova, M., Protopopov, A., DePinho, R. A., Bernstein, D., Meeker, A. K. et al. (2013). Role of telomere dysfunction in cardiac failure in Duchenne muscular dystrophy. *Nat. Cell Biol.* **15**, 895-904.
- Muntoni, F., Mateddu, A. and Serra, G. (1991). Passive avoidance behaviour deficit in the mdx mouse. *Neuromuscul. Disord.* **1**, 121-123.
- Nakamura, A., Yoshida, K., Fukushima, K., Ueda, H., Urasawa, N., Koyama, J., Yazaki, Y., Yazaki, M., Sakai, T., Haruta, S. et al. (2008). Follow-up of three patients with a large in-frame deletion of exons 45-55 in the Duchenne muscular dystrophy (DMD) gene. *J. Clin. Neurosci.* **15**, 757-763.
- Nakamura, A., Kobayashi, M., Kuraoka, M., Yuasa, K., Yugeta, N., Okada, T. and Takeda, S. (2013). Initial pulmonary respiration causes massive diaphragm damage and hyper-CKemia in Duchenne muscular dystrophy dog. *Sci. Rep.* **3**, 2183.
- Nakamura, K., Fujii, W., Tsuboi, M., Tanihata, J., Teramoto, N., Takeuchi, S., Naito, K., Yamanouchi, K. and Nishihara, M. (2014). Generation of muscular dystrophy model rats with a CRISPR/Cas system. *Sci. Rep.* **4**, 5635.
- Nardes, F., Araújo, A. P. and Ribeiro, M. G. (2012). Mental retardation in Duchenne muscular dystrophy. *J. Pediatr. (Rio J.)* **88**, 6-16.
- Neri, M., Torelli, S., Brown, S., Ugo, I., Sabatelli, P., Merlini, L., Spitali, P., Rimessi, P., Gualandi, F., Sewry, C. et al. (2007). Dystrophin levels as low as 30% are sufficient to avoid muscular dystrophy in the human. *Neuromuscul. Disord.* **17**, 913-918.
- Nguyen, F., Cherel, Y., Guigand, L., Goubault-Leroux, I. and Wyers, M. (2002). Muscle lesions associated with dystrophin deficiency in neonatal golden retriever puppies. *J. Comp. Pathol.* **126**, 100-108.
- Nicholson, L. V., Johnson, M. A., Bushby, K. M. and Gardner-Medwin, D. (1993a). Functional significance of dystrophin positive fibres in Duchenne muscular dystrophy. *Arch. Dis. Child.* **68**, 632-636.

- Nicholson, L. V., Johnson, M. A., Bushby, K. M., Gardner-Medwin, D., Curtis, A., Ginjnar, I. B., den Dunnen, J. T., Welch, J. L., Butler, T. J., Bakker, E. et al. (1993b). Integrated study of 100 patients with Xp21 linked muscular dystrophy using clinical, genetic, immunochemical, and histopathological data. Part 1. Trends across the clinical groups. *J. Med. Genet.* **30**, 728-736.
- Nishimura, D., Sakai, H., Sato, T., Sato, F., Nishimura, S., Toyama-Sorimachi, N., Bartsch, J. W. and Sehara-Fujisawa, A. (2015). Roles of ADAM8 in elimination of injured muscle fibers prior to skeletal muscle regeneration. *Mech. Dev.* **135**, 58-67.
- Nitahara-Kasahara, Y., Hayashita-Kinoh, H., Chiyo, T., Nishiyama, A., Okada, H., Takeda, S. and Okada, T. (2014). Dystrophic mdx mice develop severe cardiac and respiratory dysfunction following genetic ablation of the anti-inflammatory cytokine IL-10. *Hum. Mol. Genet.* **23**, 3990-4000.
- Nonneman, D. J., Brown-Brandt, T., Jones, S. A., Wiedmann, R. T. and Rohrer, G. A. (2012). A defect in dystrophin causes a novel porcine stress syndrome. *BMC Genomics* **13**, 233.
- Odom, G. L., Gregorevic, P., Allen, J. M., Finn, E. and Chamberlain, J. S. (2008). Microtrophin delivery through rAAV6 increases lifespan and improves muscle function in dystrophic dystrophin/utrophin-deficient mice. *Mol. Ther.* **16**, 1539-1545.
- Odom, G. L., Gregorevic, P., Allen, J. M. and Chamberlain, J. S. (2011). Gene therapy of mdx mice with large truncated dystrophins generated by recombination using rAAV6. *Mol. Ther.* **19**, 36-45.
- Ohshima, S., Shin, J. H., Yuasa, K., Nishiyama, A., Kira, J., Okada, T. and Takeda, S. (2009). Transduction efficiency and immune response associated with the administration of AAV8 vector into dog skeletal muscle. *Mol. Ther.* **17**, 73-80.
- Opar, A. (2012). Exon-skipping drug pulls ahead in muscular dystrophy field. *Nat. Med.* **18**, 1314.
- Ousterout, D. G., Perez-Pinera, P., Thakore, P. I., Kabadi, A. M., Brown, M. T., Qin, X., Fedrigo, O., Mouly, V., Tremblay, J. P. and Gersbach, C. A. (2013). Reading frame correction by targeted genome editing restores dystrophin expression in cells from Duchenne muscular dystrophy patients. *Mol. Ther.* **21**, 1718-1726.
- Ousterout, D. G., Kabadi, A. M., Thakore, P. I., Perez-Pinera, P., Brown, M. T., Majoros, W. H., Reddy, T. E. and Gersbach, C. A. (2014). Correction of dystrophin expression in cells from Duchenne Muscular Dystrophy patients through genomic excision of Exon 51 by zinc finger nucleases. *Mol. Ther.* [Epub ahead of print] doi: 10.1038/mt.2014.234.
- Pacak, C. A., Mah, C. S., Thattaliyath, B. D., Conlon, T. J., Lewis, M. A., Cloutier, D. E., Zolotukhin, I., Tarantal, A. F. and Byrne, B. J. (2006). Recombinant adeno-associated virus serotype 9 leads to preferential cardiac transduction in vivo. *Circ. Res.* **99**, e3-e9.
- Pan, X., Yue, Y., Zhang, K., Lostal, W., Shin, J. H. and Duan, D. (2013). Long-term robust myocardial transduction of the dog heart from a peripheral vein by adeno-associated virus serotype-8. *Hum. Gene Ther.* **24**, 584-594.
- Pane, M., Lombardo, M. E., Alfieri, P., D'Amico, A., Bianco, F., Vasco, G., Piccini, G., Mallardi, M., Romeo, D. M., Ricotti, V. et al. (2012). Attention deficit hyperactivity disorder and cognitive function in Duchenne muscular dystrophy: phenotype-genotype correlation. *J. Pediatr.* **161**, 705-709 e1.
- Parames, S. F., Coletta-Yudice, E. D., Nogueira, F. M., Nering de Sousa, M. B., Hayashi, M. A., Lima-Landman, M. T., Lapa, A. J. and Souccar, C. (2014). Altered acetylcholine release in the hippocampus of dystrophin-deficient mice. *Neuroscience* **269**, 173-183.
- Partridge, T. and Lu, Q. L. (2008). The enigma of the 'dystrophin revertant' muscle fibre. In *Recent Advances in Skeletal Muscle Differentiation* (ed. T. Kunihiro and S. Takeda), pp. 93-107. Kerala: Research Signpost.
- Pastoret, C. and Sebillé, A. (1995). Mdx mice show progressive weakness and muscle deterioration with age. *J. Neurol. Sci.* **129**, 97-105.
- Patria, S. Y., Alimsardjono, H., Nishio, H., Takeshima, Y., Nakamura, H. and Matsuo, M. (1996). A case of Becker muscular dystrophy resulting from the skipping of four contiguous exons (71-74) of the dystrophin gene during mRNA maturation. *Proc. Assoc. Am. Physicians* **108**, 308-314.
- Perronnet, C., Chagneau, C., Le Blanc, P., Samson-Desvignes, N., Mornet, D., Laroche, S., De La Porte, S. and Vaillend, C. (2012). Upregulation of brain utrophin does not rescue behavioral alterations in dystrophin-deficient mice. *Hum. Mol. Genet.* **21**, 2263-2276.
- Phelps, S. F., Hauser, M. A., Cole, N. M., Rafael, J. A., Hinkle, R. T., Faulkner, J. A. and Chamberlain, J. S. (1995). Expression of full-length and truncated dystrophin mini-genes in transgenic mdx mice. *Hum. Mol. Genet.* **4**, 1251-1258.
- Poussin, G., Mathis, C., Alexopoulos, L. G., Messinis, D. E., Dulize, R. H. J., Belcastro, V., Melas, I. N., Sakellaropoulos, T., Rhrissorakrai, K., Bilal, E. et al. (2014). The species translation challenge – a systems biology perspective on human and rat bronchial epithelial cells. *Sci. Data* **1**, 140009.
- Rafael, J. A., Tinsley, J. M., Potter, A. C., Deconinck, A. E. and Davies, K. E. (1998). Skeletal muscle-specific expression of a utrophin transgene rescues utrophin-dystrophin deficient mice. *Nat. Genet.* **19**, 79-82.
- Rafael-Fortney, J. A., Chimanji, N. S., Schill, K. E., Martin, C. D., Murray, J. D., Ganguly, R., Stangland, J. E., Tran, T., Xu, Y., Canan, B. D. et al. (2011). Early treatment with lisinopril and spirinolactone preserves cardiac and skeletal muscle in Duchenne muscular dystrophy mice. *Circulation* **124**, 582-588.
- Ragot, T., Vincent, N., Chafey, P., Vigne, E., Gilgenkrantz, H., Couton, D., Cartaud, J., Briand, P., Kaplan, J. C., Perricaudet, M. et al. (1993). Efficient adenovirus-mediated transfer of a human minidystrophin gene to skeletal muscle of mdx mice. *Nature* **361**, 647-650.
- Rando, T. A., Disatnik, M. H. and Zhou, L. Z. (2000). Rescue of dystrophin expression in mdx mouse muscle by RNA/DNA oligonucleotides. *Proc. Natl. Acad. Sci. USA* **97**, 5363-5368.
- Ricotti, V., Roberts, R. G. and Muntoni, F. (2011). Dystrophin and the brain. *Dev. Med. Child Neurol.* **53**, 12.
- Rodino-Klapac, L. R., Haidet, A. M., Kota, J., Handy, C., Kaspar, B. K. and Mendell, J. R. (2009). Inhibition of myostatin with emphasis on follistatin as a therapy for muscle disease. *Muscle Nerve* **39**, 283-296.
- Rooney, J. E., Welsch, J. V., Dechert, M. A., Flintoff-Dye, N. L., Kaufman, S. J. and Burkin, D. J. (2006). Severe muscular dystrophy in mice that lack dystrophin and alpha7 integrin. *J. Cell Sci.* **119**, 2185-2195.
- Rousseau, J., Chapdelaine, P., Boisvert, S., Almeida, L. P., Corbeil, J., Montpetit, A. and Tremblay, J. P. (2011). Endonucleases: tools to correct the dystrophin gene. *J. Gene Med.* **13**, 522-537.
- Rutledge, E. A., Halbert, C. L. and Russell, D. W. (1998). Infectious clones and vectors derived from adeno-associated virus (AAV) serotypes other than AAV type 2. *J. Virol.* **72**, 309-319.
- Sacco, A., Mourikioti, F., Tran, R., Choi, J., Llewellyn, M., Kraft, P., Shkreli, M., Delp, S., Pomerantz, J. H., Artandi, S. E. et al. (2010). Short telomeres and stem cell exhaustion model Duchenne muscular dystrophy in mdx/mTR mice. *Cell* **143**, 1059-1071.
- Sampaoli, M., Blot, S., D'Antona, G., Granger, N., Tonlorenzi, R., Innocenzi, A., Mogno, P., Thibaud, J. L., Galvez, B. G., Barthélémy, I. et al. (2006). Mesoangioblast stem cells ameliorate muscle function in dystrophic dogs. *Nature* **444**, 574-579.
- Sarig, R., Mezger-Lallemand, V., Gitelman, I., Davis, C., Fuchs, O., Yaffe, D. and Nudel, U. (1999). Targeted inactivation of Dp71, the major non-muscle product of the DMD gene: differential activity of the Dp71 promoter during development. *Hum. Mol. Genet.* **8**, 1-10.
- Schatzberg, S. J., Olby, N. J., Breen, M., Anderson, L. V., Langford, C. F., Dickens, H. F., Wilton, S. D., Zeiss, C. J., Binns, M. M., Kornegay, J. N. et al. (1999). Molecular analysis of a spontaneous dystrophin 'knockout' dog. *Neuromuscul. Disord.* **9**, 289-295.
- Schinkel, S., Bauer, R., Bekeredjian, R., Stucka, R., Rutschow, D., Lochmüller, H., Kleinschmidt, J. A., Katus, H. A. and Müller, O. J. (2012). Long-term preservation of cardiac structure and function after adeno-associated virus serotype 9-mediated microdystrophin gene transfer in mdx mice. *Hum. Gene Ther.* **23**, 566-575.
- Schmidt, W. M., Uddin, M. H., Dysek, S., Moser-Thier, K., Pirker, C., Höger, H., Ambros, I. M., Ambros, P. F., Berger, W. and Bittner, R. E. (2011). DNA damage, somatic aneuploidy, and malignant sarcoma susceptibility in muscular dystrophies. *PLoS Genet.* **7**, e1002042.
- Sekiguchi, M., Zushida, K., Yoshida, M., Maekawa, M., Kamichi, S., Yoshida, M., Sahara, Y., Yuasa, S., Takeda, S. and Wada, K. (2009). A deficit of brain dystrophin impairs specific amygdala GABAergic transmission and enhances defensive behaviour in mice. *Brain* **132**, 124-135.
- Selsby, J. T., Morine, K. J., Pendrak, K., Barton, E. R. and Sweeney, H. L. (2012). Rescue of dystrophic skeletal muscle by PGC-1 $\alpha$  involves a fast to slow fiber type shift in the mdx mouse. *PLoS ONE* **7**, e30063.
- Sharp, N. J., Kornegay, J. N., Van Camp, S. D., Herbstreith, M. H., Secore, S. L., Kettle, S., Hung, W. Y., Constantinou, C. D., Dykstra, M. J., Roses, A. D. et al. (1992). An error in dystrophin mRNA processing in golden retriever muscular dystrophy, an animal homologue of Duchenne muscular dystrophy. *Genomics* **13**, 115-121.
- Shelton, G. D. and Engvall, E. (2005). Canine and feline models of human inherited muscle diseases. *Neuromuscul. Disord.* **15**, 127-138.
- Shimatsu, Y., Katagiri, K., Furuta, T., Nakura, M., Tanioka, Y., Yuasa, K., Tomohiro, M., Kornegay, J. N., Nonaka, I. and Takeda, S. (2003). Canine X-linked muscular dystrophy in Japan (CXMDJ). *Exp. Anim.* **52**, 93-97.
- Shimatsu, Y., Yoshimura, M., Yuasa, K., Urasawa, N., Tomohiro, M., Nakura, M., Tanigawa, M., Nakamura, A. and Takeda, S. (2005). Major clinical and histopathological characteristics of canine X-linked muscular dystrophy in Japan, CXMDJ. *Acta Myol.* **24**, 145-154.
- Shin, J.-H., Bostick, B., Yue, Y. and Duan, D. (2010). Duchenne cardiomyopathy gene therapy. In *Muscle Gene Therapy* (ed. D. Duan), pp. 141-162. New York, NY: Springer Science + Business Media, LLC.
- Shin, J. H., Bostick, B., Yue, Y., Hajjar, R. and Duan, D. (2011a). SERCA2a gene transfer improves electrocardiographic performance in aged mdx mice. *J. Transl. Med.* **9**, 132.
- Shin, J. H., Nitahara-Kasahara, Y., Hayashita-Kinoh, H., Ohshima-Hosoyama, S., Kinoshita, K., Chiyo, T., Okada, H., Okada, T. and Takeda, S. (2011b). Improvement of cardiac fibrosis in dystrophic mice by rAAV9-mediated microdystrophin transduction. *Gene Ther.* **18**, 910-919.
- Shin, J. H., Yue, Y., Smith, B. and Duan, D. (2012a). Humoral immunity to AAV-6, 8, and 9 in normal and dystrophic dogs. *Hum. Gene Ther.* **23**, 287-294.
- Shin, J. H., Yue, Y., Srivastava, A., Smith, B., Lai, Y. and Duan, D. (2012b). A simplified immune suppression scheme leads to persistent micro-dystrophin expression in Duchenne muscular dystrophy dogs. *Hum. Gene Ther.* **23**, 202-209.
- Shin, J. H., Greer, B., Hakim, C. H., Zhou, Z., Chung, Y. C., Duan, Y., He, Z. and Duan, D. (2013a). Quantitative phenotyping of Duchenne muscular dystrophy dogs by comprehensive gait analysis and overnight activity monitoring. *PLoS ONE* **8**, e59875.
- Shin, J. H., Pan, X., Hakim, C. H., Yang, H. T., Yue, Y., Zhang, K., Terjung, R. L. and Duan, D. (2013b). Microdystrophin ameliorates muscular dystrophy in the canine model of duchenne muscular dystrophy. *Mol. Ther.* **21**, 750-757.
- Scicinski, P., Peng, Y., Ryder-Cook, A. S., Barnard, E. A., Darlison, M. G. and Barnard, P. J. (1989). The molecular basis of muscular dystrophy in the mdx mouse: a point mutation. *Science* **244**, 1578-1580.

- Siffringer, M., Uhlenberg, B., Lammel, S., Hanke, R., Neumann, B., von Moers, A., Koch, I. and Speer, A. (2004). Identification of transcripts from a subtraction library which might be responsible for the mild phenotype in an intrafamilially variable course of Duchenne muscular dystrophy. *Hum. Genet.* **114**, 149-156.
- Smith, K. (2011). Feline muscular dystrophy: parallels between cats and people. *Vet. Rec.* **168**, 507-508.
- Smith, B. F., Kornegay, J. N. and Duan, D. (2007). Independent canine models of Duchenne muscular dystrophy due to intronic insertions of repetitive DNA. *Mol. Ther.* **15**, S51.
- Smith, B. F., Yue, Y., Woods, P. R., Kornegay, J. N., Shin, J. H., Williams, R. R. and Duan, D. (2011). An intronic LINE-1 element insertion in the dystrophin gene aborts dystrophin expression and results in Duchenne-like muscular dystrophy in the corgi breed. *Lab. Invest.* **91**, 216-231.
- Snow, W. M., Anderson, J. E. and Jakobson, L. S. (2013). Neuropsychological and neurobehavioral functioning in Duchenne muscular dystrophy: a review. *Neurosci. Biobehav. Rev.* **37**, 743-752.
- Spitali, P. and Aartsma-Rus, A. (2012). Splice modulating therapies for human disease. *Cell* **148**, 1085-1088.
- Spurney, C., Shimizu, R., Morgenroth, L. P., Kolski, H., Gordish-Dressman, H., Clemens, P. R.; CINRG Investigators (2014). Cooperative International Neuromuscular Research Group Duchenne Natural History Study demonstrates insufficient diagnosis and treatment of cardiomyopathy in Duchenne muscular dystrophy. *Muscle Nerve* **50**, 250-256.
- Stedman, H. H., Sweeney, H. L., Shrager, J. B., Maguire, H. C., Panettieri, R. A., Petrof, B., Narusawa, M., Leferovich, J. M., Sladky, J. T. and Kelly, A. M. (1991). The mdx mouse diaphragm reproduces the degenerative changes of Duchenne muscular dystrophy. *Nature* **352**, 536-539.
- Stenina, M. A., Krivov, L. I., Voevodin, D. A. and Yarygin, V. N. (2013). Phenotypic differences between mdx black mice and mdx albino mice. Comparison of cytokine levels in the blood. *Bull. Exp. Biol. Med.* **155**, 376-379.
- Stinckens, A., Georges, M. and Buys, N. (2011). Mutations in the myostatin gene leading to hypermuscularity in mammals: indications for a similar mechanism in fish? *Anim. Genet.* **42**, 229-234.
- Taylor, P. J., Betts, G. A., Maroulis, S., Gilissen, C., Pedersen, R. L., Mowat, D. R., Johnston, H. M. and Buckley, M. F. (2010). Dystrophin gene mutation location and the risk of cognitive impairment in Duchenne muscular dystrophy. *PLoS ONE* **5**, e8803.
- Thomas, G. D. (2013). Functional muscle ischemia in Duchenne and Becker muscular dystrophy. *Front. Physiol.* **4**, 381.
- Tinsley, J. M., Potter, A. C., Phelps, S. R., Fisher, R., Trickett, J. I. and Davies, K. E. (1996). Amelioration of the dystrophic phenotype of mdx mice using a truncated utrophin transgene. *Nature* **384**, 349-353.
- Tinsley, J., Deconinck, N., Fisher, R., Kahn, D., Phelps, S., Gillis, J. M. and Davies, K. (1998). Expression of full-length utrophin prevents muscular dystrophy in mdx mice. *Nat. Med.* **4**, 1441-1444.
- Townsend, D., Blankinship, M. J., Allen, J. M., Gregorevic, P., Chamberlain, J. S. and Metzger, J. M. (2007). Systemic administration of micro-dystrophin restores cardiac geometry and prevents dobutamine-induced cardiac pump failure. *Mol. Ther.* **15**, 1086-1092.
- Townsend, D., Yasuda, S., Li, S., Chamberlain, J. S. and Metzger, J. M. (2008). Emergent dilated cardiomyopathy caused by targeted repair of dystrophic skeletal muscle. *Mol. Ther.* **16**, 832-835.
- Tozawa, T., Itoh, K., Yaoi, T., Tando, S., Umekage, M., Dai, H., Hosoi, H. and Fushiki, S. (2012). The shortest isoform of dystrophin (Dp40) interacts with a group of presynaptic proteins to form a presumptive novel complex in the mouse brain. *Mol. Neurobiol.* **45**, 287-297.
- Tuffery-Giraud, S., Bérout, C., Leturcq, F., Yaou, R. B., Hamroun, D., Michel-Calemard, L., Moizard, M. P., Bernard, R., Cossée, M., Boisseau, P. et al. (2009). Genotype-phenotype analysis in 2,405 patients with a dystrophinopathy using the UMD-DMD database: a model of nationwide knowledgebase. *Hum. Mutat.* **30**, 934-945.
- Vaillend, C. and Ungerer, A. (1999). Behavioral characterization of mdx3cv mice deficient in C-terminal dystrophins. *Neuromuscul. Disord.* **9**, 296-304.
- Vaillend, C., Rendon, A., Misslin, R. and Ungerer, A. (1995). Influence of dystrophin-gene mutation on mdx mouse behavior. I. Retention deficits at long delays in spontaneous alternation and bar-pressing tasks. *Behav. Genet.* **25**, 569-579.
- Vaillend, C., Billard, J. M., Claudepierre, T., Rendon, A., Dutar, P. and Ungerer, A. (1998). Spatial discrimination learning and CA1 hippocampal synaptic plasticity in mdx and mdx3cv mice lacking dystrophin gene products. *Neuroscience* **86**, 53-66.
- Vaillend, C., Ungerer, A. and Billard, J. M. (1999). Facilitated NMDA receptor-mediated synaptic plasticity in the hippocampal CA1 area of dystrophin-deficient mice. *Synapse* **33**, 59-70.
- Vaillend, C., Billard, J. M. and Laroche, S. (2004). Impaired long-term spatial and recognition memory and enhanced CA1 hippocampal LTP in the dystrophin-deficient Dmd(mdx) mouse. *Neurobiol. Dis.* **17**, 10-20.
- Vaillend, C., Perronnet, C., Ros, C., Gruszczynski, C., Goyenvallé, A., Laroche, S., Danos, O., Garcia, L. and Peltekian, E. (2010). Rescue of a dystrophin-like protein by exon skipping in vivo restores GABA<sub>A</sub>-receptor clustering in the hippocampus of the mdx mouse. *Mol. Ther.* **18**, 1683-1688.
- Valentine, B. A. and Cooper, B. J. (1991). Canine X-linked muscular dystrophy: selective involvement of muscles in neonatal dogs. *Neuromuscul. Disord.* **1**, 31-38.
- Valentine, B. A., Cooper, B. J., Cummings, J. F. and deLahunta, A. (1986). Progressive muscular dystrophy in a golden retriever dog: light microscope and ultrastructural features at 4 and 8 months. *Acta Neuropathol.* **71**, 301-310.
- Valentine, B. A., Cooper, B. J., de Lahunta, A., O'Quinn, R. and Blue, J. T. (1988). Canine X-linked muscular dystrophy. An animal model of Duchenne muscular dystrophy: clinical studies. *J. Neurol. Sci.* **88**, 69-81.
- Valentine, B. A., Blue, J. T. and Cooper, B. J. (1989a). The effect of exercise on canine dystrophic muscle. *Ann. Neurol.* **26**, 588.
- Valentine, B. A., Cooper, B. J. and Gallagher, E. A. (1989b). Intracellular calcium in canine muscle biopsies. *J. Comp. Pathol.* **100**, 223-230.
- Valentine, B. A., Cummings, J. F. and Cooper, B. J. (1989c). Development of Duchenne-type cardiomyopathy. Morphologic studies in a canine model. *Am. J. Pathol.* **135**, 671-678.
- Valentine, B. A., Kornegay, J. N. and Cooper, B. J. (1989d). Clinical electromyographic studies of canine X-linked muscular dystrophy. *Am. J. Vet. Res.* **50**, 2145-2147.
- Valentine, B. A., Blue, J. T., Shelley, S. M. and Cooper, B. J. (1990a). Increased serum alanine aminotransferase activity associated with muscle necrosis in the dog. *J. Vet. Intern. Med.* **4**, 140-143.
- Valentine, B. A., Cooper, B. J., Cummings, J. F. and de Lahunta, A. (1990b). Canine X-linked muscular dystrophy: morphologic lesions. *J. Neurol. Sci.* **97**, 1-23.
- Valentine, B. A., Chandler, S. K., Cummings, J. F. and Cooper, B. J. (1991). In vitro characteristics of normal and dystrophic skeletal muscle from dogs. *Am. J. Vet. Res.* **52**, 104-107.
- Valentine, B. A., Winand, N. J., Pradhan, D., Moise, N. S., de Lahunta, A., Kornegay, J. N. and Cooper, B. J. (1992). Canine X-linked muscular dystrophy as an animal model of Duchenne muscular dystrophy: a review. *Am. J. Med. Genet.* **42**, 352-356.
- Vallese, D., Nüchtern, E., Duguez, S., Ferry, A., Trollet, C., Aamiri, A., Vosschenrich, C. A., Fichtbauer, E. M., Di Santo, J. P., Vitiello, L. et al. (2013). The Rag2<sup>fl2rb</sup>Dmd<sup>-/-</sup> mouse: a novel dystrophic and immunodeficient model to assess innovating therapeutic strategies for muscular dystrophies. *Mol. Ther.* **21**, 1950-1957.
- van Deutekom, J. C., Janson, A. A., Ginjaar, I. B., Frankhuizen, W. S., Aartsma-Rus, A., Bremmer-Bout, M., den Dunnen, J. T., Koop, K., van der Kooi, A. J., Goemans, N. M. et al. (2007). Local dystrophin restoration with antisense oligonucleotide PRO051. *N. Engl. J. Med.* **357**, 2677-2686.
- van Putten, M., Hulsker, M., Nadarajah, V. D., van Heiningen, S. H., van Huizen, E., van Iterson, M., Admiraal, P., Messemaker, T., den Dunnen, J. T., 't Hoen, P. A. et al. (2012a). The effects of low levels of dystrophin on mouse muscle function and pathology. *PLoS ONE* **7**, e31937.
- van Putten, M., Kumar, D., Hulsker, M., Hoogaars, W. M., Plomp, J. J., van Opstal, A., van Iterson, M., Admiraal, P., van Ommen, G. J., 't Hoen, P. A. et al. (2012b). Comparison of skeletal muscle pathology and motor function of dystrophin and utrophin deficient mouse strains. *Neuromuscul. Disord.* **22**, 406-417.
- van Putten, M., Hulsker, M., Young, C., Nadarajah, V. D., Heemskerck, H., van der Weerd, L., 't Hoen, P. A., van Ommen, G. J. and Aartsma-Rus, A. M. (2013). Low dystrophin levels increase survival and improve muscle pathology and function in dystrophin/utrophin double-knockout mice. *FASEB J.* **27**, 2484-2495.
- Varki, A. (2010). Colloquium paper: uniquely human evolution of sialic acid genetics and biology. *Proc. Natl. Acad. Sci. USA* **107** Suppl. 2, 8939-8946.
- Verhaart, I. E. and Aartsma-Rus, A. (2012). Gene therapy for Duchenne muscular dystrophy. *Curr. Opin. Neurol.* **25**, 588-596.
- Vulin, A., Barthélémy, I., Goyenvallé, A., Thibaud, J. L., Beley, C., Griffith, G., Benchaour, R., le Hir, M., Unterfinger, Y., Lorain, S. et al. (2012). Muscle function recovery in golden retriever muscular dystrophy after AAV1-U7 exon skipping. *Mol. Ther.* **20**, 2120-2133.
- Wagner, K. R., McPherron, A. C., Winik, N. and Lee, S. J. (2002). Loss of myostatin attenuates severity of muscular dystrophy in mdx mice. *Ann. Neurol.* **52**, 832-836.
- Wakefield, P. M., Tinsley, J. M., Wood, M. J., Gilbert, R., Karpati, G. and Davies, K. E. (2000). Prevention of the dystrophic phenotype in dystrophin/utrophin-deficient muscle following adenovirus-mediated transfer of a utrophin minigene. *Gene Ther.* **7**, 201-204.
- Wakefield, S. E., Dimberg, E. L., Moore, S. A. and Tseng, B. S. (2009). Dystrophinopathy presenting with arrhythmia in an asymptomatic 34-year-old man: a case report. *J. Med. Case Rep.* **3**, 8625.
- Walmsley, G. L., Arechavala-Gomez, V., Fernandez-Fuente, M., Burke, M. M., Nagel, N., Holder, A., Stanley, R., Chandler, K., Marks, S. L., Muntoni, F. et al. (2010). A Duchenne muscular dystrophy gene hot spot mutation in dystrophin-deficient Cavalier King Charles spaniels is amenable to exon 51 skipping. *PLoS ONE* **5**, e8647.
- Walsh, S., Nygren, J., Pontén, A. and Jovinge, S. (2011). Myogenic reprogramming of bone marrow derived cells in a W<sup>41</sup>Dmd(mdx) deficient mouse model. *PLoS ONE* **6**, e27500.
- Wang, B., Li, J. and Xiao, X. (2000). Adeno-associated virus vector carrying human minidystrophin genes effectively ameliorates muscular dystrophy in mdx mouse model. *Proc. Natl. Acad. Sci. USA* **97**, 13714-13719.
- Wang, Z., Zhu, T., Qiao, C., Zhou, L., Wang, B., Zhang, J., Chen, C., Li, J. and Xiao, X. (2005). Adeno-associated virus serotype 8 efficiently delivers genes to muscle and heart. *Nat. Biotechnol.* **23**, 321-328.
- Wang, Z., Kuhr, C. S., Allen, J. M., Blankinship, M., Gregorevic, P., Chamberlain, J. S., Tapscott, S. J. and Storb, R. (2007). Sustained AAV-mediated dystrophin expression in a canine model of Duchenne muscular dystrophy with a brief course of immunosuppression. *Mol. Ther.* **15**, 1160-1166.
- Wang, Y., Marino-Enriquez, A., Bennett, R. R., Zhu, M., Shen, Y., Eilers, G., Lee, J. C., Henze, J., Fletcher, B. S., Gu, Z. et al. (2014). Dystrophin is a tumor suppressor in human cancers with myogenic programs. *Nat. Genet.* **46**, 601-606.

- Warner, L. E., DelloRusso, C., Crawford, R. W., Rybakova, I. N., Patel, J. R., Ervasti, J. M. and Chamberlain, J. S. (2002). Expression of Dp260 in muscle tethers the actin cytoskeleton to the dystrophin-glycoprotein complex and partially prevents dystrophy. *Hum. Mol. Genet.* **11**, 1095-1105.
- Wasala, N. B., Bostick, B., Yue, Y. and Duan, D. (2013). Exclusive skeletal muscle correction does not modulate dystrophic heart disease in the aged mdx model of Duchenne cardiomyopathy. *Hum. Mol. Genet.* **22**, 2634-2641.
- Wein, N., Vulin, A., Falzarano, M. S., Szigartyo, C. A., Maiti, B., Findlay, A., Heller, K. N., Uhlén, M., Bakthavachalu, B., Messina, S. et al. (2014). Translation from a DMD exon 5 IRES results in a functional dystrophin isoform that attenuates dystrophinopathy in humans and mice. *Nat. Med.* **20**, 992-1000.
- Wells, D. J., Wells, K. E., Asante, E. A., Turner, G., Sunada, Y., Campbell, K. P., Walsh, F. S. and Dickson, G. (1995). Expression of human full-length and minidystrophin in transgenic mdx mice: implications for gene therapy of Duchenne muscular dystrophy. *Hum. Mol. Genet.* **4**, 1245-1250.
- Wentink, G. H., van der Linde-sipman, J. S., Meijer, A. E. F. H., Kamphuisen, H. A. C., van Vorstenbosch, C. J. A. H. V., Hartman, W. and Hendriks, H. J. (1972). Myopathy with a possible recessive X-linked inheritance in a litter of Irish Terriers. *Vet. Pathol.* **9**, 328-349.
- West, N. A., Yang, M. L., Weitzenkamp, D. A., Andrews, J., Meaney, F. J., Oleszek, J., Miller, L. A., Matthews, D. and DiGiuseppi, C. (2013). Patterns of growth in ambulatory males with Duchenne muscular dystrophy. *J. Pediatr.* **163**, 1759-1763 e1.
- Winand, N. J., Edwards, M., Pradhan, D., Berian, C. A. and Cooper, B. J. (1994a). Deletion of the dystrophin muscle promoter in feline muscular dystrophy. *Neuromuscul. Disord.* **4**, 433-445.
- Winand, N. J., Pradhan, D. and Cooper, B. J. (1994b). Molecular characterization of severe Duchenne-type muscular dystrophy in a family of Rottweiler dogs. In *Molecular Mechanism of Neuromuscular Disease*. Tucson, AZ: Muscular Dystrophy Association.
- Wood, M. J. (2013). To skip or not to skip: that is the question for Duchenne muscular dystrophy. *Mol. Ther.* **21**, 2131-2132.
- Wu, B., Moulton, H. M., Iversen, P. L., Jiang, J., Li, J., Li, J., Spurney, C. F., Sali, A., Guerron, A. D., Nagaraju, K. et al. (2008). Effective rescue of dystrophin improves cardiac function in dystrophin-deficient mice by a modified morpholino oligomer. *Proc. Natl. Acad. Sci. USA* **105**, 14814-14819.
- Wu, B., Li, Y., Morcos, P. A., Doran, T. J., Lu, P. and Lu, Q. L. (2009). Octa-guanidine morpholino restores dystrophin expression in cardiac and skeletal muscles and ameliorates pathology in dystrophic mdx mice. *Mol. Ther.* **17**, 864-871.
- Wu, B., Xiao, B., Cloer, C., Shaban, M., Sali, A., Lu, P., Li, J., Nagaraju, K., Xiao, X. and Lu, Q. L. (2011). One-year treatment of morpholino antisense oligomer improves skeletal and cardiac muscle functions in dystrophic mdx mice. *Mol. Ther.* **19**, 576-583.
- Xu, R., Camboni, M. and Martin, P. T. (2007). Postnatal overexpression of the CT GalNAc transferase inhibits muscular dystrophy in mdx mice without altering muscle growth or neuromuscular development: evidence for a utrophin-independent mechanism. *Neuromuscul. Disord.* **17**, 209-220.
- Yamamoto, K., Yamada, D., Kabuta, T., Takahashi, A., Wada, K. and Sekiguchi, M. (2010). Reduction of abnormal behavioral response to brief restraint by information from other mice in dystrophin-deficient mdx mice. *Neuromuscul. Disord.* **20**, 505-511.
- Yang, H. T., Shin, J. H., Hakim, C. H., Pan, X., Terjung, R. L. and Duan, D. (2012). Dystrophin deficiency compromises force production of the extensor carpi ulnaris muscle in the canine model of Duchenne muscular dystrophy. *PLoS ONE* **7**, e44438.
- Yin, H., Moulton, H. M., Seow, Y., Boyd, C., Boutilier, J., Iversen, P. and Wood, M. J. (2008). Cell-penetrating peptide-conjugated antisense oligonucleotides restore systemic muscle and cardiac dystrophin expression and function. *Hum. Mol. Genet.* **17**, 3909-3918.
- Yin, H., Saleh, A. F., Betts, C., Camelliti, P., Seow, Y., Ashraf, S., Arzumanov, A., Hammond, S., Merritt, T., Gait, M. J. et al. (2011). Pip5 transduction peptides direct high efficiency oligonucleotide-mediated dystrophin exon skipping in heart and phenotypic correction in mdx mice. *Mol. Ther.* **19**, 1295-1303.
- Yokota, T., Lu, Q. L., Partridge, T., Kobayashi, M., Nakamura, A., Takeda, S. and Hoffman, E. (2009). Efficacy of systemic morpholino exon-skipping in Duchenne dystrophy dogs. *Ann. Neurol.* **65**, 667-676.
- Yoshimura, M., Sakamoto, M., Ikemoto, M., Mochizuki, Y., Yuasa, K., Miyagoe-Suzuki, Y. and Takeda, S. (2004). AAV vector-mediated microdystrophin expression in a relatively small percentage of mdx myofibers improved the mdx phenotype. *Mol. Ther.* **10**, 821-828.
- Yuasa, K., Yoshimura, M., Urasawa, N., Ohshima, S., Howell, J. M., Nakamura, A., Hijikata, T., Miyagoe-Suzuki, Y. and Takeda, S. (2007). Injection of a recombinant AAV serotype 2 into canine skeletal muscles evokes strong immune responses against transgene products. *Gene Ther.* **14**, 1249-1260.
- Yue, Y., Li, Z., Harper, S. Q., Davisson, R. L., Chamberlain, J. S. and Duan, D. (2003). Microdystrophin gene therapy of cardiomyopathy restores dystrophin-glycoprotein complex and improves sarcolemma integrity in the mdx mouse heart. *Circulation* **108**, 1626-1632.
- Yue, Y., Skimming, J. W., Liu, M., Strawn, T. and Duan, D. (2004). Full-length dystrophin expression in half of the heart cells ameliorates beta-isoproterenol-induced cardiomyopathy in mdx mice. *Hum. Mol. Genet.* **13**, 1669-1675.
- Yue, Y., Ghosh, A., Long, C., Bostick, B., Smith, B. F., Kornegay, J. N. and Duan, D. (2008). A single intravenous injection of adeno-associated virus serotype-9 leads to whole body skeletal muscle transduction in dogs. *Mol. Ther.* **16**, 1944-1952.
- Yugeta, N., Urasawa, N., Fujii, Y., Yoshimura, M., Yuasa, K., Wada, M. R., Nakura, M., Shimatsu, Y., Tomohiro, M., Takahashi, A. et al. (2006). Cardiac involvement in Beagle-based canine X-linked muscular dystrophy in Japan (CXMDJ): electrocardiographic, echocardiographic, and morphologic studies. *BMC Cardiovasc. Disord.* **6**, 47.
- Zatz, M., Pavanello, R. C., Lazar, M., Yamamoto, G. L., Lourenço, N. C., Cerqueira, A., Nogueira, L. and Vainzof, M. (2014). Milder course in Duchenne patients with nonsense mutations and no muscle dystrophin. *Neuromuscul. Disord.* **24**, 986-989.
- Zhang, Y. and Duan, D. (2012). Novel mini-dystrophin gene dual adeno-associated virus vectors restore neuronal nitric oxide synthase expression at the sarcolemma. *Hum. Gene Ther.* **23**, 98-103.
- Zhang, Y., Yue, Y., Li, L., Hakim, C. H., Zhang, K., Thomas, G. D. and Duan, D. (2013). Dual AAV therapy ameliorates exercise-induced muscle injury and functional ischemia in murine models of Duchenne muscular dystrophy. *Hum. Mol. Genet.* **22**, 3720-3729.
- Zhou, L., Rafael-Fortney, J. A., Huang, P., Zhao, X. S., Cheng, G., Zhou, X., Kaminski, H. J., Liu, L. and Ransohoff, R. M. (2008). Haploinsufficiency of utrophin gene worsens skeletal muscle inflammation and fibrosis in mdx mice. *J. Neurol. Sci.* **264**, 106-111.
- Zucconi, E., Valadares, M. C., Vieira, N. M., Bueno, C. R., Jr, Secco, M., Jazedje, T., da Silva, H. C., Vainzof, M. and Zatz, M. (2010). Ringo: discordance between the molecular and clinical manifestation in a golden retriever muscular dystrophy dog. *Neuromuscul. Disord.* **20**, 64-70.

**Supplementary Table 1. Animal models for DMD**

<b>Non-mammalian</b>	<b>Mutation</b>	<b>Comments</b>	<b>Reference</b>
C. elegans		Various models available.	Reviewed in Chamberlain and Benian, 2000
Drosophila		Various models available.	Reviewed in Lloyd and Taylor, 2010
Zebrafish		Dystrophin-null sapje model has served as an excellent high-throughput system for drug screening.	Reviewed in Kunkel et al., 2006; Berger and Currie, 2012
<b>Murine*</b>	<b>Mutation</b>	<b>Comments</b>	<b>Reference</b>
<b>Dystrophin-deficient mice</b>			
Mdx	Exon 23 point mutation	Most widely used model. On the C57BL/10 background. Available from the Jackson Laboratory (JL#001801).	Bulfield et al., 1984
Albino Mdx	Same as mdx	Mdx on the Albino background.	Krivov et al, 2009
Mdx/BALB/c	Same as mdx	Mdx on the BALB/c background.	Schmidt et al., 2011
Mdx/BL6	Same as mdx	Mdx on the C57BL/6 background. This strain has been used to generate IL-10/dystrophin dko mice (Nitahara-Kasahara et al., 2014) and myostatin/dystrophin dko mice (Wagner et al., 2002).	Duan et al., unpublished
Mdx/C3H	Same as mdx	Mdx on the C3H background.	Schmidt et al., 2011
Mdx/DBA2	Same as mdx	Mdx on the DBA2 background. More severe dystrophic phenotype. Available from the Jackson Laboratory (JL#013141).	Fukada et al., 2010
Mdx/FVB	Same as mdx	Mdx on the FVB background.	Wasala et al., 2015
Mdx2cv	Intron 42 point mutation	Chemically induced mutation. On the C57BL/6 background. Fewer revertant fibers. Available from the Jackson Laboratory (JL#002388).	Chapman et al., 1989
Mdx3cv	Intron 65 point mutation	Chemically induced mutation. On the C57BL/6 background. All dystrophin isoforms are eliminated but a near-full-length dystrophin is expressed at ~5% of the wild type level. Available from the Jackson Laboratory (JL#002377).	Chapman et al., 1989
Mdx4cv	Exon 53 point mutation	Chemically induced mutation. On the C57BL/6 background. Fewer revertant fibers. Available from the Jackson Laboratory (JL#002378).	Chapman et al., 1989
Mdx5cv	Exon 10 point mutation	Chemically induced mutation. On the C57BL/6 background. Skeletal muscle disease is more severe. Available from the Jackson Laboratory (JL#002388).	Chapman et al., 1989

CRKHR1	Unsequenced, dystrophin deficiency confirmed by immunofluorescence staining	ENU chemically induced mutation on the C3H background, screened for and found to have an elevated CK, centrally nucleated myofibers and dystrophin deficiency.	Aigner et al., 2009
Mdx52	Exon 52 deletion	Targeted inactivation. On the C57BL/6 background. Hot-spot mutation.	Araki et al., 1997
Mdx $\beta$ geo	Insertion of the $\beta$ -geo gene trap cassette in intron 63	LacZ replaced the CR and CT domain. All dystrophin isoforms are mutated. The full-length dystrophin-LacZ fusion protein is not detectable but Dp71-LacZ fusion protein can be detected.	Wertz and Füchtbauer., 1998
DMD-null	Entire DMD gene deletion	Generated by Cre-loxP technology.	Kudoh et al., 2005
Dp71-null	Insertion of a $\beta$ -geo cassette in intron 62. It disrupts Dp71 unique exon 1	Selective elimination of Dp71. Dp71 promoter driven LacZ expression. Similar LacZ expression pattern as mdx $\beta$ geo but muscle is not dystrophic. Dp71 deficiency is associated with early cataract formation in mice.	Sarig et al., 1999; Fort et al., 2014
Dup2	Exon 2 duplication	The only duplication mutation model. On the C57Bl/6 background.	Wein et al., 2014
<b>Immune deficient mdx mice</b>			
NSG-mdx4cv	Prkdc and IL2rg double deficient on the mdx4cv background	B cell, T cell and NK cell deficient. Innate immunity deficient. Multiple cytokine signaling pathway deficient. NSG mice are available from the Jackson Laboratory (JL#005557).	Arpke et al., 2013
Rag2 <sup>-/-</sup> Il2rb <sup>-/-</sup> Dmd <sup>-/-</sup>	Rag2 and IL2rb double deficient on the mdx $\beta$ geo background	B cell, T cell and NK cell deficient. Multiple cytokine signaling pathway deficient. No revertant fiber. Rag2/Il2rb double knock out strain is available from Taconic (#4111).	Bencze et al., 2012; Vallese et al., 2013
Scid mdx	DNA-dependent protein kinase catalytic subunit deficient (prkdc) on the mdx background	B cell and T cell deficient. Available from the Jackson Laboratory (JL#018018).	Farini et al., 2007
W41 mdx	C-kit receptor deficient on the mdx background	Haematopoietic deficient. Good for study bone marrow cell therapy in the absence of myeloablation by irradiation.	Walsh et al., 2011
<b>Phenotypic dko mice</b>			
$\alpha$ 7/dystrophin dko or mdx/ $\alpha$ 7 <sup>-/-</sup>	$\alpha$ 7-Integrin/dystrophin double deficient	Severe dystrophic phenotype. Two independent lines exist. One is generated by Mayer and colleagues. The other is generated in the Burkin lab.	Rooney et al., 2006; Guo et al., 2006
Adbn <sup>-/-</sup> mdx	$\alpha$ -Dystrobrevin/dystrophin double deficient	Severe dystrophic phenotype.	Grady et al., 1999
Cmah-mdx	Cmah/dystrophin double deficient	Severe dystrophic phenotype. Humanized model. Available from the the Jackson Laboratory (JL#017929).	Chandrasekharan et al., 2010
d-Dko	$\delta$ -Sarcoglycan/dystrophin double deficient	Severe dystrophic phenotype.	Li et al., 2009

Desmin <sup>-/-</sup> mdx4cv	Desmin/dystrophin double deficient	Severe dystrophic phenotype.	Banks et al., 2014
Dmd <sup>mdx</sup> /Large <sup>myd</sup>	like-glycosyltransferase (LARGE)/dystrophin double deficient	Severe dystrophic phenotype.	Martins et al., 2013
DMD-null; Adam8 <sup>-/-</sup>	ADAM8 deficient and entire DMD gene deletion	This mouse is on the DMD-null background (Kudoh et al., 2005). ADAM8 deficiency hinders invasion of neutrophils into the damaged myofiber. As a consequence, injured myofibers are not efficiently removed in dystrophin-null muscle.	Nishimura et al., 2014
Dysferlin/dystrophin dko	Dysferlin/dystrophin double deficient	Severe dystrophic phenotype. Two independent lines exist. One is a cross between naturally occurring dysferlin-null A/J mice and mdx5cv mice. The other is a cross between dysferlin knockout mice and mdx mice.	Han et al., 2011; Hosur et al., 2012
IL-10 <sup>-/-</sup> /mdx	Interleukin-10/dystrophin double deficient	Severe dystrophic phenotype. Prominent cardiomyopathy.	Nitahara-Kasahara et al., 2014
mdx/mTR	Telomerase RNA/dystrophin double deficient	Severe dystrophic phenotype. Two strains available at the Jackson Laboratory. One is on the mdx4cv background (JL#023535). The other is on the mdx background (JL#018915).	Sacco et al., 2010
mdx:MyoD <sup>-/-</sup>	MyoD/dystrophin double deficient	Severe dystrophic phenotype. MyoD is only expressed in skeletal muscle. Interestingly, dko mice show severe dilated cardiomyopathy.	Megeney et al., 1996
mdx:utrophin <sup>-/-</sup> (Grady strain) or mdx/utrophin <sup>-/-</sup> (Deconinck strain)	Utrophin/dystrophin double deficient	Severe dystrophic phenotype. Two independent strains exist. Both are available at the Jackson Laboratory. In the Grady strain (Utrntm1Jrs Dmdmdx), all utrophin isoforms are inactivated by a targeted mutation at the utrophin CR domain (JL#016622). In the Deconinck strain (Utrntm1Ked Dmdmdx), only the largest utrophin isoform is inactivated by a targeted mutation at utrophin exon 7 (JL#014563).	Deconinck et al., 1997; Grady et al., 1997
PAI-1 <sup>-/-</sup> mdx	Plasminogen activator inhibitor-1 (PAI-1)/dystrophin double deficient	Dko mice show early onset fibrosis and higher CK than mdx.	Ardite et al., 2012
<b>Dko mice with phenotype similar to mdx</b>			
msDKO	Cytosolic $\gamma$ -actin/dystrophin double deficient	Phenotype similar to that of mdx.	Prins et al., 2008
iNOS-null mdx or iNOS/Dys DKO	iNOS/dystrophin double deficient	Phenotype similar to that of mdx. Two independent strains exist. The Tidball lab strain is on the mdx background. The Duan lab strain is on the mdx4cv background.	Villalta et al., 2009; Li et al., 2011a
PVKO-mdx	Parvalbumin/dystrophin double deficient	Phenotype similar to that of mdx.	Raymackers et al., 2003
<b>Dko mice with reduced disease</b>			

cIAP1 <sup>-/-</sup> ;mdx	Cellular inhibitor of apoptosis 1 (cIAP1)/dystrophin double deficient	Reduced disease. Soleus pathology reduced. Diaphragm function improved.	Enwere et al., 2013
Fib <sup>-/-</sup> mdx	Fibrinogen/dystrophin double deficient	Reduced disease. Inflammation and degeneration reduced. Regeneration, grip strength and treadmill improved.	Vidal et al., 2012
Finp1 <sup>-/-</sup> mdx4CV	Folliculin interacting protein-1 (Fnip1) deficient mice on the mdx4cv background.	Disease reduced due to Finp1-deficiency associated switch to type I fiber. Central nucleation and the CK level are reduced. Membrane integrity improved.	Reyes et al., 2014 December 29 (online publication ahead of print)
Mdx-casp	Caspase-12/dystrophin double deficient	Reduced disease. Muscle force improved. Myofiber degeneration reduced but central nucleation, CK and fibrosis not changed.	Moorwood and Barton et al., 2014
mdx/Mkp5 <sup>-/-</sup>	Mitogen-activated protein kinases phosphatase-5 (Mkp5)/dystrophin double deficient	Reduced disease. Reduced degeneration, CK. Improved regeneration, grip strength and EDL force.	Shi et al., 2013
mdx/myd88 <sup>-/-</sup>	Myeloid differentiation primary response protein 88 (myd88)/dystrophin double deficient	Reduced disease. Skeletal muscle disease is reduced in 12-m-old mice but not in 2 to 4-m-old mice. Heart disease is reduced in 10 to 12-m-old mice.	Henriques-Pons et al., 2014
mdx/q <sup>-/-</sup>	Protein kinase C q (PKCq)/dystrophin double deficient	Reduced disease. Reduced degeneration and inflammation. Improved regeneration and treadmill performance.	Madaro et al, 2012
mdx/sgk1 <sup>-/-</sup>	Serum-and glucocorticoid-induced kinase 1 (sgk1) and dystrophin double deficient	Reduced disease. Improved specific force, muscle fatigueability, and histology. Normalization of fibrosis.	Steinberger et al., 2014
mdx-Xist <sup>Δhs</sup>	Xist/dystrophin double knockout	Variable level of dystrophin expression as low as 5%.	van Putten et al., 2013
Mstn <sup>-/-</sup> /mdx	Myostatin/dystrophin double deficient	Reduced disease. Limb muscle is more muscular and stronger. Diaphragm fibrosis is reduced.	Wagner et al 2002
OPN DMM	Osteopontin (OPN)/dystrophin double deficient	Reduced disease. Improved regeneration and grip strength. Reduced inflammation and fibrosis.	Vetrone et al., 2009
<b>Transgenic mdx mice</b>			
Full-length dystrophin transgenic mdx	Transgenic over-expression of full-length dystrophin in the mdx background	Multiple lines were generated by different labs. All show protection. 50-fold over-expression is not toxic to skeletal muscle.	Cox et al., 1993; Phelps et al., 1995; Wells et al., 1995
Dp71 transgenic mdx	Transgenic over-expression of Dp71 in the mdx background	More severe disease confirmed by two independent lines made in two different labs.	Cox et al., 1994; Greenberg et al., 1994
Dp116 transgenic mdx4cv	Transgenic over-expression of Dp116 in the mdx4cv background	More severe disease.	Judge et al., 2006
Dp116:mdx:utrophin <sup>-/-</sup>	Transgenic over-expression of Dp116 in the utrophin/dystrophin dko background	Improved growth, mobility and lifespan but no change in histopathology, specific force and CK.	Judge et al., 2011

Dp260 transgenic mdx	Transgenic over-expression of Dp260 in the mdx background	Reduced but not completely prevented histopathology. Improved resistance to eccentric contraction injury but did not improve specific force.	Warner et al., 2002
Dp260 in mdx/utrn <sup>-/-</sup>	Transgenic over-expression of Dp260 in the utrophin/dystrophin dko background	Severe lethal phenotype is converted to mild myopathy.	Gaedigk et al., 2006
Δ17-48 transgenic mdx	Transgenic over-expression of the naturally occurring Δ17-48 mini-dystrophin gene in the mdx background	Two independent lines were generated. Both showed muscle protection.	Phelps et al., 1995; Wells et al., 1992 and 1995
ΔH2-R19 transgenic mdx	Transgenic over-expression of the synthetic ΔH2-R19 mini-dystrophin gene in the mdx background	Completely reduced histopathology and normalized muscle force but did not restore sarcolemmal nNOS.	Harper et al., 2002
Cardiac-specific ΔH2-R19 transgenic mdx	Transgenic over-expression of the synthetic ΔH2-R19 mini-dystrophin gene in the heart of mdx mice	Effectively protected but did not fully normalize the heart.	Bostick et al., 2009
ΔH2-R15 transgenic mdx	Transgenic over-expression of the synthetic ΔH2-R15 mini-dystrophin gene in the mdx background	Complete correction of the dystrophic phenotype including nNOS and functional ischemia.	Lai et al., 2009; Hakim and Duan 2013
Micro-dystrophin transgenic	Transgenic over-expression of various synthetic micro-dystrophin genes in the mdx background	Many lines are established for different microgenes. ΔR4-23 and ΔR4-23/C yield excellent protection but they don't restore nNOS. Hinge 2 in these two microgenes compromises function. ΔR2-15/R18-19/R20-23/C contains hinge 3 and is the only microgene capable of restoring nNOS.	Harper et al., 2002; Li et al., 2011b; Sakamoto et al., 2002, Hakim et al., 2013; Wang et al., 2008; Ferrer et al 2004
Fiona	Transgenic over-expression of full-length utrophin in the mdx background	Excellent protection but does not restore nNOS.	Tinsley et al., 1998; Li et al., 2010
Laminin α1 transgenic mdx	Transgenic over-expression of the laminin α1 chain in the mdx background	Used to study laminin-111 protein therapy. Phenotype appeared to be very similar to mdx, without any benefit or harm.	Gawlik et al., 2011
<b>Canine</b>	<b>Mutation</b>	<b>Comments</b>	<b>References</b>
Alaskan malamute dystrophic dog	Unknown but dystrophin deficiency is confirmed	Case report.	Ito et al., 2011
CKCS-MD	Intron 50 point mutation resulting in exon 50 exclusion from the mRNA	Spontaneous mutation in the Cavalier King Charles Spaniel (CKCS) breed. Small breed. Hot-spot mutation. Colony maintained at Royal Veterinary College, UK.	Walmsley et al., 2010
Cocker spaniel dystrophic dog	Deletion of four nucleotides in exon 65	No colony established.	Kornegay et al., 2012

CXMDj	Same as GRMD	GRMD crossed to the beagle background. Small breed. Reduced phenotype. Colony maintained at the National Center of Neurology and Psychiatry, Japan.	Shimatsu et al., 2003
GLRMD	Same as GRMD	Hybrid background of golden retriever and Labrador retriever.	Miyazato et al., 2011
Grand Basset Griffon Vendeen dystrophic dog	Unknown but dystrophin deficiency is confirmed	Case report.	Klarenbeek et al., 2007
GRMD	Intron 6 point mutation resulting in the exclusion of exon 7 from the mRNA	Spontaneous mutation in the golden retriever (GR) breed. Similar disease as human patients. Most widely used dog model. Multiple colonies exist worldwide.	Valentine et al., 1986; Cooper et al., 1988; Kornegay et al., 1988
GSHP MD	Whole gene deletion	Spontaneous mutation in the German short haired pointer (GSHP) breed.	Schatzberg et al., 1999
Hybrid cDMD dogs with mixed genetic background and multiple mutations	Various	Generated by artificial insemination by crossing different cDMD breeds. Resembles genetic diversity seen in human patients.	Fine et al., 2011; Miyazato et al., 2011; Shin et al., 2013a; Shin et al 2013b; Yang et al 2012;
Japanese spitz dystrophic dog	Inversion between intron 19 of dystrophin gene and retinitis pigmentosa GTPase regulator gene (RPGN)	Case report.	Jones et al., 2004; Atencia-Fernandez et al., 2015
Labrador Retriever BMD dog	Unknown	Case report. Low-level uniform expression of a ~135 kDa dystrophin protein. Mild phenotype. This is the only reported BMD dog case.	Baroncelli et al., 2014
Labrador Retriever dystrophic dog	Unknown but dystrophin deficiency is confirmed	Case report.	Bergman et al., 2002
Labrador Retriever dystrophic dog	Repetitive element insertion in intron 19	Spontaneous mutation. Colony maintained at the University of Missouri and Auburn University.	Smith et al., 2007
Lurcher dystrophic dog	Unknown but dystrophin deficiency is confirmed	Case report of two pups in the same litter. Possible response to L-carnitine supplementation in one of the pups.	Giannasi et al., 2015
Miniature schnauzer dystrophic dog	Unknown but dystrophin deficiency is confirmed	Case report.	Paola et al., 1993
Norfolk Terrier dystrophy	Unknown but dystrophin deficiency is confirmed	No colony established.	Beltran et al., 2014
Old English sheepdog dystrophic dog	Unknown but dystrophin deficiency is confirmed	Case report.	Wieczorek et al., 2006
Rat terrier dystrophic dog	Unknown but dystrophin deficiency is confirmed	Case report. Unusual hypertrophic presentation in the cervical and proximal limb muscles.	Wetterman et al., 2000
Rottweiler dystrophic dog	Nonsense point mutation in exon 58	No colony established.	Kornegay et al., 2012; Winand et al 1994b

Tibetan terrier dystrophic dog	Exons 8-29 deletion	No colony established.	Kornegay et al., 2012
Weimaraner dystrophic dog	Unknown but dystrophin deficiency is confirmed	Case report.	Baltzer et al., 2007
Welsh Corgi MD	LINE-1 insertion in intron 13	Spontaneous mutation. Colony maintained at the University of Missouri and Auburn University.	Smith et al., 2011

Other Mammalian	Mutation	Comments	References
DMD rat #1	Exon 3-6 deletion using the CRISPR/Cas technology	New model.	Nakamura et al., 2014
DMD rat #2	Frame shifting 11 bp deletion in exon 23 using TALEN technology, creates premature stop codon	New model. 5% revertant fiber expression. More severe skeletal muscle fibrosis than <i>mdx</i> . Fibrotic lesions in myocardium, though showed concentric hypertrophy rather than eccentric.	Larcher et al., 2014
DMD cat #1	Dp427 promoter and exon 1 deletion	Spontaneous mutation. Prominent muscle hypertrophy. Independent cases have been reported in USA and UK.	Winand et al., 1994a; Carpenter et al., 1989; Blunden and Gower., 2011
DMD cat #2	Similar but not identical deletion as in DMD cat #1	Spontaneous mutation. Primary symptom is regurgitation due to megaesophagus. However, there is no muscle hypertrophy.	Gambino et al., 2014
BMD pig	Exon 41 missense mutation (changing arginine to tryptophan)	Spontaneous mutation. Dystrophin expression is reduced to ~30% of normal. The primary clinical manifestation is stress-induced sudden death. Minimum dystrophic symptom.	Nonneman et al., 2012
DMD Pig #1	Engineered deletion of exon 52	Hot-spot deletion. Marked utrophin upregulation.	Klymiuk et al., 2013
DMD Pig #2	Cre-LoxP engineered deletion of exon 52.	Hot-spot deletion.	Rogers and Swart., 2014

\*, The name of the mouse model is according to the first publication that described the model.

## Reference list for Supplementary Table 1

**Aigner, B., Rathkolb, B., Klawns, M., Sedlmeier, R., Klempt, M., Wagner, S., Michel, D., Mayer, U., Klopstock, T., de Angelis, M. H. et al.** (2009). Generation of N-ethyl-N-nitrosourea-induced mouse mutants with deviations in plasma enzyme activities as novel organ-specific disease models. *Exp Physiol* **94**, 412-21.

**Araki, E., Nakamura, K., Nakao, K., Kameya, S., Kobayashi, O., Nonaka, I., Kobayashi, T. and Katsuki, M.** (1997). Targeted disruption of exon 52 in the mouse dystrophin gene induced muscle degeneration similar to that observed in Duchenne muscular dystrophy. *Biochem Biophys Res Commun* **238**, 492-7.

**Ardite, E., Perdiguero, E., Vidal, B., Gutarra, S., Serrano, A. L. and Munoz-Canoves, P.** (2012). PAI-1-regulated miR-21 defines a novel age-associated fibrogenic pathway in muscular dystrophy. *J Cell Biol* **196**, 163-75.

**Arpke, R. W., Darabi, R., Mader, T. L., Zhang, Y., Toyama, A., Lonetree, C. L., Nash, N., Lowe, D. A., Perlingeiro, R. C. and Kyba, M.** (2013). A new immuno-, dystrophin-deficient model, the NSG-mdx(4Cv) mouse, provides evidence for functional improvement following allogeneic satellite cell transplantation. *Stem Cells* **31**, 1611-20.

**Atencia-Fernandez, S., Shiel, R.E., Mooney, C.T., Nolan, C.M.** (2015). Muscular dystrophy in the Japanese Spitz: an inversion disrupts the *DMD* and *RPGR* genes. *Anim Genet.* [Epub ahead of print] doi: 10.1111/age. 12266.

**Baltzer, W. I., Calise, D. V., Levine, J. M., Shelton, G. D., Edwards, J. F. and Steiner, J. M.** (2007). Dystrophin-deficient muscular dystrophy in a Weimaraner. *J Am Anim Hosp Assoc* **43**, 227-32.

**Banks, G. B., Combs, A. C., Odom, G. L., Bloch, R. J. and Chamberlain, J. S.** (2014). Muscle structure influences utrophin expression in mdx mice. *PLoS Genet* **10**, e1004431.

**Baroncelli, A. B., Abellonio, F., Pagano, T. B., Esposito, I., Peirone, B., Papparella, S. and Paciello, O.** (2014). Muscular dystrophy in a dog resembling human becker muscular dystrophy. *J Comp Pathol* **150**, 429-33.

**Beltran, E., Shelton, G. D., Guo, L. T., Dennis, R., Sanchez-Masian, D., Robinson, D. and De Risio, L.** (2014). Dystrophin-deficient muscular dystrophy in a Norfolk terrier. *J Small Anim Pract*, 2014 Oct 29. doi: 10.1111/jsap.12292. [Epub ahead of print].

**Bencze, M., Negroni, E., Vallese, D., Yacoub-Youssef, H., Chaouch, S., Wolff, A., Aamiri, A., Di Santo, J. P., Chazaud, B., Butler-Browne, G. et al.** (2012). Proinflammatory macrophages enhance the regenerative capacity of human myoblasts by modifying their kinetics of proliferation and differentiation. *Mol Ther* **20**, 2168-79.

**Berger, J. and Currie, P. D.** (2012). Zebrafish models flex their muscles to shed light on muscular dystrophies. *Dis Model Mech* **5**, 726-32.

**Bergman, R. L., Inzana, K. D., Monroe, W. E., Shell, L. G., Liu, L. A., Engvall, E. and Shelton, G. D.** (2002). Dystrophin-deficient muscular dystrophy in a Labrador retriever. *J Am Anim Hosp Assoc* **38**, 255-61.

**Blunden, A. S. and Gower, S.** (2011). Hypertrophic feline muscular dystrophy: diagnostic overview and a novel immunohistochemical diagnostic method using formalin-fixed tissue. *Vet Rec* **168**, 510.

**Bostick, B., Yue, Y., Long, C., Marschalk, N., Fine, D. M., Chen, J. and Duan, D.** (2009). Cardiac expression of a mini-dystrophin that normalizes skeletal muscle force only partially restores heart function in aged Mdx mice. *Mol Ther* **17**, 253-61.

**Bulfield, G., Siller, W. G., Wight, P. A. and Moore, K. J.** (1984). X chromosome-linked muscular dystrophy (mdx) in the mouse. *Proc Natl Acad Sci U S A* **81**, 1189-92.

**Carpenter, J. L., Hoffman, E. P., Romanul, F. C., Kunkel, L. M., Rosales, R. K., Ma, N. S., Dasbach, J. J., Rae, J. F., Moore, F. M., McAfee, M. B. et al.** (1989). Feline muscular dystrophy with dystrophin deficiency. *Am J Pathol* **135**, 909-19.

**Chamberlain, J. S. and Benian, G. M.** (2000). Muscular dystrophy: the worm turns to genetic disease. *Curr Biol* **10**, R795-7.

**Chandrasekharan, K., Yoon, J. H., Xu, Y., deVries, S., Camboni, M., Janssen, P. M., Varki, A. and Martin, P. T.** (2010). A human-specific deletion in mouse Cmah increases disease severity in the mdx model of Duchenne muscular dystrophy. *Sci Transl Med* **2**, 42ra54.

**Chapman, V. M., Miller, D. R., Armstrong, D. and Caskey, C. T.** (1989). Recovery of induced mutations for X chromosome-linked muscular dystrophy in mice. *Proc Natl Acad Sci U S A* **86**, 1292-6.

**Cooper, B. J., Winand, N. J., Stedman, H., Valentine, B. A., Hoffman, E. P., Kunkel, L. M., Scott, M. O., Fischbeck, K. H., Kornegay, J. N., Avery, R. J. et al.** (1988). The homologue of the Duchenne locus is defective in X-linked muscular dystrophy of dogs. *Nature* **334**, 154-6.

**Cox, G. A., Cole, N. M., Matsumura, K., Phelps, S. F., Hauschka, S. D., Campbell, K. P., Faulkner, J. A. and Chamberlain, J. S.** (1993). Overexpression of dystrophin in transgenic mdx mice eliminates dystrophic symptoms without toxicity [see comments]. *Nature* **364**, 725-9.

**Cox, G. A., Sunada, Y., Campbell, K. P. and Chamberlain, J. S.** (1994). Dp71 can restore the dystrophin-associated glycoprotein complex in muscle but fails to prevent dystrophy. *Nat Genet* **8**, 333-9.

**Deconinck, A. E., Rafael, J. A., Skinner, J. A., Brown, S. C., Potter, A. C., Metzinger, L., Watt, D. J., Dickson, J. G., Tinsley, J. M. and Davies, K. E.** (1997). Utrophin-dystrophin-deficient mice as a model for Duchenne muscular dystrophy. *Cell* **90**, 717-27.

**Enwere, E. K., Boudreault, L., Holbrook, J., Timusk, K., Earl, N., LaCasse, E., Renaud, J. M. and Korneluk, R. G.** (2013). Loss of cIAP1 attenuates soleus muscle pathology and improves diaphragm function in mdx mice. *Hum Mol Genet* **22**, 867-78.

**Farini, A., Merigalli, M., Belicchi, M., Battistelli, M., Parolini, D., D'Antona, G., Gavina, M., Ottoboni, L., Constantin, G., Bottinelli, R. et al.** (2007). T and B lymphocyte depletion has a marked effect on the fibrosis of dystrophic skeletal muscles in the scid/mdx mouse. *J Pathol* **213**, 229-38.

**Ferrer, A., Foster, H., Wells, K. E., Dickson, G. and Wells, D. J.** (2004). Long-term expression of full-length human dystrophin in transgenic mdx mice expressing internally deleted human dystrophins. *Gene Ther* **11**, 884-93.

**Fine, D. M., Shin, J. H., Yue, Y., Volkmann, D., Leach, S. B., Smith, B. F., McIntosh, M. and Duan, D.** (2011). Age-matched comparison reveals early

electrocardiography and echocardiography changes in dystrophin-deficient dogs. *Neuromuscul Disord* **21**, 453-61.

**Fort, P. E., Darche, M., Sahel, J. A., Rendon, A. and Tadayoni, R.** (2014). Lack of dystrophin protein Dp71 results in progressive cataract formation due to loss of fiber cell organization. *Mol Vis* **20**, 1480-90.

**Fukada, S., Morikawa, D., Yamamoto, Y., Yoshida, T., Sumie, N., Yamaguchi, M., Ito, T., Miyagoe-Suzuki, Y., Takeda, S., Tsujikawa, K. et al.** (2010). Genetic background affects properties of satellite cells and mdx phenotypes. *Am J Pathol* **176**, 2414-24.

**Gaedigk, R., Law, D. J., Fitzgerald-Gustafson, K. M., McNulty, S. G., Nsumu, N. N., Modrcin, A. C., Rinaldi, R. J., Pinson, D., Fowler, S. C., Bilgen, M. et al.** (2006). Improvement in survival and muscle function in an mdx/utrn(-/-) double mutant mouse using a human retinal dystrophin transgene. *Neuromuscul Disord* **16**, 192-203.

**Gambino, A. N., Mouser, P. J., Shelton, G. D. and Winand, N. J.** (2014). Emergent presentation of a cat with dystrophin-deficient muscular dystrophy. *J Am Anim Hosp Assoc* **50**, 130-5.

**Gawlik, K. I., Oliveira, B. M. and Durbeej, M.** (2011). Transgenic expression of Laminin alpha1 chain does not prevent muscle disease in the mdx mouse model for Duchenne muscular dystrophy. *Am J Pathol* **178**, 1728-37.

**Giannasi, C., Tappin, S.W., Guo, L.T., Shelton, G.D., Palus, V.** (2015). Dystrophin-deficient muscular dystrophy in two lurcher siblings. *J Small Anim Pract* [Epub ahead of print] doi: 10.1111/jsap.12331.

**Grady, R. M., Grange, R. W., Lau, K. S., Maimone, M. M., Nichol, M. C., Stull, J. T. and Sanes, J. R.** (1999). Role for alpha-dystrobrevin in the pathogenesis of dystrophin-dependent muscular dystrophies. *Nat Cell Biol* **1**, 215-20.

**Grady, R. M., Teng, H., Nichol, M. C., Cunningham, J. C., Wilkinson, R. S. and Sanes, J. R.** (1997). Skeletal and cardiac myopathies in mice lacking utrophin and dystrophin: a model for Duchenne muscular dystrophy. *Cell* **90**, 729-38.

**Greenberg, D. S., Sunada, Y., Campbell, K. P., Yaffe, D. and Nudel, U.** (1994). Exogenous Dp71 restores the levels of dystrophin associated proteins but does not alleviate muscle damage in mdx mice. *Nat Genet* **8**, 340-4.

**Guo, C., Willem, M., Werner, A., Raivich, G., Emerson, M., Neyses, L. and Mayer, U.** (2006). Absence of alpha7 integrin in dystrophin-deficient mice causes a myopathy similar to Duchenne muscular dystrophy. *Hum Mol Genet* **15**, 989-98.

**Hakim, C. H. and Duan, D.** (2013). Truncated dystrophins reduce muscle stiffness in the extensor digitorum longus muscle of mdx mice. *J Appl Physiol* **114**, 482-9.

**Han, R., Rader, E. P., Levy, J. R., Bansal, D. and Campbell, K. P.** (2011). Dystrophin deficiency exacerbates skeletal muscle pathology in dysferlin-null mice. *Skelet Muscle* **1**, 35.

**Harper, S. Q., Hauser, M. A., DelloRusso, C., Duan, D., Crawford, R. W., Phelps, S. F., Harper, H. A., Robinson, A. S., Engelhardt, J. F., Brooks, S. V. et al.** (2002). Modular flexibility of dystrophin: implications for gene therapy of Duchenne muscular dystrophy. *Nat Med* **8**, 253-61.

**Henriques-Pons, A., Yu, Q., Rayavarapu, S., Cohen, T. V., Ampong, B., Cha, H. J., Jahnke, V., Van der Meulen, J., Wang, D., Jiang, W. et al.** (2014). Role of Toll-like receptors in the pathogenesis of dystrophin-deficient skeletal and heart muscle. *Hum*

*Mol Genet* **23**, 2604-17.

**Hosur, V., Kavirayani, A., Riefler, J., Carney, L. M., Lyons, B., Gott, B., Cox, G. A. and Shultz, L. D.** (2012). Dystrophin and dysferlin double mutant mice: a novel model for rhabdomyosarcoma. *Cancer Genet* **205**, 232-41.

**Ito, D., Kitagawa, M., Jeffery, N., Okada, M., Yoshida, M., Kobayashi, M., Nakamura, A. and Watari, T.** (2011). Dystrophin-deficient muscular dystrophy in an Alaskan malamute. *Vet Rec* **169**, 127.

**Jones, B. R., Brennan, S., Mooney, C. T., Callanan, J. J., McAllister, H., Guo, L. T., Martin, P. T., Engvall, E. and Shelton, G. D.** (2004). Muscular dystrophy with truncated dystrophin in a family of Japanese Spitz dogs. *J Neurol Sci* **217**, 143-9.

**Judge, L. M., Arnett, A. L., Banks, G. B. and Chamberlain, J. S.** (2011). Expression of the dystrophin isoform Dp116 preserves functional muscle mass and extends lifespan without preventing dystrophy in severely dystrophic mice. *Hum Mol Genet* **20**, 4978-90.

**Judge, L. M., Haraguchi, M. and Chamberlain, J. S.** (2006). Dissecting the signaling and mechanical functions of the dystrophin-glycoprotein complex. *J Cell Sci* **119**, 1537-46.

**Klarenbeek, S., Gerritzen-Bruning, M. J., Rozemuller, A. J. and van der Lugt, J. J.** (2007). Canine X-linked muscular dystrophy in a family of Grand Basset Griffon Vendéen dogs. *J Comp Pathol* **137**, 249-52.

**Klymiuk, N., Blutke, A., Graf, A., Krause, S., Burkhardt, K., Wuensch, A., Krebs, S., Kessler, B., Zakhartchenko, V., Kurome, M. et al.** (2013). Dystrophin-deficient pigs provide new insights into the hierarchy of physiological derangements of dystrophic muscle. *Hum Mol Genet* **22**, 4368-82.

**Kornegay, J. N., Bogan, J. R., Bogan, D. J., Childers, M. K., Li, J., Nghiem, P., Detwiler, D. A., Larsen, C. A., Grange, R. W., Bhavaraju-Sanka, R. K. et al.** (2012). Canine models of Duchenne muscular dystrophy and their use in therapeutic strategies. *Mamm Genome* **23**, 85-108.

**Kornegay, J. N., Tuler, S. M., Miller, D. M. and Levesque, D. C.** (1988). Muscular dystrophy in a litter of golden retriever dogs. *Muscle Nerve* **11**, 1056-64.

**Krivov, L. I., Stenina, M. A., Yarygin, V. N., Polyakov, A. V., Savchuk, V. I., Obrubov, S. A. and Komarova, N. V.** (2009). A new genetic variant of mdx mice: study of the phenotype. *Bull Exp Biol Med* **147**, 625-9.

**Kudoh, H., Ikeda, H., Kakitani, M., Ueda, A., Hayasaka, M., Tomizuka, K. and Hanaoka, K.** (2005). A new model mouse for Duchenne muscular dystrophy produced by 2.4 Mb deletion of dystrophin gene using Cre-loxP recombination system. *Biochem Biophys Res Commun* **328**, 507-16.

**Kunkel, L. M., Bachrach, E., Bennett, R. R., Guyon, J. and Steffen, L.** (2006). Diagnosis and cell-based therapy for Duchenne muscular dystrophy in humans, mice, and zebrafish. *J Hum Genet* **51**, 397-406.

**Lai, Y., Thomas, G. D., Yue, Y., Yang, H. T., Li, D., Long, C., Judge, L., Bostick, B., Chamberlain, J. S., Terjung, R. L. et al.** (2009). Dystrophins carrying spectrin-like repeats 16 and 17 anchor nNOS to the sarcolemma and enhance exercise performance in a mouse model of muscular dystrophy. *J. Clin. Invest.* **119**, 624-635.

**Larcher, T., Lafoux, A., Tesson, L., Remy, S., Thepenier, V., Francois, V., Le Guiner, C., Goubin, H., Dutilleul, M., Guigand, L. et al.** (2014). Characterization of

dystrophin deficient rats: a new model for Duchenne muscular dystrophy. *PLoS One* **9**, e110371.

**Li, D., Bareja, A., Judge, L., Yue, Y., Lai, Y., Fairclough, R., Davies, K. E., Chamberlain, J. S. and Duan, D.** (2010). Sarcolemmal nNOS anchoring reveals a qualitative difference between dystrophin and utrophin. *J Cell Sci* **123**, 2008-13.

**Li, D., Long, C., Yue, Y. and Duan, D.** (2009). Sub-physiological sarcoglycan expression contributes to compensatory muscle protection in mdx mice. *Hum Mol Genet* **18**, 1209-20.

**Li, D., Shin, J. H. and Duan, D.** (2011a). iNOS ablation does not improve specific force of the extensor digitorum longus muscle in dystrophin-deficient mdx4cv mice. *PLoS One* **6**, e21618.

**Li, D., Yue, Y., Lai, Y., Hakim, C. H. and Duan, D.** (2011b). Nitrosative stress elicited by nNOS $\mu$  delocalization inhibits muscle force in dystrophin-null mice. *J Pathol* **223**, 88-98.

**Lloyd, T. E. and Taylor, J. P.** (2010). Flightless flies: *Drosophila* models of neuromuscular disease. *Ann N Y Acad Sci* **1184**, e1-20.

**Madaro, L., Pelle, A., Nicoletti, C., Crupi, A., Marrocco, V., Bossi, G., Soddu, S. and Bouche, M.** (2012). PKC theta ablation improves healing in a mouse model of muscular dystrophy. *PLoS One* **7**, e31515.

**Martins, P. C., Ayub-Guerrieri, D., Martins-Bach, A. B., Onofre-Oliveira, P., Malheiros, J. M., Tannus, A., de Sousa, P. L., Carlier, P. G. and Vainzof, M.** (2013). Dmdmdx/Largemyd: a new mouse model of neuromuscular diseases useful for studying physiopathological mechanisms and testing therapies. *Dis Model Mech* **6**, 1167-74.

**Megeney, L. A., Kablar, B., Garrett, K., Anderson, J. E. and Rudnicki, M. A.** (1996). MyoD is required for myogenic stem cell function in adult skeletal muscle. *Genes Dev* **10**, 1173-83.

**Miyazato, L. G., Moraes, J. R., Beretta, D. C. and Kornegay, J. N.** (2011). Muscular dystrophy in dogs: does the crossing of breeds influence disease phenotype? *Vet Pathol* **48**, 655-62.

**Moorwood, C. and Barton, E. R.** (2014). Caspase-12 ablation preserves muscle function in the mdx mouse. *Hum Mol Genet* **23**, 5325-41.

**Nakamura, K., Fujii, W., Tsuboi, M., Tanihata, J., Teramoto, N., Takeuchi, S., Naito, K., Yamanouchi, K. and Nishihara, M.** (2014). Generation of muscular dystrophy model rats with a CRISPR/Cas system. *Sci Rep* **4**, 5635.

**Nishimura, D., Sakai, H., Sato, T., Sato, F., Nishimura, S., Toyama-Sorimachi, N., Bartsch, J. W. and Sehara-Fujisawa, A.** (2014). Roles of ADAM8 in elimination of injured muscle fibers prior to skeletal muscle regeneration. *Mech Dev*.

**Nitahara-Kasahara, Y., Hayashita-Kinoh, H., Chiyo, T., Nishiyama, A., Okada, H., Takeda, S. and Okada, T.** (2014). Dystrophic mdx mice develop severe cardiac and respiratory dysfunction following genetic ablation of the anti-inflammatory cytokine IL-10. *Hum Mol Genet* **23**, 3990-4000.

**Nonneman, D. J., Brown-Brandl, T., Jones, S. A., Wiedmann, R. T. and Rohrer, G. A.** (2012). A defect in dystrophin causes a novel porcine stress syndrome. *BMC Genomics* **13**, 233.

**Paola, J. P., Podell, M. and Shelton, G. D.** (1993). Muscular dystrophy in a miniature Schnauzer. *Prog Vet Neurol* **4**, 14-8.

**Phelps, S. F., Hauser, M. A., Cole, N. M., Rafael, J. A., Hinkle, R. T., Faulkner, J. A. and Chamberlain, J. S.** (1995). Expression of full-length and truncated dystrophin mini-genes in transgenic mdx mice. *Hum Mol Genet* **4**, 1251-8.

**Prins, K. W., Lowe, D. A. and Ervasti, J. M.** (2008). Skeletal muscle-specific ablation of gamma(cyto)-actin does not exacerbate the mdx phenotype. *PLoS One* **3**, e2419.

**Raymackers, J. M., Debaix, H., Colson-Van Schoor, M., De Backer, F., Tajeddine, N., Schwaller, B., Gailly, P. and Gillis, J. M.** (2003). Consequence of parvalbumin deficiency in the mdx mouse: histological, biochemical and mechanical phenotype of a new double mutant. *Neuromuscul Disord* **13**, 376-87.

**Reyes, N. L., Banks, G. B., Tsang, M., Margineantu, D., Gu, H., Djukovic, D., Chan, J., Torres, M., Liggitt, H. D., Hirenallur, S. D. et al.** (2014). Fnip1 regulates skeletal muscle fiber type specification, fatigue resistance, and susceptibility to muscular dystrophy. *Proc Natl Acad Sci U S A*.

**Rogers, C. S. and Swart, J. R.** (2014). Animal Models of Duchenne Muscular Dystrophy, pp. 7. United States: Exemplar Genetics, LLC.

**Rooney, J. E., Welser, J. V., Dechert, M. A., Flintoff-Dye, N. L., Kaufman, S. J. and Burkin, D. J.** (2006). Severe muscular dystrophy in mice that lack dystrophin and alpha7 integrin. *J Cell Sci* **119**, 2185-95.

**Sacco, A., Mourkioti, F., Tran, R., Choi, J., Llewellyn, M., Kraft, P., Shkreli, M., Delp, S., Pomerantz, J. H., Artandi, S. E. et al.** (2010). Short Telomeres and Stem Cell Exhaustion Model Duchenne Muscular Dystrophy in mdx/mTR Mice. *Cell* **143**, 1059-71.

**Sakamoto, M., Yuasa, K., Yoshimura, M., Yokota, T., Ikemoto, T., Suzuki, M., Dickson, G., Miyagoe-Suzuki, Y. and Takeda, S.** (2002). Micro-dystrophin cDNA ameliorates dystrophic phenotypes when introduced into mdx mice as a transgene. *Biochem Biophys Res Commun* **293**, 1265-72.

**Sarig, R., Mezger-Lallemand, V., Gitelman, I., Davis, C., Fuchs, O., Yaffe, D. and Nudel, U.** (1999). Targeted inactivation of Dp71, the major non-muscle product of the DMD gene: differential activity of the Dp71 promoter during development. *Hum Mol Genet* **8**, 1-10.

**Schatzberg, S. J., Olby, N. J., Breen, M., Anderson, L. V., Langford, C. F., Dickens, H. F., Wilton, S. D., Zeiss, C. J., Binns, M. M., Kornegay, J. N. et al.** (1999). Molecular analysis of a spontaneous dystrophin 'knockout' dog. *Neuromuscul Disord* **9**, 289-95.

**Schmidt, W. M., Uddin, M. H., Dysek, S., Moser-Thier, K., Pirker, C., Hoger, H., Ambros, I. M., Ambros, P. F., Berger, W. and Bittner, R. E.** (2011). DNA damage, somatic aneuploidy, and malignant sarcoma susceptibility in muscular dystrophies. *PLoS Genet* **7**, e1002042.

**Shi, H., Verma, M., Zhang, L., Dong, C., Flavell, R. A. and Bennett, A. M.** (2013). Improved regenerative myogenesis and muscular dystrophy in mice lacking Mkp5. *J Clin Invest* **123**, 2064-77.

**Shimatsu, Y., Katagiri, K., Furuta, T., Nakura, M., Tanioka, Y., Yuasa, K., Tomohiro, M., Kornegay, J. N., Nonaka, I. and Takeda, S.** (2003). Canine X-linked muscular dystrophy in Japan (CXMDJ). *Exp Anim* **52**, 93-7.

**Shin, J. H., Greer, B., Hakim, C. H., Zhou, Z., Chung, Y. C., Duan, Y., He, Z. and Duan, D.** (2013a). Quantitative phenotyping of Duchenne muscular dystrophy dogs by comprehensive gait analysis and overnight activity monitoring. *PLoS One* **8**, e59875.

**Shin, J. H., Pan, X., Hakim, C. H., Yang, H. T., Yue, Y., Zhang, K., Terjung, R. L. and Duan, D.** (2013b). Microdystrophin ameliorates muscular dystrophy in the canine model of Duchenne muscular dystrophy. *Mol Ther* **21**, 750-7.

**Smith, B. F., Kornegay, J. N. and Duan, D.** (2007). Independent canine models of Duchenne muscular dystrophy due to intronic insertions of repetitive DNA. *Mol Ther* **15**, S51.

**Smith, B. F., Yue, Y., Woods, P. R., Kornegay, J. N., Shin, J. H., Williams, R. R. and Duan, D.** (2011). An intronic LINE-1 element insertion in the dystrophin gene aborts dystrophin expression and results in Duchenne-like muscular dystrophy in the corgi breed. *Lab Invest* **91**, 216-31.

**Steinberger, M., Foller, M., Vogelgesang, S., Krautwald, M., Landsberger, M., Winkler, C. K., Kasch, J., Fuchtbauer, E. M., Kuhl, D., Voelkl, J. et al.** (2014). Lack of the serum- and glucocorticoid-inducible kinase SGK1 improves muscle force characteristics and attenuates fibrosis in dystrophic mdx mouse muscle. *Pflugers Arch.*

**Tinsley, J., Deconinck, N., Fisher, R., Kahn, D., Phelps, S., Gillis, J. M. and Davies, K.** (1998). Expression of full-length utrophin prevents muscular dystrophy in mdx mice. *Nat Med* **4**, 1441-4.

**Valentine, B. A., Cooper, B. J., Cummings, J. F. and deLahunta, A.** (1986). Progressive muscular dystrophy in a golden retriever dog: light microscope and ultrastructural features at 4 and 8 months. *Acta Neuropathol (Berl)* **71**, 301-10.

**Vallese, D., Negroni, E., Duguez, S., Ferry, A., Trollet, C., Aamiri, A., Vosshenrich, C. A., Fuchtbauer, E. M., Di Santo, J. P., Vitiello, L. et al.** (2013). The Rag2(-)Il2rb(-)Dmd(-) mouse: a novel dystrophic and immunodeficient model to assess innovating therapeutic strategies for muscular dystrophies. *Mol Ther* **21**, 1950-7.

**van Putten, M., Hulsker, M., Young, C., Nadarajah, V. D., Heemskerk, H., van der Weerd, L., t Hoen, P. A., van Ommen, G. J. and Aartsma-Rus, A. M.** (2013). Low dystrophin levels increase survival and improve muscle pathology and function in dystrophin/utrophin double-knockout mice. *FASEB J* **27**, 2484-95.

**Vetrone, S. A., Montecino-Rodriguez, E., Kudryashova, E., Kramerova, I., Hoffman, E. P., Liu, S. D., Miceli, M. C. and Spencer, M. J.** (2009). Osteopontin promotes fibrosis in dystrophic mouse muscle by modulating immune cell subsets and intramuscular TGF-beta. *J Clin Invest* **119**, 1583-94.

**Vidal, B., Ardite, E., Suelves, M., Ruiz-Bonilla, V., Janue, A., Flick, M. J., Degen, J. L., Serrano, A. L. and Munoz-Canoves, P.** (2012). Amelioration of Duchenne muscular dystrophy in mdx mice by elimination of matrix-associated fibrin-driven inflammation coupled to the alphaMbeta2 leukocyte integrin receptor. *Hum Mol Genet* **21**, 1989-2004.

**Villalta, S. A., Nguyen, H. X., Deng, B., Gotoh, T. and Tidball, J. G.** (2009). Shifts in macrophage phenotypes and macrophage competition for arginine metabolism affect the severity of muscle pathology in muscular dystrophy. *Hum Mol Genet* **18**, 482-96.

**Wagner, K. R., McPherron, A. C., Winik, N. and Lee, S. J.** (2002). Loss of myostatin attenuates severity of muscular dystrophy in mdx mice. *Ann Neurol* **52**, 832-6.

**Walmsley, G. L., Arechavala-Gomez, V., Fernandez-Fuente, M., Burke, M. M., Nagel, N., Holder, A., Stanley, R., Chandler, K., Marks, S. L., Muntoni, F. et al.** (2010). A Duchenne muscular dystrophy gene hot spot mutation in dystrophin-deficient cavalier king charles spaniels is amenable to exon 51 skipping. *PLoS One* **5**, e8647.

**Walsh, S., Nygren, J., Ponten, A. and Jovinge, S.** (2011). Myogenic reprogramming of bone marrow derived cells in a W(4)(1)Dmd(mdx) deficient mouse model. *PLoS One* **6**, e27500.

**Wang, B., Li, J., Fu, F. H., Chen, C., Zhu, X., Zhou, L., Jiang, X. and Xiao, X.** (2008). Construction and analysis of compact muscle-specific promoters for AAV vectors. *Gene Ther* **15**, 1489-99.

**Warner, L. E., DelloRusso, C., Crawford, R. W., Rybakova, I. N., Patel, J. R., Ervasti, J. M. and Chamberlain, J. S.** (2002). Expression of Dp260 in muscle tethers the actin cytoskeleton to the dystrophin-glycoprotein complex and partially prevents dystrophy. *Hum Mol Genet* **11**, 1095-105.

**Wasala, N. B., Zhang, K., Wasala, L., Hakim, H. C., Duan, D.** (2015). The FVB genetic background does not dramatically alter the dystrophic phenotype of mdx mice. *PLoS Curr Muscular Dystrophy*. in-press.

**Wein, N., Vulin, A., Falzarano, M. S., Szgyarto, C. A., Maiti, B., Findlay, A., Heller, K. N., Uhlen, M., Bakthavachalu, B., Messina, S. et al.** (2014). Translation from a DMD exon 5 IRES results in a functional dystrophin isoform that attenuates dystrophinopathy in humans and mice. *Nat Med* **20**, 992-1000.

**Wells, D. J., Wells, K. E., Asante, E. A., Turner, G., Sunada, Y., Campbell, K. P., Walsh, F. S. and Dickson, G.** (1995). Expression of human full-length and minidystrophin in transgenic mdx mice: implications for gene therapy of Duchenne muscular dystrophy. *Hum Mol Genet* **4**, 1245-50.

**Wells, D. J., Wells, K. E., Walsh, F. S., Davies, K. E., Goldspink, G., Love, D. R., Chan-Thomas, P., Dunckley, M. G., Piper, T. and Dickson, G.** (1992). Human dystrophin expression corrects the myopathic phenotype in transgenic mdx mice. *Hum Mol Genet* **1**, 35-40.

**Wertz, K. and Fuchtbauer, E. M.** (1998). Dmd(mdx-beta geo): a new allele for the mouse dystrophin gene. *Dev Dyn* **212**, 229-41.

**Wetterman, C. A., Harkin, K. R., Cash, W. C., Nietfield, J. C. and Shelton, G. D.** (2000). Hypertrophic muscular dystrophy in a young dog. *J Am Vet Med Assoc* **216**, 878-81.

**Wieczorek, L. A., Garosi, L. S. and Shelton, G. D.** (2006). Dystrophin-deficient muscular dystrophy in an old English sheepdog. *Vet Rec* **158**, 270-3.

**Winand, N. J., Edwards, M., Pradhan, D., Berian, C. A. and Cooper, B. J.** (1994a). Deletion of the dystrophin muscle promoter in feline muscular dystrophy. *Neuromuscul Disord* **4**, 433-45.

**Winand, N. J., Pradhan, D. and Cooper, B. J.** (1994b). Molecular characterization of severe Duchenne-type muscular dystrophy in a family of Rottwiler dogs. In *Molecular Mechanism of Neuromuscular Disease*. Tucson, Arizona: Muscular Dystrophy Association.

**Yang, H. T., Shin, J. H., Hakim, C. H., Pan, X., Terjung, R. L. and Duan, D.** (2012). Dystrophin deficiency compromises force production of the extensor carpi ulnaris muscle in the canine model of Duchenne muscular dystrophy. *PLoS One* **7**, e44438.

## AAV-8 Is More Efficient than AAV-9 in Transducing Neonatal Dog Heart

Xiufang Pan,<sup>1</sup> Yongping Yue,<sup>1</sup> Keqing Zhang,<sup>1</sup> Chady H. Hakim,<sup>1</sup> Kasun Kodippili,<sup>1</sup>  
Thomas McDonald,<sup>1</sup> and Dongsheng Duan<sup>1,2</sup>

### Abstract

Adeno-associated virus serotype-8 and 9 (AAV-8 and 9) are the leading candidate vectors to test bodywide neonatal muscle gene therapy in large mammals. We have previously shown that systemic injection of  $2\text{--}2.5 \times 10^{14}$  viral genome (vg) particles/kg of AAV-9 resulted in widespread skeletal muscle gene transfer in newborn dogs. However, nominal transduction was observed in the heart. In contrast, robust expression was achieved in both skeletal muscle and heart in neonatal dogs with  $7.14\text{--}9.06 \times 10^{14}$  vg particles/kg of AAV-8. To determine whether superior cardiac transduction of AAV-8 is because of the higher vector dose, we delivered  $6.14 \times 10^{14}$  and  $9.65 \times 10^{14}$  vg particles/kg of AAV-9 to newborn puppies via the jugular vein. Transduction was examined 2.5 months later. Consistent with our previous reports, we observed robust bodywide transduction in skeletal muscle. However, increased AAV dose only moderately improved heart transduction. It never reached the level achieved by AAV-8. Our results suggest that differential cardiac transduction by AAV-8 and AAV-9 is likely because of the intrinsic property of the viral capsid rather than the vector dose.

### Introduction

OVER THE LAST TWO DECADES, adeno-associated virus (AAV) has become a leading vector for gene therapy. AAV is a single-stranded DNA virus discovered in mid-1960s.<sup>1</sup> More than 100 AAV variants are now available for gene transfer studies.<sup>2,3</sup> These AAV variants are either isolated from natural resources (such as adenovirus stocks and animal tissues) or engineered in the laboratory by rational design and/or evolution. While all AAV variants have a similar icosahedral capsid, the difference in the amino acid composition has yielded distinctive biological properties that are now being capitalized for different gene therapy applications. Among these, the ability to escape from the vasculature while remaining transduction competent is particularly attractive for treating diseases like Duchenne muscular dystrophy (DMD). Muscle makes up  $\sim 40\%$  of the body mass and it is distributed all over the body. An effective therapy for DMD will require an efficient delivery of a therapeutic gene to the whole body.

The breakthrough in systemic gene delivery was made about a decade ago.<sup>4–8</sup> Studies from several laboratories show that a single intravenous injection of AAV-6, 8, or 9 leads to sustained whole-body gene transfer in rodents. Subsequent

studies in mouse models of DMD and other types of muscular dystrophies revealed excellent bodywide muscle transduction and disease amelioration.<sup>9–14</sup> We conducted the first systemic AAV gene delivery in a large mammal in 2008.<sup>15</sup> In the study, we delivered  $1\text{--}2.5 \times 10^{14}$  viral genome (vg)/kg of AAV-9 to newborn dogs. We picked AAV-9 because this serotype worked extremely well in the rodent heart. We reasoned that the cardiac tropism would help to treat cardiomyopathy, a lethal complication of muscular dystrophy. Although robust bodywide skeletal muscle transduction was observed, surprisingly, very few cardiomyocytes were transduced.<sup>15</sup> To search for alternative methods, we tested AAV-8 in a recently published study.<sup>16</sup> At the dose of  $1.35 \times 10^{14}$  vg/kg, we did not see much cardiac gene transfer. However, when the dose was increased to  $7.14\text{--}9.06 \times 10^{14}$  vg/kg, we observed widespread gene transfer throughout the entire heart. The results of the AAV-8 study suggest that the vector dose may play an important role in determining cardiac transduction efficiency in neonatal dogs.<sup>16</sup>

In the present study, we tested whether AAV-9 has a similar dose response. We delivered AAV-9 to two neonatal dogs at the dose of 6.14 and  $9.65 \times 10^{14}$  vg/kg. The increased vector dose resulted in moderate heart transduction but never reached that of AAV-8.

Departments of <sup>1</sup>Molecular Microbiology and Immunology and <sup>2</sup>Neurology, School of Medicine, The University of Missouri, Columbia, MO 65212.

## Materials and Methods

### Animals

All animal experiments were approved by the Animal Care and Use Committee of the University of Missouri and were in accordance with the National Institutes of Health guideline. Two newborn dogs, Christa and Barbara, received medium-dose ( $6.14 \times 10^{14}$  vg/kg) and high-dose ( $9.65 \times 10^{14}$  vg/kg) AAV-9 (see below for details), respectively. Both were female carriers for DMD. An age-matched female carrier dog (Generic) was used as the noninjected control (Table 1). Two more dogs (Artemis and Dojo) were used for comparison and they were from previously published studies.<sup>15,16</sup> Artemis was a female carrier dog and Dojo was a normal male dog. Artemis received  $9.06 \times 10^{14}$  vg/kg of AAV-8 and was euthanized at the age of 2.5 months. Dojo received  $2 \times 10^{14}$  vg/kg of AAV-9 and was euthanized at the age of 6 months. All experimental dogs were generated by artificial insemination at the University of Missouri and they were on a mixed genetic background of golden retriever, Labrador retriever, beagle, and Welsh corgi. The genotyping was determined by polymerase chain reaction (PCR) as we described before.<sup>17,18</sup>

### AAV preparation

In this study, recombinant AAV-9 stock was generated using the exactly same triple-plasmid transfection protocol as we did in our published neonatal dog systemic gene delivery studies.<sup>15,16,19,20</sup> The three plasmids were (1) a *cis*-plasmid containing the Rous sarcoma virus (RSV) promoter, the heat-resistant *human placental alkaline phosphatase* (AP) reporter gene, and the simian virus 40 polyadenylation signal; (2) an AAV capsid/replication protein helper plasmid (a generous gift from Dr. James Wilson at the University of Pennsylvania, Philadelphia, PA)<sup>21</sup>; and (3) an adenoviral helper plasmid (Agilent Technologies, Clara, CA). The experimental vector (AAV.RSV.AP) was purified through three rounds of isopycnic CsCl ultracentrifugation followed by three changes of HEPES buffer at 4°C for 48 hr. The endotoxin level (as determined by the limulus amoebocyte lysate assay) was within the acceptable level recommended by the Food and Drug Administration. Minor technical differences can greatly influence AAV titer determination. To this end, we have taken several precautions. Specifically, we have used the same set of primers, same quantitative PCR (qPCR) kit, same plasmid standard, same machine, and same PCR condition for viral titer determination. For each

titer determination, we run triplicated qPCRs. The average of three reactions was designated as the vector titer. Further, we have confirmed the biological activity of different batches of the vectors (the batch used in the current study versus the batches used in our previous studies) in C57/BL10 mice by local and systemic delivery.<sup>15,16</sup> There was no apparent difference in transduction efficiency when the same dose, but different batches, of vectors were injected in mice. The PCR primers used in the titer determination amplify a fragment in the RSV promoter. The forward primer is 5'-GGTTGTACGCGGTTAGGAGT. The reverse primer is 5'-GGCATGTTGCTAACTCATCG.

### Gene delivery and dog necropsy

AAV-9 from the same batch was delivered to 2-day-old conscious puppies by a single bolus injection through the jugular vein as we described before (Table 1).<sup>15,16,20</sup> Full-body necropsy was performed at the age of 2.5 months. A total of 53 skeletal muscles were collected from the head, neck, shoulder, thorax, back, abdomen, forelimb, and hind limb. These muscles included extra-ocular muscle, geniohyoid, digastricus, masseter, temporalis (Tem), tongue (Ton), sternocephalicus (Ste), sternohyoideus, cleidocervicalis, trapezius, deltoideus (Del), supraspinatus, infraspinatus, teres major, teres minor, serratus dorsalis cranialis, serratus ventralis thoracis, latissimus dorsi, superficial pectoralis (SP), deep pectoralis, inter-costal muscle, abdominal rectus (AR), external abdominal oblique, internal abdominal oblique, transversus abdominis, extensor carpi ulnaris (ECU), extensor carpi radialis (ECR), extensor digitorum lateralis, extensor digitorum communis, flexor carpi ulnaris (FCU), flexor carpi radialis (FCR), flexor digitorum superficialis, flexor digitorum deep, pronator teres, pronator quadratus, biceps brachii (BB), triceps brachii (TB), brachialis, cranial tibialis (CT), extensor digitorum longus (EDL), vastus lateralis, vastus intermedius, semitendinosus, semimembranosus, cranial sartorius (CS), rectus femoris (RF), biceps femoris (BF), gluteus, adductor, pectineus, gracilis, gastrocnemius (Gas), and levator ani muscle. The diaphragm (DPH) samples were obtained from three different locations: the sternal (DPH-S), costal (DPH-C), and lumbar (DPH-L) part of the diaphragm. AP expression in 17 represented muscles was examined to evaluate bodywide gene transfer. These include BF, CT, CS, Del, DPH, ECU, ECR, EDL, FCR, FCU, Gas, SP, Ste, BB, TB, Tem, and Ton. Heart tissues were collected from 10 locations, including the

TABLE 1. SUMMARY OF EXPERIMENTAL PROTOCOL AND DOGS

	<i>Christa</i>	<i>Barbara</i>	<i>Artemis</i> <sup>a</sup>	<i>Dojo</i> <sup>a</sup>	<i>Generic</i>
Gender	Female	Female	Female	Male	Female
Genotype	Carrier	Carrier	Carrier	Normal	Carrier
Age at the time of injection (day)	2	2	2	2	N/A
BW at the time of injection (g)	380	380	412	520	N/A
AAV serotype	AAV-9	AAV-9	AAV-8	AAV-9	N/A
Injection volume (ml/kg BW)	9.21	14.47	14.56	8	N/A
AAV dosage (vg particle/kg BW)	$6.14 \times 10^{14}$	$9.65 \times 10^{14}$	$9.06 \times 10^{14}$	$2 \times 10^{14}$	N/A
BW at 2.5 months of age (kg)	5.40	5.44	6.02	—	5.8
Age at necropsy (month)	2.5	2.5	2.5	6	2.5

AAV, adeno-associated virus; BW, body weight; N/A, not applicable; —, not available.

<sup>a</sup>Dogs used in previous published experiment.

right and left atria (RA and LA), the cranial and caudal wall of the right ventricle (RVcr and RVca), interventricular septum (IS), anterior and posterior papillary muscles (PMA and PMp), and the apex, anterior, and posterior wall of the left ventricle (LVap, LVa, and LVp). We also collected the liver, pancreas, spleen, kidney, lung, and axillary lymph nodes.

#### Blood chemistry

Blood was collected immediately before euthanasia. Laboratory biochemical test was performed at the UMC Vet Med Diagnostic Lab (Columbia, MO).

#### AP expression

Histochemical staining was carried out on 8  $\mu$ m cryosections as we described before.<sup>15,16,22,23</sup> Enzymatic activity was measured using the Stem TAG Alkaline Phosphatase Activity Assay Kit (Cell Biolabs, San Diego, CA) according to manufacturer's instruction. Before histochemical staining and enzymatic assay, endogenous heat-sensitive AP was inactivated at 65°C for 45 min to 1 hr.

#### T-cell infiltration

Eight-micrometer cryosections were cut from the extensor carpi ulnaris muscle and left ventricle. CD4<sup>+</sup> and CD8<sup>+</sup> cells were revealed using the canine-specific anti-CD4 (1:1000) and anti-CD8 (1:200) antibodies, respectively (AbD Serotec, Raleigh, NC). The quantity of CD4<sup>+</sup> or CD8<sup>+</sup> cells was determined from counting five random 10 $\times$  fields.

#### AAV genome copy

Genomic DNA was extracted from liquid-nitrogen-frozen samples. Average DNA concentration was determined from three independent measurements using the NanoDrop ND-1000 spectrophotometer (260/280 ratio was 1.8–2.0). The viral ge-

nome copy in tissue samples was determined by quantitative PCR using the Fast SYBR Green Master Mix kit (Applied Biosystems, Foster City, CA) in an ABI 7900 HT qPCR machine. An amount of 100 ng genomic DNA was used in each qPCR. The same primers used for AAV copy number quantification were used for AAV titer determination. The qPCR efficiency from all experiments was among 90–93%.  $R^2$  was >0.99.

## Results

### High-dose intravenous AAV-9 delivery did not cause adverse reaction in newborn dogs

Administration of medium-dose (Christa,  $6.14 \times 10^{14}$  vg/kg) and high-dose (Barbara,  $9.65 \times 10^{14}$  vg/kg) AAV-9 was well tolerated. Both puppies showed similar activity, behavior, food/water intake, and body weight gain as uninjected littermates. Except for the expected elevation of serum alkaline phosphatase (because of expression from AAV.RS-V.AP), the blood panel was unremarkable (Table 2).<sup>16</sup> Histological examination of major internal organs revealed a similar morphology as that of the noninjected control (Fig. 1).

### Saturated expression was observed in skeletal muscle throughout the body

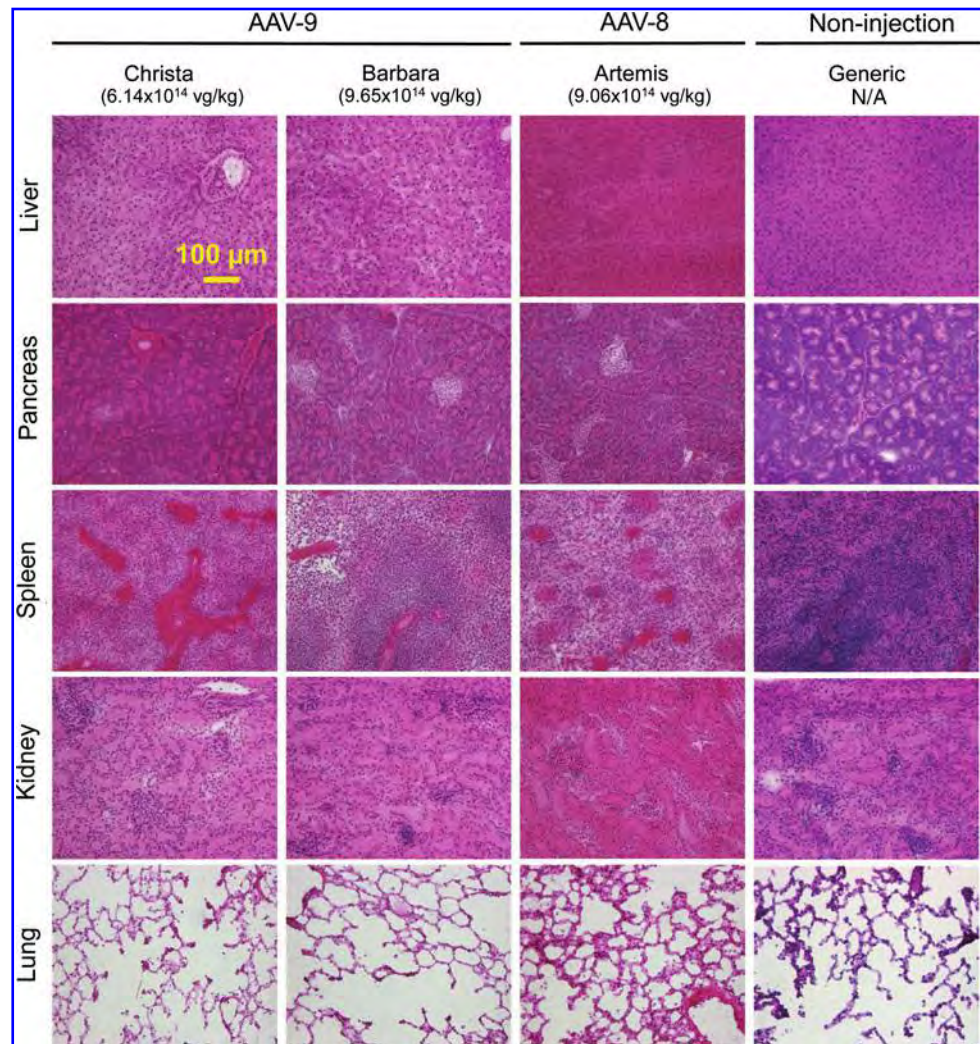
In our previous study, we demonstrated bodywide skeletal muscle transduction after intravenous injection of  $2 \times 10^{14}$  vg/kg of AAV-9 in newborn puppies.<sup>15</sup> However, gene transfer in many muscles (such as RF, CS, and AR) remains suboptimal (50–80%) (Fig. 2A).<sup>15</sup> A 3-fold increase in the vector dose (to  $6.14 \times 10^{14}$  vg/kg) resulted in complete (~100%) transduction of every limb muscle in Christa (Fig. 2A and Supplementary Fig. S1; Supplementary Data are available online at [www.liebertpub.com/hgtb](http://www.liebertpub.com/hgtb)). Boosting the dose further to  $9.65 \times 10^{14}$  vg/kg in Barbara (~5-fold higher than the dose used in Dojo) increased the vector genome

TABLE 2. BLOOD EXAMINATION RESULTS

	Age (2.5 months)			Age (1.5–3.5 months) (n=20)	
	Christa	Barbara	Artemis	Uninjected control, range	
				Uninjected control, mean $\pm$ SEM	Uninjected control, range
Calcium (mg/dl)	11.8	11.8	10.8	11.2 $\pm$ 0.1	10.5–11.9
Chloride (mEq/liter)	109	<b>113</b> <sup>a</sup>	109	106.6 $\pm$ 0.6	99–111
Phosphorus (mg/dl)	9.4	9.2	9.2	8.5 $\pm$ 0.2	7.0–10.1
Potassium (mEq/liter)	<b>7</b>	5.1	5	5.8 $\pm$ 0.1	5.2–7.1
Sodium (mEq/liter)	142	145	148	141.5 $\pm$ 0.8	133–148
Albumin (g/dl)	2.5	2.6	2.3	2.7 $\pm$ 0.1	2.1–3.6
Alkaline phosphatase (ALP) (U/liter)	<b>209</b>	<b>310</b>	<b>239</b>	147.9 $\pm$ 5.4	111–200
Alanine aminotransferase (ALT) (U/liter)	70	52	42	25.7 $\pm$ 4.4	9–97
ALP/ALT ratio	2.9	5.9	5.7	8.1 $\pm$ 1.1	1.3–22
Anion gap (mEq/liter)	20	<b>17</b>	25	22.2 $\pm$ 0.5	19–28
Cholesterol (mg/dl)	236	194	186	254.2 $\pm$ 14.7	173–427
Creatinine (mg/dl)	0.5	0.4	0.5	0.4 $\pm$ 0.0	0.2–0.7
Gamma-glutamyl transpeptidase (GGT) (U/liter)	<3	2	<3	0.9 $\pm$ 0.4	0–6
Globulin (g/dl)	2.2	2.2	1.9	2.2 $\pm$ 0.1	1.7–2.7
Glucose (mg/dl)	<b>197</b>	110	<b>88</b>	105.3 $\pm$ 2.4	89–126
Total bilirubin (mg/dl)	0.2	0.2	0.3	0.2 $\pm$ 0.0	0.1–0.4
Total CO <sub>2</sub> (mEq/liter)	20	20	19	18.6 $\pm$ 0.9	7–24
Total protein (g/dl)	4.7	4.8	4.2	4.9 $\pm$ 0.1	4.1–6.3
Urea nitrogen (mg/dl)	10	14	19	11.8 $\pm$ 1.4	4–22

<sup>a</sup>Bold font indicates the value is not within the range of uninjected control.

**FIG. 1.** High-dose AAV-9 delivery in neonatal dogs does not alter histology of major internal organs. Representative photomicrographs of HE-stained tissue sections from dogs that were injected with medium- and high-dose AAV-9 (Christa and Barbara), high-dose AAV-8 (Artemis), and non-injected dog (Generic). No abnormality was observed in the liver, pancreas, spleen, kidney, and lung. AAV, adeno-associated virus; N/A, not applicable. Color images available online at [www.liebertpub.com/hgtb](http://www.liebertpub.com/hgtb)



copy number in most muscles but it did not yield dramatically much higher AP activity in muscle lysate, suggesting a saturation effect in skeletal muscle (Fig. 2C and D, and Supplementary Fig. S1D). No AP positive cells were observed in uninjected control (Supplementary Fig. S2).

#### *Increased AAV-9 dosage yielded only moderate myocardial transduction*

The main goal of this study is to determine whether the vector dose is the primary limiting factor for AAV-9 transduction in the newborn dog heart. In our published studies ( $1\text{--}2.5 \times 10^{14}$  vg/kg), hardly any expression was detected in the heart.<sup>15</sup> In Christa ( $6.14 \times 10^{14}$  vg/kg), AP-positive cells became readily detectable by histochemical staining in the interventricular septum, left ventricle, and papillary muscle (Fig. 3A). A dose-dependent increase in AP expression was observed in almost every region of the heart in Barbara ( $9.65 \times 10^{14}$  vg/kg). Widespread AP-positive cells were seen in the left atrium, interventricular septum, papillary muscle, and left ventricle (Fig. 3A). However, it never reached the level seen in Artemis, a puppy injected with  $9.06 \times 10^{14}$  vg/kg of AAV-8 (Fig. 3A and B). Interestingly, on histochemical staining, the right heart (RA and RV) was efficiently transduced by AAV-8 but barely transduced by AAV-9 (Fig. 3A).

AAV copy number quantification revealed an interesting pattern. In the right ventricle and interventricular septum, we detected more vector genome in AAV-8-injected Artemis, consistent with high transduction. But in the right atrium, similar number of the AAV genome copy was found despite a substantially much more robust expression in the AAV-8-injected puppy (Fig. 3). Most surprisingly, in the left atrium, papillary muscle, and left ventricle, AAV copy number in Barbara ( $9.65 \times 10^{14}$  vg/kg of AAV-9) was 3–5-fold higher than that in Artemis ( $9.06 \times 10^{14}$  vg/kg of AAV-8). However, the high copy number did not result in high expression, suggesting that a significant portion of the AAV-9 genome may have been trapped in a yet-to-be-defined dead compartment and/or not converted to the transcription-competent form in cardiomyocytes and cannot express the transgene.

#### *Transduction of internal organs by systemic high-dose AAV-9 injection in newborn puppies*

AAV transduction in the liver, pancreas, spleen, lung, and kidney was examined (Fig. 4). Similar to the results of high-dose AAV-8,<sup>16</sup> very few AP-positive cells were detected in the liver, but substantial AP expression was found in the pancreas, spleen, lung, and kidney (Fig. 4).

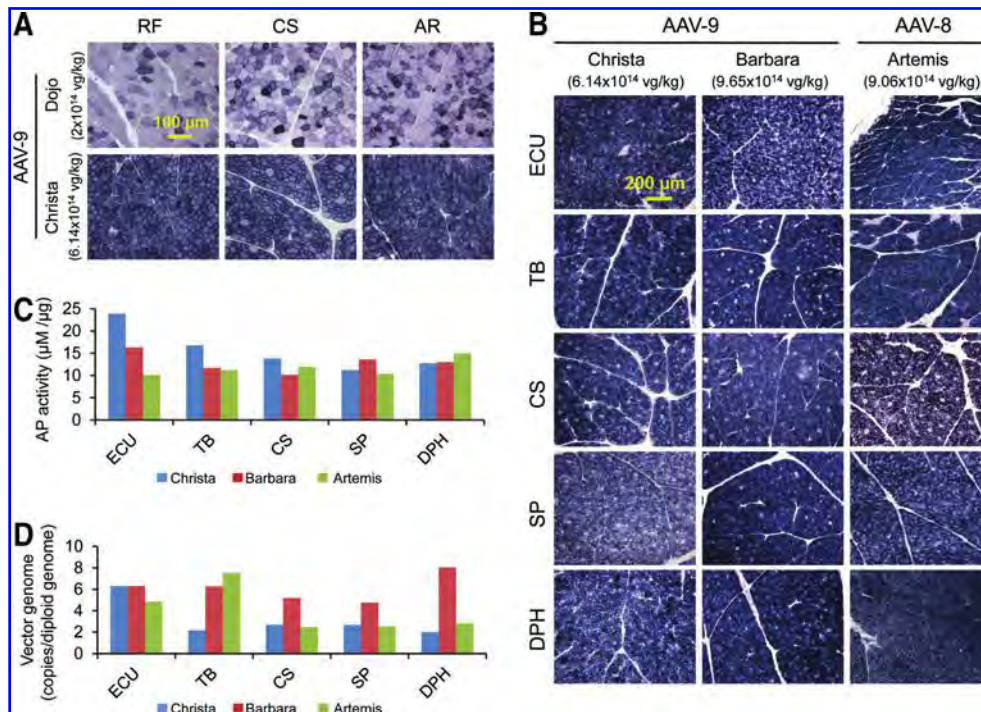


**FIG. 2.** Intravenous injection of high-dose AAV-9 results in improved skeletal muscle transduction in neonatal dogs. **(A)** Representative photomicrographs of alkaline phosphatase (AP) histochemical staining from muscles that were injected with low (Dojo,  $2 \times 10^{14}$  vg/kg) and medium (Christa,  $6.14 \times 10^{14}$  vg/kg) doses of the AAV-9 AP reporter vector. AR, abdominal rectus; CS, cranial sartorius; RF, rectus femoris. **(B)** Representative photomicrographs of skeletal muscle AP histochemical staining from AAV-9-injected dogs Christa and Barbara as well as AAV-8-injected dog Artemis. DPH, diaphragm; ECU, extensor carpi ulnaris; SP, superficial pectoralis; TB, triceps brachii. **(C)** Quantitative examination of AP activity in muscle lysate. **(D)** Comparison of the AAV vector genome copy number in different skeletal muscles. Color images available online at [www.liebertpub.com/hgtb](http://www.liebertpub.com/hgtb)

#### *Systemic AAV-9 in newborn dogs did not induce T-cell infiltration in transduced muscles*

To determine whether high-dose systemic AAV injection induced the cellular immune response in muscle, we examined the infiltration of CD4<sup>+</sup> and CD8<sup>+</sup> T-cell. Only occasional residential CD4<sup>+</sup> and CD8<sup>+</sup> T-cells were detected. There was no apparent difference in AAV-injected and noninjected dog muscles (Supplementary Fig. S3).

#### *High-dose systemic AAV injection in newborn dogs resulted in minimum transduction in draining lymph nodes*

AP expression was evaluated in the axillary lymph nodes from injected and noninjected dogs. Nominal AP expression was detected in the lymph node of AAV-9-injected puppies (Christa and Barbara) (Supplementary Fig. S4). Slightly more AP expression was seen in the puppy injected with AAV-8 (Artemis). Interestingly, there was strong AP expression in the capsule of the lymph node harvested from this puppy (Artemis) (Supplementary Fig. S4).

#### **Discussion**

In this study, we tested the hypothesis that high-dose AAV-9 can efficiently transduce the newborn dog heart. We found a positive correlation between the vector dose and transgene expression in the heart. However, cardiac transduction of AAV-9 never reached that of AAV-8.

Studies performed in rodents suggest that AAV-9 may represent a cardiac tropic serotype (reviewed in refs.<sup>24,25</sup>). Surprisingly, the heart was barely transduced when we delivered AAV-9 to newborn puppies at a dose comparable to that used in rodent studies.<sup>15</sup> To identify a serotype that can be used for dog heart gene transfer, we screened several additional AAV serotypes, including Y445F/Y731F AAV-1, Y445F AAV-6, AAV-8, and Y731F AAV-9.<sup>15,16,20</sup> Robust myocardial gene transfer was observed with AAV-8 at doses that were 3–4-fold higher than the highest dose ( $2.5 \times 10^{14}$  vg/kg) we used in the original AAV-9 study.<sup>15</sup>

The difference in the vector dose and/or the viral serotype may have contributed to the superior heart transduction by AAV-8. To dissect the underlying mechanisms, we delivered high-dose AAV-9 to two newborn puppies (Christa and Barbara). To evaluate the potential dose response, we used two doses ( $6.14 \times 10^{14}$  and  $9.65 \times 10^{14}$  vg/kg). Bodywide gene transfer in these two puppies was examined at the same time point as we did for Artemis, a dog used in the AAV-8 study.<sup>16</sup> As expected from our previous publications,<sup>15,16,20</sup> vigorous skeletal muscle transduction was observed, while liver is poorly transduced (Figs. 2 and 4, and Supplementary Fig. S1). However, unlike what we have seen with medium- to high-dose AAV-8,<sup>16</sup> heart transduction by AAV-9 only reached moderate levels at these doses (Fig. 3). For example, puppy Barbara received  $9.65 \times 10^{14}$  vg/kg of AAV-9. This is higher than the AAV-8 dose administered to puppy Artemis ( $9.06 \times 10^{14}$  vg/kg). Yet, the number of AP-positive cells seen in the heart of

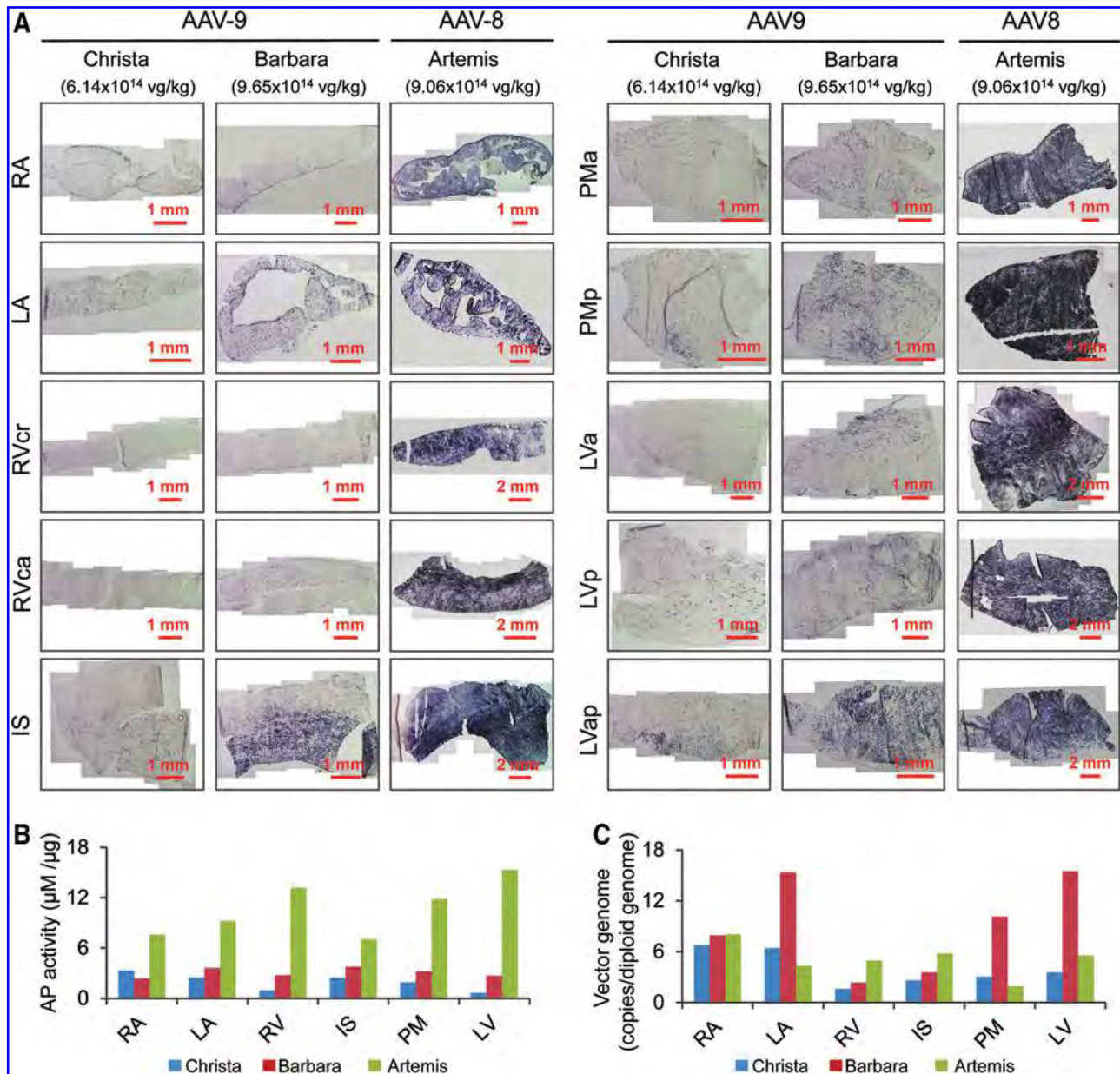


**FIG. 3.** AAV-9 is less efficient than AAV-8 in transducing neonatal dog heart. **(A)** Representative lower magnification microphotographs of AP staining in different parts of the heart, including right atrium (RA), left atrium (LA), right ventricular cranial wall (RVcr), right ventricular caudal wall (RVca), interventricular septum (IS), anterior papillary muscle (PMa), posterior papillary muscle (PMp), left ventricular anterior wall (LVa), left ventricular posterior wall (LVp), and left ventricular apex (LVap). **(B)** Quantitative examination of AP activity in muscle lysate from different parts of the heart. **(C)** AAV genome copy quantification in different parts of the heart. Color images available online at [www.liebertpub.com/hgtb](http://www.liebertpub.com/hgtb)

Barbara was substantially lower than that of Artemis (Fig. 3). While additional studies are needed to corroborate these findings (we only have a small sample size), our results suggest that some yet unidentified properties of the AAV-8 capsid may have contributed to the efficient myocardial transduction in newborn dogs by AAV-8. The crystal structure of AAV-8 capsid and AAV-9 capsid was resolved recently by the Agbandje-McKenna laboratory at the resolution of 2.6 and 2.8 angstrom, respectively.<sup>26,27</sup> Major differences between two serotypes are located in three surface variable regions. Future site-directed mutagenesis in these regions will help to pinpoint structural features that are responsible for the superior myocardial transduction by AAV-8 in newborn dogs.<sup>28</sup>

It is currently unclear why AAV-9 can effectively transduce rodent heart but not newborn dog heart. One apparent explanation would be species differences. Such species-specific changes have been shown to at least partially contribute to the phenotypic differences among dystrophin-deficient mice, dogs, and human patients.<sup>29</sup> Our findings raise a critical concern on the future translation of canine study results to DMD patients. It is our belief that animal studies may inform the design of the clinical trial rather than predict the outcome of a clinical trial.

Besides skeletal muscle and the heart, we also examined the transduction profile in major internal organs (Fig. 4). Moderate AP expression was observed in pancreas, spleen,

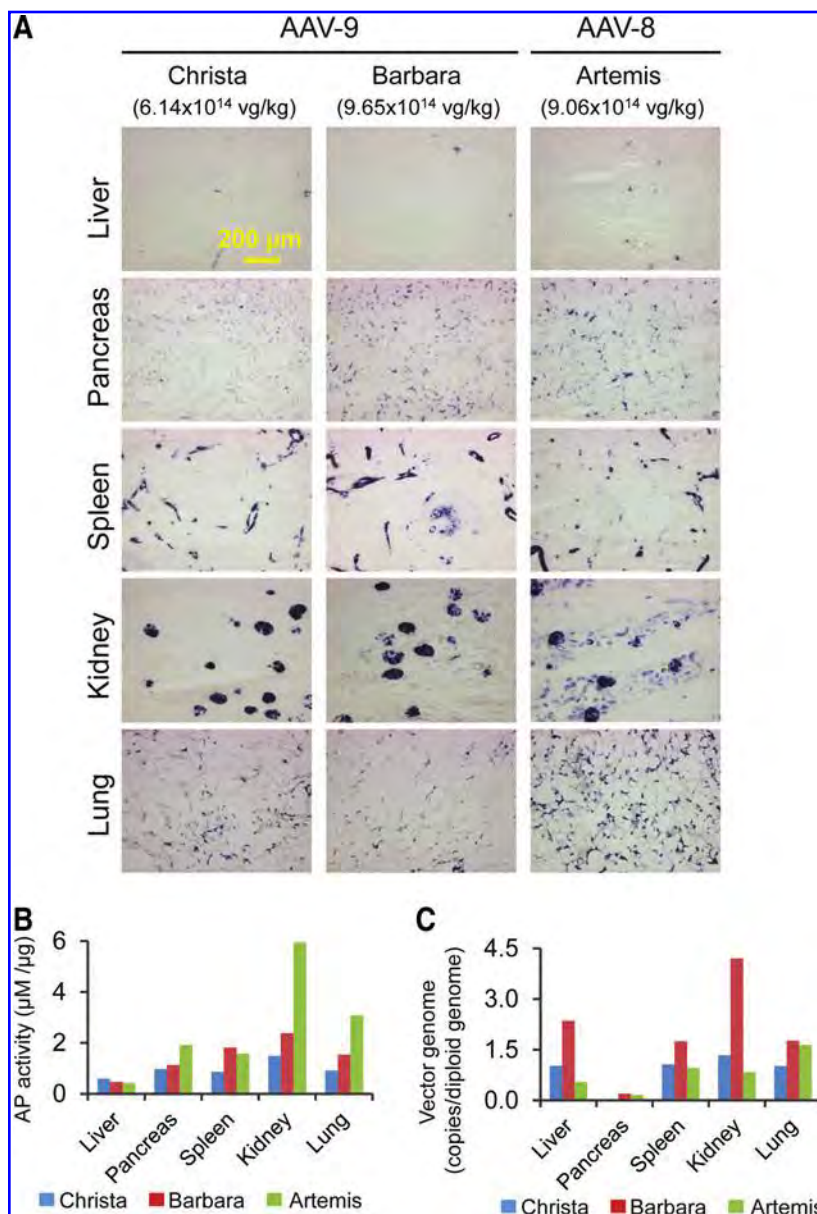


**FIG. 4.** Internal organ transduction following high-dose systemic AAV-9 injection in neonatal dogs. **(A)** Representative photomicrographs of AP histochemical staining from the liver, pancreas, spleen, kidney, and lung. **(B)** Quantitative examination of AP activity in tissue lysate from the liver, pancreas, spleen, kidney, and lung. **(C)** AAV genome copy quantification in the liver, pancreas, spleen, kidney, and lung. Color images available online at [www.liebertpub.com/hgtb](http://www.liebertpub.com/hgtb)

kidney, and lung. However, very few AP-positive cells were detected in the liver. The AP activity assay further confirmed low-level liver transduction. This is in contrary to the results of AAV genome copy quantification. Substantial amount of the vector genome was detected in the liver. We speculate that this may relate to the promoter shutdown or other yet unrecognized mechanisms that may have limited the formation of the transcriptionally competent vector genome.<sup>30–32</sup>

The safety of systemic gene delivery has always been a concern. The dosage administrated to puppy Barbara ( $9.65 \times 10^{14}$  vg/kg) is so far the highest AAV dose ever been given to a living animal. Consistent with our previous studies (from  $1 \times 10^{14}$  to  $9.06 \times 10^{14}$  vg/kg), we did not see any severe side effect in Barbara. There was no growth retardation (Table 1). Her liver and kidney function was normal (Table 2). Collectively, our data (from a total of 14 dogs) suggest that systemic AAV injection in neonatal dogs is relatively safe.<sup>15,16,20</sup>

In summary, our results suggest that AAV-9 is not a cardiotropic virus in newborn dogs. Further, our results provide additional safety data supporting neonatal gene therapy in large mammals. Highly sensitive and reproducible neonatal screening methods have developed for DMD and many other muscular dystrophies. Neonatal gene therapy will allow treatment before the onset of clinical symptoms. Recently, a clinical trial was approved to treat neonatal spinal muscular atrophy patients with systemic injection (clinical trial # NCT02122952). More neonatal gene therapy studies are expected to follow in the coming years. A detailed characterization of the transduction profile of different AAV serotypes in newborn large animals will provide necessary information to help guide these trials.

#### Acknowledgments

This work was supported by grants from the National Institutes of Health (HL-91883 and AR-49419), the Department

of Defense (MD130014), the Parent Project for Muscular Dystrophy, the Muscular Dystrophy Association, and Jesse's Journey—The Foundation for Gene and Cell Therapy.

#### Author Disclosure Statement

D.D. is a member of the scientific advisory board for Solid GT, a subsidiary of Solid Ventures. For all other authors, no competing financial interests exist.

#### References

- Atchison RW, Casto BC, Hammon WM. Adenovirus-associated defective virus particles. *Science* 1965;149:754–756.
- Vandenberghe LH, Wilson JM, Gao G. Tailoring the AAV vector capsid for gene therapy. *Gene Ther* 2009;16:311–319.
- Kotterman MA, Schaffer DV. Engineering adeno-associated viruses for clinical gene therapy. *Nat Rev Genet* 2014;15:445–451.
- Gregorevic P, Blankinship MJ, Allen JM, et al. Systemic delivery of genes to striated muscles using adeno-associated viral vectors. *Nat Med* 2004;10:828–834.
- Wang Z, Zhu T, Qiao C, et al. Adeno-associated virus serotype 8 efficiently delivers genes to muscle and heart. *Nat Biotechnol* 2005;23:321–328.
- Pacak CA, Mah CS, Thattaliyath BD, et al. Recombinant adeno-associated virus serotype 9 leads to preferential cardiac transduction *in vivo*. *Circ Res* 2006;99:e3–e9.
- Inagaki K, Fuess S, Storm TA, et al. Robust systemic transduction with AAV9 vectors in mice: efficient global cardiac gene transfer superior to that of AAV8. *Mol Ther* 2006;14:45–53.
- Bostick B, Ghosh A, Yue Y, et al. Systemic AAV-9 transduction in mice is influenced by animal age but not by the route of administration. *Gene Ther* 2007;14:1605–1609.
- Gregorevic P, Allen JM, Minami E, et al. rAAV6-microdystrophin preserves muscle function and extends lifespan in severely dystrophic mice. *Nat Med* 2006;12:787–789.
- Shin JH, Pan X, Hakim CH, et al. Microdystrophin ameliorates muscular dystrophy in the canine model of Duchenne muscular dystrophy. *Mol Ther* 2013;21:750–757.
- Lai Y, Thomas GD, Yue Y, et al. Dystrophins carrying spectrin-like repeats 16 and 17 anchor nNOS to the sarcolemma and enhance exercise performance in a mouse model of muscular dystrophy. *J Clin Invest* 2009;119:624–635.
- Goehringer C, Rutschow D, Bauer R, et al. Prevention of cardiomyopathy in delta-sarcoglycan knockout mice after systemic transfer of targeted adeno-associated viral vectors. *Cardiovasc Res* 2009;82:404–410.
- Qiao C, Li J, Zhu T, et al. Amelioration of laminin-alpha2-deficient congenital muscular dystrophy by somatic gene transfer of miniagrin. *Proc Natl Acad Sci USA* 2005;102:11999–12004.
- Xu R, DeVries S, Camboni M, Martin PT. Overexpression of Galgt2 reduces dystrophic pathology in the skeletal muscles of alpha sarcoglycan-deficient mice. *Am J Pathol* 2009;175:235–247.
- Yue Y, Ghosh A, Long C, et al. A single intravenous injection of adeno-associated virus serotype-9 leads to whole body skeletal muscle transduction in dogs. *Mol Ther* 2008;16:1944–1952.
- Pan X, Yue Y, Zhang K, et al. Long-term robust myocardial transduction of the dog heart from a peripheral vein by adeno-associated virus serotype-8. *Hum Gene Ther* 2013;24:584–594.
- Fine DM, Shin JH, Yue Y, et al. Age-matched comparison reveals early electrocardiography and echocardiography changes in dystrophin-deficient dogs. *Neuromuscul Disord* 2011;21:453–461.
- Smith BF, Yue Y, Woods PR, et al. An intronic LINE-1 element insertion in the dystrophin gene aborts dystrophin expression and results in Duchenne-like muscular dystrophy in the corgi breed. *Lab Invest* 2011;91:216–231.
- Shin JH, Yue Y, Duan D. Recombinant adeno-associated viral vector production and purification. *Methods Mol Biol* 2012;798:267–284.
- Hakim CH, Yue Y, Shin JH, et al. Systemic gene transfer reveals distinctive muscle transduction profile of tyrosine mutant AAV-1, -6, and -9 in neonatal dogs. *Mol Ther Methods Clin Dev* 2014;1:14002.
- Gao GP, Alvira MR, Wang L, et al. Novel adeno-associated viruses from rhesus monkeys as vectors for human gene therapy. *Proc Natl Acad Sci USA* 2002;99:11854–11859.
- Shin JH, Yue Y, Srivastava A, et al. A simplified immune suppression scheme leads to persistent micro-dystrophin expression in Duchenne muscular dystrophy dogs. *Hum Gene Ther* 2012;23:202–209.
- Yue Y, Shin JH, Duan D. Whole body skeletal muscle transduction in neonatal dogs with AAV-9. *Methods Mol Biol* 2011;709:313–329.
- Lai Y, Duan D. Progress in gene therapy of dystrophic heart disease. *Gene Ther* 2012;19:678–685.
- Wasala NB, Shin JH, Duan D. The evolution of heart gene delivery vectors. *J Gene Med* 2011;13:557–565.
- Nam HJ, Lane MD, Padron E, et al. Structure of adeno-associated virus serotype 8, a gene therapy vector. *J Virol* 2007;81:12260–12271.
- DiMattia MA, Nam HJ, Van Vliet K, et al. Structural insight into the unique properties of adeno-associated virus serotype 9. *J Virol* 2012;86:6947–6958.
- Agbandje-McKenna M, Kleinschmidt J. AAV capsid structure and cell interactions. *Methods Mol Biol* 2011;807:47–92.
- Chandrasekharan K, Yoon JH, Xu Y, et al. A human-specific deletion in mouse Cmah increases disease severity in the mdx model of Duchenne muscular dystrophy. *Sci Transl Med* 2010;2:42ra54.
- Leger A, Le Guiner C, Nickerson ML, et al. Adeno-associated viral vector-mediated transgene expression is independent of DNA methylation in primate liver and skeletal muscle. *PLoS One* 2011;6:e20881.
- Everett RS, Evans HK, Hodges BL, et al. Strain-specific rate of shutdown of CMV enhancer activity in murine liver confirmed by use of persistent [E1(-), E2b(-)] adenoviral vectors. *Virology* 2004;325:96–105.
- Weitzman MD, Linden RM. Adeno-associated virus biology. *Methods Mol Biol* 2011;807:1–23.

Address correspondence to:

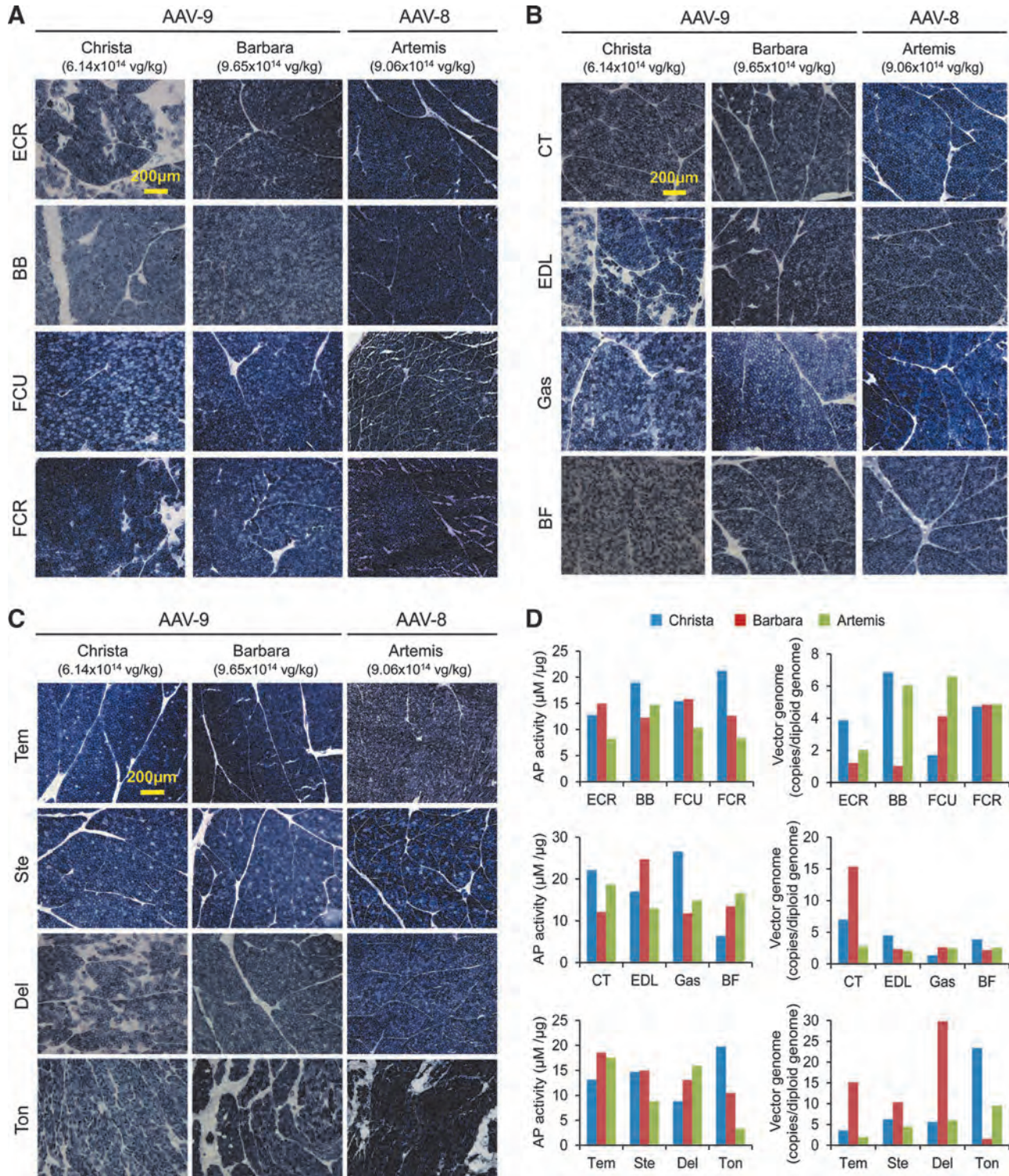
Dr. Dongsheng Duan  
 Department of Molecular Microbiology and Immunology  
 School of Medicine  
 The University of Missouri  
 1 Hospital Drive  
 Columbia, MO 65212

E-mail: duand@missouri.edu

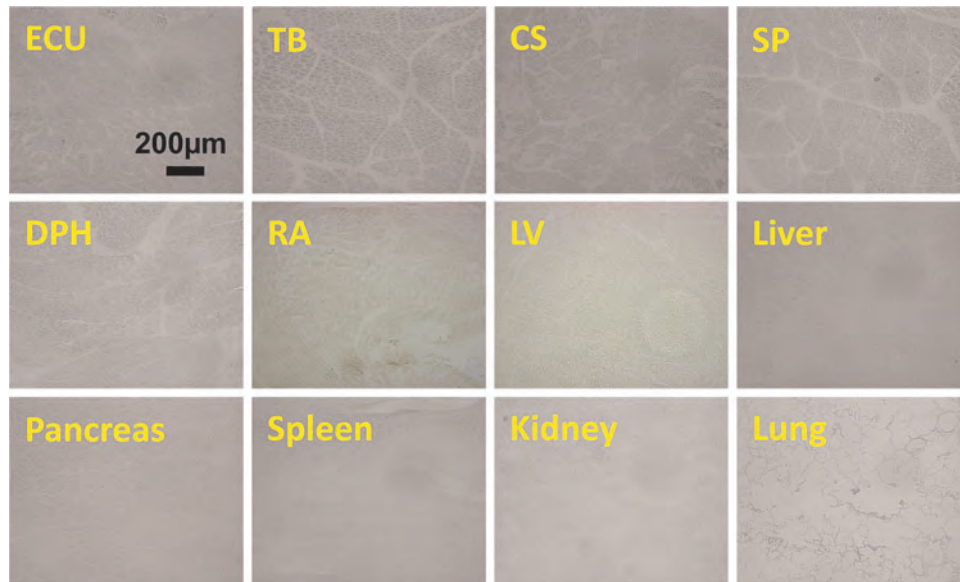
Received for publication October 21, 2014;  
 accepted after revision February 18, 2015.

Published online: March 11, 2015.

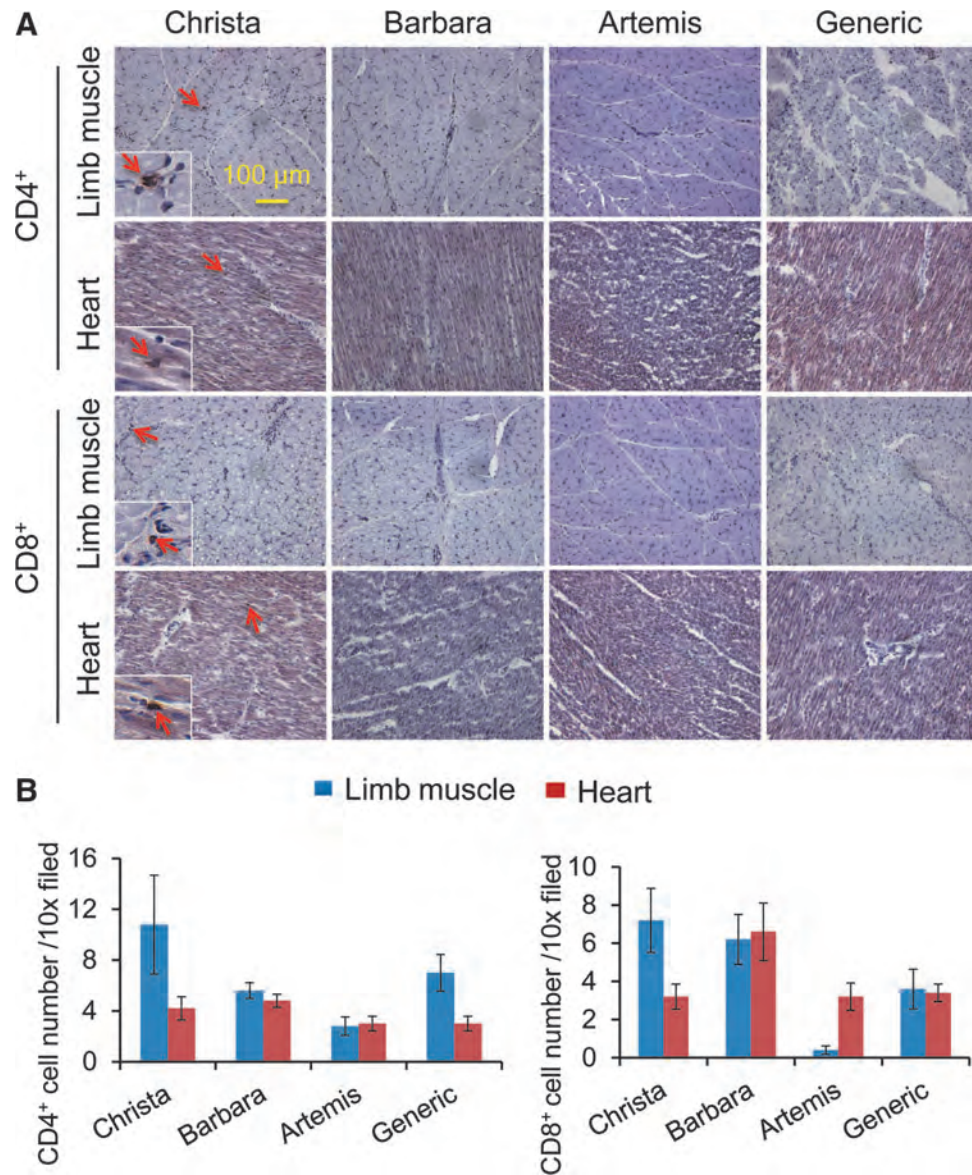
## Supplementary Data



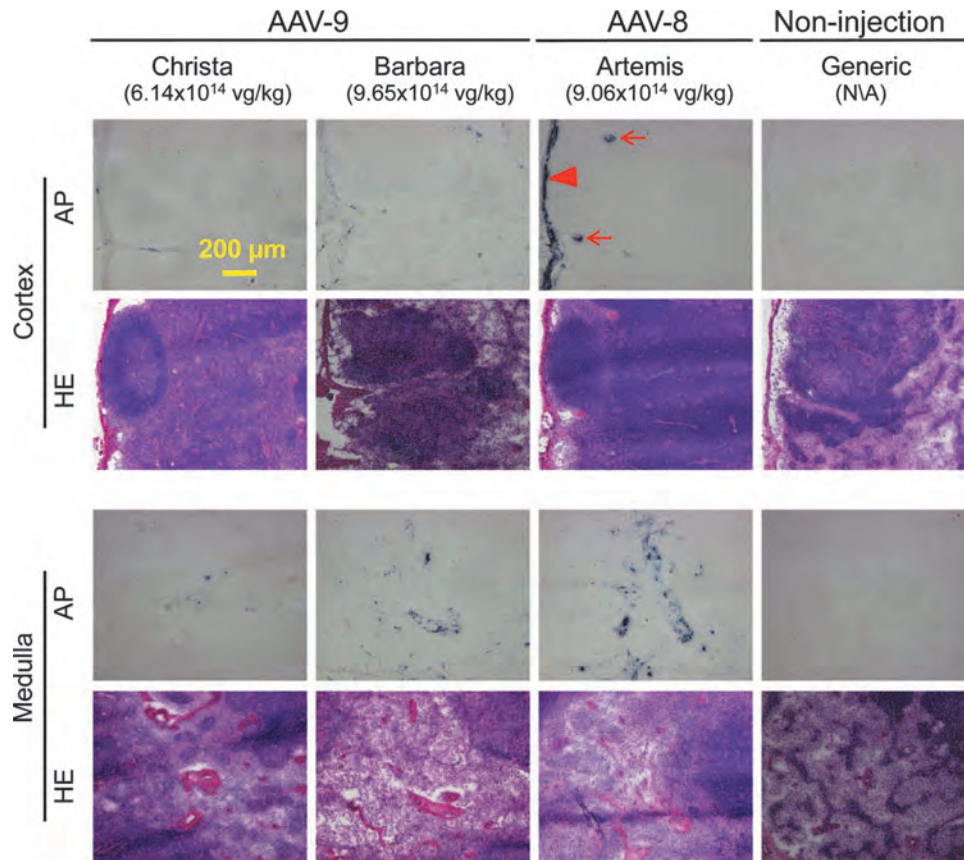
**SUPPLEMENTARY FIG. S1.** Intravenous injection of high-dose AAV-9 results in bodywide skeletal muscle transduction in neonatal dogs. **(A)** Representative photomicrographs of forelimb skeletal muscle alkaline phosphatase (AP) histochemical staining from AAV-9-injected dogs Christa and Barbara as well as AAV-8-injected dog Artemis. BB, biceps brachii; ECR, extensor carpi radialis; FCR, flexor carpi radialis; FCU, flexor carpi ulnaris. **(B)** Representative photomicrographs of hind limb skeletal muscle AP histochemical staining from AAV-9-injected dogs Christa and Barbara as well as AAV-8-injected dog Artemis. BF, biceps femoris; CT, cranial tibialis; EDL, extensor digitorum longus; Gas, gastrocnemius. **(C)** Representative photomicrographs of AP histochemical staining of others skeletal muscles from AAV-9-injected dogs Christa and Barbara as well as AAV-8-injected dog Artemis. Del, deltoid; Ste, sternocephalicus; Tem, temporalis; Ton, tongue. **(D)** Quantitative examination of AP activity in muscle lysate and AAV vector genome copy number in different skeletal muscles. AAV, adeno-associated virus.



**SUPPLEMENTARY FIG. S2.** Lack of AP expression in a noninjected dog. Representative AP histochemical staining photomicrographs of skeletal muscles, heart, and internal organs from Generic, an age-matched dog that did not receive AAV injection. CS, cranial sartorius; DPH, diaphragm; ECU, extensor carpi ulnaris; LV, left ventricle; RA, right atrium; SP, superficial pectoralis; TB, triceps brachii.



**SUPPLEMENTARY FIG. S3.** High-dose AAV-9 and AAV-8 systemic injection in neonatal dogs does not induce T-cell infiltration in striated muscles. **(A)** Representative photomicrographs of immunohistostaining for CD4<sup>+</sup> and CD8<sup>+</sup> cells in limb muscles and the heart. Arrow, rare occurring residential T-cells; box insert, high-power magnification of positively stained residential T-cells in the respective image. **(B)** Quantitative examination of T-cell number in limb muscles and the heart.



**SUPPLEMENTARY FIG. S4.** High-dose AAV-9 and AAV-8 systemic injection in neonatal dogs does not show remarkable transduction in lymph nodes. Representative microphotographs of AP histochemical staining and HE staining from the cortex (upper panels) and medulla (lower panels) of the lymph node. AP-positive staining is seen in the capsule (arrowhead) and the trabecula (arrow) in the cortex of the lymph node from AAV-8-injected dog (Artemis) and in the medulla of the lymph node from AAV-8- and AAV-9-injected dogs.

# Duchenne Muscular Dystrophy Gene Therapy in the Canine Model

Dongsheng Duan

## Abstract

Duchenne muscular dystrophy (DMD) is an X-linked lethal muscle disease caused by dystrophin deficiency. Gene therapy has significantly improved the outcome of dystrophin-deficient mice. Yet, clinical translation has not resulted in the expected benefits in human patients. This translational gap is largely because of the insufficient modeling of DMD in mice. Specifically, mice lacking dystrophin show minimum dystrophic symptoms, and they do not respond to the gene therapy vector in the same way as human patients do. Further, the size of a mouse is hundredfolds smaller than a boy, making it impossible to scale-up gene therapy in a mouse model. None of these limitations exist in the canine DMD (cDMD) model. For this reason, cDMD dogs have been considered a highly valuable platform to test experimental DMD gene therapy. Over the last three decades, a variety of gene therapy approaches have been evaluated in cDMD dogs using a number of nonviral and viral vectors. These studies have provided critical insight for the development of an effective gene therapy protocol in human patients. This review discusses the history, current status, and future directions of the DMD gene therapy in the canine model.

## Duchenne Muscular Dystrophy and the Canine Duchenne Muscular Dystrophy Model

**D**UCHENNE MUSCULAR DYSTROPHY (DMD) is a fatal muscle disease caused by null mutations in the *dystrophin* gene, a 2.4 mb gene in the X-chromosome.<sup>1,2</sup> DMD occurs in ~1 in 5,000 male births.<sup>3</sup> Affected boys show delayed motor skill development between ages 2 and 5. They lose ambulation in their early teens and die around age 20 because of cardiorespiratory failure (Table 1).<sup>4</sup> The current standard of care includes steroids, palliative support, and symptom management.<sup>5,6</sup> Unfortunately, these therapies cannot solve the fundamental problem of dystrophin deficiency in DMD. Gene therapy has the potential to bring back the missing protein and radically change the disease course.<sup>7</sup>

Dystrophin is a 427 kDa subsarcolemmal protein. It has four major functional domains: the N-terminal, rod, cysteine-rich, and C-terminal domains (Fig. 1). The N-terminal domain binds to  $\gamma$ -actin. The rod domain constitutes of 24 spectrin-like repeats and four intervening hinges. Repeats 1–3 have been suggested to interact with the membrane lipid bilayer. Repeats 11–15 form the second actin-binding domain. Repeats 16 and 17 contain the neuronal nitric oxide synthase (nNOS)-binding motif. Repeats 20–23 interact with microtubule. Hinges are thought to provide flexibility

to the dystrophin protein. The cysteine-rich domain and a part of hinge 4 bind to the transmembrane glycoprotein dystroglycan that interacts with laminin in the extracellular matrix (ECM). The C-terminal domain interacts with dystrobrevin and syntrophin. Through interaction with dystroglycan and actin/microtubule, dystrophin links the ECM with the cytoskeleton and provides mechanic stability to muscle cells during contraction. Dystrophin also mediates muscle signaling through its interaction with nNOS, syntrophin, and dystrobrevin. Transmembrane protein sarcoglycans and sarcospan further strengthen the structure connection between the cytoskeleton and the ECM. The dystrophin-associated glycoprotein complex (DGC) formed by dystrophin and its partners provides essential support for normal muscle structure and function (Fig. 1).

More than 60 dystrophin-deficient animal models have been reported in the literature.<sup>8</sup> These models have played a pivotal role in elucidating the biological function of dystrophin and pathogenic mechanisms of DMD. They are also essential for the establishment of the scientific premise for DMD gene therapy.<sup>9–11</sup> The majority of the proof-of-principle gene therapy studies are conducted in the *mdx* mouse, a spontaneous dystrophin-deficient mouse strain with a nonsense mutation in the exon 23 of the dystrophin gene.<sup>12,13</sup> Several gene therapy strategies have effectively

Department of Molecular Microbiology and Immunology, Department of Neurology School of Medicine, University of Missouri, Columbia, MO 65212.

TABLE 1. A COMPARISON OF CANINE AND HUMAN DUCHENNE MUSCULAR DYSTROPHY

	<i>Canine DMD</i>	<i>Human DMD</i>
<b>General</b>		
Mutation type	Point mutations, deletions, insertions	Mainly deletions (~60%) and duplications (~10%)
Lifespan reduction	By 75%	By 75%
Disease course	Progressive and severe	Progressive and severe
Birth body weight	Same as a normal puppy	Same as a normal baby
Neonatal death	15–30%	Rare
Onset of disease	Birth (weak milk sucking or death) to 3 months (activity reduction)	2–5 years; patients cannot reach motor development milestones
Ambulation	Rarely lost	Wheelchair-bound by early teenage
Growth retardation	Common	Rare unless the patient is on steroids
Kyphosis	Yes	Yes
Muscle wasting	Yes	Yes
Limb muscle hypertrophy	Cranial sartorius	Calf muscle
<b>Histopathology</b>		
Pathology at birth	Minimal	Minimal
Limb muscle fibrosis	Yes	Yes
Centronucleation	Limited	Limited
<b>Limb muscle MRI</b>		
Abductor	N/A	Affected
Biceps femoris	Affected	Affected, prominent fat replacement
Cranial tibialis	N/A	Relatively spared
Gluteus	N/A	Affected
Gracilis	Affected	Often preserved
Sartorius	Hypertrophic	Relatively spared
Semitendinosus	Severely affected	Less affected
<b>Heart</b>		
Abnormal ECG	Frequent	Frequent
Function reduction	Detectable by 6 months of age	Evident by 16 years of age
Death from heart failure	Seldom	More common than used to
<b>Cognitive defect</b>		
Prevalence	N/A	One-third of patients
Correlation with gene mutation	N/A	Often involves dystrophin C-terminus
Correlation with muscle disease	N/A	No correlation
<b>Gene therapy tested</b>		
Gene replacement and RNA repair	Full-length dystrophin plasmid, adenovirus minidystrophin, gutted adenovirus full-length dystrophin, AAV microdystrophin, AAV exon skipping, AON exon skipping	Full-length dystrophin plasmid, AAV microdystrophin, AON exon skipping
DNA repair	Only been tested in one GRMD dog	N/A
Dystrophin independent	N/A	AAV follistatin tested in BMD patients

AAV, adeno-associated virus; AON, antisense oligonucleotide; BMD, Becker muscular dystrophy; DMD, Duchenne muscular dystrophy; GRMD, golden retriever muscular dystrophy; N/A, no information available.

ameliorated muscle pathology and enhanced muscle force in mdx mice. However, translation to patients has encountered great difficulties. A major reason for the delay in translation is the inherent limitations of the mdx model. For example, mdx mice show very mild clinical symptoms and they cannot accurately model the immune response to the gene therapy vector. The huge body size difference between a mouse and a boy also presents a significant scale-up challenge.

Concurrent with the discovery of the mdx mouse,<sup>14</sup> a canine DMD (cDMD) model was established.<sup>15,16</sup> This dystrophic dog is a golden retriever. Hence, it is called the golden retriever muscular dystrophy (GRMD) dog. The GRMD dog carries a point mutation (adenine to guanine transition) in the intron 6 of the *dystrophin* gene. This mutation disrupts nor-

mal splicing. As a consequence, exon 7 is excluded from the final messenger RNA. Connection of exons 6 and 8 introduces a frameshift mutation. Dystrophin translation is aborted in exon 8 because of the premature stop codon in the mutated transcript.<sup>15</sup> Since then, dystrophin-deficient dogs have been described in many other breeds.<sup>15,17–33</sup> The majority of these reports are descriptive case studies. *Dystrophin* mutations have been determined in some breeds. However, research colonies have only been established in a few breeds (GRMD, beagle with GRMD mutation, corgi with intron 13 insertion, Labrador retriever with intron 19 insertion, and Cavalier King Charles spaniel with exon 50 point mutation).<sup>8,34</sup> DMD is a worldwide disease occurring in every race and every country. The genetic background of

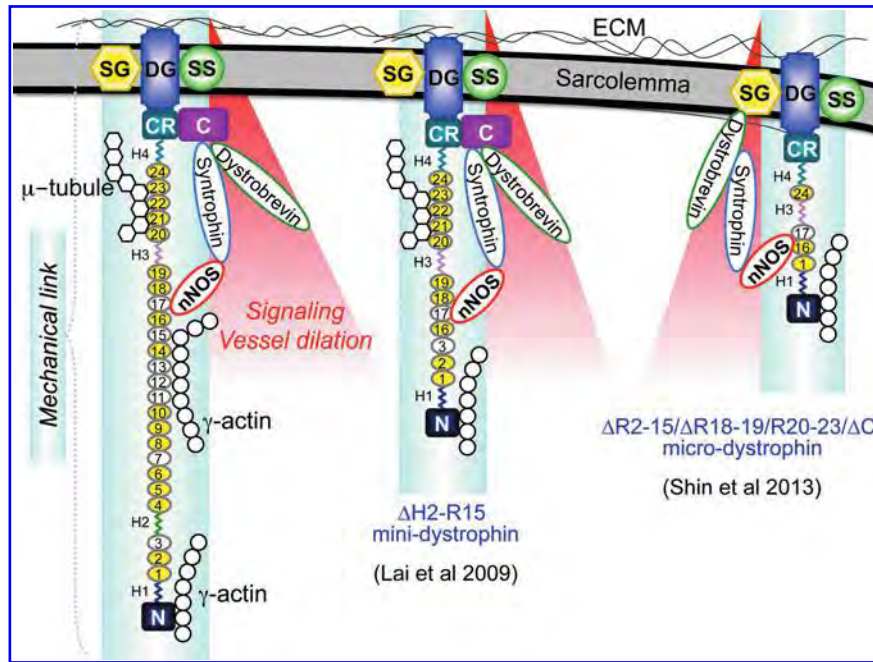


**FIG. 1.** Dystrophin, minidystrophin, microdystrophin, and the DGC. Dystrophin and its associated proteins constitute the DGC. The DGC provides mechanical support and signaling function for muscle. Nitric oxide generated by nNOS dilates the vasculature during muscle contraction to meet metabolic needs of the muscle. Minidystrophins are about half the size of full-length dystrophin. The representative  $\Delta$ H2-R15 minidystrophin protein contains all the known functional domain of the full-length protein (see reference 73). Microdystrophins are about one-third the size of full-length dystrophin. The representative  $\Delta$ R2-15/ $\Delta$ R18-19/ $\Delta$ R20-23/ $\Delta$ C microdystrophin protein restored sarcolemmal nNOS expression in mdx mice and improved muscle function in adult dystrophic dogs (see reference 40). C, dystrophin C-terminal domain; CR, dystrophin cysteine-rich domain; DGC, dystroglycan complex; ECM, extracellular matrix; H, hinge in the middle rod domain of dystrophin; N, dystrophin N-terminal domain; SG, sarcoglycan complex; SS, sarcospan. Numerical numbers refer to the number of spectrin-like repeats in the dystrophin rod domain. Note, the lipid-binding property of spectrin-like repeats 1–3 is not depicted.

the patients is highly variable and complex. A pure breed cannot model this heterogeneity. To overcome this shortcoming, we have generated hybrid DMD dogs.<sup>35–40</sup> These dogs carry the genetic information from several breeds and thus can better reflect the human condition.

In contrast to mdx mice, dystrophin-deficient dogs share many clinical features of human patients (Table 1). At birth, affected puppies are often weak and cannot compete with littermates for milk. As they reach 2–3 months of age (~3 years of age in humans), they begin to show signs of limb muscle weakness such as frequent rests, difficulty in walking, and reduced activity. The condition continues to deteriorate. Conspicuous muscular dystrophy is seen around 6 months of age. Typical symptoms at this age include excessive salivation, stunted growth, muscle wasting, abnormal gait, joint contracture, dysphagia, and aspiration pneumonia. By 3 years of age (~20 years of age in humans), affected dogs either die from cardiorespiratory complications or are euthanized because of poor health condition (Table 1). The cDMD model not only shares symptomatic similarity to human patients, but also has histological lesions resembling those of human patients. For example, limb muscle fibrosis is a common feature in DMD patients. This is observed in cDMD dogs but not in mdx mice. Centronucleation is not a prominent feature in patients because of poor muscle regeneration. This is reflected in cDMD dog muscle but not in mdx muscle.

Besides clinical manifestations and histology, the dog also has the advantage to simulate the immune response observed

in DMD patients in gene therapy. Adeno-associated virus (AAV) is the most advanced viral vector for DMD gene therapy. However, AAV-mediated DMD gene therapy has been deterred by the cellular immune response.<sup>41,42</sup> For example, muscle injection results in persistent AAV transduction in mdx mice. But nominal transduction is detected in DMD patients following direct injection.<sup>43</sup> Similar to human patients, intramuscular injection also induces robust immune rejection in affected dogs (Table 2).<sup>44–46</sup> For this reason, the canine model will be very useful to dissect the underlying mechanisms of the immune response and to develop creative strategies to evade immune surveillance.

Scale-up is a significant challenge in human gene therapy. There are issues related to vector purity, procedure safety, vector dose and dose regimen, host response, metabolic rate and body weight of the host, and so on. Large-scale vector production may amplify contaminations that are negligible in small-scale preparations.<sup>47</sup> Infusion of trillions of viral particles to a dystrophic boy may lead to unexpected inflammatory and/or immune response and possibly fatal complications.<sup>48</sup> A phenotypic large animal model (such as cDMD dogs) will be ideal to address these issues.

Collectively, given the biological and immunological similarities between dystrophic dogs and DMD patients, also given the advantage for scale-up, the cDMD model represents a highly valuable tool for the development and fine-tuning of gene therapy protocols before the human trial.

TABLE 2. CELLULAR IMMUNE RESPONSE TO ADENO-ASSOCIATED VIRUS IN THE CANINE DUCHENNE MUSCULAR DYSTROPHY MODEL

Serotype	Dog age	Route of delivery	CTL	Comments	References
AAV-1	Young adult	Local limb muscle injection and limb perfusion	No	The vector does not express a protein.	Vulin et al. (2012) <sup>9</sup>
AAV-2	Not tested in cDMD dogs	Local limb muscle injection <sup>a</sup>	Yes <sup>a</sup>	CTL to either capsid (Wang et al. 2007) <sup>44</sup> or transgene (Yuasa et al. 2007) <sup>a,45</sup>	Yuasa et al. (2007) <sup>a,45</sup> Wang et al. (2007) <sup>a,44</sup>
AAV-6	Adult	Local limb muscle injection	Yes	CTL to capsid. CTL is reduced by immune suppression and elimination of the contaminating capsid gene.	Wang et al. (2007) <sup>44,124</sup> , 2014 <sup>129</sup> ), Shin et al. (2012) <sup>37</sup>
AAV-6	Young adult	Local injection to heart	No	The vector does not express a protein.	Bish et al. (2012) <sup>102</sup> , Barbash et al. (2013) <sup>101</sup>
AAV-8	Young adult	Local limb muscle injection and limb perfusion	Yes	Local injection resulted in at least 1 m expression. Intravascular delivery led to at least 2 m expression but there was a clear trend of expression reduction over time.	Ohshima et al. (2008) <sup>131</sup>
AAV-8	Young adult	Local limb muscle injection	No	Single-dog study. Expression lasted for at least 2 m.	Koo et al. (2011) <sup>133</sup>
AAV-8	Young adult	Limb perfusion	No	The vector does not express a protein.	Le Guiner et al. (2014) <sup>100</sup>
AAV-9	Neonatal	Intravenous injection	No?	Severe innate immune response. No CD4+ and CD8+ T cell infiltration.	Kornegay et al. (2010) <sup>84</sup>
Y731F AAV-9	Adult	Local limb muscle injection	Yes	CD4+ and CD8+ T cell infiltration despite transient immune suppression. But saturated expression was observed for at least 2 m.	Shin et al. (2013) <sup>40</sup>

<sup>a</sup>Study performed in normal dog muscle.  
cDMD, canine DMD; CTL, cytotoxic T lymphocyte.

### Current Status of DMD Gene Therapy in the Canine Model

Discovery of the *dystrophin* gene opens the door to correct DMD by gene therapy.<sup>49</sup> The 2.4 mb full-length *dystrophin* gene contains 79 exons, and it produces a 11.5 kb cDNA. Since dystrophin deficiency underlies DMD pathogenesis, the majority of gene therapy approaches have been centered on the restoration of dystrophin expression. Currently, there are three distinctive classes of approaches, including gene replacement, gene repair, and dystrophin-independent gene therapy. All these approaches have been evaluated in the cDMD model.

#### *Dystrophin replacement therapy in the cDMD model*

Direct injection of a plasmid to muscle is perhaps the simplest method. However, it is very inefficient. Only a few dystrophin-positive cells (less than 1%) were observed after intramuscular injection of dystrophin plasmids to either newborn or adult GRMD dogs.<sup>50–52</sup> Limited expression and immune cell infiltration were observed following electrotransfer of canine dystrophin plasmids to GRMD muscle.<sup>53,54</sup>

Adenovirus is the first viral vector used for delivering dystrophin to the canine muscle. Since the first-generation adenoviral vector has a packaging capacity of 8.2 kb,<sup>55</sup> investigators used a 6.2 kb, minimized *dystrophin* gene called the  $\Delta 17$ –48 minigene.<sup>56</sup> This minigene is isolated from a very mild patient who was ambulant at age 61.<sup>57</sup> A large portion of the rod do-

main (from exon 17 to 48) is absent in this minidystrophin because of an in-frame deletion. Compared with plasmid injection, adenoviral delivery to neonatal GRMD puppies resulted in significantly much more efficient transduction.<sup>58,59</sup> However, minidystrophin expression did not last long because of strong cellular immune responses to the adenoviral vector and human minidystrophin. Application of immune suppressive drug cyclosporine only moderately prolonged gene transfer.<sup>58</sup> Guttated adenoviral vector has a carrying capacity up to 35 kb.<sup>60</sup> It offers a great opportunity to deliver the full-length cDNA. Gilbert et al. generated a full-length human dystrophin gutted adenoviral vector and tested it in GRMD puppies. Unfortunately, only limit transduction was observed.<sup>61</sup>

AAV is a 4.7 kb single-stranded DNA virus. AAV-based gene replacement therapy has shown unprecedented clinical success in treating inherited diseases.<sup>62</sup> However, there is a major limiting factor to use AAV in DMD gene therapy. The maximum packaging capacity of the AAV vector is 5 kb. This excludes the possibility of delivering the full-length dystrophin cDNA or even a truncated *minidystrophin* gene with the AAV vector.<sup>63</sup> To overcome this hurdle, investigators engineered super small microdystrophin. The microgene carries only one-third of the dystrophin coding sequence (~4 kb).<sup>64,65</sup> Unlike the  $\Delta 17$ –48 minigene, there is no human precedent of a functional microgene. Although patients with super-large in-frame deletions have been identified and expression of micro-size dystrophin has been confirmed in some cases, unfortunately, these patients invariably displayed severe clinical

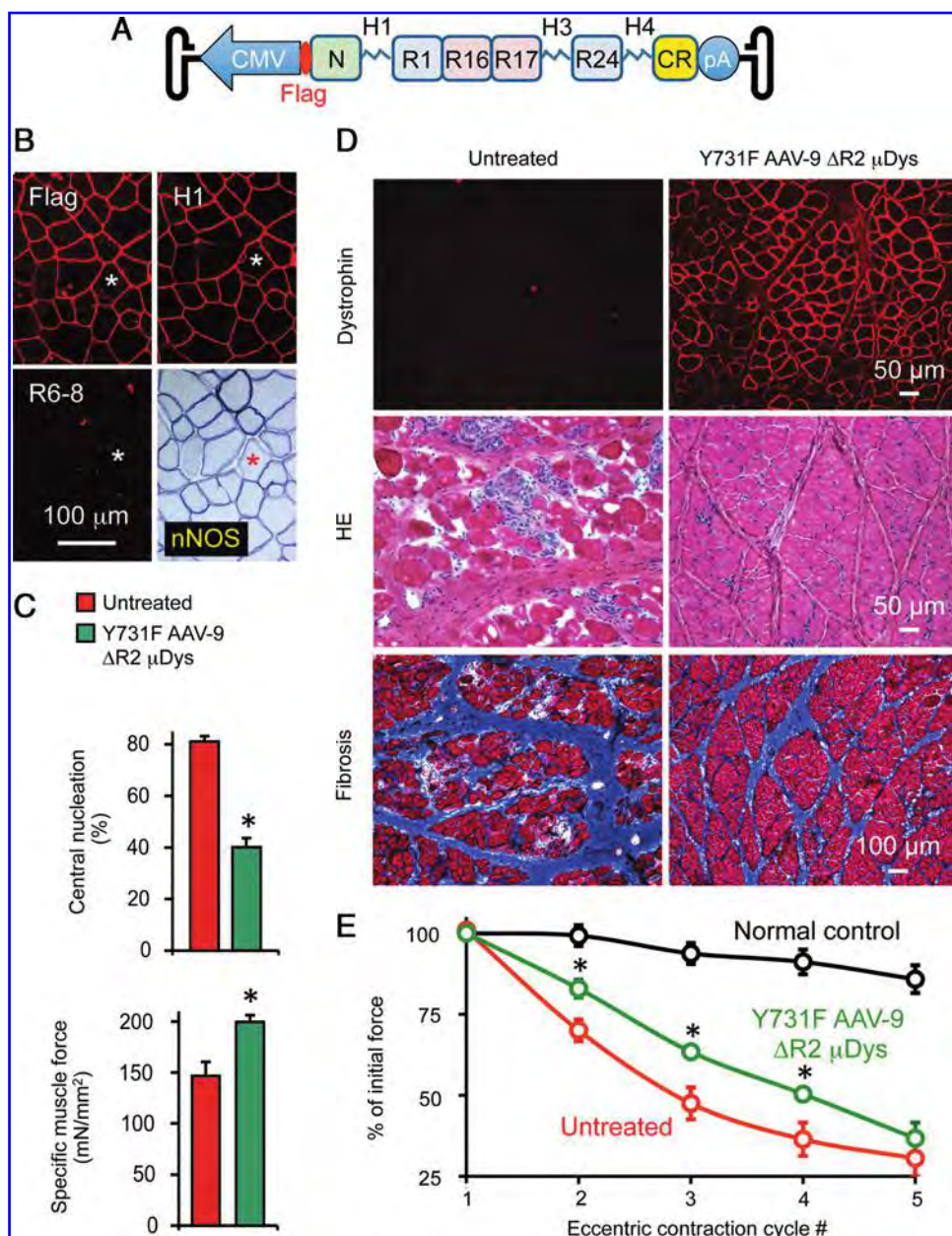
disease.<sup>66-69</sup> Since a spontaneous functional microgene does not exist, researchers have built a series of artificial microgenes based on our understanding on dystrophin. To determine the therapeutic potential of the microgene, various configurations of AAV microdystrophin vectors were injected in mdx mice. The majority of these rationally designed microgene vectors significantly protected mouse skeletal muscle and the heart.<sup>70-82</sup> Surprisingly, when microdystrophin was initially tested in the cDMD model, it did not deliver therapeutic benefits.<sup>83</sup> In one case, the phenotype of the treated dogs even became much worse.<sup>84</sup>

Over the last few years, several critical but previously unrecognized aspects of dystrophin biology are elucidated. Specifically, it is found that (1) minidystrophins with paired spectrin-like repeats are functionally superior to the ones with odd number repeats<sup>82</sup>; (2) hinge 2 negatively influences microdystrophin function<sup>85</sup>; (3) spectrin-like repeats 16 and 17 (R16/17) are required to anchor nNOS to the sarcolemma

to prevent functional ischemia<sup>73,86</sup>; and (4) codon optimization can significantly improve microdystrophin function.<sup>87</sup> To determine whether incorporation of these new developments can enhance the performance of the microgene in muscles of large mammals, we generated the  $\Delta R2-15/\Delta R18-19/\Delta R20-23/\Delta C$  microgene.<sup>73,88</sup> This microgene has four spectrin-like repeats. Among which, two of the repeats are R16 and R17. We have also replaced hinge 2 with hinge 3 (Fig. 2). We delivered the codon-optimized canine version of this microgene to mdx mice and dystrophic dogs using tyrosine-engineered AAV-9.<sup>40</sup> Systemic gene transfer restored sarcolemmal nNOS expression and enhanced muscle function in mdx mice. (Fig. 2B and C)<sup>40</sup>

In six random-bred dystrophic dogs (10-28 months old), direct muscle injection resulted in saturated microdystrophin expression and dramatic histological improvement. Macrophage infiltration, fibrosis, and calcification were all greatly reduced (Fig. 2D).<sup>40</sup> Importantly, treatment significantly protected the

**FIG. 2.** Y731F AAV-9-mediated  $\Delta R2-15/\Delta R18-19/\Delta R20-23/\Delta C$  microdystrophin expression ameliorated skeletal muscle disease in mdx mice and adult DMD dogs. (A) Schematic outline of the  $\Delta R2-15/\Delta R18-19/\Delta R20-23/\Delta C$  microgene ( $\Delta R2 \mu Dys$ ) AAV vector. The microgene is driven by the ubiquitous CMV promoter. A flag tag is fused to the N-terminal end of the microgene for unequivocal determination of microgene expression. (B) Evaluation of the  $\Delta R2 \mu Dys$  expression in mdx mice. Representative serial muscle sections were stained for the Flag tag, hinge 1, repeats 6-8, and nNOS activity. \*The same myofiber in serial sections. R6-8 is absent in  $\Delta R2 \mu Dys$ . (C)  $\Delta R2 \mu Dys$  therapy significantly reduced pathological central nucleation and enhanced specific muscle force in mdx mice. \* $p < 0.05$ . (D)  $\Delta R2 \mu Dys$  therapy greatly improved overall histology, reduced muscle inflammation, and fibrosis in adult dystrophic dogs. The untreated and AAV-treated sides are the left and right sides of the extensor carpi ulnaris muscles of the same dog, respectively. (E)  $\Delta R2 \mu Dys$  therapy significantly preserved muscle force during eccentric contraction in affected dogs. \* $p < 0.05$ . AAV, adeno-associated virus; DMD, Duchenne muscular dystrophy.



dystrophic muscle from eccentric contraction-induced force loss, a physiological hallmark of DMD (Fig. 2E).<sup>40</sup> Our data suggest that microdystrophin may ameliorate muscular dystrophy in a large mammal, potentially in human patients. Our data also suggest that the  $\Delta R2-15/\Delta R18-19/\Delta R20-23/\Delta C$  microgene is an excellent candidate gene for treating DMD. Interestingly, soon after the publication of our study, Baroncelli et al. discovered a 3-year-old dog with a mild Becker muscular dystrophy (BMD) phenotype.<sup>29</sup> On Western blot, the authors detected a micro-size dystrophin migrating at 130–140 kDa. Further investigations may reveal the location of the deletion in this BMD dog and provide critical insight to the design of next-generation microgene.

#### *Dystrophin repair therapy in the cDMD model*

The reading-frame rule explains the correlation between the mutation in the *dystrophin* gene and the clinical presentation in patients.<sup>9,90</sup> Frame-shift mutation results in a complete loss of dystrophin and severe phenotype. However, patients with in-frame mutation often express a smaller but partially functional protein. These patients manifest a much milder clinical disease and are classified as BMD. The reading-frame rule suggests that lethal DMD can be converted to less severe BMD if an out-of-frame transcript can be converted to an in-frame transcript. Based on this theory, investigators have developed exon skipping. In this strategy, antisense oligonucleotides (AONs) are used to modulate the splicing machinery so that certain exons are excluded from the mRNA. The modified mRNA produces an internally deleted dystrophin protein similar to that observed in BMD patients.

Initial exon skipping studies were conducted using 2'-O-methylated phosphorothioate (2OMe-PS) and phosphorodiamidate morpholino oligomers (PMO). These AONs worked very well in cultured muscle cells obtained from different breeds of dystrophic dogs.<sup>19,91,92</sup> Local injection also resulted in exon skipping in GRMD and beagle-background GRMD dogs.<sup>92,93</sup> While a single AON seems sufficient for exon skipping in myoblasts,<sup>19,92</sup> interestingly, a cocktail of AONs is required for efficient exon skipping in canine muscle *in vivo*.<sup>92</sup> To test whole-body exon skipping, Yokota et al. delivered the PMO cocktail to beagle-background GRMD dogs by intravenous injection.<sup>92</sup> Systemic therapy resulted in widespread dystrophin expression and clinical improvement. Short half-life and limited tissue penetration are the major limitations of 2OMe-PS and PMO. To overcome these obstacles, various modified AONs are developed.<sup>94</sup> These modified AONs are conjugated with cell-penetrating peptides or polymers. Conjugation significantly enhances the tissue uptake of AONs in mdx mice. However, so far only the *vivo*-morpholino (PMO conjugated with the octaguanidine dendrimer) has been tested in the dog model by local injection.<sup>95</sup> As expected, the *vivo*-morpholino resulted in robust, much persistent exon skipping.<sup>95</sup>

An alternative approach to improve exon skipping is to deliver the AON with an AAV vector.<sup>96</sup> In this approach, the U7 promoter is used to drive the expression of an AON that is fused to the U7 small nuclear RNA (snRNA).<sup>97,98</sup> The snRNA allows efficient targeting of the AON to the spliceosome in the nucleus. AAV allows efficient tissue penetration and continuous production of the AON. Two different studies evaluated the AAV U7 approach for skeletal muscle gene therapy in GRMD

dogs. Vulin et al. co-expressed two AONs (one for exon 6 skipping and the other for exon 8 skipping) in one vector using AAV-1 (AAV1-U7E6/8).<sup>99</sup> Exclusion of exons 6 and 8 results in an in-frame  $\Delta 6-8$  transcript. Investigators performed local injection and forelimb perfusion in six 5–15-month-old dogs and multimuscle injection in the hindlimb of four 3-week-old puppies. Efficient dystrophin restoration (20–80% positive myofibers) was observed up to 10 months after injection. Treatment reduced the number of calcified myofibers and improved parameters of magnetic resonance imaging (MRI). Further, specific muscle force was enhanced in treated puppies.<sup>99</sup> Le Guiner et al. delivered the same set of AONs to fifteen 3–4-month-old juvenile GRMD dogs by forelimb perfusion.<sup>100</sup> Instead of AAV-1, the authors used AAV-8 (AAV8-U7E6/8). At 2–3.5 months after injection, the authors observed high-level dystrophin expression (10–80% positive myofibers), reduced regeneration and fibrosis (but no change in inflammation and calcification), and improvement in MRI parameters. In dogs with  $\geq 40\%$  dystrophin-positive myofibers, treatment also prevented progressive force decline.<sup>100</sup>

Two independent groups examined AAV-6-mediated exon skipping in the heart of GRMD dogs using exactly the same U7E6/8 construct developed by Vulin et al.<sup>99,101,102</sup> AAV-6 U7E6/8 was delivered by multiple transendocardial injection in young adult dogs (5–13 months old). Both groups achieved expected exon skipping and dystrophin restoration. Bish et al. followed 5 dogs for 13 months and observed a clear reduction of myocardial fibrosis and an improvement of the peak circumferential strain in cardiac MRI.<sup>102</sup> Barbash et al. followed 5 treated dogs for 3 months and demonstrated the stabilization of left ventricular ejection fraction by cardiac MRI.<sup>101</sup>

Besides exon skipping, gene repair therapy can also be used to correct the mutation itself. Oligonucleotide-mediated gene correction and nuclease-based gene editing are two primary approaches. However, these DNA-level gene repair strategies are largely unexplored in the canine model. So far, only one study tried a chimeric RNA/DNA oligonucleotide in one 6-week-old GRMD puppy.<sup>103</sup> The authors showed evidence of gene correction up to 1 year after therapy.

#### *Dystrophin-independent gene therapy in the cDMD model*

A number of cellular proteins have been shown to modify the dystrophic phenotype.<sup>104</sup> These include utrophin,  $\alpha 7\beta 1$ -integrin, myostatin, insulin-like growth factor-1, cytotoxic T cell GalNAc transferase, sarcoplasmic reticulum calcium ATPase (SERCA), peroxisome proliferator-activated receptor gamma coactivator 1 $\alpha$ , osteopontin, and latent transforming growth factor- $\beta$  (TGF- $\beta$ ) binding protein 4. Many of these have been confirmed in mouse studies by gene knock, transgenic overexpression, and AAV-mediated gene transfer. However, only two of the modifiers have been tested in the cDMD model.

Utrophin is a dystrophin homologous protein. It shares structural and functional similarity to dystrophin. A minimized utrophin has been developed based on the  $\Delta 17-48$  *minidystrophin* gene. Cerletti et al. injected the miniutrophin adenoviral vector to 2-day-old GRMD puppies.<sup>105</sup> In immune-suppressed animals, they achieved a 15% transduction efficiency and significant reduction of fibrosis at 2 months after treatment. The highly abbreviated microutrophin

gene has also been generated recently.<sup>86,106</sup> Therapeutic effect of microtrophin remains to be tested in affected dogs.

Myostatin is a TGF- $\beta$  family muscle growth regulator.<sup>107</sup> Myostatin inhibition has been shown to increase muscle size and reduce myopathy in mdx mice.<sup>108</sup> Spontaneous mutation in the myostatin gene also leads to muscle hypertrophy in whippet dogs.<sup>109</sup> To determine whether myostatin inhibition can ameliorate muscle disease in GRMD dogs, Bish et al. expressed a secreted dominant negative myostatin peptide in the liver of four 9–10-month-old GRMD dogs using AAV-8.<sup>110</sup> Thirteen months after injection, they observed the expected increase in muscle mass. Furthermore, treatment reduced the serum creatine kinase level and muscle fibrosis. More recently, Cotten et al. crossed GRMD dogs with the myostatin-deficient whippets.<sup>111</sup> The myostatin level was reduced in myostatin heterozygous GRMD dogs. Surprisingly, these dogs displayed a more severe phenotype. The discrepancy between Bish et al.'s study and Cotten et al.'s study remains to be explained. However, it should be pointed out

that an increase in the myofiber size could be counterproductive in dystrophin-null muscle because the higher surface-to-volume ratio may result in higher sarcolemmal stress during contraction.

SERCA overexpression protects heart and muscle in rodent models of muscular dystrophy.<sup>112,116</sup> AAV-mediated SERCA expression has also improved cardiac function in various canine models of heart failure.<sup>117,118</sup> Based on these results, it is possible that AAV SERCA therapy may also reduce muscle disease in cDMD dogs.

### Systemic AAV Delivery in Dogs

DMD affects all muscles in the body. Only whole-body gene therapy can truly change the outcome of the disease. Systemic gene delivery has been established in mice using AAV-1, 6, 8, and 9 since 2004.<sup>72,119,120</sup> However, only a few studies have evaluated intravascular AAV delivery in dogs. We demonstrated the first successful systemic gene

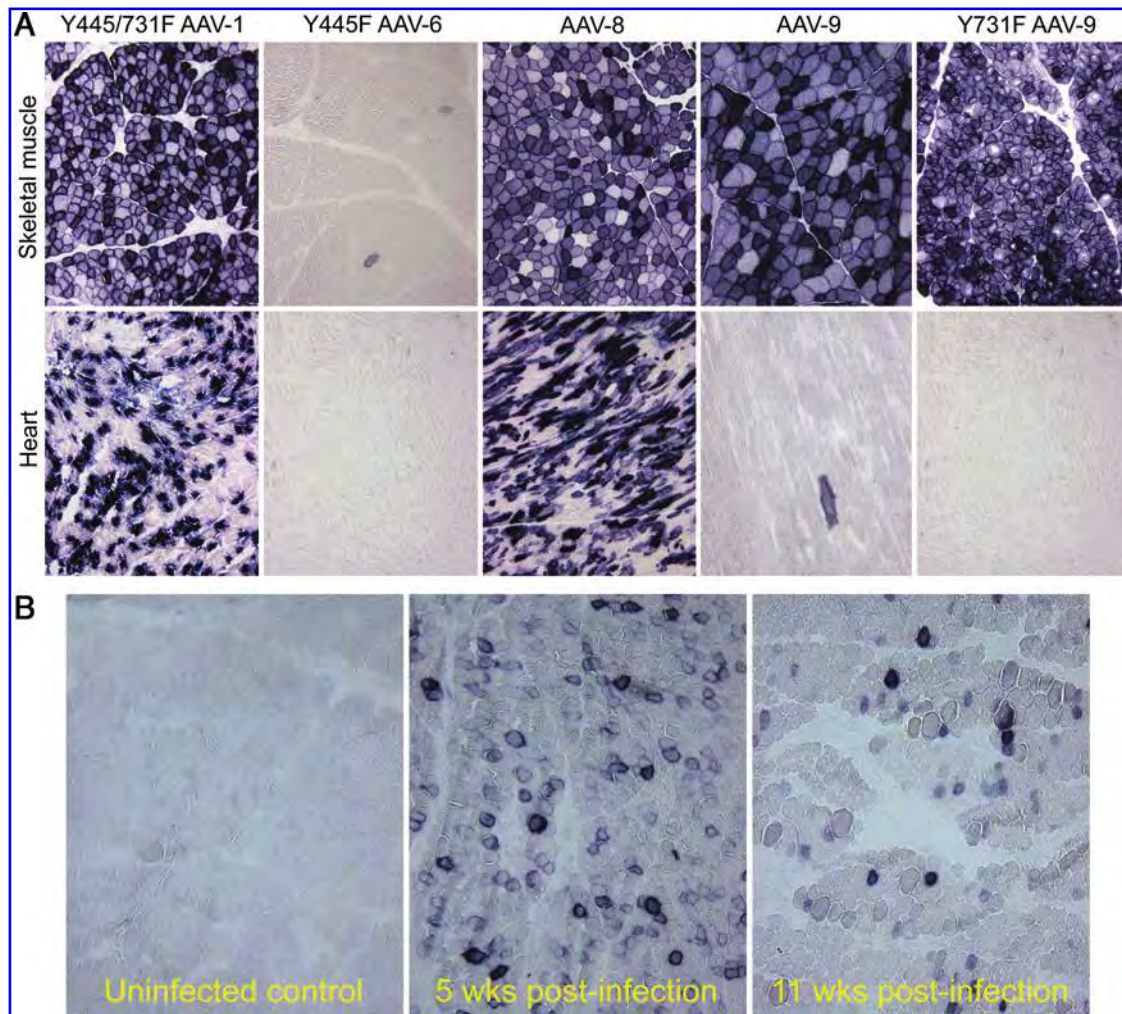


**FIG. 3.** Systemic AAV delivery in neonatal dogs. **(A)** Comparison of five different AAV variants in normal neonatal dogs. AAV-8 and tyrosine-engineered Y445/731F AAV-1 resulted in robust transduction in both skeletal muscle and the heart. AAV-9 and its variant Y731 AAV-9 effectively transduced only skeletal muscle. Y445F AAV-6 barely transduced striated muscle in neonatal dogs. **(B)** Evaluation of systemic AAV-9 gene transfer in neonatal affected dogs. An AAV-9 alkaline phosphatase reporter gene vector was injected to a 2-day-old affected puppy through the jugular vein. Efficient transduction was observed at 5 weeks postinfection. Transduction was still observed at the 11 weeks of age. However, expression appeared reduced.

transfer in newborn dogs in 2008 using AAV-9 (Fig. 3).<sup>46</sup> AAV-9 has been considered as a “cardiotropic” vector because of its efficient myocardial transduction in rodents.<sup>120,121</sup> Unexpectedly, the dog heart was barely transduced by AAV-9.<sup>46</sup> Over the last few years, we tested additional AAV serotypes and identified AAV-8 and Y445/731F AAV-1 as the preferred vectors for whole-body (heart and skeletal muscle) gene transfer in neonatal dogs (Fig. 3A).<sup>122,123</sup> We also tested AAV-6. Interestingly, little muscle transduction was observed.<sup>123</sup> This is in sharp contrast to what has been shown with direct AAV-6 injection in dog muscle.<sup>101,102,124</sup> We believe that the difference is likely because of (1) the high-level preexisting AAV-6 neutralization antibody in the canine circulation,<sup>36,125</sup> or (2) the presence of galectin 3 binding protein (G3BP) in dog serum.<sup>126</sup> It has been shown that G3BP can cause AAV-6 particle aggregation and compromise transduction.<sup>126</sup>

Few studies have evaluated bodywide gene transfer in the cDMD model (Fig. 3B). Kornegay et al. delivered an AAV-9 microdystrophin vector to newborn GRMD puppies via the jugular vein.<sup>84</sup> Injection resulted in widespread transduction. Unfortunately, these puppies also developed a fulminant inflammatory response and had to be euthanized. We recently explored systemic AAV-9 injection in adolescent dystrophic dogs.<sup>127</sup> Gene transfer resulted in bodywide transduction in striated muscles without any untoward reaction.

### Cellular Immune Response to AAV-Mediated Gene Transfer in the Canine Model

Host immune response is undoubtedly one of the greatest hurdles in gene therapy. It is influenced by the viral capsid, vector dose and purity, method of vector production and purification, delivery route, animal age and preexisting immunity, expression cassette (such as the promoter and microRNA142-3p-binding site), transgene product, regime of immune suppression, the species tested, and even the species origin of the transgene. Many studies have examined AAV immune reaction in normal and dystrophic dog muscle (Table 2). While it is generally thought that AAV can induce the cytotoxic T lymphocyte (CTL) response in canine muscle, there are important controversies that remain to be reconciled.

Vulin et al. found that intramuscular ( $3.5 \times 10^{12}$  vg) or intravascular ( $1.4 \times 10^{13}$  vg) injection of an AAV-1 vector that does not express a protein did not elicit the CTL response in GRMD dogs.<sup>99</sup> However, Wang et al. detected a strong T cell response to AAV-1 capsid in normal dog muscle after injection of a much lower dose ( $5 \times 10^{11}$  vg) of a canine factor IX vector.<sup>128</sup>

Two different groups reported cellular immune reaction to AAV-2 following direct muscle injection in normal dogs.<sup>44,45</sup> Results of Yuasa et al. suggest that the immune response is against the transgene product (LacZ).<sup>45</sup> But Wang et al. showed that the immune response is independent of the transgene product.<sup>44</sup> Wang et al. observed robust mononuclear cell infiltration even with empty capsids.<sup>44</sup>

AAV-6 has been shown to induce capsid-specific T cell infiltration in skeletal muscle of normal and affected dogs following direct injection.<sup>44,124</sup> A similar capsid-specific immune response was detected when AAV-6 was injected to the heart of nondystrophic dogs.<sup>117</sup> In support of these observations, transient immune suppression significantly pro-

longed transgene expression.<sup>37,117,124</sup> Further, elimination of the contaminating AAV-6 capsid gene reduced the immune response.<sup>129</sup> Surprisingly, transendocardial injection of AAV-6 to normal or affected dog heart did not induce T cell reaction.<sup>101,102,130</sup>

Initial study with AAV-8 revealed transient expression and T cell infiltration in dog skeletal muscle irrespective of muscular dystrophy.<sup>131</sup> Interestingly, vascular delivery seemed less immunogenic and resulted in somewhat longer expression.<sup>131</sup> Since then, several groups have tested AAV-8 in normal<sup>132</sup> and affected dogs.<sup>100,133,134</sup> In contrast to the initial report by Ohshima et al., these later studies did not detect cellular immune reaction. Koo et al. expressed a canine-microdystrophin in a 9-week-old affected dog without immune suppression.<sup>133</sup> Robust expression lasted for at least 2 months without the evidence of immune rejection. Three groups performed limb perfusion in normal,<sup>132</sup> GRMD,<sup>100</sup> and myotubularin myopathy dogs<sup>134</sup> in the absence of immune suppressive drugs.<sup>100</sup> Persistent transduction was observed up to 1 year (the longest time point) without any signs of the CTL response.

It is currently unclear why the observed immune responses to AAV-8 are different between Ohshima et al.’s study and other studies. It is possible that the use of the tissue-specific promoter and the species-specific transgene may have played a role. Ohshima et al. used a ubiquitous promoter, while Childers et al. and Koo et al. used the muscle-specific promoter. Ohshima et al. expressed LacZ and human microdystrophin, while Childers et al., Koo et al., and Qiao et al. expressed canine proteins. In the Le Guiner et al.’s study, no protein product was expressed. Regarding the species specificity of the transgene, an AAV-6 study also reached the same conclusion.<sup>124</sup> Recently, several laboratories compared the immunity of AAV-8 to that of other AAV serotypes (AAV-1, 2, and 5 and rh32.33).<sup>124,131,135–140</sup> Interestingly, all these studies suggest that AAV-8 is less immunogenic. Future mechanistic studies may reveal the molecular underpinning of the unique immune privilege demonstrated by AAV-8.

Direct injection of AAV-9 evokes a strong cellular immune response in adult dog muscle.<sup>46</sup> But this response is absent in neonatal dogs.<sup>46</sup> We recently found that local delivery of a CMV-driving canine microgene also induced CD4+ and CD8+ T cell infiltration in adult DMD dogs despite the use of transient immune suppression.<sup>40</sup> Nevertheless, we still observed robust expression for at least 2 months (the end of the study). So far, systemic AAV-9 injection has only been evaluated in newborn puppies. We achieved high-level persistent transduction in normal puppies.<sup>46,123</sup> However, when the same technique was used in affected puppies, investigators observed a serious innate immune response that was so severe to require the termination of the study.<sup>84</sup> The reason for this unexpected reaction is not clear. One possibility could be the use of a ubiquitous promoter and the human microgene.

### Summary and Perspectives

Mdx mice and cDMD dogs were discovered simultaneously 30 years ago. However, the research use of the canine model has significantly lagged behind that of mdx mice. Using “mdx, gene therapy” and “GRMD, gene therapy” as key words, 620 and 27 records are retrieved in PubMed. That is to say that, for every 100 studies performed

in mdx mice, there are only ~4–5 studies performed using the canine model. Besides the high cost in maintaining these severely disabled cDMD dogs, the lack of a comprehensive and accurate characterization of the model also hinders the use of the cDMD model. There are several issues in this regard. First, a large-size population study on the natural history of the cDMD model remains to be conducted. Since most colonies only have a limited number of dogs, collaborative efforts from different laboratories will be needed to establish a solid baseline. Second, we need to develop standardized assays to reliably determine the outcomes of experimental interventions. This is especially important for cross-colony comparison. Numerous tools and protocols exist to study mouse muscle force. However, there aren't many options for dog muscle function evaluation. In fact, until recently, there is even no physiological assay to measure the contractility of a single dog muscle.<sup>38</sup> Misinterpretation of the data has also been noticed because of insufficient understanding on dog-specific reagents (such as the antibody).<sup>141,142</sup>

In terms of gene therapy, we believe that the cDMD model will provide critical insights on issues that are very difficult to address or cannot be addressed in mdx mice, for example, the amount of the AAV vector needed to achieve bodywide transduction in a large mammal. Another important issue is the minimum level of dystrophin expression needed to protect muscle in a large mammal. Three recent AAV exon skipping studies have offered some clues. Vulin et al. found that 20–50% dystrophin-positive cells might be sufficient to improve muscle force.<sup>99</sup> Le Guiner et al. reported that a correction of 33%, 35%, and 40% of myofibers might result in histopathology amelioration, MRI improvement, and muscle function preservation, respectively.<sup>100</sup> Bish et al. showed that a level of 15–20% of normal dystrophin might offer some heart protection.<sup>102</sup> This value is quite close to what has been observed in mdx mice.<sup>143,144</sup> However, in the case microdystrophin, the level seems different between mice and dogs. Takeda and colleagues found that microdystrophin expression in 20% myofibers could not protect dog muscle although the same level expression improved muscle function in mdx mice.<sup>79,131</sup> Besides answering these basic gene therapy questions, the cDMD model will also be essential to determine whether strategies that are shown to protect mouse muscle can or cannot treat muscular dystrophy in large mammals. New technologies that have (such as the use of the dual-AAV system to express a 6–8 kb *minidystrophin* gene)<sup>145–147</sup> or have not (such as the use of nuclease to correct *dystrophin* gene mutation *in vivo*)<sup>148–150</sup> been tested in mice may ultimately require corroboration in the canine model.

As we move forward from treating mdx mice to treating affected large mammals, great caution should be taken to not overinterpret the data. Results from canine studies may inform the design of the clinical trial, but they cannot fully predict what will happen in human patients because of many species-related differences. Nevertheless, a large therapeutic margin in the cDMD model may more likely translate to DMD patients.

### Acknowledgments

DMD research in the Duan lab is supported by the National Institutes of Health (AR-49419, HL-91883), De-

partment of Defense (MD130014), Muscular Dystrophy Association, Parent Project Muscular Dystrophy, Jesse's Journey—The Foundation for Gene and Cell Therapy, Hope for Javier, Kansas City Area Life Sciences Institute, and the University of Missouri.

### Author Disclosure Statement

D.D. is a member of the scientific advisory board for Solid GT, a subsidiary of Solid Ventures.

### References

- Hoffman EP, Brown RH Jr., Kunkel LM. Dystrophin: the protein product of the Duchenne muscular dystrophy locus. *Cell* 1987;51:919–928.
- Koenig M, Hoffman EP, Bertelson CJ, et al. Complete cloning of the Duchenne muscular dystrophy (DMD) cDNA and preliminary genomic organization of the DMD gene in normal and affected individuals. *Cell* 1987;50:509–517.
- Mendell JR, Lloyd-Puryear M. Report of MDA muscle disease symposium on newborn screening for Duchenne muscular dystrophy. *Muscle Nerve* 2013;48:21–26.
- Emery AEH, Muntoni F. *Duchenne Muscular Dystrophy*, 3rd ed. (Oxford University Press, New York, NY). 2003.
- Kinnett K, Cripe LH. Transforming Duchenne care: meeting 25–26 June 2012, Ft. Lauderdale, Florida, USA. *Neuromuscul Disord* 2013;23:690–695.
- Bushby K, Finkel R, Birnkrant DJ, et al. Diagnosis and management of Duchenne muscular dystrophy, part 2: implementation of multidisciplinary care. *Lancet Neurol* 2010;9:177–189.
- Rodino-Klapac LR, Chicoine LG, Kaspar BK, Mendell JR. Gene therapy for Duchenne muscular dystrophy: expectations and challenges. *Arch Neurol* 2007;64:1236–1241.
- McGreevy JW, Hakim CH, McIntosh MA, Duan D. Animal models of Duchenne muscular dystrophy: from basic mechanisms to gene therapy. *Dis Model Mech* 2015. [Epub ahead of print]
- Duan D. Duchenne muscular dystrophy gene therapy: lost in translation? *Res Rep Biol* 2011;2:31–42.
- Foster H, Popplewell L, Dickson G. Genetic therapeutic approaches for Duchenne muscular dystrophy. *Hum Gene Ther* 2012;23:676–687.
- Chamberlain JS. Gene therapy of muscular dystrophy. *Hum Mol Genet* 2002;11:2355–2362.
- Banks GB, Chamberlain JS. The value of mammalian models for Duchenne muscular dystrophy in developing therapeutic strategies. *Curr Top Dev Biol* 2008;84:431–453.
- Sicinski P, Geng Y, Ryder-Cook AS, et al. The molecular basis of muscular dystrophy in the mdx mouse: a point mutation. *Science* 1989;244:1578–1580.
- Bulfield G, Siller WG, Wight PA, Moore KJ. X chromosome-linked muscular dystrophy (mdx) in the mouse. *Proc Natl Acad Sci USA* 1984;81:1189–1192.
- Cooper BJ, Winand NJ, Stedman H, et al. The homologue of the Duchenne locus is defective in X-linked muscular dystrophy of dogs. *Nature* 1988;334:154–156.
- Valentine BA, Cooper BJ, Cummings JF, deLahunta A. Progressive muscular dystrophy in a golden retriever dog: light microscope and ultrastructural features at 4 and 8 months. *Acta Neuropathol (Berl)* 1986;71:301–310.

17. Shimatsu Y, Yoshimura M, Yuasa K, et al. Major clinical and histopathological characteristics of canine X-linked muscular dystrophy in Japan, CXMDJ. *Acta Myol* 2005;24:145–154.
18. Valentine BA, Cooper BJ, de Lahunta A, et al. Canine X-linked muscular dystrophy—an animal model of Duchenne muscular dystrophy: clinical studies. *J Neurol Sci* 1988; 88:69–81.
19. Walmsley GL, Arechavala-Gomez V, Fernandez-Fuente M, et al. A Duchenne muscular dystrophy gene hot spot mutation in dystrophin-deficient cavalier king charles spaniels is amenable to exon 51 skipping. *PLoS One* 2010;5:e8647.
20. Schatzberg SJ, Olby NJ, Breen M, et al. Molecular analysis of a spontaneous dystrophin ‘knockout’ dog. *Neuromuscul Disord* 1999;9:289–295.
21. Kornegay JN, Tuler SM, Miller DM, Levesque DC. Muscular dystrophy in a litter of golden retriever dogs. *Muscle Nerve* 1988;11:1056–1064.
22. Klarenbeek S, Gerritzen-Bruning MJ, Rozemuller AJ, van der Lugt JJ. Canine X-linked muscular dystrophy in a family of Grand Basset Griffon Vendéen dogs. *J Comp Pathol* 2007;137:249–252.
23. Jones BR, Brennan S, Mooney CT, et al. Muscular dystrophy with truncated dystrophin in a family of Japanese Spitz dogs. *J Neurol Sci* 2004;217:143–149.
24. Bergman RL, Inzana KD, Monroe WE, et al. Dystrophin-deficient muscular dystrophy in a Labrador retriever. *J Am Anim Hosp Assoc* 2002;38:255–261.
25. Paola JP, Podell M, Shelton GD. Muscular dystrophy in a miniature Schnauzer. *Prog Vet Neurol* 1993;4:14–18.
26. Wiczorek LA, Garosi LS, Shelton GD. Dystrophin-deficient muscular dystrophy in an old English sheepdog. *Vet Rec* 2006;158:270–273.
27. Wetterman CA, Harkin KR, Cash WC, et al. Hypertrophic muscular dystrophy in a young dog. *J Am Vet Med Assoc* 2000;216:878–881.
28. Baltzer WI, Calise DV, Levine JM, et al. Dystrophin-deficient muscular dystrophy in a Weimaraner. *J Am Anim Hosp Assoc* 2007;43:227–232.
29. Baroncelli AB, Abellonio F, Pagano TB, et al. Muscular dystrophy in a dog resembling human Becker muscular dystrophy. *J Comp Pathol* 2014;150:429–433.
30. Ito D, Kitagawa M, Jeffery N, et al. Dystrophin-deficient muscular dystrophy in an Alaskan malamute. *Vet Rec* 2011;169:127.
31. Smith BF, Yue Y, Woods PR, et al. An intronic LINE-1 element insertion in the dystrophin gene aborts dystrophin expression and results in Duchenne-like muscular dystrophy in the corgi breed. *Lab Invest* 2011;91:216–231.
32. Smith BF, Kornegay JN, Duan D. Independent canine models of Duchenne muscular dystrophy due to intronic insertions of repetitive DNA. *Mol Ther* 2007;15:S51.
33. Beltran E, Shelton GD, Guo LT, et al. Dystrophin-deficient muscular dystrophy in a Norfolk terrier. *J Small Anim Pract* 2014. [Epub ahead of print]; doi:10.1111/jsap.12292.
34. Kornegay JN, Bogan JR, Bogan DJ, et al. Canine models of Duchenne muscular dystrophy and their use in therapeutic strategies. *Mam Genome* 2012;23:85–108.
35. Fine DM, Shin JH, Yue Y, et al. Age-matched comparison reveals early electrocardiography and echocardiography changes in dystrophin-deficient dogs. *Neuromuscul Disord* 2011;21:453–461.
36. Shin JH, Yue Y, Smith B, Duan D. Humoral immunity to AAV-6, 8, and 9 in normal and dystrophic dogs. *Hum Gene Ther* 2012;23:287–294.
37. Shin JH, Yue Y, Srivastava A, et al. A simplified immune suppression scheme leads to persistent micro-dystrophin expression in Duchenne muscular dystrophy dogs. *Hum Gene Ther* 2012;23:202–209.
38. Yang HT, Shin JH, Hakim CH, et al. Dystrophin deficiency compromises force production of the extensor carpi ulnaris muscle in the canine model of Duchenne muscular dystrophy. *PLoS One* 2012;7:e44438.
39. Shin JH, Greer B, Hakim CH, et al. Quantitative phenotyping of Duchenne muscular dystrophy dogs by comprehensive gait analysis and overnight activity monitoring. *PLoS One* 2013;8:e59875.
40. Shin JH, Pan X, Hakim CH, et al. Microdystrophin ameliorates muscular dystrophy in the canine model of Duchenne muscular dystrophy. *Mol Ther* 2013;21:750–757.
41. Basner-Tschakarjan E, Mingozzi F. Cell-mediated immunity to AAV vectors, evolving concepts and potential solutions. *Front Immunol* 2014;5:350.
42. Mendell JR, Rodino-Klapac L, Sahenk Z, et al. Gene therapy for muscular dystrophy: lessons learned and path forward. *Neurosci Lett* 2012;527:90–99.
43. Mendell JR, Campbell K, Rodino-Klapac L, et al. Dystrophin immunity in Duchenne’s muscular dystrophy. *N Engl J Med* 2010;363:1429–1437.
44. Wang Z, Allen JM, Riddell SR, et al. Immunity to adeno-associated virus-mediated gene transfer in a random-bred canine model of Duchenne muscular dystrophy. *Hum Gene Ther* 2007;18:18–26.
45. Yuasa K, Yoshimura M, Urasawa N, et al. Injection of a recombinant AAV serotype 2 into canine skeletal muscles evokes strong immune responses against transgene products. *Gene Ther* 2007;14:1249–1260.
46. Yue Y, Ghosh A, Long C, et al. A single intravenous injection of adeno-associated virus serotype-9 leads to whole body skeletal muscle transduction in dogs. *Mol Ther* 2008;16:1944–1952.
47. Wright JF. Manufacturing and characterizing AAV-based vectors for use in clinical studies. *Gene Ther* 2008;15: 840–848.
48. Wilson JM. Progress in the commercial-scale production of adeno-associated viral vectors. *Hum Gene Ther* 2009; 20:695.
49. Kunkel LM. 2004 William Allan award address. cloning of the DMD gene. *Am J Hum Genet* 2005;76:205–214.
50. Howell JM, Fletcher S, O’Hara A, et al. Direct dystrophin and reporter gene transfer into dog muscle *in vivo*. *Muscle Nerve* 1998;21:159–165.
51. Thioudellet C, Blot S, Squiban P, et al. Current protocol of a research phase I clinical trial of full-length dystrophin plasmid DNA in Duchenne/Becker muscular dystrophies. Part I: rationale. *Neuromuscul Disord* 2002;12:S49–S51.
52. Duan D. Myodys, a full-length dystrophin plasmid vector for Duchenne and Becker muscular dystrophy gene therapy. *Curr Opin Mol Ther* 2008;10:86–94.
53. Pichavant C, Chapdelaine P, Cerri DG, Bizario JC, Tremblay JP. Electrotransfer of the full-length dog dystrophin into mouse and dystrophic dog muscles. *Hum Gene Ther* 2010;21:1591–1601.
54. Pichavant C, Chapdelaine P, Cerri DG, et al. Expression of dog microdystrophin in mouse and dog muscles by gene therapy. *Mol Ther* 2010;18:1002–1009.

55. Danthinne X, Imperiale MJ. Production of first generation adenovirus vectors: a review. *Gene Ther* 2000;7:1707–1714.
56. Ragot T, Vincent N, Chafey P, et al. Efficient adenovirus-mediated transfer of a human minidystrophin gene to skeletal muscle of mdx mice. *Nature* 1993;361:647–650.
57. England SB, Nicholson LV, Johnson MA, et al. Very mild muscular dystrophy associated with the deletion of 46% of dystrophin. *Nature* 1990;343:180–182.
58. Howell JM, Lochmuller H, O'Hara A, et al. High-level dystrophin expression after adenovirus-mediated dystrophin minigene transfer to skeletal muscle of dystrophic dogs: prolongation of expression with immunosuppression. *Hum Gene Ther* 1998;9:629–634.
59. O'Hara AJ, Howell JM, Taplin RH, et al. The spread of transgene expression at the site of gene construct injection. *Muscle Nerve* 2001;24:488–495.
60. Parks RJ, Graham FL. A helper-dependent system for adenovirus vector production helps define a lower limit for efficient DNA packaging. *J Virol* 1997;71:3293–3298.
61. Gilbert R, Nalbantoglu J, Howell JM, et al. Dystrophin expression in muscle following gene transfer with a fully deleted (“guttled”) adenovirus is markedly improved by trans-acting adenoviral gene products. *Hum Gene Ther* 2001;12:1741–1755.
62. Mingozzi F, High KA. Therapeutic *in vivo* gene transfer for genetic disease using AAV: progress and challenges. *Nat Rev Genet* 2011;12:341–355.
63. Lai Y, Yue Y, Duan D. Evidence for the failure of adeno-associated virus serotype 5 to package a viral genome > or = 8.2 kb. *Mol Ther* 2010;18:75–79.
64. Scott J, Li S, Harper S, et al. Viral vectors for gene transfer of micro-, mini-, or full-length dystrophin. *Neuromuscul Disord* 2002;12:S23.
65. Dickson G, Roberts M, Wells D, Fabb S. Recombinant micro-genes and dystrophin viral vectors. *Neuromuscul Disord* 2002;12:S40.
66. Arikawa-Hirasawa E, Koga R, Tsukahara T, et al. A severe muscular dystrophy patient with an internally deleted very short (110 kD) dystrophin: presence of the binding site for dystrophin-associated glycoprotein (DAG) may not be enough for physiological function of dystrophin. *Neuromuscul Disord* 1995;5:429–438.
67. Den Dunnen JT, Grootsholten PM, Bakker E, et al. Topography of the Duchenne muscular dystrophy (DMD) gene: FIGE and cDNA analysis of 194 cases reveals 115 deletions and 13 duplications. *Am J Hum Genet* 1989;45:835–847.
68. Fanin M, Freda MP, Vitiello L, et al. Duchenne phenotype with in-frame deletion removing major portion of dystrophin rod: threshold effect for deletion size? *Muscle Nerve* 1996;19:1154–1160.
69. Koenig M, Beggs AH, Moyer M, et al. The molecular basis for Duchenne versus Becker muscular dystrophy: correlation of severity with type of deletion. *Am J Hum Genet* 1989;45:498–506.
70. Yue Y, Li Z, Harper SQ, et al. Microdystrophin gene therapy of cardiomyopathy restores dystrophin-glycoprotein complex and improves sarcolemma integrity in the mdx mouse heart. *Circulation* 2003;108:1626–1632.
71. Gregorevic P, Allen JM, Minami E, et al. rAAV6-microdystrophin preserves muscle function and extends lifespan in severely dystrophic mice. *Nat Med* 2006;12:787–789.
72. Gregorevic P, Blankinship MJ, Allen JM, et al. Systemic delivery of genes to striated muscles using adeno-associated viral vectors. *Nat Med* 2004;10:828–834.
73. Lai Y, Thomas GD, Yue Y, et al. Dystrophins carrying spectrin-like repeats 16 and 17 anchor nNOS to the sarcolemma and enhance exercise performance in a mouse model of muscular dystrophy. *J Clin Invest* 2009;119:624–635.
74. Gregorevic P, Blankinship MJ, Allen JM, Chamberlain JS. Systemic microdystrophin gene delivery improves skeletal muscle structure and function in old dystrophic mdx mice. *Mol Ther* 2008;16:657–664.
75. Bostick B, Yue Y, Lai Y, et al. Adeno-associated virus serotype-9 microdystrophin gene therapy ameliorates electrocardiographic abnormalities in mdx mice. *Hum Gene Ther* 2008;19:851–856.
76. Bostick B, Shin J-H, Yue Y, Duan D. AAV-microdystrophin therapy improves cardiac performance in aged female mdx mice. *Mol Ther* 2011;19:1826–1832.
77. Liu M, Yue Y, Harper SQ, et al. Adeno-associated virus-mediated microdystrophin expression protects young mdx muscle from contraction-induced injury. *Mol Ther* 2005;11:245–256.
78. Yue Y, Liu M, Duan D. C-terminal truncated microdystrophin recruits dystrobrevin and syntrophin to the dystrophin-associated glycoprotein complex and reduces muscular dystrophy in symptomatic utrophin/dystrophin double knock-out mice. *Mol Ther* 2006;14:79–87.
79. Yoshimura M, Sakamoto M, Ikemoto M, et al. AAV vector-mediated microdystrophin expression in a relatively small percentage of mdx myofibers improved the mdx phenotype. *Mol Ther* 2004;10:821–828.
80. Fabb SA, Wells DJ, Serpente P, Dickson G. Adeno-associated virus vector gene transfer and sarcolemmal expression of a 144 kDa micro-dystrophin effectively restores the dystrophin-associated protein complex and inhibits myofibre degeneration in nude/mdx mice. *Hum Mol Genet* 2002;11:733–741.
81. Wang B, Li J, Xiao X. Adeno-associated virus vector carrying human minidystrophin genes effectively ameliorates muscular dystrophy in mdx mouse model. *Proc Natl Acad Sci USA* 2000;97:13714–13719.
82. Harper SQ, Hauser MA, DelloRusso C, et al. Modular flexibility of dystrophin: implications for gene therapy of Duchenne muscular dystrophy. *Nat Med* 2002;8:253–261.
83. Sampaolesi M, Blot S, D'Antona G, et al. Mesoangioblast stem cells ameliorate muscle function in dystrophic dogs. *Nature* 2006;444:574–579.
84. Kornegay JN, Li J, Bogan JR, et al. Widespread muscle expression of an AAV9 human mini-dystrophin vector after intravenous injection in neonatal dystrophin-deficient dogs. *Mol Ther* 2010;18:1501–1508.
85. Banks GB, Judge LM, Allen JM, Chamberlain JS. The polyproline site in hinge 2 influences the functional capacity of truncated dystrophins. *PLoS Genet* 2010;6:e1000958.
86. Lai Y, Zhao J, Yue Y, Duan D. alpha2 and alpha3 helices of dystrophin R16 and R17 frame a microdomain in the alpha1 helix of dystrophin R17 for neuronal NOS binding. *Proc Natl Acad Sci USA* 2013;110:525–530.
87. Foster H, Sharp PS, Athanasopoulos T, et al. Codon and mRNA sequence optimization of microdystrophin trans-

- genes improves expression and physiological outcome in dystrophic mdx mice following AAV2/8 gene transfer. *Mol Ther* 2008;16:1825–1832.
88. Li D, Yue Y, Lai Y, et al. Nitrosative stress elicited by nNOSmu delocalization inhibits muscle force in dystrophin-null mice. *J Pathol* 2011;223:88–98.
  89. Monaco AP, Bertelson CJ, Liechti-Gallati S, et al. An explanation for the phenotypic differences between patients bearing partial deletions of the DMD locus. *Genomics* 1988;2:90–95.
  90. Beggs AH, Hoffman EP, Snyder JR, et al. Exploring the molecular basis for variability among patients with Becker muscular dystrophy: dystrophin gene and protein studies. *Am J Hum Genet* 1991;49:54–67.
  91. McClorey G, Moulton HM, Iversen PL, et al. Antisense oligonucleotide-induced exon skipping restores dystrophin expression *in vitro* in a canine model of DMD. *Gene Ther* 2006;13:1373–1381.
  92. Yokota T, Lu QL, Partridge T, et al. Efficacy of systemic morpholino exon-skipping in Duchenne dystrophy dogs. *Ann Neurol* 2009;65:667–676.
  93. Fletcher S, Ly T, Duff RM, et al. Cryptic splicing involving the splice site mutation in the canine model of Duchenne muscular dystrophy. *Neuromuscul Disord* 2001;11:239–243.
  94. Douglas AG, Wood MJ. Splicing therapy for neuromuscular disease. *Mol Cell Neurosci* 2013;56:169–185.
  95. Yokota T, Nakamura A, Nagata T, et al. Extensive and prolonged restoration of dystrophin expression with vivomorpholino-mediated multiple exon skipping in dystrophic dogs. *Nucleic Acid Ther* 2012;22:306–315.
  96. Goyenvalle A, Vulin A, Fougereousse F, et al. Rescue of dystrophic muscle through U7 snRNA-mediated exon skipping. *Science* 2004;306:1796–1799.
  97. Gorman L, Suter D, Emerick V, et al. Stable alteration of pre-mRNA splicing patterns by modified U7 small nuclear RNAs. *Proc Natl Acad Sci USA* 1998;95:4929–4934.
  98. Suter D, Tomasini R, Reber U, et al. Double-target antisense U7 snRNAs promote efficient skipping of an aberrant exon in three human beta-thalassemic mutations. *Hum Mol Genet* 1999;8:2415–2423.
  99. Vulin A, Barthelemy I, Goyenvalle A, et al. Muscle function recovery in golden retriever muscular dystrophy after AAV1-U7 exon skipping. *Mol Ther* 2012;20:2120–2133.
  100. Le Guiner C, Montus M, Servais L, et al. Forelimb treatment in a large cohort of dystrophic dogs supports delivery of a recombinant AAV for exon skipping in Duchenne patients. *Mol Ther* 2014;22:1923–1935.
  101. Barbash IM, Cecchini S, Faranesh AZ, et al. MRI roadmap-guided transendocardial delivery of exon-skipping recombinant adeno-associated virus restores dystrophin expression in a canine model of Duchenne muscular dystrophy. *Gene Ther* 2013;20:274–282.
  102. Bish LT, Sleeper MM, Forbes SC, et al. Long-term restoration of cardiac dystrophin expression in golden retriever muscular dystrophy following rAAV6-mediated exon skipping. *Mol Ther* 2012;20:580–589.
  103. Bartlett RJ, Stockinger S, Denis MM, et al. *In vivo* targeted repair of a point mutation in the canine dystrophin gene by a chimeric RNA/DNA oligonucleotide. *Nat Biotechnol* 2000;18:615–622.
  104. Swaggart KA, McNally EM. Modifiers of heart and muscle function: where genetics meets physiology. *Exp Physiol* 2014;99:621–626.
  105. Cerletti M, Negri T, Cozzi F, et al. Dystrophic phenotype of canine X-linked muscular dystrophy is mitigated by adenovirus-mediated utrophin gene transfer. *Gene Ther* 2003;10:750–757.
  106. Odom GL, Gregorevic P, Allen JM, et al. Microtrophin delivery through rAAV6 increases lifespan and improves muscle function in dystrophic dystrophin/utrophin-deficient mice. *Mol Ther* 2008;16:1539–1545.
  107. Lee SJ. Regulation of muscle mass by myostatin. *Annu Rev Cell Dev Biol* 2004;20:61–86.
  108. Bogdanovich S, Krag TO, Barton ER, et al. Functional improvement of dystrophic muscle by myostatin blockade. *Nature* 2002;420:418–421.
  109. Mosher DS, Quignon P, Bustamante CD, et al. A mutation in the myostatin gene increases muscle mass and enhances racing performance in heterozygote dogs. *PLoS Genet* 2007;3:e79.
  110. Bish LT, Sleeper MM, Forbes SC, et al. Long-term systemic myostatin inhibition via liver-targeted gene transfer in golden retriever muscular dystrophy. *Hum Gene Ther* 2011;22:1499–1509.
  111. Cotten SW, Kornegay JN, Bogan DJ, et al. Genetic myostatin decrease in the golden retriever muscular dystrophy model does not significantly affect the ubiquitin proteasome system despite enhancing the severity of disease. *Am J Transl Res* 2014;6:43–53.
  112. Shin JH, Bostick B, Yue Y, et al. SERCA2a gene transfer improves electrocardiographic performance in aged mdx mice. *J Transl Med* 2011;9:132.
  113. Ferretti R, Marques MJ, Pertille A, Santo Neto H. Sarcoplasmic-endoplasmic-reticulum  $Ca^{2+}$ -ATPase and calsequestrin are overexpressed in spared intrinsic laryngeal muscles of dystrophin-deficient mdx mice. *Muscle Nerve* 2009;39:609–615.
  114. Goonasekera SA, Lam CK, Millay DP, et al. Mitigation of muscular dystrophy in mice by SERCA overexpression in skeletal muscle. *J Clin Invest* 2011;121:1044–1052.
  115. Morine KJ, Sleeper MM, Barton ER, Sweeney HL. Overexpression of SERCA1a in the mdx diaphragm reduces susceptibility to contraction-induced damage. *Hum Gene Ther* 2010;21:1735–1739.
  116. Bouyon S, Roussel V, Fromes Y. SERCA2a gene therapy can improve symptomatic heart failure in delta-sarcoglycan-deficient animals. *Hum Gene Ther* 2014;25:694–704.
  117. Zhu X, McTiernan CF, Rajagopalan N, et al. Immunosuppression decreases inflammation and increases AAV6-hSERCA2a-mediated SERCA2a expression. *Hum Gene Ther* 2012;23:722–732.
  118. Mi YF, Li XY, Tang LJ, et al. Improvement in cardiac function after sarcoplasmic reticulum  $Ca^{2+}$ -ATPase gene transfer in a beagle heart failure model. *Chin Med J* 2009;122:1423–1428.
  119. Wang Z, Zhu T, Qiao C, et al. Adeno-associated virus serotype 8 efficiently delivers genes to muscle and heart. *Nat Biotechnol* 2005;23:321–328.
  120. Bostick B, Ghosh A, Yue Y, et al. Systemic AAV-9 transduction in mice is influenced by animal age but not by the route of administration. *Gene Ther* 2007;14:1605–1609.
  121. Pacak CA, Mah CS, Thattaliyath BD, et al. Recombinant adeno-associated virus serotype 9 leads to preferential cardiac transduction *in vivo*. *Circ Res* 2006;99:e3–9.
  122. Pan X, Yue Y, Zhang K, et al. Long-term robust myocardial transduction of the dog heart from a peripheral

- vein by adeno-associated virus serotype-8. *Hum Gene Ther* 2013;24:584–594.
123. Hakim CH, Yue Y, Shin JH, et al. Systemic gene transfer reveals distinctive muscle transduction profile of tyrosine mutant AAV-1, -6, and -9 in neonatal dogs. *Mol Ther Methods Clin Dev* 2014;1:14002.
  124. Wang Z, Kuhr CS, Allen JM, et al. Sustained AAV-mediated dystrophin expression in a canine model of Duchenne muscular dystrophy with a brief course of immunosuppression. *Mol Ther* 2007;15:1160–1166.
  125. Rapti K, Louis-Jeune V, Kohlbrenner E, et al. Neutralizing antibodies against AAV serotypes 1, 2, 6, and 9 in sera of commonly used animal models. *Mol Ther* 2011;20:73–83.
  126. Denard J, Beley C, Kotin R, et al. Human galectin 3 binding protein interacts with recombinant adeno-associated virus type 6. *J Virol* 2012;86:6620–6631.
  127. Yue Y, Pan X, Hakim CH, et al. Safe and bodywide muscle gene transfer in young adult Duchenne muscular dystrophy dogs. *New Directions in Biology and Disease of Skeletal Muscle*, 2014, Chicago, Illinois, June 29–July 22, 2014.
  128. Wang Z, Storb R, Lee D, et al. Immune responses to AAV in canine muscle monitored by cellular assays and non-invasive imaging. *Mol Ther* 2010;18:617–624.
  129. Wang Z, Halbert CL, Lee D, et al. Elimination of contaminating cap genes in AAV vector virions reduces immune responses and improves transgene expression in a canine gene therapy model. *Gene Ther* 2014;21:363–370.
  130. Bish LT, Sleeper MM, Brainard B, et al. Percutaneous transendocardial delivery of self-complementary adeno-associated virus 6 achieves global cardiac gene transfer in canines. *Mol Ther* 2008;16:1953–1959.
  131. Ohshima S, Shin JH, Yuasa K, et al. Transduction efficiency and immune response associated with the administration of AAV8 vector into dog skeletal muscle. *Mol Ther* 2009;17:73–80.
  132. Qiao C, Li J, Zheng H, et al. Hydrodynamic limb vein injection of AAV8 canine myostatin propeptide gene in normal dogs enhances muscle growth. *Hum Gene Ther* 2009;20:1–10.
  133. Koo T, Okada T, Athanasopoulos T, et al. Long-term functional adeno-associated virus-microdystrophin expression in the dystrophic CXMDj dog. *J Gene Med* 2011;13:497–506.
  134. Childers MK, Joubert R, Poulard K, et al. Gene therapy prolongs survival and restores function in murine and canine models of myotubular myopathy. *Sci Transl Med* 2014;6:220ra210.
  135. Vandenberghe LH, Wang L, Somanathan S, et al. Heparin binding directs activation of T cells against adeno-associated virus serotype 2 capsid. *Nat Med* 2006;12:967–971.
  136. Lu Y, Song S. Distinct immune responses to transgene products from rAAV1 and rAAV8 vectors. *Proc Natl Acad Sci USA* 2009;106:17158–17162.
  137. Wang L, Figueredo J, Calcedo R, et al. Cross-presentation of adeno-associated virus serotype 2 capsids activates cytotoxic T cells but does not render hepatocytes effective cytolytic targets. *Hum Gene Ther* 2007;18:185–194.
  138. Xin KQ, Mizukami H, Urabe M, et al. Induction of robust immune responses against human immunodeficiency virus is supported by the inherent tropism of adeno-associated virus type 5 for dendritic cells. *J Virol* 2006;80:11899–11910.
  139. Mays LE, Vandenberghe LH, Xiao R, et al. Adeno-associated virus capsid structure drives CD4-dependent CD8+ T cell response to vector encoded proteins. *J Immunol* 2009;182:6051–6060.
  140. Faust SM, Bell P, Cutler BJ, et al. CpG-depleted adeno-associated virus vectors evade immune detection. *J Clin Invest* 2013;123:2994–3001.
  141. Rozkalne A, Adkin C, Meng J, et al. Mouse regenerating myofibers detected as false-positive donor myofibers with anti-human spectrin. *Hum Gene Ther* 2014;25:73–81.
  142. Kodippili K, Vince L, Shin JH, et al. Characterization of 65 epitope-specific dystrophin monoclonal antibodies in canine and murine models of Duchenne muscular dystrophy by immunostaining and western blot. *PLoS One* 2014;9:e88280.
  143. Wells DJ, Wells KE, Asante EA, et al. Expression of human full-length and minidystrophin in transgenic mdx mice: implications for gene therapy of Duchenne muscular dystrophy. *Hum Mol Genet* 1995;4:1245–1250.
  144. Phelps SF, Hauser MA, Cole NM, et al. Expression of full-length and truncated dystrophin mini-genes in transgenic mdx mice. *Hum Mol Genet* 1995;4:1251–1258.
  145. Odom GL, Gregorevic P, Allen JM, Chamberlain JS. Gene therapy of mdx mice with large truncated dystrophins generated by recombination using rAAV6. *Mol Ther* 2011;19:36–45.
  146. Zhang Y, Duan D. Novel mini-dystrophin gene dual adeno-associated virus vectors restore neuronal nitric oxide synthase expression at the sarcolemma. *Hum Gene Ther* 2012;23:98–103.
  147. Zhang Y, Yue Y, Li L, et al. Dual AAV therapy ameliorates exercise-induced muscle injury and functional ischemia in murine models of Duchenne muscular dystrophy. *Hum Mol Genet* 2013;22:3720–3729.
  148. Ousterout DG, Kabadi AM, Thakore PI, et al. Correction of dystrophin expression in cells from Duchenne muscular dystrophy patients through genomic excision of exon 51 by zinc finger nucleases. *Mol Ther* 2014. [Epub ahead of print]; doi: 10.1038/mt.2014.234.
  149. Ousterout DG, Perez-Pinera P, Thakore PI, et al. Reading frame correction by targeted genome editing restores dystrophin expression in cells from Duchenne muscular dystrophy patients. *Mol Ther* 2013;21:1718–1726.
  150. Long C, McAnally JR, Shelton JM, et al. Prevention of muscular dystrophy in mice by CRISPR/Cas9-mediated editing of germline DNA. *Science* 2014;345:1184–1188.

Address correspondence to:

*Dr. Dongsheng Duan*  
 Department of Molecular Microbiology and Immunology  
 University of Missouri School of Medicine  
 One Hospital Dr. M610G, MSB  
 Columbia, MO 65212

*E-mail:* duand@missouri.edu

Received for publication January 12, 2015;  
 accepted January 13, 2015.

Published online: January 14, 2015.

## CORRESPONDENCE

# Early loss of ambulation is not a representative clinical feature in Duchenne muscular dystrophy dogs: remarks on the article of Barthélémy et al.

Dongsheng Duan<sup>1,2,\*</sup>, Chady H. Hakim<sup>1</sup>, Carlos E. Ambrosio<sup>3</sup>, Bruce F. Smith<sup>4,5</sup> and H. Lee Sweeney<sup>6</sup>

**Table 1. Complete loss of ambulation is not a clinical feature in young adult DMD dogs**

Investigator (or reference paper)	Colony location	Strain background	Mutation	Sample size	Loss of ambulation by 6 months	
					Number	Percentage (%)
Carlos Ambrosio	Brazil	Golden retriever	Intron 6 point mutation (GRMD)	160	1	0.63
Dongsheng Duan	Columbia, MO	Golden retriever	Intron 6 point mutation (GRMD)	130	0	0.00
		Corgi	Intron 13 insertion			
		Labrador	Intron 19 insertion			
		Hybrid	Mixed			
Bruce Smith	Auburn, AL	Corgi	Intron 13 insertion	30	0	0.00
		Labrador	Intron 19 insertion			
		Labradoodle	Unknown			
		Springer	Unknown			
Lee Sweeney	Philadelphia, PA	Golden retriever	Intron 6 point mutation (GRMD)	35	0	0.00
Valentine et al., 1988	Ithaca, NY	Golden retriever	Intron 6 point mutation (GRMD)	25	0	0.00
		Golden retriever/ Beagle hybrid	Intron 6 point mutation (GRMD)			
<b>Total</b>				<b>380</b>	<b>1</b>	<b>0.26</b>
Barthélémy et al., 2014	France	Golden retriever	Intron 6 point mutation (GRMD)	61	15	24.59

Remarks on the article of Barthélémy et al.: Predictive markers of clinical outcome in the GRMD dog model of Duchenne muscular dystrophy  
Dystrophin-deficient dogs are the most commonly used large animal model for Duchenne muscular dystrophy (DMD), a lethal muscle disease currently without an effective therapy. Tremendous progress has been made over the last few years in the development of novel pharmacological and genetic therapies for DMD. Validation of these exciting findings in DMD dogs will pave the way to future clinical tests in affected humans. Unfortunately, our understanding on disease progression in affected dogs remains limited. To better characterize

the natural history of the disease in dogs, Barthélémy et al. studied golden retriever muscular dystrophy (GRMD) dogs in their colony (Barthélémy et al., 2014). In the GRMD dog, dystrophin expression is abolished owing to a point mutation in intron 6 of the dystrophin gene (Cooper et al., 1988). Sixty-one GRMD dogs were followed starting from 2 months of age. By the age of 6 months, 15 dogs (24.59%) lost ambulation. These dogs were classified as the severe form. Two additional dogs lost ambulation at ~7.3 months. The remaining 44 dogs were ambulant throughout their lives and were classified as the mild form. A comparison of the blood and gait data at the beginning of the study (when dogs were 2 months old) identified three biomarkers that, when used together, can accurately predict the phenotype (mild or severe) that the dogs will have at 6 months of age. Specifically, an increase of peripheral CD4<sup>+</sup>CD49d<sup>Hi</sup> T cells, a decrease of the spontaneous gait speed and a reduction of the stride frequency were found to associate with early loss of ambulation. The results of this study have important implications in designing preclinical studies in dogs. For example, if a treatment can prevent the early loss of ambulation in dogs with severe-type disease, it might suggest that the candidate treatment has the therapeutic value.

When GRMD dogs were initially characterized in the late 1980s, Valentine et al. pointed out that a “complete loss of ambulatory function, which occurs in all DMD patients, is not a feature of CXMD (canine X-linked muscular dystrophy)” (Valentine et al., 1988). To

<sup>1</sup>Department of Molecular Microbiology and Immunology, School of Medicine, The University of Missouri, Columbia, MO 65212, USA. <sup>2</sup>Department of Neurology, School of Medicine, The University of Missouri, Columbia, MO 65212, USA. <sup>3</sup>Department of Veterinary Medicine, Faculty of Animal Science and Food Engineering, University of São Paulo, Pirassununga 05508-070, Brazil. <sup>4</sup>Scott-Ritchey Research Center, College of Veterinary Medicine, Auburn University, Auburn, AL 36849, USA. <sup>5</sup>Department of Pathobiology, College of Veterinary Medicine, Auburn University, Auburn, AL 36849, USA. <sup>6</sup>Department of Physiology, School of Medicine, The University of Pennsylvania, Philadelphia, PA 19104, USA.

\*Author for correspondence (duand@missouri.edu)

This is an Open Access article distributed under the terms of the Creative Commons Attribution License (<http://creativecommons.org/licenses/by/3.0/>), which permits unrestricted use, distribution and reproduction in any medium provided that the original work is properly attributed.

determine whether the loss of ambulation at a young age is a clinical marker for dystrophin-deficient dogs in general, we reviewed data from four different DMD colonies that are located in Brazil and the USA (Table 1). These dogs carry different mutations in the dystrophin gene and are on different strain backgrounds (including GRMD) (Table 1). Although a high neonatal mortality rate (17-37%) was noted, as initially reported by Valentine et al. (28%), we did not see a high rate of ambulation loss at 6 months of age (Table 1). From a total of 380 affected dogs, only one dog (0.26%) lost its walking ability by the age of 6 months. Our data suggest that there are important phenotypic differences in different DMD dog colonies. Currently, dystrophin deficiency has been reported in more than 20 dog breeds (McGreevy et al., 2015). In addition to the colonies mentioned in this paper (Table 1), experimental DMD dog colonies have also been established in a number of other institutions in Australia, Japan, the United Kingdom and the USA (McGreevy et al., 2015). The age of ambulation loss in affected dogs in these colonies has not been reported. It is possibly that variations between the colony located at the Veterinary School of Alfort, France (Barthélémy et al., 2014) and the four colonies we have surveyed (Table 1) could exist. Future studies are needed to gain the consensus and to identify the factors that might have contributed to the inter-colony variation (such as the genetic background of the strain, the level of inbreeding and the specific type of dystrophin gene mutation). In the meantime, caution should be taken when interpreting and extrapolating the ambulation data observed in the French colony. Additional multicenter studies are

warranted to establish a solid baseline to guide translational study using the canine model.

#### Funding

The canine DMD colonies are supported by the Department of Defense MD130014 (D.D.), Hope for Javier (D.D.), Jesse's Journey – The Foundation for Gene and Cell Therapy (D.D.), Kansas City Area Life Sciences Institute (D.D.), Muscular Dystrophy Association (D.D.), National Institutes of Health AR-49419 and AR057209 (B.F.S. and D.D.) and HL-91883 (D.D.), Parent Project Muscular Dystrophy (D.D. and H.L.S.), São Paulo Research Foundation (FAPESP) 2012/01060-4 and 2007/51222-2 (C.E.A.), Scott-Ritchey Research Center (B.F.S.), and the University of Missouri (D.D.).

#### Competing interests

D.D. is a member of the scientific advisory board for Solid GT, a subsidiary of Solid Ventures. Other authors have no conflict of interest.

#### References

- Barthélémy, I., Pinto-Mariz, F., Yada, E., Desquilbet, L., Savino, W., Silva-Barbosa, S. D., Faussat, A. M., Mouly, V., Voit, T., Blot, S. et al. (2014). Predictive markers of clinical outcome in the GRMD dog model of Duchenne Muscular Dystrophy. *Dis. Model. Mech.* **7**, 1253-1261.
- Cooper, B. J., Winand, N. J., Stedman, H., Valentine, B. A., Hoffman, E. P., Kunkel, L. M., Scott, M. O., Fischbeck, K. H., Kornegay, J. N., Avery, R. J. et al. (1988). The homologue of the Duchenne locus is defective in X-linked muscular dystrophy of dogs. *Nature* **334**, 154-156.
- McGreevy, J. W., Hakim, C. H., McIntosh, M. A. and Duan, D. (2015). Animal models of Duchenne muscular dystrophy: from basic mechanisms to gene therapy. *Dis. Model. Mech.* **8**, 195-213.
- Valentine, B. A., Cooper, B. J., de Lahunta, A., O'Quinn, R. and Blue, J. T. (1988). Canine X-linked muscular dystrophy – an animal model of Duchenne muscular dystrophy: clinical studies. *J. Neurol. Sci.* **88**, 69-81.

## ORIGINAL ARTICLE

# Safe and bodywide muscle transduction in young adult Duchenne muscular dystrophy dogs with adeno-associated virus

Yongping Yue<sup>1,†</sup>, Xiufang Pan<sup>1,†</sup>, Chady H. Hakim<sup>1,†</sup>, Kasun Kodippili<sup>1</sup>, Keqing Zhang<sup>1</sup>, Jin-Hong Shin<sup>1,‡</sup>, Hsiao T. Yang<sup>3</sup>, Thomas McDonald<sup>1</sup> and Dongsheng Duan<sup>1,2,\*</sup>

<sup>1</sup>Department of Molecular Microbiology and Immunology, School of Medicine, <sup>2</sup>Department of Neurology and <sup>3</sup>Department of Biomedical Sciences, College of Veterinary Medicine, The University of Missouri, Columbia, MO, USA

\*To whom correspondence should be addressed at: Department of Molecular Microbiology and Immunology, The University of Missouri School of Medicine, One Hospital Dr. M610G, MSB, Columbia, MO 65212, USA. Tel: +1-573-884-9584; Fax: +1-573-882-4287; Email: duand@missouri.edu

## Abstract

The ultimate goal of muscular dystrophy gene therapy is to treat all muscles in the body. Global gene delivery was demonstrated in dystrophic mice more than a decade ago using adeno-associated virus (AAV). However, translation to affected large mammals has been challenging. The only reported attempt was performed in newborn Duchenne muscular dystrophy (DMD) dogs. Unfortunately, AAV injection resulted in growth delay, muscle atrophy and contracture. Here we report safe and bodywide AAV delivery in juvenile DMD dogs. Three ~2-m-old affected dogs received intravenous injection of a tyrosine-engineered AAV-9 reporter or micro-dystrophin ( $\mu$ Dys) vector at the doses of  $1.92\text{--}6.24 \times 10^{14}$  viral genome particles/kg under transient or sustained immune suppression. DMD dogs tolerated injection well and their growth was not altered. Hematology and blood biochemistry were unremarkable. No adverse reactions were observed. Widespread muscle transduction was seen in skeletal muscle, the diaphragm and heart for at least 4 months (the end of the study). Nominal expression was detected in internal organs. Improvement in muscle histology was observed in  $\mu$ Dys-treated dogs. In summary, systemic AAV gene transfer is safe and efficient in young adult dystrophic large mammals. This may translate to bodywide gene therapy in pediatric patients in the future.

## Introduction

Localized gene transfer has resulted in miraculous improvements for diseases that affect a single organ (1,2). However, such therapies will unlikely change the disease course when afflicted tissues are distributed throughout the body as in the case of Duchenne muscular dystrophy (DMD), a lethal X-linked muscle disease caused by dystrophin deficiency (3). The ultimate cure for DMD requires bodywide gene therapy. Vascular delivery

has the potential of global muscle transduction. However, infusion of trillions of viral particles may lead to unexpected responses and even fatal complications (4,5).

The first successful whole body gene transfer was conducted in rodent models of muscular dystrophy more than a decade ago using adeno-associated virus (AAV). Investigators from several laboratories demonstrated that a single intravascular injection of AAV-6, 8 or 9 reached every muscle in the body (6–8). More

<sup>†</sup>The authors equally contributed to this work.

<sup>‡</sup>Present address: Pusan National University Yangsan Hospital, Yangsan, Republic of Korea.

Received: May 12, 2015. Revised: July 20, 2015. Accepted: July 28, 2015

© The Author 2015. Published by Oxford University Press. All rights reserved. For Permissions, please email: journals.permissions@oup.com

recently, systemic AAV delivery was achieved in skeletal and cardiac muscle of aged dystrophic mice (9–11). Despite marvelous results in rodents, bodywide gene transfer has been problematic in diseased large mammals (12).

Systemic gene transfer in a large mammal was initially tested in normal neonatal dogs (13,14). Intravenous injection of  $2 \times 10^{14}$  viral genome (vg) particles/kg of AAV-9 resulted in broad skeletal muscle transduction in puppies (13). The same technique was subsequently found to be effective for other AAV serotypes (15–17). In these studies, persistent expression was achieved for up to 1 year (the end of the study) at a dose as high as  $9.7 \times 10^{14}$  vg particles/kg without any toxicity. Unfortunately, translation to the canine DMD model has met with great difficulties (18). Kornegay *et al.* delivered  $1.5 \times 10^{14}$  vg particles/kg of AAV-9 to two 4-day-old affected puppies through the jugular vein. Surprisingly, treated dogs developed massive inflammatory myopathy, contracture and growth retardation (5). The results of Kornegay *et al.* question the feasibility of systemic AAV gene therapy in dystrophic large mammals.

Recent studies suggest that replacing surface exposed tyrosine residue on AAV capsid may reduce immunogenicity and enhance transduction (19,20). We tested Y731F AAV-9, a surface tyrosine mutated AAV-9 variant in adult DMD dogs and observed robust expression following direct muscle injection (21). Here we tested the hypothesis that Y731F AAV-9 can result in whole body muscle transduction in juvenile DMD dogs. A human placental alkaline phosphatase (AP) reporter vector or a potentially therapeutic  $\mu$ Dys vector were injected intravenously at a dose up to  $6.24 \times 10^{14}$  vg particles/kg under transient or sustained immune suppression. All three dogs tolerated injection and immune suppression well. No adverse reactions were observed. Necropsy at the age of 5.5–6 months revealed robust skeletal muscles transduction throughout the body and widespread gene transfer in the heart. Our results demonstrated for the first time that systemic AAV delivery in a diseased large mammal is safe and effective. Similar approaches may be used to treat pediatric muscular dystrophy patients in the future.

## Results

### A single intravenous injection of Y731F AAV-9 resulted in efficient skeletal muscle transduction throughout the body and widespread gene transfer in the heart

Dog Bouchelle was injected with  $1.92 \times 10^{14}$  vg particles/kg ( $7.09 \times 10^{14}$  vg particles total) of a Rous sarcoma virus (RSV) promoter-driving AP reporter AAV vector (Table 1). This dog also received 5-week transient immune suppression (Fig. 1A) (21,22).

The injection procedure went smoothly. The dog tolerated immune suppression and large-dose AAV well. No change was noted in the activity, behavior, food/water consumption and vital signs of the dog throughout the entire experiment. The body weight also showed stable growth (Table 1 and Fig. 1B). Compared with that of the baseline (before the start of immune suppression), post-injection blood chemistry was in general unremarkable (Fig. 1C, and Supplementary Material, Table S1). There was a slight increase in blood urine nitrogen (but still within the normal range), a trend of higher creatine (but still within the normal range), and transient elevation of blood AP (Fig. 1C). However, we did not detect any clinically meaningful events. One-month muscle biopsy showed strong AP expression and abundant vector genomes (Fig. 1D and E). Bouchelle was euthanized at 3.5 months after gene transfer. AAV transduction was evaluated by histochemical staining, enzymatic activity assay

**Table 1.** Experimental dog summary

Dog name	Bouchelle	Stephan	Brooke
Dystrophin gene mutation	Intron 19 insertion	Intron 6 point mutation	Intron 13 insertion
Gender	Male	Female	Male
Body weight at injection (kg)	3.7	3.5	3.2
Body weight at necropsy (kg)	10.6	10.6	11.3
Promoter	RSV	CMV	CMV
Transgene	Human AP reporter gene	Canine $\mu$ -dystrophin	Canine $\mu$ -dystrophin
Total AAV injected (vg particles)	$7.09 \times 10^{14}$	$1.77 \times 10^{15}$	$2.0 \times 10^{15}$
Vector dose (vg particles/kg BW)	$1.92 \times 10^{14}$	$5.04 \times 10^{14}$	$6.24 \times 10^{14}$
Vector volume (ml/kg BW)	4.9	5.7	6.2
Age at AAV injection (month)	2.0	1.8	1.8
Age at biopsy (month)	3.0	2.8	2.8
Age at necropsy (month)	5.5	5.3	5.8

and vector genome quantification (Figs 2 and 3). We observed widespread AP expression and vector genome in every muscle (Fig. 2). On average, ~25% (range, 5–80%) myofibers were transduced. The extensor carpi ulnaris (ECU) muscle had the lowest expression (AP positive myofiber, 5%; AP activity,  $0.84 \mu\text{M}/\mu\text{g}$ ). The highest transduction was seen in the extraocular muscle (EOM) (AP positive myofiber, 80%; AP activity,  $215 \mu\text{M}/\mu\text{g}$ ; AAV genome copy number, 26.2 copies/diploid genome). Respiratory failure and heart failure are the leading causes of death in DMD. Encouragingly, high-level AP expression was detected in the diaphragm, intercostal muscle and heart (Fig. 2).

### Systemic Y731F AAV-9 injection resulted in minimal expression in internal organs

On histochemical staining, we did not detect AP expression in the liver and testis (Fig. 3A). In the kidney, we found very few AP positive cells in the glomerulus (Fig. 3A). In the lung, AP positive cells were seen in alveolar cells. In the pancreas, we noticed strong AP expression in smooth muscle and some expression in acini (Fig. 3B). However, minimal expression was observed in islets of Langerhans (Supplementary Material, Fig. S1). Robust transduction was observed in the microvasculature in muscles (Fig. 3C). The peripheral nerves (including large nerves such as sciatic nerve and small nerve branches inside muscle) showed very high AP expression (Fig. 3D and E). The spinal cord was also transduced at high efficiency (Fig. 3E). Some AP expression was seen in the hippocampus, but minimal AP expression was detected in the cerebrum and cerebellum (Fig. 3E). Consistent with AP staining results, the AP activity assay in tissue lysate revealed minimal expression in internal organs except for the sciatic nerve and spinal cord (Fig. 3F). Despite the dramatic difference in AP expression, surprisingly, similar amount of the AAV genome was detected in internal organs (Fig. 3F). In fact, the AAV genome copy number in internal organs was quite comparable to that in muscles (Figs 2D and 3F).

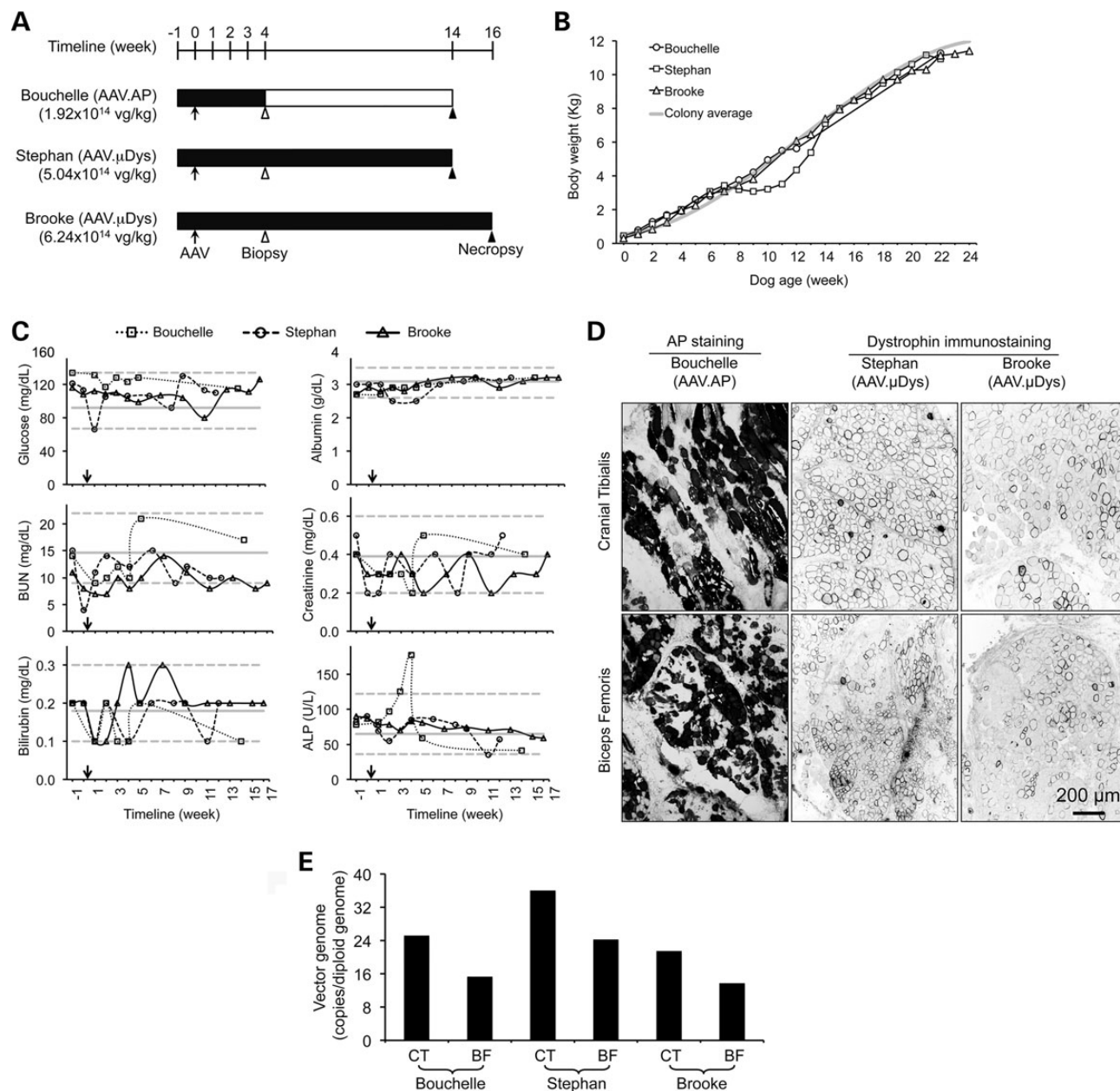


**Figure 1.** Experimental protocol, growth curve, blood biochemistry and biopsy results. (A) Schematic overview of the study. Arrow, AAV injection; open arrowhead, biopsy; filled arrowhead, necropsy; filled box, the dog is under immune suppression. (B) The growth curve of individual dogs. The colony average is shown in gray ( $N \geq 70$ ). (C) Selected blood biochemistry results. Complete data can be found in Supplementary Material, Table S1. Dotted gray lines, the maximal and minimal values for age-matched untreated DMD dogs in our colony ( $N = 31$ ). Solid gray line, the average value of age-matched untreated DMD dogs in our colony ( $N = 31$ ). (D) Representative AP histochemical staining photomicrographs and dystrophin immunofluorescence staining photomicrographs from the CT and BF muscles obtained at biopsy. (E) Vector genome copy number quantification from biopsied muscle samples.

### Bodywide gene transfer was achieved with a $\mu$ Dys vector

Next, we delivered a  $\mu$ Dys AAV vector to affected dogs Stephan ( $5.04 \times 10^{14}$  vg particles/kg,  $1.77 \times 10^{15}$  vg particles total) and Brooke ( $6.24 \times 10^{14}$  vg particles/kg,  $2.00 \times 10^{15}$  vg particles total) (Table 1). In this vector, a flag-tagged codon-optimized canine  $\Delta R2-15/\Delta R18-19/\Delta R20-23/\Delta C$   $\mu$ Dys gene was expressed from the cytomegalovirus (CMV) promoter (21). Immune suppression was extended until the end of study in these two dogs. Stephan and Brooke tolerated AAV administration and immune suppression well. Brooke showed normal growth as expected. Stephan

showed a slower growth between weeks 8 and 10, but its growth curve returned to the levels of Bouchelle and Brooke by week 14. No clinically meaningful adverse reactions were noted. Post-injection blood examination showed a profile similar to that of Bouchelle (Fig. 1C, and Supplementary Material, Table S1). Essentially, all laboratory parameters were within the range of other affected dogs in our colony. One-month biopsy revealed robust  $\mu$ Dys expression (Fig. 1D). Necropsy was performed at 3.5 (Stephan) and 4 (Brooke) months after injection. Consistent with the findings of Bouchelle, we observed efficient gene transfer in

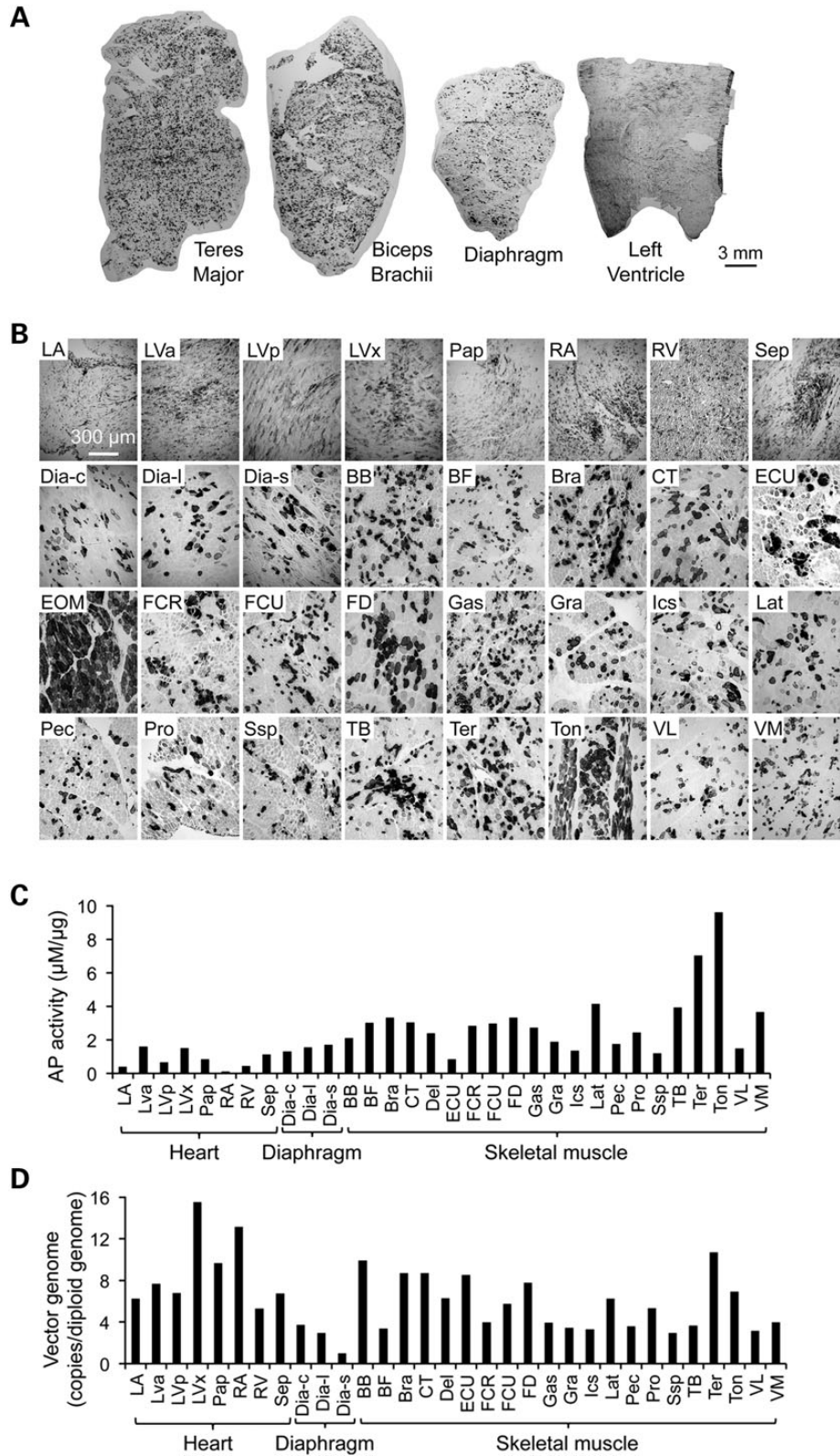


**Figure 2.** A single intravenous injection of an AP reporter AAV vector leads to global muscle transduction in a juvenile dystrophic dog. (A) Representative full-view AP staining photographs of the indicated muscle. (B) Representative AP histochemical staining photomicrographs of the heart and skeletal muscles. (C) AP activity. (D) AAV vector genome quantification. Abbreviations for the heart: LA, left atrium; LVa, left ventricle anterior; LVp, left ventricle posterior; LVx, left ventricle apex; Pap, papillary muscle; RA, right atrium; RV, right ventricle; Sep, interventricular septum. Abbreviations for the diaphragm: Dia-c, diaphragm costal part; Dia-l, diaphragm lumbar part; Dia-s, diaphragm sternal part. Abbreviations for skeletal muscles: BB, biceps brachii; BF, biceps femoris; Bra, brachialis; CT, cranial tibialis; Del, deltoideus; ECU, extensor carpi ulnaris; FCR, flexor carpi radialis; FCU, flexor carpi ulnaris; FD, flexor digitorum; Gas, gastrocnemius; Gra, gracilis; Ics, intercostalis; Lat, latissimus; Pec, pectoralis; Pro, pronator; Ssp, supraspinatus; TB, triceps brachii; Ter, Teres; Ton, tongue; VL, vastus lateralis; VM, vastus medialis.

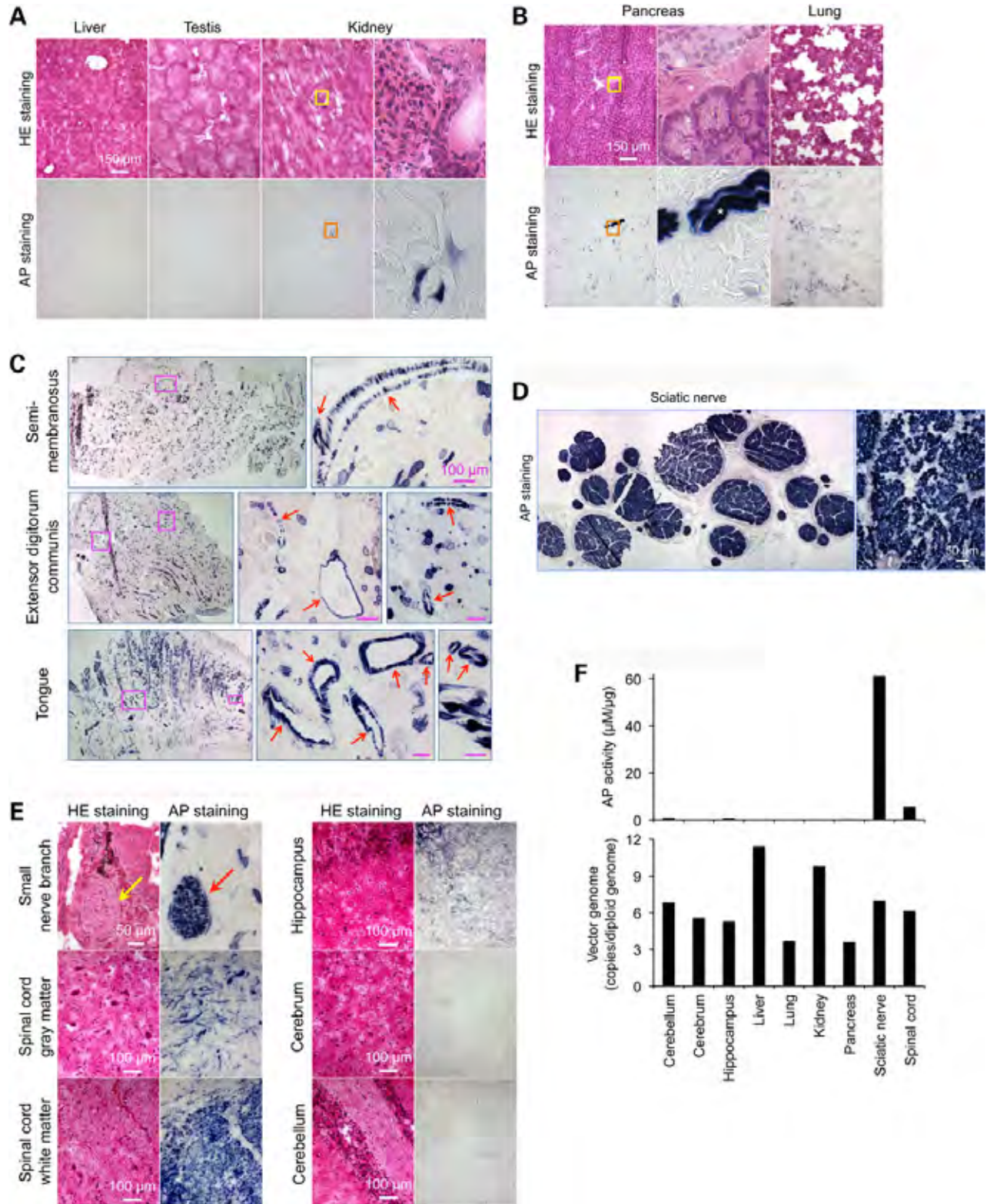


**Figure 3.** Systemic Y731F AAV-9 injection results in minimal transgene expression in internal organs despite robust expression in peripheral nerve, spinal cord and microvasculature. (A) Representative HE and AP histochemical staining photomicrographs of the liver, testis and kidney. (B) Representative HE and AP histochemical staining photomicrographs of the pancreas and lung. Asterisk, smooth muscle. (C) Representative AP histochemical staining photomicrographs of muscle revealing strong staining in the microvasculature (red arrows). All arrow bars stand for 100  $\mu\text{m}$ . (D) Representative AP histochemical staining photomicrographs of the sciatic nerve. Left panel, full-view image; right panel, high magnification image. (E) Representative HE and AP histochemical staining photomicrographs of a small nerve branch (arrow) inside muscle, spinal cord (gray matter and white matter), hippocampus, cerebrum and cerebellum. (F) AP activity and AAV vector genome quantification in the indicated tissues.

striated muscles all over the body in Stephan and Brooke at necropsy (Fig. 4). Interestingly, despite a 25% difference in the vector dose ( $5.04 \times 10^{14}$  vg particles/kg in Stephan versus  $6.24 \times 10^{14}$  vg particles/kg in Brooke), we observed quite comparable levels of transduction in two dogs. Immunostaining with a flag antibody revealed correct sarcolemmal localization of  $\mu$ Dys (Fig. 4A and B). Quantitatively,  $\mu$ Dys-positive cells reached ~25% (range, 5–60%) (Fig. 4E). Similar to Bouchelle (Fig. 2), the EOM showed the highest transduction (50–60%) while the ECU muscle had the least  $\mu$ Dys expression (5%) (Fig. 4A, B and E). Respiratory muscles (diaphragm, intercostal muscle and abdominal muscle) were also highly transduced with 23–48% myofibers showed  $\mu$ Dys expression. Western blot with a dystrophin antibody confirmed  $\mu$ Dys expression at the expected size in striated muscles (Fig. 4F

and G). The AAV vector genome was detected in every muscle (Fig. 3G and H). No  $\mu$ Dys was detected in internal organs (Supplementary Material, Fig. S2).

**$\mu$ Dys expression reduced histopathology**

In Bouchelle, the dog that received the AP reporter vector, all muscles showed classic dystrophic pathology such as abundant inflammatory cell infiltration, dark-stained hyalinized/hypercontracted myofibers, necrotic myofibers, angulated myofibers, large hypertrophic myofibers, excessively small myofibers and increased endomysial and perimysial connective tissue deposition (Fig. 5A, and Supplementary Material, Fig. S3). For dogs that received the  $\mu$ Dys vector (Stephan and Brooke), two different

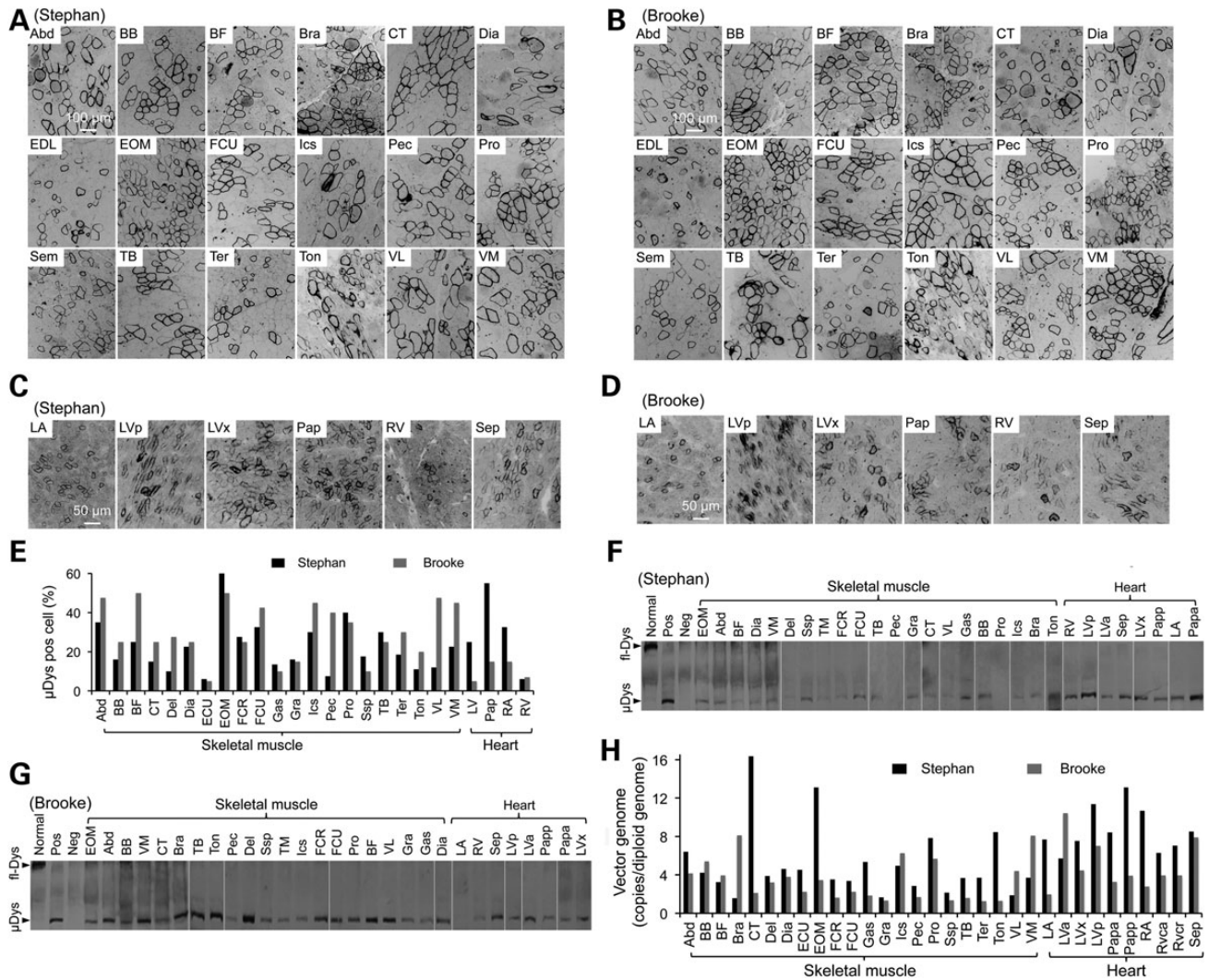


**Figure 4.** A single intravenous injection results in bodywide muscle expression of a flag-tagged  $\mu$ Dys gene in young adult dystrophic dogs. (A) Representative flag immunostaining of skeletal muscles from dog Stephan. (B) Representative flag immunostaining of skeletal muscles from dog Brooke. (C) Representative flag immunostaining of the heart from dog Stephan. (D) Representative flag immunostaining of the heart from dog Brooke. (E) Percentage of  $\mu$ Dys-positive myofibers. (F) Representative dystrophin western blot from dog Stephan. Positive and negative western blot controls are ECU muscles with and without  $\mu$ Dys AAV injection, respectively. (G) Representative dystrophin western blot from dog Brooke. Positive and negative western blot controls are ECU muscles with and without  $\mu$ Dys AAV injection, respectively. (H) AAV vector genome quantification. Abbreviations for skeletal muscles: Abd, abdominus; BB, biceps brachii; BF, biceps femoris; Bra, brachialis; CT, cranial tibialis; Del, deltoideus; Dia, diaphragm; ECU, extensor carpi ulnaris; EDL, extensor digitorum longus; EOM, extraocular muscle; FCR, flexor carpi radialis; FCU, flexor carpi ulnaris; fl-Dys, full-length dystrophin; Gas, gastrocnemius; Gra, gracilis; Ics, intercostalis; Pec, pectoralis; Pro, pronator; Sem, semitendinosus; Ssp, supraspinatus; TB, triceps brachii; Ter, Teres; Ton, tongue; VL, vastus lateralis; VM, vastus medialis. Abbreviations for the heart: LA, left atrium; LV, left ventricle; LVa, left ventricle anterior; LVp, left ventricle posterior; LVx, left ventricle apex; Pap, papillary muscle; Papa, anterior papillary muscle; Papp, posterior papillary muscle; RA, right atrium; RV, right ventricle; Rvca, caudal part of the right ventricle; RVcr, cranial part of the right ventricle; Sep, interventricular septum.

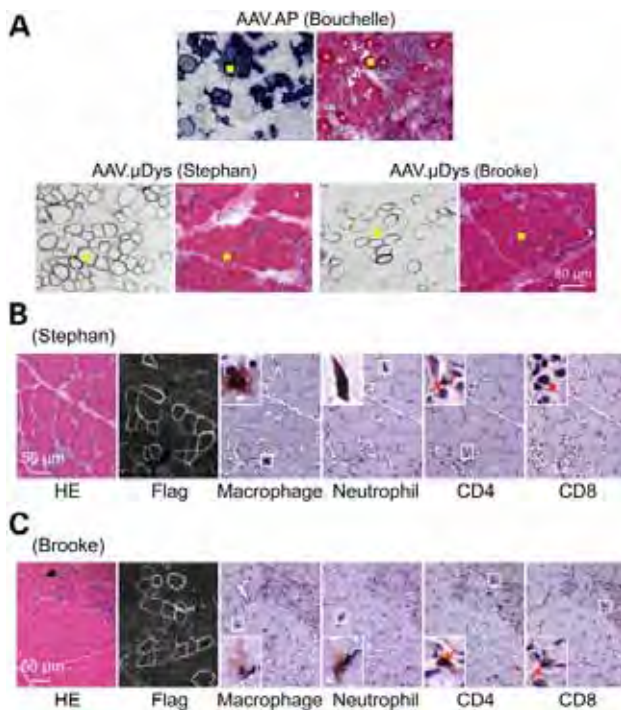


**Figure 5.**  $\mu$ Dys expression ameliorates muscle pathology in young adult dystrophic dogs. (A) Representative muscle serial sections stained for transgene expression (AP staining for AAV.AP injected dog Bouchelle and flag immunostaining for AAV. $\mu$ Dys injected dog Stephan and Brooke) and general morphology (HE staining). The yellow square marks the same myofiber in serial sections. Asterisk, heavily stained hyalinized/hypercontracted myofiber; arrow, angular myofiber; solid arrowhead, necrotic myofiber; open arrowhead, degenerative myofiber; pound sign, fibrotic tissue deposition. An enlarged view of the HE stained photomicrography of the AAV.AP infected dog is shown in Supplementary Material, Figure S3. (B) Representative HE staining, Flag immunostaining and immune cell immunohistochemical staining on muscle serial sections from AAV  $\mu$ Dys injected dog Stephan. Insets are the enlarged view of the boxed areas. Arrow, CD4+ or CD8+ T cell. (C) Representative HE staining, Flag immunostaining and immune cell immunohistochemical staining on muscle serial sections from AAV  $\mu$ Dys injected dog Brooke. Insets are the enlarged view of the boxed areas. Arrow, CD4+ or CD8+ T cell.

profiles were observed. The majority of muscles had  $\geq 25\%$   $\mu$ Dys-positive cells (such as the abdominal muscle, biceps femoris (BF), cranial tibialis (CT) and triceps brachii (TB)). These muscles appeared to have relatively uniform myofiber size and much less inflammation (Fig. 5). Hyalinized/hypercontracted myofibers were rarely detected in these muscles. On detailed immunohistochemical characterization, we observed very few macrophages, neutrophils, CD4+ T cells and CD8+ T cells (Fig. 5B and C). Further, these inflammatory cells were restricted to small loci (Fig. 5B and C). A different profile was seen in the ECU muscle. This muscle had the lowest expression (5%) (Fig. 4E). Its histology was identical to that of untreated or AAV.AP injected DMD dogs (data not shown). On *in situ* force measurement, we did not see any improvement (data not shown).

To study overall improvement in  $\mu$ Dys-treated dogs, we examined the serum CK level but did not see a consistent trend (Supplementary Material, Table S1, and Fig. S4).

## Discussion

In this study, we demonstrated for the first time that systemic AAV gene transfer is feasible in a young adult dystrophic large

mammal. Bodywide delivery to skeletal and cardiac muscle was confirmed in three affected dogs using two different AAV vectors. Notably, efficient whole body muscle transduction was not associated with any serious complications. All treated dogs tolerated gene transfer well and maintained the expected body weight growth (Fig. 1B). This is encouraging considering the fact that up to  $2 \times 10^{15}$  vg AAV particles were delivered to dogs that have ongoing massive muscle degeneration, necrosis and inflammation.

Systemic gene delivery has been a long-standing barrier in the field of gene therapy. This barrier was partially broken a decade ago when a series of studies from several laboratories showed robust whole body gene transfer in rodents with AAV-6, 8 and 9 at the dose of  $\sim 0.5\text{--}2 \times 10^{14}$  vg particles/kg body weight (6–8,23). Yet, scaling-up systemic AAV delivery to large mammals remains a formidable challenge (18). There are several obstacles. First, the thick basement membrane in large mammals may significantly limit vector spread from the microvasculature. It is thus expected that systemic transduction efficiency in large mammals will be reduced compared with that of mice. In support of this notion, the vector dose ( $1 \times 10^{14}$  vg/kg) that leads to bodywide gene transfer in adult mice yields much lower transduction in newborn dogs (8,13). The second obstacle is the large-scale AAV production. Besides the high cost and intense labor, negligible contaminants will become a significant safety concern when trillions of viral particles are administered. A third obstacle is our body's response to the infused virus. Unexpected inflammatory and/or immune response may lead to fatal complications as demonstrated in the tragic death of Jesse Gelsinger in a 1998 clinical trial and in the premature termination of the study reported by Kornegay et al. (4,5). Lastly, although AAV is much less immunogenic than vectors based on some other viruses (such as adenovirus), affected dogs often mount a furious immune response to AAV. This may further worsen untoward immune rejection to the AAV vector and/or AAV transduced myofibers (1,24). Taken together, development of systemic AAV gene transfer in adult dystrophic dogs represents an unprecedented challenge.

In light of the clinical need for bodywide gene therapy for DMD, we explored the safety and feasibility of intravenous AAV injection in the canine model, the best large animal model for DMD (25). To gain a comprehensive view on both muscle and non-muscle gene transfer, we first tested an AP reporter vector at a dose close to the effective dose we have used in normal neonatal puppies ( $\sim 2 \times 10^{14}$  vg/kg) (Table 1) (13,16). Consistent with the results of our newborn dog studies (13,16), single intravenous injection yielded bodywide skeletal muscle transduction in the juvenile DMD dog (Fig. 2). In newborn puppies, saturated transduction was observed in every skeletal muscle (13,16). However, in the young adult dystrophic dog, only the EOM showed near complete transduction (80%). We have previously found that myocardium expression from AAV-9 and Y731F AAV-9 was selectively blocked at some undefined post-entry steps in newborn dogs (13,16,17). In these published studies, we detected the AAV genome in the heart but AP positive cells were rarely observed. In striking contrast, efficient AP expression was seen in the heart of the young adult dystrophic dog suggesting that certain age and/or disease-related changes in the cardiomyocytes may have facilitated cardiac AAV-9 transduction in the juvenile DMD dog.

The cellular mechanism of systemic AAV muscle transduction is poorly understood. However, it is generally believed that viral particles have to cross the blood vessels to reach muscle. Consistent with this notion, we observed efficient microvasculature transduction in muscle (Fig. 3E). It has been shown that AAV-9 can cross the blood–brain barrier and transduce the

central nerve system (26,27). We indeed observed a high-level transduction in the spinal cord. Intriguingly, there was nominal AP expression in the cerebrum and cerebellum (Fig. 3D). Nevertheless, the peripheral nerves (including large nerves such as the sciatic nerve and small nerve branches such as these inside muscle) were effectively transduced (Fig. 3C and D).

Following systemic gene transfer, a significant amount of viral particles is often sponged in the liver. Zincarelli *et al.* compared nine AAV serotypes (AAV-1 to AAV-9) in mice and found that AAV-9 yielded the highest expression in the liver. In sharp contrast, we did not see strong liver expression in either normal newborn puppies or adult dystrophic dogs (Fig. 3) (13,15–17). There was also minimal expression in the testis, kidney, pancreas and lung (Fig. 3). Interestingly, we detected a high abundance of the AAV genome in internal organs (Fig. 3). Our results suggest that there may exist important species differences in AAV transduction. The inconsistency between the AAV genome copy number and the level of transgene expression in the liver is somewhat unexpected. The exact mechanisms behind this peculiar finding remain to be dissected. We speculate that it may relate to promoter silencing or inefficient conversion of the single-stranded AAV genome to the double stranded transcription competent form in the dog liver.

To confirm and expand our findings with the reporter AAV vector, we next performed a dose escalation study with a  $\mu$ Dys vector in two affected dogs. One dog received a total of  $1.77 \times 10^{15}$  vg AAV particles ( $5.04 \times 10^{14}$  vg/kg) and the other received  $2 \times 10^{15}$  vg AAV particles ( $6.24 \times 10^{14}$  vg/kg) (Table 1). These doses are lower than the highest doses we have delivered to newborn normal dogs ( $9.65 \times 10^{14}$  vg/kg) (17). However, as to our knowledge, they are the highest AAV doses ever been delivered to a diseased large mammal. Considering the potential immunogenicity of dystrophin (24,28), we extended immune suppression to the end of the study (Fig. 1A). Despite prolonged immune suppression and the increased AAV dose, we did not see adverse reactions in either dog. Blood examination did not show any evidence of liver or kidney damage (Fig. 1C, and Supplementary Material, Table S1). Together with the results of the AP vector injected dog, we conclude that there is minimal risk for systemic AAV gene transfer in adolescent dystrophic dogs.

To verify bodywide muscle transduction in  $\mu$ Dys vector injected dogs, we performed immunostaining and western blot (Fig. 4). These studies revealed the correct sarcolemmal localization and expected molecular size of  $\mu$ Dys (Fig. 4). Consistent with what we saw in the AP vector injected dog, widespread  $\mu$ Dys expression was detected in every muscle including the heart (Fig. 4). Although there were muscle-to-muscle differences, on average transduction efficiency reached ~25%.

The dog Brooke was injected with a dose 25% greater than what was administered to the dog Stephan (Table 1). We initially expected Brooke to have higher expression. However, this turned out not to be the case. On biopsy, Stephan seemed to have a slightly better expression and it also had more AAV genome copy (Fig. 1). The necropsy samples from Brooke's skeletal muscle, in general, had expression higher than those from Stephan's (Fig. 4). But Stephan appeared to have a better expression in the heart (Fig. 4). Interestingly, compared with Stephan, Brooke had a lower AAV genome copy number in most skeletal muscle and heart samples. We suspect that individual differences (such as gender, body weight at injection, vector dose, necropsy age and other yet unknown factors) may have contributed to these observations.

The EOM consistently showed the highest expression in all three treated dogs. The exact mechanism(s) underlying preferential

EOM transduction is yet to be elucidated. But it should be pointed out that this muscle indeed carries some unique biological features. For example, it is the only muscle in the dog body with the type IIB myofiber (29) (Duan D, unpublished observation).

In the neonatal study conducted by Kornegay and colleagues, dogs were not administered with immune suppressive drugs. We have previously shown that transient immune suppression is necessary to achieve efficient local AAV transduction in DMD dog muscles (21,22). Based on the same premise, we applied transient immune suppression in this study (Fig. 1A). Interestingly, two recent reports showed effective AAV-1 and AAV-8 delivery of an oligonucleotide via regional intravascular administration in dystrophic dogs without using immunosuppression (30,31). Future side-by-side comparison is needed to clarify the role of the AAV serotype (AAV-1 and AAV-8 versus AAV-9) and the transgene product (oligonucleotides versus proteins) in vascular delivery in DMD dogs.

Since our long-term goal is systemic DMD gene therapy, we examined muscle pathology in all three injected dogs. As expected, delivery of a reporter gene AAV vector yielded no protection (Fig. 5A). The muscle still displayed characteristic dystrophic features. Two dogs received  $\mu$ Dys therapy (Fig. 4). Different levels of mosaic expression were observed in various muscles in these dogs. The extensor carp ulnaris muscle had 5%  $\mu$ Dys-positive myofibers. Neither morphology nor function was improved in this muscle. However, we noticed an encouraging trend of pathology amelioration in muscles that had  $\mu$ Dys expression in more than 25% myofibers (Fig. 5). This result is consistent with the reports from other groups (30–34). Collectively, these data suggest that threshold non-uniform dystrophin expression can protect muscle. Despite histology improvement in many muscles, we did not see consistent reduction in serum creatine kinase. This could either be because not all muscles were protected at the current doses or because the sample size is too small in our study. Future large-scale high-dose studies are warranted to thoroughly evaluate whole body  $\mu$ Dys therapy in dystrophic dogs. Alternatively, other AAV serotypes should be explored to identify capsids that are more potent. It should also be pointed out that we have only followed AAV injected dogs for 3–3.5 months. Future long-term studies are warranted to assess the extent and persistence of systemic delivery in affected dogs.

In summary, we have demonstrated for the first time that intravenous Y731F AAV-9 administration can lead to efficient bodywide muscle transduction in young adult dystrophic dogs. The procedure is safe at the dose as high as  $6.24 \times 10^{14}$  vg particles/kg body weight ( $2 \times 10^{15}$  vg particles per dog). While our study has opened the door to the possibility of bodywide AAV  $\mu$ Dys gene therapy in young DMD patients in the future, additional works are needed to assess long-term safety and efficacy. Nevertheless, preliminary reports from systemic AAV-9 delivery in spinal muscular atrophy patients have yielded encouraging safety data (trial # NCT02122952) supporting continuous development of systemic AAV gene therapy for human diseases.

## Materials and Methods

### Animals

All animal experiments were approved by the Animal Care and Use Committees of the University of Missouri and were in accordance with the National Institutes of Health guidelines. Three dystrophin-deficient dogs were used in this study (Table 1). All three dogs were seronegative for AAV-9 before injection. Each dog carried a different null mutation in the dystrophin gene (18).

Specifically, the dog Bouchelle had a repetitive element insertion in the intron 19 of the dystrophin gene. This insertion introduced a nonsense mutation, which abolished dystrophin expression (18). In the dog Stephan, a point mutation in intron 6 disrupted dystrophin RNA splicing and the resulting transcript contained frame-shift mutation and a premature stop codon (35). In the dog Brooke, the long interspersed repetitive element-1 was inserted in the intron 13 of the dystrophin gene. Insertion created a new exon containing an in-frame stop codon (36). All experimental dogs were generated by artificial insemination and were on a mixed genetic background of golden retriever, Labrador retriever, beagle and Welsh corgi. The genotyping was determined by polymerase chain reaction (PCR) as we previously described (36,37).

### Recombinant Y731F tyrosine mutant AAV-9 production and gene delivery

The Y731F AAV-9 capsid-packaging construct has been published before (21,38). The AP reporter vector was published before (13,16). In this vector, the ubiquitous RSV promoter controls AP expression. This plasmid has been described previously. The canine micro-dystrophin AAV stock (CMV, $\mu$ Dys) was produced using our published construct pSJ46 (21). In the CMV, $\mu$ Dys vector, the codon-optimized canine  $\Delta$ R2-15/ $\Delta$ R18-19/ $\Delta$ R20-23/ $\Delta$ C microgene was expressed under the control of the CMV promoter (21). Recombinant endotoxin-free AAV vectors were generated using the triple plasmids transfection method we described before (39). Viral titer was determined using the Fast SYBR Green Master Mix kit (Bio-Rad, Hercules, CA) by real-time quantitative PCR (qPCR) in an ABI 7900 HT qPCR machine (Applied Biosystems). For RSV-AP virus, the forward primer for viral titer quantification was 5'-GGTTGTACGCGGTTAGGAGT and the reverse primer was 5'-GGCATGTTGCTAACTCATCG. This primer set amplified a fragment in the RSV promoter. For CMV, $\mu$ Dys virus, the titer was determined by qPCR using primers that amplified exons 69 and 70 in the dystrophin CR domain. The forward primer is 5'-TTTTCTGGTTCGAGTTGCAAAAAG. The reverse primer is 5'-CCATGTTGTCCCCTCTAAGAC.

### Immune suppression

Immune suppression was applied to experimental dogs using cyclosporine (Neoral, 100 mg/ml; Novartis, East Hanover, NJ; NDC 0078-0274-22) and mycophenolate mofetil (CellCept, 200 mg/ml; Genentech, South San Francisco, CA; NDC 0004-0261-29) (21,22). Cyclosporine was administered orally at the dose of 10–20/mg/kg/day to achieve a whole blood trough level of 100–200 ng/ml. The cyclosporine level was measured at the Clinical Pathology Laboratory in the University of Missouri Hospital (Columbia, MO). The blood trough level was achieved at ~6 days after starting cyclosporine. Mycophenolate mofetil was administered orally twice a day at the dose of 20 mg/kg (40 mg/kg/day). Immune suppression was started at 1 week prior to AAV injection. Immune suppression was continued for 4 weeks after AAV injection for Bouchelle and throughout the entire experiment for Stephan and Brooke (Fig. 1).

### Gene delivery, muscle biopsy and dog necropsy

Systemic Y731F AAV-9 delivery was performed in conscious dogs by a single intravenous injection through the cephalic vein (Table 1). Biopsy was performed on the BF and CT at 1 month after AAV injection (14). Necropsy was performed at 3.5 months post-injection for Bouchelle and Stephan and 4 months

post-injection for Brooke. During necropsy, major skeletal muscles from the head (EOM, temporalis, tongue), neck (sternocephalicus), shoulder (deltoideus, supraspinatus), thorax (intercostal muscle, pectoralis), back (latissimus, teres, trapezius), abdomen (abdominal rectus), forelimb (biceps brachii, brachialis, extensor carpi radialis, ECU, extensor digitorum communis, flexor carpi radialis, flexor carpi ulnaris, flexor digitorum, pronator, TB) and hind limb (BF, cranial sartorius, CT, extensor digitorum lateralis, extensor digitorum longus, gastrocnemius, gracilis, quadriceps, rectus femoris, semimembranosus, semitendinosus, vastus lateralis and vastus medialis) as well as the diaphragm (sternal, costal and lumbar part), heart (right and left atria, right and left ventricles, papillary muscles and interventricular septum) and internal organs (liver, pancreas, spleen, lung, kidney, gonad, spinal cord, brachial plexus, sciatic nerve, cerebrum, cerebellum and hippocampus) were harvested. Two pieces of samples were collected from each tissue. One piece was frozen in liquid nitrogen-cooled isopentane in optimal cutting temperature media for cryosection and histological examinations. The other piece was snap frozen in liquid nitrogen for genomic DNA and protein extraction.

### Blood chemistry

Blood was drawn from experimental subjects before the start of immune suppression (baseline data) and periodically throughout the experiment (Supplementary Material, Table S1). The laboratory biochemical test was performed at the Veterinary Medical Diagnostic Laboratory in the University of Missouri Veterinary Medical Teaching Hospital (Columbia, MO).

### Histological examination of AP reporter gene expression

AP histochemical staining was carried out on 8- $\mu$ m-thick cryosections as we described before (13,14,22). Briefly, tissue sections were fixed in 0.5% glutaraldehyde for 10 min. After washing with 1 mM MgCl<sub>2</sub>, slides were incubated at 65°C for 45 min to inactivate endogenous AP activity. Slides were subsequently washed in a pre-staining buffer containing 100 mM Tris-HCl, pH 9.5, 50 mM MgCl<sub>2</sub>, 100 mM NaCl. Finally, slides were stained in the freshly prepared AP staining solution (165 mg/mL 5-bromo-4-chloro-3-indolylphosphate-*p*-toluidine, 330 mg/ml nitroblue tetrazolium chloride, 50 mM levamisole) for 5–20 min. Cryosections from an uninfected dog (Frank) were used as negative controls for AP staining (13).

### Examination of AP activity assay in tissue lysate

Total protein lysate was extracted as we described before (14). Protein concentration was determined using the DC protein assay kit (Bio-Rad). AP activity was measured by a colorimetric method using the Stem TAGTM alkaline phosphatase activity assay kit (Cell Biolabs, San Diego, CA). Prior to the assay, endogenous AP activity was inactivated by incubating the lysate at 65°C for 1 h.

### Examination of $\mu$ Dys expression by immunofluorescence staining

Codon-optimized flag-tagged canine  $\Delta$ R2-15/ $\Delta$ R18-19/ $\Delta$ R20-23/ $\Delta$ C  $\mu$ Dys was revealed with an anti-FLAG M2 antibody (1:400; Sigma).  $\mu$ Dys expression was also confirmed with a dystrophin C-terminal Dys-2 epitope specific antibody (1:20; Novocastra, Newcastle, UK).

## Western blot

Whole muscle lysate was loaded on an 8% sodium dodecyl sulfate-polyacrylamide gel, and protein was transferred to a polyvinylidene difluoride membrane. Dystrophin was detected with an antibody against the Dys2 epitope (1:100; Novocastra). The full-length dystrophin protein migrated at 427 kD. The canine  $\Delta R2-15/\Delta R18-19/\Delta R20-23/\Delta C$   $\mu$ Dys protein migrated at 140 kD.

## Vector genome copy number determination

Genomic DNA was extracted from freshly frozen tissue samples. The AAV genome copy was determined using the Fast SYBR Green Master Mix kit (Applied Biosystems) by qPCR in an ABI 7900 HT qPCR machine. A set of primers located within the AP gene was employed to quantify the vg copy number in Bouchelle. The forward primer is 5'-GACTGAGCCCATGACACCAA. The reverse primer is 5'-CATCTGTCTCGACCCCACTG. For Stephan and Brooke, we used a set of primers that amplified a 119 bp fragment in the CMV early enhancer. The forward primer is 5'-TTACGG TAAACTGCCCACTTG. The reverse primer is 5'-CATAAGGTCA TGTACTGGGCATAA.

## In situ muscle force assay

Prior to necropsy, the contractility of the ECU muscle was measured according to our published protocol (21,40).

## Supplementary Material

Supplementary Material is available at HMG online.

## Acknowledgements

The authors thank Dr Arun Srivastava for providing experimental Y731F AAV-9 packaging construct and Dr Ronald Terjung for helpful discussion.

## Authors' Contributions

Conceived and designed study: D.D. Performed experiments: Y.Y., X.P., C.H.H., K.K., K.Z., J.S., H.T.Y. and T.M. Analyzed data: D.D., Y.Y., X.P., C.H.H.. Wrote the paper: D.D.

**Conflict of Interest statement.** D.D. is a member of the scientific advisory board for Solid GT, LLC, a venture company founded to advance gene therapy for DMD.

## Funding

This work was supported by grants (to D.D.) from Department of Defense MD130014, Jessey's Journey-The Foundation for Cell and Gene Therapy, Hope for Javier, the National Institutes of Health HL-91883, the Gene Therapy Resource Program of the National Heart, Lung and Blood Institute located at the University of Pennsylvania, Kansas City Area Life Sciences Institute and the University of Missouri.

## References

- Mingozzi, F. and High, K.A. (2011) Therapeutic in vivo gene transfer for genetic disease using AAV: progress and challenges. *Nat. Rev. Genet.*, **12**, 341–355.
- Lewis, R. (2014) Gene therapy's second act. *Sci. Am.*, **310**, 52–57.
- Kunkel, L.M. (2005) 2004 William Allan award address. Cloning of the DMD gene. *Am. J. Hum. Genet.*, **76**, 205–214.
- Wilson, J.M. (2009) Lessons learned from the gene therapy trial for ornithine transcarbamylase deficiency. *Mol. Genet. Metab.*, **96**, 151–157.
- Kornegay, J.N., Li, J., Bogan, J.R., Bogan, D.J., Chen, C., Zheng, H., Wang, B., Qiao, C., Howard, J.F. Jr. and Xiao, X. (2010) Widespread muscle expression of an AAV9 human mini-dystrophin vector after intravenous injection in neonatal dystrophin-deficient dogs. *Mol. Ther.*, **18**, 1501–1508.
- Gregorevic, P., Blankinship, M.J., Allen, J.M., Crawford, R.W., Meuse, L., Miller, D.G., Russell, D.W. and Chamberlain, J.S. (2004) Systemic delivery of genes to striated muscles using adeno-associated viral vectors. *Nat. Med.*, **10**, 828–834.
- Wang, Z., Zhu, T., Qiao, C., Zhou, L., Wang, B., Zhang, J., Chen, C., Li, J. and Xiao, X. (2005) Adeno-associated virus serotype 8 efficiently delivers genes to muscle and heart. *Nat. Biotechnol.*, **23**, 321–328.
- Bostick, B., Ghosh, A., Yue, Y., Long, C. and Duan, D. (2007) Systemic AAV-9 transduction in mice is influenced by animal age but not by the route of administration. *Gene Ther.*, **14**, 1605–1609.
- Bostick, B., Shin, J.H., Yue, Y., Wasala, N.B., Lai, Y. and Duan, D. (2012) AAV micro-dystrophin gene therapy alleviates stress-induced cardiac death but not myocardial fibrosis in >21-m-old mdx mice, an end-stage model of Duchenne muscular dystrophy cardiomyopathy. *J. Mol. Cell. Cardiol.*, **53**, 217–222.
- Bostick, B., Shin, J.-H., Yue, Y. and Duan, D. (2011) AAV-microdystrophin therapy improves cardiac performance in aged female mdx mice. *Mol. Ther.*, **19**, 1826–1832.
- Gregorevic, P., Blankinship, M.J., Allen, J.M. and Chamberlain, J.S. (2008) Systemic microdystrophin gene delivery improves skeletal muscle structure and function in old dystrophic mdx mice. *Mol. Ther.*, **16**, 657–664.
- Duan, D. (2015) Duchenne muscular dystrophy gene therapy in the canine model. *Hum. Gene Ther. Clin. Dev.*, **26**, 57–69.
- Yue, Y., Ghosh, A., Long, C., Bostick, B., Smith, B.F., Kornegay, J.N. and Duan, D. (2008) A single intravenous injection of adeno-associated virus serotype-9 leads to whole body skeletal muscle transduction in dogs. *Mol. Ther.*, **16**, 1944–1952.
- Yue, Y., Shin, J.H. and Duan, D. (2011) Whole body skeletal muscle transduction in neonatal dogs with AAV-9. *Methods Mol. Biol.*, **709**, 313–329.
- Pan, X., Yue, Y., Zhang, K., Lostal, W., Shin, J.H. and Duan, D. (2013) Long-term robust myocardial transduction of the dog heart from a peripheral vein by adeno-associated virus serotype-8. *Hum. Gene Ther.*, **24**, 584–594.
- Hakim, C.H., Yue, Y., Shin, J.H., Williams, R.R., Zhang, K., Smith, B.F. and Duan, D. (2014) Systemic gene transfer reveals distinctive muscle transduction profile of tyrosine mutant AAV-1, -6, and -9 in neonatal dogs. *Mol. Ther. Methods Clin. Dev.*, **1**, 14002.
- Pan, X., Yue, Y., Zhang, K., Hakim, C.H., Kodippili, K., McDonald, T. and Duan, D. (2015) AAV-8 is more efficient than AAV-9 in transducing neonatal dog heart. *Hum. Gene Ther. Methods*, **26**, 54–61.
- Duan, D. (2011) Duchenne muscular dystrophy gene therapy: lost in translation? *Res. Rep. Biol.*, **2**, 31–42.
- Zhong, L., Li, B., Mah, C.S., Govindasamy, L., Agbandje-McKenna, M., Cooper, M., Herzog, R.W., Zolotukhin, I., Warrington, K.H. Jr., Weigel-Van Aken, K.A. et al. (2008) Next generation of adeno-associated virus 2 vectors: point

- mutations in tyrosines lead to high-efficiency transduction at lower doses. *Proc. Natl. Acad. Sci. USA*, **105**, 7827–7832.
20. Martino, A.T., Basner-Tschakarjan, E., Markusic, D.M., Finn, J.D., Hinderer, C., Zhou, S., Ostrov, D.A., Srivastava, A., Ertl, H.C., Terhorst, C. et al. (2013) Engineered AAV vector minimizes in vivo targeting of transduced hepatocytes by capsid-specific CD8+ T cells. *Blood*, **121**, 2224–2233.
  21. Shin, J.H., Pan, X., Hakim, C.H., Yang, H.T., Yue, Y., Zhang, K., Terjung, R.L. and Duan, D. (2013) Microdystrophin ameliorates muscular dystrophy in the canine model of Duchenne muscular dystrophy. *Mol. Ther.*, **21**, 750–757.
  22. Shin, J.H., Yue, Y., Srivastava, A., Smith, B., Lai, Y. and Duan, D. (2012) A simplified immune suppression scheme leads to persistent micro-dystrophin expression in Duchenne muscular dystrophy dogs. *Hum. Gene Ther.*, **23**, 202–209.
  23. Pacak, C.A., Mah, C.S., Thattaliyath, B.D., Conlon, T.J., Lewis, M.A., Cloutier, D.E., Zolotukhin, I., Tarantal, A.F. and Byrne, B.J. (2006) Recombinant adeno-associated virus serotype 9 leads to preferential cardiac transduction in vivo. *Circ. Res.*, **99**, e3–e9.
  24. Mendell, J.R., Campbell, K., Rodino-Klapac, L., Sahenk, Z., Shilling, C., Lewis, S., Bowles, D., Gray, S., Li, C., Galloway, G. et al. (2010) Dystrophin immunity in Duchenne's muscular dystrophy. *N. Engl. J. Med.*, **363**, 1429–1437.
  25. McGreevy, J.W., Hakim, C.H., McIntosh, M.A. and Duan, D. (2015) Animal models of Duchenne muscular dystrophy: from basic mechanisms to gene therapy. *Dis. Model. Mech.*, **8**, 195–213.
  26. Foust, K.D., Nurre, E., Montgomery, C.L., Hernandez, A., Chan, C.M. and Kaspar, B.K. (2009) Intravascular AAV9 preferentially targets neonatal neurons and adult astrocytes. *Nat. Biotechnol.*, **27**, 59–65.
  27. Zhang, H., Yang, B., Mu, X., Ahmed, S.S., Su, Q., He, R., Wang, H., Mueller, C., Sena-Estevés, M., Brown, R. et al. (2011) Several rAAV vectors efficiently cross the blood–brain barrier and transduce neurons and astrocytes in the neonatal mouse central nervous system. *Mol. Ther.*, **19**, 1440–1448.
  28. Flanigan, K., Campbell, K., Viollet, L., Wang, W., Gomez, A.M., Walker, C. and Mendell, J.R. (2013) Anti-dystrophin T cell responses in Duchenne muscular dystrophy: prevalence and a glucocorticoid treatment effect. *Hum. Gene Ther.*, **24**, 797–806.
  29. Toniolo, L., Maccatrozzo, L., Patruno, M., Caliaro, F., Mascarello, F. and Reggiani, C. (2005) Expression of eight distinct MHC isoforms in bovine striated muscles: evidence for MHC-2B presence only in extraocular muscles. *J. Exp. Biol.*, **208**, 4243–4253.
  30. Vulin, A., Barthelemy, I., Goyenvalle, A., Thibaud, J.L., Beley, C., Griffith, G., Benchaouir, R., le Hir, M., Unterfinger, Y., Lorain, S. et al. (2012) Muscle function recovery in golden retriever muscular dystrophy after AAV1-U7 exon skipping. *Mol. Ther.*, **20**, 2120–2133.
  31. Le Guiner, C., Montus, M., Servais, L., Cherel, Y., Francois, V., Thibaud, J.L., Wary, C., Matot, B., Larcher, T., Guigand, L. et al. (2014) Forelimb treatment in a large cohort of dystrophic dogs supports delivery of a recombinant AAV for exon skipping in Duchenne patients. *Mol. Ther.*, **22**, 1923–1935.
  32. Bish, L.T., Sleeper, M.M., Forbes, S.C., Wang, B., Reynolds, C., Singletary, G.E., Trafny, D., Morine, K.J., Sanmiguel, J., Cecchini, S. et al. (2012) Long-term restoration of cardiac dystrophin expression in golden retriever muscular dystrophy following rAAV6-mediated exon skipping. *Mol. Ther.*, **20**, 580–589.
  33. Yoshimura, M., Sakamoto, M., Ikemoto, M., Mochizuki, Y., Yuasa, K., Miyagoe-Suzuki, Y. and Takeda, S. (2004) AAV vector-mediated microdystrophin expression in a relatively small percentage of mdx myofibers improved the mdx phenotype. *Mol. Ther.*, **10**, 821–828.
  34. Chamberlain, J.S. (1997) Dystrophin levels required for correction of Duchenne muscular dystrophy. *Basic Appl. Myol.*, **7**, 251–255.
  35. Cooper, B.J., Winand, N.J., Stedman, H., Valentine, B.A., Hoffman, E.P., Kunkel, L.M., Scott, M.O., Fischbeck, K.H., Kornegay, J.N., Avery, R.J. et al. (1988) The homologue of the Duchenne locus is defective in X-linked muscular dystrophy of dogs. *Nature*, **334**, 154–156.
  36. Smith, B.F., Yue, Y., Woods, P.R., Kornegay, J.N., Shin, J.H., Williams, R.R. and Duan, D. (2011) An intronic LINE-1 element insertion in the dystrophin gene aborts dystrophin expression and results in Duchenne-like muscular dystrophy in the corgi breed. *Lab. Invest.*, **91**, 216–231.
  37. Fine, D.M., Shin, J.H., Yue, Y., Volkmann, D., Leach, S.B., Smith, B.F., McIntosh, M. and Duan, D. (2011) Age-matched comparison reveals early electrocardiography and echocardiography changes in dystrophin-deficient dogs. *Neuromuscul. Disord.*, **21**, 453–461.
  38. Petrs-Silva, H., Dinculescu, A., Li, Q., Min, S.H., Chiodo, V., Pang, J.J., Zhong, L., Zolotukhin, S., Srivastava, A., Lewin, A.S. et al. (2009) High-efficiency transduction of the mouse retina by tyrosine-mutant AAV serotype vectors. *Mol. Ther.*, **17**, 463–471.
  39. Shin, J.H., Yue, Y. and Duan, D. (2012) Recombinant adeno-associated viral vector production and purification. *Methods Mol. Biol.*, **798**, 267–284.
  40. Yang, H.T., Shin, J.H., Hakim, C.H., Pan, X., Terjung, R.L. and Duan, D. (2012) Dystrophin deficiency compromises force production of the extensor carpi ulnaris muscle in the canine model of Duchenne muscular dystrophy. *PLoS One*, **7**, e44438.

## Supplementary Materials

**Supplementary Table 1.** Blood test results.

**Supplementary Figure 1. Systemic Y731F AAV-9 injection results in minimal transgene expression in the islet of the pancreas.** The islet is marked by immunofluorescence staining with a polyclonal anti-insulin antibody. Top row, low-magnification images; Bottom row, high-power images of the boxed areas in the top row.

**Supplementary Figure 2. Micro-dystrophin is not detectable in internal organs follow systemic AAV. $\mu$ Dys injection.** **A**, Quantification of the AAV genome copy in internal organs of dog Stephan and Brooke. **B**, Representative western blot results showing a lack of micro-dystrophin expression in internal organs.

**Supplementary Figure 3. Systemic AAV.AP injection does not protect skeletal muscle in young adult DMD dogs.** Representative photomicrograph of HE stained cranial tibialis muscle from the dog injected with AAV.AP. This is an enlarged version of the photo shown in Figure 5A. Asterisk, heavily stained hyalinated/hypercontracted myofiber; Arrow, angular myofiber, Solid arrowhead, necrotic myofiber; Open arrowhead, degenerative myofiber, Pound sign, fibrotic tissue deposition.

**Supplementary Figure 4. Serum CK profile.** AAV injection was performed at time 0. The pre-treatment CK level was obtained right before the start of immune suppression (one week before AAV injection).

Supplementary Table 1. Blood test results

Timeline	Unit	Bouchelle							Stephan							Brooke							2 to 6-m-old untreated affected dogs												
		week	-1	1	2	3	4	5	14	-1	0	1	2	4	6	8	9	11	12	-1	0	1	2	3	4	5	7	9	11	13	15	16	Average	Min	Max
Plasma protein	g/dL	6.1	6.2	6.6	6.5	6.6	7.2	7.2	7.3	6.3	6.2	5.5	5.9	6.9	7.0	7.8	7.0	7.3	6.2	6.4	6.3	6.6	6.3	6.7	6.9	6.9	7.0	6.8	6.8	7.1	6.8	6.84	5.80	7.90	
WBC	x10 <sup>3</sup> /uL	14.13	11.13	17.73	10.40	9.93	13.38	13.69	13.56	8.47	11.46	16.81	10.99	13.86	10.73	11.93	12.99	13.28	15.65	21.15	9.92	12.52	14.39	16.25	15.25	13.78	13.85	11.51	12.36	14.82	12.26	14.59	8.34	21.13	
RBC	x10 <sup>6</sup> /uL	4.27	4.64	4.72	4.87	5.11	5.65	5.69	4.61	8	5.58	5.5	5.15	4.70	5.59	6.27	5.81	6.28	4.61	4.69	5.2	5.42	5.13	4.94	5.34	5.47	6.01	5.88	6.67	6.88	6.36	5.84	4.27	7.31	
Hgb	g/dL	9.5	10.4	10.6	11.1	11.6	12.9	12.9	11	11.1	12.9	12.7	11.5	11.1	13.2	14.8	13.5	14.6	10.9	10.9	12.2	12.4	11.6	11.3	12.3	12.1	13.7	13.2	15.1	15.3	14.2	13.56	9.50	16.70	
Hct	%	30	31	32	33	34	37	38	33	33	34	37	34	32	37	43	39	42	33	31	33	33	33	31	34	34	37	36	41	43	39	39.50	30.00	48.00	
MCV	fL	71	67	67	67	66	65	67	71	69	61	68	67	69	66	69	67	66	72	67	63	60	63	63	64	61	62	61	62	62	62	62	67.88	58.00	74.00
MCH	pg	22.2	22.4	22.5	22.8	22.7	22.8	22.7	23.9	23.3	23.1	23.1	22.3	23.6	23.6	23.6	23.2	23.2	23.6	23.2	23.5	22.9	22.6	22.9	23.0	22.1	22.8	22.4	22.6	22.2	22.3	23.22	22.10	24.50	
MCHC	g/dL	31.5	33.5	33.5	34.2	34.6	35.2	33.9	33.7	33.9	37.7	34.2	33.4	34.5	36.0	34.2	34.6	35.2	32.7	34.7	37.3	37.9	35.7	36.2	36.1	36.1	36.7	37.0	36.5	35.9	36.0	34.32	30.50	39.20	
Platelet	x10 <sup>3</sup> /uL	801	932	921	796	850	1069	806	329	278	501	569	493	416	737	749	639	637	438	626	465	573	587	561	491	508	608	445	585	517	475	732.35	409.00	977.00	
Neutro, Seg	x10 <sup>3</sup> /uL	9.47	7.35	12.59	8.01	7.05	8.56	8.35	5.56	5.59	6.76	8.41	7.25	8.87	5.37	7.64	8.18	6.91	7.51	12.90	6.25	7.01	9.79	9.26	7.32	9.78	7.89	5.87	6.80	6.97	7.48	7.68	3.51	12.68	
Neutro, Band	x10 <sup>3</sup> /uL	0.00	0.00	0.00	0.00	0.00	0.00	0.00	0.00	0.17	0.00	0.00	0.00	0.00	0.00	0.00	0.26	0.00	0.16	0.00	0	0.13	0.00	0.00	0.00	0.00	0.00	0.00	0.00	0.00	0.00	0.00	0.00	0.00	0.30
Lymphocyte	x10 <sup>3</sup> /uL	3.96	2.45	4.08	2.29	2.18	2.94	4.52	7.19	1.69	3.78	7.23	2.75	4.02	4.51	4.06	3.90	5.58	7.67	7.19	3.17	4.01	3.60	5.69	7.17	3.58	5.40	4.83	5.07	6.22	4.54	6.36	2.25	9.90	
Monocyte	x10 <sup>3</sup> /uL	0.57	0.56	0.53	0.00	0.70	1.20	0.82	0.81	0.85	0.69	0.67	0.33	0.69	0.54	0.24	0.52	0.27	0.16	0.63	0.5	1.25	0.58	0.65	0.76	0.00	0.42	0.35	0.25	1.19	0.00	0.38	0.00	1.30	
Eosinophil	x10 <sup>3</sup> /uL	0.14	0.78	0.53	0.10	0.00	0.67	0.00	0.00	0.17	0.23	0.50	0.66	0.28	0.32	0.00	0.13	0.40	0.16	0.42	0	0.13	0.43	0.65	0.00	0.41	0.14	0.46	0.25	0.44	0.25	0.25	0.00	0.72	
Basophil	x10 <sup>3</sup> /uL	0.00	0.00	0.00	0.00	0.00	0.00	0.00	0.00	0.00	0.00	0.00	0.00	0.00	0.00	0.00	0.00	0.13	0.00	0.00	0.00	0.00	0.00	0.00	0.00	0.00	0.00	0.00	0.00	0.00	0.00	0.00	0.01	0.00	0.16
Reticulocyte	%	3.5	1.6	3.1	2.2	1.4	2.2	1.1	5.4	2.4	0.8	0.5	4.2	6.2	3.1	2.6	2.7	3.3	6.6	3.3	1.5	1.6	2.7	4.0	2.0	2.2	1.9	1.6	1.7	1.9	1.6	2.59	0.70	5.50	
Glucose	mg/dL	134	131	117	128	123	128	115	121	113	66	105	106	106	92	130	113	110	116	108	112	109	110	103	99	107	104	80	114	111	126	97.78	66.00	134.00	
BUN	mg/dL	14	9	10	12	10	21	17	15	4	11	14	12	15	9	12	10	10	11	8	7	7	10	8	10	14	11	10	10	8	9	14.63	9.00	22.00	
Creatinine	mg/dL	0.4	0.3	0.3	0.3	0.2	0.5	0.4	0.5	0.2	0.2	0.4	0.3	0.4	0.2	0.4	0.4	0.3	0.4	0.3	0.3	0.3	0.4	0.3	0.2	0.3	0.4	0.2	0.3	0.3	0.4	0.39	0.20	0.60	
Sodium	mEq/L	142	141	141	142	144	142	151	145	142	141	142	145	143	146	145	143	148	143	144	144	142	143	142	145	144	144	145	145	143	143	143	143.25	139.00	150.00
Potassium	mEq/L	5.9	6.2	6.0	5.4	6.0	5.7	4.5	5.6	6	5.1	6.4	5.6	6.1	6.2	6.0	4.7	5.7	4.7	5.4	5.3	5.5	5.6	5.6	5.4	5.2	5.7	5.2	5.6	5.6	5.0	5.80	4.70	6.70	
Chloride	mEq/L	106	105	105	106	107	102	107	108	109	102	111	109	104	105	103	105	106	105	106	108	105	107	105	107	104	105	105	105	106	104	105.13	102.00	108.00	
Total CO2	mEq/L	23	20	18	20	20	24	24	20	19	16	18	18	21	25	25	19	24	22	22	19	20	19	20	19	19	19	22	23	18	20	21.80	20.00	25.00	
Anion gap	mEq/L	19	22	24	21	23	22	25	23	20	28	19	24	24	22	23	24	24	21	21	22	23	23	23	24	26	26	23	23	25	24	22.20	17.00	27.00	
Albumin	g/dL	2.7	2.7	2.9	2.9	2.9	3.0	3.2	3.0	3.0	3.0	2.5	2.5	3.0	3.1	3.2	3.1	3.2	2.7	2.9	2.8	2.9	2.8	3.0	3.1	3.2	3.2	2.9	3.1	3.2	3.2	3.09	2.60	3.50	
Total protein	g/dL	5.0	4.8	5.6	5.4	5.4	5.6	6.2	5.1	5.1	5.0	4.5	4.5	5.8	6.1	5.6	6.4	5.8	4.5	5.6	4.8	5.1	5.1	5.4	5.7	5.5	5.6	5.7	5.8	5.7	5.9	5.64	4.80	7.00	
Globulin	g/dL	2.3	2.1	2.7	2.5	2.5	2.6	3.0	2.1	2.1	2.0	2.0	2.0	2.8	3.0	2.4	3.3	2.6	1.8	2.7	2.0	2.2	2.3	2.4	2.6	2.3	2.4	2.8	2.7	2.5	2.7	2.56	1.80	3.50	
Calcium	mg/dL	11.1	10.8	10.9	11.4	10.8	13.7	10.9	11.7	11.1	10.7	10.6	11.1	11.7	11.2	11.7	10.5	11.1	12	11.8	11.4	11.5	11.6	11.7	11.7	12.7	12.6	11.8	11.8	10.8	10.8	11.31	10.40	13.20	
Phosphorus	mg/dL	9.5	8.8	9.3	8.8	9.1	7.6	7.9	10.1	7.2	6.6	6.7	8.7	8.2	8.3	8.5	6.3	7.7	9.8	8.5	7.8	8.3	8.4	9.1	9.5	8.6	8.4	8.3	8.4	7.4	8.3	8.76	6.10	10.50	
Cholesterol	mg/dL	208	271	253	252	251	283	299	272	286	259	165	206	211	271	296	419	284	207	251	282	290	267	227	222	247	284	285	290	300	279	276.85	182.00	430.00	
Bilirubin	mg/dL	0.2	0.1	0.2	0.1	0.1	0.2	0.1	0.2	0.2	0.1	0.2	0.1	0.2	0.2	0.1	0.2	0.1	0.2	0.2	0.1	0.1	0.2	0.3	0.2	0.3	0.2	0.2	0.2	0.2	0.2	0.18	0.10	0.30	
ALT	U/L	402	330	383	414	417	370	1,053	264	222	149	72	188	382	403	370	374	370	284	339	263	251	265	345	304	416	439	422	414	396	427	415.20	264.00	593.00	
ALP	U/L	78	82	97	125	177	59	41	82	90	69	55	85	86	78	72	35	57	90	87	78	78	70	83	81	72	74	70	71	61	59	64.75	31.00	122.00	
CK	U/L	27,600	16,144	25,235	19,890	11,658	31,541	N/A	32,319	10,186	4,055	5,119	7,770	31,974	17,588	13,679	12,810	30,958	30,859	15,812	11,571	14,092	22,193	13,328	22,000	15,750	25,458	17,701	20,995	22,819	19,918	46,074.13	17,772.00	209,625.00	

Blue marked, baseline level before the start of immune suppression.

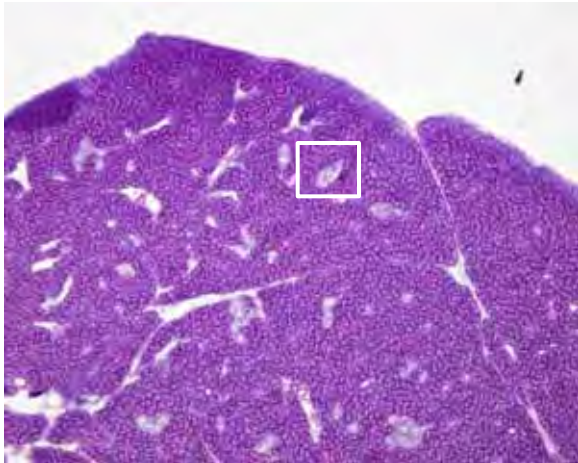
Yellow marked, mean value of 2 to 6-m-old untreated affected dogs.

Green/Orange marked, lower/higher than the minimum/maximum value, respectively, in age-matched untreated affected dogs.

Abbreviations: ALP, alkaline phosphatase; ALT, Alanine aminotransferase; BUN, Blood urea nitrogen; CK, creatine kinase; Hct, Hematocrit; Hgb, Hemoglobin; MCH, Mean corpuscular hemoglobin; MCHC, Mean corpuscular hemoglobin concentration; MCV, Mean corpuscular volume; Neutro Band; Neutro Seg, Segmented neutrophil; RBC, red blood cell; WBC, white blood cell.

Supplementary Figure 1.

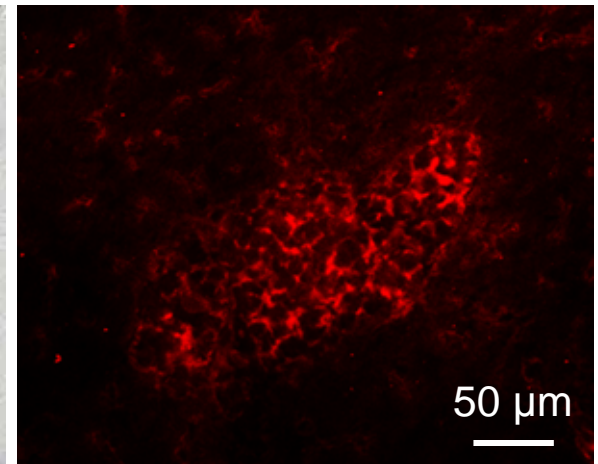
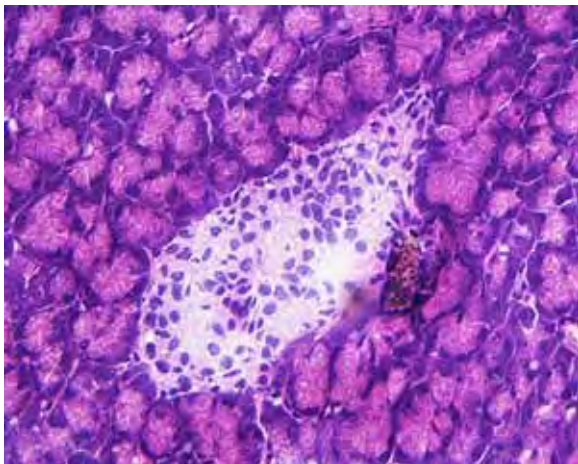
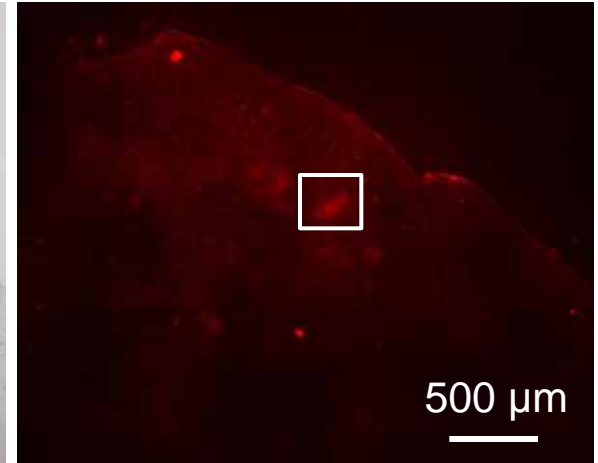
HE staining



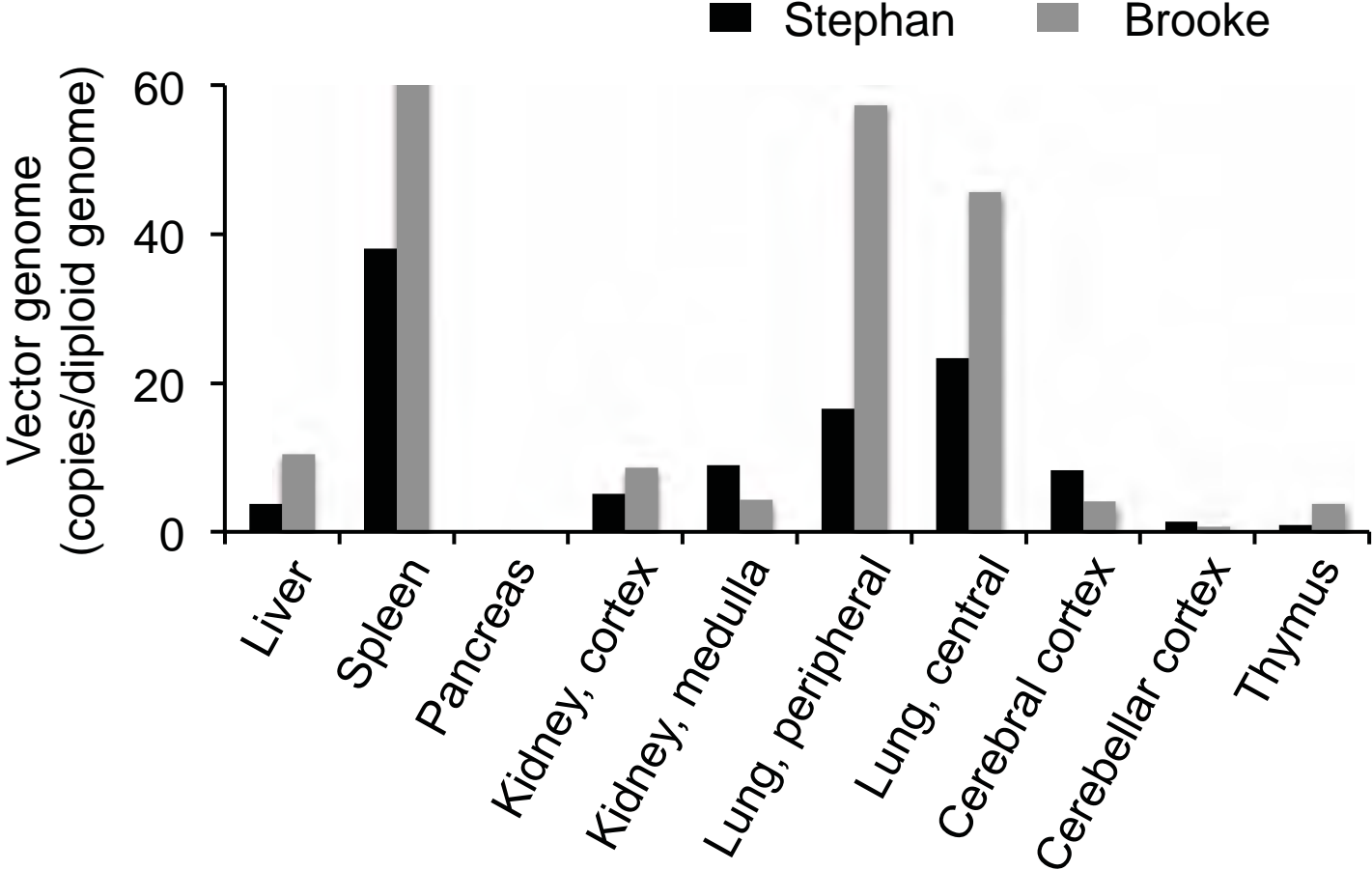
AP staining



Insulin staining

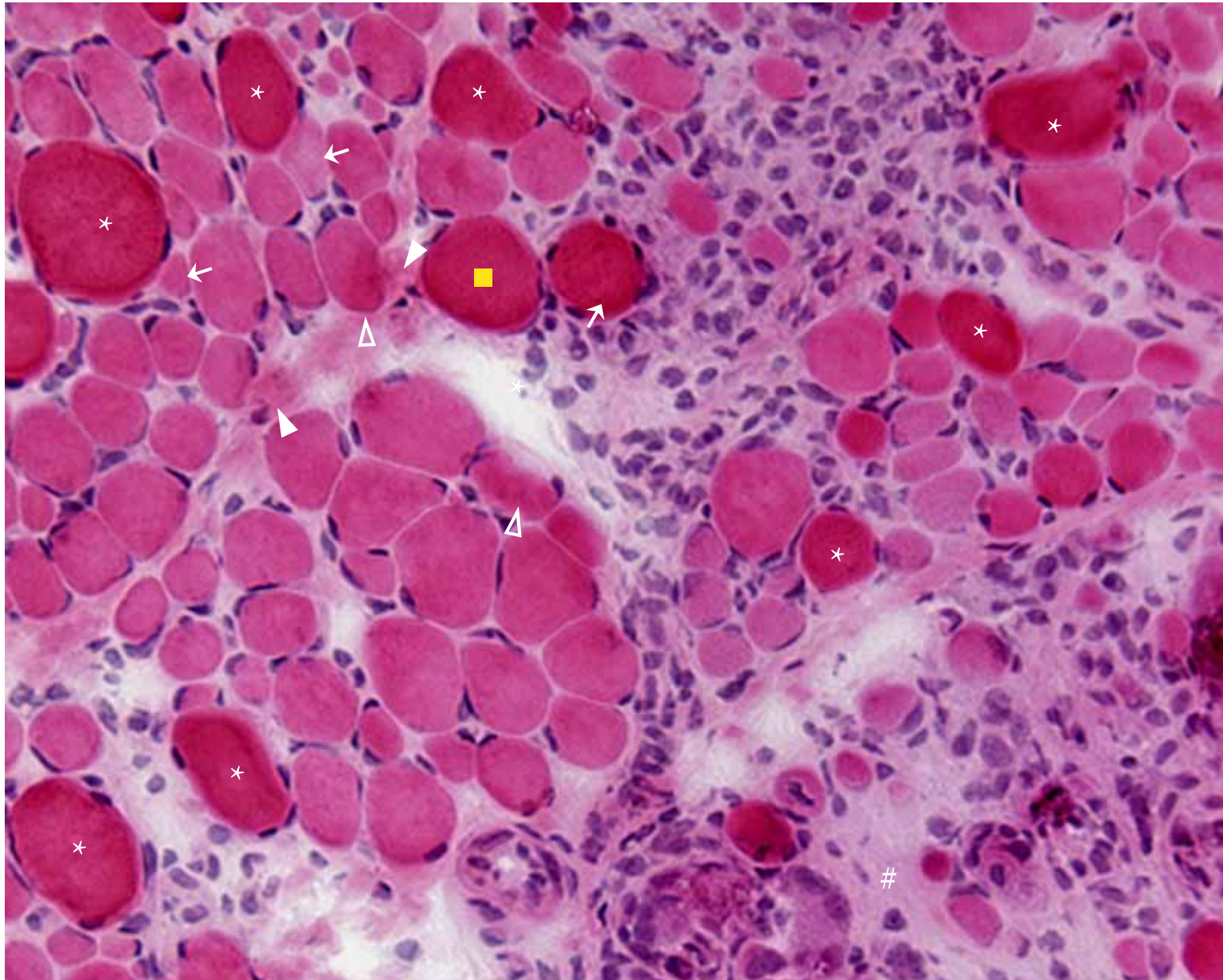


Supplementary Figure 2A

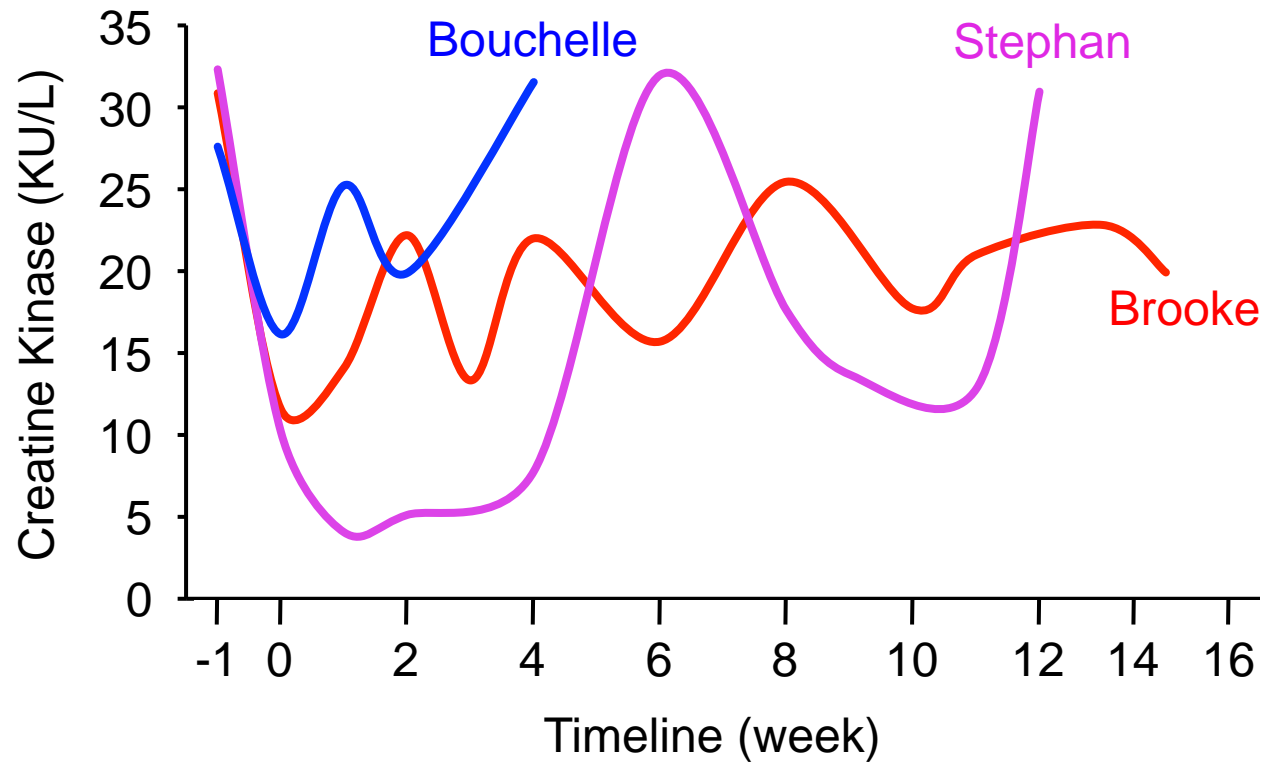




Supplementary Figure 3



Supplementary Figure 4



## Research Report

---

# Night Activity Reduction is a Signature Physiological Biomarker for Duchenne Muscular Dystrophy Dogs

Chady H. Hakim<sup>a</sup>, Austin A. Peters<sup>a</sup>, Feng Feng<sup>b</sup>, Gang Yao<sup>c</sup> and Dongsheng Duan<sup>a,\*</sup>

<sup>a</sup>*Department of Molecular Microbiology and Immunology, School of Medicine, University of Missouri, Columbia, MO, USA*

<sup>b</sup>*Department of Electrical and Computer Engineering, College of Engineering, University of Missouri, Columbia, MO, USA*

<sup>c</sup>*Department of Bioengineering, College of Engineering, University of Missouri, Columbia, MO, USA*

### Abstract.

**Background:** Duchenne muscular dystrophy (DMD) is an X-linked lethal muscle disease. Dystrophic dogs are excellent models to test novel therapies for DMD. However, the use of the dog model has been hindered by the lack of an effective method to evaluate whole-body mobility. We recently showed that night activity is a good indicator of dog mobility. However, our published method relies on frame-by-frame manual processing of a 12-hour video for each dog. This labor-intensive and time-consuming approach makes it unrealistic to use this assay as a routine outcome measurement.

**Objective:** To solve this problem, we developed an automatic video-capturing/imaging processing system. The new system reduces the data analysis time over 1,000 fold and also provides a more detailed activity profile of the dog.

**Methods:** Using the new system, we analyzed more than 120 twelve-hour recordings from 12 normal and 22 affected dogs.

**Results:** We observed similar activity profiles during repeated recording of the same dog. Throughout the night, normal dogs were in motion  $10.4 \pm 0.9\%$  of the time while affected dogs were in motion  $4.6 \pm 0.2\%$  of the time ( $p < 0.0001$ ). Further, normal dogs made significantly more movements ( $p < 0.0001$ ) while affected dogs rested significantly longer ( $p < 0.0001$ ) during the period of recording (from 6 pm to 6 am next day). Importantly, statistical significance persisted irrespective of the coat color, gender and mutation type.

**Conclusions:** Our results suggest that night activity reduction is a robust, quantitative physiological biomarker for dystrophic dogs. The new system may be applicable to study mobility in other species.

Keywords: Duchenne muscular dystrophy, DMD, dystrophin, dog, canine model, biomarker, night activity, mobility, muscle function

## INTRODUCTION

Duchenne muscular dystrophy (DMD) is a devastating muscle-wasting disease that affects boys and young men and leads to premature death [1]. DMD is caused by the loss of a subsarcolemmal cytoskeletal protein

called dystrophin. Dystrophin is an essential component of the dystrophin-associated glycoprotein (DGC) complex that preserves the integrity of the muscle cell membrane. In the absence of dystrophin, the cell membrane becomes fragile and cannot sustain shearing stress generated during muscle contraction. This results in membrane damage and myofiber degeneration. Eventually the dead muscle cells are replaced by connective tissue and affected individuals lose their mobility.

---

\*Correspondence to: Dongsheng Duan, Ph.D., Professor, Department of Molecular Microbiology and Immunology, One Hospital Dr., Columbia, 65212 MO, USA. Tel.: +1 573 884 9584; Fax: +1 573 882 4287; E-mail: duand@missouri.edu.

Current treatments for DMD are limited to corticosteroids and symptom management [2]. Tremendous progress has been made over the last decade in the development of novel pharmacologic and genetic therapies for DMD [3–5]. Most of these experimental treatments show promising efficacy in dystrophin-null mdx mice. However, mouse results often translate poorly to DMD patients due to the lack of the dystrophic phenotype in mdx mice, differences in immune responses between mice and humans, and/or the failure to scale-up from mice to large mammals [6]. Dystrophin-deficient dogs show characteristic symptoms of muscular dystrophy and dogs also have the scale-up advantage [7]. Results from studies performed in the canine DMD model may better inform the design of human trials.

Dystrophin deficiency has been described in more than 20 different dog breeds. Experimental DMD dog colonies have also been established in many places around the world [7]. However, there are limited tools to study muscle function in dogs. We recently developed an *in situ* protocol to evaluate contractility of a single dog muscle [8]. Kornegay and colleagues reported an assay for measuring hindlimb force in dogs [9]. Yet, there is no method to objectively study whole body mobility in dogs. To address this issue, we recently tested the hypothesis that spontaneous movement at night can serve as a physiological biomarker to objectively evaluate dog mobility. As a pilot study, we recorded night activity in a litter of three affected and four normal dogs [10]. We then converted the video to images (one frame every three seconds) and determined dog movement by manually quantifying differences between neighboring frames. This pilot study, though labor-intensive and time-consuming, has provided the critical preliminary data supporting our hypothesis that night activity is a useful endpoint for studying dog mobility.

Several questions were not answered in our pilot study. Specifically, it was not clear whether reproducible data could be obtained from the same dog on different days, whether dogs of different kindreds could yield consistent results, and whether reduced activity is a common finding in all dystrophic dogs irrespective of the gender and genotype type. The pilot study also had several inherent constraints such as the small sample size, cumbersome method and limited output parameters. To address all these issues, we developed a computer-based system that can automatically record and analyze spontaneous movements at night in canines. The new system allows quantification of dog mobility using a comprehensive set of metrics.

The results from the new system confirm and expand our initial observation [10]. Together these data suggest that night activity is a robust whole body mobility biomarker for dogs. The new system will greatly facilitate ongoing and future translational studies in the canine DMD model [11].

## MATERIALS AND METHODS

### *Animals*

Animal housing and experiments were approved by the Animal Care and Use Committee of the University of Missouri and were performed in accordance with guidelines of the National Institutes of Health and Department of Defense. All experimental dogs were on a mixed genetic background of golden retriever, Labrador retriever, beagle, and Welsh corgi. There are three different types of dystrophin gene mutations in affected dogs including type G (intron 6 point mutation identical to that of golden retriever muscular dystrophy dogs), type L (intron 19 insertion identical to that of Labrador retriever muscular dystrophy dogs) and type W (intron 13 insertion identical to that of Welsh corgi muscular dystrophy dogs) [12–15]. Experimental dogs were generated by in house artificial insemination. Specifically, fresh or frozen semen from an affected dog (genotype YG, YL, YW) were injected into the uterus of a carrier (genotype XG, XL, XW) twice at 48 h and 72 h post-ovulation. The dog coat color was determined according to Wikipedia ([https://en.wikipedia.org/wiki/Coat\\_%28dog%29](https://en.wikipedia.org/wiki/Coat_%28dog%29)).

The genotype was determined by polymerase chain reaction as we previously described [12, 13]. The diagnosis was further confirmed by the significantly elevated serum creatine kinase (CK) level in affected dogs. Night activity in 12 normal male (mean age,  $14.8 \pm 1.9$  months; range, 8.0 to 22.9 months), 11 affected male (mean age,  $18.2 \pm 1.3$  months; range, 9.7 to 23.3 months) and 11 affected female (mean age,  $12.6 \pm 1.8$  months; range, 6.8 to 19.9 months) dogs were recorded and analyzed. These dogs were from 27 different litters. All experimental dogs were housed in specific-pathogen free animal care facilities and kept under a 12-hour light/12-hour dark cycle.

### *Video recording equipment*

A low-light charge-coupled device (CCD) camera (PC164C, Supercircuits Inc., Austin, TX) was used for overnight video recording. The video camera was equipped with an infrared lens (Part #12VM412ASIR,

Tamron, Commack, NY) and a near infrared (NIR) light source (Part # IR045, Clover electronics USA, Cerritos, CA).

#### Video recording conditions

The dog was housed individually in a kennel (181 cm × 122 cm) with an elevated floor (Fig. 1A). The video camera was centered and secured to the ceiling on top of the kennel through a custom-made mounting bracket. Rubber dampers were added to the bracket to isolate any vibration from the ceiling to the camera. The camera and light source were positioned at 210 cm above the kennel floor to ensure a full view and even illumination of the cage floor (Fig. 1A). Spontaneous movement of the dog was recorded during the dark cycle from 6 pm to 6 am next day. During this period, there was no interference from environment cues or animal caregivers. Temperature and humidity were controlled and monitored during the recording period. The dog had free access to water but food was removed from the kennel.

#### Video recording

The CCD camera was controlled by the Overnight Dog Recording software, a program developed in Labview (National Instrument Inc., Austin, TX) (Fig. 1A). The program automatically started the recording system at 5:30 pm to warm up the hardware. Each session of recording was started at 6 pm and continued for 12 hrs. The frame rate was set to 3 frames per second. The recorded video was streamed to the hard drive of the control computer. The motion signal  $S(t)$  was defined as the signal difference between every two consecutive images. It was computed according to the following formula

$$S(t) = \frac{\sum_{i,j} |I(i, j, t + \Delta t) - I(i, j, t)|}{N_{i,j}} \quad (1)$$

where  $I(i, j, t)$  is the image pixel value at the pixel location  $(i, j)$  and acquired at the time point  $t$ .  $\Delta t$  is the time interval between two consecutive image frames.  $I(i, j, t + \Delta t)$  is the image pixel value at the pixel location  $(i, j)$  and acquired at the time point  $t + \Delta t$ .  $N_{i,j}$  is the total number of pixels in the image and it is equal to  $640 \times 480$  in our system. If the dog does not move, the two images should be the same and  $I(i, j, t)$  will be equal to  $I(i, j, t + \Delta t)$ . The motion signal  $S(t)$  will be zero. When the dog moves, the difference of the dog position results in a change of the image pixel value between  $I(i, j, t)$  and  $I(i, j, t + \Delta t)$ . The change of the

image pixel values produces a  $S(t)$  value to reflect the movement.

#### Processing of the recorded video

The recorded  $S(t)$  was analyzed by the *Overnight Dog-Video Analyzer*, a software program developed in Matlab (Mathworks Inc., Natick, MA) (Fig. 1A). Ideally, the baseline should be zero when the dog is not moving. However the recorded baseline always fluctuated and drifted with time due to various noises from the video recording system and environment (such as air ventilation, building vibration and thermal noise of the electronics). To correct the baseline drift, the signal baseline was extracted by removing all motion-induced signal peaks from the raw signal. The missing baseline segments corresponding to the removed motion signals were reconstructed using a piecewise cubic interpolation algorithm. The resulting baseline was further smoothed by applying a 7th order Savitzky-Golay filter followed by a median filter, both with a window size of 1.1 sec (33 data points). This reconstructed baseline was then subtracted from the raw signal to create a flat baseline. Finally, a motion threshold was applied to remove noisy spikes that were not considered as true motion signals (Fig. 1B). Signals that are above this threshold were considered as motion spikes.

#### Definition of the movement and rest

The processed motion signals showed three types of motion spike(s) including a single motion spike, a stretch of continuous non-interrupted spikes and a stretch of spikes with  $\leq 10$  sec interruptions between neighbouring spikes (Fig. 1C). The 10 sec value was chosen based on a pilot study. Each identifiable type of spike (or spikes) was defined as a single movement. The interval between two consecutive movements was defined as rest. By definition, a rest is always longer than 10 sec.

#### Motion quantification metrics

A series of metrics were used to comprehensively evaluate dog night activity. These included the percentage of time in motion (%; the percentage of the time the dog was in motion during the entire 12-hour recording period), amplitude of the movement (arbitrary unit; relative signal strength of a motion spike), number of movement per hour (Nm/hr), average duration of a single movement (sec) and average duration of a single rest (sec). Based on the duration, a movement was

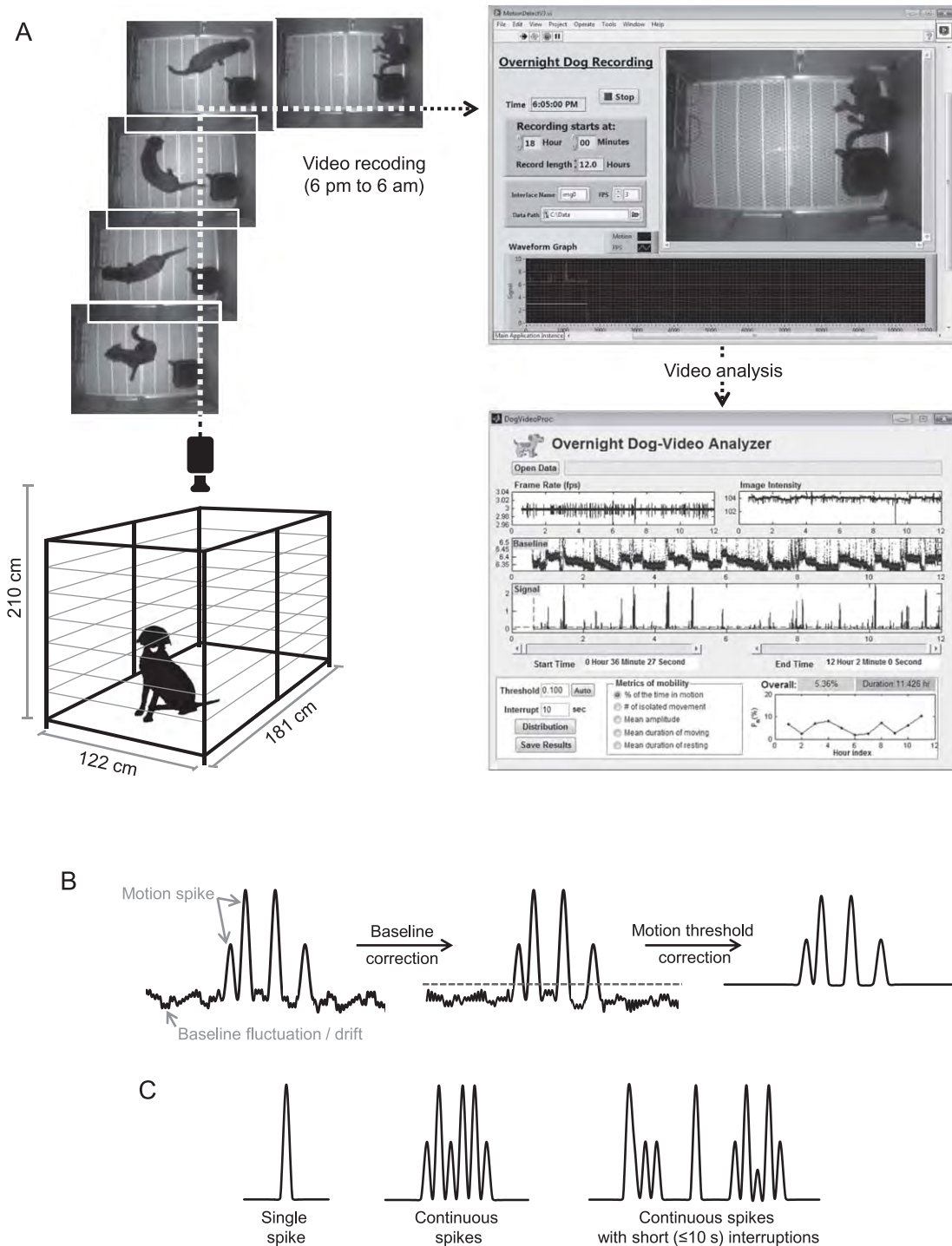


Fig. 1. Dog night activity evaluation system. A, Overview of the system. The experimental dog was housed in the recording kennel. The CCD camera was installed to the ceiling allowing full visualization of the entire floor. Dog activity was recorded from 6 pm to 6 am next day by the “overnight dog recording” system. The signals were sent to the “overnight dog-video analyzer” for activity evaluation. B, Video processing outline. First, the baseline drift of the raw motion signals was corrected. Then noisy spikes were eliminated by the motion threshold (gray dotted line). C, A cartoon illustration of three types of motion spike(s): a single isolated spike, a stretch of continuous spikes and a stretch of spikes with short ( $\leq 10$  s) interruptions.

further divided into short-duration movement ( $\leq 10$ s) and long-duration movement ( $> 10$ s). To gain more detailed understanding on the movement, we further quantify the frequency of short and long-duration movements per hour and expressed these parameters as “number of short movement/hour” and “number of long movement/hour”, respectively.

### Statistical analysis

Data are presented as mean  $\pm$  standard error of mean. Statistical difference was assessed with the Student's *t*-test followed by Bonferroni correction to correct familywise error caused by multiple two-group comparisons. The *p* value is presented in the figure legend.

## RESULTS

### Night activity analyzer is a robust system to evaluate dog mobility

To objectively evaluate dog mobility, we intentionally performed recording at night when there was neither human nor environment interference. To eliminate potential influences from changes in temperature and humidity, we also maintained a constant temperature ( $23.8 \pm 0.2^\circ\text{C}$ ) and humidity ( $40.2 \pm 1.5\%$ ) in the kennel.

To determine whether our newly developed software can consistently record and analyze dog activity, we performed repeated recording. Specifically, the same dog was recorded multiple times during an 11-day

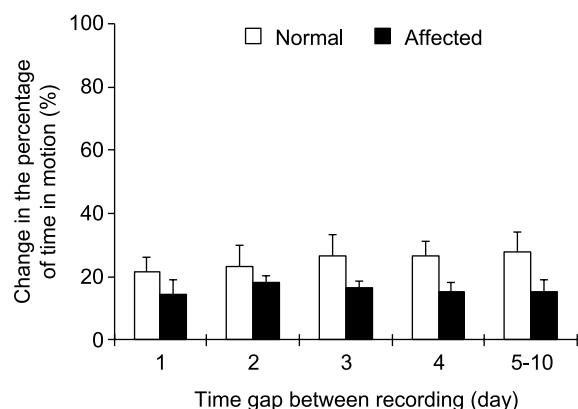


Fig. 2. Repeated recording yielded consistent results from the same dog. The dog was recorded at different nights (either continuously every night or at alternating nights). The results of subsequent recordings were compared to that of the first night. The graph shows repeated recording results from 11 normal dogs and 10 affected dogs.

period (2 to 10 times, either daily or in different days). The percentage of time in motion was quantified for each recording and compared with the first night recording. Consistent activity was observed for both normal and affected dogs during repeated recording (Fig. 2). For normal dogs, the difference (compared with the result of the first night recording) was  $\leq 28\%$  when the same dog was recorded at different nights. For affected dogs, the difference (compared with the result of the first night recording) was  $\leq 18\%$  when the same dog was recorded at different nights.

### Dystrophin deficiency significantly reduced night activity in affected dogs

To determine whether night activity can serve as a robust physiological biomarker for DMD dogs, we initiated a comprehensive study with a large cohort of crossbred dogs. These included 12 male normal dogs (age  $14.7 \pm 1.9$  months) and 22 mixed-gender affected dogs (age  $15.4 \pm 1.24$  months). They came from 27 different litters. Figure 3A showed representative processed 12-hr recordings from a normal and an affected dog. Throughout the night, normal dogs were in motion  $10.4 \pm 0.9\%$  of the time while affected dogs were in motion only  $4.6 \pm 0.2\%$  of the time ( $p < 0.00001$ ) (Fig. 3B). In other words, normal dogs moved approximately 75 min and affected dogs moved approximately 33 min during 12-hr recording. On average, normal dogs moved  $28.3 \pm 1.3$  times per hour while affected dogs only moved  $14.1 \pm 0.4$  times per hour ( $p < 0.00001$ ) (Fig. 3C). Additional analysis showed that normal dogs not only made significantly more short movements but also made significantly more long movements ( $p < 0.00001$ ) (Fig. 3D and E). Interestingly, the average amplitude of movement was similar between normal ( $0.60 \pm 0.08$ ) and affected ( $0.56 \pm 0.04$ ) dogs ( $p = 0.68$ ) (Fig. 3F). Further, there was no significant difference in the average duration of movement between normal and affected dogs (Fig. 3G). In contrast to the duration of movement, the average duration of rest in affected dogs ( $243.1 \pm 0.6$  sec) was significantly longer than that of normal dogs ( $111.5 \pm 4.5$  sec) ( $p < 0.00001$ ) (Fig. 3H).

As a consequence of crossbreeding, our study dogs displayed different coat colors which produced different pixel intensities in the video. To determine whether the coat color influenced the outcome, we grouped normal and affected dogs based on their color. Affected dogs consistently showed reduced activity irrespective of the coat color (Supplementary Figure 1).

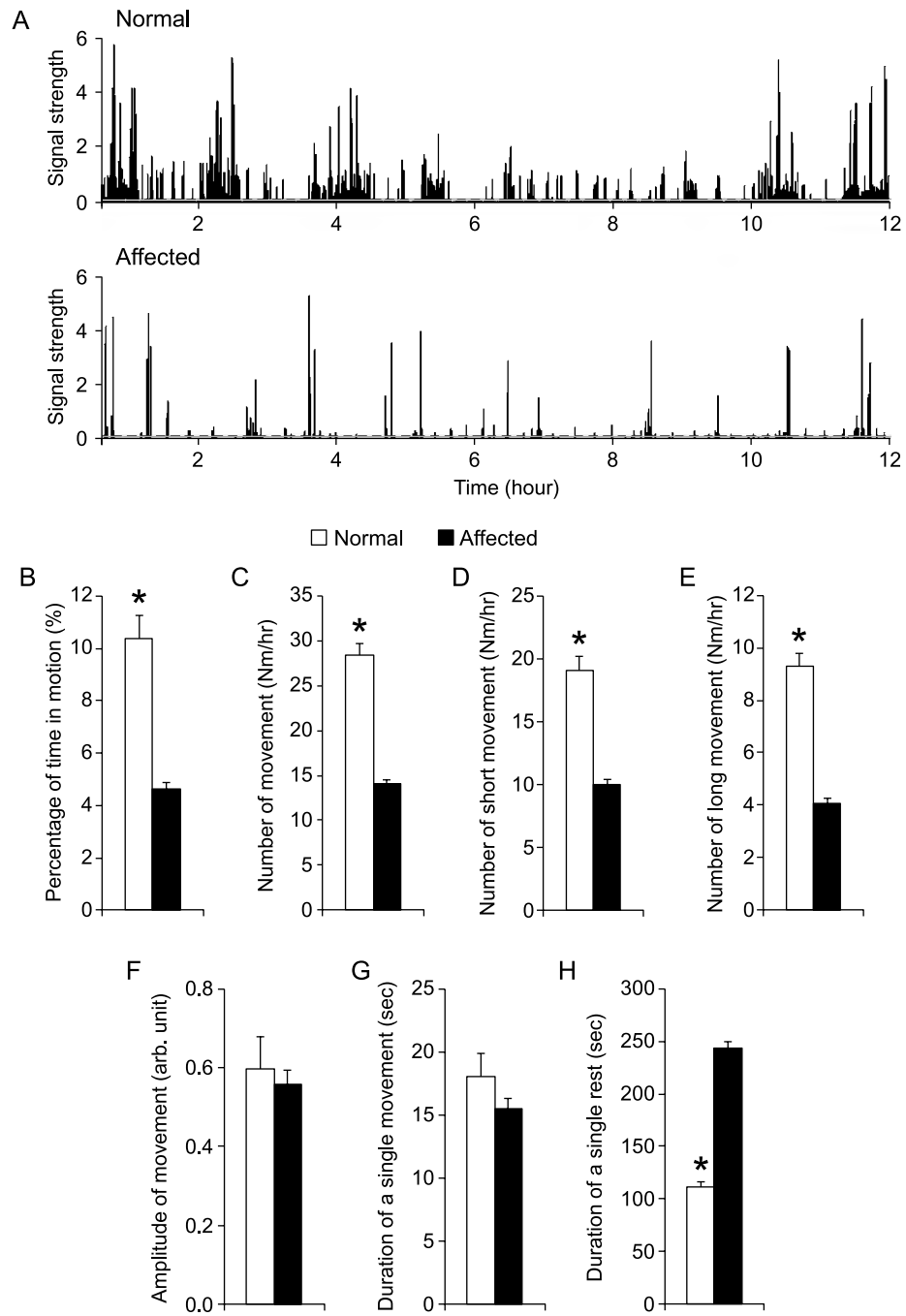


Fig. 3. Night activity was significantly reduced in affected dogs. A, Representative processed motion signals from a normal (top panel) and an affected dog (bottom panel). The normal dog showed more activity than the affected dog. Dotted line, motion threshold. B to H, A quantitative comparison of indicated night activity property between normal ( $n = 12$ ) and affected ( $n = 22$ ) dogs. Asterisk,  $p < 0.0001$ .

#### *Gender had minimal impact on night activity*

The normal group consisted of male dogs only while the affected group included both male and female dogs. To determine whether gender had confounded our ini-

tial analysis (Fig. 3), we removed female dogs from the affected group and re-analyzed the data (Fig. 4). Impressively, normal male and affected male comparison resulted in a pattern nearly identical to that of the initial analysis (Figs. 3 and 4).

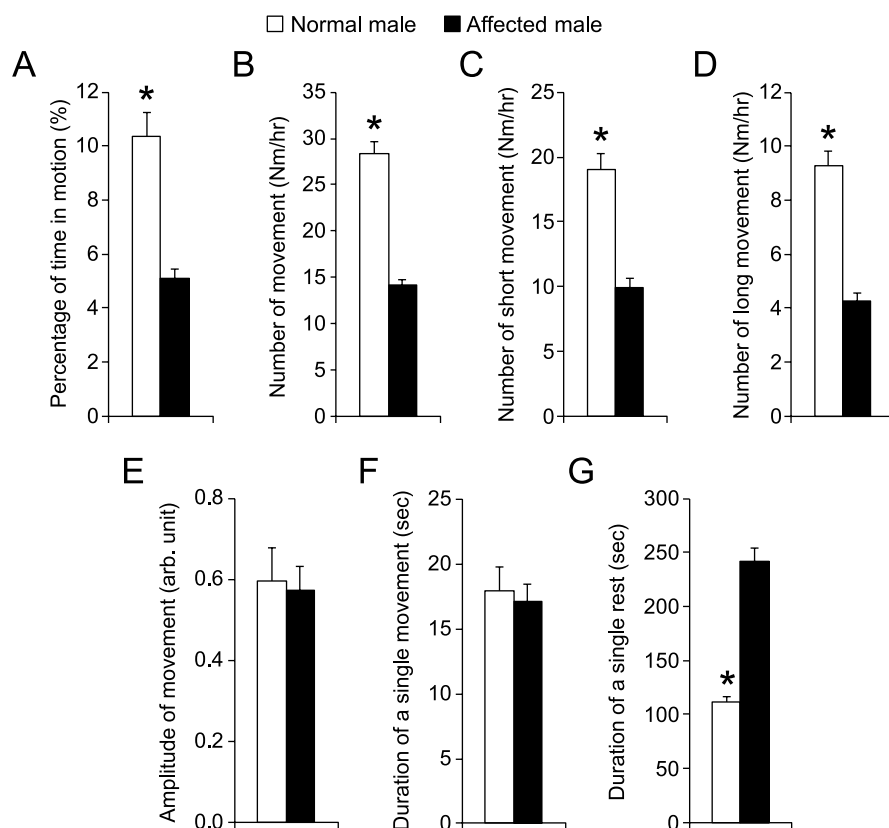


Fig. 4. Comparison of night activity between normal and affected male dogs.  $n=12$  for normal male,  $n=11$  for affected male. Asterisk,  $p<0.0001$ .

To further characterize the potential influence of the gender, we compared results of male affected and female affected dogs (Fig. 5). Affected male dogs showed slightly more movement than affected female dogs (the percentage of time in motion was  $5.1 \pm 0.4\%$  and  $4.1 \pm 0.3\%$  for affected male and female, respectively;  $p=0.03$ ) (Fig. 5A). This appeared to have resulted from a slightly longer movement time in males (the average duration of a single movement was  $17.1 \pm 1.4$  sec and  $13.8 \pm 0.8$  sec for affected male and affected female, respectively;  $p=0.05$ ). No difference was noticed in other parameters between affected male dogs and affected female dogs.

#### *Affected dogs showed reduced night activity irrespective of the mutation type*

There are three different types of dystrophin gene mutations in our affected dogs including type G, L and W [13–15]. In our study, all affected males carried type G mutation in their X-chromosome. However, all affected females carried two different types of

dystrophin gene mutations, one on each chromosome. Comparison between male and female affected dogs (Fig. 4) suggests that the type of gene mutation had minimal impact on night activity. To confirm this observation, we performed detailed analysis in female affected dogs. Among 11 affected females, six had the genotype of LW and four had GW. No difference was seen in any metrics between LW and GW affected dogs (Fig. 6).

## DISCUSSION

In this study, we developed a robust automatic video capturing/processing system to quantify dog mobility at night. A large cohort of crossbred normal and DMD dogs were evaluated using this system. We found that normal dogs had significantly more movements and shorter rests. In contrast, affected dogs displayed a significantly reduced night activity irrespective of the coat color, gender and type of mutations in the dystrophin gene.

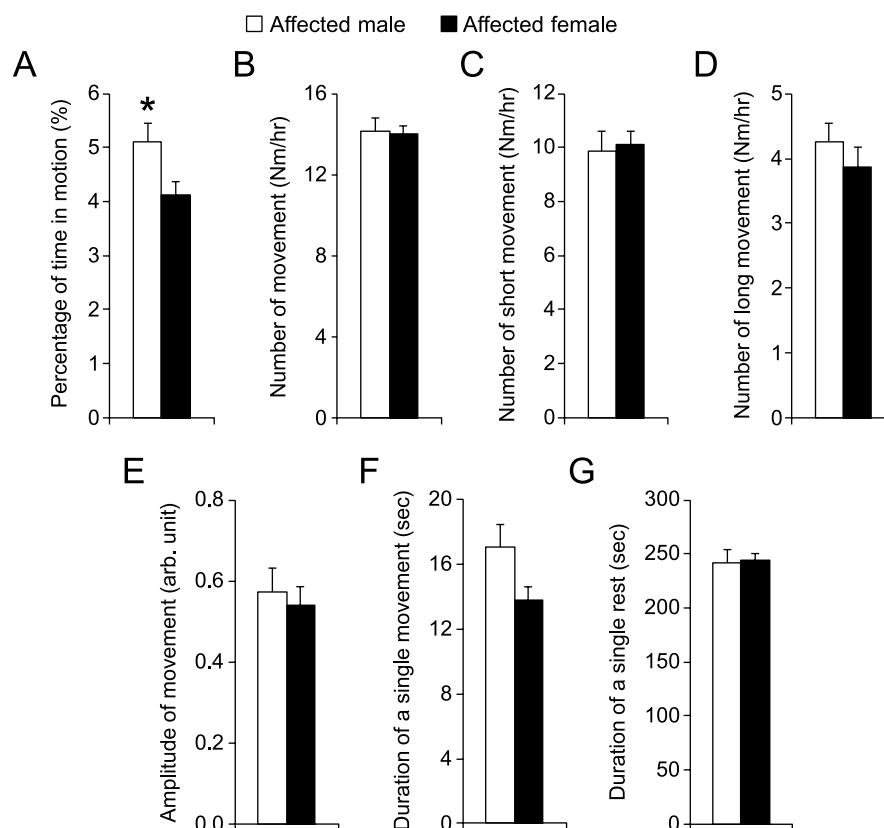


Fig. 5. Comparison of night activity between male and female affected male dogs.  $n = 11$  for affected male,  $n = 11$  for affected female. Asterisk,  $p < 0.0001$ .

Dystrophin-deficient dogs have been considered an excellent large animal model for DMD because of their striking clinical and pathological similarity to human patients. However, the research use of affected dogs has been limited by the lack of physiological assays that can reliably quantify muscle function. To address this issue, investigators have begun to adopt *in situ* protocols that are commonly used in rodent studies [8, 9, 16, 17]. While these methods allow detailed characterization of the contractile profile of a single muscle or a group of muscles, there are important limitations. First, these assays require the subject be anesthetized. Unfortunately, DMD patients and affected dogs are especially vulnerable to anesthesia-associated risks such as sudden cardiac arrest and rhabdomyolysis [18–21]. Second, these assays are often limited to limb muscle and cannot provide information on whole body mobility. Third, some of these assays (such as single muscle *in situ* force measurement) are terminal assays and can only be performed once in a subject before euthanization [8]. Non-invasive goniometry and accelerometry were developed recently to evaluate the

range of motion of a joint and the gait pattern [10, 22–25]. These non-invasive assays had minimum risks and they can also be performed repeatedly in the same dog to monitor disease progression or responses to experimental therapy. However, the results obtained from kinematic studies could be influenced by training, environment, experiment conditions (such as the use of treats) and people involved in the study (caregivers and investigators). These interferences may introduce subjective bias. A truly objective assay would require evaluating dog mobility in its natural status (without the need of dog training and without interference from the environment and people). We reasoned that monitoring dog activity at night might accomplish this goal. We hypothesized that muscle degeneration and inflammation should compromise night movement in affected dogs. To test this hypothesis, we conducted a pilot study and quantified night video recordings frame-by-frame manually [10]. To minimize the labor and the potential influence of the genetic background and age, we only evaluated three affected and four normal dogs from the same litter. Despite the small sample size, we

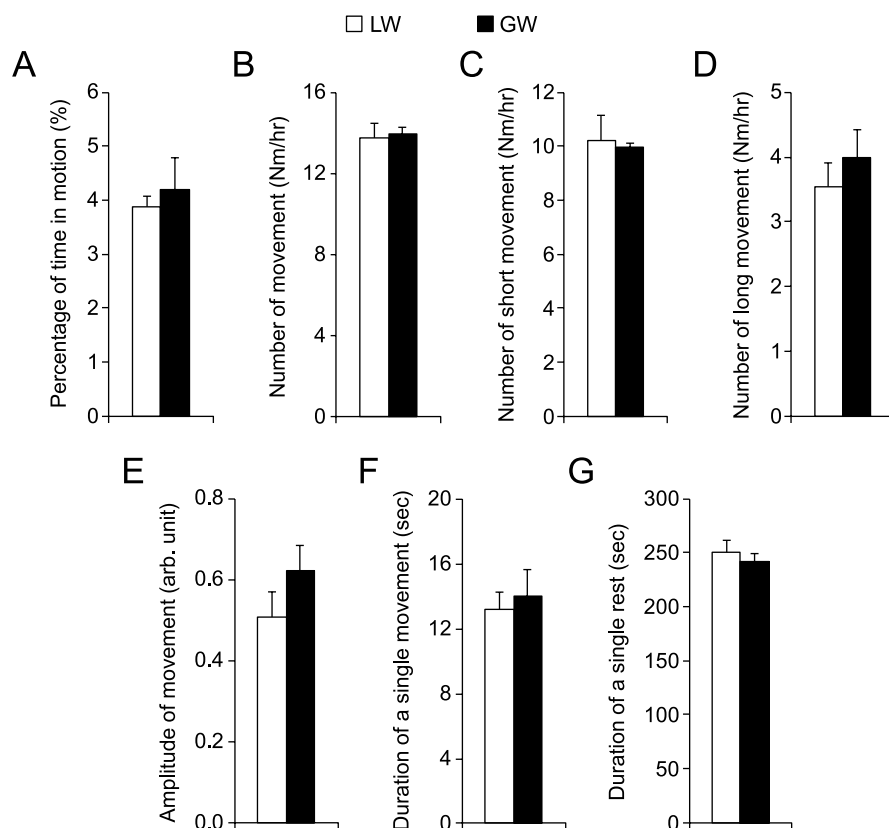


Fig. 6. Comparison of night activity in female affected dogs that had different mutations in the dystrophin gene. LW, affected female dogs with one X-chromosome carrying intron 19 insertion and another X-chromosome carrying intron 13 insertion. GW, affected female dogs with one X-chromosome carrying intron 6 point mutation and another X-chromosome carrying intron 13 insertion. Asterisk,  $p < 0.0001$ .

found that the relative movement of affected dogs was significantly reduced [10].

To confirm this preliminary finding, we decided to expand the study to a large cohort of adult dogs from different litters. In preparation for this large sample-size study and also to facilitate easy application of the protocol by other investigators in the future, we streamlined the video recording and analysis procedures. Instead of manual recording and analysis, we developed the *Overnight Dog Recording* software and the *Overnight Dog-Video Analyzer* to control the entire process of video recording and to perform subsequent video quantification (Fig. 1). These software programs greatly reduce the labor. Further, they yield a set of metrics for comprehensive analysis. We can now not only quantify overall movement (percent of time in motion and number of movements) during the entire 12-hour recording period but also perform a detailed analysis of each individual movement (such as the type, amplitude and duration of the movement). A robust reliable protocol should yield consistent results on repeated

measurements. We tested the same dog at different days (Fig. 2). Despite some changes (especially for the normal dog), overall there were minimal day-to-day variations suggesting our new system is highly reliable.

The ultimate goal of our study is to determine whether the muscle health of the dog correlates with night activity. We studied 34 dogs from 27 litters of different kindreds. As expected for diurnal animals, dogs were in sleep (without movement) most part of the night (Fig. 3A and B). Consistent with the data of the pilot study [10], night mobility of affected dogs was significantly reduced (Fig. 3). This is reflected in the total amount of time in motion, number of movements and duration of the rest. Overall, the percent of time in motion and number of movements was reduced by 50% while the duration of the rest was doubled in affected dogs. Surprisingly, the amplitude and the duration of the movements were not altered in affected dogs. The exact reasons for these observations are not clear but they may relate to neuronal control of sleep (hence cannot be influenced by muscle health). Alternatively,

they may reflect inherent limitations of the software. For example, the current version of the software cannot discriminate a small-scale fast movement (such as the rapid wriggling of the dog tail) and a large-scale slow movement (such as when a dog moves its entire body slowly over a short distance).

DMD is a worldwide disease. It affects all human races. While the vast majority of DMD patients are male, female could also be affected if the dystrophin gene in both X-chromosomes is mutated or when random X-chromosome inactivation is skewed in a carrier [26–28]. Further, more than 7,000 different mutations have been reported in the dystrophin gene [29]. A robust assay for DMD should differentiate normal versus affected irrespective of their skin color, gender and the type of mutation the patient has. To this end, we analyzed on the impact of the coat color, sex and gene mutation (Figs. 4 to 6, Supplementary Figure 1). None of these factors significantly changed the outcome.

There are also several limitations. First, the loss of dystrophin also affects cognitive functions. It is possible that the observed differences may reflect a combined effect of dystrophin deficiency in muscle as well as in the central nerve system. Second, the muscle groups involved in different types of movement (such as short movement versus long movement, single spike versus continuous spikes) remain to be defined. Third, the results are obtained from a single colony. Additional studies are needed to see if similar findings exist in other dystrophic dog colonies. Fourth, we observed statistically significant differences between normal and affected dogs. However, our study did not establish the overnight activity as a valid surrogate end point. Future studies are needed to determine if a therapy that increases muscle force also results in improvement in overnight activity.

In summary, our results suggest that night activity reduction is a signature functional biomarker for DMD dogs. The newly developed video system is an easy-to-use, cost-effective and highly reliable platform to objectively study dog (and potentially other species) mobility. The night activity monitoring should be included in future studies to help assess disease progression and therapeutic intervention in the canine DMD model.

#### COMPETING FINANCIAL INTERESTS

D.D. is a member of the scientific advisory board for Solid GT, LLC, a venture company founded to advance gene therapy for DMD.

#### ACKNOWLEDGMENTS

This work was supported by grants (to D.D.) from National Institutes of Health NS-90634, Department of Defense MD130014, Jesse's Journey-The Foundation for Cell and Gene Therapy, and Hope for Javier. Authors thank Duan lab members for the help of caring for affected dogs.

#### SUPPLEMENTARY MATERIAL

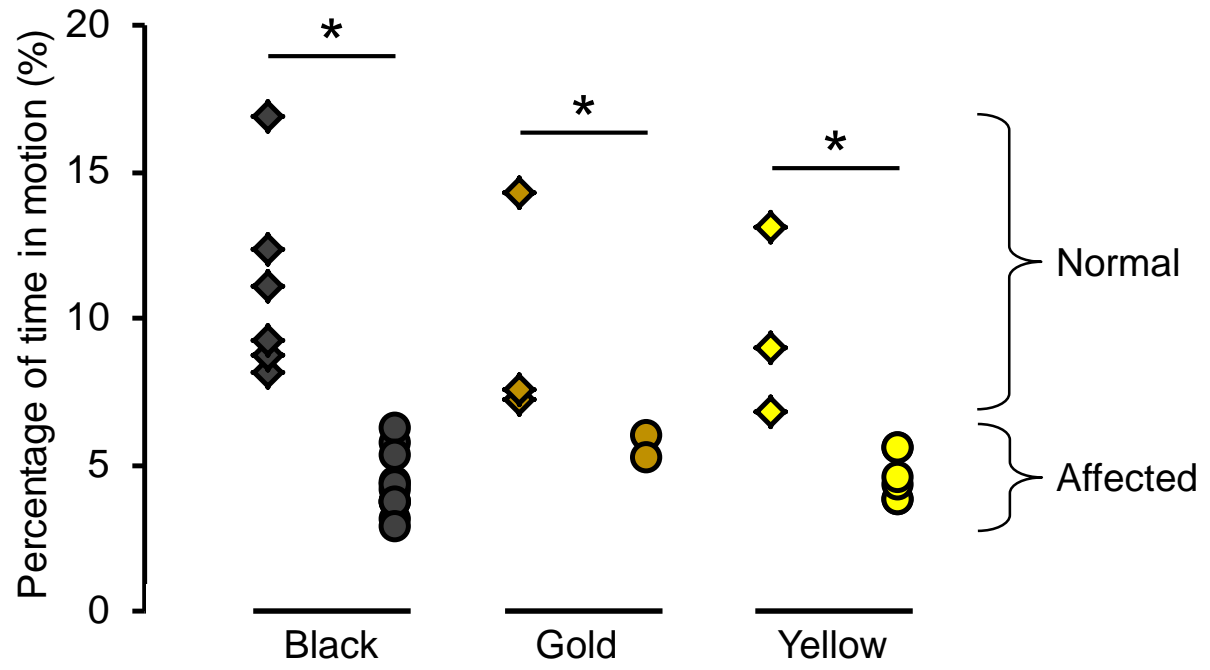
The supplementary table and figure are available in the electronic version of this article: <http://dx.doi.org/10.3233/JND-150114>.

#### REFERENCES

- [1] O'Brien KF, Kunkel LM. Dystrophin and muscular dystrophy: Past, present, and future. *Mol Genet Metab*. 2001;74(1-2):75-88.
- [2] Bushby K, Finkel R, Birnkrant DJ, Case LE, Clemens PR, Cripe L, et al. Diagnosis and management of Duchenne muscular dystrophy, part 1: Diagnosis, and pharmacological and psychosocial management. *Lancet Neurol*. 2010;9(1):77-93.
- [3] Rodino-Klapac LR, Mendell JR, Sahenk Z. Update on the treatment of Duchenne muscular dystrophy. *Curr Neurol Neurosci Rep*. 2013;13(3):332.
- [4] Leung DG, Wagner KR. Therapeutic advances in muscular dystrophy. *Ann Neurol*. 2013;74(3):404-11.
- [5] Verhaart IE, Aartsma-Rus A. Gene therapy for Duchenne muscular Dystrophy. *Curr Opin Neurol*. 2012;25(5):588-96.
- [6] Duan D. Duchenne muscular dystrophy gene therapy: Lost in translation? *Res and Rep in Biol*. 2011;2:31-42.
- [7] McGreevy JW, Hakim CH, McIntosh MA, Duan D. Animal models of Duchenne muscular dystrophy: From basic mechanisms to gene therapy. *Dis Model Mech*. 2015;8(3):195-213.
- [8] Yang HT, Shin JH, Hakim CH, Pan X, Terjung RL, Duan D. Dystrophin deficiency compromises force production of the extensor carpi ulnaris muscle in the canine model of Duchenne muscular dystrophy. *PLoS One*. 2012;7(9):e44438.
- [9] Childers MK, Grange RW, Kornegay JN. *In vivo* Canine muscle function assay. *J Vis Exp*. 2011(50):pii 2623.
- [10] Shin JH, Greer B, Hakim CH, Zhou Z, Chung YC, Duan Y, et al. Quantitative phenotyping of Duchenne muscular dystrophy dogs by comprehensive gait analysis and overnight activity monitoring. *PLoS One*. 2013;8(3):e59875.
- [11] Duan D. Duchenne muscular dystrophy gene therapy in the canine model. *Hum Gene Ther Clin Dev*. 2015;26(1):57-69.
- [12] Fine DM, Shin JH, Yue Y, Volkmann D, Leach SB, Smith BF, et al. Age-matched comparison reveals early electrocardiography and echocardiography changes in dystrophin-deficient dogs. *Neuromuscul Disord*. 2011;21(7):453-61.
- [13] Smith BF, Yue Y, Woods PR, Kornegay JN, Shin JH, Williams RR, et al. An intronic LINE-1 element insertion in the dystrophin gene aborts dystrophin expression and results in Duchenne-like muscular dystrophy in the corgi breed. *Lab Invest*. 2011;91(2):216-31.
- [14] Sharp NJ, Kornegay JN, Van Camp SD, Herbstreith MH, Secore SL, Kettle S, et al. An error in dystrophin mRNA processing in golden retriever muscular dystrophy,

- an animal homologue of Duchenne muscular dystrophy. *Genomics*. 1992;13(1):115-21.
- [15] Smith BF, Wrighten R. Animal models for inherited muscle diseases. In: Duan D, editor. *Muscle gene therapy*. New York: Springer Science + Business Media, LLC; 2010, pp. 1-21.
- [16] Hakim CH, Wasala NB, Duan D. Evaluation of muscle function of the extensor digitorum longus muscle *ex vivo* and tibialis anterior muscle *in situ* in mice. *J Vis Exp*. 2013;(72):e50183.
- [17] Hakim CH, Li D, Duan D. Monitoring murine skeletal muscle function for muscle gene therapy. *Methods Mol Biol*. 2011;709:75-89.
- [18] Segura LG, Lorenz JD, Weingarten TN, Scavonetto F, Bojanic K, Selcen D, et al. Anesthesia and Duchenne or Becker muscular dystrophy: Review of 117 anesthetic exposures. *Paediatric Anaesth*. 2013;23(9):855-64.
- [19] Hayes J, Veyckemans F, Bissonnette B. Duchenne muscular dystrophy: An old anesthesia problem revisited. *Paediatr Anaesth*. 2008;18(2):100-6.
- [20] Girshin M, Mukherjee J, Clowney R, Singer LP, Wasnick J. The postoperative cardiovascular arrest of a 5-year-old male: An initial presentation of Duchenne's muscular dystrophy. *Paediatr Anaesth*. 2006;16(2):170-3.
- [21] Nathan A, Ganesh A, Godinez RI, Nicolson SC, Greeley WJ. Hyperkalemic cardiac arrest after cardiopulmonary bypass in a child with unsuspected Duchenne muscular dystrophy. *Anesth Analg*. 2005;100(3):672-4.
- [22] Barthelemy I, Barrey E, Thibaud JL, Uriarte A, Voit T, Blot S, et al. Gait analysis using accelerometry in dystrophin-deficient dogs. *Neuromuscul Disord*. 2009;19(11):788-96.
- [23] Marsh AP, Eggebeen JD, Kornegay JN, Markert CD, Childers MK. Kinematics of gait in golden retriever muscular dystrophy. *Neuromuscul Disord*. 2010;20(1):16-20.
- [24] Gaiad TP, Silva MB, Silva GC, Caromano FA, Miglino MA, Ambrosio CE. Physical therapy assessment tools to evaluate disease progression and phenotype variability in golden retriever muscular dystrophy. *Res Vet Sci*. 2011;91(2):188-93.
- [25] Gaiad TP, Araujo KP, Serrao JC, Miglino MA, Ambrosio CE. Motor physical therapy affects muscle collagen type I and decreases gait speed in dystrophin-deficient dogs. *PLoS One*. 2014;9(4):e93500.
- [26] Leyser M, Marques FJ, Elias MA, Diniz Gonsalves MC, da Silva OS, Jr., Carvalho RS, et al. Classic manifestations of Duchenne dystrophy in a young female patient: A case report. *Eur J Paediatr Neurol*. 2013;17(2):212-8.
- [27] Seemann N, Selby K, McAdam L, Biggar D, Kolski H, Goobie S, et al. Symptomatic dystrophinopathies in female children. *Neuromuscul Disord*. 2011;21(3):172-7.
- [28] Schanzer A, Rau I, Kress W, Kohler A, Neubauer B, Hahn A. Duchenne muscular dystrophy in a 4-year-old girl due to heterozygous frame shift deletion of the dystrophin gene and skewed X-inactivation. *Klin Padiatr*. 2012;224(4):256-8.
- [29] Bladen CL, Salgado D, Monges S, Foncuberta ME, Kekou K, Kosma K, et al. The TREAT-NMD DMD global database: Analysis of more than 7000 Duchenne muscular dystrophy mutations. *Hum Mutat*. 2015;36(4):395-402.

Supplementary Figure 1



## Perspective on Adeno-Associated Virus Capsid Modification for Duchenne Muscular Dystrophy Gene Therapy

Michael E. Nance and Dongsheng Duan\*

Department of Molecular Microbiology and Immunology, School of Medicine, University of Missouri, Columbia, Missouri.

Duchenne muscular dystrophy (DMD) is a X-linked, progressive childhood myopathy caused by mutations in the *dystrophin* gene, one of the largest genes in the genome. It is characterized by skeletal and cardiac muscle degeneration and dysfunction leading to cardiac and/or respiratory failure. Adeno-associated virus (AAV) is a highly promising gene therapy vector. AAV gene therapy has resulted in unprecedented clinical success for treating several inherited diseases. However, AAV gene therapy for DMD remains a significant challenge. Hurdles for AAV-mediated DMD gene therapy include the difficulty to package the full-length dystrophin coding sequence in an AAV vector, the necessity for whole-body gene delivery, the immune response to dystrophin and AAV capsid, and the species-specific barriers to translate from animal models to human patients. Capsid engineering aims at improving viral vector properties by rational design and/or forced evolution. In this review, we discuss how to use the state-of-the-art AAV capsid engineering technologies to overcome hurdles in AAV-based DMD gene therapy.

### INTRODUCTION

DUCHENNE MUSCULAR DYSTROPHY (DMD) is the most common childhood muscle disease. It is characterized by progressive muscle weakness, loss of ambulation, and premature death caused by respiratory muscle and/or heart failure. DMD results from the loss of dystrophin, an essential cytoskeletal protein that protects muscle from contraction-induced injury (Fig. 1A). Soon after the discovery of the *dystrophin* gene,<sup>1,2</sup> it was postulated that expression of a functional *dystrophin* gene in muscle may provide a cure for this relentless disease.<sup>3</sup> Over the years, a number of nonviral and viral vectors have been explored to deliver the *dystrophin* gene. Currently, adeno-associated virus (AAV) stands out as the leading candidate vector.<sup>4,5</sup>

AAV is a dependent parvovirus with an ~5 kb single-stranded linear DNA genome.<sup>6</sup> Wild-type AAV has two major open reading frames (ORFs) flanked by two inverted terminal repeats (ITRs). The 5' and 3' ORFs encode replication and capsid proteins, respectively.<sup>7</sup> The ITR contains 145 nucleotides and serves as the AAV genome replication

origin and packaging signal (Fig. 1B). In recombinant AAV, viral ORFs are replaced by the exogenous gene expression cassette, while the replication and capsid proteins are provided *in trans* (Figs. 1C and D). AAV has many appealing features as a gene therapy vector. For example, it has broad tissue tropism and high transduction efficiency. AAV can result in long-term persistent episomal expression.<sup>8,9</sup> In addition, wild-type AAV is not associated with any known human diseases, and recombinant AAV vectors have shown an excellent safety profile in many clinical trials.

Despite many appealing features, recombinant AAV vectors face several challenges for DMD gene therapy. First, AAV has a fairly limited packaging capacity. Two-thirds of the dystrophin coding sequence has to be removed in order to fit into an AAV particle. Second, the dystrophic muscle is an extremely hostile microenvironment for gene transfer (Fig. 1A). Myofiber degeneration and necrosis may result in the loss of the vector genome.<sup>10,11</sup> Inflammation in the muscle further intensifies the immune response. Third, muscle consists of ~40–50% the body mass and is spread

\*Correspondence: Dr. Dongsheng Duan, Department of Molecular Microbiology and Immunology, University of Missouri School of Medicine, One Hospital Dr. M610G, MSB, Columbia, MO 65212. E-mail: duand@missouri.edu

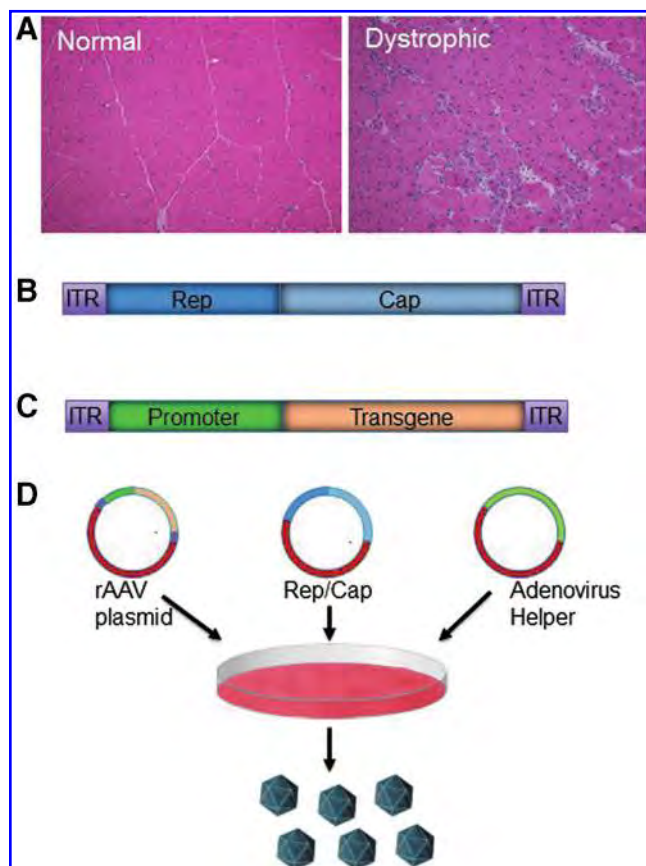


**Figure 1.** Adeno-associated viral vector (AAV) for Duchenne muscular dystrophy (DMD) gene therapy. The ultimate goal of AAV-mediated DMD gene therapy is to deliver a therapeutic gene using the gutless recombinant AAV (rAAV) to achieve bodywide, robust, and persistent gene transfer in highly inflammatory and degenerative dystrophic muscle and heart to improve muscle and heart function, life quality, and lifespan. **(A)** Representative histology images from normal (left panel) and dystrophic (right panel) muscle. Normal muscle has well-organized, uniform myofibers with peripherally placed nuclei. Dystrophic muscle shows myofiber disorganization, centrally localized nuclei, and abundant infiltration of inflammatory cells. **(B)** Schematic outline of the wild-type AAV genome. The wild-type AAV has an ~4.6–4.8 kb genome. It contains a *Rep* gene for viral replication and a *Cap* gene to generate viral capsid. Two inverted terminal repeats (ITRs) are positioned at the ends of the viral genome. ITR serves as the replication origin and packaging signal. **(C)** Schematic outline of the rAAV genome. The AAV vector is essentially gutted. A therapeutic expression cassette replaces the wild-type *Rep* and *Cap* genes. The only viral component in the rAAV genome is ITR. **(D)** The most commonly used AAV vector production method is triple-plasmid transfection in 293 cells. A *cis* rAAV plasmid carries the rAAV genome. A *trans* Rep/Cap plasmid expresses the replication and capsid proteins. Because the reproductive life cycle of AAV requires the help of adenovirus, an adenovirus helper plasmid is included in the transfection cocktail. AAV vector is purified using isopycnic ultracentrifugation and/or chromatography. Color images available online at [www.liebertpub.com/hum](http://www.liebertpub.com/hum)

throughout the body. An effective gene therapy will require efficient systemic delivery to a variety of muscle groups, including the heart and diaphragm. Bodywide gene transfer brings in the issue of vector genome sequestration in nonmuscle tissues and off-target transduction. Fourth, 30–80% of the human population has preexisting serum antibodies to various AAV serotypes. There is also a high-level cross-reactivity among different AAV serotypes.<sup>12</sup> Capsids with distinctive serological properties will be needed to bypass these obstacles. Last but not least is the species-specific barrier. This not only refers to the scale-up of AAV production and delivery to large species (dogs, pigs, nonhuman primates, and humans), but also includes species-unique AAV transduction biology and possibly the differences in dystrophin structure and function among different species.

The biological properties (such as tropism and immunity) of the viral vectors are mainly determined by the viral capsid. The AAV capsid is composed of three overlapping capsid proteins called viral protein 1 (VP1), VP2, and VP3. The mature virion contains ~5 copies of VP1, ~5 copies of VP2, and ~50 copies of VP3 in a 1:1:10 ratio. Together, 60 copies of capsid proteins form a  $T=1$  icosahedral particle with 5-fold, 3-fold, and 2-fold axes of sym-

metry.<sup>13</sup> There are nine highly conserved regions (defined as regions A–I) in each AAV capsid protein. Region A is an  $\alpha$ -helix ( $\alpha$ A). Regions B–I are  $\beta$ -sheets. These  $\beta$ -sheets are arranged as a jelly-roll  $\beta$ -barrel. Between the  $\beta$ -sheets are intervening loops. These loops form much of the outer surface of an assembled AAV particle. Importantly, they are composed of variable amino acid sequences and hence are amenable to genetic manipulation.<sup>14</sup>

Capsid engineering refers to intentional modification of hypervariable loops (and possibly other regions) of the capsid to achieve a desired biological property. Currently, there are two major approaches: rational design and directed evolution. In rational design, existing knowledge of the capsid structure/function is used to guide genetic engineering to achieve predetermined outcomes. In directed evolution, investigators apply selective pressure(s) to a random capsid library to drive the evolution of the most adapted capsid. The beauty of directed evolution is that it does not require prior knowledge on the structure or function of the capsid. Directed evolution also has the advantage of integrating multiple selective pressures simultaneously to achieve desired features. Most importantly, directed evolution may result in unique capsid variants that are impossible to program using the rational design approach.

In this review, we summarize the state-of-the-art capsid engineering technologies and discuss the potential to apply these technologies to overcome major barriers in AAV-mediated DMD gene therapy. It should be noted that strategies based on

AAV genome engineering (such as the dual AAV vector) and expression cassette optimization (such as the use of a tissue-specific promoter, transgene codon optimization, and microRNA targeting sequence) have also been used to improve AAV vectors for DMD gene therapy. Since these mechanisms are not based on capsid modification, we opt to not include them in this review.

## AAV CAPSID ENGINEERING BY RATIONAL DESIGN

Rational design depends on accruing insight into structure–function relationships between the primary amino acid sequence, assembled quaternary structure, and biological phenotype of the AAV capsid. Defined structures for 12 naturally occurring or modified AAV serotype/variants have been resolved in recent years using X-ray crystallography and/or cryo-electron microscopy. These include AAV-1,<sup>15</sup> AAV-2,<sup>16–22</sup> AAV-3B,<sup>23,24</sup> AAV-4,<sup>25,26</sup> AAV-5,<sup>27–30</sup> AAV-6,<sup>31,32</sup> AAV-7,<sup>33</sup> AAV-8,<sup>34–38</sup> AAV-9,<sup>39–41</sup> AAVrh32.33,<sup>42</sup> AAV-DJ,<sup>43,44</sup> and AAV-rh8.<sup>172</sup> The structural information of these AAV capsids as well as their interaction with respective cellular receptor/co-receptors have provided the necessary framework to logically design tailored vectors. Successful application of educated capsid design has been used to alter tissue tropism (targeting or de-targeting), avoid immune recognition, and improve postentry processing.

### Engineering to enhance AAV uptake in muscle

Bodywide muscle delivery is a prominent challenge in developing a viable therapy for DMD, especially since muscle occupies such a large volume of the body. Further complicating the picture, significant amount of vectors can be sequestered by non-muscle tissues (such as the liver and spleen), hence reducing the effective dose in muscle. Consequently, an effective gene therapy for DMD will inevitably require a large quantity of AAV vectors (up to  $10^{15}$ – $10^{16}$  viral genome particles per patient).<sup>45,46</sup> This not only exposes the body to a large antigen load but also puts an increased demand on vector production. Controlling AAV tropism to favor skeletal and cardiac muscle could minimize some of these concerns.

Two strategies are often used to improve AAV uptake in muscle. In one approach, a muscle homing peptide is inserted on the surface of the capsid to facilitate the entry of AAV into muscle cells. In the second approach, enhanced muscle targeting is achieved by modulating AAV interaction with its natural receptors. In the discussion below, we illustrate both strategies.

**Peptide insertion to improve muscle homing.** Inserting a tissue-specific peptide ligand to the capsid is a convenient method to alter AAV tropism. When considering peptide insertion, there are two key questions: where should the peptide be inserted and what peptide(s) should be inserted? Ideally, insertion should not alter capsid assembly, vector genome packaging, and the overall yield of vector production. The insertion site should also facilitate proper peptide presentation such that the peptide can effectively interact with its receptor. For muscle gene therapy, apparently, a muscle targeting peptide would be preferred.

Identifying sites amenable to peptide insertion has been the focus of a considerable amount of research. During early years, this was achieved by the “hit-or-miss” approach or scanning mutagenesis. Yang and colleagues inserted a single chain CD34 antibody in front of VP1, VP2, or VP3 of AAV-2.<sup>47</sup> Fusion to the N-terminus of VP2, but not VP1 and VP3, resulted in particles capable of infecting previously nonpermissible CD34 cells.<sup>47</sup> It is currently unclear why this strategy did not work for VP1 and VP3. However, in terms of VP1, it may relate to the unique biological property of the VP1 N-terminal region. This region not only contains the nuclear localization signal<sup>48</sup> but also contains phospholipase A2 activity that is essential for AAV infectivity.<sup>49,50</sup> Some recent studies suggest that the VP1 N-terminal region undergoes structural changes in the endosome and this change is essential for viral trafficking to the nucleus.<sup>51,52</sup> To identify regions that are suitable for peptide insertion, Rabinowitz et al. and Wu et al. performed independent scanning mutagenesis across the entire capsid region of AAV-2.<sup>53,54</sup> They found many sites that can tolerate peptide insertion. For example, Wu et al. successfully enhanced AAV-2 infection in lung epithelial cells by inserting an expanded serpin receptor ligand (10 residues) at residue 138 of the AAV-2 capsid. Warrington et al. inserted larger peptides such as fractalkine chemokine (76 residues) and leptin (146 residues) at exactly the same location (residue 138 of the AAV-2 capsid). Surprisingly, these insertions abolished VP3 production and viral particle assembly.<sup>55</sup> Collectively, in addition to the location, the size and/or amino acid composition of the peptide may also play an important role.

The resolution of the parvovirus structure has opened the door to rationally select the peptide insertion site.<sup>56–59</sup> Girod et al. were the first to successfully use this approach.<sup>60</sup> They inserted an integrin ligand peptide (14 residues) to a putative loop region of AAV-2 and achieved efficient transduction in AAV-2 resistant cells that expressed the

integrin receptor.<sup>60</sup> Grifman et al. successfully targeted tumor cell lines by inserting an NGR peptide, which binds CD-13, a marker for tumor angiogenesis.<sup>61</sup> In another study, Shi et al. identified potential insertion sites on a computer-simulated AAV structure.<sup>62</sup> They successfully inserted the 15-residue luteinizing hormone receptor ligand into AAV-2 capsid and enhanced transduction of ovarian carcinoma cells.

With the availability of the AAV-2 atomic structure, it has become possible to precisely select a site for peptide insertion.<sup>16,17</sup> For example, residues 587 and 588 (AAV-2 numbering) are located within a flexible loop on the external surface of the AAV-2 particle.<sup>63–73</sup> Insertion at these two locations will likely allow good presentation of the peptide without substantially compromising virion assembly and stability. As the crystal structures of many AAV serotypes are now available, designing tailored peptide insertion in these serotypes may improve their transduction efficiency and specificity.<sup>74,75</sup>

A major goal of DMD gene therapy is to achieve efficient transduction of skeletal and cardiac muscles. Insertion of muscle-homing peptides may improve targeted delivery of AAV to muscle and at the same time limit uptake in other tissues (Table 1). Ideally, a muscle-targeting peptide should (1) bind with high affinity to a muscle-specific receptor, (2) disrupt binding to the natural AAV receptor/co-receptors (such as the heparan sulfate receptor for AAV-2) (Table 2), and (3) incorporate on the surface of the capsid without altering assembly and infectivity. High-affinity ligands may occur naturally (e.g., transferrin and  $\alpha$ -bungarotoxin)<sup>76</sup> or may be isolated using phage biopanning (Table 2).<sup>65,67,77–83</sup> The success of *in vivo* biopanning depends on the delivery method (systemic versus local) and selection criteria. For DMD, systemic injection is a preferable selective pressure as a therapeutic vector will most likely be administered intravenously. Phage biopanning has been particularly successful for isolating peptides specific to skeletal and cardiac muscle. For example, Samoylova and Smith isolated a 7-residue muscle-targeting peptide (ASSLNIA) (Table 2).<sup>78</sup> Yu et al. inserted this peptide between residues 587 and 588 in AAV-2.<sup>68</sup> The modified vector displayed enhanced skeletal and cardiac muscle uptake.<sup>68</sup> Targeting the heart is particularly important in DMD as ~90% DMD patients develop cardiomyopathy. While intracardiac injection of AAV dystrophin constructs partially restores the dystrophin complex to the heart,<sup>84</sup> a cardiac muscle targeting peptide could provide a less invasive approach for cardiac delivery. To this end, Ying and colleagues

applied *in vivo* biopanning on organotypic cultures of heart tissue and obtained a unique isolate (VNSTRLP) capable of myocardial targeting.<sup>67</sup>

Altering capsid structural motifs involved in receptor interactions. Ligand–receptor interaction is a major determinant of viral tissue tropism. In the case of AAV, the ligand refers to the special structural motifs on the surface of the capsid that interact with cellular receptor/co-receptors. The ligand is often called the “footprint.”<sup>20,85</sup> An AAV footprint does not have to be a series of contiguous amino acid residues. More often, a footprint is composed of a cluster of three-dimensionally related amino acids. For example, the footprint of AAV-2 is made of basic residues R484, R487, K527, K532, R585, and R588.<sup>73,86,87</sup>

Cellular receptors for at least eight different AAV serotypes have been identified (Table 2). These receptors consist of various carbohydrates on the cell surface, in particular, N-linked  $\alpha$ -2,3 sialic acid for AAV-1 and AAV-5,<sup>88,89</sup> heparan sulfate proteoglycan for AAV-2 and AAV-3,<sup>90,91</sup> O-linked  $\alpha$ -2,3 sialic acid for AAV-4,<sup>92</sup> N-linked  $\alpha$ -2,6 sialic acid for AAV-6,<sup>88</sup> and N-linked galactose for AAV-9<sup>93,94</sup> (Table 2).

Several studies have explored the possibility of modifying AAV tropism through the alteration of AAV footprint–cellular receptor interaction. The AAV-2 footprint interacts with its receptor heparan sulfate proteoglycan. Heparan sulfate proteoglycan binding correlates with liver transduction.

**Table 1.** AAV receptor and co-receptor(s)

Serotype	Receptor	Co-receptor(s)	Reference
AAV-1	N-linked $\alpha$ -2,3 sialic acid		Wu et al. <sup>88</sup>
AAV-2	Heparin sulfate proteoglycan	$\alpha$ 5 $\beta$ 1-integrin, hFGFR1, $\alpha$ V $\beta$ 5-integrin, hHGFR, LamR	Qing et al. <sup>166</sup> , Summerford et al. <sup>91</sup>
AAV-3	Heparin sulfate proteoglycan	hFGFR, hHGFR, LamR	Handa et al. <sup>90</sup> ; Lerch et al. <sup>168</sup> ; Ling et al. <sup>167</sup>
AAV-4	O-linked $\alpha$ -2,3 sialic acid	Unknown	Kaludov et al. <sup>92</sup>
AAV-5	N-linked $\alpha$ -2,3 sialic acid	PDGFR	Di Pasquale et al. <sup>169</sup> ; Walters et al. <sup>89</sup>
AAV-6	N-linked $\alpha$ -2,6 sialic acid	EGFR	Wu et al. <sup>88</sup>
AAV-7	Unknown	Unknown	
AAV-8	Unknown	LamR	Akache et al. <sup>170</sup>
AAV-9	Galactose	LamR	Akache et al. <sup>170</sup> ; Bell et al. <sup>94</sup> ; Shen et al. <sup>93</sup>

EGFR, epidermal growth factor receptor; hFGFR1, human fibroblast growth factor receptor 1; hHGFR, human hepatocyte growth factor receptor; LamR, 37/67kDa laminin receptor; PDGFR, platelet-derived growth factor receptor; AAV, adeno-associated virus.

**Table 2.** Muscle-targeting peptides

Reference	Peptide name	Peptide sequence	Length	Comment
Barry et al. <sup>77</sup>	Peptide 20.1	TPHSLYEDLKRQMMQLGRH L	20-mer	This peptide targets fibroblasts and myoblasts but not differentiated myotubes <i>in vitro</i> .
	Peptide T.1	TGGETSGIKKAPYASTTRNR	20-mer	This peptide targets differentiated myotubes.
	Peptide T.2	SHHGVAQVLDLGGGADFKSI A	20-mer	This peptide targets differentiated myotubes.
Flint et al. <sup>79</sup>	Peptide (P5)	PYDQLRH	7-mer	This peptide targets C2C12 muscle cell line <i>in vitro</i> .
	Peptide (P6)	KAMHQMQ	7-mer	This peptide targets C2C12 muscle cell line <i>in vitro</i> .
	Peptide (P9)	YASINPM	7-mer	This peptide targets C2C12 muscle cell line <i>in vitro</i> and rat skeletal muscle <i>in vivo</i> .
		NPSQVKH	7-mer	This peptide targets rat laryngeal muscle <i>in vivo</i> .
Samoylova and Smith <sup>78</sup> ; Yu et al. <sup>68</sup>		ASSLNIA	7-mer	This peptide targets C2C12 muscle cell <i>in vitro</i> and mouse skeletal and cardiac muscle <i>in vivo</i> .
Ghosh and Barry <sup>80</sup>	Peptide 12.51	TARGEHKEEELI	12-mer	This peptide targets C2C12 muscle cell line <i>in vitro</i> .
McGuire et al. <sup>81</sup>	Peptide PCM.1	WLSEAGPVVTVRALRGTGS W	20-mer	This peptide targets primary cardiomyocytes <i>in vitro</i> and murine heart <i>in vivo</i> .
Seow et al., 2010 <sup>171</sup>	Peptide T9	SKTFNTHPQSTP	12-mer	This peptide targets C2C12 muscle cells <i>in vitro</i> and mdx heart and quadriceps muscle <i>in vivo</i> .
Ying et al. <sup>67</sup>		PSVSPRP and VNSTRLP	7-mers	This peptide targets rat heart slices <i>in vitro</i> and mouse heart <i>in vivo</i> .
		EGRVRPP and GTFSRAP	7-mers	This peptide targets rat cardiomyocytes <i>in vitro</i> and mouse heart <i>in vivo</i> .
Gao et al. <sup>82</sup>	Peptide M12	RRQPPRSISSHP	12-mer	This peptide targets C2C12 muscle cell line <i>in vitro</i> and skeletal and heart muscle <i>in vivo</i> .

Theoretically, alteration of the AAV-2 footprint should reduce heparan sulfate proteoglycan binding and hence decrease liver transduction. To test this hypothesis, Asokan and colleagues replaced a section of AAV-2 footprint (from residue 585–590, RGNRQA) with corresponding residues from AAV-8 (QQNTAP).<sup>95</sup> The chimeric capsids indeed showed reduced liver uptake. AAV-9 enters a cell through binding to N-linked galactose on the surface of the cell. This interaction is thought to underlie systemic transduction of AAV-9. The residues responsible for galactose binding in AAV-9 were identified recently.<sup>41,96,97</sup> Engraftment of these residues to AAV-2 (Q464V, A467P, D469N, I470M, R471A, D472V, S474G, Y500F, S501A, and D514N) indeed resulted in galactose binding and significantly improved systemic gene transfer efficiency of AAV-2.<sup>96,97</sup>

Another approach to modulate AAV interaction with its receptor is to conditionally hide the receptor binding residues. Judd et al. invented such a gating system for AAV-2.<sup>98</sup> To block the interaction of AAV-2 with its receptor, they inserted a short peptide between R585 and R588. They also engineered matrix metallo-protease (MMP) cleavage sites at the end of this short peptide. In the presence of MMP, the inserted peptide was removed and the heparan sulfate proteoglycan binding motif of AAV-2 was reconstituted allowing receptor recognition and viral uptake.<sup>98</sup> This type of capsid modification will be very useful for DMD gene therapy because inflammation is a prominent

feature of DMD and MMP is highly expressed in inflamed tissues.

### Rational modification to circumvent immune responses

As we alluded to earlier, immune responses constitute a critical barrier to DMD gene therapy.<sup>12,99</sup> Preexisting neutralizing antibodies may nullify AAV in the circulation. Capsid- or transgene product-specific T-cell responses can result in the elimination of AAV-transduced cells. While molecular mechanisms of the immune response remain to be fully elucidated, the immunological hurdle must be addressed in order to achieve successful DMD gene therapy. As the focus of this review is on capsid modifications, we will limit our discussion to capsid-related immune responses.

Alteration of neutralizing antibody binding epitopes to improve transduction in seropositive subjects. Preexisting neutralizing antibodies at levels as low as 1:2 are sufficient to attenuate AAV transduction in animal models.<sup>100,101</sup> A significant portion of the human population (~30–80%) has preexisting neutralizing antibodies to AAV.<sup>12</sup> This precludes a large percentage of patients from AAV therapy unless new vectors with enhanced antibody evasion become available. Several strategies have been developed to identify capsid epitopes that interact with neutralizing antibodies. Peptide display and scanning have been used to identify linear epitopes that reside in continuous amino acid residues.<sup>102,103</sup>

However, to fish out conformational epitopes that reside in noncontiguous amino acid residues, one has to use nondenatured intact viral particles.<sup>103</sup>

Capsid mutagenesis has been used to identify both linear and conformational neutralizing antibody binding motifs in AAV. For example, Huttner et al. applied the peptide insertion approach and found that AAV-2 residues 534, 573, and 587 are important for neutralization escaping.<sup>104</sup> Adachi et al. mapped the epitopes for AAV-1 and AAV-9 neutralization antibody binding to 452-QSGSAQ-457 and 453-GSGQN-457, respectively, by screening double-alanine mutants.<sup>96</sup> Antibody–capsid interactions can also be visualized with cryo-electron microscopy and three-dimensional image reconstruction.<sup>37,105,106</sup> High-resolution imaging shows that capsid epitopes tend to localize around the threefold protrusions and overlap with key regions involved in receptor recognition and tropism.<sup>105</sup> This information suggests that perhaps capsid engineering to improve tropism may simultaneously alter antibody recognition. In summary, delineating specific antibody recognition sites and targeted mutagenesis may yield new capsid variants that can be used in patients with preexisting immunity to existing serotypes.

Engineering AAV vectors to reduce cellular immune responses. The dystrophic muscle presents a formidable inflammatory environment for AAV gene therapy (Fig. 1A). Expression of major histocompatibility complexes (MHC) is upregulated in dystrophic muscles.<sup>107</sup> Cytokines and chemokines released from degenerative/necrotic myofibers may

recruit more immune cells to muscle and further aggravate inflammation.

Both capsid-specific and dystrophin-specific cellular immune responses have been implicated in transduction loss in dystrophic muscle.<sup>108–110</sup> Capsid-specific T-cell responses depend on AAV endosomal escape and subsequent proteasome processing (Fig. 2).<sup>111,112</sup> Therefore, capsid modifications to de-target the proteasome may be a useful method to reduce capsid T-cell responses. Zhong et al. found that AAV capsid was degraded by the ubiquitin–proteasome system upon phosphorylation of surface-exposed tyrosine (Y) residues.<sup>113,114</sup> Replacement of these residues with phenylalanine (F) aborted phosphorylation.<sup>115</sup> Martino and colleagues evaluated immunological benefits of tyrosine mutated AAV-2.<sup>116</sup> They found that the mutant vector showed reduced MHC presentation and less killing of hepatocytes in a liver gene transfer study (Fig. 2).<sup>116</sup> It is currently unclear whether tyrosine mutants will fare better in dystrophic muscle in terms of the T-cell response. However, some tyrosine-mutated AAV serotypes have shown promise for intramuscular injection in mouse muscle (Y445F or Y731F AAV-6) or body-wide muscle delivery in newborn dogs (Y445F/Y731F AAV-1).<sup>45,117</sup> We recently found that Y731F AAV-9 resulted in robust local and systemic muscle gene transfer in adult DMD dogs.<sup>46,118</sup> It is possible that tyrosine-mutated AAV capsids may prove useful to DMD gene therapy. In addition to tyrosine, surface-exposed serine, threonine, and lysine residues are also targets for phosphorylation. Sen and colleagues showed reduced ubiquitination and enhanced hepatic transduction when these

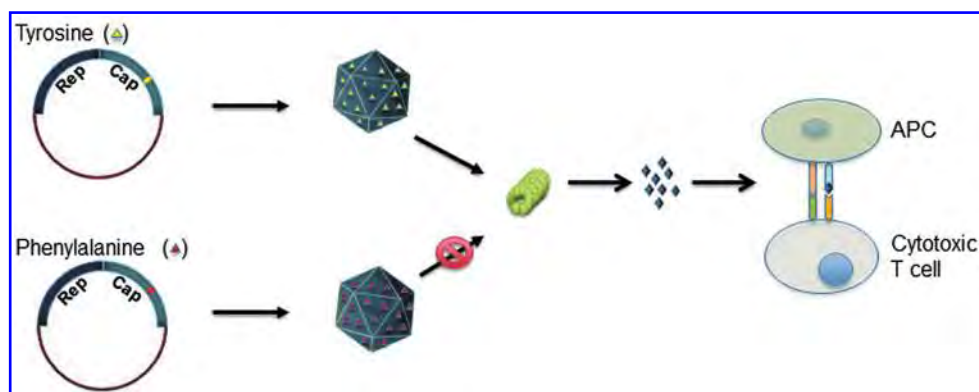


**Figure 2.** Engineering AAV vector by tyrosine substitution for proteasome evasion. Capsid-induced T-cell response is a major barrier for AAV-mediated DMD gene therapy. Viral capsids are degraded in the proteasome in the host cell cytoplasm. Degraded peptide fragments are transported into the endoplasmic reticulum and loaded into major histocompatibility complexes (MHC) class I molecules on the surface of antigen presenting cells (APC). The peptide–MHC I complex traffics to the cell membrane where peptide is recognized by the T-cell receptor leading to T-cell activation. The tyrosine residue on the surface of the viral capsid plays an important role in this process. Substitution of surface-exposed tyrosine by phenylalanine may reduce MHC presentation and T-cell immunity. Color images available online at [www.liebertpub.com/hum](http://www.liebertpub.com/hum)

residues were substituted in AAV-1, 5, and 8.<sup>119–122</sup> Additional studies are needed to determine whether these modifications offer immunological advantages in inflamed dystrophic muscle.

Uptake by antigen-presenting cells (such as macrophages) is a premise for the induction of cellular immune responses.<sup>123–125</sup> Strategies that can minimize macrophage uptake may improve AAV transduction in dystrophic muscle. CD47 glycoprotein is a surface marker for “self” in all human cells. Interaction of CD47 with signal regulatory protein- $\alpha$  on macrophages prevents uptake of “self” cells by macrophages.<sup>126</sup> Recently, a 21-residue peptide was found to mediate this self-recognition.<sup>127</sup> Incorporation of this peptide to nanoparticles reduced phagocytic clearance and enhanced gene delivery.<sup>127</sup> It is foreseeable that insertion of this peptide to the surface loops of AAV capsids may reduce macrophage uptake and improve AAV transduction in DMD muscle.

### AAV CAPSID ENGINEERING THROUGH DIRECTED EVOLUTION

Directed evolution harnesses natural selection to identify capsids with desired phenotypes. In this manner, it is possible to develop AAV vectors capable of coping with multiple selective pressures without any prior knowledge of the capsid structure.<sup>128</sup> Like natural selection, directed evolution requires a diverse starting population to increase the odds of identifying rare, desirable variants. This translates into the creation of a diverse capsid library. Theoretically, the more diverse the library, the more likely you will find a variant that can meet your need. A key technical challenge of directed evolution is the ability to retrieve the capsid coding sequence based on the phenotype of the capsid protein. For example, one may have identified an attractive neutralization escaping capsid variant. In order to package a therapeutic gene into this capsid variant, the exact coding sequence for this particular capsid variant must be fished out from millions of capsid coding sequences in the library. This could be quite challenging if not impossible. An ingenious solution is to have this capsid variant carrying its own coding sequence in its genome. Genomes can then be extracted from the capsids after selection. We will discuss various strategies used by different groups and a surprising but pleasant new discovery on capsid–genome correlation. The last step in directed evolution is to apply selective pressures to enrich capsid variants with desirable properties, and finally to isolate the fa-

vored capsid variant. We will discuss screening strategies that may help isolation of new AAV capsids for DMD gene therapy.

### Methods for library creation

Below we summarized the most commonly used strategies for AAV capsid library generation. More information can be found in a recent review article by Kotterman and Schaffer.<sup>128</sup>

**Error-prone polymerase chain reaction.** Error-prone polymerase chain reaction (EP-PCR) is a relatively simple method to randomly mutate a DNA sequence. This is achieved by enhancing the inherent polymerase error rate. The Taq polymerase has an inherent cumulative error rate of  $\sim 10^{-3}$  per nucleotide favoring A-to-G and T-to-C mutations yielding from 1 to 20 mutations per 1,000 bases.<sup>129–131</sup> This error rate may be further enhanced by incorporating high levels of  $Mn^{2+}$  or  $Mg^{2+}$  in the PCR or, alternatively, providing disproportionate amounts of deoxynucleotides.  $Mn^{2+}$  and  $Mg^{2+}$  help to stabilize noncomplementary strands, while disproportionate deoxynucleotides leads to unequal base pair incorporation. Additionally, nontraditional bases such as 8-oxo-GTP or dITP may be introduced to the PCR products.<sup>132,133</sup> Using these techniques, it is possible to generate an AAV capsid library with a complexity of approximately  $10^7$  variants.<sup>134</sup>

**Mosaic capsids.** The construction of mosaic capsids provides an alternative to EP-PCR for increasing the library diversity. To generate mosaic capsids, cultured cells are transfected with AAV helper plasmids expressing capsid genes from different serotypes, the adenovirus helper plasmid and a rAAV plasmid. This results in the incorporation of viral protein monomers from different serotypes during capsid assembling (Fig. 3A). The resulting viral capsids are mosaic capsids because they contain capsid units from several serotypes. Since not all capsid monomer combinations are viable,<sup>135</sup> the diversity is limited for this approach.

**PCR-based *in vitro* recombination.** PCR-based *in vitro* recombination methods create highly diverse chimeric libraries. It takes the advantage of high sequence similarity among different AAV serotypes to develop capsids of various combinations of the original parental sequences. Three most commonly used PCR strategies are staggered extension, overlap extension, and DNA shuffling.

**Staggered extension PCR.** Staggered extension PCR (StEP) provides a simple method to generate

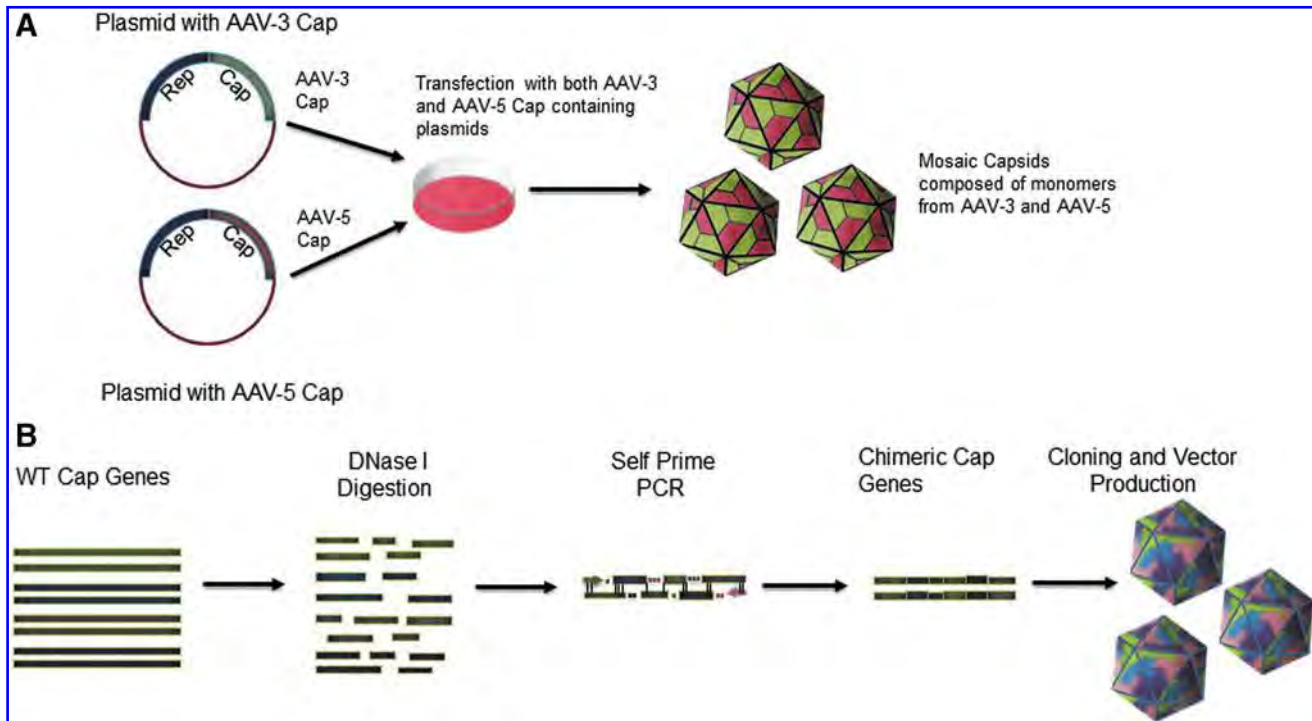
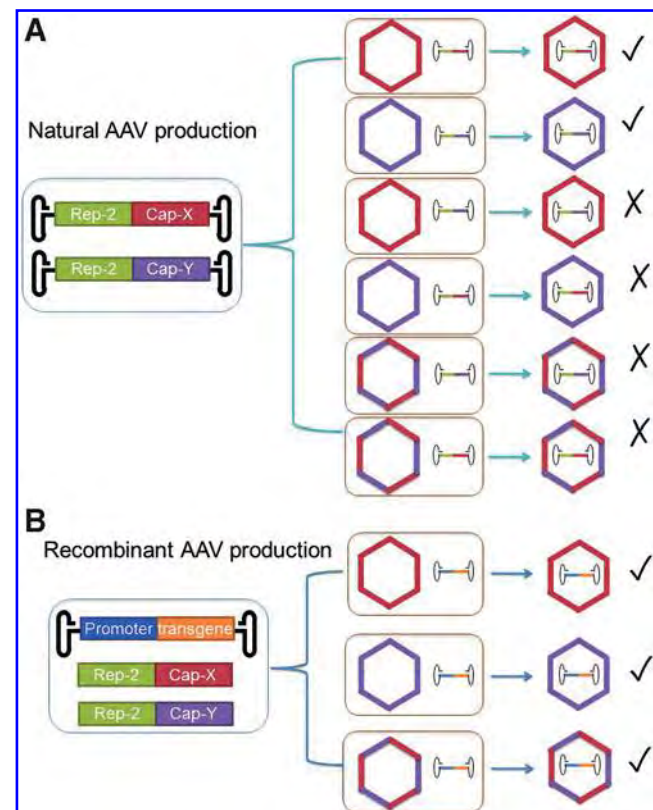


**Figure 3.** Generation of mosaic capsid library and DNA-shuffled capsid library. **(A)** Mosaic capsids are produced by co-transfection of the *Cap* gene from several AAV serotypes (in the example here, AAV-3 and AAV-5). During viral production, viral protein monomers from different serotypes are incorporated in the capsids to form mosaic capsids. **(B)** In DNA shuffling, AAV capsid genes from several serotypes are fragmented by DNase I. Homology between different capsid genes allows re-ligation through self-priming PCR. This haphazard re-assembly results in a library of chimeric capsids containing fragments from different serotypes. Color images available online at [www.liebertpub.com/hum](http://www.liebertpub.com/hum)

**Figure 4.** Capsid–genome correlation in AAV production. **(A)** Natural AAV production refers to AAV production using a *cis* plasmid that contains a wild-type-like AAV genome. In this genome, the *Rep* and *Cap* genes are flanked by the ITRs. In the presence of multiple different *cis* plasmids, the capsid produced by a particular *Cap* gene will package only the viral genome containing this *Cap* gene. There is a tight capsid–genome correlation. In the example here, two *cis* plasmids are used for AAV production, one carries the *Cap-X* gene (marked in red color) and the other carries the *Cap-Y* gene (marked in purple color). The Rep-2/*Cap-X* genome (green/red) will be packaged only inside capsids X (the red colored capsid). The Rep-2/*Cap-Y* genome (green/purple) will be packaged only inside capsids Y (the purple colored capsid). The Rep-2/*Cap-X* genome (green/red) will not be packaged inside capsids Y (the purple colored capsid), neither will the Rep-2/*Cap-Y* genome (green/purple) be packaged inside capsids X (the red colored capsid). In addition, this system will not generate chimeric viral particles in which the viral genome is packaged in chimeric capsids. **(B)** Recombinant AAV production refers to AAV production using a *cis* plasmid that contains a recombinant AAV genome (a genome in which a foreign expression cassette is flanked by the ITR). In recombinant AAV production, viral replication protein and capsid protein are produced from a *trans* plasmid that does not contain the ITR. In the example here, the recombinant AAV genome can be packaged in the capsid X, the capsid Y, or a mosaic capsid. The capsid–genome correlation is lost during recombinant AAV production. Color images available online at [www.liebertpub.com/hum](http://www.liebertpub.com/hum)



chimeras by altering the annealing and extension phases in a standard PCR. By reducing the annealing and extension period, staggered extension produces incomplete PCR fragments, which, due to the high sequence homology of AAV capsids, are able to anneal and self-prime on other parent templates.<sup>136</sup> Through reiterative cycles of staggered extension, capsid sequences from various parent templates are linked together to form chimeras.<sup>137,138</sup>

**Overlap extension PCR.** This method is usually used to insert specific mutation at specific points in a sequence or to stitch smaller DNA fragments into a larger fragment. In overlap extension PCR, primers with a 5' overhang complementary to the opposite parent template amplify parent templates yielding fragments with overlapping 5' regions. Primer-less PCR combines the individual amplicons into a larger gene sequence based on the overlapping regions. Terminal flanking primers are then used to amplify the entire sequence.<sup>139</sup> This method takes advantage of homologous 5' sequences between PCR products allowing parental templates to be sown together. In as few as 5–10 cycles of overlap extension followed by 30 cycles of flanking primer amplification, it is possible to fuse 2–7 parental capsid fragments.<sup>140</sup> Overlap extension PCR is particularly useful for inserting amino acids from one serotype into the capsid of another serotype.

**DNA shuffling.** DNA shuffling involves the fragmentation of related genetic sequences by DNase I digestion and subsequent recombination based on sequence homology in a reassembly PCR.<sup>141,142</sup> In recursive cycles of DNA shuffling, selective pressure is applied to enrich the recombinant population that has desirable characteristics (Fig. 3B). To shuffle AAV capsids, parental capsid sequences are PCR amplified with primers containing unique restriction sites on the 5' ends. The unique restriction sites are for cloning each capsid into a common backbone containing the wild-type ITRs and the AAV-2 replication gene. In a subsequent PCR, the capsid sequences are amplified, pooled, and digested briefly with DNase I. Because of sequence homology, fragments are able to undergo template switching and self-priming, allowing the *in vitro* recombination of homologous sequences. Unique restriction sites allow the assembled capsid sequences to be cloned into the common plasmid backbone for virus production.<sup>143</sup>

### Capsid–genome correlation

In order to retrieve the AAV genome that encodes the desired capsid, it is important that each capsid encapsulates only its own coding genome during packaging. Several strategies have been developed

to address this issue. Schaffer and colleagues used limiting dilution.<sup>144</sup> Basically, they controlled the amount of plasmids used in transfection to achieve one proviral plasmid per cell. In this case, the AAV vector made in each cell will likely carry only its own genome. Alternatively, Muller and colleagues utilized a shuttle vector system by transfecting the capsid plasmid library with wild-type capsid.<sup>65</sup> Using a low multiplicity of infection, shuttle vectors theoretically deliver only one genome to each cell. Recently, the Weber laboratory encountered a surprising observation when comparing AAV production using natural or recombinant proviral AAV plasmids (Fig. 4).<sup>145</sup> Natural proviral AAV plasmids contain the 5'-ITR, replication gene, capsid gene, and 3'-ITR. Weber and colleagues found excellent capsid–genome correlation when they transfected a mixture of natural proviral AAV plasmids from different serotypes at the dose of 5,000–50,000 plasmids/cell. Essentially, 75–80% of capsids packaged only their own coding genome (Fig. 4A). This is surprising because there are hundreds of proviral plasmids in each cell and these plasmids encode different capsids.<sup>145</sup> In contrast to natural proviral AAV plasmids, recombinant AAV proviral plasmids contain the 5'-ITR, transgene expression cassette, and 3'-ITR. For the production of recombinant AAV, the AAV replication and capsid genes are provided *in trans* using ITR-deficient plasmids. When Nonnenmacher et al. transfected a recombinant AAV proviral plasmid with ITR-null capsid plasmids from different serotypes, the tight capsid–genome correlation was lost (Fig. 4B). It is currently unclear why a capsid packages only the “correct (its own)” genome in the case of natural AAV reproduction. Nevertheless, this new observation suggests that capsid–genome correlation may not be a big concern as previously thought. If the capsid library is made in natural AAV plasmids, one may not need to perform limiting dilution or to use shuttle vectors.

### Evolution of novel capsids for DMD gene therapy

In natural selection, environmental pressure creates a selective advantage for phenotypes with higher fitness. Likewise, selective pressures applied to capsid libraries should force the survival of one or a few dominant capsids that can handle the specific selective pressure. Directed AAV evolution can be performed in cultured cells *in vitro* or in live animals *in vivo*. Selective pressure can also be applied to the capsid library before (e.g., preincubation of the library with antibodies or antisera) or after AAV is delivered to cells/animals.

Directed evolution to improve muscle tropism. Directed evolution is particularly well suited for creating AAV variants with enhanced tissue specificity. Simultaneous application of positive (e.g., muscle uptake) and negative (e.g., restricted liver uptake) pressures can dramatically improve targeting and de-targeting. Using a shuffled capsid library of AAV-1, 2, 3B, 4, 6, 7, 8, and 9, Yang and colleagues isolated a chimeric vector called AAV-M41.<sup>146</sup> AAV-M41 displayed enhanced cardiac tropism comparable to that of AAV-9, the so-called “cardiotropic” AAV. But in contrast to AAV-9, AAV-M41 resulted in minimum liver transduction.<sup>146</sup> The Asokan laboratory utilized EP-PCR to mutate AAV-9 capsids and screened for vectors with enhanced muscle transduction.<sup>147</sup> A resultant vector, AAV-9.45, displayed significantly increased transgene expression in the heart and skeletal muscle. Interestingly, AAV-9.45 was de-targeted from the liver, a feature similar to that of AAV-M41.

Directed evolution has also been used to identify novel capsids that can transduce difficult targets such as nonpermissive melanoma cells.<sup>148</sup> Failure to transduce muscle progenitor cells (such as satellite cells) by conventional AAV serotypes represents a major challenge in DMD gene therapy.<sup>149</sup> Directed evolution may yield capsids with enhanced transduction efficiency in satellite cells.

A major challenge in gene therapy is to reproduce animal study results in human patients.<sup>150–152</sup> The traditional approach is to confirm rodent results in large animal models before the initiation of human trials. Scaling up from small to large animals gives investigators a good chance to gauge the impact of the body size. However, this cannot address species-specific reactions. The xenograft model may provide a platform to test promising candidate vectors in human tissues or to identify viral capsids with enhanced tropism in human cells. Lisowski and colleagues screened a shuffled capsid library of AAV-1, 2, 3B, 4–6, 8, and 9 in a human liver xenograft model. In this model, human hepatocytes were engrafted in the liver of immune-deficient mice. After several rounds of *in vivo* selection, the authors isolated a chimeric vector called AAV-LK03. This vector showed preferred transduction of human but not mouse hepatocytes.<sup>153</sup> A human skeletal muscle xenograft model was developed by the Wagner laboratory recently.<sup>154</sup> This model recapitulated dystrophic muscle pathology. Future directed evolution in this model could potentially yield AAV capsids suitable for muscular dystrophy gene therapy.

Directed evolution to modify immune reactivity. Another important application of directed evolution is to develop immune-evasive vectors. By screening against human neutralizing sera, directed evolution has yielded vectors that are resistant to preexisting neutralizing antibodies. Schaffer’s group was the first to test this strategy. Maheshri et al. included a neutralizing sera preincubation step before screening EP-PCR- and StEP-derived libraries.<sup>155</sup> This strategy led to the isolation of AAV-r2.4 and r2.15. Both showed improved transgene expression in the presence of the neutralizing antibody in *in vitro* and *in vivo* tests. In another study, Schaffer’s lab used a library generated by DNA shuffling. They then selected against pooled intravenous immunoglobulin (IVIG). This led to the isolation of several vectors (AAV-cA2, cA3, cA4) that are highly resistant to IVIG challenge.<sup>144</sup> Similarly, Perabo and colleagues used preincubation with human sera to screen an EP-PCR capsid library for retained infectivity.<sup>134</sup> Capsids with mutations (R459G/K and N551D) showed increased resistance to human neutralizing sera. Neutralizing antibody screening can also be used in combination with tissue-selective pressures. For example, Grimm and colleagues developed a shuffled library from AAV-2, 4, 5, 8, and 9 and then screened this library on human hepatocytes and antisera.<sup>156</sup> A resultant vector, AAV-DJ, displayed enhanced liver tropism and resistance to neutralizing sera. This study suggests that combined use of multiple selective pressures may yield vectors with multiple desired features. So far, none of these immune evasive capsids has been tested in clinical trials. Future study with sera from DMD patients may reveal the utility of these capsids for DMD gene therapy.

### **CAPSID MODIFICATION TO INCREASE AAV PACKAGING CAPACITY FOR DMD GENE THERAPY**

The *dystrophin* gene is one of the largest genes in the genome. The 2.4 mb gene carries 79 exons and an 11.2 kb protein coding sequence.<sup>157</sup> This greatly exceeds the packaging capacity of AAV. Dual- and tri-AAV vectors are currently under development to deliver a larger *dystrophin* gene via interviral genome recombination.<sup>158,159</sup> An alternative approach is to increase the payload of each individual viral particle. One study suggests that AAV-5, the phylogenetically most divergent AAV serotype, may package an 8.2 kb vector genome.<sup>160</sup> However, subsequent studies from several laboratories suggest that this is not the case.<sup>161–163</sup>

AAV belongs to the dependent genera of parvovirus. All parvovirus shares a similar structure. Interestingly, some members appear to have a more flexible capsid.<sup>164</sup> For example, human bocavirus-1 (a member of autonomous genera of parvovirus) carries a viral genome of 5,543 nucleotides. This is 18.5% larger than that of the AAV-2 genome (4,679 nucleotides). Yan et al. recently tested cross-genera packaging of an AAV genome in human bocavirus-1.<sup>165</sup> The chimeric AAV-2/human bocavirus-1 vector indeed packaged a larger genome than conventional AAV. It is possible that further interrogation along this line may lead to the development of oversize AAV vectors suitable for DMD gene therapy.

### PERSPECTIVE ON AAV CAPSID ENGINEERING FOR DMD GENE THERAPY

Capsid engineering has contributed significantly to the development of better, more efficient, and specific viral vectors. As we have discussed throughout this review, there is a wide array of methodologies for altering the biological properties of AAV capsids. With the continual understanding of AAV capsid structure–function relationship, improved library generation, and creative screen-

ing methods, we may develop AAV vectors that better fit the needs of DMD gene therapy. In this regard, low-immunogenic, large-capacity, and human muscle-specific capsids will be particularly appealing. It is tempting to speculate that a more integrated approach, combining several rational and directed evolution approaches, may lead to the development of one or several AAV capsids that can meet the needs of DMD gene therapy.

### ACKNOWLEDGMENTS

DMD research in the Duan lab is supported by the National Institutes of Health NS-90634, Department of Defense, Muscular Dystrophy Association, Parent Project Muscular Dystrophy, Jesse's Journey—The Foundation for Gene and Cell Therapy, Hope for Javier, Kansas City Area Life Sciences Institute, and the University of Missouri.

### AUTHOR DISCLOSURE

D.D. is a member of the scientific advisory board for Solid GT, a subsidiary of Solid Ventures. The Duan lab received funding support from Solid Ventures for research not related to AAV capsid modification.

## REFERENCES

- Kunkel LM. 2004 William Allan Award address. Cloning of the DMD gene. *Am J Hum Genet* 2005;76:205–214.
- Kunkel LM, Monaco AP, Hoffman E, et al. Molecular studies of progressive muscular dystrophy (Duchenne). *Enzyme* 1987;38:72–75.
- Rossiter BJ, Stirpe NS, Caskey CT. Report of the MDA gene therapy conference, Tucson, Arizona, September 27–28, 1991. *Neurology* 1992;42:1413–1418.
- Seto JT, Bengtsson NE, Chamberlain JS. Therapy of genetic disorders—novel therapies for Duchenne muscular dystrophy. *Curr Pediatr Rep* 2014;2:102–112.
- Duan D. Duchenne muscular dystrophy gene therapy in the canine model. *Hum Gene Ther Clin Dev* 2015;26:57–69.
- Carter BJ. Adeno-associated virus and the development of adeno-associated virus vectors: A historical perspective. *Mol Ther* 2004;10:981–989.
- Flotte TR, Berns KI. Adeno-associated virus: A ubiquitous commensal of mammals. *Hum Gene Ther* 2005;16:401–407.
- Duan D, Sharma P, Yang J, et al. Circular intermediates of recombinant adeno-associated virus have defined structural characteristics responsible for long term episomal persistence in muscle. *J Virol* 1998;72:8568–8577.
- Schnepf BC, Jensen RL, Chen CL, et al. Characterization of adeno-associated virus genomes isolated from human tissues. *J Virol* 2005;79:14793–14803.
- Le Hir M, Goyenvall A, Peccate C, et al. AAV genome loss from dystrophic mouse muscles during AAV-U7 snRNA-mediated exon-skipping therapy. *Mol Ther* 2013;21:1551–1558.
- Dupont JB, Tournaire B, Georger C, et al. Short-lived recombinant adeno-associated virus transgene expression in dystrophic muscle is associated with oxidative damage to transgene mRNA. *Mol Ther Methods Clin Dev* 2015;2:15010.
- Calcedo R, Wilson JM. Humoral immune response to AAV. *Front Immunol* 2013;4:341.
- Agbandje-McKenna M, Kleinschmidt J. AAV capsid structure and cell interactions. *Methods Mol Biol* 2011;807:47–92.
- Drouin LM, Agbandje-McKenna M. Adeno-associated virus structural biology as a tool in vector development. *Future Virol* 2013;8:1183–1199.
- Miller EB, Gurda-Whitaker B, Govindasamy L, et al. Production, purification and preliminary X-ray crystallographic studies of adeno-associated virus serotype 1. *Acta Crystallogr F Struct Biol Crystall Commun* 2006;62:1271–1274.
- Kronenberg S, Kleinschmidt JA, Bottcher B. Electron cryo-microscopy and image reconstruction of adeno-associated virus type 2 empty capsids. *EMBO Rep* 2001;2:997–1002.
- Xie Q, Bu W, Bhatia S, et al. The atomic structure of adeno-associated virus (AAV-2), a vector for human gene therapy. *Proc Natl Acad Sci USA* 2002;99:10405–10410.
- Xie Q, Somasundaram T, Bhatia S, et al. Structure determination of adeno-associated virus 2: Three complete virus particles per asymmetric unit. *Acta Crystallogr D Biol Crystallogr* 2003;59:959–970.
- Xie Q, Hare J, Turnigan J, et al. Large-scale production, purification and crystallization of wild-type adeno-associated virus-2. *J Virol Methods* 2004;122:17–27.
- Zhang F, Aguilera J, Beaudet JM, et al. Characterization of interactions between heparin/glycosaminoglycan and adeno-associated virus. *Biochemistry* 2013;52:6275–6285.

21. O'Donnell J, Taylor KA, Chapman MS. Adeno-associated virus-2 and its primary cellular receptor—Cryo-EM structure of a heparin complex. *Virology* 2009;385:434–443.
22. McCraw DM, O'Donnell JK, Taylor KA, et al. Structure of adeno-associated virus-2 in complex with neutralizing monoclonal antibody A20. *Virology* 2012;431:40–49.
23. Lerch TF, Xie Q, Ongley HM, et al. Twinned crystals of adeno-associated virus serotype 3b prove suitable for structural studies. *Acta Crystallogr F Struct Biol Crystall Commun* 2009;65:177–183.
24. Lerch TF, Xie Q, Chapman MS. The structure of adeno-associated virus serotype 3B (AAV-3B): Insights into receptor binding and immune evasion. *Virology* 2010;403:26–36.
25. Kaludov N, Padron E, Govindasamy L, et al. Production, purification and preliminary X-ray crystallographic studies of adeno-associated virus serotype 4. *Virology* 2003;306:1–6.
26. Govindasamy L, Padron E, McKenna R, et al. Structurally mapping the diverse phenotype of adeno-associated virus serotype 4. *J Virol* 2006;80:11556–11570.
27. Walters RW, Agbandje-McKenna M, Bowman VD, et al. Structure of adeno-associated virus serotype 5. *J Virol* 2004;78:3361–3371.
28. Afione S, DiMattia MA, Halder S, et al. Identification and mutagenesis of the AAV5 sialic acid binding region. *J Virol* 2015;89:1660–1072.
29. Govindasamy L, DiMattia MA, Gurda BL, et al. Structural insights into adeno-associated virus serotype 5. *J Virol* 2013;87:11187–11199.
30. DiMattia M, Govindasamy L, Levy HC, et al. Production, purification, crystallization and preliminary X-ray structural studies of adeno-associated virus serotype 5. *Acta Crystallogr F Struct Biol Crystall Commun* 2005;61:917–921.
31. Xie Q, Lerch TF, Meyer NL, et al. Structure-function analysis of receptor-binding in adeno-associated virus serotype 6 (AAV-6). *Virology* 2011;420:10–19.
32. Xie Q, Ongley HM, Hare J, et al. Crystallization and preliminary X-ray structural studies of adeno-associated virus serotype 6. *Acta Crystallogr F Struct Biol Crystall Commun* 2008;64:1074–1078.
33. Quesada O, Gurda B, Govindasamy L, et al. Production, purification and preliminary X-ray crystallographic studies of adeno-associated virus serotype 7. *Acta Crystallogr F Struct Biol Crystall Commun* 2007;63:1073–1076.
34. Lane MD, Nam HJ, Padron E, et al. Production, purification, crystallization and preliminary X-ray analysis of adeno-associated virus serotype 8. *Acta Crystallogr F Struct Biol Crystall Commun* 2005;61:558–561.
35. Nam HJ, Lane MD, Padron E, et al. Structure of adeno-associated virus serotype 8, a gene therapy vector. *J Virol* 2007;81:12260–12271.
36. Nam HJ, Gurda BL, McKenna R, et al. Structural studies of adeno-associated virus serotype 8 capsid transitions associated with endosomal trafficking. *J Virol* 2011;85:11791–11799.
37. Gurda BL, Raupp C, Popa-Wagner R, et al. Mapping a neutralizing epitope onto the capsid of adeno-associated virus serotype 8. *J Virol* 2012;86:7739–7751.
38. Raupp C, Naumer M, Muller OJ, et al. The threefold protrusions of adeno-associated virus type 8 are involved in cell surface targeting as well as postattachment processing. *J Virol* 2012;86:9396–9408.
39. Mitchell M, Nam HJ, Carter A, et al. Production, purification and preliminary X-ray crystallographic studies of adeno-associated virus serotype 9. *Acta Crystallogr F Struct Biol Crystall Commun* 2009;65:715–718.
40. DiMattia MA, Nam HJ, Van Vliet K, et al. Structural insight into the unique properties of adeno-associated virus serotype 9. *J Virol* 2012;86:6947–6958.
41. Bell CL, Gurda BL, Van Vliet K, et al. Identification of the galactose binding domain of the adeno-associated virus serotype 9 capsid. *J Virol* 2012;86:7326–7333.
42. Mikals K, Nam HJ, Van Vliet K, et al. The structure of AAVrh32.33, a novel gene delivery vector. *J Struct Biol* 2014;186:308–317.
43. Lerch TF, O'Donnell JK, Meyer NL, et al. Structure of AAV-DJ, a retargeted gene therapy vector: Cryo-electron microscopy at 4.5 Å resolution. *Structure* 2012;20:1310–1320.
44. Xie Q, Spilman M, Meyer NL, et al. Electron microscopy analysis of a disaccharide analog complex reveals receptor interactions of adeno-associated virus. *J Struct Biol* 2013;184:129–135.
45. Hakim CH, Yue Y, Shin JH, et al. Systemic gene transfer reveals distinctive muscle transduction profile of tyrosine mutant AAV-1, -6, and -9 in neonatal dogs. *Mol Ther Methods Clin Dev* 2014;1:14002.
46. Yue Y, Pan X, Hakim CH, et al. Safe and bodywide muscle transduction in young adult Duchenne muscular dystrophy dogs with adeno-associated virus. *Hum Mol Genet* 2015;24:5880–5890.
47. Yang Q, Mamounas M, Yu G, et al. Development of novel cell surface CD34-targeted recombinant adeno-associated virus vectors for gene therapy. *Hum Gene Ther* 1998;9:1929–1937.
48. Hoque M, Ishizu K, Matsumoto A, et al. Nuclear transport of the major capsid protein is essential for adeno-associated virus capsid formation. *J Virol* 1999;73:7912–7915.
49. Girod A, Wobus CE, Zadori Z, et al. The VP1 capsid protein of adeno-associated virus type 2 is carrying a phospholipase A2 domain required for virus infectivity. *J Gen Virol* 2002;83:973–978.
50. Stahnke S, Lux K, Uhrig S, et al. Intrinsic phospholipase A2 activity of adeno-associated virus is involved in endosomal escape of incoming particles. *Virology* 2011;409:77–83.
51. Venkatakrishnan B, Yarbrough J, Domsic J, et al. Structure and dynamics of adeno-associated virus serotype 1 VP1-unique N-terminal domain and its role in capsid trafficking. *J Virol* 2013;87:4974–4984.
52. Sonntag F, Bleker S, Leuchs B, et al. Adeno-associated virus type 2 capsids with externalized VP1/VP2 trafficking domains are generated prior to passage through the cytoplasm and are maintained until uncoating occurs in the nucleus. *J Virol* 2006;80:11040–11054.
53. Rabinowitz JE, Xiao W, Samulski RJ. Insertional mutagenesis of AAV2 capsid and the production of recombinant virus. *Virology* 1999;265:274–285.
54. Wu P, Xiao W, Conlon T, et al. Mutational analysis of the adeno-associated virus type 2 (AAV2) capsid gene and construction of AAV2 vectors with altered tropism. *J Virol* 2000;74:8635–8647.
55. Warrington KH, Jr., Gorbatyuk OS, Harrison JK, et al. Adeno-associated virus type 2 VP2 capsid protein is nonessential and can tolerate large peptide insertions at its N terminus. *J Virol* 2004;78:6595–6609.
56. Agbandje-McKenna M, Llamas-Saiz AL, Wang F, et al. Functional implications of the structure of the murine parvovirus, minute virus of mice. *Structure* 1998;6:1369–1381.
57. McKenna R, Olson NH, Chipman PR, et al. Three-dimensional structure of Aleutian mink disease parvovirus: Implications for disease pathogenicity. *J Virol* 1999;73:6882–6891.
58. Agbandje M, Kajigaya S, McKenna R, et al. The structure of human parvovirus B19 at 8 Å resolution. *Virology* 1994;203:106–115.
59. Tsao J, Chapman MS, Agbandje M, et al. The three-dimensional structure of canine parvovirus and its functional implications. *Science* 1991;251:1456–1464.
60. Girod A, Ried M, Wobus C, et al. Genetic capsid modifications allow efficient re-targeting of adeno-associated virus type 2. *Nat Med* 1999;5:1052–1056.
61. Grifman M, Trepel M, Speece P, et al. Incorporation of tumor-targeting peptides into recombinant adeno-associated virus capsids. *Mol Ther* 2001;3:964–975.
62. Shi W, Arnold GS, Bartlett JS. Insertional mutagenesis of the adeno-associated virus type 2 (AAV2) capsid gene and generation of AAV2 vectors targeted to alternative cell-surface receptors. *Hum Gene Ther* 2001;12:1697–1711.
63. Perabo L, Goldnau D, White K, et al. Heparan sulfate proteoglycan binding properties of adeno-associated virus retargeting mutants and consequences for their *in vivo* tropism. *J Virol* 2006;80:7265–7269.

64. Perabo L, Buning H, Kofler DM, et al. *In vitro* selection of viral vectors with modified tropism: The adeno-associated virus display. *Mol Ther* 2003;8:151–157.
65. Muller OJ, Kaul F, Weitzman MD, et al. Random peptide libraries displayed on adeno-associated virus to select for targeted gene therapy vectors. *Nat Biotechnol* 2003;21:1040–1046.
66. Naumer M, Popa-Wagner R, Kleinschmidt JA. Impact of capsid modifications by selected peptide ligands on recombinant adeno-associated virus serotype 2-mediated gene transduction. *J Gen Virol* 2012;93:2131–2141.
67. Ying Y, Muller OJ, Goehringer C, et al. Heart-targeted adeno-associated viral vectors selected by *in vivo* biopanning of a random viral display peptide library. *Gene Ther* 2010;17:980–990.
68. Yu CY, Yuan Z, Cao Z, et al. A muscle-targeting peptide displayed on AAV2 improves muscle tropism on systemic delivery. *Gene Ther* 2009;16:953–962.
69. Michelfelder S, Kohlschutter J, Skorupa A, et al. Successful expansion but not complete restriction of tropism of adeno-associated virus by *in vivo* biopanning of random virus display peptide libraries. *PLoS One* 2009;4:e5122.
70. Michelfelder S, Lee MK, deLima-Hahn E, et al. Vectors selected from adeno-associated viral display peptide libraries for leukemia cell-targeted cytotoxic gene therapy. *Exp Hematol* 2007;35:1766–1776.
71. White AF, Mazur M, Sorscher EJ, et al. Genetic modification of adeno-associated viral vector type 2 capsid enhances gene transfer efficiency in polarized human airway epithelial cells. *Hum Gene Ther* 2008;19:1407–1414.
72. White SJ, Nicklin SA, Buning H, et al. Targeted gene delivery to vascular tissue *in vivo* by tropism-modified adeno-associated virus vectors. *Circulation* 2004;109:513–519.
73. Opie SR, Warrington KH, Jr., Agbandje-McKenna M, Zolotukhin S, Muzyczka N. Identification of amino acid residues in the capsid proteins of adeno-associated virus type 2 that contribute to heparan sulfate proteoglycan binding. *J Virol* 2003;77:6995–7006.
74. Varadi K, Michelfelder S, Korff T, et al. Novel random peptide libraries displayed on AAV serotype 9 for selection of endothelial cell-directed gene transfer vectors. *Gene Ther* 2012;19:800–809.
75. Michelfelder S, Varadi K, Raupp C, et al. Peptide ligands incorporated into the threefold spike capsid domain to re-direct gene transduction of AAV8 and AAV9 *in vivo*. *PLoS One* 2011;6:e23101.
76. Feero WG, Li S, Rosenblatt JD, et al. Selection and use of ligands for receptor-mediated gene delivery to myogenic cells. *Gene Ther* 1997;4:664–674.
77. Barry MA, Dower WJ, Johnston SA. Toward cell-targeting gene therapy vectors: Selection of cell-binding peptides from random peptide-presenting phage libraries. *Nat Med* 1996;2:299–305.
78. Samoylova TI, Smith BF. Elucidation of muscle-binding peptides by phage display screening. *Muscle Nerve* 1999;22:460–466.
79. Flint PW, Li ZB, Lehar M, et al. Laryngeal muscle surface receptors identified using random phage library. *Laryngoscope* 2005;115:1930–1937.
80. Ghosh D, Barry MA. Selection of muscle-binding peptides from context-specific peptide-presenting phage libraries for adenoviral vector targeting. *J Virol* 2005;79:13667–13672.
81. McGuire MJ, Samli KN, Johnston SA, et al. *In vitro* selection of a peptide with high selectivity for cardiomyocytes *in vivo*. *J Mol Biol* 2004;342:171–182.
82. Gao X, Zhao J, Han G, et al. Effective dystrophin restoration by a novel muscle-homing peptide-morpholino conjugate in dystrophin-deficient mdx mice. *Mol Ther* 2014;22:1333–1341.
83. Waterkamp DA, Muller OJ, Ying Y, et al. Isolation of targeted AAV2 vectors from novel virus display libraries. *J Gene Med* 2006;8:1307–1319.
84. Yue Y, Li Z, Harper SQ, Davison RL, et al. Microdystrophin gene therapy of cardiomyopathy restores dystrophin-glycoprotein complex and improves sarcolemma integrity in the mdx mouse heart. *Circulation* 2003;108:1626–1632.
85. Mietzsch M, Broecker F, Reinhardt A, et al. Differential adeno-associated virus serotype-specific interaction patterns with synthetic heparins and other glycans. *J Virol* 2014;88:2991–3003.
86. Kern A, Schmidt K, Leder C, et al. Identification of a heparin-binding motif on adeno-associated virus type 2 capsids. *J Virol* 2003;77:11072–11081.
87. Levy HC, Bowman VD, Govindasamy L, et al. Heparin binding induces conformational changes in adeno-associated virus serotype 2. *J Struct Biol* 2009;165:146–156.
88. Wu Z, Miller E, Agbandje-McKenna M, et al. Alpha<sub>2,3</sub> and alpha<sub>2,6</sub> N-linked sialic acids facilitate efficient binding and transduction by adeno-associated virus types 1 and 6. *J Virol* 2006;80:9093–9103.
89. Walters RW, Yi SM, Keshavjee S, et al. Binding of adeno-associated virus type 5 to 2,3-linked sialic acid is required for gene transfer. *J Biol Chem* 2001;276:21021–21026.
90. Handa A, Muramatsu S, Qiu J, et al. Adeno-associated virus (AAV)-3-based vectors transduce haematopoietic cells not susceptible to transduction with AAV-2-based vectors. *J Gen Virol* 2000;81:2077–2084.
91. Summerford C, Samulski RJ. Membrane-associated heparan sulfate proteoglycan is a receptor for adeno-associated virus type 2 virions. *J Virol* 1998;72:1438–1445.
92. Kaludov N, Brown KE, Walters RW, et al. Adeno-associated virus serotype 4 (AAV4) and AAV5 both require sialic acid binding for hemagglutination and efficient transduction but differ in sialic acid linkage specificity. *J Virol* 2001;75:6884–6893.
93. Shen S, Bryant KD, Brown SM, et al. Terminal N-linked galactose is the primary receptor for adeno-associated virus 9. *J Biol Chem* 2011;286:13532–13540.
94. Bell CL, Vandenberghe LH, Bell P, et al. The AAV9 receptor and its modification to improve *in vivo* lung gene transfer in mice. *J Clin Invest* 2011;121:2427–2435.
95. Asokan A, Conway JC, Phillips JL, et al. Reengineering a receptor footprint of adeno-associated virus enables selective and systemic gene transfer to muscle. *Nat Biotechnol* 2010;28:79–82.
96. Adachi K, Enoki T, Kawano Y, et al. Drawing a high-resolution functional map of adeno-associated virus capsid by massively parallel sequencing. *Nat Commun* 2014;5:3075.
97. Shen S, Horowitz ED, Troupes AN, et al. Engraftment of a galactose receptor footprint onto adeno-associated viral capsids improves transduction efficiency. *J Biol Chem* 2013;288:28814–28823.
98. Judd J, Ho ML, Tiwari A, et al. Tunable protease-activatable virus nanonodes. *ACS Nano* 2014;8:4740–4746.
99. Louis Jeune V, Joergensen JA, Hajjar RJ, et al. Pre-existing anti-adeno-associated virus antibodies as a challenge in AAV gene therapy. *Hum Gene Ther Methods* 2013;24:59–67.
100. Scallan CD, Jiang H, Liu T, et al. Human immunoglobulin inhibits liver transduction by AAV vectors at low AAV2 neutralizing titers in SCID mice. *Blood* 2006;107:1810–1817.
101. Rapti K, Louis-Jeune V, Kohlbrenner E, et al. Neutralizing antibodies against AAV serotypes 1, 2, 6, and 9 in sera of commonly used animal models. *Mol Ther* 2011;20:73–83.
102. Moskalenko M, Chen L, van Roey M, et al. Epitope mapping of human anti-adeno-associated virus type 2 neutralizing antibodies: Implications for gene therapy and virus structure. *J Virol* 2000;74:1761–1766.
103. Wobus CE, Hugle-Dorr B, Girod A, et al. Monoclonal antibodies against the adeno-associated virus type 2 (AAV-2) capsid: Epitope mapping and identification of capsid domains involved in AAV-2-cell interaction and neutralization of AAV-2 infection. *J Virol* 2000;74:9281–9293.
104. Huttner NA, Girod A, Perabo L, et al. Genetic modifications of the adeno-associated virus type 2 capsid reduce the affinity and the neutralizing effects of human serum antibodies. *Gene Ther* 2003;10:2139–2147.
105. Tseng YS, Gurda BL, Chipman P, et al. Adeno-associated virus serotype 1 (AAV1)- and AAV5-antibody complex structures reveal evolutionary

- commonalities in parvovirus antigenic reactivity. *J Virol* 2015;89:1794–1808.
106. Gurda BL, DiMattia MA, Miller EB, et al. Capsid antibodies to different adeno-associated virus serotypes bind common regions. *J Virol* 2013; 87:9111–9124.
  107. Englund P, Lindroos E, Nennesmo I, et al. Skeletal muscle fibers express major histocompatibility complex class II antigens independently of inflammatory infiltrates in inflammatory myopathies. *Am J Pathol* 2001;159:1263–1273.
  108. Mendell JR, Campbell K, Rodino-Klapac L, et al. Dystrophin immunity in Duchenne's muscular dystrophy. *N Engl J Med* 2010;363:1429–1437.
  109. Ferrand M, Galy A, Boisgerault F. A dystrophic muscle broadens the contribution and activation of immune cells reacting to rAAV gene transfer. *Gene Ther* 2014;21:828–839.
  110. Cordier L, Gao GP, Hack AA, et al. Muscle-specific promoters may be necessary for adeno-associated virus-mediated gene transfer in the treatment of muscular dystrophies. *Hum Gene Ther* 2001;12:205–215.
  111. He Y, Weinberg MS, Hirsch M, et al. Kinetics of adeno-associated virus serotype 2 (AAV2) and AAV8 capsid antigen presentation *in vivo* are identical. *Hum Gene Ther* 2013;24:545–553.
  112. Li C, He Y, Nicolson S, et al. Adeno-associated virus capsid antigen presentation is dependent on endosomal escape. *J Clin Invest* 2013;123: 1390–1401.
  113. Zhong L, Zhao W, Wu J, et al. A dual role of EGFR protein tyrosine kinase signaling in ubiquitination of AAV2 capsids and viral second-strand DNA synthesis. *Mol Ther* 2007;15:1323–1330.
  114. Zhong L, Li B, Jayandharan G, et al. Tyrosine-phosphorylation of AAV2 vectors and its consequences on viral intracellular trafficking and transgene expression. *Virology* 2008;381:194–202.
  115. Zhong L, Li B, Mah CS, et al. Next generation of adeno-associated virus 2 vectors: Point mutations in tyrosines lead to high-efficiency transduction at lower doses. *Proc Natl Acad Sci USA* 2008;105:7827–7832.
  116. Martino AT, Basner-Tschakarjan E, Markusic DM, et al. Engineered AAV vector minimizes *in vivo* targeting of transduced hepatocytes by capsid-specific CD8<sup>+</sup> T cells. *Blood* 2013;121: 2224–2233.
  117. Qiao C, Zhang W, Yuan Z, et al. AAV6 capsid tyrosine to phenylalanine mutations improve gene transfer to skeletal muscle. *Hum Gene Ther* 2010;21:1343–1348.
  118. Shin JH, Pan X, Hakim CH, et al. Microdystrophin ameliorates muscular dystrophy in the canine model of Duchenne muscular dystrophy. *Mol Ther* 2013;21:750–757.
  119. Sen D, Gadkari RA, Sudha G, et al. Targeted modifications in adeno-associated virus serotype 8 capsid improves its hepatic gene transfer efficiency *in vivo*. *Hum Gene Ther Methods* 2013;24:104–116.
  120. Sen D, Balakrishnan B, Gabriel N, et al. Improved adeno-associated virus (AAV) serotype 1 and 5 vectors for gene therapy. *Sci Rep* 2013;3:1832.
  121. Aslanidi GV, Rivers AE, Ortiz L, et al. High-efficiency transduction of human monocyte-derived dendritic cells by capsid-modified recombinant AAV2 vectors. *Vaccine* 2012;30:3908–3917.
  122. Aslanidi GV, Rivers AE, Ortiz L, et al. Optimization of the capsid of recombinant adeno-associated virus 2 (AAV2) vectors: The final threshold? *PLoS One* 2013;8:e59142.
  123. Mays LE, Wang L, Lin J, et al. AAV8 induces tolerance in murine muscle as a result of poor APC transduction, T cell exhaustion and minimal MHC1 upregulation on target cells. *Mol Ther* 2014;22:28–41.
  124. Zhang Y, Chirmule N, Gao G, et al. CD40 ligand-dependent activation of cytotoxic T lymphocytes by adeno-associated virus vectors *in vivo*: Role of immature dendritic cells. *J Virol* 2000;74: 8003–8010.
  125. Jooss K, Yang Y, Fisher KJ, et al. Transduction of dendritic cells by DNA viral vectors directs the immune response to transgene products in muscle fibers. *J Virol* 1998;72:4212–4223.
  126. Tsai RK, Discher DE. Inhibition of “self” engulfment through deactivation of myosin-II at the phagocytic synapse between human cells. *J Cell Biol* 2008;180:989–1003.
  127. Rodriguez PL, Harada T, Christian DA, et al. Minimal “self” peptides that inhibit phagocytic clearance and enhance delivery of nanoparticles. *Science* 2013;339:971–975.
  128. Kotterman MA, Schaffer DV. Engineering adeno-associated viruses for clinical gene therapy. *Nat Rev Genet* 2014;15:445–451.
  129. Cadwell RC, Joyce GF. Randomization of genes by PCR mutagenesis. *PCR Methods Appl* 1992;2: 28–33.
  130. Cadwell RC, Joyce GF. Mutagenic PCR. *PCR Methods Appl* 1994;3:S136–S140.
  131. Cadwell RC, Joyce GF. Mutagenic PCR. *CSH Protoc* 2006;prot4143.
  132. Cirino PC, Mayer KM, Umeno D. Generating mutant libraries using error-prone PCR. *Methods Mol Biol* 2003;231:3–9.
  133. Pritchard L, Corne D, Kell D, et al. A general model of error-prone PCR. *J Theor Biol* 2005;234: 497–509.
  134. Perabo L, Endell J, King S, et al. Combinatorial engineering of a gene therapy vector: Directed evolution of adeno-associated virus. *J Gene Med* 2006;8:155–162.
  135. Rabinowitz JE, Bowles DE, Faust SM, et al. Cross-dressing the virion: The transcapsidation of adeno-associated virus serotypes functionally defines subgroups. *J Virol* 2004;78:4421–4432.
  136. Aguinaldo AM, Arnold FH. Staggered extension process (StEP) *in vitro* recombination. *Methods Mol Biol* 2003;231:105–110.
  137. Zhao H, Giver L, Shao Z, et al. Molecular evolution by staggered extension process (StEP) *in vitro* recombination. *Nat Biotechnol* 1998;16:258–261.
  138. Zhao H, Zha W. *In vitro* “sexual” evolution through the PCR-based staggered extension process (StEP). *Nat Protoc* 2006;1:1865–1871.
  139. Luo F, Du X, Weng T, et al. Efficient multi-site-directed mutagenesis directly from genomic template. *J Biosci* 2012;37:965–969.
  140. Luo WG, Liu HZ, et al. Simultaneous splicing of multiple DNA fragments in one PCR reaction. *Biol Proced Online* 2013;15:9.
  141. Stemmer WP. Rapid evolution of a protein *in vitro* by DNA shuffling. *Nature* 1994;370:389–391.
  142. Stemmer WP. DNA shuffling by random fragmentation and reassembly: *In vitro* recombination for molecular evolution. *Proc Natl Acad Sci USA* 1994;91:10747–10751.
  143. Kienle E, Senis E, Borner K, et al. Engineering and evolution of synthetic adeno-associated virus (AAV) gene therapy vectors via DNA family shuffling. *J Vis Exp* 2012;62:e3819.
  144. Koerber JT, Jang JH, Schaffer DV. DNA shuffling of adeno-associated virus yields functionally diverse viral progeny. *Mol Ther* 2008;16:1703–1709.
  145. Nonnenmacher M, van Bakel H, Hajjar RJ, et al. High capsid-genome correlation facilitates creation of AAV libraries for directed evolution. *Mol Ther* 2015;23:675–682.
  146. Yang L, Jiang J, Drouin LM, et al. A myocardium tropic adeno-associated virus (AAV) evolved by DNA shuffling and *in vivo* selection. *Proc Natl Acad Sci USA* 2009;106:3946–3951.
  147. Pulicherla N, Shen S, Yadav S, et al. Engineering liver-detargeted AAV9 vectors for cardiac and musculoskeletal gene transfer. *Mol Ther* 2011;19:1070–1078.
  148. Li W, Asokan A, Wu Z, et al. Engineering and selection of shuffled AAV genomes: A new strategy for producing targeted biological nanoparticles. *Mol Ther* 2008;16:1252–1260.
  149. Arnett AL, Konieczny P, Ramos JN, et al. Adeno-associated viral (AAV) vectors do not efficiently target muscle satellite cells. *Mol Ther Methods Clin Dev* 2014;1. pii: 14038.
  150. Perrin S. Preclinical research: Make mouse studies work. *Nature* 2014;507:423–425.
  151. Collins FS, Tabak LA. Policy: NIH plans to enhance reproducibility. *Nature* 2014;505:612–613.
  152. Perel P, Roberts I, Sena E, et al. Comparison of treatment effects between animal experiments

- and clinical trials: Systematic review. *Brit Med J* 2007;334:197.
153. Lisowski L, Dane AP, Chu K, et al. Selection and evaluation of clinically relevant AAV variants in a xenograft liver model. *Nature* 2014;506:382–386.
  154. Zhang Y, King OD, Rahimov F, et al. Human skeletal muscle xenograft as a new preclinical model for muscle disorders. *Hum Mol Genet* 2014;23:3180–3188.
  155. Maheshri N, Koerber JT, Kaspar BK, et al. Directed evolution of adeno-associated virus yields enhanced gene delivery vectors. *Nat Biotechnol* 2006;24:198–204.
  156. Grimm D, Lee JS, Wang L, et al. *In vitro* and *in vivo* gene therapy vector evolution via multi-species interbreeding and retargeting of adeno-associated viruses. *J Virol* 2008;82:5887–5911.
  157. Koenig M, Hoffman EP, Bertelson CJ, et al. Complete cloning of the Duchenne muscular dystrophy (DMD) cDNA and preliminary genomic organization of the DMD gene in normal and affected individuals. *Cell* 1987;50:509–517.
  158. Lostal W, Kodippili K, Yue Y, et al. Full-length dystrophin reconstitution with adeno-associated viral vectors. *Hum Gene Ther* 2014;25:552–562.
  159. Zhang Y, Yue Y, Li L, et al. Dual AAV therapy ameliorates exercise-induced muscle injury and functional ischemia in murine models of Duchenne muscular dystrophy. *Hum Mol Genet* 2013;22:3720–3729.
  160. Allocca M, Doria M, Petrillo M, et al. Serotype-dependent packaging of large genes in adeno-associated viral vectors results in effective gene delivery in mice. *J Clin Invest* 2008;118:1955–1964.
  161. Lai Y, Yue Y, Duan D. Evidence for the failure of adeno-associated virus serotype 5 to package a viral genome > or = 8.2 kb. *Mol Ther* 2010;18:75–79.
  162. Wu Z, Yang H, Colosi P. Effect of genome size on AAV vector packaging. *Mol Ther* 2010;18:80–86.
  163. Dong B, Nakai H, Xiao W. Characterization of genome integrity for oversized recombinant AAV vector. *Mol Ther* 2010;18:87–92.
  164. Carrasco C, Castellanos M, de Pablo PJ, Mateu MG. Manipulation of the mechanical properties of a virus by protein engineering. *Proc Natl Acad Sci USA* 2008;105:4150–4155.
  165. Yan Z, Keiser NW, Song Y, et al. A novel chimeric adeno-associated virus 2/human bocavirus 1 parvovirus vector efficiently transduces human airway epithelia. *Mol Ther* 2013;21:2181–2194.
  166. Qing K, Mah C, Hansen J, et al. Human fibroblast growth factor receptor 1 is a coreceptor for infection by adeno-associated virus 2. *Nat Med* 1999;5:71–77.
  167. Ling C, Lu Y, Kalsi JK, et al. Human hepatocyte growth factor receptor is a cellular co-receptor for adeno-associated virus serotype 3. *Hum Gene Ther* 2010;21:1741–1747.
  168. Lerch TF, Chapman MS. Identification of the heparin binding site on adeno-associated virus serotype 3B. *Virology* 2012;423:6–13.
  169. Di Pasquale G, Davidson BL, Stein CS, et al. Identification of PDGFR as a receptor for AAV-5 transduction. *Nat Med* 2003;9:1306–1312.
  170. Akache B, Grimm D, Pandey K, et al. The 37/67-kilodalton laminin receptor is a receptor for adeno-associated virus serotypes 8, 2, 3, and 9. *J Virol* 2006;80:9831–9836.
  171. Seow Y, Yin H, Wood MJ. Identification of a novel muscle targeting peptide in mdx mice. *Peptides* 2010;31:1873–1877.
  172. Halder S, Van Vliet K, Smith JK, et al. Structure of neurotropic adeno-associated virus AAVrh.8. *Journal of structural biology* 2015;192:21–36.

Received for publication July 22, 2015;  
accepted after revision September 1, 2015.

Published online: September 16, 2015.

REVIEW

## Prospect of gene therapy for cardiomyopathy in hereditary muscular dystrophy

Yongping Yue<sup>a</sup>, Ibrahim M. Binalsheikh<sup>b</sup>, Stacey B. Leach<sup>c</sup>, Timothy L. Domeier<sup>d</sup> and Dongsheng Duan<sup>a,e</sup>

<sup>a</sup>Department of Molecular Microbiology and Immunology, School of Medicine, University of Missouri, Columbia, MO, USA; <sup>b</sup>Department of Child Health, School of Medicine, University of Missouri, Columbia, MO, USA; <sup>c</sup>Department of Veterinary Medicine and Surgery, College of Veterinary Medicine, University of Missouri, Columbia, MO, USA; <sup>d</sup>Department of Medical Pharmacology and Physiology, School of Medicine, University of Missouri, Columbia, MO, USA; <sup>e</sup>Department of Neurology, School of Medicine, University of Missouri, Columbia, MO, USA

### ABSTRACT

**Introduction:** Cardiac involvement is a common feature in muscular dystrophies. It presents as heart failure and/or arrhythmia. Traditionally, dystrophic cardiomyopathy is treated with symptom-relieving medications. Identification of disease-causing genes and investigation on pathogenic mechanisms have opened new opportunities to treat dystrophic cardiomyopathy with gene therapy. Replacing/repairing the mutated gene and/or targeting the pathogenic process/mechanisms using alternative genes may attenuate heart disease in muscular dystrophies.

**Areas covered:** Duchenne muscular dystrophy is the most common muscular dystrophy. Duchenne cardiomyopathy has been the primary focus of ongoing dystrophic cardiomyopathy gene therapy studies. Here, we use Duchenne cardiomyopathy gene therapy to showcase recent developments and to outline the path forward. We also discuss gene therapy status for cardiomyopathy associated with limb-girdle and congenital muscular dystrophies, and myotonic dystrophy.

**Expert opinion:** Gene therapy for dystrophic cardiomyopathy has taken a slow but steady path forward. Preclinical studies over the last decades have addressed many fundamental questions. Adeno-associated virus-mediated gene therapy has significantly improved the outcomes in rodent models of Duchenne and limb-girdle muscular dystrophies. Validation of these encouraging results in large animal models will pave the way for future human trials.

### ARTICLE HISTORY

Received 24 October 2015  
Accepted 20 November 2015  
Published online 16  
December 2015

### KEYWORDS

AAV; adeno-associated virus; gene therapy; cardiomyopathy; Duchenne muscular dystrophy; DMD; dystrophin; capsid engineering; vector; capsid; muscular dystrophy; gene therapy; heart failure; limb-girdle muscular dystrophy; congenital muscular dystrophy; myotonic dystrophy

### 1. Clinical presentation, pathogenic mechanism, and therapeutic challenge of dystrophic cardiomyopathy

Dystrophic cardiomyopathy refers to cardiac manifestations of muscular dystrophies. Muscular dystrophies are a clinically, genetically, and biochemically heterogeneous group of disorders. They are characterized by progressive muscle wasting, force loss, and dystrophic muscle pathology.[1,2] Muscular dystrophies can be classified in many different ways, such as the age of onset (congenital/neonatal, adolescent, or adult), disease progression (rapid or slow), the muscle groups involved (such as limb-girdle, facioscapulohumeral, and oculopharyngeal, etc.), and the mode of inheritance (such as X-linked or autosomal, recessive or dominant). Some muscular dystrophies are named after people who discovered the disease (such as Duchenne muscular dystrophy (DMD), Becker muscular dystrophy (BMD), and Emery–Dreifuss muscular dystrophy, etc.). Despite the unique clinical features of each type of muscular dystrophy, cardiac involvement has been a

common finding in most muscular dystrophies and often represents a major cause of morbidity and mortality.[3–7] Interestingly, the cardiac phenotype varies in different types of muscular dystrophies and even in different patients or disease stages of the same type of muscular dystrophy. Some present with dilated/hypertrophic/restrictive cardiomyopathy with eventual heart failure, while others exhibit conduction defects leading to arrhythmias and sudden cardiac death. In the case of DMD and BMD, MRI studies have revealed a unique pattern of subepicardial fibrosis predominantly in the left ventricular lateral wall.[8–10]

The pathogenic mechanisms of dystrophic cardiomyopathy are not completely understood.[11,12] However, it may at least involve destabilization of the cardiomyocyte membrane, or sarcolemma. Unlike other cells in the body, muscle cells undergo continuous calcium-regulated contraction/relaxation cycles. A consequence of this unique physiology is the repeated cycles of shrinking and expansion of the cell. This dynamic deformation process places

## Article highlights

- Cardiomyopathy is a common complication in inherited muscular dystrophies.
- Gene therapy holds great promise to reduce heart-related morbidity and mortality in muscular dystrophies.
- AAV is the most effective cardiac gene delivery vector.
- Micro-dystrophin and sarcoglycan gene therapies have significantly improved the cardiac outcome in animal models of DMD and LGMD, respectively.
- Targeting pathogenic mechanisms with disease gene-independent gene therapy opens exciting new opportunities.
- Preclinical test in large animal models will pave the way to human trials.

This box summarizes key points contained in the article.

enormous stress on the sarcolemma. Such stress is especially problematic for cardiomyocytes because of the repetitive pumping activity of the heart. To relieve contraction-induced stress, muscle cells have evolved specialized trans-membrane protein complexes such as the dystrophin-associated glycoprotein complex (DGC) and the integrin complex. These protein complexes constitute physical connections between the cytoskeleton and the extracellular matrix. Mutations in the genes encoding the components of these complexes result in various forms of muscular dystrophies. Failure to maintain sarcolemmal integrity leads to membrane leakage, myocyte degeneration, necrosis, and eventual replacement by fibrofatty tissue. Clearly, strengthening the destabilized sarcolemma holds the key for treating dystrophic cardiomyopathy. Unfortunately, this cannot be achieved with conventional medical/surgical treatments.[13] Gene therapy, however, provides a great opportunity to address this therapeutic challenge.

## 2. Strategies to deliver a therapeutic gene to a dystrophic heart

Disease-causing genes for many muscular dystrophies have been discovered. The identification of the genetic underpinning makes it possible to treat dystrophic cardiomyopathy with gene therapy. The first step of gene therapy is delivery of a therapeutic gene to the heart. A number of viral and nonviral vectors have been tested. [14] So far, the most effective and least immunogenic vector is the adeno-associated virus (AAV). AAV is a 20-nm single-stranded DNA virus.[15] Recombinant AAV vectors contain no wild-type viral genes. The vector genome can be readily packaged into naturally existing or synthetic capsids to meet specific therapeutic needs. The nano-size AAV particle creates a packaging

dilemma. The maximal carrying capacity of a single AAV particle is 5 kb.[16] This is too small for many genes required for muscular dystrophy gene therapy (such as the dystrophin gene and the dysferlin gene). To overcome this limitation, we and others have invented a series of dual and tri-AAV vectors.[17] The basic idea is to fragment a large therapeutic gene and package each segment into an AAV particle. The full-length gene is reconstituted by cellular recombination machinery after co-infection. These multi-vector strategies have made it possible to deliver the 6–8-kb mini-dystrophin gene and even the 12-kb full-length dystrophin coding sequence to dystrophin-deficient mdx mice, the most commonly used animal models for DMD.[18–22]

Over the years, a number of different strategies have been developed to achieve effective AAV gene transfer in dystrophic hearts. Early studies were mainly based on AAV-2 using invasive and complicated methods such as direct myocardial injection,[23] intracavity injection,[24] transcatheter perfusion,[25] and ex vivo coronary perfusion.[26] The identification and development of novel AAV capsids has opened the door to transduce dystrophic hearts with peripheral vein injections.[27–32] This simple method not only greatly reduces the risks associated invasive heart gene transfer but also allows simultaneous treatment of both cardiac and skeletal muscle disease in muscular dystrophy.

The tissue tropism of the AAV vector is largely determined by the viral capsids. Experimenting with natural and engineered AAV capsids has proven to be a fruitful approach in identifying cardiotropic AAV vectors. For example, a comparison of AAV-1 to AAV-9 revealed AAV-9 as the most potent vector for the mouse heart. [33] Indeed, AAV-9 results in robust, widespread myocardial transduction in mdx mice irrespective of the age and the route of delivery (intravenous or intra-arterial). [34–36] Directed evolution and cardiotropic peptide insertion have also yielded novel AAV variants with enhanced cardiac transduction in rodent models of limb-girdle muscular dystrophy (LGMD) 2F, an extremely rare type of muscular dystrophy caused by  $\delta$ -sarcoglycan deficiency.[32,37,38]

## 3. Disease gene-specific gene therapy

### 3.1. Dystrophin-based Duchenne cardiomyopathy gene therapy

The dystrophin gene was the first muscular dystrophy-associated gene cloned by the positional cloning approach.[39] Its mutation leads to DMD. The 2.4-mb full-length dystrophin gene contains 79 exons and it

transcribes into a ~12-kb cDNA. The full-length dystrophin protein has four major functional domains, including the N-terminal, rod, cysteine-rich, and C-terminal domains. The N-terminal domain binds to cytosolic  $\gamma$ -actin. The rod domain consists of 24 spectrin-like repeats. Within the rod domain, there are several important subdomains, including one for  $\gamma$ -actin-binding, one for neuronal nitric oxide synthase (nNOS)-binding, and one for microtubule-binding.[40–43] The cysteine-rich domain links dystrophin to the extracellular matrix through dystroglycan, a transmembrane glycoprotein. The C-terminal domain binds to syntrophin and dystrobrevin.

The enormous size of the dystrophin gene presents a delivery challenge, because it is beyond the packaging capacity of most viral vectors. Interestingly, some naturally existing, internally deleted dystrophins (e.g.  $\Delta 17$ –48) are quite functional.[44] These mini-dystrophin genes are about 6–8-kb in length, and their expression in humans and animals has greatly mitigated skeletal muscle disease.[19–21,44–47] The therapeutic implication of mini-dystrophin in the heart has only been investigated in transgenic mice.[48] We expressed mini-dystrophin specifically in the heart of mdx mice. This cardiac-restricted expression completely corrected cardiac histopathology, improved exercise performance, and enhanced myocardial contractility.[48] Whether mini-dystrophin gene therapy can achieve similar effectiveness remains to be seen. In this regard, dual AAV vectors have been developed to express the mini-dystrophin gene.[18–21,49–51] Further, systemic injection of dual AAV vectors has been shown to transduce the myocardium at high efficiency in mdx mice.[52,53]

A single vector therapy would be more advantageous. To package dystrophin into AAV, highly abbreviated micro-dystrophin genes have been developed. The microgene is about 3.5–4 kb in length and contains ~30% of the dystrophin coding sequence. In contrast to mini-dystrophin, micro-dystrophin does not carry the C-terminal domain. Additionally, it has a shorter rod domain with only four to five spectrin-like repeats. AAV-mediated micro-dystrophin gene therapy has been extensively studied in various mouse models and more recently in the canine model.[47,54–59] Direct or systemic AAV microgene therapy significantly ameliorated skeletal muscle disease in dystrophic mice and dogs. The first study to evaluate the therapeutic effect of micro-dystrophin in the heart was performed by Yue et al.[24] In this study, an AAV-5 microgene vector was directly injected into the cardiac cavity of neonatal mdx mice. Micro-dystrophin restored the DGC complex in the heart and enhanced the membrane stability of

cardiomyocytes.[24] In subsequent studies, newly developed AAV capsids (such as AAV-6 and AAV-9) were utilized to deliver micro-dystrophin to the heart through peripheral vein injection.[34–36,54,60–62] Of particular interest are studies by Bostick et al., in which an AAV-9 microgene vector was delivered to the heart of aged female mdx mice. This study is noteworthy because aged female mdx mice develop a cardiac phenotype nearly identical to that observed in dilated cardiomyopathy of human patients.[34,35,63,64] Despite the advanced heart disease in very old mice, surprisingly, cardiomyocytes were efficiently transduced.[34,35] The average lifespan of mdx mice is ~22 months.[65,66] In preterminal mdx mice (16–20 m old), microgene therapy reduced myocardial fibrosis, improved the electrocardiographic profile, and enhanced hemodynamic function.[34] In terminal-aged mdx mice (>21 m old), neither fibrosis nor hemodynamic function was improved.[35] However, some ECG parameters were partially corrected, and dobutamine stress-induced acute cardiac death was reduced.[35]

Expression of a full-length or near-full-length dystrophin protein may lead to a better recovery. This is feasible with tri-AAV vectors, but the efficiency is too low to be of practical use currently.[22] Editing the mutated RNA transcript or genome offers alternative approaches to reach this goal. Exon skipping is a potent method to achieve RNA-level editing. Briefly, antisense oligonucleotides (AONs) are delivered to modulate RNA splicing so that the mutated (and sometimes adjacent) exons are removed. The resulting mRNA, though abbreviated, is in-frame and can yield a near-full-length protein.[67] Several chemically distinctive classes of AONs have been developed, including 2-O-methylated phosphorothioated (2-OMePS), phosphorodiamidate morpholino oligomers (PMOs), peptide/polymer/nanoparticle-conjugated PMOs, and most recently tricycle-DNA (tcDNA). 2-OMePS and PMOs are currently in clinical trials.[68–73] However, these AONs cannot reach the heart.[74–76] Peptide/polymer/nanoparticle-conjugated PMOs can induce exon-skipping in the heart of mdx mice and improve heart function.[77–87] However, there are issues related to potential toxicity and immunogenicity.[88] The newly developed tcDNA represents the most advanced AON formulation.[89] Because of its unique pharmacological property, systemic delivery of tcDNA–AONs resulted in phenomenal uptake in many tissues, including the heart and brain. Treatment in mdx mice and more severe utrophin/dystrophin double knockout (u-dko) mice improved cardiac, respiratory, and behavioral functions.[89] Importantly, no overt toxicity was detected with tcDNA.[89] An alternative strategy to

deliver AONs is to use the AAV vector. AAV-9-mediated systemic AON delivery resulted in high, efficient dystrophin expression in the heart of u-dko mice.[90] More recently, two independent groups achieved long-term dystrophin restoration in the heart of the canine DMD model with AAV-6-mediated local exon-skipping.[91,92]

Compared to RNA editing with exon-skipping, targeted editing of the mutated dystrophin gene has just entered an exciting time due to recent development of highly versatile genome engineering tools such as zinc-finger nucleases (ZFNs), transcription activator-like effector nucleases (TALENs), and most importantly, the clustered regularly interspaced palindromic repeat (CRISPR)-associated endonuclease 9 (Cas9).[93] A series of elegant studies from the Gersbach laboratory has provided compelling proof-of-concept evidence in restoring dystrophin expression in cells from DMD patients using these new technologies.[94–96] It is highly anticipated that genome editing will soon be used to treat skeletal muscle disease and cardiomyopathy in animal models of DMD.[97]

### **3.2. Disease gene-based therapy for cardiomyopathy in other muscular dystrophies**

#### **3.2.1. Targeting disease gene to treat LGMD cardiomyopathy**

LGMD refers to a group of muscle disorders with a wide range of clinical and genetic heterogeneity.[98,99] Based on the inheritance pattern, they are classified as autosomal dominant type 1 (LGMD1) and autosomal recessive type 2 (LGMD2). Each type of LGMD is further classified according to the time the disease gene was discovered. For LGMD1, the goal of the gene therapy is to decrease the expression of the mutated gene. This can be achieved with RNA interference (RNAi) to silence the mutated gene.[100,101] So far, only one study has tested gene therapy for dominant LGMD. LGMD1A is caused by myotilin gene mutation. Liu et al. targeted mutant myotilin with an AAV-6 microRNA vector.[102] The treatment significantly reduced the expression of the mutated myotilin protein and ameliorated skeletal muscle myopathy. Although LGMD1A patients do not exhibit cardiac abnormalities,[4] the RNAi approach described by Liu et al. may treat cardiac manifestations in other dominant myopathies such as lamin A/C gene mutation-induced LGMD1B and Emery–Dreifuss muscular dystrophy.

There has been significant progress in LGMD2 gene therapy. AAV-mediated gene therapy has been tested in animal models of at least seven different subtypes of LGMD2 (2A to 2F, and 2I). LGMD2A and 2B are caused by mutations in the calpain-3 gene and the dysferlin

gene, respectively. According to Hermans, LGMD2A and 2B do not show cardiac manifestations.[4] However, cardiomyopathy has been seen in dysferlin-deficient mice, and there are also a few reports of cardiac involvement in some LGMD2B patients.[103–106] Three different approaches have been explored to express a functional dysferlin gene. These include delivering a minimized dysferlin gene with a single AAV vector, delivering a full-length dysferlin cDNA with dual AAV vectors, and exon-skipping or pre-mRNA trans-splicing to repair the defective dysferlin RNA transcript.[107–113] Defective membrane repair has been considered as the major pathogenic mechanism for LGMD2B. The in vitro membrane repair assay has been used as a surrogate endpoint to evaluate the therapeutic efficacy. Surprisingly, a recent study by Lostal et al. found that a correction of membrane repair as measured by the in vitro assay did not correlate with the correction of muscle pathology. The authors overexpressed myoferlin, a homolog of dysferlin, in dysferlin-null mice by the transgenic approach and they also expressed the mini-dysferlin gene in 4-week-old dysferlin-null mice. Neither transgenic overexpression of myoferlin nor AAV-mediated expression of mini-dysferlin improved muscle histology, although both corrected membrane repair deficits in vitro.[114]

LGMD2C to 2F are often referred to as sarcoglycanopathies, because they are caused by mutations in the sarcoglycan genes. The most common sarcoglycanopathy is  $\alpha$ -sarcoglycan-deficient LGMD2D. Cardiac involvement is rare in LGMD2D.[6] LGMD2C, which is caused by mutations in the  $\gamma$ -sarcoglycan gene, usually exhibits mild cardiomyopathy. Deficiency of  $\beta$ -sarcoglycan and  $\delta$ -sarcoglycan results in LGMD2E and LGMD2F, respectively. These two diseases are associated with dilated cardiomyopathy.[3,6] The molecular weights of sarcoglycans are in the range of 35–50 kD. The small size makes sarcoglycan genes perfect candidates for AAV delivery. Sarcoglycanopathies were among the first few inherited diseases proposed for AAV gene therapy.[115] Recently, AAV gene therapy for LGMD2C and 2D has entered into clinical trials.[116–118] Very few studies have explored AAV  $\beta$ -sarcoglycan gene transfer for treating LGMD2E.[119,120] However, therapeutic delivery of the  $\delta$ -sarcoglycan gene by AAV has been tested extensively in the mouse and hamster models of LGMD2F. Systemic or direct myocardial delivery of the  $\delta$ -sarcoglycan gene not only reduced histological lesions in the heart (such as myocardial necrosis, inflammation, calcification, and fibrosis) but also improved heart function and extended lifespan.[38,121–125] Collectively, these preclinical studies suggest that AAV  $\delta$ -sarcoglycan gene transfer is an effective treatment for dilated cardiomyopathy in LGMD2F.

LGMD2I is caused by mutations in the fukutin-related protein (FKRP) gene. FKRP is located in the Golgi apparatus, and it is essential for post-translational glycosylation of  $\alpha$ -dystroglycan, the protein that directly interacts with the extracellular matrix in the DGC complex. More than half of LGMD2I patients have cardiac abnormalities, and a quarter of them develop heart failure.[126] Gene therapy for LGMD2I has been hindered by the lack of a good animal model. Nonsense mutations and whole-gene deletions are embryonically lethal.[127] To overcome this hurdle, Lu and colleagues recently generated an FKRP L276I knock-in mouse.[128] This nonsense mutation model mimics the clinical phenotype of LGMD2I. To determine whether systemic delivery of the FKRP gene with AAV can protect the heart, Qiao et al. performed intraperitoneal injection in newborn FKRP L276I knock-in mice using an AAV-8 vector. Dobutamine-stressed echocardiography in 7-month-old treated mice showed significantly higher ejection fraction and fractional shortening than those of untreated mice.[128]

### 3.2.2. Targeting disease gene to treat heart disease in other muscular dystrophies

Dystroglycanopathies are a group of congenital muscular dystrophies (MDC). They are caused by mutations in the genes involved in the glycosylation pathway of  $\alpha$ -dystroglycan.[129,130] Fukuyama muscular dystrophy, a dystroglycanopathy caused by retrotransposon insertion in the 3'-untranslated region of the fukutin gene, is associated with severe cardiomyopathy and congestive heart failure.[131,132] Blockade of pathogenic exon-trapping by a cocktail of AONs restored fukutin expression and  $\alpha$ -dystroglycan glycosylation in the mouse model and human cells.[132] Whether this therapy can rescue heart function remains to be determined by future studies.

FKRP gene mutation not only causes LGMD2I but also causes MDC type 1C (MDC1C). Similar to LGMD2I, cardiac involvement is also a frequent finding in MDC1C patients.[133] A mouse model for MDC1C has been generated with FKRP P448L knock-in.[134] AAV-9 mediated FKRP expression normalized  $\alpha$ -dystroglycan glycosylation in the heart of MDC1C mice. Unfortunately, cardiac function was not assessed due to mild heart disease at the age of euthanization (5 months).[134]

Myotonic dystrophy (DM), the second most common muscular dystrophy, is an autosomal dominant disease. It is caused by pathogenic RNA gain-of-function toxicity due to CTG (for DM1) or CCTG (for DM2) expansion. Cardiac conduction deficits (conduction block and arrhythmia) contribute significantly to the morbidity

and mortality.[135] About 20 different mouse models have been developed to reveal various aspects of the disease.[136] Among these, tamoxifen-inducible EpA960 mice and tetracycline-inducible GFP-DMPK-(CTG)<sub>5</sub> mice are considered as good models to test cardiac interventions for DM.[137,138] The field of DM gene therapy has been particularly active in recent years. RNAi, ribozyme, AONs, and more recently, site-specific RNA endonuclease have all been explored for DM gene therapy.[139–144] However, most of these studies have not examined therapeutic efficacy in the heart. The in vivo proof-of-principle for reversing cardiac conduction defects has only been shown in GFP-DMPK-(CTG)<sub>5</sub> mice. In this model, administration of doxycycline induced myotonia and cardiac conduction abnormalities. Discontinuation of doxycycline dramatically reduced myotonic symptoms and conduction block in the heart.[137]

## 4. Expanding the armory of dystrophic cardiomyopathy gene therapy by targeting pathogenic mechanisms

### 4.1. Dystrophin-independent Duchenne cardiomyopathy gene therapy

#### 4.1.1. Stabilization of cardiomyocyte membrane with endogenous cellular genes

Given that membrane weakening is a primary pathogenic mechanism, strategies that enhance sarcolemmal stability should theoretically ameliorate Duchenne cardiomyopathy. Utrophin is a dystrophin homolog.[145] Despite some differences,[43,146,147] utrophin shares significant structural and functional similarity to dystrophin and assembles the utrophin-associated glycoprotein complex (UGC). As is the case for dystrophin, micro-utrophin has been generated for AAV delivery.[40,148] More recently, AAV-mediated expression of jazz, an artificial zinc finger transcription factor, was found to activate the utrophin promoter and enhance utrophin expression.[149] So far, these utrophin-based strategies have only been shown to protect skeletal muscle. Their therapeutic efficacy in the heart remains to be tested experimentally. Several components of the DGC and UGC, including sarcoglycans, sarcospan, and nNOS, were recently shown to reduce the skeletal muscle phenotype in mdx mice.[66,150,151] Of these, only nNOS has been shown to treat Duchenne cardiomyopathy.[152] Specifically, Lai et al. delivered a PDZ domain-truncated version of the nNOS gene to the heart of 14-month-old mdx mice and examined the cardiac phenotype when mice reached 21 months of age. Supraphysiological  $\Delta$ PDZ-nNOS expression significantly

reduced myocardial fibrosis, inflammation, and apoptosis. Importantly, treatment partially ameliorated ECG abnormalities and improved hemodynamic performance.[152]

Besides the DGC and UGC, the integrin complex (especially  $\alpha 7\beta 1$ ) is another membrane-crossing complex that stabilizes the sarcolemma.[153] Expression of the  $\alpha 7$ -integrin gene by AAV was recently shown to reduce limb muscle disease in mdx mice and extend the life span of u-dko mice.[154,155] The cardiac benefit of AAV-mediated  $\alpha 7$ -integrin expression remains to be demonstrated.

#### 4.1.2. Treating Duchenne cardiomyopathy with calcium-regulating genes

Cytosolic calcium overload is a pivotal pathogenic event leading to muscle damage and force reduction in DMD.[156] Restoring calcium homeostasis holds great promise for treating Duchenne cardiomyopathy. The sarco/endoplasmic reticulum calcium ATPase (SERCA) is a calcium pump that removes calcium from the cytosol and transports it into the lumen of the sarcoplasmic reticulum (SR). SERCA accounts for  $\geq 70\%$  of calcium removal from the cytosol in muscle cells. SERCA2a is expressed in the heart and slow-twitch skeletal muscle. We found that SERCA2a expression is reduced in the heart of mdx mice by immunostaining.[157] When the AAV-9 SERCA2a vector was delivered to the heart of 12-m-old mdx mice, it increased myocardial SERCA2a expression and significantly improved cardiac electrophysiology.[157] Encouragingly, similar protection was observed when the AAV-9 SERCA2a vector was administered to terminal-aged (22-m-old) mdx mice.[158]

#### 4.1.3. Additional dystrophin-independent gene therapy strategies

Besides strengthening the sarcolemma and restoring calcium homeostasis, investigators have explored many other creative gene therapy strategies that are not dependent on dystrophin. These include AAV-mediated inhibition of the myostatin pathway, AAV-mediated overexpression of peroxisome proliferator-activated receptor gamma coactivator 1-alpha (PGC-1 $\alpha$ ), the cytotoxic T cell GalNAc transferase (Galgt2) and miR486, and AAV-mediated blocking of the nuclear factor kappa-light-chain-enhancer of activated B cell (NF- $\kappa$ B) signaling pathway.[159–165] However, most of these studies only demonstrated disease amelioration in skeletal muscle. Whether cardiac muscle can be protected is yet to be seen. Among these strategies, the myostatin inhibition approach is especially intriguing, because this approach aims at increasing the muscle mass. This raises two concerns: (a) muscle hypertrophy

may increase stress on the sarcolemma and hence worsen muscle disease, and (b) myostatin inhibition may lead to hypertrophic cardiomyopathy. Indeed, conflicting results have been achieved depending on the models used. In animal models for DMD (mice and dogs), myostatin inhibition has consistently improved skeletal muscle pathology and function.[163,164,166–168] In a phase I trial, AAV-mediated regional expression of the myostatin antagonist follistatin improved walking distance in five out of six BMD patients.[169] However, the results of myostatin inhibition appear less promising in preclinical studies of some other muscular dystrophies such as LGMD2B, LGMD2C, LGMD2F, and congenital muscular dystrophy type 1A (MDC1A).[170–173] Cohn et al. examined whether myostatin deficiency can cause myocardial hypertrophy in normal C57BL/6 mice and mdx mice.[174] Surprisingly, myostatin elimination did not affect heart weight and heart weight/body weight ratio in either strain.[174] A major protective mechanism of myostatin inhibition is to reverse muscle fibrosis by inducing fibroblast apoptosis.[175] For reasons yet unknown, this mechanism appears to be deficient in the heart.[174] Collectively, there is a lack of clear evidence suggesting that myostatin blockade benefits a dystrophic heart. Myostatin inhibition-based gene therapy strategies have to be carefully weighted against potential undesirable side effects.[170–173,176]

#### 4.2. Disease gene-independent gene therapy for cardiomyopathy in other muscular dystrophies

##### 4.2.1. Disease gene-independent gene therapy for dilated cardiomyopathy in LGMD2E and 2F

MicroRNAs (miRs) are regulatory noncoding RNAs. Recent studies suggest that miRs play crucial roles in myocardial remodeling.[177] Sampaolesi and colleagues found that miR669 is downregulated in the heart of  $\beta$ -sarcoglycan-null LGMD2E mice.[178] In a subsequent study, they evaluated preventive miR gene therapy in  $\beta$ -sarcoglycan knockout mice.[179] After intraventricular delivery of an AAV-2 miR669a vector to neonates, they quantified survival, cardiac fibrosis, and function at the age of 18 months. AAV-injected mice showed less myocardial fibrosis, better heart function, and significantly better survival.[179]

Several disease gene-independent approaches have been tested to treat dilated cardiomyopathy in rodent models of LGMD2F.[25] Mitsugumin 53 (MG53) is a 53-kD membrane repair protein and also a ubiquitin E3 ligase.[180] Mice lacking MG53 show increased susceptibility to sarcolemmal injury and develop a slow but progressive myopathy.[181] He et al. introduced MG53 to neonatal and young adult LGMD2F hamsters with

AAV-8. Supraphysiological MG53 expression in the heart and limb muscle partially reduced the serum creatine kinase level, stabilized the sarcolemma, and slowed muscle degeneration and fibrosis. It also improved treadmill performance and heart function.[182] Since sarcolemmal disruption is a common pathogenic process, it is suggested that MG53 therapy may serve as a broadband therapeutic for a wide range of muscular dystrophies.[180] Unfortunately, there are some important safety concerns for long-term use. In one study, authors noticed elevation of hepatic enzymes due to leaky MG53 expression in the liver.[182] Most alarmingly, two recent studies found that the E3 ligase function of MG53 targets the muscle insulin receptor and insulin-receptor substrate 1 for degradation.[183,184] Transgenic overexpression of MG53 in striated muscle and heart resulted in metabolic syndrome and diabetic cardiomyopathy, respectively.[183,185]

Defects in SR calcium cycling play a pivotal role in the pathogenesis of inherited and acquired cardiomyopathy.[186] As eluded before, SERCA2a is the primary calcium pump in the heart. AAV-mediated SERCA2a overexpression ameliorates some cardiac manifestations in the mdx model of Duchenne cardiomyopathy.[157,158] The activity of SERCA2a is regulated by phospholamban. Unphosphorylated phospholamban inhibits SERCA2a activity but phosphorylated phospholamban does not. A single amino acid change (Ser16 Glu) locks phospholamban in a conformation that resembles the phosphorylated form. Hoshijima et al. delivered this pseudo-phosphorylated phospholamban to the heart of  $\delta$ -sarcoglycan-deficient hamsters using AAV-2.[25] Chronic expression of pseudo-phosphorylated phospholamban markedly improved heart function in this LGMD2F-dilated cardiomyopathy model.[25]

Apoptosis has been implicated in the progression of heart failure. In particular, activation of apoptosis signal-regulating kinase 1 (ASK1) induces cardiomyocytes apoptosis. Hikoso et al. tested whether delivery of the dominant mutant form of ASK1 can reduce cardiomyopathy in the LGMD2F hamster model.[187] They delivered dominant mutant ASK1 by AAV-2 via transcatheter perfusion to 10-week-old affected hamsters. Evaluation at the age of 24 weeks revealed remarkable improvements of systolic and diastolic function as well as a reduction of chamber dilation and myocardial fibrosis.

#### 4.2.2. Disease gene-independent gene therapy for cardiomyopathy in other muscular dystrophies

Merosin (laminin  $\alpha$ 2) is an extracellular matrix protein. Deficiency in merosin leads to MDC1A. Although

MDC1A patients usually do not have clinically significant cardiomyopathy,[4] cardiac involvement has been documented in atypical patients and laminin  $\alpha$ 2-null dy/dy mice.[188–191] Agrin is also an extracellular matrix protein, but it has no structural similarity to laminin  $\alpha$ 2. Interestingly, AAV-1 mediated systemic expression of a miniature version of agrin greatly reduced myocardial fibrosis in dy/dy mice.[192]

LGMD2I and MDC1C are caused by mutations in the FKR gene, and both diseases display prominent cardiac manifestations. FKR knock-in mice L276I and P448L have been developed to model LGMD2I and MDC1C, respectively.[128,134] The pathway of  $\alpha$ -dystroglycan glycosylation involves a series of glycosyltransferases. Like-acetylglucosaminyltransferase (LARGE) acts downstream of FKR. Activation of a downstream enzyme presumably should correct the disease phenotype caused by upstream enzyme deficiency. Vannoy indeed found that AAV-mediated LARGE overexpression not only reduced myopathy in LARGE-deficient MDC mice but also improved  $\alpha$ -dystroglycan glycosylation in the heart and skeletal muscle of FKR P448L knock-in mice.[193]

## 5. Expert opinion

The cloning of the dystrophin gene in 1986 started a flood of discoveries on genes whose mutations cause various forms of muscular dystrophies.[39] All of a sudden, it appears that we may cure many muscular dystrophies and their associated cardiomyopathies by either fixing the mutated gene or introducing a functional copy of the normal gene. While conceptually straightforward, the journey thus far has turned out to be long and winding. Research in dystrophic cardiomyopathy and its gene therapy has made significant progress in the last decade.[194–196] Several fundamental issues have been addressed. These include the establishment of a large collection of animal models to test experimental gene therapy in various forms of dystrophic cardiomyopathy, the development of non-invasive AAV delivery methods to efficiently transduce the heart, and the expansion of therapeutic schemes from simply delivering a functional cDNA to dystrophic muscle to the modulation of the RNA/DNA structure and expression using a variety of coding and noncoding sequences, even oligonucleotides. Some critical parameters for dystrophic cardiomyopathy gene therapy have also been clarified. For example, studies in the mdx model of Duchenne cardiomyopathy have provided compelling evidence that we may achieve a near-wild-type protection by treating half of the cardiomyocytes instead of every single cell.[63,197] On the

other hand, debates on whether treating skeletal muscle disease will alleviate or aggravate cardiomyopathy have settled down on the conclusion that both should be treated either together or separately.[76,198,199]

There is no doubt that Duchenne cardiomyopathy gene therapy has led the way for the entire field. First, a number of models have been generated for Duchenne cardiomyopathy gene therapy studies such as aged mdx mice, Cmah/mdx mice, u-dko mice, myoD/dystrophin double-knockout mice, and telomerase RNA/dystrophin double-null mdx/mTR mice.[63,64,200–204] Importantly, most of these rodent models are commercially available.[205] In terms of large animal models, besides the commonly used golden retriever muscular dystrophy dogs (GRMDs), additional dog models have been identified and colonies established.[206–209] Second, we have successfully treated the cardiac phenotype in symptomatic u-dko mice and aged mdx mice using micro-dystrophin and exon-skipping.[34,89] We even achieved widespread myocardial AAV gene transfer and some ECG improvements in terminal-stage mdx mice.[35] For scaling up, efficient myocardial transduction has been achieved in newborn dogs and adult affected dogs with systemic and percutaneous transendocardial AAV delivery.[57,91,92,210,211] Third, many previously underappreciated disease targets (such as nNOS and SERCA2a) and revolutionary technologies (such as tcDNA, ZENs, TALENs, and CRISPR/Cas9) are now on the horizon for Duchenne cardiomyopathy gene therapy. Despite this substantial progress, we still do not have answers to a lot of important questions. For example, it is not clear whether supra-physiological dystrophin expression in the heart is toxic, whether there are heart-specific domain(s) in the dystrophin gene that should be included in micro-dystrophin, and whether cardiotropic features of some existing AAV serotypes can cross the species boundary and result in efficient heart transduction in humans. For this last point, some recent developments in the generation of the xenograft model using dystrophic human muscle and forced evolution of human tissue tropic AAV capsids may provide some hints.[32,212,213] It should be noted that emerging new technologies such as genome editing with CRISPR/Cas9 not only brings in new hopes, they are also accompanied with new questions such as potential toxicity from off-target editing.

There is a long to-do list for the field of dystrophic cardiomyopathy gene therapy. Some of these may include (1) continued development and characterization of large animal models for dystrophic cardiomyopathy. In light of recent success in creating rat, pig, and monkey models using the CRISPR/Cas9 technology, model generation may no longer represent a formidable barrier as it was before [214]; (2) thorough evaluation of the most

promising gene therapy strategies in large animal models.[215] Lack of solid large animal data has been an important factor limiting the translation of rodent study results to human patients. In this regard, there is an urgent need to thoroughly evaluate therapeutic efficacy in large mammals. For example, treating heart disease with tcDNA exon-skipping and AAV micro-dystrophin gene therapy in dystrophin-deficient dogs [216]; (3) establishment of cardiac-specific biomarkers that can be used to monitor disease progression and responses to gene therapy in animal models of dystrophic cardiomyopathy; (4) investigations of gene therapy for cardiac manifestations in muscular dystrophies other than DMD and LGMD2F. For many of these muscular dystrophies, gene therapy strategies have been developed for treating skeletal muscle myopathy. We need to test if similar approaches can attenuate cardiac disease.

In summary, gene therapy for dystrophic cardiomyopathy has taken a slow but steady path toward preclinical and eventually clinical studies. These efforts will undoubtedly be complicated by issues related to vector manufacturing, host immune responses, and the lack of enough patients for large-scale clinical trials due to the relatively low incidence of the disease. Nevertheless, we already have a solid foundation. The future of dystrophic cardiomyopathy gene therapy is very bright.

### Financial and competing interests disclosure

*D Duan is a member of the scientific advisory board for Solid GT, a subsidiary of Solid Biosciences. DMD research in the Duan lab is supported by the National Institutes of Health (NS-90634 and HL91883), Department of Defense (MD130014), Muscular Dystrophy Association, Parent Project Muscular Dystrophy, Jesse's Journey-The Foundation for Gene and Cell Therapy, Hope for Javier and the University of Missouri. The authors have no other relevant affiliations or financial involvement with any organization or entity with a financial interest in or financial conflict with the subject matter or materials discussed in the manuscript. This includes employment, consultancies, honoraria, stock ownership or options, expert testimony, grants or patents received or pending, or royalties.*

### References

Papers of special note have been highlighted as either of interest (\*) or of considerable interest (\*\*\*) to readers.

1. Mercuri E, Muntoni F. Muscular dystrophies. *Lancet*. 2013;381(9869):845–860.
2. Emery AE. The muscular dystrophies. *Lancet*. 2002;359(9307):687–695.
3. Dellefave LM, McNally EM. Cardiomyopathy in neuromuscular disorders. *Prog Ped Cardio*. 2007;24:35–46.
4. Hermans MC, Pinto YM, Merkies IS, et al. Hereditary muscular dystrophies and the heart. *Neuromuscul Disord*. 2010;20(8):479–492.

5. Cox GF, Kunkel LM. Dystrophies and heart disease. *Curr Opin Cardiol.* 1997;12(3):329–343.
6. Goodwin FC, Muntoni F. Cardiac involvement in muscular dystrophies: molecular mechanisms. *Muscle Nerve.* 2005;32(5):577–588.
7. Finsterer J, Stollberger C. Cardiac involvement in primary myopathies. *Cardiology.* 2000;94(1):1–11.
8. Silva MC, Meira ZM, Gurgel Giannetti J, et al. Myocardial delayed enhancement by magnetic resonance imaging in patients with muscular dystrophy. *J Am Coll Cardiol.* 2007;49(18):1874–1879.
9. Bilchick KC, Salerno M, Plitt D, et al. Prevalence and distribution of regional scar in dysfunctional myocardial segments in Duchenne muscular dystrophy. *J Cardiovasc Magn Resonance.* 2011;13:20.
10. Tandon A, Villa CR, Hor KN, et al. Myocardial fibrosis burden predicts left ventricular ejection fraction and is associated with age and steroid treatment duration in Duchenne muscular dystrophy. *J Am Heart Assoc.* 2015;4(4):e001338.
11. Rahimov F, Kunkel LM. The cell biology of disease: cellular and molecular mechanisms underlying muscular dystrophy. *J Cell Biol.* 2013;201(4):499–510.
12. Guiraud S, Aartsma-Rus A, Vieira NM, et al. The pathogenesis and therapy of muscular dystrophies. *Annu Rev Genomics Hum Genet.* 2015;16:281–308.
13. McNally EM, Kaltman JR, Benson DW, et al. Contemporary cardiac issues in Duchenne muscular dystrophy. *Circulation.* 2015;131(18):1590–1598.
14. Wasala NB, Shin JH, Duan D. The evolution of heart gene delivery vectors. *J Gene Med.* 2011;13(10):557–565.
15. Carter BJ. Adeno-associated virus and the development of adeno-associated virus vectors: a historical perspective. *Mol Ther.* 2004;10(6):981–989.
16. Lai Y, Yue Y, Duan D. Evidence for the failure of adeno-associated virus serotype 5 to package a viral genome > or = 8.2 kb. *Mol Ther.* 2010;18(1):75–79.
17. Ghosh A, Duan D. Expanding adeno-associated viral vector capacity: a tale of two vectors. *Biotechnol Genet Eng Rev.* 2007;24:165–177.
18. Ghosh A, Yue Y, Lai Y, et al. A hybrid vector system expands aden-associated viral vector packaging capacity in a transgene independent manner. *Mol Ther.* 2008;16(1):124–130.
19. Lai Y, Yue Y, Liu M, et al. Efficient in vivo gene expression by trans-splicing adeno-associated viral vectors. *Nat Biotechnol.* 2005;23(11):1435–1439.
20. Zhang Y, Yue Y, Li L, et al. Dual AAV therapy ameliorates exercise-induced muscle injury and functional ischemia in murine models of Duchenne muscular dystrophy. *Hum Mol Genet.* 2013;22(18):3720–3729.
21. Odom GL, Gregorevic P, Allen JM, et al. Gene therapy of mdx mice with large truncated dystrophins generated by recombination using rAAV6. *Mol Ther.* 2011;19(1):36–45.
22. Lostal W, Kodippili K, Yue Y, et al. Full-length dystrophin reconstitution with adeno-associated viral vectors. *Hum Gene Ther.* 2014;25(6):552–562.
23. Toyo-oka T, Kawada T, Xi H, et al. Gene therapy prevents disruption of dystrophin-related proteins in a model of hereditary dilated cardiomyopathy in hamsters. *Heart Lung Circ.* 2002;11(3):174–181.
24. Yue Y, Li Z, Harper SQ, et al. Microdystrophin gene therapy of cardiomyopathy restores dystrophin-glycoprotein complex and improves sarcolemma integrity in the mdx mouse heart. *Circulation.* 2003;108(13):1626–1632.
  - **This is the first study demonstrating the potential of micro-dystrophin gene therapy to treat Duchenne cardiomyopathy in an animal model.**
25. Hoshijima M, Ikeda Y, Iwanaga Y, et al. Chronic suppression of heart-failure progression by a pseudophosphorylated mutant of phospholamban via in vivo cardiac rAAV gene delivery. *Nat Med.* 2002;8(8):864–871.
  - **This study suggests that restoration of calcium homeostasis in the heart is a promising strategy to treat dystrophic cardiomyopathy.**
26. Li J, Wang D, Qian S, et al. Efficient and long-term intracardiac gene transfer in delta-sarcoglycan-deficiency hamster by adeno-associated virus-2 vectors. *Gene Ther.* 2003;10(21):1807–1813.
27. Kotterman MA, Schaffer DV. Engineering adeno-associated viruses for clinical gene therapy. *Nat Rev Genet.* 2014;15(7):445–451.
28. Gregorevic P, Blankinship MJ, Allen JM, et al. Systemic delivery of genes to striated muscles using adeno-associated viral vectors. *Nat Med.* 2004;10(8):828–834.
  - **This is the first study demonstrating systemic gene delivery in an animal model of muscular dystrophy.**
29. Wang Z, Zhu T, Qiao C, et al. Adeno-associated virus serotype 8 efficiently delivers genes to muscle and heart. *Nat Biotechnol.* 2005;23(3):321–328.
30. Pacak CA, Mah CS, Thattaliyath BD, et al. Recombinant adeno-associated virus serotype 9 leads to preferential cardiac transduction in vivo. *Circ Res.* 2006;99(4):e3–9.
31. Bostick B, Ghosh A, Yue Y, et al. Systemic AAV-9 transduction in mice is influenced by animal age but not by the route of administration. *Gene Ther.* 2007;14(22):1605–1609.
32. Nance ME, Duan D. Perspective on adeno-associated virus (AAV) capsid modification for Duchenne muscular dystrophy gene therapy. *Hum Gene Ther.* 2015 Oct 15. [Epub ahead of print].
33. Zincarelli C, Soltys S, Rengo G, et al. Analysis of AAV serotypes 1–9 mediated gene expression and tropism in mice after systemic injection. *Mol Ther.* 2008;16(6):1073–1080.
34. Bostick B, Shin J-H, Yue Y, et al. AAV-microdystrophin therapy improves cardiac performance in aged female mdx mice. *Mol Ther.* 2011;19(10):1826–1832.
  - **This is the first study demonstrating improvement of cardiac contractility following AAV-mediated micro-dystrophin gene therapy in a model of dilated Duchenne cardiomyopathy.**
35. Bostick B, Shin JH, Yue Y, et al. AAV micro-dystrophin gene therapy alleviates stress-induced cardiac death but not myocardial fibrosis in >21-m-old mdx mice, an end-stage model of Duchenne muscular dystrophy cardiomyopathy. *J Mol Cell Cardiol.* 2012;53(2):217–222.
  - **This study demonstrates that AAV micro-dystrophin gene therapy can reduce stress-induced cardiac death in terminal-aged mdx mice.**
36. Bostick B, Yue Y, Lai Y, et al. Adeno-associated virus serotype-9 microdystrophin gene therapy ameliorates

- electrocardiographic abnormalities in mdx mice. *Hum Gene Ther.* 2008;19(8):851–856.
37. Ying Y, Muller OJ, Goehringer C, et al. Heart-targeted adeno-associated viral vectors selected by in vivo bio-panning of a random viral display peptide library. *Gene Ther.* 2010;17(8):980–990.
38. Yang L, Jiang J, Drouin LM, et al. A myocardium tropic adeno-associated virus (AAV) evolved by DNA shuffling and in vivo selection. *Proc Natl Acad Sci USA.* 2009;106(10):3946–3951.
39. Kunkel LM. 2004 William Allan award address. cloning of the DMD gene. *Am J Hum Genet.* 2005;76(2):205–214.
- **This article provides an excellent review on the cloning of the dystrophin gene.**
40. Lai Y, Zhao J, Yue Y, et al. alpha2 and alpha3 helices of dystrophin R16 and R17 frame a microdomain in the alpha1 helix of dystrophin R17 for neuronal NOS binding. *Proc Natl Acad Sci USA.* 2013;110(2):525–530.
41. Lai Y, Thomas GD, Yue Y, et al. Dystrophins carrying spectrin-like repeats 16 and 17 anchor nNOS to the sarcolemma and enhance exercise performance in a mouse model of muscular dystrophy. *J Clin Invest.* 2009;119(3):624–635.
- **This study demonstrates the importance of dystrophin spectrin-like repeats 16 and 17 for Duchenne muscular dystrophy gene therapy.**
42. Rybakova IN, Amann KJ, Ervasti JM. A new model for the interaction of dystrophin with F-actin. *J Cell Biol.* 1996;135(3):661–672.
43. Belanto JJ, Mader TL, Eckhoff MD, et al. Microtubule binding distinguishes dystrophin from utrophin. *Proc Natl Acad Sci USA.* 2014;111(15):5723–5728.
44. England SB, Nicholson LV, Johnson MA, et al. Very mild muscular dystrophy associated with the deletion of 46% of dystrophin. *Nature.* 1990;343(6254):180–182.
- **This study demonstrates for the first time that an abbreviated dystrophin gene may benefit DMD patients.**
45. Phelps SF, Hauser MA, Cole NM, et al. Expression of full-length and truncated dystrophin mini-genes in transgenic mdx mice. *Hum Mol Genet.* 1995;4(8):1251–1258.
46. Wells DJ, Wells KE, Asante EA, et al. Expression of human full-length and minidystrophin in transgenic mdx mice: implications for gene therapy of Duchenne muscular dystrophy. *Hum Mol Genet.* 1995;4(8):1245–1250.
47. Harper SQ, Hauser MA, DelloRusso C, et al. Modular flexibility of dystrophin: implications for gene therapy of Duchenne muscular dystrophy. *Nat Med.* 2002;8(3):253–261.
- **This study reveals the critical structure-function relationship of the dystrophin gene and the implication for Duchenne muscular dystrophy gene therapy.**
48. Bostick B, Yue Y, Long C, et al. Cardiac expression of a mini-dystrophin that normalizes skeletal muscle force only partially restores heart function in aged mdx mice. *Mol Ther.* 2009;17(2):253–261.
49. Lai Y, Yue Y, Bostick B, et al. Delivering large therapeutic genes for muscle gene therapy. In: Duan D, ed. *Muscle gene therapy.* New York (NY): Springer Science + Business Media, LLC; 2010. p. 205–218.
50. Duan D. From the smallest virus to the biggest gene: marching towards gene therapy for Duchenne muscular dystrophy. *Discov Med.* 2006;6(33):103–108.
51. Zhang Y, Duan D. Novel mini-dystrophin gene dual adeno-associated virus vectors restore neuronal nitric oxide synthase expression at the sarcolemma. *Hum Gene Ther.* 2012;23(1):98–103.
52. Ghosh A, Yue Y, Duan D. Efficient transgene reconstitution with hybrid dual AAV vectors carrying the minimized bridging sequence. *Hum Gene Ther.* 2011;22(1):77–83.
53. Ghosh A, Yue Y, Shin J-H, et al. Systemic trans-splicing AAV delivery efficiently transduces the heart of adult mdx mouse, a model for Duchenne muscular dystrophy. *Hum Gene Ther.* 2009;20(11):1319–1328.
54. Gregorevic P, Allen JM, Minami E, et al. rAAV6-microdystrophin preserves muscle function and extends lifespan in severely dystrophic mice. *Nat Med.* 2006;12(7):787–789.
55. Wang B, Li J, Xiao X. Adeno-associated virus vector carrying human minidystrophin genes effectively ameliorates muscular dystrophy in mdx mouse model. *Proc Natl Acad Sci USA.* 2000;97(25):13714–13719.
56. Liu M, Yue Y, Harper SQ, et al. Adeno-associated virus-mediated microdystrophin expression protects young mdx muscle from contraction-induced injury. *Mol Ther.* 2005;11(2):245–256.
57. Yue Y, Pan X, Hakim CH, et al. Safe and bodywide muscle transduction in young adult Duchenne muscular dystrophy dogs with adeno-associated virus. *Hum Mol Genet.* 2015;24(20):5880–5890.
- **This study opens the door of systemic AAV gene therapy in a large mammal with muscular dystrophy.**
58. Shin JH, Pan X, Hakim CH, et al. Microdystrophin ameliorates muscular dystrophy in the canine model of Duchenne muscular dystrophy. *Mol Ther.* 2013;21(4):750–757.
59. Koo T, Okada T, Athanasopoulos T, et al. Long-term functional adeno-associated virus-microdystrophin expression in the dystrophic CXMDj dog. *J Gene Med.* 2011;13(9):497–506.
60. Townsend D, Blankinship MJ, Allen JM, et al. Systemic administration of micro-dystrophin restores cardiac geometry and prevents dobutamine-induced cardiac pump failure. *Mol Ther.* 2007;15(6):1086–1092.
61. Schinkel S, Bauer R, Bekeredjian R, et al. Long-term preservation of cardiac structure and function after adeno-associated virus serotype 9-mediated microdystrophin gene transfer in mdx mice. *Hum Gene Ther.* 2012;23(6):566–575.
62. Shin JH, Nitahara-Kasahara Y, Hayashita-Kinoh H, et al. Improvement of cardiac fibrosis in dystrophic mice by rAAV9-mediated microdystrophin transduction. *Gene Ther.* 2011;18(9):910–919.
63. Bostick B, Yue Y, Long C, et al. Prevention of dystrophin-deficient cardiomyopathy in twenty-one-month-old carrier mice by mosaic dystrophin expression or complementary dystrophin/utrophin expression. *Circ Res.* 2008;102(1):121–130.
- **This study demonstrates that genetic correction of 50% cardiomyocytes may be sufficient to treat dystrophic cardiomyopathy. This study also demonstrates that aged female mdx mice have dilated cardiomyopathy.**
64. Bostick B, Yue Y, Duan D. Gender influences cardiac function in the mdx model of Duchenne cardiomyopathy. *Muscle Nerve.* 2010;42(4):600–603.

65. Chamberlain JS, Metzger J, Reyes M, et al. Dystrophin-deficient mdx mice display a reduced life span and are susceptible to spontaneous rhabdomyosarcoma. *Faseb J*. 2007;21(9):2195–2204.
66. Li D, Long C, Yue Y, et al. Sub-physiological sarcoglycan expression contributes to compensatory muscle protection in mdx mice. *Hum Mol Genet*. 2009;18(7):1209–1220.
67. Aartsma-Rus A. Overview on DMD exon skipping. *Methods Mol Biol*. 2012;867:97–116.
68. Goemans NM, Tulinius M, Van Den Akker JT, et al. Systemic Administration of PRO051 in Duchenne's Muscular Dystrophy. *N Engl J Med*. 2011;364(16):1513–1522.
69. Van Deutekom JC, Janson AA, Ginjaar IB, et al. Local dystrophin restoration with antisense oligonucleotide PRO051. *N Engl J Med*. 2007;357(26):2677–2686.
- **This is the first study demonstrating exon-skipping in human patients.**
70. Cirak S, Arechavala-Gomez V, Guglieri M, et al. Exon skipping and dystrophin restoration in patients with Duchenne muscular dystrophy after systemic phosphorodiamidate morpholino oligomer treatment: an open-label, phase 2, dose-escalation study. *Lancet*. 2011;378(9791):595–605.
71. Kinali M, Arechavala-Gomez V, Feng L, et al. Local restoration of dystrophin expression with the morpholino oligomer AVI-4658 in Duchenne muscular dystrophy: a single-blind, placebo-controlled, dose-escalation, proof-of-concept study. *Lancet Neurol*. 2009;8(10):918–928.
72. Mendell J, Rodino-Klapac LR, Sahenk Z, et al. Eteplirsen for the treatment of Duchenne muscular dystrophy. *Ann Neurol*. 2013;74(5):637–647.
73. Voit T, Topaloglu H, Straub V, et al. Safety and efficacy of drisapersen for the treatment of Duchenne muscular dystrophy (DEMAND II): an exploratory, randomised, placebo-controlled phase 2 study. *Lancet Neurol*. 2014;13(10):987–996.
74. Alter J, Lou F, Rabinowitz A, et al. Systemic delivery of morpholino oligonucleotide restores dystrophin expression bodywide and improves dystrophic pathology. *Nat Med*. 2006;12(2):175–177.
75. Malerba A, Boldrin L, Dickson G. Long-term systemic administration of unconjugated morpholino oligomers for therapeutic expression of dystrophin by exon skipping in skeletal muscle: implications for cardiac muscle integrity. *Nucleic Acid Ther*. 2011;21(4):293–298.
76. Crisp A, Yin H, Goyenvalle A, et al. Diaphragm rescue alone prevents heart dysfunction in dystrophic mice. *Hum Mol Genet*. 2011;20(3):413–421.
77. Wu B, Moulton HM, Iversen PL, et al. Effective rescue of dystrophin improves cardiac function in dystrophin-deficient mice by a modified morpholino oligomer. *Proc Natl Acad Sci USA*. 2008;105(39):14814–14819.
78. Yin H, Lu Q, Wood M. Effective exon skipping and restoration of dystrophin expression by peptide nucleic acid antisense oligonucleotides in mdx mice. *Mol Ther*. 2008;16(1):38–45.
79. Yin H, Moulton HM, Seow Y, et al. Cell-penetrating peptide-conjugated antisense oligonucleotides restore systemic muscle and cardiac dystrophin expression and function. *Hum Mol Genet*. 2008;17(24):3909–3918.
80. Jearawiriyapaisarn N, Moulton HM, Buckley B, et al. Sustained dystrophin expression induced by peptide-conjugated morpholino oligomers in the muscles of mdx mice. *Mol Ther*. 2008;16(9):1624–1629.
81. Wu B, Li Y, Morcos PA, et al. Octa-guanidine morpholino restores dystrophin expression in cardiac and skeletal muscles and ameliorates pathology in dystrophic mdx mice. *Mol Ther*. 2009;17(5):864–871.
82. Ferlini A, Sabatelli P, Fabris M, et al. Dystrophin restoration in skeletal, heart and skin arrector pili smooth muscle of mdx mice by ZM2 NP-AON complexes. *Gene Ther*. 2010;17(3):432–438.
83. Jearawiriyapaisarn N, Moulton HM, Sazani P, et al. Long-term improvement in mdx cardiomyopathy after therapy with peptide-conjugated morpholino oligomers. *Cardiovasc Res*. 2010;85(3):444–453.
84. Yin H, Moulton HM, Betts C, et al. A fusion peptide directs enhanced systemic dystrophin exon skipping and functional restoration in dystrophin-deficient mdx mice. *Hum Mol Genet*. 2009;18(22):4405–4414.
85. Yin H, Moulton HM, Betts C, et al. Functional rescue of dystrophin-deficient mdx mice by a chimeric peptide-PMO. *Mol Ther*. 2010;18(10):1822–1829.
86. Yin H, Saleh AF, Betts C, et al. Pip5 transduction peptides direct high efficiency oligonucleotide-mediated dystrophin exon skipping in heart and phenotypic correction in mdx mice. *Mol Ther*. 2011;19(7):1295–1303.
87. Wu B, Xiao B, Cloer C, et al. One-year treatment of morpholino antisense oligomer improves skeletal and cardiac muscle functions in dystrophic mdx mice. *Mol Ther*. 2011;19(3):576–583.
88. Amantana A, Moulton HM, Cate ML, et al. Pharmacokinetics, biodistribution, stability and toxicity of a cell-penetrating peptide-morpholino oligomer conjugate. *Bioconjug Chem*. 2007;18(4):1325–1331.
89. Goyenvalle A, Griffith G, Babbs A, et al. Functional correction in mouse models of muscular dystrophy using exon-skipping tricyclo-DNA oligomers. *Nat Med*. 2015;21(3):270–275.
- **This study demonstrates that newly developed tricyclo oligomers can significantly improve exon-skipping in animal models of muscular dystrophy.**
90. Goyenvalle A, Babbs A, Wright J, et al. Rescue of severely affected dystrophin/utrophin-deficient mice through scAAV-U7snRNA-mediated exon skipping. *Hum Mol Genet*. 2012;21(11):2559–2571.
91. Bish LT, Sleeper MM, Forbes SC, et al. Long-term restoration of cardiac dystrophin expression in golden retriever muscular dystrophy following rAAV6-mediated exon skipping. *Mol Ther*. 2012;20(3):580–589.
- **This study suggests that AAV-mediated exon-skipping can treat dystrophic cardiomyopathy in a large animal model.**
92. Barbash IM, Cecchini S, Faranesh AZ, et al. MRI roadmapped transendocardial delivery of exon-skipping recombinant adeno-associated virus restores dystrophin expression in a canine model of Duchenne muscular dystrophy. *Gene Ther*. 2013;20(3):274–282.
93. Gaj T, Gersbach CA, Barbas CF 3rd. ZFN, TALEN, and CRISPR/Cas-based methods for genome engineering. *Trends Biotechnol*. 2013;31(7):397–405.

94. Ousterout DG, Kabadi AM, Thakore PI, et al. Multiplex CRISPR/Cas9-based genome editing for correction of dystrophin mutations that cause Duchenne muscular dystrophy. *Nat Commun*. 2015;6:6244.
- **This study demonstrates the feasibility of genome editing as a therapy for Duchenne muscular dystrophy.**
95. Ousterout DG, Kabadi AM, Thakore PI, et al. Correction of dystrophin expression in cells from Duchenne muscular dystrophy patients through genomic excision of exon 51 by zinc finger nucleases. *Mol Ther*. 2015;23(3):523–532.
96. Ousterout DG, Perez-Pinera P, Thakore PI, et al. Reading frame correction by targeted genome editing restores dystrophin expression in cells from Duchenne muscular dystrophy patients. *Mol Ther*. 2013;21(9):1718–1726.
97. Nelson CE, Ousterout DG, Robinson-Hamm J, et al. Correction of the dystrophin gene by the CRISPR/Cas9 system in a mouse model of muscular dystrophy. *Mol Ther*. 2015;23(Suppl 1):S157–8.
98. Nigro V, Savarese M. Genetic basis of limb-girdle muscular dystrophies: the 2014 update. *Acta Myol*. 2014;33(1):1–12.
99. Guglieri M, Straub V, Bushby K, et al. Limb-girdle muscular dystrophies. *Curr Opin Neurol*. 2008;21(5):576–584.
100. Wallace LM, Garwick SE, Harper SQ. RNAi therapy for dominant muscular dystrophies and other myopathies. In: Duan D, ed. *Muscle gene therapy*. New York (NY): Springer Science + Business Media, LLC; 2010. p. 99–115.
101. Liu J, Harper SQ. RNAi-based gene therapy for dominant limb girdle muscular dystrophies. *Curr Gene Ther*. 2012;12(4):307–314.
102. Liu J, Wallace LM, Garwick-Coppens SE, et al. RNAi-mediated gene silencing of mutant myotilin improves myopathy in LGMD1A mice. *Mol Ther Nucleic Acids*. 2014;3:e160.
- **This study reveals the potential of using RNA interference to treat dominant muscular dystrophy.**
103. Han R, Bansal D, Miyake K, et al. Dysferlin-mediated membrane repair protects the heart from stress-induced left ventricular injury. *J Clin Invest*. 2007;117(7):1805–1813.
104. Chase TH, Cox GA, Burzenski L, et al. Dysferlin deficiency and the development of cardiomyopathy in a mouse model of limb-girdle muscular dystrophy 2B. *Am J Pathol*. 2009;175(6):2299–2308.
105. Wenzel K, Geier C, Qadri F, et al. Dysfunction of dysferlin-deficient hearts. *J Mol Med*. 2007;85(11):1203–1214.
106. Kuru S, Yasuma F, Wakayama T, et al. [A patient with limb girdle muscular dystrophy type 2B (LGMD2B) manifesting cardiomyopathy]. *Rinsho Shinkeigaku*. 2004;44(6):375–378.
107. Lostal W, Bartoli M, Bourg N, et al. Efficient recovery of dysferlin deficiency by dual adeno-associated vector-mediated gene transfer. *Hum Mol Genet*. 2010;19(10):1897–1907.
108. Krahn M, Wein N, Bartoli M, et al. A naturally occurring human minidysferlin protein repairs sarcolemmal lesions in a mouse model of dysferlinopathy. *Sci Transl Med*. 2010;2(50):50ra69.
109. Aartsma-Rus A, Singh KH, Fokkema IF, et al. Therapeutic exon skipping for dysferlinopathies? *Eur J Hum Genet*. 2010;18(8):889–894.
110. Pryadkina M, Lostal W, Bourg N, et al. A comparison of AAV strategies distinguishes overlapping vectors for efficient systemic delivery of the 6.2 kb Dysferlin coding sequence. *Molecular Ther Methods Clin Dev*. 2015;2:15009.
111. Philippi S, Lorain S, Beley C, et al. Dysferlin rescue by spliceosome-mediated pre-mRNA trans-splicing targeting introns harbouring weakly defined 3' splice sites. *Hum Mol Genet*. 2015;24(14):4049–4060.
112. Sondergaard PC, Griffin DA, Pozsgai ER, et al. AAV. Dysferlin overlap vectors restore function in dysferlinopathy animal models. *Ann Clin Transl Neurol*. 2015;2(3):256–270.
113. Wein N, Avril A, Bartoli M, et al. Efficient bypass of mutations in dysferlin deficient patient cells by antisense-induced exon skipping. *Hum Mutat*. 2010;31(2):136–142.
114. Lostal W, Bartoli M, Roudaut C, et al. Lack of correlation between outcomes of membrane repair assay and correction of dystrophic changes in experimental therapeutic strategy in dysferlinopathy. *PLoS One*. 2012;7(5):e38036.
115. Stedman H, Wilson JM, Finke R, et al. Phase I clinical trial utilizing gene therapy for limb girdle muscular dystrophy: alpha-, beta-, gamma-, or delta-sarcoglycan gene delivered with intramuscular instillations of adeno-associated vectors. *Hum Gene Ther*. 2000;11(5):777–790.
116. Herson S, Hentati F, Rigolet A, et al. A phase I trial of adeno-associated virus serotype 1-gamma-sarcoglycan gene therapy for limb girdle muscular dystrophy type 2C. *Brain*. 2012;135(Pt 2):483–492.
117. Mendell JR, Rodino-Klapac LR, Rosales XQ, et al. Sustained alpha-sarcoglycan gene expression after gene transfer in limb-girdle muscular dystrophy, type 2D. *Ann Neurol*. 2010;68(5):629–638.
118. Mendell JR, Rodino-Klapac LR, Rosales-Quintero X, et al. Limb-girdle muscular dystrophy type 2D gene therapy restores alpha-sarcoglycan and associated proteins. *Ann Neurol*. 2009;66(3):290–297.
- **This study demonstrates the therapeutic potential of AAV therapy for limb girdle muscular dystrophy in human patients.**
119. Dressman D, Araishi K, Imamura M, et al. Delivery of alpha- and beta-sarcoglycan by recombinant adeno-associated virus: efficient rescue of muscle, but differential toxicity. *Hum Gene Ther*. 2002;13(13):1631–1646.
120. Pozsgai ER, Griffin DA, Heller KN, et al. Beta-Sarcoglycan gene transfer decreases fibrosis and restores force in LGMD2E mice. *Gene Ther*. 2015 Aug 20. [Epub ahead of print].
121. Zhu T, Zhou L, Mori S, et al. Sustained whole-body functional rescue in congestive heart failure and muscular dystrophy hamsters by systemic gene transfer. *Circulation*. 2005;112(17):2650–2659.
- **This study demonstrates the feasibility of systemic AAV gene therapy to treat heart disease associated with limb girdle muscular dystrophy.**
122. Vitiello C, Faraso S, Sorrentino NC, et al. Disease rescue and increased lifespan in a model of cardiomyopathy and muscular dystrophy by combined AAV treatments. *PLoS One*. 2009;4(3):e5051.
123. Goehring C, Rutschow D, Bauer R, et al. Prevention of cardiomyopathy in delta-sarcoglycan knockout mice

- after systemic transfer of targeted adeno-associated viral vectors. *Cardiovasc Res.* 2009;82(3):404–410.
124. Kawada T, Nakazawa M, Nakauchi S, et al. Rescue of hereditary form of dilated cardiomyopathy by rAAV-mediated somatic gene therapy: amelioration of morphological findings, sarcolemmal permeability, cardiac performances, and the prognosis of TO-2 hamsters. *Proc Natl Acad Sci USA.* 2002;99(2):901–906.
  125. Hoshijima M, Hayashi T, Jeon YE, et al. Delta-sarcoglycan gene therapy halts progression of cardiac dysfunction, improves respiratory failure, and prolongs life in myopathic hamsters. *Circ Heart Fail.* 2011;4(1):89–97.
  126. Poppe M, Bourke J, Eagle M, et al. Cardiac and respiratory failure in limb-girdle muscular dystrophy 2I. *Ann Neurol.* 2004;56(5):738–741.
  127. Chan YM, Keramaris-Vrantsis E, Lidov HG, et al. Fukutin-related protein is essential for mouse muscle, brain and eye development and mutation recapitulates the wide clinical spectrums of dystroglycanopathies. *Hum Mol Genet.* 2010;19(20):3995–4006.
  128. Qiao C, Wang CH, Zhao C, et al. Muscle and heart function restoration in a limb girdle muscular dystrophy 2I (LGMD2I) mouse model by systemic FKRP gene delivery. *Mol Ther.* 2014;22(11):1890–1899.
  129. Barresi R, Campbell KP. Dystroglycan: from biosynthesis to pathogenesis of human disease. *J Cell Sci.* 2006;119(Pt 2):199–207.
  130. Godfrey C, Foley AR, Clement E, et al. Dystroglycanopathies: coming into focus. *Curr Opin Genet Dev.* 2011;21(3):278–285.
  131. Nakanishi T, Sakauchi M, Kaneda Y, et al. Cardiac involvement in Fukuyama-type congenital muscular dystrophy. *Pediatrics.* 2006;117(6):e1187–92.
  132. Taniguchi-Ikeda M, Kobayashi K, Kanagawa M, et al. Pathogenic exon-trapping by SVA retrotransposon and rescue in Fukuyama muscular dystrophy. *Nature.* 2011;478(7367):127–131.
  133. Pane M, Messina S, Vasco G, et al. Respiratory and cardiac function in congenital muscular dystrophies with alpha dystroglycan deficiency. *Neuromuscul Disord.* 2012;22(8):685–689.
  134. Xu L, Lu PJ, Wang CH, et al. Adeno-associated virus 9 mediated FKRP gene therapy restores functional glycosylation of alpha-dystroglycan and improves muscle functions. *Mol Ther.* 2013;21(10):1832–1840.
  135. Chaudhry SP, Frishman WH. Myotonic dystrophies and the heart. *Cardiol Rev.* 2012;20(1):1–3.
  136. Gomes-Pereira M, Cooper TA, Gourdon G. Myotonic dystrophy mouse models: towards rational therapy development. *Trends Mol Med.* 2011;17(9):506–517.
  137. Mahadevan MS, Yadava RS, Yu Q, et al. Reversible model of RNA toxicity and cardiac conduction defects in myotonic dystrophy. *Nat Genet.* 2006;38(9):1066–1070.
    - **This study shows the proof-of-principle for reversing cardiac defects in myotonic dystrophy.**
  138. Orengo JP, Chambon P, Metzger D, et al. Expanded CTG repeats within the DMPK 3' UTR causes severe skeletal muscle wasting in an inducible mouse model for myotonic dystrophy. *Proc Natl Acad Sci USA.* 2008;105(7):2646–2651.
  139. Klein AF, Dastidar S, Furling D, et al. Therapeutic approaches for dominant muscle diseases: highlight on myotonic dystrophy. *Curr Gene Ther.* 2015;15(4):329–337.
  140. Gao Z, Cooper TA. Antisense oligonucleotides: rising stars in eliminating RNA toxicity in myotonic dystrophy. *Hum Gene Ther.* 2013;24(5):499–507.
  141. Zhang W, Wang Y, Dong S, et al. Treatment of type 1 myotonic dystrophy by engineering site-specific RNA endonucleases that target (CUG)(n) repeats. *Mol Ther.* 2014;22(2):312–320.
  142. Wheeler TM, Leger AJ, Pandey SK, et al. Targeting nuclear RNA for in vivo correction of myotonic dystrophy. *Nature.* 2012;488(7409):111–115.
  143. Lee JE, Bennett CF, Cooper TA. RNase H-mediated degradation of toxic RNA in myotonic dystrophy type 1. *Proc Natl Acad Sci USA.* 2012;109(11):4221–4226.
  144. Wheeler TM, Sobczak K, Lueck JD, et al. Reversal of RNA dominance by displacement of protein sequestered on triplet repeat RNA. *Science.* 2009;325(5938):336–339.
  145. Blake DJ, Tinsley JM, Davies KE. Utrophin: a structural and functional comparison to dystrophin. *Brain Pathol.* 1996;6(1):37–47.
  146. Li D, Bareja A, Judge L, et al. Sarcolemmal nNOS anchoring reveals a qualitative difference between dystrophin and utrophin. *J Cell Sci.* 2010;123(Pt 12):2008–2013.
  147. Rybakova IN, Humston JL, Sonnemann KJ, et al. Dystrophin and utrophin bind actin through distinct modes of contact. *J Biol Chem.* 2006;281(15):9996–10001.
  148. Odom GL, Gregorevic P, Allen JM, et al. Microtrophin delivery through rAAV6 increases lifespan and improves muscle function in dystrophic dystrophin/utrophin-deficient mice. *Mol Ther.* 2008;16(9):1539–1545.
  149. Strimpakos G, Corbi N, Pisani C, et al. Novel adeno-associated viral vector delivering the utrophin gene regulator jazz counteracts dystrophic pathology in mdx mice. *J Cell Physiol.* 2014;229(9):1283–1291.
  150. Peter AK, Marshall JL, Crosbie RH. Sarcospan reduces dystrophic pathology: stabilization of the utrophin-glycoprotein complex. *J Cell Biol.* 2008;183(3):419–427.
  151. Wehling M, Spencer MJ, Tidball JG. A nitric oxide synthase transgene ameliorates muscular dystrophy in mdx mice. *J Cell Biol.* 2001;155(1):123–132.
  152. Lai Y, Zhao J, Yue Y, et al. Partial restoration of cardiac function with  $\Delta$ PDZ nNOS in aged mdx model of Duchenne cardiomyopathy. *Hum Mol Genet.* 2014;23(12):3189–3199.
    - **This study demonstrates the feasibility of nNOS-based gene therapy for treating Duchenne cardiomyopathy.**
  153. Burkin DJ, Kaufman SJ. The alpha7beta1 integrin in muscle development and disease. *Cell Tissue Res.* 1999;296(1):183–190.
  154. Heller KN, Montgomery CL, Janssen PM, et al. AAV-mediated overexpression of human alpha7 integrin leads to histological and functional improvement in dystrophic mice. *Mol Ther.* 2013;21(3):520–525.
  155. Heller KN, Montgomery CL, Shontz KM, et al. Human alpha7 integrin gene (ITGA7) delivered by adeno-associated virus extends survival of severely affected dystrophin/utrophin-deficient mice. *Hum Gene Ther.* 2015;26(10):647–656.
  156. Burr AR, Molkentin JD. Genetic evidence in the mouse solidifies the calcium hypothesis of myofiber

- death in muscular dystrophy. *Cell Death Differ.* 2015;22(9):1402–1412.
157. Shin JH, Bostick B, Yue Y, et al. SERCA2a gene transfer improves electrocardiographic performance in aged mdx mice. *J Transl Med.* 2011;9:132.
  158. Wasala NB, Yue Y, Duan D AAV-SERCA2a gene therapy ameliorated dystrophin phenotype in mdx mice. 2015 Association for Clinical and Translational Science (ACTS) Annual Conference. Washington (DC); 2015.
  159. Tang Y, Reay DP, Salay MN, et al. Inhibition of the IKK/NF-kappaB pathway by AAV gene transfer improves muscle regeneration in older mdx mice. *Gene Ther.* 2010;17(12):1476–1483.
  160. Yang Q, Tang Y, Imbrogno K, et al. AAV-based shRNA silencing of NF-kappaB ameliorates muscle pathologies in mdx mice. *Gene Ther.* 2012;19(12):1196–1204.
  161. Selsby JT, Morine KJ, Pendrak K, et al. Rescue of dystrophic skeletal muscle by PGC-1alpha involves a fast to slow fiber type shift in the mdx mouse. *PLoS One.* 2012;7(1):e30063.
  162. Xu R, Camboni M, Martin PT. Postnatal overexpression of the CT GalNAc transferase inhibits muscular dystrophy in mdx mice without altering muscle growth or neuromuscular development: evidence for a utrophin-independent mechanism. *Neuromuscul Disord.* 2007;17(3):209–220.
  163. Bish LT, Sleeper MM, Forbes SC, et al. Long-term systemic myostatin inhibition via liver-targeted gene transfer in golden retriever muscular dystrophy. *Hum Gene Ther.* 2011;22(12):1499–1509.
  164. Haidet AM, Rizo L, Handy C, et al. Long-term enhancement of skeletal muscle mass and strength by single gene administration of myostatin inhibitors. *Proc Natl Acad Sci USA.* 2008;105(11):4318–4322.
  165. Alexander MS, Casar JC, Motohashi N, et al. MicroRNA-486-dependent modulation of DOCK3/PDEN/AKT signaling pathways improves muscular dystrophy-associated symptoms. *J Clin Invest.* 2014;124(6):2651–2667.
  166. Bogdanovich S, Krag TO, Barton ER, et al. Functional improvement of dystrophic muscle by myostatin blockade. *Nature.* 2002;420(6914):418–421.
  167. Wagner KR, McPherron AC, Winik N, et al. Loss of myostatin attenuates severity of muscular dystrophy in mdx mice. *Ann Neurol.* 2002;52(6):832–836.
  168. Nakatani M, Takehara Y, Sugino H, et al. Transgenic expression of a myostatin inhibitor derived from follistatin increases skeletal muscle mass and ameliorates dystrophic pathology in mdx mice. *Faseb J.* 2008;22(2):477–487.
  169. Mendell JR, Sahenk Z, Malik V, et al. A phase I/IIa follistatin gene therapy trial for Becker muscular dystrophy. *Mol Ther.* 2015;23(1):192–201.
    - **This study demonstrates therapeutic potential of follistatin gene therapy in BMD patients.**
  170. Li ZF, Shelton GD, Engvall E. Elimination of myostatin does not combat muscular dystrophy in dy mice but increases postnatal lethality. *Am J Pathol.* 2005;166(2):491–497.
  171. Bogdanovich S, McNally EM, Khurana TS. Myostatin blockade improves function but not histopathology in a murine model of limb-girdle muscular dystrophy 2C. *Muscle Nerve.* 2008;37(3):308–316.
  172. Parsons SA, Millay DP, Sargent MA, et al. Age-dependent effect of myostatin blockade on disease severity in a murine model of limb-girdle muscular dystrophy. *Am J Pathol.* 2006;168(6):1975–1985.
  173. Lee YS, Lehar A, Sebald S, et al. Muscle hypertrophy induced by myostatin inhibition accelerates degeneration in dysferlinopathy. *Hum Mol Genet.* 2015;24(20):5711–5719.
  174. Cohn RD, Liang HY, Shetty R, et al. Myostatin does not regulate cardiac hypertrophy or fibrosis. *Neuromuscul Disord.* 2007;17(4):290–296.
  175. Bo Li Z, Zhang J, Wagner KR. Inhibition of myostatin reverses muscle fibrosis through apoptosis. *J Cell Sci.* 2012;125(Pt 17):3957–3965.
  176. Relizani K, Mouisel E, Giannesini B, et al. Blockade of ActRIIB signaling triggers muscle fatigability and metabolic myopathy. *Mol Ther.* 2014;22(8):1423–1433.
  177. Quiat D, Olson EN. MicroRNAs in cardiovascular disease: from pathogenesis to prevention and treatment. *J Clin Invest.* 2013;123(1):11–18.
  178. Crippa S, Cassano M, Messina G, et al. miR669a and miR669q prevent skeletal muscle differentiation in postnatal cardiac progenitors. *J Cell Biol.* 2011;193(7):1197–1212.
  179. Quattrocchi M, Crippa S, Montecchiani C, et al. Long-term miR-669a therapy alleviates chronic dilated cardiomyopathy in dystrophic mice. *J Am Heart Assoc.* 2013;2(4):e000284.
  180. Alloush J, Weisleder N. TRIM proteins in therapeutic membrane repair of muscular dystrophy. *JAMA Neurol.* 2013;70(7):928–931.
  181. Cai C, Masumiya H, Weisleder N, et al. MG53 nucleates assembly of cell membrane repair machinery. *Nat Cell Biol.* 2009;11(1):56–64.
  182. He B, Tang RH, Weisleder N, et al. Enhancing muscle membrane repair by gene delivery of MG53 ameliorates muscular dystrophy and heart failure in delta-sarcoglycan-deficient hamsters. *Mol Ther.* 2012;20(4):727–735.
  183. Song R, Peng W, Zhang Y, et al. Central role of E3 ubiquitin ligase MG53 in insulin resistance and metabolic disorders. *Nature.* 2013;494(7437):375–379.
  184. Yi JS, Park JS, Ham YM, et al. MG53-induced IRS-1 ubiquitination negatively regulates skeletal myogenesis and insulin signalling. *Nat Commun.* 2013;4:2354.
  185. Liu F, Song R, Feng Y, et al. Upregulation of MG53 induces diabetic cardiomyopathy through transcriptional activation of peroxisome proliferation-activated receptor alpha. *Circulation.* 2015;131(9):795–804.
  186. Hoshijima M, Knoll R, Pashmforoush M, et al. Reversal of calcium cycling defects in advanced heart failure toward molecular therapy. *J Am Coll Cardiol.* 2006;48(9 Suppl 1):A15–23.
  187. Hikoso S, Ikeda Y, Yamaguchi O, et al. Progression of heart failure was suppressed by inhibition of apoptosis signal-regulating kinase 1 via transcortical gene transfer. *J Am Coll Cardiol.* 2007;50(5):453–462.
  188. Carboni N, Marrosu G, Porcu M, et al. Dilated cardiomyopathy with conduction defects in a patient with partial merosin deficiency due to mutations in the laminin-alpha2-chain gene: a chance association or a novel phenotype? *Muscle Nerve.* 2011;44(5):826–828.
  189. Spyrou N, Philpot J, Foale R, et al. Evidence of left ventricular dysfunction in children with merosin-deficient congenital muscular dystrophy. *Am Heart J.* 1998;136(3):474–476.

190. Marques J, Duarte ST, Costa S, et al. Atypical phenotype in two patients with LAMA2 mutations. *Neuromuscul Disord.* 2014;24(5):419–424.
191. Rash SM, Wanitkin S, Shiota T, et al. Congenital muscular dystrophy mouse model dy/dy has hypertrophic cardiomyopathy by echocardiography. *Pediatr Res.* 1998;43:26.
192. Qiao C, Li J, Zhu T, et al. Amelioration of laminin-alpha2-deficient congenital muscular dystrophy by somatic gene transfer of miniagrin. *Proc Natl Acad Sci USA.* 2005;102(34):11999–12004.
193. Vannoy CH, Xu L, Keramaris E, et al. Adeno-associated virus-mediated overexpression of LARGE rescues alpha-dystroglycan function in dystrophic mice with mutations in the fukutin-related protein. *Hum Gene Ther Methods.* 2014;25(3):187–196.
194. Duan D. Challenges and opportunities in dystrophin-deficient cardiomyopathy gene therapy. *Hum Mol Genet.* 2006;15(Spec No 2):R253–61.
- **This is the first comprehensive review on dystrophic cardiomyopathy gene therapy.**
195. Lai Y, Duan D. Progress in gene therapy of dystrophic heart disease. *Gene Ther.* 2012;19(6):678–685.
196. Shin J-H, Bostick B, Yue Y, et al. Duchenne cardiomyopathy gene therapy. In: Duan D, ed. *Muscle gene therapy.* New York (NY): Springer Science + Business Media, LLC; 2010. p. 141–162.
197. Yue Y, Skimming JW, Liu M, et al. Full-length dystrophin expression in half of the heart cells ameliorates beta-isoproterenol-induced cardiomyopathy in mdx mice. *Hum Mol Genet.* 2004;13(15):1669–1675.
198. Townsend D, Yasuda S, Li S, et al. Emergent dilated cardiomyopathy caused by targeted repair of dystrophic skeletal muscle. *Mol Ther.* 2008;16(5):832–835.
199. Wasala NB, Bostick B, Yue Y, et al. Exclusive skeletal muscle correction does not modulate dystrophic heart disease in the aged mdx model of Duchenne cardiomyopathy. *Hum Mol Genet.* 2013;22(13):2634–2641.
200. Mourkioti F, Kustan J, Kraft P, et al. Role of telomere dysfunction in cardiac failure in Duchenne muscular dystrophy. *Nat Cell Biol.* 2013;15(8):895–904.
201. Deconinck AE, Rafael JA, Skinner JA, et al. Utrrophin-dystrophin-deficient mice as a model for Duchenne muscular dystrophy. *Cell.* 1997;90(4):717–727.
202. Grady RM, Teng H, Nichol MC, et al. Skeletal and cardiac myopathies in mice lacking utrophin and dystrophin: a model for Duchenne muscular dystrophy. *Cell.* 1997;90(4):729–738.
203. Megeney LA, Kablar B, Perry RL, et al. Severe cardiomyopathy in mice lacking dystrophin and MyoD. *Proc Natl Acad Sci USA.* 1999;96(1):220–225.
204. Chandrasekharan K, Yoon JH, Xu Y, et al. A human-specific deletion in mouse Cmah increases disease severity in the mdx model of Duchenne muscular dystrophy. *Sci Transl Med.* 2010;2(42):42ra54.
205. McGreevy JW, Hakim CH, McIntosh MA, et al. Animal models of Duchenne muscular dystrophy: from basic mechanisms to gene therapy. *Dis Model Mech.* 2015;8(3):195–213.
- **This is a comprehensive review on animal models for Duchenne muscular dystrophy.**
206. Smith BF, Kornegay JN, Duan D. Independent canine models of Duchenne muscular dystrophy due to intronic insertions of repetitive DNA. *Mol Ther.* 2007;15(Supplement 1):S51.
207. Smith BF, Wrighten R. Animal models for inherited muscle diseases. In: Duan D, ed. *Muscle gene therapy.* New York (NY): Springer Science + Business Media, LLC; 2010. p. 1–21.
208. Smith BF, Yue Y, Woods PR, et al. An intronic LINE-1 element insertion in the dystrophin gene aborts dystrophin expression and results in Duchenne-like muscular dystrophy in the corgi breed. *Lab Invest.* 2011;91(2):216–231.
209. Walmsley GL, Arechavala-Gomez V, Fernandez-Fuente M, et al. A Duchenne muscular dystrophy gene hot spot mutation in dystrophin-deficient cavalier king charles spaniels is amenable to exon 51 skipping. *PLoS One.* 2010;5(1):e8647.
210. Pan X, Yue Y, Zhang K, et al. Long-term robust myocardial transduction of the dog heart from a peripheral vein by adeno-associated virus serotype-8. *Hum Gene Ther.* 2013;24(6):584–594.
211. Pan X, Yue Y, Zhang K, et al. AAV-8 is more efficient than AAV-9 in transducing neonatal dog heart. *Hum Gene Ther Methods.* 2015;26(4):54–61.
212. Zhang Y, King OD, Rahimov F, et al. Human skeletal muscle xenograft as a new preclinical model for muscle disorders. *Hum Mol Genet.* 2014;23(12):3180–3188.
213. Lisowski L, Dane AP, Chu K, et al. Selection and evaluation of clinically relevant AAV variants in a xenograft liver model. *Nature.* 2014;506(7488):382–386.
214. Chen Y, Zheng Y, Kang Y, et al. Functional disruption of the dystrophin gene in rhesus monkey using CRISPR/Cas9. *Hum Mol Genet.* 2015;24(13):3764–3774.
215. Duan D. Duchenne muscular dystrophy gene therapy: lost in translation? *Res Rep Biol.* 2011;2:31–42.
216. Duan D. Duchenne muscular dystrophy gene therapy in the canine model. *Hum Gene Ther Clin Dev.* 2015;26(1):57–69.

# Dystrophin Gene Replacement and Gene Repair Therapy for Duchenne Muscular Dystrophy in 2016: An Interview

Dongsheng Duan\*

Department of Molecular Microbiology and Immunology & Department of Neurology, School of Medicine, and Department of Bioengineering, The University of Missouri, Columbia, Missouri.

After years of relentless efforts, gene therapy has now begun to deliver its therapeutic promise in several diseases. A number of gene therapy products have received regulatory approval in Europe and Asia. Duchenne muscular dystrophy (DMD) is an X-linked inherited lethal muscle disease. It is caused by mutations in the *dystrophin* gene. Replacing and/or repairing the mutated *dystrophin* gene holds great promises to treated DMD at the genetic level. Last several years have evidenced significant developments in preclinical experimentations in murine and canine models of DMD. There has been a strong interest in moving these promising findings to clinical trials. In light of rapid progress in this field, the Parent Project Muscular Dystrophy (PPMD) recently interviewed me on the current status of DMD gene therapy and readiness for clinical trials. Here I summarized the interview with PPMD.

**Parent Project Muscular Dystrophy (PPMD):** What is gene therapy?

**Dr. Dongsheng Duan:** Gene therapy refers to therapies that use nucleic acids as the “drug” to treat and/or prevent inherited or acquired diseases. Nucleic acids can be DNA, RNA, or oligonucleotides. Nucleic acids can be naked or encapsidated in a viral or nonviral carrier.

Gene therapy can be classified as either disease gene-dependent or disease gene-independent therapies. In the former, treatment aims at the gene that encodes the protein (in the case of Duchenne, this would be dystrophin). The mutated gene can be repaired or replaced. In the case of dominant mutation, the mutated gene can be silenced. Disease gene-independent therapies take advantage of disease-modifying genes that either are functional substitutes of the diseased gene or are genes that intervening downstream pathogenic processes (in the case of Duchenne, utrophin and follistatin are examples of gene-independent therapies). Disease gene-independent therapies also involve strategies that target noncoding region of the genome (such as microRNA therapy).

**PPMD:** Can you define the key terminology used in gene therapy—such as transgene, serotype, and vector?

**Dr. Duan:** A transgene means the gene that is being transferred. In the context of gene therapy, it usually refers to the gene that is used for therapy. For example, Duchenne muscular dystrophy (DMD) is caused by mutations in the *dystrophin* gene. A functional *dystrophin* gene can thus be transferred to diseased muscle cells to treat DMD. Here the transgene is the normal dystrophin gene.

In the context of gene therapy, a vector means the vehicle that is used to transport the nucleic acid “drug” to target cells. Gene therapy vectors are classified as viral vectors (meaning they are derived from a virus) or nonviral vectors (meaning they are not derived from a virus). Some of the most commonly used viral vectors include adeno-associated virus (AAV), adenovirus, retrovirus, and lentivirus.

The serotype refers to the serologically distinguishable feature of a virus. When a virus infects our body, the body will generate a unique set of antibodies against the invading virus. These antibodies can be detected in the serum. A virus can thus be classified into different types according to the antibodies detected in the serum. The serotype is often used to classify different members of the same family virus. For example, the family of AAV virus has different serotypes such as AAV serotype-1, 2, 8, and 9 (abbreviated as AAV-1, 2, 8, and 9).

\*Correspondence: Dr. Dongsheng Duan, Department of Molecular Microbiology and Immunology, One Hospital Drive, Columbia, MO 65212. E-mail: duand@missouri.edu

**PPMD:** How is a gene therapy vector delivered to the cells where it is needed and what does it do once there?

**Dr. Duan:** A gene therapy vector can be delivered to our cells either *ex vivo* or *in vivo*. In *ex vivo* delivery, investigators first isolate the target cells (e.g., bone marrow stem cells) from the body. They then mix the target cells and the vector in a container outside the body (e.g., in a petri dish) to allow the vector to get into the cells. The cells that carry the vector are then isolated and put back to the body. *In vivo* delivery refers to directly deliver the vector to the body. This can be achieved either locally to a specific location (e.g., via intramuscular injection to a muscle) or systemically to whole body (e.g., via intravenous injection).

After a vector is delivered to a tissue, the vector will enter the cell through receptors and co-receptors that are located on the surface of the cell. Once inside the cell, the vector will release the therapeutic gene it carries into the nucleus. In a typical AAV vector, the therapeutic gene is in a single-stranded DNA format. This format cannot direct cells to make the protein. In order to express the protein, the incoming AAV genome has to be converted to a double-stranded transcription-competent DNA molecule. The vast majority of the AAV genome is converted into a double-stranded sealed circle. A very tiny fraction of AAV may integrate into the chromosome. Most often, it does not cause a safety concern.<sup>1</sup> However, in a retroviral or lentiviral vector, the vector genome enters the cell as an RNA molecule. The RNA molecule is subsequently reverse transcribed into a DNA molecule and integrates into the chromosome. The integration of a retroviral vector in the human genome has been shown to cause leukemia in several clinical trials.<sup>2,3</sup> A new generation of retro/lentiviral vectors has been developed to minimize this safety concern.<sup>4</sup>

**PPMD:** There appears to be considerable progress recently in developing gene therapy for several genetic disorders. Can you give us some insights into that progress in eye and blood diseases?

**Dr. Duan:** Over the last few years, gene therapy has begun to deliver its therapeutic promise in several diseases. One example is AAV-2-mediated gene therapy for Leber's congenital amaurosis 2 (LCA2). This is a rare inherited retinal degenerative disease. Affected children lose their vision because of mutations in a gene called *Rep65*. Investigators in the United States and United Kingdom put a normal *Rep65* gene in an AAV-2 vector and then injected the vector into the eye of patients with LCA2. Treated

patients were able to regain their vision. Some patients still maintain their improved vision at eight years after gene therapy.<sup>5</sup>

Another major breakthrough is AAV-8-mediated gene therapy for hemophilia B. Hemophilia B is caused by mutations in a gene that encodes coagulation factor IX. To treat hemophilia B, scientists packaged a normal *factor IX* gene in an AAV-8 vector and injected intravenously to patients with severe hemophilia B. Factor IX produced from the AAV-8 vector significantly improved clinical outcomes without causing serious side effects. Therapeutic effect has maintained for more than four years in treated patients.<sup>6,7</sup>

**PPMD:** Have any gene therapy products received regulatory approval?

**Dr. Duan:** Several gene therapy products have been approved by regulatory agencies. In 2003, China approved the first gene therapy product called *Gendicine*.<sup>8</sup> This is an adenovirus vector for cancer therapy. In 2005, China approved *Oncorin*, another adenoviral vector for cancer gene therapy.<sup>9</sup> In 2007, the Philippines approved *Rexin-G*, a retroviral vector for cancer gene therapy.<sup>10</sup> In 2011, Russia approved *Neovasculgen*, a nonviral vector for treating peripheral arterial disease.<sup>11,12</sup> In 2012, European Medical Agency approved *Glybera*, an AAV-1 vector for treating a rare genetic disease called lipoprotein lipase deficiency.<sup>13,14</sup> On October 27, 2015, FDA approved *Imlygic*, an oncolytic herpes virus vector. This is the first commercial gene therapy product approved in the United States.<sup>15,16</sup> On October 10, 2015, a biotech company called Spark Therapeutics announced the results of its phase III trial on an AAV-2 vector for treating a form of childhood blindness. There were no serious adverse events. Treated patients showed significant vision improvement. Spark Therapeutics will seek regulatory approval from FDA in 2016 to market their gene therapy product. If successful, this will become the first AAV gene therapy approved by FDA.<sup>5</sup>

**PPMD:** What's the rationale for gene therapy in Duchenne? How does a gene delivered via gene therapy help ameliorate the progression of DMD? What's the potential impact for Duchenne patients?

**Dr. Duan:** The fundamental problem in DMD is the absence of dystrophin, an essential muscle protein. This is caused by mutations in the *dystrophin* gene.<sup>17,18</sup> Basically, mutations abort dystrophin production. Delivery of a new functional *dystrophin* gene or repair of the mutated *dystro-*

*phin* gene should restore dystrophin production in muscle and prevent muscle cells from dying. Gene therapy is expected to stop or slow down the progression of muscular dystrophy, improve life quality, and extend the life span of affected boys. If gene therapy is applied early enough, it may “cure” the disease.

**PPMD:** Gene therapy was tried years ago in muscular dystrophy, but suffered some setbacks from clinical trials in other diseases? Are we in better shape now and why?

**Dr. Duan:** Soon after the discovery of the *dystrophin* gene, scientists had begun to test gene therapy. Early studies used plasmid (nonviral vector), retrovirus, and adenovirus. These were performed in cultured muscle cells and dystrophin-deficient mdx mice. During this period, adenovirus delivery of a *mini-dystrophin* gene (which is derived from a very mild Becker patient) was at the forefront (see Note).<sup>19</sup> Unfortunately, adenovirus induces strong cellular immune responses and the mini-dystrophin produced from the adenovirus vector did not last long. In 1998, the entire field of gene therapy was put on hold because of the death of 18-year-old Jesse Gelsinger, who died from an adenovirus gene therapy trial for an inherited liver disease.<sup>20</sup>

Several gene therapy studies have been conducted in muscular dystrophy patients since that time. The first clinical trial for muscular dystrophy was published in 2004. This trial used a nonviral plasmid vector called *Myodys*.<sup>21</sup> It delivers a full-length dystrophin coding sequence. Investigators injected the plasmid directly into a muscle in DMD patients. Unfortunately, therapy yielded minimal dystrophin expression.<sup>22</sup>

The clinical trial of AAV gene therapy for muscular dystrophy was initially proposed in 2000 to treat limb girdle muscular dystrophy.<sup>23</sup> However, the first AAV gene therapy for muscular dystrophy was not reported until 2009.<sup>24</sup> In this study, Dr. Mendell and colleagues injected an AAV-1 vector that carried the *alpha-sarcoglycan* gene to the muscle of patients with limb girdle muscular dystrophy 2D and observed persistent expression of the therapeutic alpha-sarcoglycan in injected muscle for 6 months.<sup>24</sup> Another AAV trial was reported in 2010 for DMD.<sup>25</sup> This trial used an engineered AAV-2.5 vector that carried a highly minimized synthetic *dystrophin* gene. Unfortunately, dystrophin expression was barely observed in injected muscle. Detailed investigations suggest that the lack of expression was barely because of the immune response. The immune response to a gene

therapy product first caught the attention in 2006 when an AAV-2 vector that carried *factor IX* gene was delivered to the liver of patients with hemophilia B.<sup>26</sup> Investigators initially observed a therapeutic level factor IX production in the blood. But it did not last because treated liver cells were rejected by the immune system a few weeks later. It is now clear that the gene delivery vehicle (AAV virus capsid), cargo (transgene), or the protein produced from the therapeutic transgene can all illicit immune responses. To achieve long-term persistent gene therapy, we need to overcome the immune response barrier.

The invention of antisense oligonucleotide (AON)-mediated exon skipping opens the door to repair the messenger RNA, the molecule that translates the language of the gene (DNA) into a protein.<sup>27</sup> In exon skipping, the mutated part of dystrophin is skipped and a shortened version of dystrophin is produced. The first exon skipping trial on DMD patients was published in 2007.<sup>28</sup> In that trial, AONs were directly injected into patient's muscle. Since then, there has been significant progress in exon skipping. Several trials have been conducted in Europe and the United States to achieve systemic exon skipping. The major hurdles in current exon skipping include its low efficiency, transient nature, and failure to treat the heart. The US Food and Drug Administration (FDA) recently reviewed the new drug application (NDA) for two exon-skipping drugs, one from BioMarin Pharmaceutical (Kyndrisa; drisapersen) and the other from Sarepta Therapeutics (eteplirsen; AVI-4658). Both drugs aim at skipping exon 51 which could benefit ~13% DMD patients. On January 14, 2016, the FDA issued a complete response on BiomaMarin's NDA application and stated the FDA could not approve the NDA in its present form ([www.drugs.com/history/kyndrisa.html](http://www.drugs.com/history/kyndrisa.html)). According to a FDA briefing document published on November 24, 2015 ([www.fda.gov/downloads/advisorycommittees/committeesmeetingmaterials/drugs/peripheralandcentralnervoussystemdrugsadvisorycommittee/ucm473737.pdf](http://www.fda.gov/downloads/advisorycommittees/committeesmeetingmaterials/drugs/peripheralandcentralnervoussystemdrugsadvisorycommittee/ucm473737.pdf)), the major issues are the lack of clinical efficacy, failure to show increased dystrophin expression by western blot, and some concerns on the safety (such as renal toxicity). On January 22, 2016, the FDA published a briefing document on Sarepta's NDA application for eteplirsen ([www.fda.gov/downloads/advisorycommittees/committeesmeetingmaterials/drugs/peripheralandcentralnervoussystemdrugsadvisorycommittee/ucm481911.pdf](http://www.fda.gov/downloads/advisorycommittees/committeesmeetingmaterials/drugs/peripheralandcentralnervoussystemdrugsadvisorycommittee/ucm481911.pdf)). Significant concerns were raised by the FDA on clinical efficacy and dystrophin levels but not on the safety of the drug. Sarepta has since submitted four-year clinical effective data. According to a news release from

Sarepta<sup>29</sup>, the FDA will further review the data and reach a conclusion on whether eteplirsen will be approved, conditionally approved, or not approved by May 2, 2016.

Looking forward, the field is in a much stronger position than it was ever before. For example, we have identified major hurdles in exon skipping and AAV gene therapy, and we have also developed novel strategies to overcome these hurdles. In terms of exon skipping, new AONs with superior chemical properties (such as tricycle-DNA AONs) have greatly improved correction in deep muscles such as the diaphragm and the heart without causing toxicity in mouse models of DMD.<sup>30</sup> Methods have also been developed to use AAV to deliver AONs for long-term widespread correction. In terms of AAV gene therapy, transient immune suppression protocols (before, at the time of, or after gene delivery) have been developed and have shown success in the hemophilia B trial and in dog DMD models. Novel AAV capsids with improved properties are also being engineered to meet the specific needs of DMD gene therapy.<sup>31</sup>

**PPMD:** Which Duchenne patients could potentially benefit from gene therapy? Early versus late-stage boys? Ambulatory versus nonambulatory?

**Dr. Duan:** Broadly speaking, gene therapy has the potential to benefit every DMD patient. Systemic bodywide gene therapy in early stage boys (especially before they lose large amount of muscle) may prevent muscle from deterioration and dramatically change the disease course. Clinical observations in mild Becker patients suggest that a successful gene therapy may allow ambulation to the age of 60s.<sup>19</sup> For late-stage boys, the goal of gene therapy is to improve life quality. Localized gene therapy in limb muscles may improve their function for holding and grasping and allow use of a keyboard. Cardiac gene therapy may also improve the heart function of late-stage boys.

**PPMD:** What attributes of the dystrophin gene and protein make it amenable to gene therapy (e.g., size of the gene, spectrin repeat region, proof-of-concept from large Becker muscular dystrophy deletions)?

**Dr. Duan:** The *dystrophin* gene is one of the largest genes in the genome. It has a size of 2.4 mb (mega base) and is beyond the carrying capacity of any viral vector.<sup>32</sup> A gene is composed of protein-coding exons and nonprotein coding introns. Dystrophin has 79 exons. The protein-coding region (also called cDNA) of dystrophin has a size of 11.2 kb (kilo

base).<sup>33</sup> The dystrophin protein has a size of 427 kD (kilo Dalton).<sup>34</sup> Ideally, delivery of a full-length dystrophin cDNA will yield the production of a full-length dystrophin protein and the maximum protection of muscle. This can be achieved with a nonviral vector (such as a plasmid), gutted adenovirus, and tri-AAV vectors.<sup>21,35,36</sup> Currently, these strategies are not ready for clinical development because of issues related to delivery efficiency, the immune response, vector purification, and so on.

The full-length dystrophin protein can be divided into four domains. These are the N-terminal, rod, cysteine-rich, and C-terminal domains. The rod domain can be further divided into 24 spectrin-like repeats and 4 hinges (1 hinge sits between the N-terminal domain and the rod domain, 1 hinge sits between the rod domain and the cysteine-rich domain, and the other 2 hinges intervene spectrin-like repeats). It is now clear that not all the domains are absolutely required for muscle protection. Studies in mildly affected Becker patients suggest that deletion of a fairly large piece of the rod domain is not associated with major deleterious consequences to muscle function.

Knowledge learned from Becker patients inspired scientists to develop an abbreviated/truncated *dystrophin* gene for DMD gene therapy. There are two major classes of abbreviated *dystrophin* genes.<sup>37</sup> One is called the *mini-dystrophin* gene and the other is called the *microdystrophin* gene. The *mini-dystrophin* gene (minigene) is about 6 to 8 kb in size and it results in the production of a mini-dystrophin protein that is about the half size of the full-length protein (see Note). Based on clinical observations in Becker patients, there is a high likelihood that minigene therapy will improve muscle health in DMD patients.<sup>19,38–41</sup> The *microdystrophin* gene (microgene) is about 3.5 to 4 kb in size and it results in the production of a microdystrophin protein that is about one-third the size of the full-length protein (see note). In addition to the truncation in the rod domain, the C-terminal domain is also deleted in the microgene. Although studies in mouse and dog models of DMD suggest that the microgene can ameliorate muscle disease and improve muscle force, no human precedent has been identified for the super-small microgene.<sup>42,43</sup> We will not know whether the microgene can treat DMD patients until a clinical trial is conducted. The beauty of the microgene is that it can fit into the AAV vector, which has a maximal packaging capacity of 5 kb. To deliver a mini-dystrophin gene with AAV, the gene has to be split into two pieces and separately delivered by two independent AAV vectors (the dual-AAV

approach); using this approach would increase the complexity of therapy development.<sup>44</sup>

**PPMD:** Can you briefly describe what exon skipping is and how it compares and contrasts with gene therapy as a potential treatment for Duchenne?

**Dr. Duan:** Three different gene therapy methods can be used to restore dystrophin expression. These are gene repair, exon skipping, and *dystrophin* gene replacement. Gene repair strategies can be used either to fix the mutation and recover a full-length *dystrophin* gene, or covert a Duchenne mutation into a Becker mutation. For the former, it requires homologous recombination (which is very inefficient in mature muscle cells) and a template of the normal sequence. Further, it may work only for patients with small mutations (such as point mutation and small deletions). To covert a Duchenne into a Becker, the mutated region (and sometimes its surrounding regions) is removed and remaining parts are ligated together. This will yield a dystrophin protein with a slightly reduced size but still functional.

Exon skipping is another repair strategy, but it does not repair the mutated gene. The mutated gene generates mutated RNA molecules. In exon skipping, the mutated region is removed by AONs from the RNA molecule while it is being processed inside the cell. Because the mutated gene will continually generate mutated RNAs, one has to continually deliver AONs to the cells in order to achieve long-term therapy. In other words, one may consider exon skipping as a “transient” gene repair therapy.

Gene replacement therapy has the longest history. It is often referred to as “gene therapy.” In this case, the original mutated *dystrophin* gene remains in the genome. A normal copy of the dystrophin gene or an engineered synthetic *dystrophin* gene is delivered to muscle to produce a functional dystrophin protein. As long as the therapeutic transgene persists in the body, it should continually produce dystrophin. Because of the packaging limitations of viral vectors, most gene replacement therapies are aimed at delivering the abbreviated versions of the *dystrophin* gene.

Compared with the naturally existing *mini-dystrophin* genes (in Becker patients) and the shortened *dystrophin* gene/RNA generated by gene repair/exon skipping, a synthetic *dystrophin* gene may have some advantages. For example, scientists may use molecular engineering techniques to generate synthetic *dystrophin* genes that are structurally and functionally superior. Further,

viral vectors can be engineered to produce much more dystrophin than a cell can produce with its own gene. Nevertheless, *dystrophin* gene replacement therapy also has a drawback. The endogenous *dystrophin* gene expresses the physiological amount of dystrophin at selected tissues at defined times. These specificities are usually lost in gene replacement therapy.

**PPMD:** We’ve heard of recent progress in gene editing using CRISPR/Cas9 technology—there was even an article on gene editing in a recent *New Yorker*. Can you briefly describe the gene editing approach; how is it similar and different from gene therapy?

**Dr. Duan:** Gene editing is another term for gene repair. Traditionally, gene editing has been very inefficient because of the lack of a good gene-editing tool. The CRISPR/Cas9 technology is a newly developed gene-editing system that originates from the bacterial defense mechanism. The CRISPR/Cas9 technology allows scientists to cut the genome at the desired locations with a guider RNA that has a sequence complementary to the DNA target. Using the CRISPR/Cas9 technology, Gersbach and colleagues have successfully restored dystrophin expression in muscle cells isolated from DMD patients.<sup>45</sup> Recently, Cohn and colleagues also demonstrated correction of a duplication mutation in muscle cells from patients.<sup>46</sup> An important concern is whether what have been achieved in cultured cells in a petri dish can be replicated in a live muscle. To this end, several groups have reported exciting new development demonstrating that it is feasible to perform CRISPR/Cas9 therapy in a live muscle in an intact mdx mouse.<sup>47–49</sup> Importantly, CRISPR/Cas9 treatment significantly reduced dystrophic pathology and improved muscle contractility. Despite these encouraging progresses, we have to realize that the technology itself is still at its infant stage. There are a lot of hurdles before it can be tested in human patients. Some of these include the immune response to the bacterial-derived Cas9 protein and off-target cutting.

**PPMD:** What are your latest findings in delivering a microdystrophin systemically in an animal model?

**Dr. Duan:** DMD affects all muscles in the body. A big challenge of DMD gene therapy is to treat all muscles in the body. Such whole-body therapy was shown possible in rodents more than 10 years ago.<sup>50,51</sup> However, the body size of a mouse is approximately 1000-fold smaller than that of a boy. It has been daunting to try to scale-up from a mouse to a larger mammal (such as a dog that has a body size

closer to a boy). We initially demonstrated the feasibility of systemic delivery in newborn dogs.<sup>52–54</sup> But this did not work well in neonatal affected dogs because of unexpected side effects.<sup>43,55</sup> Recently, we have finally accomplished the scale-up of systemic AAV delivery to juvenile DMD dogs and published the results in October 2015 in *Human Molecular Genetics*.<sup>56</sup> We achieved efficient AAV delivery of either a marker gene or a therapeutic *microdystrophin* gene to every muscle in the body of several young muscular dystrophy dogs. No toxicity was observed, and microdystrophin-treated muscles showed fewer lesions on histology examination.<sup>56</sup>

**PPMD:** Since DMD muscles undergo degeneration and regeneration, and satellite or other muscle precursor cells will be incorporated into fibers attempting regeneration, does your approach deliver dystrophin to these precursor cells?

**Dr. Duan:** Treating muscle precursor cells (or muscle stem cells) has been an important goal of DMD gene therapy. However, directly delivering an AAV microdystrophin vector to muscle stem cells may have limited effect. This is because AAV mainly exists as episomal circular molecules in a cell. As a stem cell begins to divide, AAV vectors will be diluted and eventually lost in progeny cells after many rounds of cell division.

This problem can be overcome by delivering a therapeutic *dystrophin* gene with an integrating virus such as lentivirus. A tiny fraction of AAV vectors may also integrate into the genome but the integration efficiency is much lower than that of a retrovirus or lentivirus.

Another solution is to use AAV to deliver gene repair tools to muscle stem cells. In this case, the repaired *dystrophin* gene will persist for good in daughter cells.<sup>48</sup>

**PPMD:** You used young dogs in your study. What do you see for a therapeutic window for gene therapy in DMD? That is, what age range do you see benefiting from the gene therapy approach?

**Dr. Duan:** As a first step toward systemic AAV *microdystrophin* gene therapy in a large mammal, we intentionally used young dogs that are 2 to 3 months of age. There are several considerations. The first is the amount of AAV vectors needed for the therapy. The amount of vectors that can treat one adult dog is sufficient to treat several young dogs. Although the industrial-scale AAV production is being developed, it is beyond the budget limit of an academic lab. The

second is the age. We choose an age when affected dogs just begin to show symptoms. This roughly correlates to 2 to 4 years of age in affected boys when they begin to show delay in their motor milestones and are diagnosed. At this stage, muscle damage is mild and early intervention may yield the best effect.

With this being said, we don't think age will be a limitation for systemic AAV gene therapy. Our group and Chamberlain laboratories have shown that systemic therapy in aged mdx mice ( $\geq 18$  months old; this corresponds to  $\geq 60$  years of age in humans) can still improve skeletal muscle and heart function.<sup>57–59</sup>

**PPMD:** Are you evaluating respiratory muscles, like the diaphragm, and the heart in your studies? Can these muscles benefit from gene therapy?

**Dr. Duan:** We achieved good gene transfer in the heart and respiratory muscles (including the diaphragm, intercostal muscle, and abdominal muscle). Based on our previous studies in the mouse model, we believe these muscles will benefit from the therapy.

**PPMD:** You now have established proof-of-concept for a microdystrophin delivered systemically in dogs; how do you see that progressing toward trials?

**Dr. Duan:** This is a critical milestone in the eventual application of bodywide gene therapy in Duchenne patients. Bodywide AAV delivery has been demonstrated in the rodent models of muscular dystrophy since 2004. However, systemic gene transfer has never been achieved in an adult subject of a large mammal. The enormous amount of vectors needed for each animal ( $>10^{15}$  particles) not only implies a huge cost in vector production but also represents a significant safety concern. Scale-up AAV production may amplify contaminations that are negligible in small-scale ( $<10^{13}$  particles) preparations. Importantly, unexpected inflammatory and/or immune response to the infusion of trillions of viral particles may lead to fatal complications as demonstrated in the tragic death of Jesse Gelsinger in a 1998 clinical trial.<sup>20</sup> On top of these, the ongoing massive myofiber necrosis and inflammation in adult dystrophic dogs may further worsen untoward immune responses. The excellent safety profile we saw in our study suggests that above-mentioned issues are likely manageable.

In our study, we tested only three dogs (one received a reporter gene AAV vector and two received the microdystrophin AAV vector). There is a need to expand the study to see if the success can be reproduced in a large number of dystrophic dogs.

DMD is a life-long disease. However, the longest time point in our study was four months. It is thus important to conduct long-term study to see if there are delayed immune responses or unexpected toxicity. In our study, we observed microdystrophin expression in 5% to 60% of muscle cells in different muscles. Additional studies are needed to further improve gene transfer efficiency to eventually achieve near-saturated dystrophin expression in the majority of muscles in the body. It should also be noted that in our study we evaluated only muscle histology; further studies are needed to see if systemic AAV gene therapy can improve muscle function. Last but not least, in our study we tested only one version of microdystrophin. Although this is so far the only microdystrophin that has been shown to provide physiological benefits in a large mammal, the improvement in muscle force is limited. Additional studies are needed to engineer more potent microdystrophins.

**PPMD:** You have a grant from PPMD to develop a gene therapy approach to deliver the sarco/endoplasmic reticulum calcium ATPase (*SERCA*) gene; can you tell us what the rationale is there and what progress you have made?

**Dr. Duan:** In DMD, a pivotal event downstream of dystrophin deficiency is the elevation of calcium in the cytoplasm of muscle cells. Elevated cytosolic calcium triggers proteolysis and muscle cell death.<sup>60</sup> Strategies that can reduce calcium overload in muscle cells will restore calcium homeostasis and reduce muscle disease. *SERCA* is the calcium pump that removes cytosolic calcium in muscle. With the funding from PPMD, we have tested whether AAV delivery of the *SERCA* gene can treat muscular dystrophy in animal models. We found that intravenous injection of the AAV *SERCA* vector to mdx mice significantly improved skeletal muscle force and heart function. Our next step is to test this highly promising therapy in affected dogs.

Duchenne patients do not have dystrophin in their body. Dystrophin generated by gene repair or gene replacement therapy could be considered as a foreign molecule by our immune system and hence mount an immune response to reject cells that contain the newly generated dystrophin protein. This will not be a concern for *SERCA* gene therapy because *SERCA* already exists in patient body.

**PPMD:** What preclinical steps need to be taken before an investigational new drug (IND) application can be filed for a gene therapy trial with systemic delivery of dystrophin?

**Dr. Duan:** A number of IND-enabling studies are needed before an IND can be issued. These include toxicity studies in small and large animals, generation of good manufacturing practices (GMP)-quality AAV vectors, pharmacokinetic and pharmacodynamics studies, and randomized blinded studies with sufficient sample size to confirm and validate systemic AAV therapy in dogs. It should also be noted that, in our study, we have used a canine *microdystrophin* gene. For clinical trial we need to develop a human-version *microdystrophin* gene.

**PPMD:** Delivering a gene therapy vector to all muscles affected in Duchenne has been one of the key challenges in developing this potential therapy. Can you tell us how research has progressed from the single-muscle injections that have been done in clinical trials toward systemic delivery?

**Dr. Duan:** Single-muscle injection is the foundation for systemic delivery. When gene therapy was initially tested in mdx mice, investigators performed single-muscle injection. The first attempt to achieve systemic delivery involved co-administration of vessel-perfusing agents such as histamine. The identification of new AAV serotypes that can escape from the vasculature and reach muscle cells has opened the door to “true” systemic delivery. Initial tests were performed in dystrophic mice and hamsters and then in neonatal dogs. Our study now suggests that systemic delivery can also be achieved in juvenile dystrophic dogs.

Single-muscle injection has been used in most of the muscular dystrophy clinical trials to date. Only one study has tested systemic delivery in human patients with a neuromuscular disease. In this trial (by AveXis, a biotech firm in Dallas), Drs. Mendell and Kaspar and colleagues delivered an AAV-9 vector to infants who suffered from a severe form of spinal muscular atrophy. According to the report by Dr. Mendell on October 5, 2015, at the International Congress of the World Muscle Society, nine patients have received therapy. The therapy appears to be generally safe and well tolerated. Signs of clinical improvement have also been noted (<http://avexis.com/data-ongoing-study-avxs-101-spinal-muscular-atrophy-type-1-presented-world-muscle-congress/>).

**PPMD:** Prior clinical trials of gene therapy in Duchenne have encountered immunological reactions that have impaired efficacy. What is being done to address that issue?

**Dr. Duan:** In our study in dystrophic dogs, we found that a five-week transient immune sup-

pression seemed to have made the trick. In hemophilia B trial and spinal muscular dystrophy trials, transient application of large dosage of steroids was found to be effective. Another important aspect is to screen patients for preexisting immunity to the viral vector and the therapeutic gene product. In our study, we screen affected dogs for the preexisting neutralization antibody to AAV-9 and we only used dogs that were seronegative for AAV-9 (meaning these dogs have never been exposed to AAV-9). It should be noted that additional efforts are needed before we can completely solve the problem of the immune response. In this regard, several new strategies that are being tested in laboratories (such as plasmapheresis and AAV capsid engineering) have shown promise.

**PPMD:** In scaling up to do clinical trials in Duchenne, vector production may be a limitation. How is the problem of having sufficient vector to do clinical trials and, later, to treat large numbers of Duchenne patients being addressed?

**Dr. Duan:** Vector manufacture has been recognized as a key bottleneck to scale-up of systemic AAV therapy in human patients.<sup>61,62</sup> Classic AAV production protocol requires transient transfection of three different plasmids to HEK 293 cells that are cultured in a petri dish. AAV is then purified from culture medium and cell lysate using ultracentrifugation. Numerous strategies have been tested to scale-up AAV production and purification. Some examples include the use of the infection approach with the baculovirus-based system or herpes virus-based system, and producer cell lines. Cell culture has also been expanded from the petri dish to roller bottles, cell factors, and bioreactors. Chromatography-based purification strategy has also been developed for different AAV serotypes. Most importantly, robust vector characterization and analytical quality control protocols and standards have been developed or are being developed and validated.

**PPMD:** What about commercial partners that would be needed to bring a therapy through regulatory approval and to market? Can you tell us about your partnership with SOLID GT and how that may move gene therapy toward clinical trials in Duchenne?

**Dr. Duan:** Industry investment is essential to bring an experimental vector into a gene therapy product. Funding from biopharmaceutical partners

will offset the high cost of clinical studies. Solid GT is a subsidiary of Solid Biosciences and was started by parents of a boy with DMD. As stated in the company's website (<http://solidbio.com/gt/>), it "is dedicated to the development of durable disease-modifying interventions for Duchenne Muscular Dystrophy through gene therapy." Solid GT is currently pursuing systemic AAV *microdystrophin* gene therapy. According to the company's website "Solid GT is conducting a number of key studies that will enable us to enter the clinic within two years." "These studies include efficacy, safety and dose ranging assessments" in mdx mice and dystrophic dogs. We have been involved in the animal studies. The results so far are very promising. Besides animal studies, Solid GT is also working with academic and corporate partners to refine and scale-up AAV manufacturing technology, and is addressing a number of other key aspects of this program, in preparation for upcoming human clinical trials. On November 3, 2015, Solid GT announced that it has raised \$42.5 million in series B financing to advance gene therapy for DMD ([www.businesswire.com/news/home/20151103006362/en/Solid-GT-Raises-42.5-Million-Series-Financing](http://www.businesswire.com/news/home/20151103006362/en/Solid-GT-Raises-42.5-Million-Series-Financing)).

## NOTE

Early on, all truncated dystrophins are called mini-dystrophin. In 2002, Dr. Jeff Chamberlain coined the term "micro-dystrophin" to refer to the abbreviated dystrophins that are about one-third the size of the full-length dystrophin protein. Micro-dystrophin does not contain a complete C-terminal domain. The micro-dystrophin genes are 3.5 to 4-kb in size and can fit into a single AAV vector. The original term "mini-dystrophin" is now reserved for the abbreviated dystrophins that are at least half the size of the full-length dystrophin protein. Mini-dystrophin often contains the complete C-terminal domain. The minidystrophin genes are 6 to 8-kb in size and cannot fit into a single AAV vector. Dual AAV vectors are required to deliver the mini-dystrophin gene.

The micro-dystrophin gene is often abbreviated as the microgene. The mini-dystrophin gene is often abbreviated as the minigene. "Micro-dystrophin" and "mini-dystrophin" are also spelled as "micro-dystrophin" and "minidystrophin", respectively.

For this historic reason, some of the early versions of the microgene (these that were published before 2002) have been called the minigene. For example the  $\Delta 3849$ ,  $\Delta 3990$  and  $\Delta 4173$  minigenes developed in Dr. Xiao Xiao's laboratory are actually microgenes.

## ACKNOWLEDGMENTS

DMD research in the Duan Lab is supported by the National Institutes of Health (NS-90634, AR-67985, AR-69085), Department of Defense (MD130014), Muscular Dystrophy Association, Parent Project Muscular Dystrophy, Jesse's Journey—The Foundation for Gene and Cell

Therapy, Hope for Javier, and the University of Missouri.

## AUTHOR DISCLOSURE

D.D. is a member of the scientific advisory board and an equity holder of Solid GT, a subsidiary of Solid Biosciences.

## REFERENCES

- Berns KI, Byrne BJ, Flotte TR, et al. Adeno-associated virus type 2 and hepatocellular carcinoma? *Hum Gene Ther* 2015;26:779–781.
- Wilson JM. Adverse events in gene transfer trials and an agenda for the new year. *Hum Gene Ther* 2008;19:1–2.
- Board of the European Society of Gene and Cell Therapy. Case of leukaemia associated with X-linked severe combined immunodeficiency gene therapy trial in London. *Hum Gene Ther* 2008;19:3–4.
- Naldini L. Gene therapy returns to centre stage. *Nature* 2015;526:351–360.
- Ledford H. Success against blindness encourages gene therapy researchers. *Nature* 2015;526:487–488.
- Brimble MA, Reiss UM, Nathwani AC, Davidoff AM. New and improved AAVenues: Current status of hemophilia B gene therapy. *Expert Opin Biol Ther* 2016;16:79–92.
- High KA, Anguela XM. Adeno-associated viral vectors for the treatment of hemophilia. *Hum Mol Genet* 2015. [Epub ahead of print]
- Wilson JM. Gendicine: The first commercial gene therapy product. *Hum Gene Ther* 2005;16:1014–1015.
- Ma G, Shimada H, Hiroshima K, et al. Gene medicine for cancer treatment: Commercially available medicine and accumulated clinical data in China. *Drug Des Dev Ther* 2009;2:115–122.
- Gordon EM, Hall FL. Rexin-G, a targeted genetic medicine for cancer. *Expert Opin Biol Ther* 2010;10:819–832.
- Willyard C. Limb-saving medicines sought to prevent amputations. *Nat Med* 2012;18:328.
- Deev RV, Bozo IY, Mzhavanadze ND, et al. pCMV-vegf165 intramuscular gene transfer is an effective method of treatment for patients with chronic lower limb ischemia. *J Cardiovasc Pharmacol Ther* 2015;20:473–482.
- Bryant LM, Christopher DM, Giles AR, et al. Lessons learned from the clinical development and market authorization of Glybera. *Hum Gene Ther Clin Dev* 2013;24:55–64.
- Melchiorri D, Pani L, Gasparini P, et al. Regulatory evaluation of Glybera in Europe—two committees, one mission. *Nat Rev Drug Discov* 2013;12:719.
- FDA. FDA approves first-of-its-kind product for the treatment of melanoma. FDA News Release October 27, 2015. [www.fda.gov/NewsEvents/Newsroom/PressAnnouncements/ucm469571.htm](http://www.fda.gov/NewsEvents/Newsroom/PressAnnouncements/ucm469571.htm)
- Greig SL. Talimogene laherparepvec: First global approval. *Drugs* 2016;76:147–154.
- Kunkel LM. 2004 William Allan award address. Cloning of the DMD gene. *Am J Hum Genet* 2005;76:205–214.
- Bladen CL, Salgado D, Monges S, et al. The TREAT-NMD DMD global database: Analysis of more than 7000 Duchenne muscular dystrophy mutations. *Hum Mutat* 2015;36:395–402.
- England SB, Nicholson LV, Johnson MA, et al. Very mild muscular dystrophy associated with the deletion of 46% of dystrophin. *Nature* 1990;343:180–182.
- Wilson JM. Lessons learned from the gene therapy trial for ornithine transcarbamylase deficiency. *Mol Genet Metab* 2009;96:151–157.
- Duan D. Myodys, a full-length dystrophin plasmid vector for Duchenne and Becker muscular dystrophy gene therapy. *Curr Opin Mol Ther* 2008;10:86–94.
- Romero NB, Braun S, Benveniste O, et al. Phase I study of dystrophin plasmid-based gene therapy in Duchenne/Becker muscular dystrophy. *Hum Gene Ther* 2004;15:1065–1076.
- Stedman H, Wilson JM, Finke R, et al. Phase I clinical trial utilizing gene therapy for limb girdle muscular dystrophy: Alpha-, beta-, gamma-, or delta-sarcoglycan gene delivered with intramuscular instillations of adeno-associated vectors. *Hum Gene Ther* 2000;11:777–790.
- Mendell JR, Rodino-Klapac LR, Rosales-Quintero X, et al. Limb-girdle muscular dystrophy type 2D gene therapy restores alpha-sarcoglycan and associated proteins. *Ann Neurol* 2009;66:290–297.
- Mendell JR, Campbell K, Rodino-Klapac L, et al. Dystrophin immunity in Duchenne's muscular dystrophy. *N Engl J Med* 2010;363:1429–1437.
- Manno CS, Arruda VR, Pierce GF, et al. Successful transduction of liver in hemophilia by AAV-Factor IX and limitations imposed by the host immune response. *Nat Med* 2006;12:342–347.
- Spitali P, Aartsma-Rus A. Splice modulating therapies for human disease. *Cell* 2012;148:1085–1088.
- van Deutekom JC, Janson AA, Ginjaar IB, et al. Local dystrophin restoration with antisense oligonucleotide PRO051. *N Engl J Med* 2007;357:2677–2686.
- <http://investorrelations.sarepta.com/phoenix.zhtml?c=64231&p=irol-newsArticle&ID=2136367>. Accessed on March 12, 2016.
- Goyenvalle A, Griffith G, Babbs A, et al. Functional correction in mouse models of muscular dystrophy using exon-skipping tricyclo-DNA oligomers. *Nat Med* 2015;21:270–275.
- Nance ME, Duan D. Perspective on adeno-associated virus (AAV) capsid modification for Duchenne muscular dystrophy gene therapy. *Hum Gene Ther* 2015;26:786–800.
- Koenig M, Hoffman EP, Bertelson CJ, et al. Complete cloning of the Duchenne muscular dystrophy (DMD) cDNA and preliminary genomic organization of the DMD gene in normal and affected individuals. *Cell* 1987;50:509–517.
- Koenig M, Monaco AP, Kunkel LM. The complete sequence of dystrophin predicts a rod-shaped cytoskeletal protein. *Cell* 1988;53:219–226.
- Hoffman EP, Brown RH Jr., Kunkel LM. Dystrophin: The protein product of the Duchenne muscular dystrophy locus. *Cell* 1987;51:919–928.
- Lostal W, Kodippili K, Yue Y, Duan D. Full-length dystrophin reconstitution with adeno-associated viral vectors. *Hum Gene Ther* 2014;25:552–562.
- DelloRusso C, Scott JM, Hartigan-O'Connor D, et al. Functional correction of adult mdx mouse muscle using gutted adenoviral vectors expressing full-length dystrophin. *Proc Natl Acad Sci U S A* 2002;99:12979–12984.
- Scott J, Li S, Harper S, et al. Viral vectors for gene transfer of micro-, mini-, or full-length dystrophin. *Neuromuscul Disord* 2002;12 Suppl:S23.
- Winnard AV, Klein CJ, Coovert DD, et al. Characterization of translational frame exception patients in Duchenne/Becker muscular dystrophy. *Hum Mol Genet* 1993;2:737–744.
- Matsumura K, Burghes AH, Mora M, et al. Immunohistochemical analysis of dystrophin-associated proteins in Becker/Duchenne muscular dystrophy with huge in-frame deletions in the NH2-terminal and rod domains of dystrophin. *J Clin Invest* 1994;93:99–105.
- Mirabella M, Galluzzi G, Manfredi G, et al. Giant dystrophin deletion associated with congenital cataract and mild muscular dystrophy. *Neurology* 1998;51:592–595.

41. Nicholson LV, Johnson MA, Bushby KM, et al. Integrated study of 100 patients with Xp21 linked muscular dystrophy using clinical, genetic, immunochemical, and histopathological data. Part 3. Differential diagnosis and prognosis. *J Med Genet* 1993;30:745–751.
42. Chamberlain JS. Gene therapy of muscular dystrophy. *Hum Mol Genet* 2002;11:2355–2362.
43. Duan D. Duchenne muscular dystrophy gene therapy in the canine model. *Hum Gene Ther Clin Dev* 2015;26:57–69.
44. Duan D. From the smallest virus to the biggest gene: Marching towards gene therapy for Duchenne muscular dystrophy. *Discov Med* 2006;6:103–108.
45. Ousterout DG, Kabadi AM, Thakore PI, et al. Multiplex CRISPR/Cas9-based genome editing for correction of dystrophin mutations that cause Duchenne muscular dystrophy. *Nat Commun* 2015; 6:6244.
46. Wojtal D, Kemaladewi DU, Malam Z, et al. Spell checking nature: Versatility of CRISPR/Cas9 for developing treatments for inherited disorders. *Am J Hum Genet* 2016;98:1–12.
47. Nelson CE, Hakim CH, Ousterout DG, et al. *In vivo* genome editing improves muscle function in a mouse model of Duchenne muscular dystrophy. *Science* 2016;351:493–407.
48. Tabebordbar M, Zhu K, Cheng JK, et al. *In vivo* gene editing in dystrophic mouse muscle and muscle stem cells. *Science* 2016;351:407–411.
49. Long C, Amoasii L, Mireault AA, et al. Postnatal genome editing partially restores dystrophin expression in a mouse model of muscular dystrophy. *Science* 2016;351:400–403.
50. Gregorevic P, Blankinship MJ, Allen JM, et al. Systemic delivery of genes to striated muscles using adeno-associated viral vectors. *Nat Med* 2004;10:828–834.
51. Wang Z, Zhu T, Qiao C, et al. Adeno-associated virus serotype 8 efficiently delivers genes to muscle and heart. *Nat Biotechnol* 2005;23:321–328.
52. Yue Y, Ghosh A, Long C, et al. A single intravenous injection of adeno-associated virus serotype-9 leads to whole body skeletal muscle transduction in dogs. *Mol Ther* 2008;16:1944–1952.
53. Pan X, Yue Y, Zhang K, et al. Long-term robust myocardial transduction of the dog heart from a peripheral vein by adeno-associated virus serotype-8. *Hum Gene Ther* 2013;24:584–594.
54. Hakim CH, Yue Y, Shin JH, et al. Systemic gene transfer reveals distinctive muscle transduction profile of tyrosine mutant AAV-1, -6, and -9 in neonatal dogs. *Mol Ther Methods Clin Dev* 2014;1:14002.
55. Kornegay JN, Li J, Bogan JR, et al. Widespread muscle expression of an AAV9 human mini-dystrophin vector after intravenous injection in neonatal dystrophin-deficient dogs. *Mol Ther* 2010; 18:1501–1508.
56. Yue Y, Pan X, Hakim CH, et al. Safe and bodywide muscle transduction in young adult Duchenne muscular dystrophy dogs with adeno-associated virus. *Hum Mol Genet* 2015;24:5880–5890.
57. Gregorevic P, Blankinship MJ, Allen JM, et al. Systemic microdystrophin gene delivery improves skeletal muscle structure and function in old dystrophic mdx mice. *Mol Ther* 2008;16:657–664.
58. Bostick B, Shin J-H, Yue Y, et al. AAV-microdystrophin therapy improves cardiac performance in aged female mdx mice. *Mol Ther* 2011;19:1826–1832.
59. Bostick B, Shin JH, Yue Y, et al. AAV micro-dystrophin gene therapy alleviates stress-induced cardiac death but not myocardial fibrosis in >21-m-old mdx mice, an end-stage model of Duchenne muscular dystrophy cardiomyopathy. *J Mol Cell Cardiol* 2012;53:217–222.
60. Burr AR, Molkentin JD. Genetic evidence in the mouse solidifies the calcium hypothesis of myofiber death in muscular dystrophy. *Cell Death Differ* 2015;22:1402–1412.
61. van der Loo JC, Wright JF. Progress and challenges in viral vector manufacturing. *Hum Mol Genet* 2015. [Epub ahead of print]
62. Kotin RM. Large-scale recombinant adeno-associated virus production. *Hum Mol Genet* 2011;20:R2–R6.

## ARTICLE

# 100-fold but not 50-fold dystrophin overexpression aggravates electrocardiographic defects in the mdx model of Duchenne muscular dystrophy

Yongping Yue<sup>1</sup>, Nalinda B Wasala<sup>1</sup>, Brian Bostick<sup>1</sup> and Dongsheng Duan<sup>1,2,3</sup>

Dystrophin gene replacement holds the promise of treating Duchenne muscular dystrophy. Supraphysiological expression is a concern for all gene therapy studies. In the case of Duchenne muscular dystrophy, Chamberlain and colleagues found that 50-fold overexpression did not cause deleterious side effect in skeletal muscle. To determine whether excessive dystrophin expression in the heart is safe, we studied two lines of transgenic mdx mice that selectively expressed a therapeutic *minidystrophin* gene in the heart at 50-fold and 100-fold of the normal levels. In the line with 50-fold overexpression, minidystrophin showed sarcolemmal localization and electrocardiogram abnormalities were corrected. However, in the line with 100-fold overexpression, we not only detected sarcolemmal minidystrophin expression but also observed accumulation of minidystrophin vesicles in the sarcoplasm. Excessive minidystrophin expression did not correct tachycardia, a characteristic feature of Duchenne muscular dystrophy. Importantly, several electrocardiogram parameters (QT interval, QRS duration and the cardiomyopathy index) became worse than that of mdx mice. Our data suggests that the mouse heart can tolerate 50-fold minidystrophin overexpression, but 100-fold overexpression leads to cardiac toxicity.

*Molecular Therapy — Methods & Clinical Development* (2016) **3**, 16045; doi:10.1038/mtm.2016.45; published online 6 July 2016

## INTRODUCTION

Duchenne muscular dystrophy (DMD) is the most common childhood lethal muscle disease caused by dystrophin deficiency. This X-linked disease mainly affects boys and young men. Introducing a functional dystrophin gene back to muscle by gene therapy holds a great promise to treat DMD. Ideally, for gene therapy one would like to express the full-length gene or the full-length cDNA from the endogenous promoter. This will allow for spatially and temporally regulated expression of a full-length protein to meet developmental and physiological needs of muscle. Unfortunately, the *dystrophin* gene is one of the largest genes in the mammalian genome. It greatly exceeds the packaging limit of most viral gene delivery vectors. This not only excludes the use of the full-length gene or cDNA as the therapeutic gene but also excludes the use of the endogenous dystrophin promoter in the expression cassette. To overcome these hurdles, investigators are forced to express a synthetic *mini/micro dystrophin* gene from a constitutive promoter (either ubiquitous or muscle-specific). A likely consequence of this approach is unchecked expression and the production of excessive amount of dystrophin. From the safety standpoint, it is essential to determine whether supraphysiological expression of a therapeutic mini/micro dystrophin gene can lead to deleterious side effects.

Despite intensive research and exciting progresses in the field of dystrophin gene replacement therapy, so far only one study has examined potential toxicity of dystrophin overexpression. Cox *et al.* generated a strain of full-length dystrophin overexpression transgenic mice on the background of dystrophin-null mdx mice.<sup>1</sup> The authors found that the dystrophin level in transgenic mice was 50-fold higher than that of normal mice. Despite excessive amount of dystrophin, surprisingly, skeletal muscle morphology and force were completely normal. This study suggests that skeletal muscle can tolerate supraphysiological levels of dystrophin.<sup>1</sup>

Heart disease is a leading cause of morbidity and mortality in DMD. To treat DMD heart disease, we need to deliver a functional dystrophin gene to the heart. It is thus important to determine whether supraphysiological dystrophin expression in the heart is safe. To address this critical question, we developed cardiac transgenic mdx mice that selectively overexpressed the *ΔH2-R19 minidystrophin* gene in the heart.<sup>2</sup> This minidystrophin gene has previously being shown to protect both skeletal muscle and the heart in mdx mice.<sup>2–4</sup> In a line of 50-fold overexpression, we observed the expected benefits of the *minidystrophin* gene.<sup>2</sup> However, cardiac toxicity was detected in a line that showed

<sup>1</sup>Department of Molecular Microbiology and Immunology, School of Medicine, The University of Missouri, Columbia, Missouri, USA; <sup>2</sup>Department of Neurology, School of Medicine, The University of Missouri, Columbia, Missouri, USA; <sup>3</sup>Department of Bioengineering, The University of Missouri, Columbia, Missouri, USA.  
Correspondence: D Duan (duand@missouri.edu)

Received 10 March 2016; accepted 18 May 2016

100-fold overexpression. Our results suggest that dystrophin overexpression in the heart is likely safe as long as it does not exceed 50-fold of the wild type level.

## RESULTS

Generation of cardiac  $\Delta$ H2-R19 minidystrophin overexpression transgenic mdx mice

To achieve heart specific overexpression of the therapeutic  $\Delta$ H2-R19 minidystrophin gene, we used the 5.5 kb murine  $\alpha$ -myosin heavy chain ( $\alpha$ MHC) promoter.<sup>5-7</sup> This is the most commonly used promoter for cardiac transgenic studies and it drives transgene expression throughout the entire heart. Importantly, depending on the copy number, one can achieve a broad range of gene expression including supraphysiological expression with this promoter.<sup>8-24</sup> We obtained a total of 10 founder lines and nine lines were backcrossed to the congenic background of mdx mice.<sup>2</sup> In this study, we focused on lines 26 and 29.

Characterization of cardiac minidystrophin overexpressing transgenic mice

To determine the copy number of the minidystrophin gene in lines 26 and 29, we performed Southern blot. The 3.4 kb diagnostic band was detected in both lines (Figure 1a). On quantification, lines

26 and 29 contained  $328.7 \pm 11.5$  and  $5.3 \pm 0.2$  copies of the  $\Delta$ H2-R19 minidystrophin gene, respectively (Figure 1b).

Next we examined the protein level by western blot. Both lines yielded the expected 220 kDa  $\Delta$ H2-R19 minidystrophin band (Figure 1c). When compared with the level of full-length dystrophin in normal BL10 mice, the minidystrophin protein in lines 26 and 29 were  $102.6 \pm 4.3$  and  $50.8 \pm 2.3$  fold higher than that of normal mice, respectively (Figure 1d).

On immunofluorescence staining,  $\Delta$ H2-R19 minidystrophin showed the expected sarcolemmal localization in the heart of line 29 mice (Figure 1e). However, minidystrophin was detected in both sarcolemma and sarcoplasm in cardiomyocytes of line 26 (Figure 1e, Supplementary Figure S1). On high magnification, sarcoplasmic minidystrophin staining displayed as small vesicles (Figure 1e).

Evaluation of heart histology and ECG in cardiac minidystrophin overexpression transgenic mice

On hematoxylin/eosin staining and Masson trichrome staining, heart histology of transgenic mice was indistinguishable from that of normal mice (see Supplementary Figure S2). To evaluate physiological consequences of minidystrophin overexpression, we performed 12 lead electrocardiogram (ECG) in 6-m-old mice. A characteristic change in DMD patients and mdx mice is tachycardia.<sup>2,25-28</sup> The heart

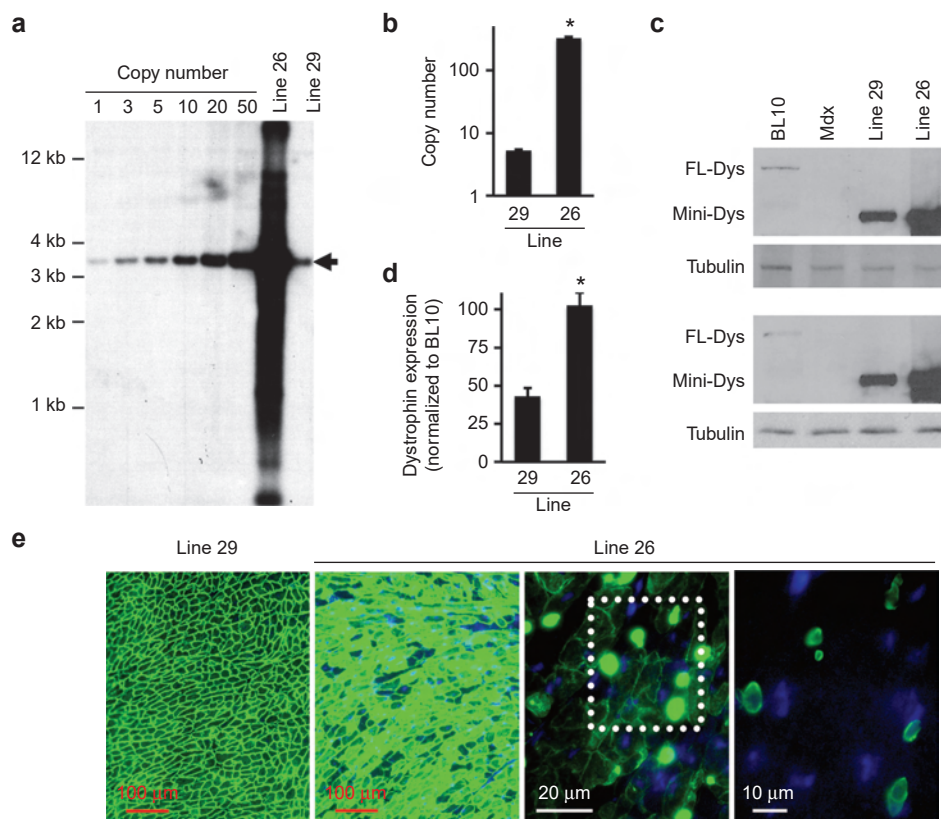


**Figure 1** Transgenic overexpression of a therapeutic minidystrophin gene in the heart of mdx mice. (a) A representative Southern blot photomicrograph. Arrow, the 3.4 kb diagnostic band for transgenic mice. (b) Quantification of the minidystrophin gene copy number in transgenic mice. (c) Two representative dystrophin western blots of the heart of BL10, mdx and transgenic mice. (d) Quantification of minidystrophin expression. The level of expression was normalized to the loading control and BL10 control. (e) Representative dystrophin immunofluorescence staining from the heart of transgenic lines 26 and 29. The left panel (low-power images of line 29 heart) and the second to the left panel (low-power images of line 26 heart) had the identical exposure conditions. The middle panel of line 26 images shows a short-exposure, high-power photomicrograph. Excessively expressed dystrophin forms inclusion body inside cardiomyocytes. The right panel of line 26 images is an enlarged view of the boxed region of the middle panel and it was taken with a much reduced exposure time. The cytosolic dystrophin inclusion bodies appear as vesicles. Nuclei were stained with 4',6'-diamidino-2-phenylindole (DAPI) (blue color). Asterisk, significantly different from the other group.

rate was normalized in line 29 but not in line 26 (Figure 2). In fact, line 26 showed the same heart rate as that of mdx mice. The only ECG abnormality that was corrected in both lines was the PR interval (Figure 2b). When compared with BL10, mdx had a longer QT interval and QRS duration. These defects were completely corrected in line 29. Surprisingly, both parameters got worse in line 26. They were even significantly longer than those of mdx mice (Figure 2b). The Q-wave amplitude showed a peculiar trend. Line 26 was significantly shallower than all other strains. The cardiomyopathy index was used to

evaluate overall electrophysiology in the heart. It was normalized in line 29 but was significantly higher than that of mdx in line 26.

**DISCUSSION**

In this study, we examined the consequences of supraphysiological level minidystrophin expression in the heart of mdx mice. We found that 50-fold overexpression ameliorated ECG defects. In contrast, 100-fold overexpression not only failed to improve the outcome of the most of the ECG parameters but also aggravated abnormalities in several measures (such as the QT interval, QRS duration and cardiomyopathy index). Our results suggest that the murine heart has a quite impressive tolerance to dystrophin overexpression (up to 50-fold). However, when the level of expression becomes excessively high (e.g., 100-fold), it will lead to cardiac toxicity. Specifically, overexpressed dystrophin formed aberrant cytosolic dystrophin vesicles and aggravated ECG abnormalities.

There has been significant progress in the development of DMD gene replacement therapy over the last few years. In particular, adeno-associated virus (AAV)-mediated *microdystrophin* gene delivery has yielded highly promising efficacy data in the murine and canine models.<sup>29,30</sup> Several clinical trials are currently in planning.<sup>31</sup> Despite these advances, one critical question remains incompletely answered. Specifically, how much dystrophin is too much? In other words, will dystrophin overexpression cause a problem? This is highly relevant because dystrophin is expressed from a constitutive promoter (either ubiquitous or muscle-specific) in all gene replacement therapy vectors and AAV is a long lasting virus.<sup>32</sup> To address this question, the Chamberlain laboratory, Seattle, WA studied transgenic mdx mice that had 50-fold dystrophin overexpression. Strikingly, no structural or functional abnormalities were found in skeletal muscle suggesting supraphysiological dystrophin expression is safe in skeletal muscle.<sup>1</sup>

Cardiac complications greatly compromise the life quality of DMD patients. A significant portion of patients dies from heart failure or sudden cardiac death. Hence, an effective DMD gene replacement therapy requires efficient delivery of a therapeutic dystrophin gene to the heart. Overexpression-induced cardiotoxicity is well documented in the literature.<sup>11,14–16,20,33</sup> For example, two fold overexpression of the green fluorescence protein, six fold overexpression of the adenosine receptor and 27-fold overexpression of myosin light chain 1 result in dilated cardiomyopathy.<sup>14–16</sup> Interestingly, depending on the protein being overexpressed, the heart seems to show different levels of tolerance. For example, 16-fold overexpression of myosin light chain 1 is not toxic.<sup>14</sup> Unfortunately, the tolerant range for dystrophin has never been determined. To address this unmet need, we generated cardiac dystrophin overexpressing mice. Since future clinical trials will likely use the abbreviated *dystrophin* gene, we overexpressed a therapeutic *minidystrophin* gene. Consistent with the finding of Cox *et al.*,<sup>1</sup> we did not detect any toxicity in the line with 50-fold minidystrophin overexpression. However, there was clear evidence of toxicity by the ECG assay when expression reached 100-fold of the normal. Based on these findings, we conclude that the heart has a relatively high safety margin for dystrophin overexpression. More specifically, 50-fold minidystrophin overexpression is not toxic to the mouse heart.

Several groups have tested AAV-mediated *dystrophin* gene replacement therapy for Duchenne cardiomyopathy in the mouse model.<sup>25,34–40</sup> Despite widespread expression throughout the entire heart, in none of these studies, AAV-mediated expression exceeded 10-fold of the normal dystrophin level. We have achieved cardiac AAV transduction in dogs and more recently demonstrated efficient

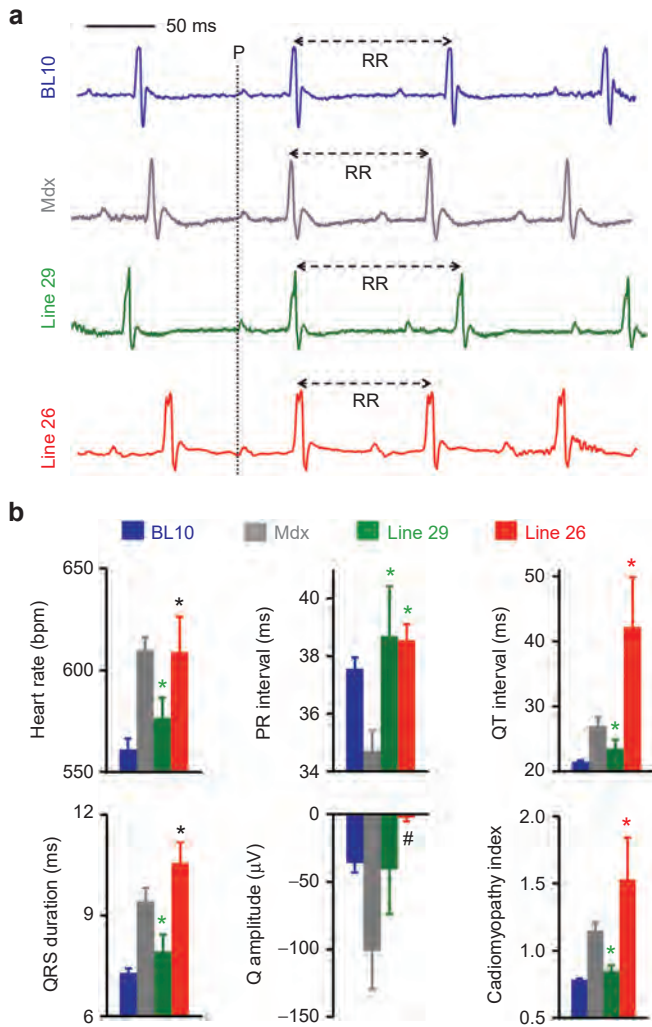


**Figure 2** 100-fold overexpression of the therapeutic ΔH2-R19 minidystrophin gene in the heart of transgenic line 26 worsened electrocardiogram (ECG) defects seen in mdx mice. (a) Representative ECG tracing from BL10, mdx, transgenic line 29 (50-fold overexpression) and line 26 (100-fold overexpression) mice. The dotted vertical line indicates the starting position of the P-wave. Respiratory rate (RR) duration (time between two neighboring heart beats) is clearly reduced in mdx mice and line 26, suggesting the presence of tachycardia in these two strains. In line 29, RR duration is similar to that of BL10 mice. (b) Quantitative comparison of the ECG profile from BL10, mdx, line 29, and line 26. Sample size: n = 10 for BL10 mice, n = 9 for mdx mice, n = 17 for line 29, and n = 13 for line 26. Green asterisk, results from transgenic mice are normalized to that of BL10 mice; black asterisk, results from transgenic mice are similar to that of mdx mice; red asterisk, results from transgenic mice are significantly worse than that of mdx mice; Pound sign, results from Line 26 mice are significantly different from all other lines (BL10, mdx and Line 29).

AAV micro-dystrophin expression in the heart of DMD dogs.<sup>29,41–43</sup> Two independent groups have also demonstrated AAV-mediated exon-skipping in dystrophic dog hearts.<sup>44,45</sup> Yet, it is still a great challenge to obtain saturated myocardial AAV transduction in the heart of a large mammal. We believe that with the current AAV technology, supraphysiologic dystrophin overexpression may not constitute a serious concern for Duchenne cardiomyopathy gene therapy. However, the development of novel AAV capsids, expression cassette and/or gene delivery methods may lead to significantly much higher transduction efficiency in the future.<sup>46–48</sup> The maximal tolerable dystrophin level described in our study will serve as an important reference to guide future studies.

The toxicity seen in the line of 100-fold overexpression suggests that a level higher than 50-fold may also cause harmful changes in skeletal muscle. Indeed, Harper *et al.* observed similar dystrophin aggregation vesicles in the quadriceps muscle of a microdystrophin transgenic line that specifically overexpressed the  $\Delta R2-R21+H3$  microgene in skeletal muscle.<sup>3</sup> On quantification of centrally located myonuclei of 6-m-old mice, the authors found  $\leq 1\%$ , 64% and 52% in BL10 (normal control), mdx, and  $\Delta R2-R21+H3$  microgene overexpression transgenic mice, respectively. Interestingly, in another line that expressed the  $\Delta R4-R23$ , a structurally similar microgene (both microgenes have 4 repeats and 1 hinge), the percent of central nucleation was  $<1\%$ . Although the authors did not quantify the level of overexpression, a rough evaluation based on the western blots in the paper suggests that the lines  $\Delta R2-R21+H3$  and  $\Delta R4-R23$  had a dystrophin level of  $\sim 90$ -fold and  $\sim 10$ -fold of BL10, respectively.

It is currently unclear how 100-fold dystrophin overexpression resulted in cardiac toxicity. We suspect that it may likely relate to the accumulation of excessive amount of dystrophin inclusion bodies in the cytosol. However, we believe the heart may tolerate limited levels of cytosolic dystrophin expression. In support of this notion, we did notice some dystrophin staining in the cytoplasm of cardiomyocytes in transgenic line 29 mice. Chamberlain also observed similar cytosolic dystrophin expression in the heart of their full-length dystrophin transgenic mice.<sup>1</sup> Besides the dystrophin level, it is also possible that the toxicity seen in line 26 may relate to the positional effect of transgene integration. Insertion may have either activated or shut down expression of other important cellular protein(s) and consequently result in toxicity. Nevertheless, the data of the current study as well as that of Cox *et al.* suggest that moderate dystrophin overexpression is relatively safe in muscle.<sup>1</sup> Tight control of dystrophin expression may not be necessary in DMD gene therapy.

## MATERIALS AND METHODS

### Experimental animals

All animal experiments were approved by the institutional animal care and use committee and were in accordance with NIH guidelines. All experimental mice were housed in a specific pathogen-free facility and kept under a 12 hours light (25 lux)/12 hours dark cycle with free access to food and water. C57Bl/10SnJ (BL10) and dystrophin-deficient C57Bl/10ScSn-*Dmd*<sup>mdx</sup>/J (*mdx*) mice were purchased from the Jackson Laboratory (Bar Harbor, ME).

The cardiac specific minidystrophin transgenic mice were generated at the University of Missouri transgenic core. The expression cassette consists of the  $\alpha$ MHC promoter (a gift from Dr Jeffrey Robbins, Division of Molecular Cardiovascular Biology, Cincinnati Children's Hospital Research Foundation, Cincinnati, OH), the  $\Delta H2-R19$  minidystrophin gene (a gift from Dr Jeffrey Chamberlain at the University of Washington, Seattle, WA) and the bovine growth hormone polyadenylation signal.<sup>3,5,7</sup> A total of 10 founders were identified and nine founders were backcrossed with mdx mice for 5–7 generations.<sup>2</sup> In this study, we evaluated incipient congenic mice from lines 26 and 29. Only male mice were used in the study. The ECG assay was performed in 6-m-old male mice.

### Southern blot

Genomic DNA was extracted from the tail using a previously described high salt precipitation protocol.<sup>49</sup> A 414-bp BamH I (exon 4)/EcoR V (exon 7) double digested DNA fragment was used as the template for the Southern probe. Tail genomic DNA was digested with BamH I. After transfer to a nylon membrane, the blot was hybridized with a <sup>32</sup>P-labelled probe according to a previously published protocol.<sup>49</sup> The diagnostic band migrated at 3.4 kb. For the copy number control, the plasmid used for making transgenic mice was digested with BamH I and loaded on the same gel.

### Immunostaining

Dystrophin immunofluorescence staining was performed essentially as we described before using a mouse monoclonal antibody against the C-terminal domain of dystrophin (Dys-2; 1:30; Vector Laboratories, Burlingame, CA).<sup>36,50</sup> Slides were viewed using a Nikon E800 fluorescence microscope. Photomicrographs were taken with a Qimage REtiga 1,300 camera (Burnaby, BC, Canada).<sup>51</sup>

### Western blot

Membrane protein enriched microsomal preparation was extracted from the heart according to our published protocol.<sup>52–54</sup> 50  $\mu$ g protein was separated on a 6% sodium dodecyl sulfate-polyacrylamide gel. After electrophoresis, protein was transferred to a polyvinylidene fluoride membrane. The membrane was probed with the Dys-2 antibody (1:100). For the loading control, we used the  $\alpha$ -tubulin antibody (1:3,000; clone B-5-1-2; Sigma, St Louis, MO). Western blot quantification was performed using ImageJ (<http://rsbweb.nih.gov/ij/>). The relative intensity of the respective protein band was normalized to the corresponding loading control in the same blot. To determine the relative expression level of minidystrophin, the relative band intensity of transgenic mice was further normalized to that of full-length dystrophin in BL10 mice in the same blot. We would like to point out that the full-length dystrophin protein might transfer to the membrane less efficiently than the minidystrophin protein during western analysis due to the large size of the full-length protein (427 kDa). To overcome this technical problem, we have conducted overnight transfer in western blot analysis. Furthermore, we confirmed efficient transfer by the lack of Coomassie blue staining of the polyacrylamide gel after transfer. Despite these efforts, we cannot completely exclude the possibility of incomplete transfer of trivial amount of full-length protein. There is still a very small likelihood that we may have underestimated the quantity of full-length dystrophin. Hence, the relative overexpression of minidystrophin could be slightly lower.

### ECG

A 12-lead ECG assay was performed with an ECG recording system from AD Instruments (Model MLA0112S; Colorado Springs, CO) as described in the *Standard Operating Procedures (SOPs) for Duchenne Animal Models-Cardiac Protocols* ([http://www.parentprojectmd.org/site/PageServer?pagename=Advance\\_researchers\\_sops](http://www.parentprojectmd.org/site/PageServer?pagename=Advance_researchers_sops)).<sup>54,55</sup> Briefly, cardiac electric activity signals were processed with a single channel bioamplifier (Model ML132; AD Instruments). Averaged value from at least 1 minute continuous recording was used for ECG analysis by LabChart software (AD Instruments). The amplitude of the Q-wave was analyzed using the lead I tracing. The remaining ECG parameters were analyzed using lead II tracing results. The cardiomyopathy index is determined by dividing the QT interval by the PQ segment.

### Statistical analysis

Data are presented as mean  $\pm$  SEM. Statistical analysis was performed with the Prism software (GraphPad, San Diego, CA). Statistical significance between two groups was determined by the Student's *t*-test. Statistical significance among different groups was determined by one-way analysis of variance followed by Tukey's *post hoc* analysis. Difference was considered statistically significant when  $P < 0.05$ .

### CONFLICT OF INTEREST

D.D. is a member of the scientific advisory board for and an equity holder of Solid GT, a subsidiary of Solid Biosciences.

## ACKNOWLEDGMENTS

We thank Chun Long for technical assistance. This work was supported by grants from the National Institutes of Health (HL-91883, NS-90634), Department of Defense (MD130014), Jesse's Journey-The Foundation for Gene and Cell Therapy. N.W. was partially supported by the life science fellowship, University of Missouri.

## REFERENCES

- Cox, GA, Cole, NM, Matsumura, K, Phelps, SF, Hauschka, SD, Campbell, KP *et al.* (1993). Overexpression of dystrophin in transgenic mdx mice eliminates dystrophic symptoms without toxicity. *Nature* **364**: 725–729.
- Bostick, B, Yue, Y, Long, C, Marschalk, N, Fine, DM, Chen, J *et al.* (2009). Cardiac expression of a minidystrophin that normalizes skeletal muscle force only partially restores heart function in aged Mdx mice. *Mol Ther* **17**: 253–261.
- Harper, SQ, Hauser, MA, DelloRusso, C, Duan, D, Crawford, RW, Phelps, SF *et al.* (2002). Modular flexibility of dystrophin: implications for gene therapy of Duchenne muscular dystrophy. *Nat Med* **8**: 253–261.
- Lai, Y, Thomas, GD, Yue, Y, Yang, HT, Li, D, Long, C *et al.* (2009). Dystrophins carrying spectrin-like repeats 16 and 17 anchor nNOS to the sarcolemma and enhance exercise performance in a mouse model of muscular dystrophy. *J Clin Invest* **119**: 624–635.
- Gulick, J, Subramaniam, A, Neumann, J and Robbins, J (1991). Isolation and characterization of the mouse cardiac myosin heavy chain genes. *J Biol Chem* **266**: 9180–9185.
- Sánchez, A, Jones, WK, Gulick, J, Doetschman, T and Robbins, J (1991). Myosin heavy chain gene expression in mouse embryoid bodies. An *in vitro* developmental study. *J Biol Chem* **266**: 22419–22426.
- Subramaniam, A, Jones, WK, Gulick, J, Wert, S, Neumann, J and Robbins, J (1991). Tissue-specific regulation of the alpha-myosin heavy chain gene promoter in transgenic mice. *J Biol Chem* **266**: 24613–24620.
- Robbins, J, Palermo, J and Rindt, H (1995). *In vivo* definition of a cardiac specific promoter and its potential utility in remodeling the heart. *Ann NY Acad Sci* **752**: 492–505.
- Milano, CA, Allen, LF, Rockman, HA, Dolber, PC, McMinn, TR, Chien, KR *et al.* (1994). Enhanced myocardial function in transgenic mice overexpressing the beta 2-adrenergic receptor. *Science* **264**: 582–586.
- Palermo, J, Gulick, J, Colbert, M, Fewell, J and Robbins, J (1996). Transgenic remodeling of the contractile apparatus in the mammalian heart. *Circ Res* **78**: 504–509.
- Colbert, MC, Hall, DG, Kimball, TR, Witt, SA, Lorenz, JN, Kirby, ML *et al.* (1997). Cardiac compartment-specific overexpression of a modified retinoic acid receptor produces dilated cardiomyopathy and congestive heart failure in transgenic mice. *J Clin Invest* **100**: 1958–1968.
- Sato, Y, Ferguson, DG, Sako, H, Dorn, GW II, Kadambi, VJ, Yatani, A *et al.* (1998). Cardiac-specific overexpression of mouse cardiac calsequestrin is associated with depressed cardiovascular function and hypertrophy in transgenic mice. *J Biol Chem* **273**: 28470–28477.
- Kadambi, VJ and Kranias, EG (1998). Genetically engineered mice: model systems for left ventricular failure. *J Card Fail* **4**: 349–361.
- James, J, Osinska, H, Hewett, TE, Kimball, T, Kleivitsky, R, Witt, S *et al.* (1999). Transgenic over-expression of a motor protein at high levels results in severe cardiac pathology. *Transgenic Res* **8**: 9–22.
- Huang, WY, Aramburu, J, Douglas, PS and Izumo, S (2000). Transgenic expression of green fluorescence protein can cause dilated cardiomyopathy. *Nat Med* **6**: 482–483.
- Black, RG Jr, Guo, Y, Ge, ZD, Murphree, SS, Prabhu, SD, Jones, WK *et al.* (2002). Gene dosage-dependent effects of cardiac-specific overexpression of the A3 adenosine receptor. *Circ Res* **91**: 165–172.
- Matsui, T, Li, L, Wu, JC, Cook, SA, Nagoshi, T, Picard, MH *et al.* (2002). Phenotypic spectrum caused by transgenic overexpression of activated Akt in the heart. *J Biol Chem* **277**: 22896–22901.
- Hahn, HS, Yussman, MG, Toyokawa, T, Marreez, Y, Barrett, TJ, Hilty, KC *et al.* (2002). Ischemic protection and myofibrillar cardiomyopathy: dose-dependent effects of *in vivo* deltaPKC inhibition. *Circ Res* **91**: 741–748.
- Pontén, A, Li, X, Thorén, P, Aase, K, Sjöblom, T, Ostman, A *et al.* (2003). Transgenic overexpression of platelet-derived growth factor-C in the mouse heart induces cardiac fibrosis, hypertrophy, and dilated cardiomyopathy. *Am J Pathol* **163**: 673–682.
- Habets, PE, Clout, DE, Lekanne Deprez, RH, van Roon, MA, Moorman, AF and Christoffels, VM (2003). Cardiac expression of Gal4 causes cardiomyopathy in a dose-dependent manner. *J Muscle Res Cell Motil* **24**: 205–209.
- Eigenthaler, M, Engelhardt, S, Schinke, B, Kobsar, A, Schmitteckert, E, Gambaryan, S *et al.* (2003). Disruption of cardiac Ena-VASP protein localization in intercalated disks causes dilated cardiomyopathy. *Am J Physiol Heart Circ Physiol* **285**: H2471–H2481.
- Gergs, U, Boknik, P, Buchwalow, I, Fabritz, L, Matus, M, Justus, I *et al.* (2004). Overexpression of the catalytic subunit of protein phosphatase 2A impairs cardiac function. *J Biol Chem* **279**: 40827–40834.
- Li, J, McLerie, M and Lopatin, AN (2004). Transgenic upregulation of IK1 in the mouse heart leads to multiple abnormalities of cardiac excitability. *Am J Physiol Heart Circ Physiol* **287**: H2790–H2802.
- Wheeler, MT, Allikian, MJ, Heydemann, A, Hadhazy, M, Zarnegar, S and McNally, EM (2004). Smooth muscle cell-extrinsic vascular spasm arises from cardiomyocyte degeneration in sarcoglycan-deficient cardiomyopathy. *J Clin Invest* **113**: 668–675.
- Bostick, B, Yue, Y, Lai, Y, Long, C, Li, D and Duan, D (2008). Adeno-associated virus serotype-9 microdystrophin gene therapy ameliorates electrocardiographic abnormalities in mdx mice. *Hum Gene Ther* **19**: 851–856.
- Shin, JH, Bostick, B, Yue, Y, Hajjar, R and Duan, D (2011). SERCA2a gene transfer improves electrocardiographic performance in aged mdx mice. *J Transl Med* **9**: 132.
- Markham, LW, Spicer, RL and Cripe, LH (2005). The heart in muscular dystrophy. *Pediatr Ann* **34**: 531–535.
- McNally, EM, Kaltman, JR, Benson, DW, Canter, CE, Cripe, LH, Duan, D, *et al.* (2015). Contemporary cardiac issues in Duchenne muscular dystrophy. *Circulation* **131**: 1590–1598.
- Yue, Y, Pan, X, Hakim, CH, Kodippili, K, Zhang, K, Shin, JH *et al.* (2015). Safe and bodywide muscle transduction in young adult Duchenne muscular dystrophy dogs with adeno-associated virus. *Hum Mol Genet* **24**: 5880–5890.
- Duan, D (2015). Duchenne muscular dystrophy gene therapy in the canine model. *Hum Gene Ther Clin Dev* **26**: 57–69.
- Bengtsson, NE, Seto, JT, Hall, JK, Chamberlain, JS and Odom, GL (2016). Progress and prospects of gene therapy clinical trials for the muscular dystrophies. *Hum Mol Genet* **25**(R1): R9–R17.
- Buchlis, G, Podsakoff, GM, Radu, A, Hawk, SM, Flake, AW, Mingozzi, F *et al.* (2012). Factor IX expression in skeletal muscle of a severe hemophilia B patient 10 years after AAV-mediated gene transfer. *Blood* **119**: 3038–3041.
- Milano, CA, Dolber, PC, Rockman, HA, Bond, RA, Venable, ME, Allen, LF *et al.* (1994). Myocardial expression of a constitutively active alpha 1B-adrenergic receptor in transgenic mice induces cardiac hypertrophy. *Proc Natl Acad Sci USA* **91**: 10109–10113.
- Bostick, B, Shin, JH, Yue, Y and Duan, D (2011). AAV-microdystrophin therapy improves cardiac performance in aged female mdx mice. *Mol Ther* **19**: 1826–1832.
- Bostick, B, Shin, JH, Yue, Y, Wasala, NB, Lai, Y and Duan, D (2012). AAV micro-dystrophin gene therapy alleviates stress-induced cardiac death but not myocardial fibrosis in >21-m-old mdx mice, an end-stage model of Duchenne muscular dystrophy cardiomyopathy. *J Mol Cell Cardiol* **53**: 217–222.
- Yue, Y, Li, Z, Harper, SQ, Davisson, RL, Chamberlain, JS and Duan, D (2003). Microdystrophin gene therapy of cardiomyopathy restores dystrophin-glycoprotein complex and improves sarcolemma integrity in the mdx mouse heart. *Circulation* **108**: 1626–1632.
- Gregorevic, P, Allen, JM, Minami, E, Blankinship, MJ, Haraguchi, M, Meuse, L *et al.* (2006). rAAV6-microdystrophin preserves muscle function and extends lifespan in severely dystrophic mice. *Nat Med* **12**: 787–789.
- Townsend, D, Blankinship, MJ, Allen, JM, Gregorevic, P, Chamberlain, JS and Metzger, JM (2007). Systemic administration of micro-dystrophin restores cardiac geometry and prevents dobutamine-induced cardiac pump failure. *Mol Ther* **15**: 1086–1092.
- Schinkel, S, Bauer, R, Bekeredjian, R, Stucka, R, Rutschow, D, Lochmüller, H *et al.* (2012). Long-term preservation of cardiac structure and function after adeno-associated virus serotype 9-mediated microdystrophin gene transfer in mdx mice. *Hum Gene Ther* **23**: 566–575.
- Shin, JH, Nishihara-Kasahara, Y, Hayashita-Kinoh, H, Ohshima-Hosoyama, S, Kinoshita, K, Chiyo, T *et al.* (2011). Improvement of cardiac fibrosis in dystrophic mice by rAAV9-mediated microdystrophin transduction. *Gene Ther* **18**: 910–919.
- Pan, X, Yue, Y, Zhang, K, Hakim, CH, Kodippili, K, McDonald, T *et al.* (2015). AAV-8 is more efficient than AAV-9 in transducing neonatal dog heart. *Hum Gene Ther Methods* **26**: 54–61.
- Pan, X, Yue, Y, Zhang, K, Lostal, W, Shin, JH and Duan, D (2013). Long-term robust myocardial transduction of the dog heart from a peripheral vein by adeno-associated virus serotype-8. *Hum Gene Ther* **24**: 584–594.
- Hakim, CH, Yue, Y, Shin, JH, Williams, RR, Zhang, K, Smith, BF *et al.* (2014). Systemic gene transfer reveals distinctive muscle transduction profile of tyrosine mutant AAV-1, -6, and -9 in neonatal dogs. *Mol Ther Methods Clin Dev* **1**: 14002.
- Bish, LT, Sleeper, MM, Forbes, SC, Wang, B, Reynolds, C, Singletary, GE *et al.* (2012). Long-term restoration of cardiac dystrophin expression in golden retriever muscular dystrophy following rAAV6-mediated exon skipping. *Mol Ther* **20**: 580–589.
- Barbash, IM, Cecchini, S, Faranesh, AZ, Virag, T, Li, L, Yang, Y *et al.* (2013). MRI roadmapped transendocardial delivery of exon-skipping recombinant adeno-associated virus restores dystrophin expression in a canine model of Duchenne muscular dystrophy. *Gene Ther* **20**: 274–282.
- Duan, D, Yue, Y, Yan, Z and Engelhardt, JF (2000). A new dual-vector approach to enhance recombinant adeno-associated virus-mediated gene expression through intermolecular cis activation. *Nat Med* **6**: 595–598.
- Zhong, L, Li, B, Mah, CS, Govindasamy, L, Agbandje-McKenna, M, Cooper, M *et al.* (2008). Next generation of adeno-associated virus 2 vectors: point mutations in tyrosines lead to high-efficiency transduction at lower doses. *Proc Natl Acad Sci USA* **105**: 7827–7832.
- Nance, ME and Duan, D (2015). Perspective on adeno-associated virus capsid modification for Duchenne muscular dystrophy gene therapy. *Hum Gene Ther* **26**: 786–800.

49. Duan, D, Yue, Y, Zhou, W, Labe, B, Ritchie, TC, Grosschedl, R *et al.* (1999). Submucosal gland development in the airway is controlled by lymphoid enhancer binding factor 1 (LEF1). *Dev* **126**: 4441–4453.
50. Yue, Y, Liu, M and Duan, D (2006). C-terminal-truncated microdystrophin recruits dystrobrevin and syntrophin to the dystrophin-associated glycoprotein complex and reduces muscular dystrophy in symptomatic utrophin/dystrophin double-knockout mice. *Mol Ther* **14**: 79–87.
51. Wasala, NB, Bostick, B, Yue, Y and Duan, D (2013). Exclusive skeletal muscle correction does not modulate dystrophic heart disease in the aged mdx model of Duchenne cardiomyopathy. *Hum Mol Genet* **22**: 2634–2641.
52. Yue, Y, Skimming, JW, Liu, M, Strawn, T and Duan, D (2004). Full-length dystrophin expression in half of the heart cells ameliorates beta-isoproterenol-induced cardiomyopathy in mdx mice. *Hum Mol Genet* **13**: 1669–1675.
53. Lai, Y, Yue, Y, Liu, M, Ghosh, A, Engelhardt, JF, Chamberlain, JS *et al.* (2005). Efficient *in vivo* gene expression by trans-splicing adeno-associated viral vectors. *Nat Biotechnol* **23**: 1435–1439.
54. Bostick, B, Yue, Y, Long, C and Duan, D (2008). Prevention of dystrophin-deficient cardiomyopathy in twenty-one-month-old carrier mice by mosaic dystrophin expression or complementary dystrophin/utrophin expression. *Circ Res* **102**: 121–130.
55. Bostick, B, Yue, Y and Duan, D (2011). Phenotyping cardiac gene therapy in mice. *Methods Mol Biol* **709**: 91–104.



This work is licensed under a Creative Commons Attribution-NonCommercial-NoDerivs 4.0 International License. The images or other third party material in this article are included in the article's Creative Commons license, unless indicated otherwise in the credit line; if the material is not included under the Creative Commons license, users will need to obtain permission from the license holder to reproduce the material. To view a copy of this license, visit <http://creativecommons.org/licenses/by-nc-nd/4.0/>

©Y Yue *et al.* (2016)

Supplementary Information accompanies this paper on the *Molecular Therapy—Methods & Clinical Development* website (<http://www.nature.com/mtm>)



ELSEVIER



# Systemic delivery of adeno-associated viral vectors

Dongsheng Duan<sup>1,2,3,4</sup>

For diseases like muscular dystrophy, an effective gene therapy requires bodywide correction. Systemic viral vector delivery has been attempted since early 1990s. Yet a true success was not achieved until mid-2000 when adeno-associated virus (AAV) serotype-6, 8 and 9 were found to result in global muscle transduction in rodents following intravenous injection. The simplicity of the technique immediately attracts attention. Marvelous whole body amelioration has been achieved in rodent models of many diseases. Scale-up in large mammals also shows promising results. Importantly, the first systemic AAV-9 therapy was initiated in patients in April 2014. Recent studies have now begun to reveal molecular underpinnings of systemic AAV delivery and to engineer new AAV capsids with superior properties for systemic gene therapy.

## Addresses

<sup>1</sup> Department of Molecular Microbiology and Immunology, School of Medicine, The University of Missouri, Columbia, MO 65212, USA

<sup>2</sup> Department of Neurology, School of Medicine, The University of Missouri, Columbia, MO 65212, USA

<sup>3</sup> Department of Bioengineering, The University of Missouri, Columbia, MO 65212, USA

<sup>4</sup> Department of Biomedical Sciences, College of Veterinary Medicine, The University of Missouri, Columbia, MO 65212, USA

Corresponding author: Duan, Dongsheng ([duand@missouri.edu](mailto:duand@missouri.edu))

Current Opinion in Virology 2016, 21:16–25

This review comes from a themed issue on **Viral gene therapy vector–host interactions**

Edited by **David Markusic** and **Roland Herzog**

<http://dx.doi.org/10.1016/j.coviro.2016.07.006>

1879-6257/© 2016 Elsevier B.V. All rights reserved.

## Introduction

Many life-threatening diseases affect a number of organs or affect tissues that are widely distributed. A successful gene therapy for these diseases requires a viral vector that can effectively reach all target cells throughout the body. Since our vessels are a built-in and ready-to-use system for bodywide transportation, a convenient strategy to achieve systemic delivery would be infusion of a therapeutic viral vector into the circulation. For this seeming straightforward method to work, a viral vector has to reach the target area, get out from the vasculature and infect the diseased cells.

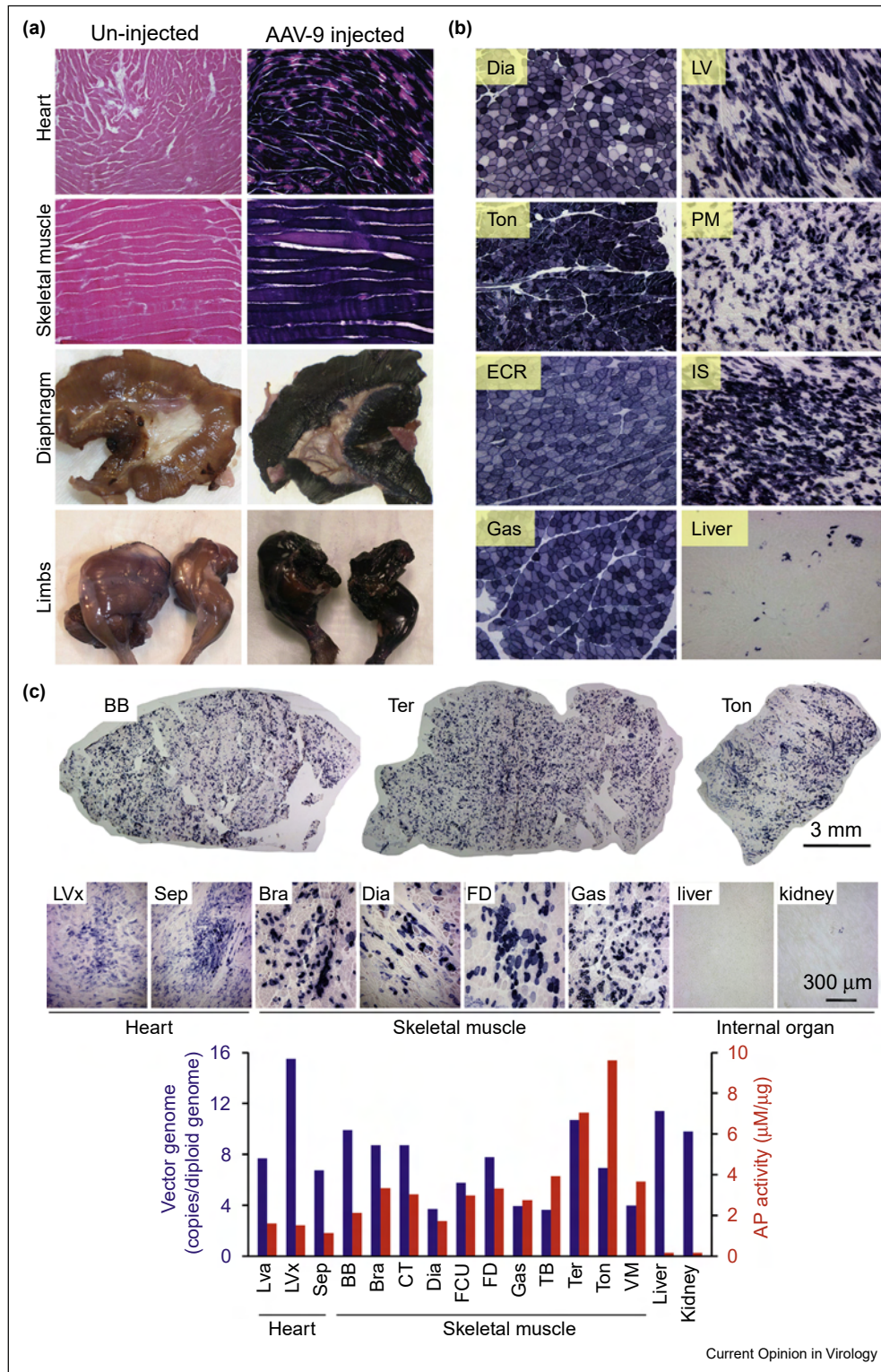
A report in 1992 claimed to have achieved ‘widespread long-term gene transfer’ to striated muscles in newborn mice using recombinant adenovirus [1]. The authors delivered adenovirus intravenously to 2–5-day-old mice and detected some expression in the liver, lung, heart and skeletal muscle. While the adenoviral vector had indeed spread to various tissues and organs, there were only sporadic transduction in skeletal muscle and ~0.2% transduction in the heart. This is far from 20 to 50% gene transfer efficiency required to treat skeletal muscle disease and cardiomyopathy in diseases like Duchenne muscular dystrophy (DMD) [2,3]. Several strategies were developed to overcome the endothelial barrier for systemic adenovirus delivery. These include the application of the vessel dilator and permeabilizer, hydrodynamic injection and viral capsid modification [4–6]. Despite improved intravascular transduction of a single limb with pressurized infusion and endothelial permeabilization, adenoviral vectors eventually lose the favor for systemic delivery due to severe immune responses and fatal complications [7].

Over the last two decades, adeno-associated virus (AAV) has emerged and now become the most preferred vector for gene therapy [8\*,9\*,10\*,11]. AAV is a single stranded DNA virus discovered in 1965 [12]. It persists mainly as episomal molecules in infected tissues [13–15]. More than 12 different serotypes and hundreds of capsid variants have been isolated from adenoviral stocks and animal tissues or engineered in laboratories. In contrast to adenovirus, intramuscular injection of recombinant AAV serotype-2 (AAV-2) resulted in yearlong robust transduction with nominal cellular immune responses [16,17]. Strategies that have been shown to enhance adenoviral intravascular delivery (such as pharmacological vessel permeabilization and forced extravasation) also resulted in uniform whole limb muscle transduction by AAV-2 [4,18]. However, there remains a significant gap to achieve whole body gene transfer from peripheral vessels. A bona fide breakthrough in systemic gene delivery has to wait until new AAV serotypes are isolated.

## Systemic gene delivery with AAV in rodents

In early days of AAV vector development, most studies are focused on AAV-2. Isolation of new serotypes has greatly expanded the repertoire [19–21]. Rutledge *et al.* isolated AAV-6 from an adenovirus stock [22]. Gao *et al.* isolated AAV-8 and AAV-9 from tissues of rhesus monkey and human, respectively [23\*\*,24]. These three serotypes open the door to a successful systemic delivery. Gregorevic *et al.* showed efficient whole body striated muscle transduction in mice after tail vein

Figure 1



Systemic AAV delivery results in bodywide gene transfer in rodents and large mammals. Peripheral vascular delivery provides a method that allows an AAV vector to reach most, if not every, part of the body. **(a)** Bodywide muscle transduction in mice following tail vein delivery of an alkaline phosphatase (AP) reporter gene AAV-9 vector. **(b)** Robust and persistent (up to one year) skeletal muscle and myocardial transduction after jugular vein injection of an AAV-8 AP vector in a neonatal dog. **(c)** Tyrosine mutant AAV-9 results in whole body striated muscle transduction in young adult dystrophic dogs. Top panel, representative full-view images from selected skeletal muscles; middle panel, representative

Table 1

## Comparison of AAV-2 with AAV-1, 6, 7, 8 and 9 for systemic delivery

	AAV-1	AAV-2	AAV-6	AAV-7	AAV-8	AAV-9	References
<i>In vitro</i> capsid stability	Moderate	Low	?	?	Moderate	?	[140]
Blood clearance	Fast	Fast	Fast	Fast	Fast	Slow	[31*,94]
Transcytosis	?	Poor	Poor	?	High	High	[99,100*,101]
Direct muscle transduction efficiency	High	Moderate	Very high	High	Moderate	High–very high	[23**,129]
Systemic transduction efficiency	High	Low	High	High	High–very high	Very high	[26**,30,31*,32]
Unique features		Very efficient in cultured cells			Low immunity <sup>a</sup>	Cardiotropic in rodents <sup>b</sup> ; Cross BBB <sup>c</sup>	

<sup>a</sup> See Refs. [40,82\*] and [79,141–146].

<sup>b</sup> See Refs. [27\*,28\*,29\*, 30,31\*, 32].

<sup>c</sup> See Refs. [85\*\*,86–89]. BBB, blood–brain–barrier.

injection of AAV-6 and the vascular endothelium growth factor for transient microvasculature permeabilization [25\*\*]. Wang *et al.* achieved widespread saturated transduction of the heart as well as axial and appendicular muscles in mice and hamsters via systemic delivery of AAV-8 [26\*\*]. Shortly after, successful bodywide systemic gene transfer was established for AAV-9 (Figure 1) [27\*,28\*,29\*]. Interestingly, peripheral delivery of AAV-9 resulted in superior myocardial and central nervous system transduction. It is now clear that other AAV serotypes (such as AAV-1 and AAV-7) can also lead to systemic transduction (Table 1) [26\*\*,30,31\*]. Nevertheless, AAV-9 remains the most potent serotype for systemic delivery in rodents [30,31\*,32].

The establishment of systemic AAV delivery technique immediately raises the possibility for bodywide correction in rodent models of human diseases. Today, impressive results have been reported in neonatal, adult and even aged animals. Some of these examples include AAV-1 mediated gene therapy for Pompe disease, limb-girdle muscular dystrophy (LGMD) and myotonic dystrophy [33–35], AAV-6 mediated gene therapy for DMD and facioscapulohumeral muscular dystrophy [25\*\*,36\*,37,38], AAV-8-mediated gene therapy for DMD, LGMD and atherosclerosis [26\*\*,39–41], and AAV-9 mediated gene therapy for cardiomyopathy, lysosomal storage disorders and neuronal diseases [42,43,44\*,45–51].

The maximal packaging capacity of an AAV vector is ~5-kb [52–55]. This limits the use of AAV for a number of diseases including DMD and dysferlin-deficient myopathy. Various dual AAV strategies have been developed to overcome this hurdle (reviewed in [56–58]). Optimized dual AAV vectors have reach transduction efficiency of

the single AAV vector [59,60]. Ghosh *et al.* provided the first proof-of-principle evidence for efficient systemic dual AAV delivery in normal and diseased mice [61\*,62]. Subsequent studies from several laboratories showed unequivocal evidence that systemic dual AAV therapy is a viable option for bodywide alleviation for DMD and dysferlin-deficient myopathy [63–65].

### Scale-up systemic AAV delivery in large mammals

The remarkable success in rodents and the convenience of the technique have stimulated tremendous interests in adopting systemic AAV delivery to large mammals. The first successful systemic AAV delivery to a large mammal was achieved with AAV-9 in newborn canines (Figure 1) [66\*]. Surprisingly, despite spectacular bodywide skeletal muscle transduction, few cardiomyocytes were transduced [66\*]. In sharp contrast, AAV-8 yielded robust transduction of both skeletal and cardiac muscles in dog puppies (Figure 1) [67,68]. AAV-1 and AAV-6 are two other serotypes that have shown good systemic transduction in rodents [26\*\*,30,31\*]. Recent studies suggest that mutating surface-exposed tyrosine can significantly enhance AAV transduction [69,70]. Hakim *et al.* tested tyrosine modified AAV-1 and AAV-6 in neonatal dogs [71]. Interestingly, AAV-1 showed high efficient whole body striated muscle transduction but AAV-6 resulted in little muscle transduction (Figure 1). Two groups explored systemic AAV-9 delivery in newborn DMD puppies [72,73\*]. Gene transfer was observed in multiple muscles up to 4 months of age. However, Kornegay *et al.* encountered a catastrophic inflammatory response potentially linked to the transgene product [73\*]. Contrary to Kornegay *et al.*, Hinderer *et al.* reasoned that neonatal period could be a window to induce immune tolerance to the transgene product [74].

(Figure 1 Legend Continued) high-power images from selected skeletal muscles, heart and internal organs; bottom panel, quantification of the AAV genome and AP expression in selective tissues. BB, biceps brachii; Bra, brachialis; Dia, diaphragm; CT, cranial tibialis; ECR, extensor carpi radialis; FCU, flexor carpi ulnaris; FD, flexor digitorum; Gas, gastrocnemius; IS, interstitial septum; LV, left ventricle; LVa, left ventricle anterior portion; LVx, left ventricle apex; PM, papillary muscle; Sep, septum; TB, triceps brachii; Ter, teres; Ton, tongue; VM, vastus medialis.

Indeed, they were able to achieve this goal by systemic delivery of low-dose AAV-8 (30-fold lower than used by Kornegay *et al.*) in rhesus monkeys and type I mucopolysaccharidosis dogs [74].

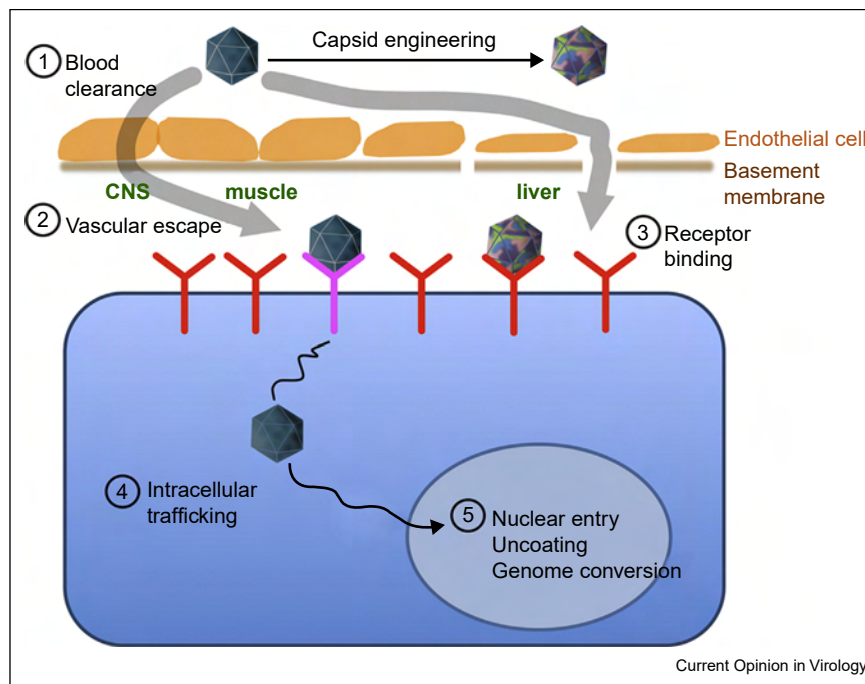
Very few studies have evaluated systemic AAV delivery to adult large mammals. An early work in cynomolgus monkeys suggests that even very low-dose AAV ( $\leq 5 \times 10^{10}$  particles/kg) can result in vector genome accumulation in the spleen and expression in the lymph nodes [75]. Intriguingly, regional intravascular delivery of AAV to nonhuman primates is devoid of cellular immunotoxicity [76–78]. Several groups have shown successful regional limb perfusion with AAV-1 and 8 in normal and diseased dogs [79–81,82\*]. A breakthrough of systemic AAV transfer in a diseased adult large mammal has not been achieved until recently. Yue *et al.* injected tyrosine mutant AAV-9 to young adult DMD dogs from a peripheral vein and observed efficient global skeletal and cardiac muscle transduction without serious complications (Figure 1) [83\*\*]. Hakim *et al.* further extended this result demonstrating systemic delivery of an AAV-9 micro-dystrophin vector can lead to near saturated expression for at least 12 months without any toxicity in adult affected dogs [84].

The most exciting progress is the ongoing clinical trial in neonatal spinal muscular atrophy (SMA) patients using AAV-9 by Drs. Mendel, Kaspar and colleagues (clinical trial ID: NCT02122952) [85\*\*]. SMA is caused by mutations in the survival motor neuron 1 (SMN1) gene. Earlier studies from several groups have revealed remarkable therapeutic benefits in newborn SMA mice with AAV-9 mediated systemic SMN1 gene therapy [86–89]. In this game-changing clinical trial, fifteen 1 to 8-m-old patients received intravenous injection of up to  $2 \times 10^{14}$  particles/kg of the AAV-9 SMN1 vector. Some patients have been treated for almost two years. There was no major safety concerns. Importantly, high-dose group patients showed clinical improvement [85\*\*].

### Mechanistic insights of systemic AAV delivery

A better understanding on the mechanisms of systemic AAV transduction is essential to further improve this important gene therapy technology. The major rate-limiting steps may include interaction with serum proteins, blood clearance, vessel escape, attachment, endocytosis, intracellular processing, nuclear entry and vector genome conversion (Figure 2, Table 1). The last five steps have been extensively reviewed elsewhere and will not be discussed here [90,91].

Figure 2



Rate-limiting steps in systemic AAV delivery. The major rate-limiting steps include interaction with serum proteins (such as neutralizing antibodies), blood clearance, vessel escape, attachment, endocytosis, intracellular processing, nuclear entry and vector genome conversion. Capsid engineering can yield new AAV variants with enhanced systemic delivery properties. Numerical numbers highlight five rate-limiting barriers. Capillaries in the central nerve system (CNS) are sealed by the blood–brain barrier. Transcytosis is the only way for AAV to exit the vasculature in CNS. Capillaries in the liver and spleen are fenestrated and discontinuous. This allows for efficient paracellular diffusion of AAV into the parenchyma. Capillaries in muscles may allow for limited paracellular transport of AAV. However, transcytosis may likely be the primary pathway for AAV to get to muscle.

Interaction of AAV with circulating proteins greatly influences the outcome of systemic delivery. Inactivation by pre-existing neutralizing antibodies has been well documented. Recently, Denard *et al.* found that some blood proteins bind to certain AAV serotypes in a species-specific manner [92,93]. In particular, AAV-6 interacts with the galectin 3 binding protein in human and dog sera but not macaque and mouse sera. This interaction aggregates AAV particles and hampers systemic delivery [92]. On the other side, AAV-6 interacts with the C-reactive protein in mouse but not human sera. Instead of inhibition, this interaction boosts systemic delivery [93].

Blood clearance varies dramatically among AAV serotypes [31\*,94]. While rapid clearance may not necessarily abort systemic delivery, prolongation of the circulation time certainly enhances it [31\*,94,95,96\*]. In this regard, delayed clearance has been suggested as a primary reason underlying pronounced systemic delivery of AAV-9 [94]. Shen *et al.* investigated the underlying mechanisms for extended persistence of AAV-9 in blood and found that it is due to the low abundance of the AAV-9 receptor, hence reduced tissue binding [95]. It is very likely that the blood clearance of AAV is regulated by many factors. Additional studies may reveal these yet unknown factors. On the other side, future studies are also needed to explain why fast blood clearance of some AAV serotypes (such as AAV-8) has minimal impact on systemic delivery (Table 1).

Depending on the architecture of capillary, AAV may get out from blood via two different pathways, paracellular or transcellular (Figure 2). Paracellular transport refers to the escape of a virus from the circulation through the space between adjacent endothelial cells. Capillaries in the liver and spleen are fenestrated and discontinuous (Figure 2). In these tissues, AAV can readily diffuse out through large gaps between endothelial cells. This paracellular mechanism contributes to the accumulation of the AAV genome in the liver following systemic delivery [25\*\*,27\*,30,31\*,83\*\*,97].

In the central nerve system, the tight junctions between neighboring endothelial cells form the highly selective blood-brain barrier (Figure 2). In this case, the only way to escape from the circulation is transcellular transcytosis (Figure 2). In this process, AAV is taken into endothelial cells in specialized vesicles [98]. These vesicles traffic to the other side of the cell and release the virus into the interstitium. AAV transcytosis has been documented *in vitro* [99,100\*,101]. Interestingly, AAV-8 and 9 show efficient transcytosis but AAV-6 does not [100\*,101,102]. Recent studies have revealed two distinctive mechanisms of transcytosis, dependent or independent of caveolae [103]. Kotchey *et al.* found that systemic AAV-9 transduction is not compromised in caveolin-1 knockout mice. Since AAV-9 displays unparalleled superior neuronal tissue transduction when delivered through the

peripheral vein [104], it is very likely that transvascular transport of AAV-9 is through caveolae-independent transcytosis [94].

### Re-engineering AAV for improved systemic delivery

Despite the great promise of systemic delivery, the current technology remains limited. For example, a large proportion of humans are seropositive for known AAV serotypes [105,106]. Further, systemic delivery often leads to gene transfer in non-target tissues and organs. AAV transduction is largely determined by the viral capsid, especially variable loops on the surface [107,108\*,109]. Several strategies have been used to develop novel capsids for improved systemic delivery. These include (1) isolation and reconstruction from existing or ancestral species [110,111], and (2) modification by rational design and directed evolution [112\*,113].

Many new AAV isolates have been tested for systemic delivery recently. These studies have revealed some unique organism, organ, tissue, or cell-type specific transduction patterns after intravascular delivery. For example, AAV-3B showed superior hepatotropism in the primate but not rodent liver [114–116]. AAV-4 showed selective cardiopulmonary tropism [117]. AAV-rh8 and rh10 are as efficient as AAV-9 in crossing the blood-brain barrier [118].

A hurdle to systemic AAV delivery is the high prevalence (40–80%) of pre-existing immunity in human populations (reviewed in [119]). While some successes have been achieved with the application of immune suppressive drugs (such as anti-CD20 antibody rituximab) and plasmapheresis [120–122], modification of the antigenic epitope on the capsid may yield neutralizing-resistant ‘designer’ AAV variants. Several approaches have been used to map the neutralizing antibody binding epitopes for different AAV serotypes (reviewed in [123]). These studies suggest that protrusions around the 3-fold axis and 2/5-fold wall participate in interactions with neutralizing antibodies [123]. Targeted mutagenesis of these residues may circumvent preexisting immunity [124,125]. An alternative and highly effective method to targeted mutagenesis is forced evolution in the presence of high amounts of neutralizing antibodies (such as pooled immunoglobulins from human donors) (reviewed in [112\*,126]). This approach has allowed isolation of neutralizing antibody escaping AAV variants AAV-r2.15 by Maheshri *et al.* and AAV-DJ by Grimm *et al.* [127\*,128]. More recently, Li *et al.* found that capsid variants isolated following *in vitro* selection in human serum had poor *in vivo* transduction strength although they were able to escape neutralization [129]. *In vivo* selection in the presence of the patient serum may yield escaping-capsids with better *in vivo* performance [129].

Blood clearance is a rate-limiting barrier in systemic delivery. The determinants for AAV-9 blood clearance were reported recently [94,95,130]. These mainly consist of surface-exposed amino acids and overlap with the receptor footprint. Mutations in these residues substantially shorten the circulation half-life and reduce systemic transduction [94,95,130].

Delivery of a viral vector through the bloodstream will likely spread the virus to untoward tissues/organs. This raises safety concerns. Sequestration of AAV in these non-target locations also reduces the amount of vectors that can be delivered to the targets and hence has significant implications on the effective vector dose needed for systemic therapy. Tissue/cell-specific AAV will help resolve this problem. A series of tropism-modified AAV capsid variants have been developed using either *in vivo* evolution or educated engineering. These capsid chimeras are highly desirable for systemic gene therapy of various diseases, for example, liver-detargeted vectors for muscular dystrophy [96\*,130–132], liver-enhanced vectors for hemophilia [128,133\*], myocardium tropic vectors for cardiomyopathy [134], central nerve system-enhanced vectors for neurodegenerative diseases [135].

AAV uses cell surface carbohydrates as its binding receptors [136]. The nature and abundance of these extracellular glycans vary dramatically between different species and at different developmental stages. Since AAV attachment is a determining factor in systemic delivery, cautions should be taken to extrapolate re-engineered capsids for different applications [102,115,116,137].

## Conclusion

The non-invasive nature and the convenience of peripheral vascular delivery promise a straightforward approach to treating a number of diseases. Many barriers have been overcome. However, there remain significant hurdles to translate the promise of systemic delivery into clinical benefits in human patients. Further, new challenges will surface as we learn more about AAV (such as the discovery of the universal AAV receptor) and begin to apply systemic delivery to new technologies (such as gene editing with the CRISPR technology) [138\*,139]. The study on systemic viral vector delivery has just reached its prime time and the best is yet to come.

## Acknowledgements

The research in the Duan lab is supported by the National Institutes of Health (NS-90634, AR-69085, AR-67985 and AR-70517), Department of Defense (MD130014 and MD150133), Muscular Dystrophy Association, Jesse's Journey-The Foundation for Gene and Cell Therapy, Parent Project Muscular Dystrophy, Hope for Javier, Solid GT LLC and the University of Missouri.

*Disclosure:* D.D. is a member of the scientific advisory board for Solid GT, LLC and an equity holder of Solid GT, LLC. The Duan lab has received research supports from Solid GT, LLC.

## References and recommended reading

Papers of particular interest, published within the period of review, have been highlighted as:

- of special interest
- of outstanding interest

1. Stratford-Perricaudet LD, Makeh I, Perricaudet M, Briand P: **Widespread long-term gene transfer to mouse skeletal muscles and heart.** *J Clin Invest* 1992, **90**:626-630.
  2. Chamberlain JS: **Gene therapy of muscular dystrophy.** *Hum Mol Genet* 2002, **11**:2355-2362.
  3. Duan D: **Challenges and opportunities in dystrophin-deficient cardiomyopathy gene therapy.** *Hum Mol Genet* 2006, **15**(Spec No 2):R253-R261.
  4. Greelish JP, Su LT, Lankford EB, Burkman JM, Chen H, Konig SK, Mercier IM, Desjardins PR, Mitchell MA, Zheng XG *et al.*: **Stable restoration of the sarcoglycan complex in dystrophic muscle perfused with histamine and a recombinant adeno-associated viral vector.** *Nat Med* 1999, **5**:439-443.
  5. Douglas JT, Curiel DT: **Strategies to accomplish targeted gene delivery to muscle cells employing tropism-modified adenoviral vectors.** *Neuromuscul Disord* 1997, **7**:284-298.
  6. Cho WK, Ebihara S, Nalbantoglu J, Gilbert R, Massie B, Holland P, Karpati G, Petrof BJ: **Modulation of Starling forces and muscle fiber maturity permits adenovirus-mediated gene transfer to adult dystrophic (mdx) mice by the intravascular route.** *Hum Gene Ther* 2000, **11**:701-714.
  7. Wilson JM: **Lessons learned from the gene therapy trial for ornithine transcarbamylase deficiency.** *Mol Genet Metab* 2009, **96**:151-157.
  8. Muzyczka N: **Use of adeno-associated virus as a general transduction vector for mammalian cells.** *Curr Top Microbiol Immunol* 1992, **158**:97-129.
- This review article summarizes the very early stage of AAV vector development.
9. Carter BJ: **Adeno-associated virus and the development of adeno-associated virus vectors: a historical perspective.** *Mol Ther* 2004, **10**:981-989.
- This is a comprehensive review of the history of AAV vector development.
10. Samulski RJ, Muzyczka N: **AAV-mediated gene therapy for research and therapeutic purposes.** *Annu Rev Virol* 2014, **1**:427-451.
- This is a comprehensive review of AAV transduction biology.
11. Muzyczka N, Berns KI: **AAV's golden jubilee.** *Mol Ther* 2015, **23**:807-808.
  12. Atchison RW, Casto BC, Hammon WM: **Adenovirus-associated defective virus particles.** *Science* 1965, **149**:754-756.
  13. Duan D, Sharma P, Yang J, Yue Y, Dudus L, Zhang Y, Fisher KJ, Engelhardt JF: **Circular intermediates of recombinant adeno-associated virus have defined structural characteristics responsible for long term episomal persistence in muscle.** *J Virol* 1998, **72**:8568-8577.
  14. Schnepf BC, Jensen RL, Chen CL, Johnson PR, Clark KR: **Characterization of adeno-associated virus genomes isolated from human tissues.** *J Virol* 2005, **79**:14793-14803.
  15. Penaud-Budloo M, Le Guiner C, Nowrouzi A, Toromanoff A, Cheral Y, Chenuaud P, Schmidt M, von Kalle C, Rolling F, Moullier P *et al.*: **Adeno-associated virus vector genomes persist as episomal chromatin in primate muscle.** *J Virol* 2008, **82**:7875-7885.
  16. Xiao X, Li J, Samulski RJ: **Efficient long-term gene transfer into muscle tissue of immunocompetent mice by adeno-associated virus vector.** *J Virol* 1996, **70**:8098-8108.
  17. Kessler PD, Podsakoff GM, Chen X, McQuiston SA, Colosi PC, Matelis LA, Kurtzman GJ, Byrne BJ: **Gene delivery to skeletal muscle results in sustained expression and systemic delivery of a therapeutic protein.** *Proc Natl Acad Sci U S A* 1996, **93**:14082-14087.

18. Su LT, Gopal K, Wang Z, Yin X, Nelson A, Kozyak BW, Burkman JM, Mitchell MA, Low DW, Bridges CR *et al.*: **Uniform scale-independent gene transfer to striated muscle after transvenular extravasation of vector.** *Circulation* 2005, **112**:1780-1788.
19. Wu Z, Asokan A, Samulski RJ: **Adeno-associated virus serotypes: vector toolkit for human gene therapy.** *Mol Ther* 2006, **14**:316-327.
20. Gao G, Vandenberghe LH, Wilson JM: **New recombinant serotypes of AAV vectors.** *Curr Gene Ther* 2005, **5**:285-297.
21. Vandenberghe LH, Wilson JM, Gao G: **Tailoring the AAV vector capsid for gene therapy.** *Gene Ther* 2009, **16**:311-319.
22. Rutledge EA, Halbert CL, Russell DW: **Infectious clones and vectors derived from adeno-associated virus (AAV) serotypes other than AAV type 2.** *J Virol* 1998, **72**:309-319.
23. Gao GP, Alvira MR, Wang L, Calcedo R, Johnston J, Wilson JM: **Novel adeno-associated viruses from rhesus monkeys as vectors for human gene therapy.** *Proc Natl Acad Sci U S A* 2002, **99**:11854-11859.
- This study opens the door of isolating new AAV variants from mammalian tissues. Several AAV serotypes discovered in this study (such as AAV-8 and AAV-9) show excellent systemic delivery property and are currently in human trials.
24. Gao G, Vandenberghe LH, Alvira MR, Lu Y, Calcedo R, Zhou X, Wilson JM: **Clades of adeno-associated viruses are widely disseminated in human tissues.** *J Virol* 2004, **78**:6381-6388.
25. Gregorevic P, Blankinship MJ, Allen JM, Crawford RW, Meuse L, Miller DG, Russell DW, Chamberlain JS: **Systemic delivery of genes to striated muscles using adeno-associated viral vectors.** *Nat Med* 2004, **10**:828-834.
- This is the first report of successful systemic AAV delivery in mice. The authors utilized AAV-6. In order to achieve high efficient bodywide delivery, the authors co-administrated VEGF, a transient vessel permeabilizer.
26. Wang Z, Zhu T, Qiao C, Zhou L, Wang B, Zhang J, Chen C, Li J, Xiao X: **Adeno-associated virus serotype 8 efficiently delivers genes to muscle and heart.** *Nat Biotechnol* 2005, **23**:321-328.
- This is the first report demonstrating whole body systemic delivery of an AAV vector in rodents in the absence of pharmacological vessel permeabilization.
27. Inagaki K, Fuess S, Storm TA, Gibson GA, McTiernan CF, Kay MA, Nakai H: **Robust systemic transduction with AAV9 vectors in mice: efficient global cardiac gene transfer superior to that of AAV8.** *Mol Ther* 2006, **14**:45-53.
- The study shows robust myocardial transduction of AAV-9 suggesting AAV-9 is cardiotropic in rodent heart.
28. Pacak CA, Mah CS, Thattaliyath BD, Conlon TJ, Lewis MA, Cloutier DE, Zolotukhin I, Tarantal AF, Byrne BJ: **Recombinant adeno-associated virus serotype 9 leads to preferential cardiac transduction in vivo.** *Circ Res* 2006, **99**:e3-e9.
- See annotation to Ref. [27\*].
29. Bostick B, Ghosh A, Yue Y, Long C, Duan D: **Systemic AAV-9 transduction in mice is influenced by animal age but not by the route of administration.** *Gene Ther* 2007, **14**:1605-1609.
- See annotation to Ref. [27\*].
30. Bish LT, Morine K, Sleeper MM, Sanmiguel J, Wu D, Gao G, Wilson JM, Sweeney HL: **Adeno-associated virus (AAV) serotype 9 provides global cardiac gene transfer superior to AAV1, AAV6, AAV7, and AAV8 in the mouse and rat.** *Hum Gene Ther* 2008, **19**:1359-1368.
31. Zincarelli C, Soltys S, Rengo G, Rabinowitz JE: **Analysis of AAV serotypes 1-9 mediated gene expression and tropism in mice after systemic injection.** *Mol Ther* 2008, **16**:1073-1080.
- This study reports side-by-side comparison of systemic delivery efficiency of AAV-1 to AAV-9. This study suggests that AAV-9 is superior to other serotypes.
32. Prasad KM, Xu Y, Yang Z, Acton ST, French BA: **Robust cardiomyocyte-specific gene expression following systemic injection of AAV: in vivo gene delivery follows a Poisson distribution.** *Gene Ther* 2011, **18**:43-52.
33. Bisset DR, Stepniak-Konieczna EA, Zavaljevski M, Wei J, Carter GT, Weiss MD, Chamberlain JR: **Therapeutic impact of systemic AAV-mediated RNA interference in a mouse model of myotonic dystrophy.** *Hum Mol Genet* 2015, **24**:4971-4983.
34. Mah C, Pacak CA, Cresawn KO, Deruisseau LR, Germain S, Lewis MA, Cloutier DA, Fuller DD, Byrne BJ: **Physiological correction of Pompe disease by systemic delivery of adeno-associated virus serotype 1 vectors.** *Mol Ther* 2007, **15**:501-507.
35. Fougereousse F, Bartoli M, Poupiot J, Arandel L, Durand M, Guerchet N, Gicquel E, Danos O, Richard I: **Phenotypic correction of alpha-sarcoglycan deficiency by intra-arterial injection of a muscle-specific serotype 1 rAAV vector.** *Mol Ther* 2007, **15**:53-61.
36. Gregorevic P, Allen JM, Minami E, Blankinship MJ, Haraguchi M, Meuse L, Finn E, Adams ME, Froehner SC, Murry CE *et al.*: **rAAV6-microdystrophin preserves muscle function and extends lifespan in severely dystrophic mice.** *Nat Med* 2006, **12**:787-789.
- This study shows systemic AAV-6 therapy ameliorated dystrophic phenotype in dystrophin/utrophin double knockout mice.
37. Gregorevic P, Blankinship MJ, Allen JM, Chamberlain JS: **Systemic microdystrophin gene delivery improves skeletal muscle structure and function in old dystrophic mdx mice.** *Mol Ther* 2008, **16**:657-664.
38. Bortolanza S, Nonis A, Sanvito F, Maciotta S, Sitia G, Wei J, Torrente Y, Di Serio C, Chamberlain JR, Gabellini D: **AAV6-mediated systemic shRNA delivery reverses disease in a mouse model of facioscapulohumeral muscular dystrophy.** *Mol Ther* 2011, **19**:2055-2064.
39. Nishiyama A, Ampong BN, Ohshima S, Shin JH, Nakai H, Imamura M, Miyagoe-Suzuki Y, Okada T, Takeda S: **Recombinant adeno-associated virus type 8-mediated extensive therapeutic gene delivery into skeletal muscle of alpha-sarcoglycan-deficient mice.** *Hum Gene Ther* 2008, **19**:719-730.
40. Qiao C, Li J, Jiang J, Zhu X, Wang B, Xiao X: **Myostatin propeptide gene delivery by adeno-associated virus serotype 8 vectors enhances muscle growth and ameliorates dystrophic phenotypes in mdx mice.** *Hum Gene Ther* 2008, **19**:241-254.
41. Khan JA, Cao M, Kang BY, Liu Y, Mehta JL, Hermonat PL: **Systemic human Netrin-1 gene delivery by adeno-associated virus type 8 alters leukocyte accumulation and atherogenesis in vivo.** *Gene Ther* 2011, **18**:437-444.
42. Goehringer C, Rutschow D, Bauer R, Schinkel S, Weichenhan D, Bekeredjian R, Straub V, Kleinschmidt JA, Katus HA, Muller OJ: **Prevention of cardiomyopathy in delta-sarcoglycan knockout mice after systemic transfer of targeted adeno-associated viral vectors.** *Cardiovasc Res* 2009, **82**:404-410.
43. Bostick B, Yue Y, Long C, Duan D: **Prevention of dystrophin-deficient cardiomyopathy in twenty-one-month-old carrier mice by mosaic dystrophin expression or complementary dystrophin/utrophin expression.** *Circ Res* 2008, **102**:121-130.
44. Bostick B, Shin J-H, Yue Y, Duan D: **AAV-microdystrophin therapy improves cardiac performance in aged female mdx mice.** *Mol Ther* 2011, **19**:1826-1832.
- This study demonstrates systemic AAV-9 delivery can treat severe dystrophic cardiomyopathy in a phenotypic model.
45. Shin JH, Nitahara-Kasahara Y, Hayashita-Kinoh H, Ohshima-Hosoyama S, Kinoshita K, Chiyo T, Okada H, Okada T, Takeda S: **Improvement of cardiac fibrosis in dystrophic mice by rAAV9-mediated microdystrophin transduction.** *Gene Ther* 2011, **18**:910-919.
46. Bostick B, Shin JH, Yue Y, Wasala NB, Lai Y, Duan D: **AAV microdystrophin gene therapy alleviates stress-induced cardiac death but not myocardial fibrosis in >21-m-old mdx mice, an end-stage model of Duchenne muscular dystrophy cardiomyopathy.** *J Mol Cell Cardiol* 2012, **53**:217-222.
47. Shin JH, Bostick B, Yue Y, Hajjar R, Duan D: **SERCA2a gene transfer improves electrocardiographic performance in aged mdx mice.** *J Transl Med* 2011, **9**:132.
48. Spampanato C, De Leonibus E, Dama P, Gargiulo A, Fraldi A, Sorrentino NC, Russo F, Nusco E, Auricchio A, Surace EM *et al.*:

**Efficacy of a combined intracerebral and systemic gene delivery approach for the treatment of a severe lysosomal storage disorder.** *Mol Ther* 2011, **19**:860-869.

49. Fu H, Dirosario J, Killedar S, Zaraspe K, McCarty DM: **Correction of neurological disease of mucopolysaccharidosis IIIB in adult mice by rAAV9 trans-blood-brain barrier gene delivery.** *Mol Ther* 2011, **19**:1025-1033.
  50. Katare R, Caporali A, Zentilin L, Avolio E, Sala-Newby G, Oikawa A, Cesselli D, Beltrami AP, Giacca M, Emanuelli C *et al.*: **Intravenous gene therapy with PIM-1 via a cardiotropic viral vector halts the progression of diabetic cardiomyopathy through promotion of prosurvival signaling.** *Circ Res* 2011, **108**:1238-1251.
  51. Dufour BD, Smith CA, Clark RL, Walker TR, McBride JL: **Intrajugular vein delivery of AAV9-RNAi prevents neuropathological changes and weight loss in Huntington's disease mice.** *Mol Ther* 2014, **22**:797-810.
  52. Dong JY, Fan PD, Frizzell RA: **Quantitative analysis of the packaging capacity of recombinant adeno-associated virus.** *Hum Gene Ther* 1996, **7**:2101-2112.
  53. Dong B, Nakai H, Xiao W: **Characterization of genome integrity for oversized recombinant AAV vector.** *Mol Ther* 2010, **18**:87-92.
  54. Lai Y, Yue Y, Duan D: **Evidence for the failure of adeno-associated virus serotype 5 to package a viral genome > or = 8.2 kb.** *Mol Ther* 2010, **18**:75-79.
  55. Wu Z, Yang H, Colosi P: **Effect of genome size on AAV vector packaging.** *Mol Ther* 2010, **18**:80-86.
  56. Chamberlain K, Riyad JM, Weber T: **Expressing transgenes that exceed the packaging capacity of adeno-associated virus capsids.** *Hum Gene Ther Methods* 2016, **27**:1-12.
  57. Hirsch ML, Wolf SJ, Samulski RJ: **Delivering transgenic DNA exceeding the carrying capacity of AAV vectors.** *Methods Mol Biol* 2016, **1382**:21-39.
  58. Ghosh A, Duan D: **Expanding adeno-associated viral vector capacity: a tale of two vectors.** *Biotechnol Genetic Eng Rev* 2007, **24**:165-177.
  59. Lai Y, Yue Y, Liu M, Ghosh A, Engelhardt JF, Chamberlain JS, Duan D: **Efficient in vivo gene expression by trans-splicing adeno-associated viral vectors.** *Nat Biotechnol* 2005, **23**:1435-1439.
  60. Trapani I, Colella P, Sommella A, Iodice C, Cesi G, de Simone S, Marrocco E, Rossi S, Giunti M, Palfi A *et al.*: **Effective delivery of large genes to the retina by dual AAV vectors.** *EMBO Mol Med* 2014, **6**:194-211.
  61. Ghosh A, Yue Y, Long C, Bostick B, Duan D: **Efficient whole-body transduction with trans-splicing adeno-associated viral vectors.** *Mol Ther* 2007, **15**:750-755.
- This study demonstrates the feasibility of systemic delivery with the dual AAV vectors.
62. Ghosh A, Yue Y, Shin J-H, Duan D: **Systemic trans-splicing AAV delivery efficiently transduces the heart of adult mdx mouse, a model for Duchenne muscular dystrophy.** *Hum Gene Ther* 2009, **20**:1319-1328.
  63. Zhang Y, Yue Y, Li L, Hakim CH, Zhang K, Thomas GD, Duan D: **Dual AAV therapy ameliorates exercise-induced muscle injury and functional ischemia in murine models of Duchenne muscular dystrophy.** *Hum Mol Genet* 2013, **22**:3720-3729.
  64. Odom GL, Gregorevic P, Allen JM, Chamberlain JS: **Gene therapy of mdx mice with large truncated dystrophins generated by recombination using rAAV6.** *Mol Ther* 2011, **19**:36-45.
  65. Lostal W, Bartoli M, Bourg N, Roudaut C, Bentaib A, Miyake K, Guerchet N, Fougereousse F, McNeil P, Richard I: **Efficient recovery of dysferlin deficiency by dual adeno-associated vector-mediated gene transfer.** *Hum Mol Genet* 2010, **19**:1897-1907.
  66. Yue Y, Ghosh A, Long C, Bostick B, Smith BF, Kornegay JN, Duan D: **A single intravenous injection of adeno-associated virus serotype-9 leads to whole body skeletal muscle transduction in dogs.** *Mol Ther* 2008, **16**:1944-1952.
- This is the first study demonstrating efficient systemic AAV delivery in a large mammalian species.
67. Pan X, Yue Y, Zhang K, Lostal W, Shin JH, Duan D: **Long-term robust myocardial transduction of the dog heart from a peripheral vein by adeno-associated virus serotype-8.** *Hum Gene Ther* 2013, **24**:584-594.
  68. Pan X, Yue Y, Zhang K, Hakim CH, Kodippili K, McDonald T, Duan D: **AAV-8 is more efficient than AAV-9 in transducing neonatal dog heart.** *Hum Gene Ther Methods* 2015, **26**:54-61.
  69. Zhong L, Li B, Mah CS, Govindasamy L, Agbandje-McKenna M, Cooper M, Herzog RW, Zolotukhin I, Warrington KH Jr, Weigel-Van Aken KA *et al.*: **Next generation of adeno-associated virus 2 vectors: point mutations in tyrosines lead to high-efficiency transduction at lower doses.** *Proc Natl Acad Sci U S A* 2008, **105**:7827-7832.
  70. Qiao C, Zhang W, Yuan Z, Shin JH, Li J, Jayandharan GR, Zhong L, Srivastava A, Xiao X, Duan D: **AAV6 capsid tyrosine to phenylalanine mutations improve gene transfer to skeletal muscle.** *Hum Gene Ther* 2010, **21**:1343-1348.
  71. Hakim CH, Yue Y, Shin JH, Williams RR, Zhang K, Smith BF, Duan D: **Systemic gene transfer reveals distinctive muscle transduction profile of tyrosine mutant AAV-1, -6, and -9 in neonatal dogs.** *Mol Ther Methods Clin Dev* 2014, **1**:14002.
  72. Duan D: **Duchenne muscular dystrophy gene therapy in the canine model.** *Hum Gene Ther Clin Dev* 2015, **26**:57-69.
  73. Kornegay JN, Li J, Bogan JR, Bogan DJ, Chen C, Zheng H, Wang B, Qiao C, Howard JF Jr, Xiao X: **Widespread muscle expression of an AAV9 human mini-dystrophin vector after intravenous injection in neonatal dystrophin-deficient dogs.** *Mol Ther* 2010, **18**:1501-1508.
- This study suggests that systemic delivery may induce catastrophic inflammatory response in a diseased large mammal.
74. Hinderer C, Bell P, Louboutin JP, Zhu Y, Yu H, Lin G, Choa R, Gurda BL, Bagel J, O'Donnell P *et al.*: **Neonatal systemic AAV induces tolerance to CNS gene therapy in MPS I dogs and nonhuman primates.** *Mol Ther* 2015, **23**:1298-1307.
  75. Mori S, Takeuchi T, Enomoto Y, Kondo K, Sato K, Ono F, Iwata N, Sata T, Kanda T: **Biodistribution of a low dose of intravenously administered AAV-2, 10, and 11 vectors to cynomolgus monkeys.** *Jpn J Infect Dis* 2006, **59**:285-293.
  76. Rodino-Klapac LR, Montgomery CL, Bremer WG, Shontz KM, Malik V, Davis N, Sprinkle S, Campbell KJ, Sahenk Z, Clark KR *et al.*: **Persistent expression of FLAG-tagged micro dystrophin in nonhuman primates following intramuscular and vascular delivery.** *Mol Ther* 2010, **18**:109-117.
  77. Toromanoff A, Adjali O, Larcher T, Hill M, Guigand L, Chenuaud P, Deschamps JY, Gauthier O, Blancho G, Vanhove B *et al.*: **Lack of immunotoxicity after regional intravenous (RI) delivery of rAAV to nonhuman primate skeletal muscle.** *Mol Ther* 2010, **18**:151-160.
  78. Toromanoff A, Chereil Y, Guilbaud M, Penaud-Budloo M, Snyder RO, Haskins ME, Deschamps JY, Guigand L, Podevin G, Arruda VR *et al.*: **Safety and efficacy of regional intravenous (r.i.) versus intramuscular (i.m.) delivery of rAAV1 and rAAV8 to nonhuman primate skeletal muscle.** *Mol Ther* 2008, **16**:1291-1299.
  79. Qiao C, Li J, Zheng H, Bogan J, Yuan Z, Zhang C, Bogan D, Kornegay J, Xiao X: **Hydrodynamic limb vein injection of AAV8 canine myostatin propeptide gene in normal dogs enhances muscle growth.** *Hum Gene Ther* 2009, **20**:1-10.
  80. Vulin A, Barthelemy I, Goyenvallé A, Thibaud JL, Beley C, Griffith G, Benchaouir R, le Hir M, Unterfinger Y, Lorain S *et al.*: **Muscle function recovery in golden retriever muscular dystrophy after AAV1-U7 exon skipping.** *Mol Ther* 2012, **20**:2120-2133.
  81. Le Guiner C, Montus M, Servais L, Chereil Y, Francois V, Thibaud JL, Wary C, Matot B, Larcher T, Guigand L *et al.*: **Forelimb treatment in a large cohort of dystrophic dogs supports delivery of a recombinant AAV for exon skipping in Duchenne patients.** *Mol Ther* 2014, **22**:1923-1935.
  82. Childers MK, Joubert R, Poulard K, Moal C, Grange RW, Doering JA, Lawlor MW, Rider BE, Jamet T, Daniele N *et al.*: **Gene**

**therapy prolongs survival and restores function in murine and canine models of myotubular myopathy.** *Sci Transl Med* 2014, **6**:220ra210.

This study suggests that isolated limb perfusion can result in bodywide improvement if the therapeutic product is an enzyme. The authors also showed that intravenous delivery of AAV-8 did not induce any immune response in the canine model of myotubular myopathy.

83. Yue Y, Pan X, Hakim CH, Kodippili K, Zhang K, Shin JH, Yang HT, ●● McDonald T, Duan D: **Safe and bodywide muscle transduction in young adult Duchenne muscular dystrophy dogs with adeno-associated virus.** *Hum Mol Genet* 2015, **24**:5880-5890.

This is the first study demonstrating successful systemic AAV delivery in young adult subjects in a large animal model of human diseases. This study sets the foundation for conducting systemic AAV therapy in boys afflicted by Duchenne muscular dystrophy.

84. Hakim CH, Pan X, Kodippili K, Blessa T, Yang HT, Yao G, Leach S, Emter C, Yue Y, Zhang K *et al.*: **Intravenous delivery of a novel micro-dystrophin vector prevented muscle deterioration in young adult canine Duchenne muscular dystrophy dogs.** *Mol Ther* 2016, **24**:S198-S199.

85. Mendell JR, Al-Zaidy S, Shell R, Arnold WD, Rodino-Klapac L, ●● Kissel JT, Prior TW, Miranda C, Lowes L, Alfano L *et al.*: **Gene therapy for spinal muscular atrophy type 1 shows potential to improve survival and motor functional outcomes.** *Mol Ther* 2016, **24**:S190.

In this meeting report, Dr. Mendell presented results of the first-in-human study on systemic AAV gene therapy in severely affected newborn spinal muscular dystrophy patients. A total of 15 patients have been treated with an AAV-9 vector at the dose of  $6.7 \times 10^{13}$  to  $2 \times 10^{14}$  for 4 months to 2 years. The results of this ongoing study suggest that systemic AAV gene therapy is safe and may dramatically change the disease course. This study opens the door for systemic AAV gene therapy for other diseases in human patients.

86. Valori CF, Ning K, Wyles M, Mead RJ, Grierson AJ, Shaw PJ, Azzouz M: **Systemic delivery of scAAV9 expressing SMN prolongs survival in a model of spinal muscular atrophy.** *Sci Transl Med* 2010, **2**:35ra42.
87. Bevan AK, Hutchinson KR, Foust KD, Braun L, McGovern VL, Schmelzer L, Ward JG, Petruska JC, Lucchesi PA, Burghes AH *et al.*: **Early heart failure in the SMNDelta7 model of spinal muscular atrophy and correction by postnatal scAAV9-SMN delivery.** *Hum Mol Genet* 2010, **19**:3895-3905.
88. Foust KD, Wang X, McGovern VL, Braun L, Bevan AK, Haidet AM, Le TT, Morales PR, Rich MM, Burghes AH *et al.*: **Rescue of the spinal muscular atrophy phenotype in a mouse model by early postnatal delivery of SMN.** *Nat Biotechnol* 2010, **28**:271-274.
89. Dominguez E, Marais T, Chatauret N, Benkhelifa-Ziyyat S, Duque S, Ravassard P, Carcenac R, Astord S, Pereira de Moura A, Voit T *et al.*: **Intravenous scAAV9 delivery of a codon-optimized SMN1 sequence rescues SMA mice.** *Hum Mol Genet* 2011, **20**:681-693.
90. Ding W, Zhang L, Yan Z, Engelhardt JF: **Intracellular trafficking of adeno-associated viral vectors.** *Gene Ther* 2005, **12**:873-880.
91. Nonnenmacher M, Weber T: **Intracellular transport of recombinant adeno-associated virus vectors.** *Gene Ther* 2012, **19**:649-658.
92. Denard J, Beley C, Kotin R, Lai-Kuen R, Blot S, Leh H, Asokan A, Samulski RJ, Moullier P, Voit T *et al.*: **Human galectin 3 binding protein interacts with recombinant adeno-associated virus type 6.** *J Virol* 2012, **86**:6620-6631.
93. Denard J, Marolleau B, Jenny C, Rao TN, Fehling HJ, Voit T, Svinartchouk F: **C-reactive protein (CRP) is essential for efficient systemic transduction of recombinant adeno-associated virus vector 1 (rAAV-1) and rAAV-6 in mice.** *J Virol* 2013, **87**:10784-10791.
94. Kotchey NM, Adachi K, Zahid M, Inagaki K, Charan R, Parker RS, Nakai H: **A potential role of distinctively delayed blood clearance of recombinant adeno-associated virus serotype 9 in robust cardiac transduction.** *Mol Ther* 2011, **19**:1079-1089.
95. Shen S, Bryant KD, Sun J, Brown SM, Troupes A, Pulicherla N, Asokan A: **Glycan binding avidity determines the systemic fate of adeno-associated virus type 9.** *J Virol* 2012, **86**:10408-10417.

96. Asokan A, Conway JC, Phillips JL, Li C, Hegge J, Sinnott R, ●● Yadav S, DiPrimio N, Nam HJ, Agbandje-McKenna M *et al.*: **Reengineering a receptor footprint of adeno-associated virus enables selective and systemic gene transfer to muscle.** *Nat Biotechnol* 2010, **28**:79-82.

This study provides the proof-of-principle to engineer AAV capsid for improved systemic delivery.

97. Gray SJ, Matagne V, Bachaboina L, Yadav S, Ojeda SR, Samulski RJ: **Preclinical differences of intravascular AAV9 delivery to neurons and glia: a comparative study of adult mice and nonhuman primates.** *Mol Ther* 2011, **19**:1058-1069.
98. Tuma P, Hubbard AL: **Transcytosis: crossing cellular barriers.** *Physiol Rev* 2003, **83**:871-932.
99. Di Pasquale G, Ostedgaard L, Vermeer D, Swaim WD, Karp P, Chiorini JA: **Bovine AAV transcytosis inhibition by tannic acid results in functional expression of CFTR in vitro and altered biodistribution in vivo.** *Gene Ther* 2012, **19**:576-581.
100. Di Pasquale G, Chiorini JA: **AAV transcytosis through barrier ●● epithelia and endothelium.** *Mol Ther* 2006, **13**:506-516.
- This study provides *in vitro* evidence of AAV transcytosis.
101. He B, Yuan Z, Qiao C, Madden V, Thakker D, Li J, Xiao X: **Transcytosis of AAV8 and AAV9 across endothelial barrier.** *Mol Ther* 2009, **17**:S175.
102. Byrne LC, Lin YJ, Lee T, Schaffer DV, Flannery JG: **The expression pattern of systemically injected AAV9 in the developing mouse retina is determined by age.** *Mol Ther* 2015, **23**:290-296.
103. Cheng JP, Nichols BJ: **Caveolae: one function or many?** *Trends Cell Biol* 2016, **26**:177-189.
104. Foust KD, Nurre E, Montgomery CL, Hernandez A, Chan CM, Kaspar BK: **Intravascular AAV9 preferentially targets neonatal neurons and adult astrocytes.** *Nat Biotechnol* 2009, **27**:59-65.
105. Calcedo R, Vandenberghe LH, Gao G, Lin J, Wilson JM: **Worldwide epidemiology of neutralizing antibodies to adeno-associated viruses.** *J Infect Dis* 2009, **199**:381-390.
106. Boutin S, Monteilhet V, Veron P, Leborgne C, Benveniste O, Montus MF, Masurier C: **Prevalence of serum IgG and neutralizing factors against adeno-associated virus (AAV) types 1, 2, 5, 6, 8, and 9 in the healthy population: implications for gene therapy using AAV vectors.** *Hum Gene Ther* 2010, **21**:704-712.
107. Van Vliet KM, Blouin V, Brument N, Agbandje-McKenna M, Snyder RO: **The role of the adeno-associated virus capsid in gene transfer.** *Methods Mol Biol* 2008, **437**:51-91.
108. Drouin LM, Agbandje-McKenna M: **Adeno-associated virus ●● structural biology as a tool in vector development.** *Future Virol* 2013, **8**:1183-1199.
- This is an excellent review article on AAV capsid structure.
109. Agbandje-McKenna M, Kleinschmidt J: **AAV capsid structure and cell interactions.** *Methods Mol Biol* 2011, **807**:47-92.
110. Santiago-Ortiz J, Ojala DS, Westesson O, Weinstein JR, Wong SY, Steinsapir A, Kumar S, Holmes I, Schaffer DV: **AAV ancestral reconstruction library enables selection of broadly infectious viral variants.** *Gene Ther* 2015, **22**:934-946.
111. Zinn E, Pacouret S, Khaychuk V, Turunen HT, Carvalho LS, Andres-Mateos E, Shah S, Shelke R, Maurer AC, Plovie E *et al.*: **In silico reconstruction of the viral evolutionary lineage yields a potent gene therapy vector.** *Cell Rep* 2015, **12**:1056-1068.
112. Kotterman MA, Schaffer DV: **Engineering adeno-associated ●● viruses for clinical gene therapy.** *Nat Rev Genet* 2014, **15**:445-451.
- This is a comprehensive review on the current status of AAV capsid engineering and clinical application of synthetic AAV variants.
113. Nance ME, Duan D: **Perspective on adeno-associated virus (AAV) capsid modification for Duchenne muscular dystrophy gene therapy.** *Hum Gene Ther* 2015, **26**:786-800.
114. Ling C, Lu Y, Kelsi JK, Jayandharan GR, Li B, Ma W, Cheng B, Gee SW, McGoogan KE, Govindasamy L *et al.*: **Human**

- hepatocyte growth factor receptor is a cellular co-receptor for AAV3.** *Hum Gene Ther* 2010, **21**:1741-1747.
115. Li S, Ling C, Zhong L, Li M, Su Q, He R, Tang Q, Greiner DL, Shultz LD, Brehm MA *et al.*: **Efficient and targeted transduction of nonhuman primate liver with systemically delivered optimized AAV3B vectors.** *Mol Ther* 2015, **23**:1867-1876.
116. Wang L, Bell P, Somanathan S, Wang Q, He Z, Yu H, McMenamin D, Goode T, Calcedo R, Wilson JM: **Comparative study of liver gene transfer with AAV vectors based on natural and engineered AAV capsids.** *Mol Ther* 2015, **23**:1877-1887.
117. Shen S, Troupes AN, Pulicherla N, Asokan A: **Multiple roles for sialylated glycans in determining the cardiopulmonary tropism of adeno-associated virus 4.** *J Virol* 2013, **87**:13206-13213.
118. Yang B, Li S, Wang H, Guo Y, Gessler DJ, Cao C, Su Q, Kramer J, Zhong L, Ahmed SS *et al.*: **Global CNS transduction of adult mice by intravenously delivered rAAVrh.8 and rAAVrh.10 and nonhuman primates by rAAVrh.10.** *Mol Ther* 2014, **22**:1299-1309.
119. Louis Jeune V, Joergensen JA, Hajjar RJ, Weber T: **Pre-existing anti-adeno-associated virus antibodies as a challenge in AAV gene therapy.** *Hum Gene Ther Methods* 2013, **24**:59-67.
120. Mingozzi F, Chen Y, Edmonson SC, Zhou S, Thurlings RM, Tak PP, High KA, Vervoordeldonk MJ: **Prevalence and pharmacological modulation of humoral immunity to AAV vectors in gene transfer to synovial tissue.** *Gene Ther* 2013, **20**:417-424.
121. Mingozzi F, Chen Y, Murphy SL, Edmonson SC, Tai A, Price SD, Metzger ME, Zhou S, Wright JF, Donahue RE *et al.*: **Pharmacological modulation of humoral immunity in a nonhuman primate model of AAV gene transfer for hemophilia B.** *Mol Ther* 2012, **20**:1410-1416.
122. Monteilhet V, Saheb S, Boutin S, Leborgne C, Veron P, Montus MF, Moulhier P, Benveniste O, Masurier C: **A 10 patient case report on the impact of plasmapheresis upon neutralizing factors against adeno-associated virus (AAV) types 1, 2, 6, and 8.** *Mol Ther* 2011, **19**:2084-2091.
123. Tseng YS, Agbandje-McKenna M: **Mapping the AAV capsid host antibody response toward the development of second generation gene delivery vectors.** *Front Immunol* 2014, **5**:9.
124. Lochrie MA, Tatsuno GP, Christie B, McDonnell JW, Zhou S, Surosky R, Pierce GF, Colosi P: **Mutations on the external surfaces of adeno-associated virus type 2 capsids that affect transduction and neutralization.** *J Virol* 2006, **80**:821-834.
125. Maersch S, Huber A, Buning H, Hallek M, Perabo L: **Optimization of stealth adeno-associated virus vectors by randomization of immunogenic epitopes.** *Virology* 2010, **397**:167-175.
126. Bartel M, Schaffer D, Buning H: **Enhancing the clinical potential of AAV vectors by capsid engineering to evade pre-existing immunity.** *Front Microbiol* 2011, **2**:204.
127. Maheshri N, Koerber JT, Kaspar BK, Schaffer DV: **Directed evolution of adeno-associated virus yields enhanced gene delivery vectors.** *Nat Biotechnol* 2006, **24**:198-204.
- This paper describes the first application of directed evolution to generate novel AAV capsids. This library-based approach allows investigators to obtain functionally superior AAV mutants without prior knowledge of the capsid structure.
128. Grimm D, Lee JS, Wang L, Desai T, Akache B, Storm TA, Kay MA: **In vitro and in vivo gene therapy vector evolution via multispecies interbreeding and retargeting of adeno-associated viruses.** *J Virol* 2008, **82**:5887-5911.
129. Li C, Wu S, Albright B, Hirsch M, Li W, Tseng YS, Agbandje-McKenna M, McPhee S, Asokan A, Samulski RJ: **Development of patient-specific AAV vectors after neutralizing antibody selection for enhanced muscle gene transfer.** *Mol Ther* 2016, **24**:53-65.
130. Adachi K, Enoki T, Kawano Y, Veraz M, Nakai H: **Drawing a high-resolution functional map of adeno-associated virus capsid by massively parallel sequencing.** *Nat Commun* 2014, **5**:3075.
131. Pulicherla N, Shen S, Yadav S, Debbink K, Govindasamy L, Agbandje-McKenna M, Asokan A: **Engineering liver-detargeted AAV9 vectors for cardiac and musculoskeletal gene transfer.** *Mol Ther* 2011, **19**:1070-1078.
132. Shen S, Horowitz ED, Troupes AN, Brown SM, Pulicherla N, Samulski RJ, Agbandje-McKenna M, Asokan A: **Engraftment of a galactose receptor footprint onto adeno-associated viral capsids improves transduction efficiency.** *J Biol Chem* 2013, **288**:28814-28823.
133. Lisowski L, Dane AP, Chu K, Zhang Y, Cunningham SC, Wilson EM, Nygaard S, Grompe M, Alexander IE, Kay MA: **Selection and evaluation of clinically relevant AAV variants in a xenograft liver model.** *Nature* 2014, **506**:382-386.
- This study describes a unique *in vivo* evolution approach in human tissue xenograft. The resulting AAV variants hold great promise for human application.
134. Yang L, Jiang J, Drouin LM, Agbandje-McKenna M, Chen C, Qiao C, Pu D, Hu X, Wang DZ, Li J *et al.*: **A myocardium tropic adeno-associated virus (AAV) evolved by DNA shuffling and in vivo selection.** *Proc Natl Acad Sci U S A* 2009, **106**:3946-3951.
135. Choudhury SR, Harris AF, Cabral DJ, Keeler AM, Sapp E, Ferreira JS, Gray-Edwards HL, Johnson JA, Johnson AK, Su Q *et al.*: **Widespread central nervous system gene transfer and silencing after systemic delivery of novel AAV-AS vector.** *Mol Ther* 2016, **24**:726-735.
136. Huang LY, Halder S, Agbandje-McKenna M: **Parvovirus glycan interactions.** *Curr Opin Virol* 2014, **7**:108-118.
137. Murlidharan G, Corriher T, Ghashghaei HT, Asokan A: **Unique glycan signatures regulate adeno-associated virus tropism in the developing brain.** *J Virol* 2015, **89**:3976-3987.
138. Pillay S, Meyer NL, Puschnik AS, Davulcu O, Diep J, Ishikawa Y, Jae LT, Wosen JE, Nagamine CM, Chapman MS *et al.*: **An essential receptor for adeno-associated virus infection.** *Nature* 2016, **530**:108-112.
- This paper describes the identification of a poorly characterized transmembrane protein KIAA0319L as a ubiquitous AAV receptor for multiple serotypes.
139. Nelson CE, Hakim CH, Ousterout DG, Thakore PI, Moreb EA, Rivera RM, Madhavan S, Pan X, Ran FA, Yan WX *et al.*: **In vivo genome editing improves muscle function in a mouse model of Duchenne muscular dystrophy.** *Science* 2016, **351**:403-407.
140. Rayaprolu V, Kruse S, Kant R, Venkatakrishnan B, Movahed N, Brooke D, Lins B, Bennett A, Potter T, McKenna R *et al.*: **Comparative analysis of adeno-associated virus capsid stability and dynamics.** *J Virol* 2013, **87**:13150-13160.
141. Vandenberghe LH, Wang L, Somanathan S, Zhi Y, Figueredo J, Calcedo R, Sanmiguel J, Desai RA, Chen CS, Johnston J *et al.*: **Heparin binding directs activation of T cells against adeno-associated virus serotype 2 capsid.** *Nat Med* 2006, **12**:967-971.
142. Lu Y, Song S: **Distinct immune responses to transgene products from rAAV1 and rAAV8 vectors.** *Proc Natl Acad Sci U S A* 2009, **106**:17158-17162.
143. Wang L, Figueredo J, Calcedo R, Lin J, Wilson JM: **Cross-presentation of adeno-associated virus serotype 2 capsids activates cytotoxic T cells but does not render hepatocytes effective cytolytic targets.** *Hum Gene Ther* 2007, **18**:185-194.
144. Ohshima S, Shin JH, Yuasa K, Nishiyama A, Kira J, Okada T, Takeda S: **Transduction efficiency and immune response associated with the administration of AAV8 vector into dog skeletal muscle.** *Mol Ther* 2009, **17**:73-80.
145. Mays LE, Wang L, Lin J, Bell P, Crawford A, Wherry EJ, Wilson JM: **AAV8 induces tolerance in murine muscle as a result of poor APC transduction, T cell exhaustion and minimal MHC1 upregulation on target cells.** *Mol Ther* 2014, **22**:28-41.
146. Koo T, Okada T, Athanasopoulos T, Foster H, Takeda S, Dickson G: **Long-term functional adeno-associated virus-microdystrophin expression in the dystrophic CXMDj dog.** *J Gene Med* 2011, **13**:497-506.

## ORIGINAL ARTICLE

# Dystrophin contains multiple independent membrane-binding domains

Junling Zhao<sup>1</sup>, Kasun Kodippili<sup>1</sup>, Yongping Yue<sup>1</sup>, Chady H. Hakim<sup>1,2</sup>,  
Lakmini Wasala<sup>1</sup>, Xiufang Pan<sup>1</sup>, Keqing Zhang<sup>1</sup>, Nora N. Yang<sup>2</sup>,  
Dongsheng Duan<sup>1,3,4,5,\*</sup> and Yi Lai<sup>1,\*</sup>

<sup>1</sup>Department of Molecular Microbiology and Immunology, School of Medicine, <sup>2</sup>National Center for Advancing Translational Sciences, NIH, Rockville, MD, USA <sup>3</sup>Department of Neurology, School of Medicine, <sup>4</sup>Department of Bioengineering and <sup>5</sup>Department of Biomedical Sciences, College of Veterinary Medicine, University of Missouri, Columbia, MO, USA

\*To whom correspondence should be addressed at: Dongsheng Duan or Yi Lai, Department of Molecular Microbiology and Immunology, One Hospital Drive, Columbia, MO 65212, USA. Tel: +573-882-8989; Fax: +573-882-4287; Email: duand@health.missouri.edu or lai@health.missouri.edu

## Abstract

Dystrophin is a large sub-sarcolemmal protein. Its absence leads to Duchenne muscular dystrophy (DMD). Binding to the sarcolemma is essential for dystrophin to protect muscle from contraction-induced injury. It has long been thought that membrane binding of dystrophin depends on its cysteine-rich (CR) domain. Here, we provide *in vivo* evidence suggesting that dystrophin contains three additional membrane-binding domains including spectrin-like repeats (R)1-3, R10-12 and C-terminus (CT). To systematically study dystrophin membrane binding, we split full-length dystrophin into ten fragments and examined subcellular localizations of each fragment by adeno-associated virus-mediated gene transfer. In skeletal muscle, R1-3, CR domain and CT were exclusively localized at the sarcolemma. R10-12 showed both cytosolic and sarcolemmal localization. Importantly, the CR-independent membrane binding was conserved in murine and canine muscles. A critical function of the CR-mediated membrane interaction is the assembly of the dystrophin-associated glycoprotein complex (DGC). While R1-3 and R10-12 did not restore the DGC, surprisingly, CT alone was sufficient to establish the DGC at the sarcolemma. Additional studies suggest that R1-3 and CT also bind to the sarcolemma in the heart, though relatively weak. Taken together, our study provides the first conclusive *in vivo* evidence that dystrophin contains multiple independent membrane-binding domains. These structurally and functionally distinctive membrane-binding domains provide a molecular framework for dystrophin to function as a shock absorber and signaling hub. Our results not only shed critical light on dystrophin biology and DMD pathogenesis, but also provide a foundation for rationally engineering minimized dystrophins for DMD gene therapy.

## Introduction

Dystrophin is an essential cytoskeletal protein in the muscle. It constitutes a primary linkage between the extracellular matrix (ECM) and the actin cytoskeleton (1,2). In muscle cells, dystrophin plays an important role in maintaining membrane integrity and preventing membrane rupture. Loss of dystrophin, as seen in

Duchenne muscular dystrophy (DMD) (3), leads to sarcolemmal leakage, myofiber degeneration and necrosis. Full-length dystrophin is a large rod-shaped protein. It contains four functional domains including N-terminus (NT), the mid-rod domain, the cysteine-rich (CR) domain and C-terminus (CT). The mid-rod domain consists of 24 spectrin-like repeats (R). Four hinges (H) are

Received: April 24, 2016. Revised: June 14, 2016. Accepted: June 27, 2016

© The Author 2016. Published by Oxford University Press.

All rights reserved. For Permissions, please email: journals.permissions@oup.com

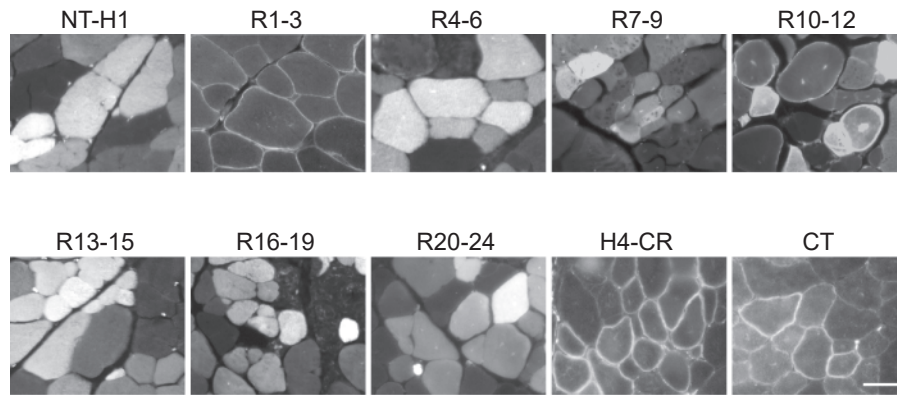


**Figure 1.** Dystrophin R1-3, R10-12, CR and CT are independent membrane-binding domains. Full-length human dystrophin was split into ten subdomains and each subdomain fused with a GFP tag. The fusion proteins were individually expressed in *mdx* muscle by AAV gene transfer. Representative GFP photomicrographs of each indicated dystrophin subdomain are shown. Dystrophin R1-3, H4-CR and CT were exclusively localized at the sarcolemma. R10-12 was found at the sarcolemma and in the cytosol. NT-H1, R4-6, R7-9, R13-15, R16-19 and R20-24 were exclusively localized in the cytosol. Scale bar: 50  $\mu$ m.

interspersed in the mid-rod domain (4). Dystrophin NT and spectrin-like repeats R11-17 bind to cytoskeletal filamentous actin (5,6). The CR domain anchors dystrophin to the muscle membrane via interaction with the transmembrane protein  $\beta$ -dystroglycan (7–9).  $\beta$ -dystroglycan further connects with basal lamina proteins to complete the axis from the ECM to the cytoskeleton (10). This mechanical linkage protects the muscle membrane from contraction-induced damages. In this well-established model, the dystrophin CR domain is solely responsible for dystrophin membrane binding (Supplementary Material, Fig. S1).

Despite compelling evidence suggesting that the CR domain mediates dystrophin-sarcolemma interaction, case reports from some rare-occurring patients suggest that dystrophin may bind to the sarcolemma through CR domain-independent mechanisms. In these patients, biochemical and genetic analyses confirmed a complete deletion of the CR domain. Yet, immunostaining showed clear sarcolemmal localization of the truncated dystrophin protein (Supplementary Material, Fig. S2B) (11–13).

To better understand how dystrophin interacts with the sarcolemma in the absence of the CR domain, we performed a comprehensive *in vivo* screening for alternative membrane binding domains (MBDs) in dystrophin. We identified R1-3, R10-12 and CT as new dystrophin MBDs in mouse muscle. We further confirmed that these MBDs are conserved in dog muscle. To determine whether these MBDs are functionally equivalent, we evaluated their ability to establish the dystrophin-associated glycoprotein complex (DGC) at the sarcolemma. Our results showed that only the CR domain and CT are capable of restoring the DGC. We also evaluated these newly discovered MBDs in the heart. We found that R1-3 and CT interact with the sarcolemma in cardiac muscle. Taken together, our studies suggest that dystrophin-sarcolemma interaction is much more complex than it has been perceived. Our findings reveal a new model of dystrophin membrane binding. This model may better explain the dynamic participation of dystrophin in maintaining the integrity of the muscle cell membrane.

## Results

### Identification of dystrophin R1-3, R10-12 and CT as new dystrophin MBDs

To thoroughly understand how dystrophin interacts with the sarcolemma, we performed a comprehensive screening in

mouse muscle. According to the fact that dystrophin has four functional domains and its mid-rod domain can be further divided into sub-regions (14), we split the full-length human dystrophin protein into ten subdomains, including NT-H1, R1-3, R4-6, R7-9, R10-12, R13-15, R16-19, R20-24, H4-CR and CT. We fused each subdomain with a green fluorescent protein (GFP) tag and individually expressed them in the tibialis anterior (TA) muscle of dystrophin-null *mdx* mice by adeno-associated virus (AAV)-mediated gene transfer (Supplementary Material, Fig. S3).

To determine subcellular localization of each dystrophin subdomain, we visualized the GFP signal under a fluorescence microscope (Fig. 1). In line with the literature, we observed the sarcolemmal localization of the H4-CR subdomain. Unexpectedly, we found that subdomains R1-3 and CT were exclusively restricted at the muscle cell membrane. Subdomains NT-H1, R4-6, R7-9, R13-15, R16-19, and R20-24 were only detected in the cytosol. Interestingly, the R10-12 subdomain was found both at the sarcolemma and in the cytoplasm (Fig. 1).

To confirm these intriguing observations, we performed immunoblot with whole muscle lysates and microsomal preparations (Fig. 2). In whole muscle lysates, we found an efficient expression of all ten dystrophin subdomains (Fig. 2A). However, only subdomains R1-3, R10-12, H4-CR and CT were detected in the membrane-enriched microsomal preparations (Fig. 2B). These data are in agreement with immunostaining results suggesting that these subdomains are indeed dystrophin MBDs.

### Preservation of the membrane-binding property of R1-3, R10-12, CR and CT in canine muscle

To examine whether the membrane-binding property of R1-3, R10-12, H4-CR and CT is conserved in different species, next we delivered the corresponding AAV vectors to dystrophic dog muscle by local injection. As controls, we also injected R7-9 and R20-24 AAV vectors. Two months later, we examined GFP expression under a fluorescence microscope. Similar to what we saw in *mdx* muscle, R1-3, H4-CR and CT subdomains were exclusively localized in the muscle membrane, while the R10-12 subdomain was found both at the sarcolemma and in the cytoplasm. Subdomains R7-9 and R20-24, which localized exclusively in the cytosol in *mdx* muscle, were only detected in the cytosol of dystrophic dog muscle (Fig. 3)

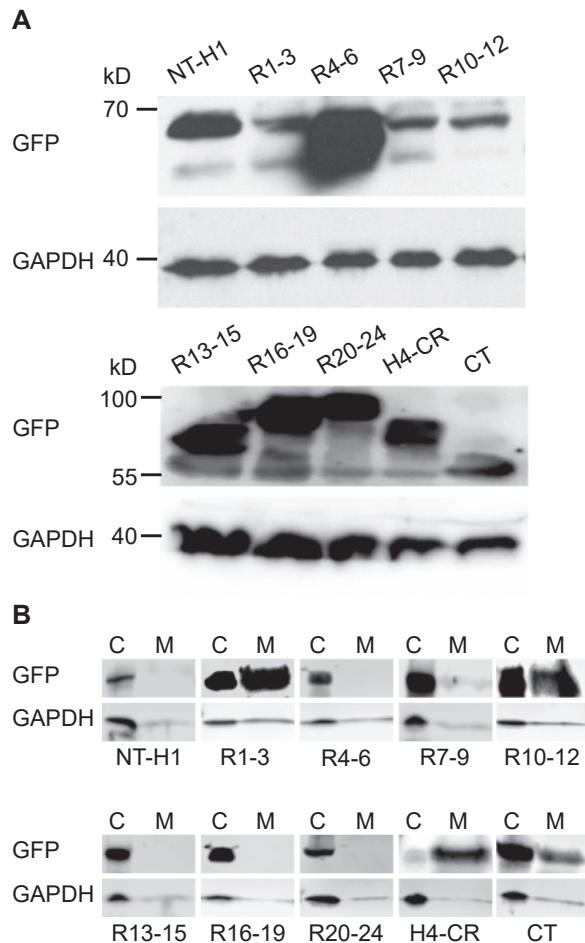


**Figure 2.** Microsomal western blot suggests the association of R1-3, R10-12, CR and CT with the sarcolemma. (A) Whole muscle lysate western blots revealing AAV-mediated expression of GFP-fused dystrophin subdomains in *mdx* muscle. (B) Detection of dystrophin R1-3, R10-12, H4-CR and CT in the membrane fraction by microsomal western blots. GAPDH marks the cytosolic fraction. (C) cytosolic fraction; M, membrane fraction.

### Independent restoration of the DGC by the CR domain and CT

In the canonical model (Supplementary Materials, Figs S1 and S4), the CR domain is solely responsible for nucleating dystroglycan, sarcoglycans, dystrobrevin and syntrophin into the DGC at the sarcolemma (15–18). To determine whether the newly identified MBDs had similar functions, we evaluated DGC components on serial muscle sections by immunostaining (Fig. 4). As expected, the H4-CR subdomain successfully restored  $\beta$ -dystroglycan,  $\beta$ -sarcoglycan, dystrobrevin and syntrophin to the sarcolemma. Surprisingly, myofibers that were transduced with the CT subdomain AAV vector also resulted in sarcolemmal localization of these DGC components. In muscles infected with R1-3 and R10-12 AAV vectors, DGC components were detected in GFP-negative revertant fibers but not in transduced GFP-positive myofibers (Fig. 4).

### Conservation of the membrane-binding property of R1-3, CR and CT in cardiac muscle

To determine whether our findings in skeletal muscle can be extended to cardiac muscle, we delivered GFP-fusion subdomain

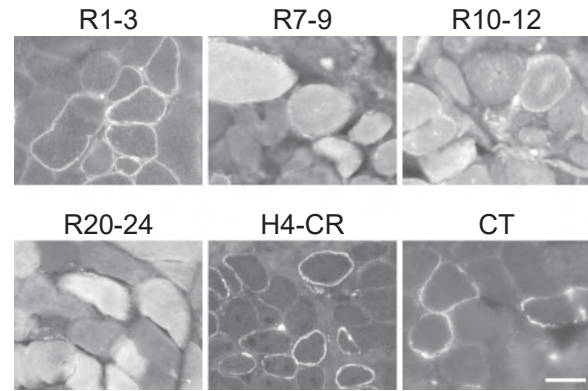


**Figure 3.** Dystrophin R1-3, R10-12, H4-CR and CT bind to the sarcolemma in canine muscle. Indicated GFP fusion dystrophin subdomains were expressed in dystrophic dog muscle by AAV gene transfer. Representative GFP photomicrographs show the membrane binding of R1-3, R10-12, H4-CR and CT and cytosolic localization of R7-9 and R20-24. R10-12 is also seen in the cytosol. Scale bar: 50  $\mu$ m.

AAV vectors via the tail vein (Fig. 5). Compared with un-injected BL10 and *mdx* controls, systemic AAV injection resulted in robust GFP signals in the myocardium. Several different patterns were observed. The H4-CR subdomain was restricted at the sarcolemma while subdomains NT-H1, R4-6, R10-12, R13-15, R16-19 showed exclusive cytosolic expression. The R1-3 subdomain was found in the cytosol and the intercalated disk. In the mice infected with the CT-GFP AAV vector, we only detected a few GFP positive cardiomyocytes. Interestingly, GFP signals in these cells were found predominantly at the sarcolemma (Fig. 5).

## Discussion

In this study, we performed the first comprehensive *in vivo* evaluation of the subcellular localizations of dystrophin subdomains. We demonstrated that in addition to the well-known CR domain, dystrophin contains several highly conserved MBDs that can independently interact with the sarcolemma. These newly identified MBDs are R1-3, R10-12 and CT (Fig. 6). The CT subdomain bound to the sarcolemma in both skeletal muscle and cardiac muscle. Further, it restored the DGC. Subdomain R1-3 showed exclusive membrane binding in skeletal muscle (Fig. 6A) but a preference for the intercalated disk in the heart (Fig. 6B). Subdomain R10-12 only demonstrated partial membrane localization in skeletal muscle (Fig. 6A).

Interaction with the sarcolemma is central to how dystrophin protects the muscle. A wealth of molecular, biochemical and structural studies has provided unequivocal proof that the CR domain anchors dystrophin to the sarcolemma via the formation of the DGC (7–9). Hence, it has been quite puzzling why dystrophins that lack the CR domain still appear to bind to the sarcolemma in some atypical patients (11–13). Studies performed in *mdx* mice suggest that these puzzling patient observations may well be true. Of notice, forced expression of fragmented dystrophins that lack the CR domain has been repeatedly detected at the sarcolemma in *mdx* mice (Supplementary Material, Fig. S2C) (19–24). Collectively, it is reasonable to hypothesize that dystrophin may carry additional membrane localization domain(s).

To better understand dystrophin-sarcolemma interaction, investigators have turned to the artificial *in vitro* systems. These studies identified a number of potential regions capable of

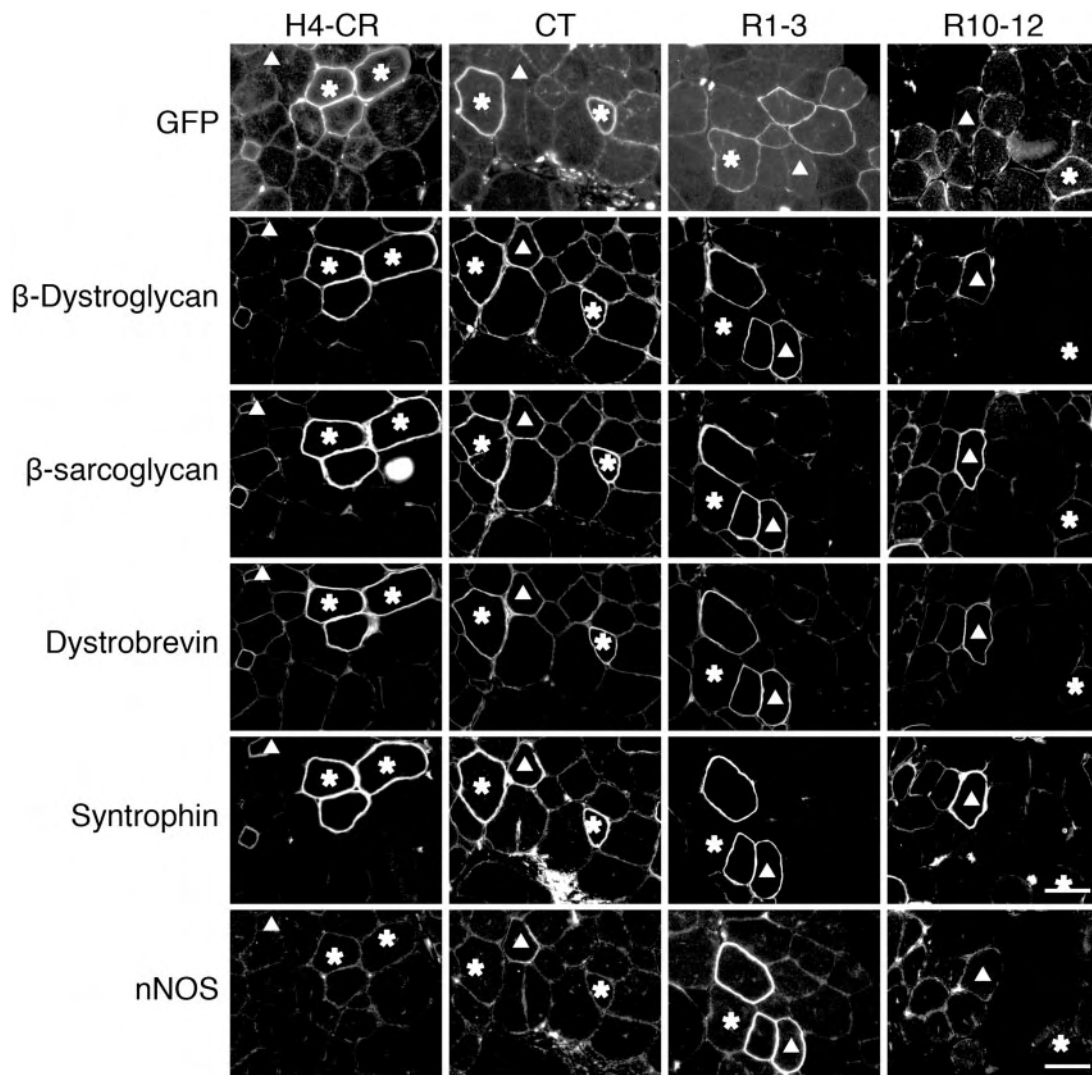


**Figure 4.** Dystrophin CT restores the DGC at the sarcolemma. Representative serial section photomicrographs of GFP and immunostaining for  $\beta$ -dystroglycan,  $\beta$ -sarcoglycan, dystrobrevin and syntrophin in *mdx* muscle expressing the indicated GFP-dystrophin subdomain fusion proteins. Asterisk, the GFP-positive myofiber in serial sections; Triangle, the GFP-negative revertant fiber in serial sections. GFP signals co-localize with DGC components in myofibers transduced by the H4-CR and CT but not R1-3 and R10-12 subdomain AAV vectors. Scale bar: 50  $\mu$ m.

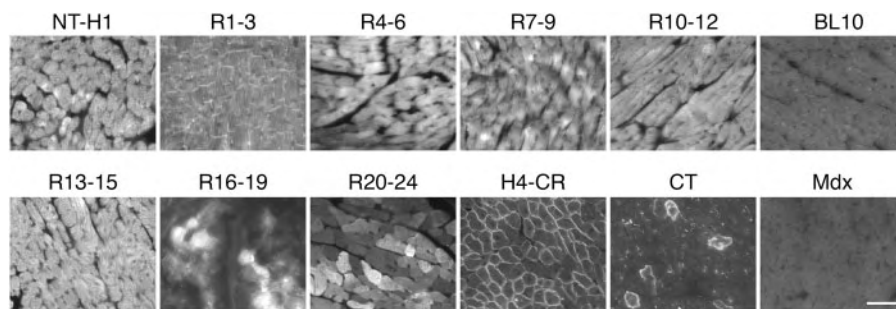


**Figure 5.** Dystrophin R1-3, CR and CT bind to the sarcolemma in the heart. Indicated GFP fusion dystrophin subdomains were delivered to the *mdx* heart by systemic AAV injection. Uninjected BL10 and *mdx* hearts were used as negative controls. Subdomain H4-CR and CT showed membrane localization. Subdomain R1-3 was found in the intercalated disk and cytosol. Remaining subdomains were only seen in the cytosol. Scale bar: 50  $\mu$ m.

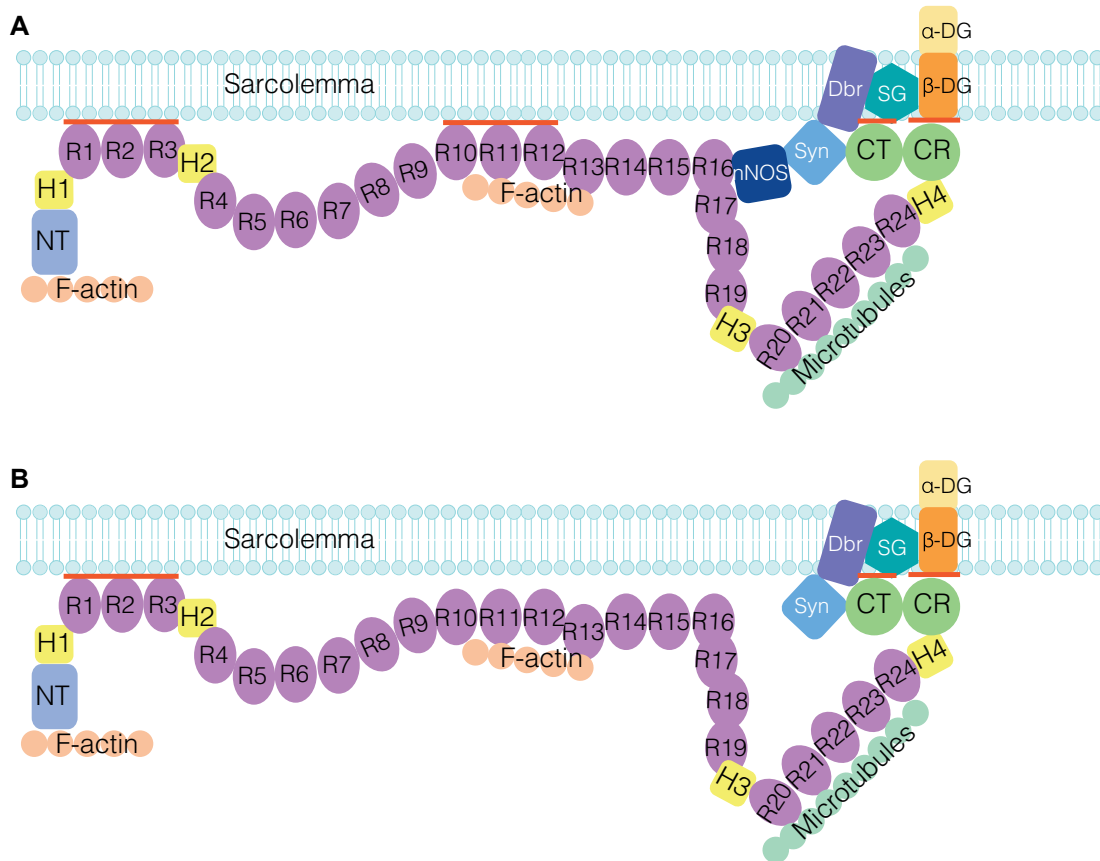


**Figure 6.** A new model of dystrophin-sarcolemma interaction. (A) In muscle, dystrophin binds to the sarcolemma through four independent membrane-binding subdomains. (B) In the heart, dystrophin binds to the sarcolemma through three independent membrane-binding domains. These subdomains are marked by thick red lines.

membrane binding such as R2, R1-3, R4-19, R11-15, R16-21 (Supplementary Material, Fig. S2D) (14,25–30). Essentially, 21 out of 24 spectrin-like repeats in the rod domain were found to carry the membrane binding property in these *in vitro* studies. Such a broad range makes it almost impossible to pinpoint the identity of true dystrophin MBDs. Considering the fact that *in vivo* performance of dystrophin spectrin-like repeats cannot be accurately predicted by *in vitro* analysis (31), it becomes even more challenging to characterize the CR domain-independent dystrophin-sarcolemma interaction in test tubes. Here, we took a systematic and unbiased approach with an emphasis on the *in vivo* interaction in rodents and large mammals. We found four structurally defined regions in dystrophin that are capable of interacting with the sarcolemma. These include the well-studied CR domain and three new MBDs (two in the rod domain and one in CT). While R1-3 and R10-12 have been implicated in some *in vitro* studies, direct binding of CT to the sarcolemma has never been reported. Intriguingly, CT also restores the DGC (Fig. 4). It is intriguing that we observed striking differences in the membrane binding behavior of the newly identified rod domain MBDs. Specifically, R1-3 is not restricted to the sarcolemma in the heart and R10-12 has no membrane binding activity in the heart (Fig. 5). This is reminiscent of different nNOS-binding properties of dystrophin in skeletal muscle and the heart (32,33). Collectively, these data suggest that dystrophin may have different functional roles in skeletal muscle and the heart.

The mechanism(s) by which these newly identified MBDs bind to the sarcolemma await future investigations. It is possible that electrostatic and/or hydrophobic interactions may play

a role. However, considering what is known about other spectrin family proteins, we suspect that such interactions may likely involve specified membrane domains (such as lipid rafts) and palmitoylation (34).

Restoration of the DGC by CT is another unexpected finding in this study. We speculate that CT may utilize its syntrophin/dystrobrevin binding motifs to recruit syntrophin and dystrobrevin first. Subsequently, these two proteins scaffold sarcoglycans and dystroglycan to the complex (Supplementary Material, Fig. S4) (35–38).

Another important area that requires further analysis is the kinetic mode of interaction between different MBDs and the sarcolemma. A recent study in the zebrafish suggests that dystrophin can associate with the sarcolemma either via stable tight interaction or via reversible dynamic shuttling between the sarcolemma and the cytosol (39). While additional studies are needed, the results of our microsomal preparation western blot seem to hint that the CR domain is responsible for stable membrane binding (GFP signals were barely detected in the cytosolic fraction) and three newly discovered MBDs may contribute to dynamic membrane binding (abundant GFP signals also presented in the cytosol) (Fig. 2B).

There are a few limitations in our study. First, we have not included hinges 2 and 3 in our constructs. Due to the structural properties of hinges (proline-rich, neither  $\alpha$ -helix nor  $\beta$ -sheet), we suspect that these hinge regions may play a nominal role in membrane binding. Nevertheless, future studies are needed to confirm this. Second, we have used an over-expression system in our studies and also the fragmented dystrophin domains are

not in their natural protein environment. It remains to be determined whether the membrane binding properties of the newly discovered MBDs are preserved under physiological concentration of dystrophin in wild type animals.

Taken together, we have discovered a new model for dystrophin membrane binding (Fig. 6). Our results offer critical insights into dystrophin function, DMD pathogenesis and gene therapy.

## Materials and Methods

### Animals

All animal experiments were approved by the Animal Care and Use Committee of the University of Missouri, and the animal use and handling were strictly in accordance with the National Institutes of Health guidelines. Dystrophin-null *mdx* mice were purchased from The Jackson Laboratory (Bar Harbor, ME). Dystrophin-deficient dogs were generated in house by artificial insemination.

### AAV production and delivery

The GFP gene was fused in-frame to the C-terminal ends of the human dystrophin subdomains (Supplementary Material, Fig. S3). The fusion constructs were cloned into the *cis* AAV packaging constructs by PCR and confirmed by sequencing. Expression was driven by the cytomegalovirus promoter and the SV40 polyadenylation signal. Y731F AAV-9 vectors were generated by transient transfection and purified through two rounds of CsCl gradient ultracentrifugation (40,41). The viral titer was determined by quantitative PCR.

AAV vectors were delivered by intramuscular injection to limb muscles to adult *mdx* mice ( $4\text{--}7 \times 10^{11}$  vg particles/muscle) and adult dystrophic dogs ( $0.8\text{--}4 \times 10^{14}$  vg particles/muscle). In dog studies, we applied 5-week transient immune suppression with cyclosporine and mycophenolate mofetil according to our published protocol (42).

### Muscle harvesting, microscopic examination and western blot

Eight weeks after injection, the animals were euthanized and muscles were harvested according to Liadaki et al through serial sucrose gradient to preserve the GFP signal (43). GFP was visualized directly under the fluorescein isothiocyanate channel using a fluorescence microscope. Immunostaining was performed as we published before (31,44). Whole muscle lysates were generated as we published before (31,44). The cytosolic and microsomal preparations were obtained with the Plasma Membrane Protein Extraction kit (ab65400, Abcam). Muscle lysates were resolved in a 6% sodium dodecyl sulfate polyacrylamide gel and transferred to a polyvinylidene difluoride membrane. Antibodies used in immunostaining and western blot are listed in Supplementary Material, Table S1.

## Supplementary Material

Supplementary Material is available at HMG online.

**Conflict of Interest statement.** D.D. is a member of the scientific advisory board for and an equity holder of Solid GT, a subsidiary of Solid Biosciences.

## Funding

This work was supported by the grants from Duchenne Parent Project, the Netherlands [to Y.L.]; the National Institutes of Health [NS90634 to D.D., AR67985 to D.D. and Y.L.]; Department of Defense [MD130014 to D.D.]; and Jesse's Journey-The Foundation for Gene and Cell Therapy [to D.D.].

## References

1. Straub, V., Rafael, J.A., Chamberlain, J.S. and Campbell, K.P. (1997) Animal models for muscular dystrophy show different patterns of sarcolemmal disruption. *J. Cell Biol.*, **139**, 375–385.
2. Petrof, B.J., Shrager, J.B., Stedman, H.H., Kelly, A.M. and Sweeney, H.L. (1993) Dystrophin protects the sarcolemma from stresses developed during muscle contraction. *Proc. Natl. Acad. Sci. USA*, **90**, 3710–3714.
3. Hoffman, E.P., Brown, R.H.J. and Kunkel, L.M. (1987) Dystrophin: the protein product of the Duchenne muscular dystrophy locus. *Cell*, **51**, 919–928.
4. Koenig, M. and Kunkel, L.M. (1990) Detailed analysis of the repeat domain of dystrophin reveals four potential hinge segments that may confer flexibility. *J. Biol. Chem.*, **265**, 4560–4566.
5. Amann, K.J., Renley, B.A. and Ervasti, J.M. (1998) A cluster of basic repeats in the dystrophin rod domain binds F-actin through an electrostatic interaction. *J. Biol. Chem.*, **273**, 28419–28423.
6. Rybakova, I.N., Amann, K.J. and Ervasti, J.M. (1996) A new model for the interaction of dystrophin with F-actin. *J. Cell Biol.*, **135**, 661–672.
7. Campbell, K.P. and Kahl, S.D. (1989) Association of dystrophin and an integral membrane glycoprotein. *Nature*, **338**, 259–262.
8. Jung, D., Yang, B., Meyer, J., Chamberlain, J.S. and Campbell, K.P. (1995) Identification and characterization of the dystrophin anchoring site on beta-dystroglycan. *J. Biol. Chem.*, **270**, 27305–27310.
9. Huang, X., Poy, F., Zhang, R., Joachimiak, A., Sudol, M. and Eck, M.J. (2000) Structure of a WW domain containing fragment of dystrophin in complex with beta-dystroglycan. *Nat. Struct. Biol.*, **7**, 634–638.
10. Ervasti, J.M. and Campbell, K.P. (1991) Membrane organization of the dystrophin-glycoprotein complex. *Cell*, **66**, 1121–1131.
11. Helliwell, T.R., Ellis, J.M., Mountford, R.C., Appleton, R.E. and Morris, G.E. (1992) A truncated dystrophin lacking the C-terminal domains is localized at the muscle membrane. *Am. J. Hum. Genet.*, **50**, 508–514.
12. Hoffman, E.P., Garcia, C.A., Chamberlain, J.S., Angelini, C., Lupski, J.R. and Fenwick, R. (1991) Is the carboxyl-terminus of dystrophin required for membrane association? A novel, severe case of Duchenne muscular dystrophy. *Ann. Neurol.*, **30**, 605–610.
13. Recan, D., Chafey, P., Leturcq, F., Hugnot, J.P., Vincent, N., Tome, F., Collin, H., Simon, D., Czernichow, P., Nicholson, L.V. and et al. (1992) Are cysteine-rich and COOH-terminal domains of dystrophin critical for sarcolemmal localization? *J. Clin. Invest.*, **89**, 712–716.
14. Le Rumeur, E., Winder, S.J. and Hubert, J.F. (2010) Dystrophin: more than just the sum of its parts. *Biochim. Biophys. Acta*, **1804**, 1713–1722.
15. Cox, G.A., Sunada, Y., Campbell, K.P. and Chamberlain, J.S. (1994) Dp71 can restore the dystrophin-associated glycoprotein complex in muscle but fails to prevent dystrophy. *Nat. Genet.*, **8**, 333–339.

16. Crawford, G.E., Faulkner, J.A., Crosbie, R.H., Campbell, K.P., Froehner, S.C. and Chamberlain, J.S. (2000) Assembly of the dystrophin-associated protein complex does not require the dystrophin COOH-terminal domain. *J. Cell Biol.*, **150**, 1399–1410.
17. Rapaport, D., Greenberg, D.S., Tal, M., Yaffe, D. and Nudel, U. (1993) Dp71, the nonmuscle product of the Duchenne muscular dystrophy gene is associated with the cell membrane. *FEBS Lett.*, **328**, 197–202.
18. Judge, L.M., Haraguchiln, M. and Chamberlain, J.S. (2006) Dissecting the signaling and mechanical functions of the dystrophin-glycoprotein complex. *J. Cell Sci.*, **119**, 1537–1546.
19. Rafael, J.A., Cox, G.A., Corrado, K., Jung, D., Campbell, K.P. and Chamberlain, J.S. (1996) Forced expression of dystrophin deletion constructs reveals structure-function correlations. *J. Cell Biol.*, **134**, 93–102.
20. Fritz, J.D., Danko, I., Roberds, S.L., Campbell, K.P., Latendresse, J.S. and Wolff, J.A. (1995) Expression of deletion-containing dystrophins in mdx muscle: implications for gene therapy and dystrophin function. *Pediatr. Res.*, **37**, 693–700.
21. Maconochie, M.K., Simpkins, A.H., Damien, E., Coulton, G., Greenfield, A.J. and Brown, S.D. (1996) The cysteine-rich and C-terminal domains of dystrophin are not required for normal costameric localization in the mouse. *Transgenic Res.*, **5**, 123–130.
22. Gardner, K.L., Kearney, J.A., Edwards, J.D. and Rafael-Fortney, J.A. (2006) Restoration of all dystrophin protein interactions by functional domains in trans does not rescue dystrophy. *Gene Ther.*, **13**, 744–751.
23. Barnabei, M.S., Sjaastad, F.V., Townsend, D., Bedada, F.B. and Metzger, J.M. (2015) Severe dystrophic cardiomyopathy caused by the enteroviral protease 2A-mediated C-terminal dystrophin cleavage fragment. *Sci. Transl. Med.*, **7**, 294ra106.
24. Dunkley, M.G., Wells, K.E., Piper, T.A., Wells, D.J. and Dickson, G. (1994) Independent localization of dystrophin N- and C-terminal regions to the sarcolemma of mdx mouse myofibres in vivo. *J. Cell Sci.*, **107**, 1469–1475.
25. Hir, S.A., Raguene-Nicol, C., Paboef, G., Nicolas, A., L Rumeur, E. and Vie, V., (2014) Cholesterol favors the anchorage of human dystrophin repeats 16 to 21 in membrane at physiological surface pressure. *Biochim. Biophys. Acta*, **1838**, 1266–1273.
26. DeWolf, C., McCauley, P., Sikorski, A.F., Winlove, C.P., Bailey, A.I., Kahana, E., Pinder, J.C. and Gratzner, W.B. (1997) Interaction of dystrophin fragments with model membranes. *Biophys. J.*, **72**, 2599–2604.
27. Le Rumeur, E., Fichou, Y., Pottier, S., Gaboriau, F., Rondeau-Mouro, C., Vincent, M., Gallay, J. and Bondon, A. (2003) Interaction of dystrophin rod domain with membrane phospholipids. Evidence of a close proximity between tryptophan residues and lipids. *J. Biol. Chem.*, **278**, 5993–6001.
28. Le Rumeur, E., Pottier, S., Da Costa, G., Metzinger, L., Mouret, L., Rocher, C., Fourage, M., Rondeau-Mouro, C. and Bondon, A. (2007) Binding of the dystrophin second repeat to membrane di-oleyl phospholipids is dependent upon lipid packing. *Biochim. Biophys. Acta*, **1768**, 648–654.
29. Legardinier, S., Hubert, J.F., Le Bihan, O., Tascon, C., Rocher, C., Raguene-Nicol, C., Bondon, A., Hardy, S. and Le Rumeur, E. (2008) Sub-domains of the dystrophin rod domain display contrasting lipid-binding and stability properties. *Biochim. Biophys. Acta*, **1784**, 672–682.
30. Legardinier, S., Raguene-Nicol, C., Tascon, C., Rocher, C., Hardy, S., Hubert, J.F. and Le Rumeur, E. (2009) Mapping of the lipid-binding and stability properties of the central rod domain of human dystrophin. *J. Mol. Biol.*, **389**, 546–558.
31. Lai, Y., Zhao, J., Yue, Y. and Duan, D. (2013) alpha2 and alpha3 helices of dystrophin R16 and R17 frame a microdomain in the alpha1 helix of dystrophin R17 for neuronal NOS binding. *Proc. Natl. Acad. Sci. U S A*, **110**, 525–530.
32. Johnson, E.K., Zhang, L., Adams, M.E., Phillips, A., Freitas, M.A., Froehner, S.C., Green-Church, K.B. and Montanaro, F. (2012) Proteomic analysis reveals new cardiac-specific dystrophin-associated proteins. *PLoS One*, **7**, e43515.
33. Lai, Y., Thomas, G.D., Yue, Y., Yang, H.T., Li, D., Long, C., Judge, L., Bostick, B., Chamberlain, J.S., Terjung, R.L. and Duan, D. (2009) Dystrophins carrying spectrin-like repeats 16 and 17 anchor nNOS to the sarcolemma and enhance exercise performance in a mouse model of muscular dystrophy. *J. Clin. Invest.*, **119**, 624–635.
34. Bennett, V. and Lorenzo, D.N. (2016) An Adaptable Spectrin/Ankyrin-Based Mechanism for Long-Range Organization of Plasma Membranes in Vertebrate Tissues. *Curr Top Membr*, **77**, 143–184.
35. Yoshida, M., Hama, H., Ishikawa-Sakurai, M., Imamura, M., Mizuno, Y., Araishi, K., Wakabayashi-Takai, E., Noguchi, S., Sasaoka, T. and Ozawa, E. (2000) Biochemical evidence for association of dystrobrevin with the sarcoglycan-sarcospan complex as a basis for understanding sarcoglycanopathy. *Hum. Mol. Genet.*, **9**, 1033–1040.
36. Suzuki, A., Yoshida, M. and Ozawa, E. (1995) Mammalian alpha 1- and beta 1-syntrophin bind to the alternative splice-prone region of the dystrophin COOH terminus. *J. Cell Biol.*, **128**, 373–381.
37. Yang, B., Jung, D., Rafael, J.A., Chamberlain, J.S. and Campbell, K.P. (1995) Identification of alpha-syntrophin binding to syntrophin triplet, dystrophin, and utrophin. *J. Biol. Chem.*, **270**, 4975–4978.
38. Bunnell, T.M., Jaeger, M.A., Fitzsimons, D.P., Prins, K.W. and Ervasti, J.M. (2008) Destabilization of the dystrophin-glycoprotein complex without functional deficits in alpha-dystrobrevin null muscle. *PLoS One*, **3**, e2604.
39. Bajanca, F., Gonzalez-Perez, V., Gillespie, S.J., Beley, C., Garcia, L., Theveneau, E., Sear, R.P. and Hughes, S.M. (2015) In vivo dynamics of skeletal muscle Dystrophin in zebrafish embryos revealed by improved FRAP analysis. *Elife*, **4**, e06541.
40. Shin, J.H., Yue, Y. and Duan, D. (2012) Recombinant adeno-associated viral vector production and purification. *Methods Mol. Biol.*, **798**, 267–284.
41. Zhong, L., Li, B., Mah, C.S., Govindasamy, L., Agbandje-McKenna, M., Cooper, M., Herzog, R.W., Zolotukhin, I., Warrington, K.H.J., Weigel-Van Aken, K.A., et al. (2008) Next generation of adeno-associated virus 2 vectors: point mutations in tyrosines lead to high-efficiency transduction at lower doses. *Proc. Natl. Acad. Sci. U S A*, **105**, 7827–7832.
42. Shin, J.H., Yue, Y., Srivastava, A., Smith, B., Lai, Y. and Duan, D. (2012) A Simplified Immune Suppression Scheme Leads to Persistent Micro-dystrophin Expression in Duchenne Muscular Dystrophy Dogs. *Hum. Gene Ther.*, **23**, 202–209.
43. Liadaki, K., Luth, E.S. and Kunkell, L.M. (2007) Co-detection of GFP and dystrophin in skeletal muscle tissue sections. *BioTechniques*, **42**, 699–700.
44. Lai, Y., Zhao, J., Yue, Y., Wasala, N.B. and Duan, D. (2014) Partial restoration of cardiac function with ΔPDZ nNOS in aged mdx model of Duchenne cardiomyopathy. *Hum. Mol. Genet.*, **23**, 3189–3199.

## Supplementary Figure Legends

**Supplementary Fig 1. The classic model of dystrophin-sarcolemma interaction.** Numerous studies suggest that dystrophin binds to the sarcolemma via its CR domain (1–8). See **Supplementary References** for full citation.

**Supplementary Fig 2. Evidence of dystrophin sarcolemmal binding in the absence of the CR domain.** **A**, Cartoon illustration of the structure of full-length dystrophin. **B**, Cartoon illustration of CR-deleted dystrophins that were found at the sarcolemma in patients (9–11). **C**, Cartoon illustration of synthetic CR-deleted dystrophin fragments that showed sarcolemmal localization in *mdx* mice (12–17). **D**, Cartoon illustration dystrophin membrane binding domains identified by *in vitro* interaction assays (18–23). Related references are marked next to the cartoon illustrations and the full citation is available in **Supplementary References**. Filled shapes: domains present; open shapes: domains absent.

**Supplementary Fig 3. Cartoon illustration of ten GFP-fused dystrophin subdomains used in the study.** The full-length human dystrophin molecule is split into ten subdomains. The numerical number range above each cartoon illustration refers to amino acid sequence numbering in the full-length human dystrophin protein. The predicted molecular weight of each fusion protein is marked. The YL numbers refer to the construct name in the Duan/Lai laboratory.

**Supplementary Fig 4. The hypothetical mechanism of CT-mediated DGC restoration.** Left side cartoon illustrates the CR domain mediated DGC restoration. Right side cartoon illustrates the hypothetical mechanism of CT-mediated DGC restoration. Specifically, direct membrane binding of the CT domain restores syntrophin and dystrobrevin to the sarcolemma (24, 25). Membrane-localized syntrophin and dystrobrevin then recruit sarcoglycans and dystroglycan to the sarcolemma (26–29). DG, dystroglycan; SG, sarcoglycans; Dbr, dystrobrevin; Syn, syntrophin.

## Supplementary References

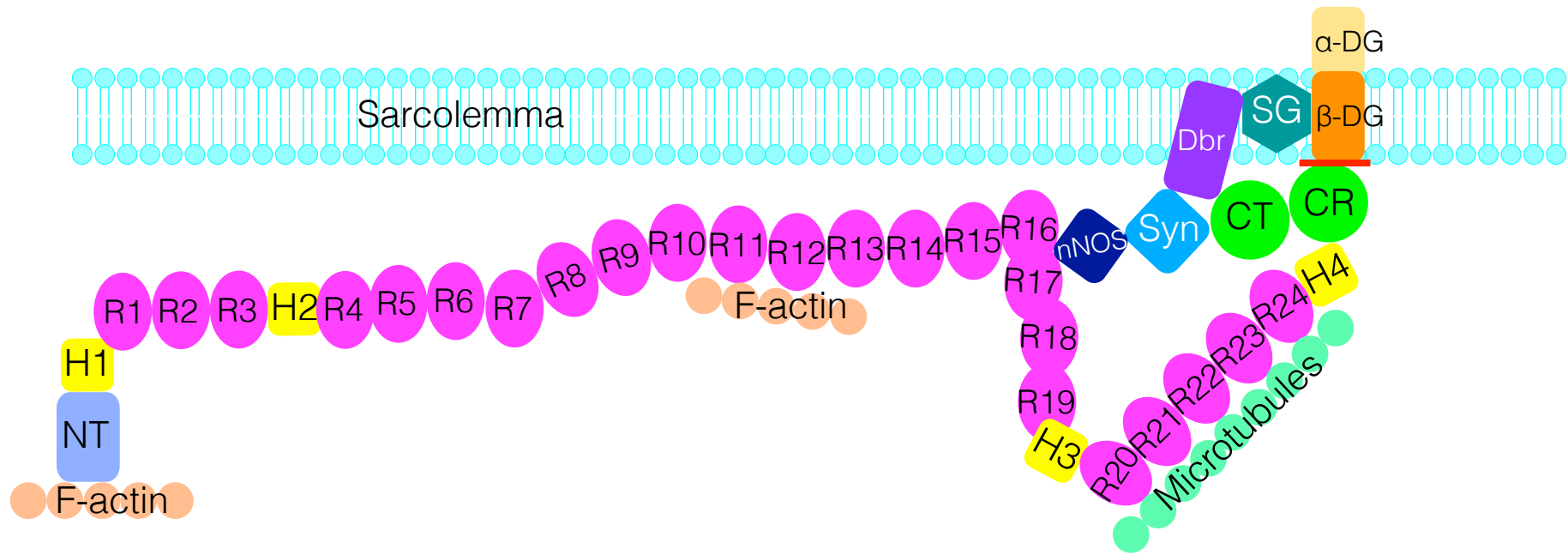
1. Suzuki, A., Yoshida, M., Yamamoto, H. and Ozawa, E. (1992) Glycoprotein-binding site of dystrophin is confined to the cysteine-rich domain and the first half of the carboxy-terminal domain. *FEBS Lett.*, **308**, 154-160.
2. Suzuki, A., Yoshida, M., Hayashi, K., Mizuno, Y., Hagiwara, Y. and Ozawa, E. (1994) Molecular organization at the glycoprotein-complex-binding site of dystrophin. Three dystrophin-associated proteins bind directly to the carboxy-terminal portion of dystrophin. *Eur. J. Biochem.*, **220**, 283-292.
3. Campbell, K.P. and Kahl, S.D. (1989) Association of dystrophin and an integral membrane glycoprotein. *Nature*, **338**, 259-262.
4. Jung, D., Yang, B., Meyer, J., Chamberlain, J.S. and Campbell, K.P. (1995) Identification and characterization of the dystrophin anchoring site on beta-dystroglycan. *J. Biol. Chem.*, **270**, 27305-27310.
5. Huang, X., Poy, F., Zhang, R., Joachimiak, A., Sudol, M. and Eck, M.J. (2000) Structure of a WW domain containing fragment of dystrophin in complex with beta-dystroglycan. *Nat. Struct. Biol.*, **7**, 634-638.
6. Ishikawa-Sakurai, M., Yoshida, M., Imamura, M., Davies, K.E. and Ozawa, E. (2004) ZZ domain is essentially required for the physiological binding of dystrophin and utrophin to beta-dystroglycan. *Hum. Mol. Genet.*, **13**, 693-702.
7. Draviam, R.A., Wang, B., Li, J., Xiao, X. and Watkins, S.C. (2006) Mini-dystrophin efficiently incorporates into the dystrophin protein complex in living cells. *J Muscle Res Cell Motil*, **27**, 53-67.
8. Einbond, A. and Sudol, M. (1996) Towards prediction of cognate complexes between the

- WW domain and proline-rich ligands. *FEBS Lett.*, **384**, 1-8.
9. Recan, D., Chafey, P., Leturcq, F., Hugnot, J.P., Vincent, N., Tome, F., Collin, H., Simon, D., Czernichow, P., Nicholson, L.V. and et, A. (1992) Are cysteine-rich and COOH-terminal domains of dystrophin critical for sarcolemmal localization? *J. Clin. Invest.*, **89**, 712-716.
  10. Hoffman, E.P., Garcia, C.A., Chamberlain, J.S., Angelini, C., Lupski, J.R. and Fenwick, R. (1991) Is the carboxyl-terminus of dystrophin required for membrane association? A novel, severe case of Duchenne muscular dystrophy. *Ann. Neurol.*, **30**, 605-610.
  11. Helliwell, T.R., Ellis, J.M., Mountford, R.C., Appleton, R.E. and Morris, G.E. (1992) A truncated dystrophin lacking the C-terminal domains is localized at the muscle membrane. *Am. J. Hum. Genet.*, **50**, 508-514.
  12. Rafael, J.A., Cox, G.A., Corrado, K., Jung, D., Campbell, K.P. and Chamberlain, J.S. (1996) Forced expression of dystrophin deletion constructs reveals structure-function correlations. *J. Cell Biol.*, **134**, 93-102.
  13. Maconochie, M.K., Simpkins, A.H., Damien, E., Coulton, G., Greenfield, A.J. and Brown, S.D. (1996) The cysteine-rich and C-terminal domains of dystrophin are not required for normal costameric localization in the mouse. *Transgenic Res*, **5**, 123-130.
  14. Gardner, K.L., Kearney, J.A., Edwards, J.D. and Rafael-Fortney, J.A. (2006) Restoration of all dystrophin protein interactions by functional domains in trans does not rescue dystrophy. *Gene Ther*, **13**, 744-751.
  15. Barnabei, M.S., Sjaastad, F.V., Townsend, D., Bedada, F.B. and Metzger, J.M. (2015) Severe dystrophic cardiomyopathy caused by the enteroviral protease 2A-mediated C-terminal dystrophin cleavage fragment. *Sci Transl Med*, **7**, 294ra106.

16. Dunckley, M.G., Wells, K.E., Piper, T.A., Wells, D.J. and Dickson, G. (1994) Independent localization of dystrophin N- and C-terminal regions to the sarcolemma of mdx mouse myofibres in vivo. *J. Cell Sci.*, **107**, 1469-1475.
17. Fritz, J.D., Danko, I., Roberds, S.L., Campbell, K.P., Latendresse, J.S. and Wolff, J.A. (1995) Expression of deletion-containing dystrophins in mdx muscle: implications for gene therapy and dystrophin function. *Pediatr Res*, **37**, 693-700.
18. Sarkis, J., Hubert, J.F., Legrand, B., Robert, E., Cheron, A., Jardin, J., Hitti, E., Le Rumeur, E. and Vie, V. (2011) Spectrin-like repeats 11-15 of human dystrophin show adaptations to a lipidic environment. *J. Biol. Chem.*, **286**, 30481-30491.
19. Legardinier, S., Raguene-Nicol, C., Tascon, C., Rocher, C., Hardy, S., Hubert, J.F. and Le Rumeur, E. (2009) Mapping of the lipid-binding and stability properties of the central rod domain of human dystrophin. *J. Mol. Biol.*, **389**, 546-558.
20. Legardinier, S., Hubert, J.F., Le Bihan, O., Tascon, C., Rocher, C., Raguene-Nicol, C., Bondon, A., Hardy, S. and Le Rumeur, E. (2008) Sub-domains of the dystrophin rod domain display contrasting lipid-binding and stability properties. *Biochim. Biophys. Acta*, **1784**, 672-682.
21. Le Rumeur, E., Pottier, S., Da Costa, G., Metzinger, L., Mouret, L., Rocher, C., Fourage, M., Rondeau-Mouro, C. and Bondon, A. (2007) Binding of the dystrophin second repeat to membrane di-oleyl phospholipids is dependent upon lipid packing. *Biochim. Biophys. Acta*, **1768**, 648-654.
22. Hir, S.A., Raguene-Nicol, C., Paboeuf, G., Nicolas, A., Le Rumeur, E. and Vie, V. (2014) Cholesterol favors the anchorage of human dystrophin repeats 16 to 21 in membrane at physiological surface pressure. *Biochim. Biophys. Acta*, **1838**, 1266-1273.

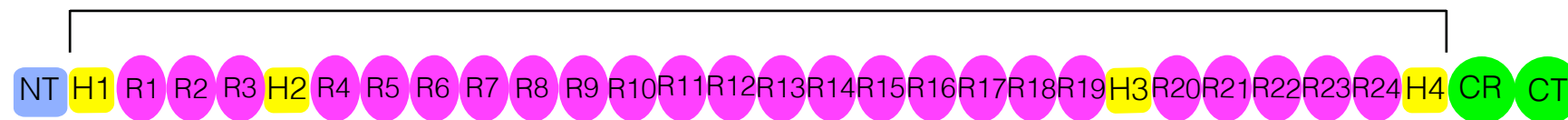
23. Le Rumeur, E., Fichou, Y., Pottier, S., Gaboriau, F., Rondeau-Mouro, C., Vincent, M., Gallay, J. and Bondon, A. (2003) Interaction of dystrophin rod domain with membrane phospholipids. Evidence of a close proximity between tryptophan residues and lipids. *J. Biol. Chem.*, **278**, 5993-6001.
24. Suzuki, A., Yoshida, M. and Ozawa, E. (1995) Mammalian alpha 1- and beta 1-syntrophin bind to the alternative splice-prone region of the dystrophin COOH terminus. *J. Cell Biol.*, **128**, 373-381.
25. Yang, B., Jung, D., Rafael, J.A., Chamberlain, J.S. and Campbell, K.P. (1995) Identification of alpha-syntrophin binding to syntrophin triplet, dystrophin, and utrophin. *J. Biol. Chem.*, **270**, 4975-4978.
26. Yoshida, M., Hama, H., Ishikawa-Sakurai, M., Imamura, M., Mizuno, Y., Araishi, K., Wakabayashi-Takai, E., Noguchi, S., Sasaoka, T. and Ozawa, E. (2000) Biochemical evidence for association of dystrobrevin with the sarcoglycan-sarcospan complex as a basis for understanding sarcoglycanopathy. *Hum. Mol. Genet.*, **9**, 1033-1040.
27. Cox, G.A., Sunada, Y., Campbell, K.P. and Chamberlain, J.S. (1994) Dp71 can restore the dystrophin-associated glycoprotein complex in muscle but fails to prevent dystrophy. *Nat. Genet.*, **8**, 333-339.
28. Rapaport, D., Greenberg, D.S., Tal, M., Yaffe, D. and Nudel, U. (1993) Dp71, the nonmuscle product of the Duchenne muscular dystrophy gene is associated with the cell membrane. *FEBS Lett.*, **328**, 197-202.
29. Judge, L.M., Haraguchiln, M. and Chamberlain, J.S. (2006) Dissecting the signaling and mechanical functions of the dystrophin-glycoprotein complex *J. Cell Sci.*, **119**, 1537-1546.

Fig S1

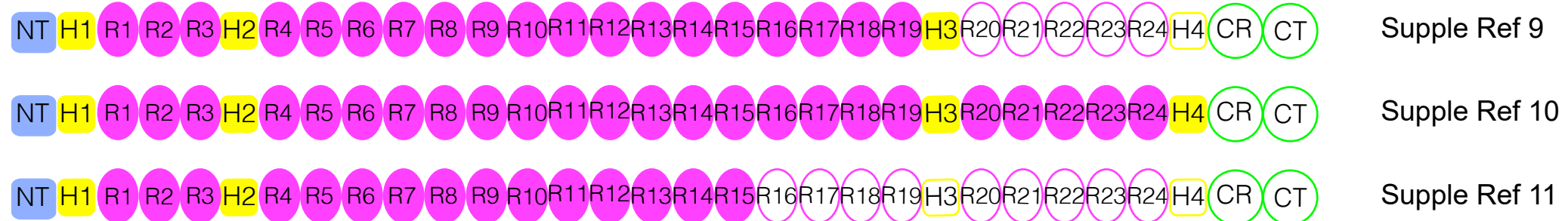


## A. Full-length dystrophin

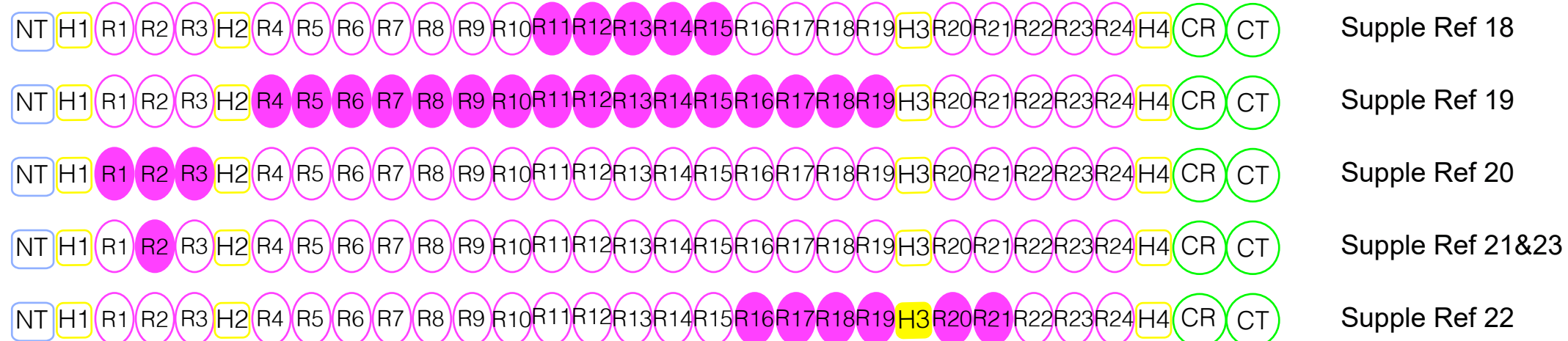
the mid-rod domain



## B. CR-deleted dystrophins that were found at the sarcolemma in human patients



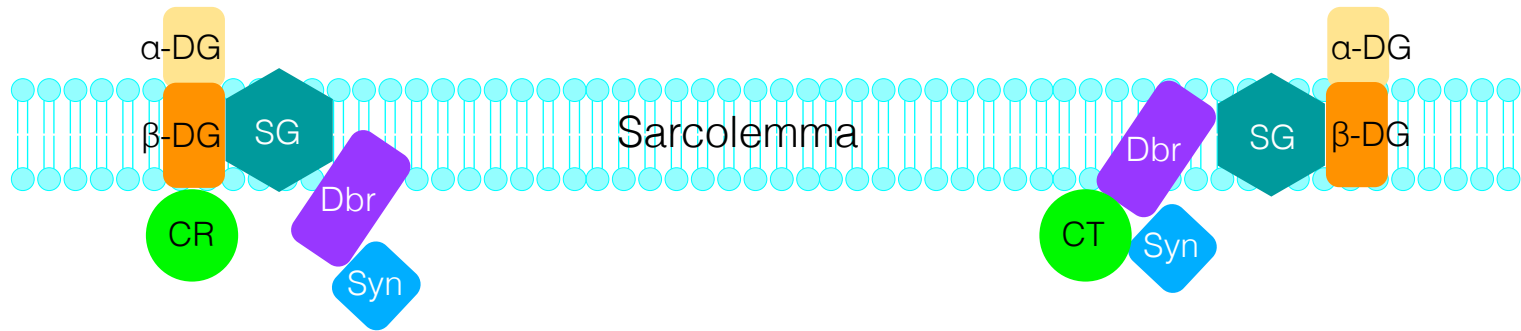
## C. Synthetic CR-deleted dystrophins that are found at the sarcolemma in mdx mice

D. Dystrophin membrane binding domains identified by *in vitro* studies

## Fig S3

NT-H1	1-336 NT-H1	GFP	65.9 kD	YL376
R1-3	337-667 R1-3	GFP	65.7 kD	YL375
R4-6	718-1045 R4-6	GFP	65.5 kD	YL367
R7-9	1046-1367 R7-9	GFP	64.9 kD	YL368
R10-12	1368-1676 R10-12	GFP	62.6 kD	YL369
R13-15	1677-1973 R13-15	GFP	62.4 kD	YL370
R16-19	1992-2423 R16-19	GFP	77.8 kD	YL371
R20-24	2471-3040 R20-24	GFP	94.1 kD	YL372
H4-CR	3041-3408 H4-CR	GFP	69.9 kD	YL410
CT	3422-3685 CT	GFP	57 kD	YL411

**Fig S4**



Restoration of DGC by the CR domain

Restoration of DGC by CT

**Table S1. Antibodies used in the study.**

<b>Antigen</b>	<b>Host</b>	<b>Catalog #</b>	<b>Company</b>	<b>Dilution</b>	<b>Experiment</b>
$\beta$ -Dystroglycan	Mouse	NCL-B-DG	Novocastra	1:50	IF
Syntrophin	Mouse	ab11425	Abcam	1:200	IF
$\beta$ -Sarcoglycan	Mouse	NCL-B-SARC	Novocastra	1:50	IF
Dystrobrevin	Mouse	610766	BD Bioscience	1:200	IF
GFP	Mouse	33-2600	Invitrogen	1:100	WB
GAPDH	Mouse	MAB374	Millipore	1:5,000	WB

IF: Immunofluorescence staining; WB: western blot.

## ORIGINAL ARTICLE

# Genomic removal of a therapeutic mini-dystrophin gene from adult mice elicits a Duchenne muscular dystrophy-like phenotype

Nalinda B. Wasala<sup>1</sup>, Yi Lai<sup>1</sup>, Jin-Hong Shin<sup>1,†</sup>, Junling Zhao<sup>1</sup>, Yongping Yue<sup>1</sup> and Dongsheng Duan<sup>1,2,3,\*</sup>

<sup>1</sup>Department of Molecular Microbiology and Immunology, School of Medicine, <sup>2</sup>Department of Neurology, School of Medicine and <sup>3</sup>Department of Bioengineering, The University of Missouri, Columbia, MO 65212, USA

\*To whom correspondence should be addressed at: Department of Molecular Microbiology and Immunology, One Hospital Dr, Columbia, MO 65212, USA. Tel: +1-573 884 9584; Fax: +1-573 882 4287; Email: duand@missouri.edu

## Abstract

Duchenne muscular dystrophy (DMD) is caused by dystrophin deficiency. A fundamental question in DMD pathogenesis and dystrophin gene therapy is whether muscle health depends on continuous dystrophin expression throughout the life. Published data suggest that transient dystrophin expression in early life might offer permanent protection. To study the consequences of adulthood dystrophin loss, we generated two strains of floxed mini-dystrophin transgenic mice on the dystrophin-null background. Muscle diseases were prevented in skeletal muscle of the YL238 strain and the heart of the SJ13 strain by selective expression of a therapeutic mini-dystrophin gene in skeletal muscle and heart, respectively. The mini-dystrophin gene was removed from the tibialis anterior (TA) muscle of 8-month-old YL238 mice and the heart of 7-month-old SJ13 mice using an adeno-associated virus serotype-9 Cre recombinase vector (AAV.CBA.Cre). At 12 and 15 months after AAV.CBA.Cre injection, mini-dystrophin expression was reduced by ~87% in the TA muscle of YL238 mice and ~64% in the heart of SJ13 mice. Mini-dystrophin reduction caused muscle atrophy, degeneration and force loss in the TA muscle of YL238 mice and significantly compromised left ventricular hemodynamics in SJ13 mice. Our results suggest that persistent dystrophin expression is essential for continuous muscle and heart protection.

## Introduction

Duchenne muscular dystrophy (DMD) is an X-linked life limiting genetic disease resulted from the loss of dystrophin (1). It affects ~1 in 5000 newborn boys (2). Patients often fail to meet their motor development milestones at 3–5 years of age and lose their mobility in early teenage. They die either from respiratory muscle failure and/or heart failure in the second and third decade of the life. Currently there is no cure. Restoration of dystrophin expression holds a great promise to treat DMD at the molecular level (3–6).

A fundamental question in DMD pathogenesis and dystrophin gene replacement therapy is whether muscle health depends on continuous dystrophin expression. If dystrophin is required for muscle health throughout the lifespan of the patient, then an effective therapy will have to depend on persistent dystrophin expression. On the other hand, if dystrophin is only required during certain developmental/growth stages, then transient expression at these stages may meet the therapeutic need. Although it is generally believed that DMD therapy

<sup>†</sup>Present address: Pusan National University Yangsan Hospital, Yangsan, Republic of Korea.

Received: January 4, 2016. Revised: March 29, 2016. Accepted: April 18, 2016

© The Author 2016. Published by Oxford University Press.

All rights reserved. For permissions, please e-mail: journals.permissions@oup.com

requires continuous dystrophin expression, experimental support for this notion is lacking. In contrast, existing evidence seems to suggest that the opposite might be true. In particular, Ghahramani Seno *et al.* (7) found that knockdown of dystrophin expression in skeletal muscle of adult normal mice did not cause overt dystrophic pathology. Hence, dystrophin might be more important in the early developmental stage and could become dispensable once this stage is over (8). Consistently, Ahmad *et al.* (9) demonstrated that sustained dystrophin production was more critical in younger growing muscle than in older muscle. Collectively, these studies suggest that dystrophin is less essential in fully developed muscle. In other words, transient restoration of dystrophin during muscle maturation (such as in young adolescent patients) might grant long-lasting protection, or even lifelong therapy. If this theory is confirmed, it will have tremendous implications on our understanding of DMD pathogenesis and the development of dystrophin replacement gene therapy.

To address this critical question, we generated floxed  $\Delta$ H2-R15 mini-dystrophin transgenic mice in the background of dystrophin-null FVB/mdx mice (10). The  $\Delta$ H2-R15 mini-dystrophin gene is a fully characterized and highly functional synthetic dystrophin gene. Transgenic expression of this minigene completely prevented dystrophic muscle pathology, restored sarcolemmal neuronal nitric oxide synthase (nNOS), normalized muscle force and improved exercise performance in mdx mice (11). Systemic gene therapy with this minigene significantly improved muscle morphology, prevented functional ischemia and enhanced muscle force in mdx mice (12). Since both skeletal muscle and the heart are compromised in DMD, we generated two independent strains of transgenic mice. In strain YL238, we selectively expressed the loxP-flanked  $\Delta$ H2-R15 mini-dystrophin gene in skeletal muscle using the human skeletal  $\alpha$ -actin (HSA) promoter (Table 1). In strain SJ13, we achieved heart-specific expression of the loxP-flanked  $\Delta$ H2-R15 mini-dystrophin gene with the  $\alpha$ -myosin heavy chain ( $\alpha$ -MHC) promoter (Table 1). As expected, expression of the  $\Delta$ H2-R15 minigene prevented skeletal muscle disease in YL238 mice and cardiomyopathy in SJ13 mice. To test whether persistent dystrophin expression is absolutely required for continuous skeletal muscle and heart protection, we removed the mini-dystrophin gene in adult transgenic mice using Cre recombinase expressed from an adeno-associated virus serotype-9 vector (AAV.CBA.Cre). We then examined dystrophin expression, muscle and heart histology and function. At 12 and 15 months after injection of the AAV.CBA.Cre vector, mini-dystrophin expression was reduced by ~87% in the skeletal muscle of YL238 mice and by ~64% in the heart of SJ13 mice, respectively. Reduction of mini-dystrophin in skeletal muscle resulted in significant degeneration, atrophy and force reduction in YL238 mice. Partial removal of mini-dystrophin from the myocardium also significantly compromised left

ventricular (LV) hemodynamics in SJ13 mice. Our results suggest that an effective gene therapy for DMD requires persistent dystrophin expression in both skeletal muscle and the heart.

## Results

### Generation of floxed skeletal muscle-specific mini-dystrophin transgenic mice

Full-length dystrophin has four functional domains including the N-terminal, rod, cysteine-rich and C-terminal domain. The rod domain can be further divided into four hinges and 24 spectrin-like repeats (Fig. 1A). Due to the limitation of viral vector packaging, the vast majority of dystrophin replacement therapies are based on abbreviated mini- or micro-dystrophins. In this study, we opt to use  $\Delta$ H2-R15 mini-dystrophin. This mini-dystrophin has a smaller rod domain due to a deletion from hinge 2 to spectrin-like repeat 15 (Fig. 1A). We have previously shown that the  $\Delta$ H2-R15 minigene can prevent muscle pathology, normalize muscle force and restore sarcolemmal nNOS in mdx and mdx4cv mice (11–13).

To generate floxed skeletal muscle-specific  $\Delta$ H2-R15 mini-dystrophin transgenic mice, we cloned two loxP sites (one before the HSA promoter and the other before the polyadenylation site) into our previously published HSA. $\Delta$ H2-R15 mini-dystrophin construct (Fig. 1B, Supplementary Material, Fig. S1A and Table S1) (11). *In vitro* test in 293 cells showed effective excision of the floxed mini-dystrophin gene from the transgenic construct by Cre recombinase (Supplementary Material, Fig. S1B). The floxed HSA. $\Delta$ H2-R15 minigene construct was microinjected to the zygotes of FVB mice. The founder mouse was identified by polymerase chain reaction and crossed to the background of dystrophin-null FVB/mdx mice (10). The resulting mice were called YL238 mice. These mice selectively expressed a floxed  $\Delta$ H2-R15 mini-dystrophin gene in skeletal muscle but not the heart (Fig. 1D, Supplementary Material, Fig. S2A). As expected, we did not see any signs of skeletal muscle pathology by hematoxylin and eosin (HE) staining (Fig. 2A). Neither was inflammation detected in skeletal muscle of YL238 mice by macrophage and neutrophil immunohistochemical staining (Fig. 2A).

### Genomic elimination of minigene significantly reduced mini-dystrophin expression in skeletal muscle but had minimal impact on the dystrophin-associated glycoprotein complex in adult YL238 mice

To study the consequences of dystrophin loss in adult skeletal muscle, we used the AAV.CBA.Cre vector. In this vector, the Cre recombinase is expressed from the ubiquitous cytomegalovirus enhancer-chicken  $\beta$ -actin promoter (CBA).  $2.7 \times 10^{12}$  viral genome (vg) particles of AAV.CBA.Cre were administered to the tibialis anterior (TA) muscle of 8-month-old male YL238 transgenic mice (Fig. 1C). We first evaluated the kinetics of the loss of mini-dystrophin by western blot (Supplementary Material, Fig. S3A). We observed a time-dependent reduction of mini-dystrophin. However, by 16 weeks after AAV.CBA.Cre injection, we still detected a substantial amount of residual mini-dystrophin (Supplementary Material, Fig. S3A). To this end, we decided to not perform terminal studies until injected mice reached 20-month-old.

Mice were euthanized at the age of 20 months. On immunostaining, AAV.CBA.Cre injected muscles showed reduced dystrophin staining intensity (Fig. 1D). On western blot, mini-dystrophin expression was also greatly decreased in

**Table 1.** Comparison of two strains of floxed mini-dystrophin transgenic mice

	YL238	SJ13
Promoter	HSA	$\alpha$ -MHC
Transgene	$\Delta$ H2-R15	$\Delta$ H2-R15
Mini-dystrophin expression	Skeletal muscle only	Heart only
Skeletal muscle protection	Yes	No
Heart protection	No	Yes
Acute cardiac death from systemic AAV.CBA.Cre injection	Yes	No

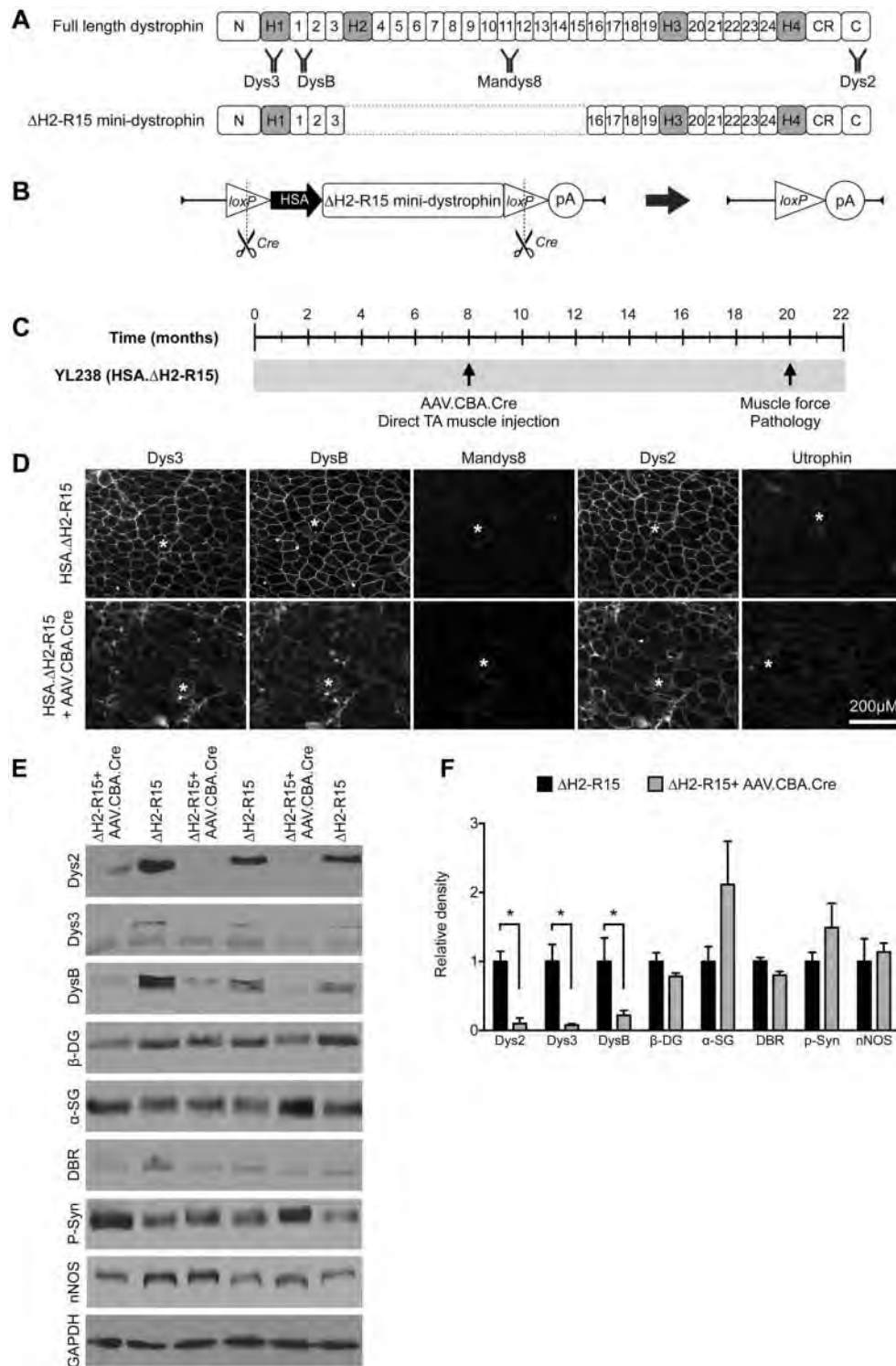


**Figure 1.** Genomic excision of the floxed HSA. $\Delta$ H2-R15 transgenic cassette leads to significant reduction of mini-dystrophin expression in skeletal muscle. (A) Schematic outline of the structure of full-length dystrophin and  $\Delta$ H2-R15 mini-dystrophin. Dys3, DysB, Mandys8 and Dys2 are four different dystrophin monoclonal antibodies used in the study. Dys2 recognizes an epitope in the dystrophin C-terminal domain. Dys3 recognizes an epitope in dystrophin hinge 1. DysB recognizes an epitope that is located between hinge 1 and dystrophin spectrin-like repeat 2. Mandys8 recognizes an epitope in dystrophin spectrin-like repeat 11, which is absent in  $\Delta$ H2-R15 mini-dystrophin. (B) Graphical representation of the floxed HSA. $\Delta$ H2-R15 transgenic cassette and Cre recombinase-mediated excision of the cassette. In YL238 transgenic mice, the expression of the  $\Delta$ H2-R15 minigene is under the control of the skeletal muscle-specific human  $\alpha$ -skeletal actin promoter (HSA). (C) Experimental outline. AAV.CBA.Cre is injected to one side of the TA muscle in 8-month-old YL238 transgenic mice. The contralateral side was mock injected and served as the untreated control. Dystrophin expression and muscle force were assessed when mice reached 20 months of age. (D) Representative photomicrographs of dystrophin and utrophin immunofluorescence staining in the TA muscles of 20-month-old YL238 mice. Asterisk, the same myofiber in serial muscle sections. (E) Representative western blots of dystrophin and components of DGC ( $\beta$ -DG,  $\beta$ -dystroglycan;  $\alpha$ -SG,  $\alpha$ -sarcoglycan; DBR, dystrobrevin; P-Syn, pan-syntrophin; nNOS, neuronal nitric oxide synthase) from the TA muscles of 20-month-old YL238 mice. (F) Densitometry quantification of western blots.  $N = 3$ . Asterisk, significantly different.

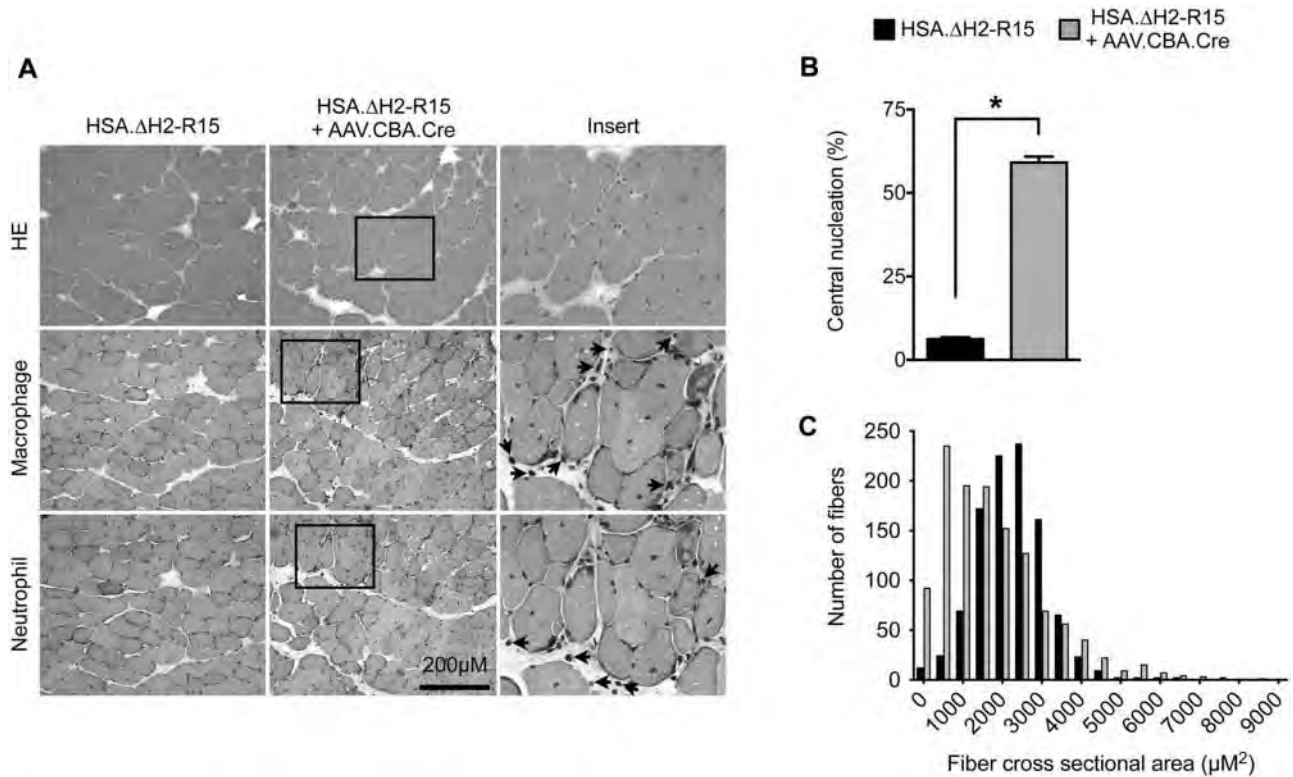


**Figure 2.** Adulthood loss of dystrophin alters skeletal muscle histology. (A) Representative photomicrographs of hematoxylin and eosin (HE) staining, and macrophage and neutrophil immunohistochemical staining from the tibialis anterior muscles of 20-m-old YL238 mice. One side of the tibialis anterior muscle received AAV.CBA.Cre. The contralateral side served as the untreated control. Dark spots on HE and immunohistochemical staining are myonuclei and infiltrating immune cells. Left panels are the enlarged view of the boxed area in the corresponding middle panels. Arrows indicate macrophages and neutrophils in respective images. (B) Quantification of centrally located myonuclei. Asterisk, significantly different. (C) Myofiber size distribution. N = 1223 myofibers for AAV.CBA.Cre injected muscle. N = 1005 myofibers for contralateral mock injected control.

AAV.CBA.Cre injected muscles (Fig. 1E). Consistent results were obtained with three independent antibodies (Dys2, Dys3 and DysB) that recognize different regions of mini-dystrophin (Fig. 1A, D and E). Quantitative densitometry analysis of western blots showed statistically significant reduction (Fig. 1F, Supplementary Material, Table S1). Compared with that of contralateral untreated muscle, AAV.CBA.Cre injection resulted in a loss of  $86.7 \pm 3.4\%$  of mini-dystrophin (the average from results of western blot using three independent antibodies).

We next examined expression of the dystrophin-associated glycoprotein complex (DGC) components and utrophin. In sharp contrast to the dramatic reduction of mini-dystrophin, there were nominal changes in the expression of  $\beta$ -dystroglycan,  $\beta$ -sarcoglycan, dystrobrevin and syntrophin (Fig. 1F, Supplementary Material, Fig. S4). On immunostaining, we did not see substantial changes in utrophin expression (Fig. 1D).

### Adulthood loss of mini-dystrophin resulted in skeletal muscle myopathy

After confirming effective mini-dystrophin removal, we examined muscle histology and function. On HE staining, we observed clear signs of myopathy in AAV.CBA.Cre injected muscles (such as great variations in the myofiber size and abundant centrally nucleated myofibers) (Fig. 2A). Immunohistochemical staining revealed macrophage, neutrophil and T cell infiltration in muscles treated with AAV.CBA.Cre (Fig. 2A,

Supplementary Material, Fig. S5A). On Masson trichrome staining, we did not detect obvious fibrosis (Supplementary Material, Fig. S5B). Quantification showed a central nucleation of  $59.1 \pm 0.6\%$  in AAV.CBA.Cre injected muscle while it was only  $6.2 \pm 0.2\%$  in contralateral untreated muscle (Fig. 2B). Removal of mini-dystrophin also skewed the distribution of the myofiber size (Fig. 2C). There was an apparent shift of the peak toward smaller size myofibers although the number of super-large myofibers was also increased in AAV.CBA.Cre injected muscles (Fig. 2C). Consistent with myofiber size quantification, the weight and cross-sectional area (CSA) of AAV.CBA.Cre injected muscles were significantly reduced (Table 2).

To evaluate physiological consequences of adulthood dystrophin removal, we measured the contractile properties of the TA muscle in situ. On single twitch, force-frequency and eccentric contraction studies, AAV.CBA.Cre injected muscles generated significantly much lower absolute force though CSA normalized specific forces were not altered (Fig. 3).

### Intravenous delivery of AAV.CBA.Cre to adult YL238 mice elicited acute cardiac death

Next, we delivered  $8 \times 10^{12}$  vg particles of AAV.CBA.Cre through the tail vein to 3-month-old YL238 mice. Our goal was to study the consequences of the loss of the therapeutic mini-dystrophin gene in all skeletal muscles in the body. To our surprise none of the injected mice survived beyond 20 days

postinjection. The majority of the injected mice (>75%) died around 13–15 days after AAV.CBA.Cre administration (Fig. 4A). Necropsy revealed severe heart damage. On HE staining, we found extensive myocardial inflammation in atrial and ventricular walls consistent with the diagnosis of acute cardiac death (Fig. 4B and C, Supplementary Material, Fig. S2A and Table S1).

### Removal of cardiac $\Delta$ H2-R15 mini-dystrophin from adult SJ13 mice by AAV.CBA.Cre recombinase altered LV hemodynamics

To study the impact of adulthood loss of the therapeutic mini-dystrophin gene in the heart, we generated SJ13 mice. We used the same approach as described for the generation of YL238 mice except that a floxed cardiac-specific mini-dystrophin transgenic construct was used. Specifically, expression of the  $\Delta$ H2-R15 mini-dystrophin was confined to the heart by the  $\alpha$ -MHC promoter and the entire expression cassette was flanked by the loxP sites (Fig. 5A, Supplementary Material, Fig. S1A).

**Table 2.** Anatomic properties of the TA muscle of 20-month-old YL238 mice

	HSA. $\Delta$ H2-R15	HSA. $\Delta$ H2R15 +AAV.CBA.Cre
Sample size (n)	11	10
TA weight (mg)	48.17 $\pm$ 2.32	40.13 $\pm$ 1.39 <sup>a</sup>
CSA (mm <sup>2</sup> )	5.41 $\pm$ 0.28	4.53 $\pm$ 0.18 <sup>a</sup>
L <sub>0</sub> (mm)	14.02 $\pm$ 0.12	13.95 $\pm$ 0.12

TA, anterior tibialis muscle; CSA, cross-sectional area; L<sub>0</sub>, optimal muscle length.

<sup>a</sup>Significantly different.

Cardiac-specific  $\Delta$ H2-R15 mini-dystrophin expression prevented myocardial inflammation and fibrosis (Fig. 5D, Supplementary Material, Fig. S6D).

To remove the  $\Delta$ H2-R15 mini-dystrophin gene, we administered  $8 \times 10^{12}$  vg particles of AAV.CBA.Cre to 7-month-old SJ13 mice via the tail vein. Early time points (up to 20 weeks post AAV.CBA.Cre injection) showed limited reduction of mini-dystrophin in the heart of SJ13 mice (Supplementary Material, Fig. S3B). To achieve the maximal level of mini-dystrophin removal from the heart, we evaluated cardiac dystrophin/DGC/utrophin expression, histology, electrocardiogram (ECG) and LV hemodynamics when mice reached 22 months of age (15 months after injection) (Fig. 5, Supplementary Material, Figs. S6 and S7 and Tables S2 and S5). On western blot, the mini-dystrophin level in the heart was reduced by  $64.32 \pm 5.32\%$  in AAV.CBA.Cre injected SJ13 mice (Fig. 5C, Supplementary Material, Table S2). Interestingly, immunostaining showed a non-homogeneous loss of mini-dystrophin expression in the heart (Fig. 5D). Although mini-dystrophin expression was greatly reduced in some cardiomyocytes, patches of mini-dystrophin positive cardiomyocytes were readily visible (Fig. 5D). Additional studies showed that AAV.CBA.Cre-mediated removal of mini-dystrophin did not change DGC expression neither did it induced utrophin upregulation in the heart (Supplementary Material, Fig. S6).

On histology examination, we did not see obvious abnormalities in the heart of AAV.CBA.Cre injected SJ13 mice (Fig. 5D, Supplementary Material, Figs S2B and S6D). There was neither inflammatory cell infiltration nor myocardial fibrosis (Fig. 5D and Supplementary Material, Fig. S6D). The body weight (BW), TA muscle weight (TW), heart weight (HW) and ventricular weight (VW) of AAV.CBA.Cre injected mice were not altered

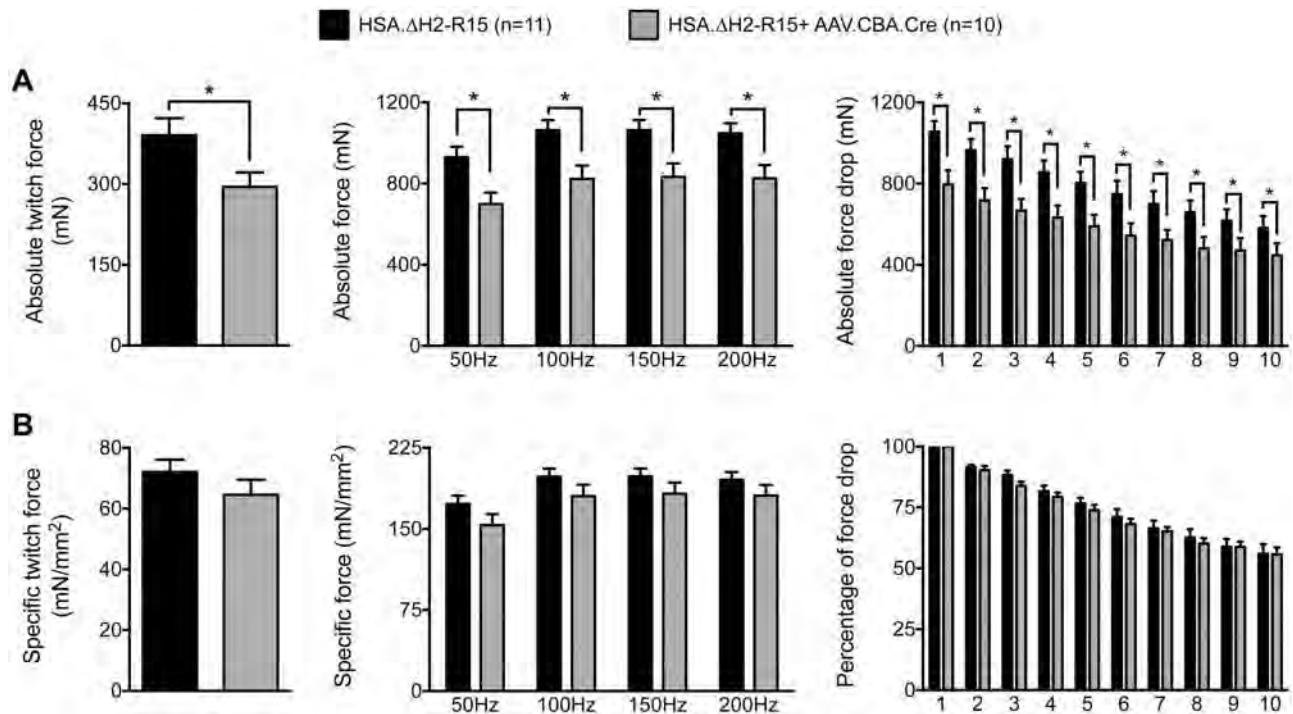


**Figure 3.** Removal of dystrophin in adult mice significantly reduces absolute muscle force. (A) Absolute muscle force. Left panel, twitch force; Middle panel, tetanic forces at different stimulation frequencies; Right panel, force drop during 10 cycles of eccentric contractions. (B) Specific muscle force. Left panel, twitch force; Middle panel, tetanic forces at different stimulation frequencies; Right panel, percentage of force drop from the baseline during 10 cycles of eccentric contractions. Asterisk, significantly different.

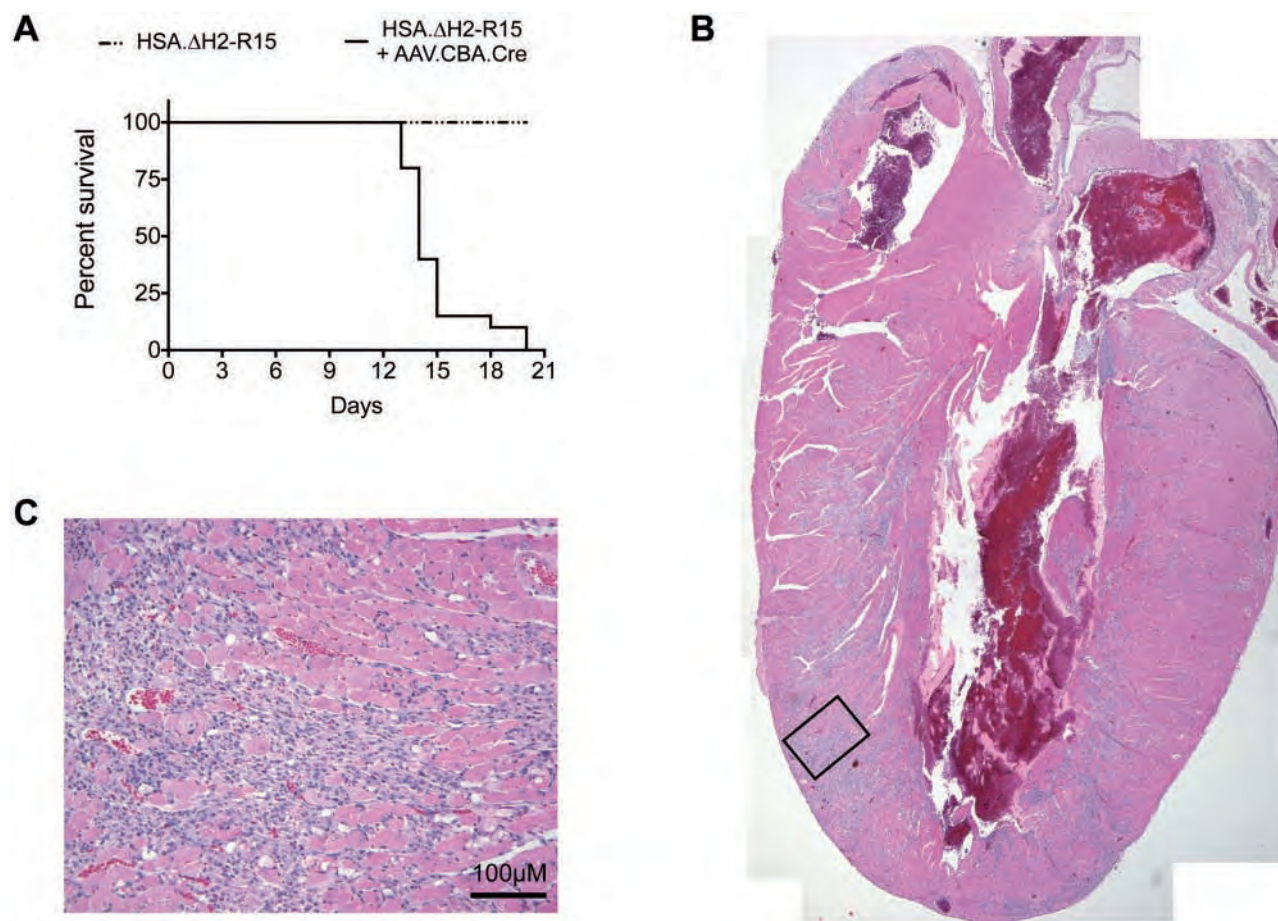


**Figure 4.** Intravenous injection of AAV.CBA.Cre results in lethal myocarditis in skeletal muscle mini-dystrophin transgenic FVB/mdx (YL238) mice. AAV.CBA.Cre was injected to adult YL238 mice at the dose of  $8 \times 10^{12}$  vg/mouse via the tail vein. Survival was monitored until all injected mice died. (A) Kaplan-Meier survival curve.  $N=20$  mice for each group. (B) Representative HE staining photomicrographs of whole heart section from a mouse died at day 15 after AAV.CBA.Cre injection. (C) Higher magnification photomicrograph of the boxed area in panel B. Abundant inflammatory cells were seen in myocardia.

(Table 3). However, the ratios of HW/BW, HW/TW and VW/TW showed a trend of increase. Importantly, the VW/BW ratio was significantly higher in SJ13 mice that received AAV.CBA.Cre injection (Table 3). On ECG examination, we clearly detected significant differences in many parameters between FVB and FVB/mdx mice (Supplementary Material, Table S3). However, no difference was observed in ECG tracing between SJ13 mice and AAV.CBA.Cre injected SJ13 mice (Supplementary Material, Fig. S7). Irrespective of AAV.CBA.Cre injection, all experimental mice showed the similar heart rate, PR interval, QRS duration, QT interval, Q amplitude and cardiomyopathy index (Supplementary Material, Fig. S7). Left ventricle catheterization was used to evaluate hemodynamic function of the heart. Compared with FVB mice, FVB/mdx mice had a significantly enlarged volume at the ends of systole and diastole (Supplementary Material, Table S4). FVB/mdx mice also showed reduced maximum pressure and ejection fraction (Supplementary Material, Table S4). All these parameters were normalized in SJ13 mice (Fig. 5E). However, the chamber size was clearly enlarged in AAV.CBA.Cre injected SJ13 mice as demonstrated by the significant increase in both end systolic and end diastolic volumes (Fig. 5E). Significant reduction in the maximum pressure and ejection fraction of AAV.CBA.Cre injected SJ13 mice suggested that the pump function of the heart was compromised in these mice (Fig. 5E). Nevertheless, there was no significant difference

in other hemodynamic parameters (such as stroke volume, cardiac output,  $dp/dt$  max,  $dp/dt$  min and Tau) between SJ13 mice and AAV.CBA.Cre injected SJ13 mice (Supplementary Material, Table S5).

## Discussion

In this study, we examined the consequences of adulthood loss of dystrophin in skeletal muscle and the heart in  $\Delta H2-R15$  mini-dystrophin transgenic FVB/mdx mice. We found that a partial loss of therapeutic mini-dystrophin is associated with significant detrimental changes in muscle structure and function. Our results suggest that dystrophin reduction alone is sufficient to induce DMD-like myopathy in adult muscle and persistent dystrophin expression is essential for long-term protection. Our results also bring in new perspective on the therapeutic significance of low-level dystrophin expression.

It is well established that the absence of dystrophin causes DMD (14,15). However, it is not clear whether myopathy seen in patients originates from congenital dystrophin deficiency during embryogenesis (16). In other words, it is not clear whether the loss of dystrophin from mature muscle alone is sufficient to cause dystrophic changes. Discrepancy between dystrophin deficiency and muscular dystrophy has been documented in the literature. At least three patients who had nonsense mutation

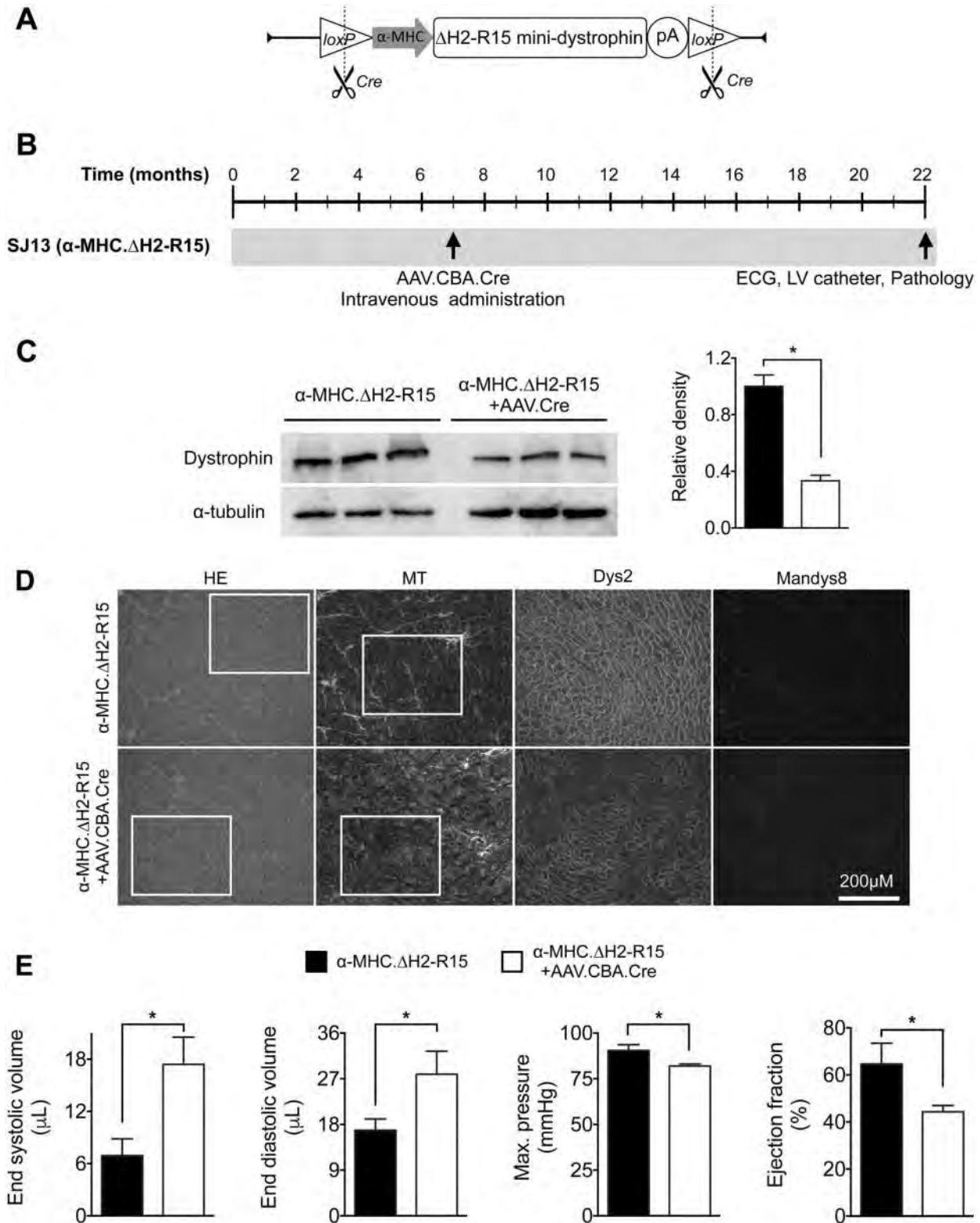


**Figure 5.** Loss of dystrophin in the heart of adult mice compromises LV hemodynamics. To evaluate the effects of loss of dystrophin in the heart of adult mice, we generated SJ13 mice. These mice selectively expressed  $\Delta$ H2-R15 mini-dystrophin in the heart from a floxed  $\alpha$ -MHC. $\Delta$ H2-R15 expression cassette. (A) Graphical representation of the floxed  $\alpha$ -MHC. $\Delta$ H2-R15 transgenic cassette. Vertical dotted lines mark Cre recombinase-mediated excision of the cassette. (B) Experimental outline. AAV.CBA.Cre was injected to 7-month-old SJ13 mice via the tail vein. Dystrophin expression and heart function were assessed when mice reached 22 months of age. (C) Representative dystrophin western blots and densitometry quantification. (D) Representative photomicrographs of HE staining, Masson trichrome staining and dystrophin immunostaining with Dys2 and Mandys8 monoclonal antibodies. Boxed areas in HE and Masson trichrome staining are enlarged in [Supplementary Material, Figure S6D](#). In AAV.CBA.Cre injected SJ13 mice, Dys2 immunostaining revealed patchy mini-dystrophin expression. (E) Selective LV hemodynamic parameters measured by cardiac catheterization in AAV.CBA.Cre injected ( $N = 5$ ) and un-injected ( $N = 6$ ) SJ13 mice. Asterisk, significantly different.

**Table 3.** Weights and weight ratios of 22-month-old SJ13 mice

	$\alpha$ -MHC. $\Delta$ H2-R15	$\alpha$ -MHC. $\Delta$ H2-R15 +AAV.CBA.Cre
Sample size (n)	9	6
Age (m)	22.91 $\pm$ 0.05	22.25 $\pm$ 0.65
BW (g)	30.68 $\pm$ 2.03	26.93 $\pm$ 1.85
TW (mg)	34.26 $\pm$ 1.46	33.46 $\pm$ 2.2
HW (mg)	143.64 $\pm$ 6.63	149.17 $\pm$ 8.06
VW (mg)	132.90 $\pm$ 5.83	139.38 $\pm$ 8.39
TW/BW (mg/g)	1.14 $\pm$ 0.06	1.26 $\pm$ 0.07
HW/BW (mg/g)	4.79 $\pm$ 0.25	5.61 $\pm$ 0.26
HW/TW (mg/g)	4.30 $\pm$ 0.26	4.51 $\pm$ 0.22
VW/BW (mg/g)	4.43 $\pm$ 0.23	5.24 $\pm$ 0.26 <sup>a</sup>
VW/TW (mg/g)	3.98 $\pm$ 0.23	4.21 $\pm$ 0.21

BW, body weight; TW, anterior tibialis muscle weight; HW, heart weight; VW, ventricle weight.

<sup>a</sup>Significantly different.

in the dystrophin gene and no detectable dystrophin in their muscle were clinically asymptomatic and/or mildly affected (17,18). Lack of histological and physiological defects in  $\leq$ 14-day-old mdx mice is another example where the absence of dystrophin is not accompanied with muscle disease (19–22). To determine whether dystrophin deficiency alone can elicit myopathy in adult muscle, Ghahramani Seno *et al.* (7) applied AAV-mediated dystrophin RNA interference (RNAi) in adult normal mice. Although they successfully reduced dystrophin expression, no overt dystrophic pathology was observed (7). Collectively, these observations appear to support the notion that dystrophin deficiency by itself may, at least in some cases, not lead to overt muscular dystrophy. Dystrophin replacement gene therapy has the potential to bring back the missing dystrophin protein in large mammals (23,24). However, current approaches may not lead to lifelong dystrophin restoration due to the cellular immune response and muscle cell turnover. Patients may end up lose their restored dystrophin again. Hence, there is a strong need to understand what will happen after therapeutic dystrophin is lost.

We designed this study to investigate whether the adulthood loss of dystrophin is associated with deleterious consequences. In Ghahramani Seno *et al.* (7) study, RNAi cannot completely eliminate dystrophin because muscle still carries a transcriptionally competent dystrophin gene in the genome. The residual dystrophin expression may at least partially account for the lack of muscle disease seen by the authors. To avoid this caveat, we decided to use the gene elimination approach in our study. Specifically, we engineered floxed mini-dystrophin transgenic FVB/mdx mice. We hypothesized that excision by Cre recombinase will eliminate the minigene from the genome and consequently completely remove mini-dystrophin from muscle. Because AAV is the most robust muscle gene transfer vector and intramuscular AAV injection is not associated with any toxicity (25), we opted to use AAV to deliver the Cre recombinase gene. In the Ghahramani Seno *et al.* (7) study, dystrophin knockdown was only performed in skeletal muscle. Considering cardiomyopathy is a leading cause of morbidity and mortality in DMD patients, we made two independent strains of floxed transgenic mdx mice (Table 1). Strain YL238 only had functional mini-dystrophin expression in skeletal muscle while strain SJ13 only had functional mini-dystrophin expression in the heart (Supplementary Material, Fig. S2). Characterization of the transgenic constructs in 293

cells confirmed digestion of the minigene by AAV.CBA.Cre (Supplementary Material, Fig. S1). To determine how long it would take to remove dystrophin expression from muscle in transgenic mice, we performed a time course study (Supplementary Material, Fig. S3). In strain YL238, reduction in mini-dystrophin expression became apparent at 8 weeks after local AAV.CBA.Cre injection. However, mini-dystrophin remained readily detectable at the 16-week time point (Supplementary Material, Fig. S3A). Systemic AAV.CBA.Cre injection was performed in strain SJ13 to knockdown myocardial mini-dystrophin expression. Surprisingly, at 20 weeks after injection we still observed substantial amount of mini-dystrophin in the heart on western blot (Supplementary Material, Fig. S3B). It has been shown that full-length dystrophin is extremely stable (7,9). Our results suggest that  $\Delta$ H2-R15 mini-dystrophin may also have a fairly long half-life. Alternatively, our results may also suggest that Cre recombinase digestion was incomplete (either not enough Cre recombinase due to poor AAV transduction or not enough digestion time). Since the dosages used in our studies are known to cause saturated gene transfer (26), we decided to extend the experiment duration until these mice reached the terminal age of their life (20–22 months) (Figs 1C and 5B).

To study dystrophin loss in skeletal muscle, we delivered AAV.CBA.Cre to 8-month-old YL238 mice and examined muscle histology and force when they reached 20 months of age. On western blot, mini-dystrophin level was reduced by  $\sim$ 87% (Fig. 1E and 1F, Supplementary Material, Table S1). In contrast to the results of AAV-mediated dystrophin knockdown by RNAi (7), we observed significant muscle atrophy, myofiber size change, degeneration/regeneration, inflammation and significant loss of absolute muscle force (Figs 2 and 3, Supplementary Material, Fig. S5 and Table S2). Our data suggest that dystrophin deficiency alone can cause skeletal muscle myopathy in an adult mammal. Loss of therapeutic dystrophin will lead to the relapse of myopathy. An effective therapy for DMD requires persistent expression.

Most of DMD patients die from respiratory muscle failure. However, these muscles (including the diaphragm, intercostal muscle, abdominal muscle and chest muscle) cannot be easily reached by direct muscle injection. To study the consequences of bodywide loss of mini-dystrophin in skeletal muscle of adult mice, we delivered AAV.CBA.Cre intravenously to YL238 mice. Unexpectedly, all injected mice died between 13 and 20 days after injection. Autopsy suggests that the death was due to acute myocarditis (Fig. 4, Supplementary Material, Fig. S2A). Chronic overexpression of Cre recombinase in cardiac Cre transgenic mice has been shown to cause cardiomyopathy at the age of 8–12 months (27). However, AAV-mediated Cre expression in the heart has not been associated with any toxicity (28,29). To troubleshoot our study, we injected the same batch of the AAV.CBA.Cre vector to SJ13 mice at the same dose. None of the injected SJ13 mice died (Supplementary Material, Fig. S2B). This new piece of data suggests that the death seen in YL238 mice was not due to AAV vector contamination, but rather, caused by the lack of dystrophin in the heart of YL238 mice. We have previously successfully delivered several different AAV vectors (such as alkaline phosphatase reporter vector and micro-dystrophin vector) to the heart of adult (and even aged) mdx mice without seeing any toxicity (30–32). Hence, we don't believe that the delivery of AAV to the heart of mdx mice *per se* is the cause of cardiac death. We suspect that, very likely, the observed cardiac death in YL238 mice is due to a combined effect of Cre toxicity and dystrophin deficiency. Future studies are needed to clarify this issue.

In our preliminary study, we found that SJ13 mice were more resistant to the genetic removal of mini-dystrophin from the heart (Supplementary Material, Fig. S3B). In the hope of achieving better dystrophin removal, we injected AAV.CBA.Cre to 7-month-old SJ13 mice and waited until they were 22-month-old (Fig. 5B). On western blot, mini-dystrophin expression in the heart was significantly reduced in mice that received AAV.CBA.Cre injection. On average, the mini-dystrophin level was reduced by ~64% (Fig. 5C, Supplementary Material, Table S2). On immunostaining, homogenous cardiac mini-dystrophin expression became patchy in AAV.CBA.Cre injected SJ13 mice (Fig. 5D). Similar to what we seen in YL238 mice, expression of the DGC components and utrophin was not altered (Figs 1C–E, Supplementary Material, Fig. S4). However, in contrast to the histological signs of myopathy seen in YL238 mice, we did not detect any overt pathological lesions in the heart of SJ13 mice following AAV.CBA.Cre injection (Fig. 5D, Supplementary Material, Fig. S6D). On ECG examination, no difference was detected either (Supplementary Material, Fig. S7). Nevertheless, signs of dilated cardiomyopathy were clearly noted (Fig. 5E, Table 3). Specifically, the VW to BW ratio (VW/BW) was significantly increased (Table 3). On hemodynamic assays, end systolic/diastolic volumes were significantly increased, and the maximum pressure and ejection fraction were significantly reduced (Fig. 5E). Collectively, our data suggest that the reduction of dystrophin alone is sufficient to induce Duchenne cardiomyopathy-like functional changes in adult mice. If we extrapolate these findings to gene therapy, it will suggest that a loss of therapeutic dystrophin after it has been expressed for a while may lead to the deterioration of an already improved heart. Continuous cardiac dystrophin expression is absolutely required to reduce cardiac morbidity and mortality in DMD.

An important goal of DMD gene therapy studies is to determine how much dystrophin is enough for muscle and heart protection. Homogenous expression of marginal level (4–5%) dystrophin starting from *in utero* has been shown to partially preserve muscle function in mdx mice and increase survival of severely affected utrophin/dystrophin double knockout mice (33–36). More recently, the Wells laboratory showed that exon-skipping restoration of 15% homogenous dystrophin expression significantly improved the eccentric contraction profile in adult mdx mice (37). In our study, we originally hoped to completely eliminate transgenic  $\Delta$ H2-R15 mini-dystrophin expression. However, this did not happen. We still got ~13 and 36% mini-dystrophin expression in skeletal muscle and heart, respectively. In skeletal muscle, we observed clear morphological evidence of myopathy but the specific muscle force and eccentric contraction profile were preserved (Figs 2 and 3B). Our results suggest that the amount of dystrophin needed for preserving muscle histology is different from that needed for preserving specific force. More dystrophin is required to preserve muscle histology (36).

For reasons yet unclear, we obtained patchy mini-dystrophin elimination in the heart on immunostaining in SJ13 mice (Fig. 5D). We have previously shown that 50% mosaic dystrophin expression and complementary utrophin upregulation are sufficient to completely prevent dilated cardiomyopathy in mdx mice (38,39). In the heart of SJ13 mice, AAV.CBA.Cre injection resulted in a loss of ~64% mini-dystrophin (Fig. 5C, Supplementary Material, Table S2). However, we did not detect evident histological change in the myocardium (Fig. 5D and Supplementary Material, Fig. S6D). The ECG profile was not altered either (Supplementary Material, Fig. S7). Nevertheless, the hemodynamic function of the left ventricle was significantly

compromised. These data have further lowered the therapeutic threshold for the protection of heart morphology and electrophysiology (from 50 to ~36%). On the other side, the rescue of the heart hemodynamics may require complementary utrophin upregulation in dystrophin-negative cardiomyocytes and/or  $\geq$ 50% dystrophin expression in the heart.

In summary, our results have provided clear evidence that an effective gene therapy for DMD depends on persistent expression of a therapeutic dystrophin gene.

## Materials and Methods

### Experimental animals

All animal experiments were approved by the institutional animal care and use committee and were in accordance with National Institutes of Health guidelines. Two FVB background founders of human  $\Delta$ H2-R15 mini-dystrophin transgenic mice were generated at the University of Missouri transgenic core. In one founder, the  $\Delta$ H2-R15 mini-dystrophin gene was driven by the skeletal muscle-specific HSA promoter. The promoter and the minigene were flanked by two unidirectional loxP repeats (Fig. 1B, Supplementary Material, Fig. S1A). This founder was subsequently crossed with dystrophin-null FVB/mdx mice (10). The resulting skeletal muscle-specific mini-dystrophin transgenic mdx mice were termed YL238 mice. In the other founder, the  $\Delta$ H2-R15 mini-dystrophin gene was driven by the cardiac-specific  $\alpha$ -MHC promoter. The entire expression cassette (promoter, minigene and pA) was flanked by two unidirectional loxP repeats (Fig. 5A, Supplementary Material, Fig. S1A). Following crossing with dystrophin-null FVB/mdx mice (10), we obtained cardiac-specific mini-dystrophin transgenic mdx mice and named these mice SJ13 mice. All mice were maintained in a specific-pathogen free animal care facility on a 12-h light (25 lux):12-h dark cycle with access to food and water *ad libitum*. In light of the gender bias in mdx skeletal muscle disease and cardiomyopathy, male mice were used in the YL238 mouse study and female mice were used in the SJ13 mouse study (40,41). Mice were euthanized following the functional assays and tissues were harvested.

### AAV.CBA.Cre production and *in vivo* delivery

The cis-plasmid for AAV.CBA.Cre production was a generous gift of Dr Weidong Xiao (Temple University, Philadelphia, PA) (42). The AAV-9 packaging plasmid was a generous gift of Dr James Wilson (University of Pennsylvania, Philadelphia, PA) (43). The AAV.CBA.Cre was packaged in AAV-9 according to our published protocol (44). For intramuscular delivery,  $2.7 \times 10^{12}$  vg (50  $\mu$ l) particles of AAV.CBA.Cre were injected into one side TA muscle using a 32G Hamilton syringe (Reno, NV). The contralateral TA muscle received saline as the untreated control. For systemic delivery,  $8 \times 10^{12}$  vg (500  $\mu$ l) particles of AAV.CBA.Cre were administered in a single bolus via the tail vein.

### Morphological studies

Dystrophin expression was evaluated by immunofluorescence staining using four independent dystrophin monoclonal antibodies including Dys2 (1:30; Vector Laboratories, Burlingame, CA), Dys3 (1:20; Leica Biosystems, Buffalo Grove, IL), DysB (1:80, clone 34C5, IgG1; Novocastra, Newcastle, UK) and Mandys8 (1:200; Sigma Aldrich, St Louis, MO). Dys2 recognizes an epitope in the dystrophin C-terminal domain. Dys3 recognizes an epitope in dystrophin

hinge 1. DysB recognizes an epitope that is located between hinge 1 and dystrophin spectrin-like repeat 2. Dys2, Dys3 and DysB react with  $\Delta$ H2-R15 mini-dystrophin (Fig. 1A). Mandys8 recognizes an epitope in dystrophin spectrin-like repeat 11, which is absent in  $\Delta$ H2-R15 mini-dystrophin (38,45). General histology was examined by HE staining. Central nucleation was quantified on six random 20 $\times$  field images for each muscle. Fiber size was quantified on digitized images using the Adobe Photoshop software (San Jose, CA). Briefly, the micrometer scale was defined with the set measurement scale option in the software. The perimeter of each individual fiber was marked using the quick selection tool. The CSA was then calculated by the software. Approximately 400 myofibers were quantified in each TA muscle. Fibrosis was examined by Masson trichrome staining as we described before (46). Macrophages (1:200; Caltag Laboratories, Burlingame, CA), neutrophils (1:80; BD Pharmingen, San Jose, CA), CD<sup>4+</sup>T cells (1:800; Affinity Bioreagent, Golden, CO) and CD<sup>8+</sup>T cells (1:800; BD Pharmingen) were examined by immunohistochemistry staining. Slides were viewed at the identical exposure setting using a Nikon E800 fluorescence microscope. Photomicrographs were taken with a Qimage Retiga 1300 camera (46).

### Western blot

TA muscles and hearts lysates were prepared as described before (47). Briefly, the tissues were snap frozen in liquid nitrogen. The frozen tissue samples were ground to fine powder in liquid nitrogen followed by homogenization in a buffer containing 10% sodium dodecyl sulfate, 5 mM Ethylenediaminetetraacetic acid, 62.5 mM Tris-HCl at pH6.8 and the protease inhibitor cocktail (Roche, Indianapolis, IN). The crude lysate were heated at 95°C for 3 min, chilled on ice for 2 min and then centrifuged at 14 000g for 2 min. Supernatant was collected as the whole muscle lysate. Protein concentration was measured using the DC protein assay kit (Bio-Rad, Hercules, CA) and 50  $\mu$ g of protein was used to load per lane for the western blot. Dystrophin was detected with Dys3 (1:50 Leica Biosystems), DysB (1:100, clone 34C5, IgG1; Novocastra) and Dys2 (1:100 Vector Laboratories) antibodies (Fig. 1A).  $\beta$ -Dystroglycan was detected with a mouse monoclonal antibody against the  $\beta$ -dystroglycan C-terminus (NCL-b-DG, 1:100; clone 43DAG1/8D5, IgG2a; Novocastra).  $\alpha$ -Sarcoglycan was detected with a mouse monoclonal antibody against  $\alpha$ -sarcoglycan amino acid residues 217–289 (VP-A105; 1:1000; clone Ad1/20A6, IgG1; Vector Laboratories). Syntrophin was detected with a pan-syntrophin mouse monoclonal antibody that recognized the syntrophin PSD-95/Dlg/ZO-1 domain (ab11425, 1:2000; clone 1351, IgG1; Abcam, Cambridge, MA). Dystrobrevin was detected with a mouse monoclonal antibody against dystrobrevin amino acid residues 249–403 (#610766, 1:000; clone 23, IgG1; BD Biosciences, San Diego, CA). nNOS was detected with a rabbit polyclonal antibody (N7280, 1:2000; Sigma Aldrich). For the loading control, we used the glyceraldehyde 3-phosphate dehydrogenase antibody (1:3000; Millipore, Billerica, MA) and  $\alpha$ -tubulin antibody (1:3000; clone B-5-1-2; Sigma) for TA muscle and heart western blot, respectively. Western blot quantification was performed using the ImageJ (<http://rsbweb.nih.gov/ij/>; last accessed January 05, 2016) or LI-COR Image Studio Version 5.0.21 software (<https://www.licor.com>; last accessed January 05, 2016). The relative intensity of the respective protein band was normalized to the corresponding loading control in the same blot. The relative band intensity in AAV.CBA.Cre treated muscles was normalized to that of untreated controls.

### TA muscle function evaluation

The TA muscle force was measured *in situ* according to our published protocol (48,49). Briefly, mice were anesthetized via intraperitoneal injection of a cocktail containing 25 mg/ml ketamine, 2.5 mg/ml xylazine and 0.5 mg/ml acepromazine at 2.5  $\mu$ l/g BW. The TA muscle and the sciatic nerve were exposed. The mouse was transferred to a custom-designed thermo-controlled platform of the footplate apparatus (48,49). After 5 min equilibration, the sciatic nerve was stimulated at the frequency of 1 Hz (20 V, 1000 mA) to elicit twitch muscle contraction using a custom-made 25G platinum electrode at 2.0–6.0 g resting tensions. The muscle length ( $L_m$ ) of the TA muscle was measured with an electronic digital caliper (Fisher Scientific, Waltham, MA, USA) at the resting tension that generated the maximal twitch force. This length was defined as the optimal muscle length ( $L_0$ ). The twitch force was measured at 1 Hz frequency followed by the force frequency assay at 50, 100, 150 and 200 Hz with 1 min resting between each contraction. Specific muscle force was determined by dividing the maximum isometric tetanic force with the muscle CSA. The CSA was calculated according to the following equation,  $CSA = (\text{muscle mass, in gram}) / [(\text{optimal fiber length, in cm}) \times (\text{muscle density, in g/cm}^3)]$ . A muscle density of 1.06 g/cm<sup>3</sup> was used in calculation. Optimal fiber length was calculated as  $0.60 \times L_0$ . In total, 0.60 represents the ratio of the fiber length to the  $L_0$  of the TA muscle. After tetanic force measurement, the muscle was rested for 5 min and then subjected to 10 rounds of eccentric contraction according to our previously published protocol (48,49). Briefly, following a tetanic contraction the TA muscle was stretched by 10%  $L_0$  at a rate 0.5  $L_0/s$ . The muscle was allowed to rest 1 min between each eccentric contraction cycle. The percentage of force drop following each round of eccentric contraction was recorded. Muscle twitch and tetanic forces and the eccentric contraction profile were measured with a 305C-LR dual-mode servomotor transducer (Aurora Scientific, Inc.). Data were processed using the Laboratory View-based DMC and DMA programs (Version 3.12, Aurora Scientific, Inc.).

### ECG and LV hemodynamic assay

A 12-lead ECG assay was performed using a commercial system from AD Instruments (Colorado Springs, CO) according to our previously published protocol (50). The Q wave amplitude was determined using the lead I tracing. Other ECG parameters were analyzed using the lead II tracing. The QTc interval was determined by correcting the QT interval with the heart rate as described by Mitchell et al. (51). The cardiomyopathy index was calculated by dividing the QT interval by the PQ segment (52). LV hemodynamics was evaluated using a closed chest approach as we previously described (50). The resulting pressure-volume (PV) loops were analyzed with the PVAN software (Millar Instruments, Houston, TX). Detailed protocols for ECG and hemodynamic assays are available at the Parent Project Muscular Dystrophy standard operating protocol web site ([http://www.parentprojectmd.org/site/PageServer?pagename=Advance\\_researchers\\_sops](http://www.parentprojectmd.org/site/PageServer?pagename=Advance_researchers_sops); last accessed January 05, 2016).

### Statistical analysis

Data are presented as mean  $\pm$  standard error of mean (s.e.m.). Statistical significance between un-injected controls and AAV.CBA.Cre injected samples were determined by the Student t-test. For data that were non-parametric, statistical analysis was performed with the Wilcoxon Rank Sum test. Difference was considered statistically significant when  $P < 0.05$ .

## Supplementary Material

Supplementary Material is available at HMG online.

## Acknowledgements

The authors thank Dr Weidong Xiao for providing the cis-plasmid used for AAV.CBA.Cre production and Dr Jim Wilson for providing AAV-9 packaging plasmid.

*Conflict of Interest statement.* D.D. is a member of the scientific advisory board for and an equity holder of Solid GT, a subsidiary of Solid Biosciences.

## Funding

This work was supported by grants from the National Institutes of Health (HL-91883, NS-90634); Department of Defense (MD130014, MD150133); Jesse's Journey-The Foundation for Gene and Cell Therapy. N.W. was partially supported by the life science fellowship, University of Missouri.

## Disclosure

D.D. is a member of the scientific advisory board for and an equity holder of Solid GT, a subsidiary of Solid Biosciences.

## References

- Kunkel, L.M. (2005) 2004 William Allan Award address. Cloning of the DMD gene. *Am. J. Hum. Genet.*, **76**, 205–214.
- Mendell, J.R. and Lloyd-Puryear, M. (2013) Report of MDA muscle disease symposium on newborn screening for Duchenne muscular dystrophy. *Muscle Nerve*, **48**, 21–26.
- Bengtsson, N.E., Seto, J.T., Hall, J.K., Chamberlain, J.S. and Odom, G.L. (2016) Progress and prospects of gene therapy clinical trials for the muscular dystrophies. *Hum. Mol. Genet.*, **25**, R9–R17.
- Duan, D. (2015) Duchenne muscular dystrophy gene therapy in the canine model. *Hum. Gene Ther. Clin. Dev.*, **26**, 57–69.
- Al-Zaidy, S., Rodino-Klapac, L. and Mendell, J.R. (2014) Gene therapy for muscular dystrophy: moving the field forward. *Pediatr. Neurol.*, **51**, 607–618.
- Kawecka, K., Theodoulides, M., Hasoglu, Y., Jarmin, S., Kymalainen, H., Le-Heron, A., Popplewell, L., Malerba, A., Dickson, G. and Athanasopoulos, T. (2015) Adeno-associated virus (AAV) mediated dystrophin gene transfer studies and exon skipping strategies for Duchenne muscular dystrophy (DMD). *Curr. Gene Ther.*, **15**, 395–415.
- Ghahramani Seno, M.M., Graham, I.R., Athanasopoulos, T., Trollet, C., Pohlschmidt, M., Crompton, M.R. and Dickson, G. (2008) RNAi-mediated knockdown of dystrophin expression in adult mice does not lead to overt muscular dystrophy pathology. *Hum. Mol. Genet.*, **17**, 2622–2632.
- Duan, D. (2008) Dystrophin knockdown mice suggest that early, transient dystrophin expression might be enough to prevent later pathology. *Neuromuscul. Disord.*, **18**, 904–905.
- Ahmad, A., Brinson, M., Hodges, B.L., Chamberlain, J.S. and Amalfitano, A. (2000) Mdx mice inducibly expressing dystrophin provide insights into the potential of gene therapy for duchenne muscular dystrophy. *Hum. Mol. Genet.*, **9**, 2507–2515.
- Wasala, N.B., Zhang, K., Wasala, L.P., Hakim, C.H. and Duan, D. (2015) The FVB background does not dramatically alter the dystrophic phenotype of mdx mice. *PLoS Curr.*, **7**, pii: e-currents.md.28266819ca28266810ec28266815fefcac28266767ea28266819a28263461c.
- Lai, Y., Thomas, G.D., Yue, Y., Yang, H.T., Li, D., Long, C., Judge, L., Bostick, B., Chamberlain, J.S., Terjung, R.L. et al. (2009) Dystrophins carrying spectrin-like repeats 16 and 17 anchor nNOS to the sarcolemma and enhance exercise performance in a mouse model of muscular dystrophy. *J. Clin. Invest.*, **119**, 624–635.
- Zhang, Y., Yue, Y., Li, L., Hakim, C.H., Zhang, K., Thomas, G.D. and Duan, D. (2013) Dual AAV therapy ameliorates exercise-induced muscle injury and functional ischemia in murine models of Duchenne muscular dystrophy. *Hum. Mol. Genet.*, **22**, 3720–3729.
- Zhang, Y. and Duan, D. (2012) Novel mini-dystrophin gene dual adeno-associated virus vectors restore neuronal nitric oxide synthase expression at the sarcolemma. *Hum. Gene Ther.*, **23**, 98–103.
- Hoffman, E.P., Brown, R.H., Jr and Kunkel, L.M. (1987) Dystrophin: the protein product of the Duchenne muscular dystrophy locus. *Cell*, **51**, 919–928.
- Bonilla, E., Samitt, C.E., Miranda, A.F., Hays, A.P., Salviati, G., DiMauro, S., Kunkel, L.M., Hoffman, E.P. and Rowland, L.P. (1988) Duchenne muscular dystrophy: deficiency of dystrophin at the muscle cell surface. *Cell*, **54**, 447–452.
- Merrick, D., Stadler, L.K., Larner, D. and Smith, J. (2009) Muscular dystrophy begins early in embryonic development deriving from stem cell loss and disrupted skeletal muscle formation. *Dis. Model. Mech.*, **2**, 374–388.
- Castro-Gago, M. (2014) Milder course in Duchenne patients with nonsense mutations and no muscle dystrophin. *Neuromuscul. Disord.*, **25**, 443.
- Zatz, M., Pavanello, R.C., Lazar, M., Yamamoto, G.L., Lourenco, N.C., Cerqueira, A., Nogueira, L. and Vainzof, M. (2014) Milder course in Duchenne patients with nonsense mutations and no muscle dystrophin. *Neuromuscul. Disord.*, **24**, 986–989.
- Grange, R.W., Gainer, T.G., Marschner, K.M., Talmadge, R.J. and Stull, J.T. (2002) Fast-twitch skeletal muscles of dystrophic mouse pups are resistant to injury from acute mechanical stress. *Am. J. Physiol. Cell Physiol.*, **283**, C1090–C1101.
- Reed, P. and Bloch, R.J. (2005) Postnatal changes in sarcolemmal organization in the mdx mouse. *Neuromuscul. Disord.*, **15**, 552–561.
- Grady, R.M., Teng, H., Nichol, M.C., Cunningham, J.C., Wilkinson, R.S. and Sanes, J.R. (1997) Skeletal and cardiac myopathies in mice lacking utrophin and dystrophin: a model for Duchenne muscular dystrophy. *Cell*, **90**, 729–738.
- Deconinck, A.E., Rafael, J.A., Skinner, J.A., Brown, S.C., Potter, A.C., Metzinger, L., Watt, D.J., Dickson, J.G., Tinsley, J.M. and Davies, K.E. (1997) Utrophin-dystrophin-deficient mice as a model for Duchenne muscular dystrophy. *Cell*, **90**, 717–727.
- Shin, J.H., Pan, X., Hakim, C.H., Yang, H.T., Yue, Y., Zhang, K., Terjung, R.L. and Duan, D. (2013) Microdystrophin ameliorates muscular dystrophy in the canine model of Duchenne muscular dystrophy. *Mol. Ther.*, **21**, 750–757.
- Yue, Y., Pan, X., Hakim, C.H., Kodippili, K., Zhang, K., Shin, J.H., Yang, H.T., McDonald, T. and Duan, D. (2015) Safe and bodywide muscle transduction in young adult Duchenne muscular dystrophy dogs with adeno-associated virus. *Hum. Mol. Genet.*, **24**, 5880–5890.
- Liu, M., Yue, Y., Harper, S.Q., Grange, R.W., Chamberlain, J.S. and Duan, D. (2005) Adeno-associated virus-mediated microdystrophin expression protects young mdx muscle from contraction-induced injury. *Mol. Ther.*, **11**, 245–256.
- Bostick, B., Ghosh, A., Yue, Y., Long, C. and Duan, D. (2007) Systemic AAV-9 transduction in mice is influenced by

- animal age but not by the route of administration. *Gene Ther.*, **14**, 1605–1609.
27. Davis, J., Maillet, M., Miano, J.M. and Molkenkin, J.D. (2012) Lost in transgenesis: a user's guide for genetically manipulating the mouse in cardiac research. *Circ. Res.*, **111**, 761–777.
  28. Iwatate, M., Gu, Y., Dieterle, T., Iwanaga, Y., Peterson, K.L., Hoshijima, M., Chien, K.R. and Ross, J. (2003) In vivo high-efficiency transcoronary gene delivery and Cre-LoxP gene switching in the adult mouse heart. *Gene Ther.*, **10**, 1814–1820.
  29. Werfel, S., Jungmann, A., Lehmann, L., Ksienzyk, J., Bekeredjian, R., Kaya, Z., Leuchs, B., Nordheim, A., Backs, J., Engelhardt, S. et al. (2014) Rapid and highly efficient inducible cardiac gene knockout in adult mice using AAV-mediated expression of Cre recombinase. *Cardiovasc. Res.*, **104**, 15–23.
  30. Bostick, B., Shin, J.H., Yue, Y., Wasala, N.B., Lai, Y. and Duan, D. (2012) AAV micro-dystrophin gene therapy alleviates stress-induced cardiac death but not myocardial fibrosis in > 21-m-old mdx mice, an end-stage model of Duchenne muscular dystrophy cardiomyopathy. *J. Mol. Cell. Cardiol.*, **53**, 217–222.
  31. Bostick, B., Shin, J.H., Yue, Y. and Duan, D. (2011) AAV-micro-dystrophin therapy improves cardiac performance in aged female mdx mice. *Mol. Ther.*, **19**, 1826–1832.
  32. Ghosh, A., Yue, Y., Shin, J.H. and Duan, D. (2009) Systemic trans-splicing AAV delivery efficiently transduces the heart of adult mdx mouse, a model for Duchenne muscular dystrophy. *Hum. Gene Ther.*, **20**, 1319–1328.
  33. van Putten, M., Hulsker, M., Nadarajah, V.D., van Heiningen, S.H., van Huizen, E., van Iterson, M., Admiraal, P., Messemaker, T., den Dunnen, J.T., t Hoen, P.A. et al. (2012) The effects of low levels of dystrophin on mouse muscle function and pathology. *PLoS One*, **7**, e31937.
  34. van Putten, M., Hulsker, M., Young, C., Nadarajah, V.D., Heemskerk, H., van der Weerd, L., t Hoen, P.A., van Ommen, G.J. and Aartsma-Rus, A.M. (2013) Low dystrophin levels increase survival and improve muscle pathology and function in dystrophin/utrophin double-knockout mice. *FASEB J.*, **27**, 2484–2495.
  35. Li, D., Yue, Y. and Duan, D. (2010) Marginal level dystrophin expression improves clinical outcome in a strain of dystrophin/utrophin double knockout mice. *PLoS One*, **5**, e15286.
  36. Li, D., Yue, Y. and Duan, D. (2008) Preservation of muscle force in mdx3cv mice correlates with low-level expression of a near full-length dystrophin protein. *Am. J. Pathol.*, **172**, 1332–1341.
  37. Godfrey, C., Muses, S., McClorey, G., Wells, K.E., Coursindel, T., Terry, R.L., Betts, C., Hammond, S., O'Donovan, L., Hildyard, J. et al. (2015) How much dystrophin is enough: the physiological consequences of different levels of dystrophin in the mdx mouse. *Hum. Mol. Genet.*, **24**, 4225–4237.
  38. Yue, Y., Skimming, J.W., Liu, M., Strawn, T. and Duan, D. (2004) Full-length dystrophin expression in half of the heart cells ameliorates beta-isoproterenol-induced cardiomyopathy in mdx mice. *Hum. Mol. Genet.*, **13**, 1669–1675.
  39. Bostick, B., Yue, Y., Long, C. and Duan, D. (2008) Prevention of dystrophin-deficient cardiomyopathy in twenty-one-month-old carrier mice by mosaic dystrophin expression or complementary dystrophin/utrophin expression. *Circ. Res.*, **102**, 121–130.
  40. Bostick, B., Yue, Y. and Duan, D. (2010) Gender influences cardiac function in the mdx model of Duchenne cardiomyopathy. *Muscle Nerve*, **42**, 600–603.
  41. Hakim, C.H. and Duan, D. (2012) Gender differences in contractile and passive properties of mdx extensor digitorum longus muscle. *Muscle Nerve*, **45**, 250–256.
  42. Wang, J., Xie, J., Lu, H., Chen, L., Hauck, B., Samulski, R.J. and Xiao, W. (2007) Existence of transient functional double-stranded DNA intermediates during recombinant AAV transduction. *Proc. Natl. Acad. Sci. U. S. A.*, **104**, 13104–13109.
  43. Gao, G., Vandenberghe, L.H., Alvira, M.R., Lu, Y., Calcedo, R., Zhou, X. and Wilson, J.M. (2004) Clades of Adeno-associated viruses are widely disseminated in human tissues. *J. Virol.*, **78**, 6381–6388.
  44. Shin, J.H., Yue, Y. and Duan, D. (2012) Recombinant adeno-associated viral vector production and purification. *Methods Mol. Biol.*, **798**, 267–284.
  45. Kodippili, K., Vince, L., Shin, J.H., Yue, Y., Morris, G.E., McIntosh, M.A. and Duan, D. (2014) Characterization of 65 epitope-specific dystrophin monoclonal antibodies in canine and murine models of duchenne muscular dystrophy by immunostaining and western blot. *PLoS One*, **9**, e88280.
  46. Wasala, N.B., Bostick, B., Yue, Y. and Duan, D. (2013) Exclusive skeletal muscle correction does not modulate dystrophic heart disease in the aged mdx model of Duchenne cardiomyopathy. *Hum. Mol. Genet.*, **22**, 2634–2641.
  47. Li, D., Long, C., Yue, Y. and Duan, D. (2009) Sub-physiological sarcoglycan expression contributes to compensatory muscle protection in mdx mice. *Hum. Mol. Genet.*, **18**, 1209–1220.
  48. Hakim, C.H., Li, D. and Duan, D. (2011) Monitoring murine skeletal muscle function for muscle gene therapy. *Methods Mol. Biol.*, **709**, 75–89.
  49. Hakim, C.H., Wasala, N.B. and Duan, D. (2013) Evaluation of muscle function of the extensor digitorum longus muscle ex vivo and tibialis anterior muscle in situ in mice. *J. Vis. Exp.*, **72**, e50183.
  50. Bostick, B., Yue, Y. and Duan, D. (2011) Phenotyping cardiac gene therapy in mice. *Methods Mol. Biol.*, **709**, 91–104.
  51. Mitchell, G.F., Jeron, A. and Koren, G. (1998) Measurement of heart rate and Q-T interval in the conscious mouse. *Am. J. Physiol.*, **274**, H747–H751.
  52. Nigro, G., Comi, L.I., Politano, L. and Nigro, G. (2004) Cardiomyopathies associated with muscular dystrophies. In Engel, A. and Franzini-Armstrong, C. (eds), *Myology: Basic and Clinical*. McGraw-Hill, Medical Pub. Division, New York, Vol. 2, pp. 1239–1256.

## Supplementary Tables

*Wasala N et al*

*Genomic removal of a therapeutic mini-dystrophin gene from adult mice elicits a Duchenne muscular dystrophy-like phenotype*

**Supplementary Table 1. Raw densitometry data of Dys2 western blot quantification shown in Figure 1F.**

Sample	Dystrophin band Density	Loading Ctrl density	Normalized to loading	Normalized to none injected ctrl	Avg. Relative density
YL238+AAV.CBA.Cre	5.682	13.344	0.4258	0.26	
YL238+AAV.CBA.Cre	0.534	18.338	0.0291	0.02	
YL238+AAV.CBA.Cre	0.437	12.029	0.0363	0.02	<b>0.10± 0.06</b>
YL238	41.231	19.305	2.1358	1.29	
YL238	26.182	18.913	1.3843	0.84	
YL238	25.935	18.071	1.4352	0.87	<b>1.00± 0.12</b>

*p value = 0.0131*

**Supplementary Table 2. Raw densitometry data of Dys2 western blot quantification shown in Figure 5C.**

<b>Sample</b>	<b>Dystrophin band Density</b>	<b>Loading Ctrl density</b>	<b>Normalized to loading</b>	<b>Normalized to none injected ctrl</b>	<b>Avg. Relative density</b>
SJ13+AAV.CBA.Cre	0.8076	0.8537	0.946	0.30	
SJ13+AAV.CBA.Cre	0.9983	0.9064	1.1013	0.35	
SJ13+AAV.CBA.Cre	0.8245	0.6862	1.2015	0.39	<b>0.35± 0.04</b>
SJ13	1.4759	0.4389	3.3624	1.08	
SJ13	1.489	0.4455	3.3422	1.08	
SJ13	1.3916	0.5322	2.6148	0.84	<b>1.00± 0.08</b>

*p value = 0.0017*

**Supplementary Table 3. Comparison of ECG assay results between FVB and FVB/mdx mice.**

	<b>FVB</b>	<b>FVB/mdx</b>
Sample size (n)	14	17
Heart rate (BPM)	555.4 ± 10.70	525.8 ± 14.60
PR interval (ms)	34.0 ± 1.51	25.4 ± 1.35 <sup>a</sup>
QRS duration (ms)	8.9 ± 0.36	11.4 ± 0.82 <sup>a</sup>
QTc interval (ms)	17.9 ± 0.75	27.9 ± 1.60 <sup>a</sup>
Cardiomyopathy index	0.9 ± 0.05	1.9 ± 0.23 <sup>a</sup>
Q amplitude	-76.4 ± 29.10	-351.2 ± 32.10 <sup>a</sup>

a, significantly different from FVB

**Supplementary Table 4. Comparison of left ventricular hemodynamics between FVB and FVB/mdx mice.**

	FVB	FVB/mdx
Sample size (n)	19	13
End systolic volume ( $\mu\text{L}$ )	6.8 $\pm$ 1.35	16.2 $\pm$ 2.43 <sup>a</sup>
End diastolic volume ( $\mu\text{L}$ )	18.9 $\pm$ 1.73	23.8 $\pm$ 2.72 <sup>a</sup>
Max pressure (mmHg)	89.4 $\pm$ 2.70	81.9 $\pm$ 2.69 <sup>a</sup>
Ejection Fraction (%)	72.5 $\pm$ 0.91	44.5 $\pm$ 3.49 <sup>a</sup>

a, significantly different from FVB

**Supplementary Table 5. Some results of the left ventricular hemodynamics in 22-m-old SJ13 mice (See Figure 5E for results that showed statistically significant difference).**

	$\alpha$ -MHC. $\Delta$ H2-R15	$\alpha$ -MHC. $\Delta$ H2-R15+ AAV.CBA.Cre
Sample size (n)	6	5
Age (m)	22.4 $\pm$ 0.1	22.0 $\pm$ 0.7
Heart rate (BPM)	550 $\pm$ 15.8	597 $\pm$ 22.8
Stroke volume ( $\mu$ l)	11.93 $\pm$ 1.9	12.75 $\pm$ 1.6
Cardiac output (mL/min)	6.7 $\pm$ 1.2	7.5 $\pm$ 0.8
dP/dt Max (KmmHg/s)	10.9 $\pm$ 0.8	9.4 $\pm$ 1.1
dP/dt Min (KmmHg/s)	-6.9 $\pm$ 0.7	-7.3 $\pm$ 0.5
Tau (msec)	10.0 $\pm$ 1.2	13.0 $\pm$ 1.7

*Abbreviations:* BPM, beats per minute; Max, maximum; Min, minimum, dP/dt, the pressure change over the time, Tau, the relaxation constant of the heart at diastole.

## Supplementary Figures

*Wasala N et al*

*Genomic removal of a therapeutic mini-dystrophin gene from adult mice elicits a Duchenne muscular dystrophy-like phenotype*

### **Supplementary Figure 1. Outline of experimental constructs and *in vitro* characterization**

**of the transgenic constructs in 293 cells.** **A**, Schematic outline of Cre mediated excision of the mini-dystrophin expression cassettes. *Top panel*, the Cre expression cassette in the AAV vector. Cre expression is driven by the ubiquitous CBA promoter. *Middle panel*, excision of the mini-dystrophin gene from the floxed HSA. $\Delta$ H2-R15 transgenic cassette in the genome. This cassette drives selective expression of the  $\Delta$ H2-R15 mini-dystrophin gene in skeletal muscle. Digestion with Cre recombinase removes the HSA promoter and the minigene from the genome. The leftover can be detected as a 422 bp band with the primer set DL1927/28 by PCR. *Bottom panel*, excision of the floxed  $\alpha$ -MHC. $\Delta$ H2-R15 transgenic cassette in the genome. This cassette drives selective expression of the  $\Delta$ H2-R15 mini-dystrophin gene in the heart. Digestion with Cre recombinase removes the entire expression cassette from the genome. The leftover can be detected as a 450 bp band with the primer set DL1925/26 by PCR. The primer set hDMD69/70 yield a 200 bp mini-dystrophin specific band. **B**, In vitro demonstration of AAV.CBA.Cre mediated excision of mini-dystrophin gene from the transgenic constructs in 293 cells. Transgenic constructs and AAV.CBA.Cre used in the study as well as the primer set used in the PCR reaction are marked for each lane. The diagnostic band for the mini-dystrophin gene is 200 bp. The diagnostic band for Cre excision of YL238 mice (HSA. $\Delta$ H2-R15) was 422 bp. The diagnostic band for Cre excision of SJ13 mice ( $\alpha$ -MHC. $\Delta$ H2-R15) was 450 bp.

**Supplementary Figure 2. AAV.CBA.Cre injection resulted in acute myocarditis in YL238**

**but not SJ13 mice. A,** Representative photomicrographs showing mini-dystrophin expression in the tibialis anterior (TA) muscle and the diaphragm in skeletal muscle-specific YL238 transgenic mice. and SJ13 mice respectively. Systemic delivery of AAV.CBA.Cre in YL238 mice resulted in acute myocarditis (HE staining in right panel) and mice died within 20 days. **B,**

Representative photomicrographs showing mini-dystrophin expression in the heart in cardiac specific SJ13 transgenic mice. Systemic delivery of AAV.CBA.Cre in SJ13 mice did not induce acute myocarditis.

**Supplementary Figure 3. Time-dependent loss of mini-dystrophin following AAV.CBA.Cre**

**injection in YL238 and SJ13 transgenic mice. A,**  $2.7 \times 10^{12}$  vg particles of AAV.CBA.Cre was injected into the tibialis anterior (TA) muscle of 8-m-old YL238 mice. The TA muscle was harvested before injection (time 0) and 4, 8, and 16 weeks after infection. Dystrophin western blot showed a time-dependent loss of mini-dystrophin. Ponceau S staining was used as the loading control. **B,**  $8 \times 10^{12}$  vg particles of AAV.CBA.Cre was injected into the tail vein of 7-m-old SJ13 mice. The heart was harvested before injection (time 0) and 4, 8, 16, and 20 weeks after infection. Dystrophin western blot showed a time-dependent slow reduction of mini-dystrophin.  $\alpha$ -Tubulin was used as the loading control.

**Supplementary Figure 4. Immunostaining evaluation of the components of the dystrophin-associated glycoprotein complex in the tibialis anterior muscle of 20-m-old YL238 mice.**

Representative photomicrographs of immunofluorescence staining for  $\beta$ -dystroglycan,  $\beta$ -sarcoglycan, dystrobrevin, pan-syntrophin and nNOS on serial muscle sections from YL238

mice (HSA. $\Delta$ H2-R15) and AAV.CBA.Cre injected YL238 mice (HSA. $\Delta$ H2-R15 + AAV.CBA.Cre). Asterisk, the same myofiber in serial sections.

**Supplementary Figure 5. Histological evaluation of fibrosis and T cell infiltration in the tibialis anterior muscle of 20-m-old YL238 mice.** Representative photomicrographs of CD4 and CD8 T cell immunohistochemical staining (**A**) and Masson trichrome staining (**B**) from YL238 mice (HSA. $\Delta$ H2-R15) and AAV.CBA.Cre injected YL238 mice (HSA. $\Delta$ H2-R15 + AAV.CBA.Cre). The high-power view images of the boxed regions in B are shown next to the low-power view images.

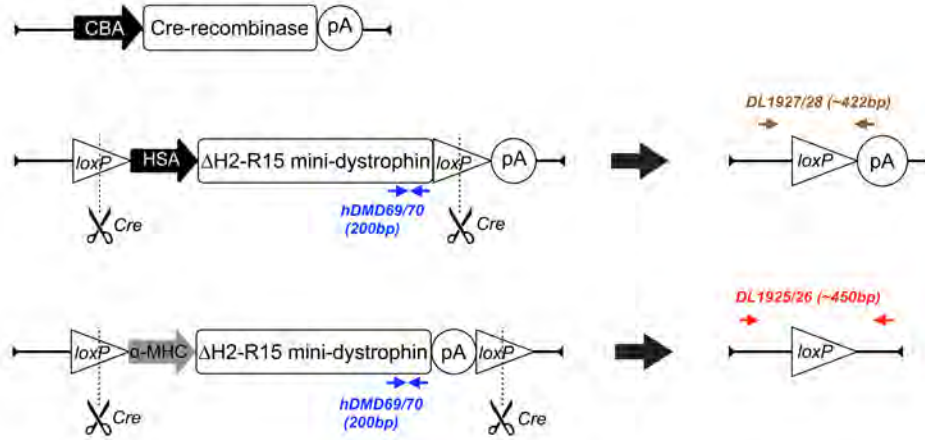
**Supplementary Figure 6. Reduction of cardiac dystrophin in adult mice did not influence the expression of the dystrophin-associated glycoprotein complex and utrophin.** **A**, Representative photomicrographs of immunofluorescence staining for  $\beta$ -dystroglycan,  $\beta$ -sarcoglycan, dystrobrevin, pan-syntrophin and utrophin. **B**, Representative western blot for  $\beta$ -dystroglycan,  $\beta$ -sarcoglycan, dystrobrevin and pan-syntrophin.  $\alpha$ -Tubulin is used as the loading control. **C**, Densitometry quantification of western blots ( $\beta$ -DG,  $\beta$ -dystroglycan;  $\beta$ -SG,  $\beta$ -sarcoglycan; DBR, dystrobrevin; p-Syn, pan-syntrophin). **D**, The high-power view images of the boxed regions in Figure 5.

**Supplementary Figure 7. Adulthood loss of cardiac dystrophin did not alter ECG parameters.** **A**, Quantitative evaluation of the heart rate, PR interval, QRS duration, Mitchell corrected QT interval (QTc), cardiomyopathy index and the Q wave amplitude. **B**,

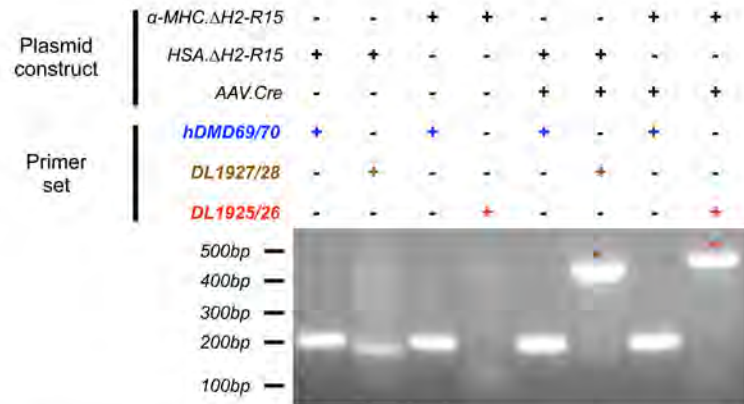
Representative lead II ECG tracing from SJ13 mice ( $\alpha$ -MHC. $\Delta$ H2-R15) and AAV.CBA.Cre injected SJ13 mice ( $\alpha$ -MHC. $\Delta$ H2-R15 + AAV.CBA.Cre).

Supp Figure 1

**A**



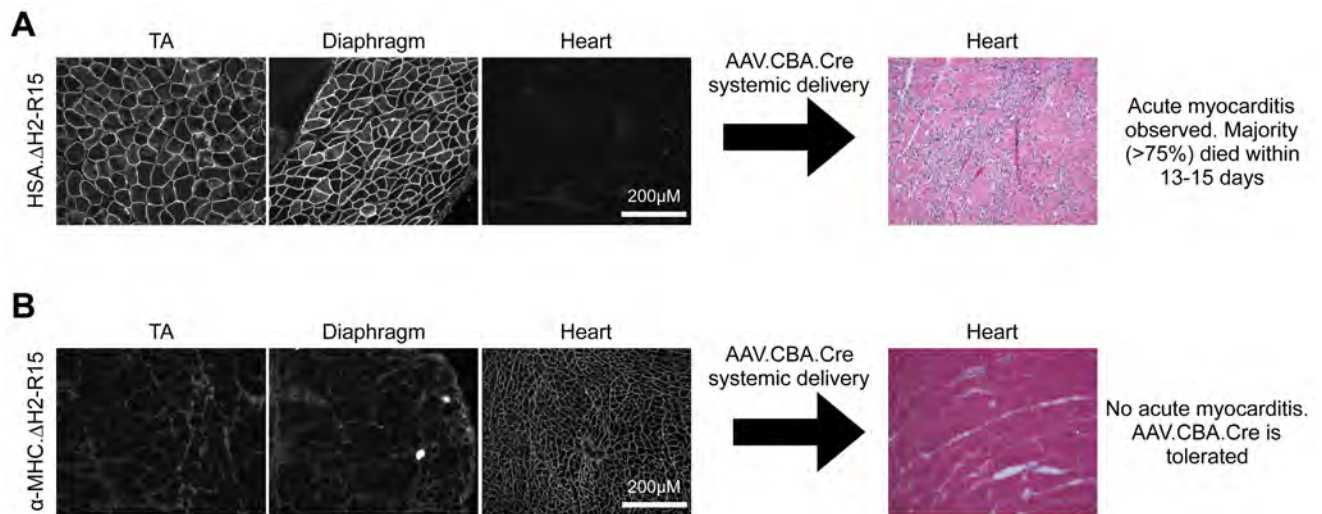
**B**



\* DL1927/28 amplicon following AAV.Cre mediated excision of HSA.ΔH2-R15 at the loxP sites

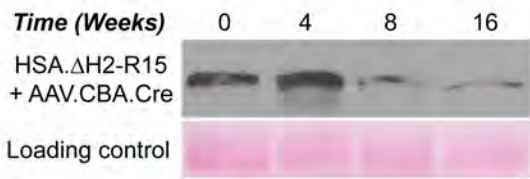
\* DL1925/26 amplicon following AAV.Cre mediated excision of α-MHC.ΔH2-R15 plasmid at the loxP sites

Supp Figure 2

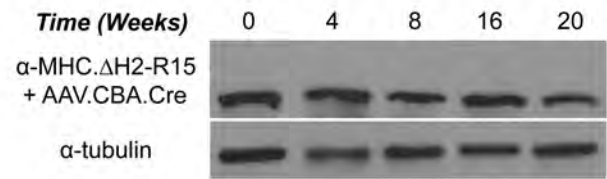


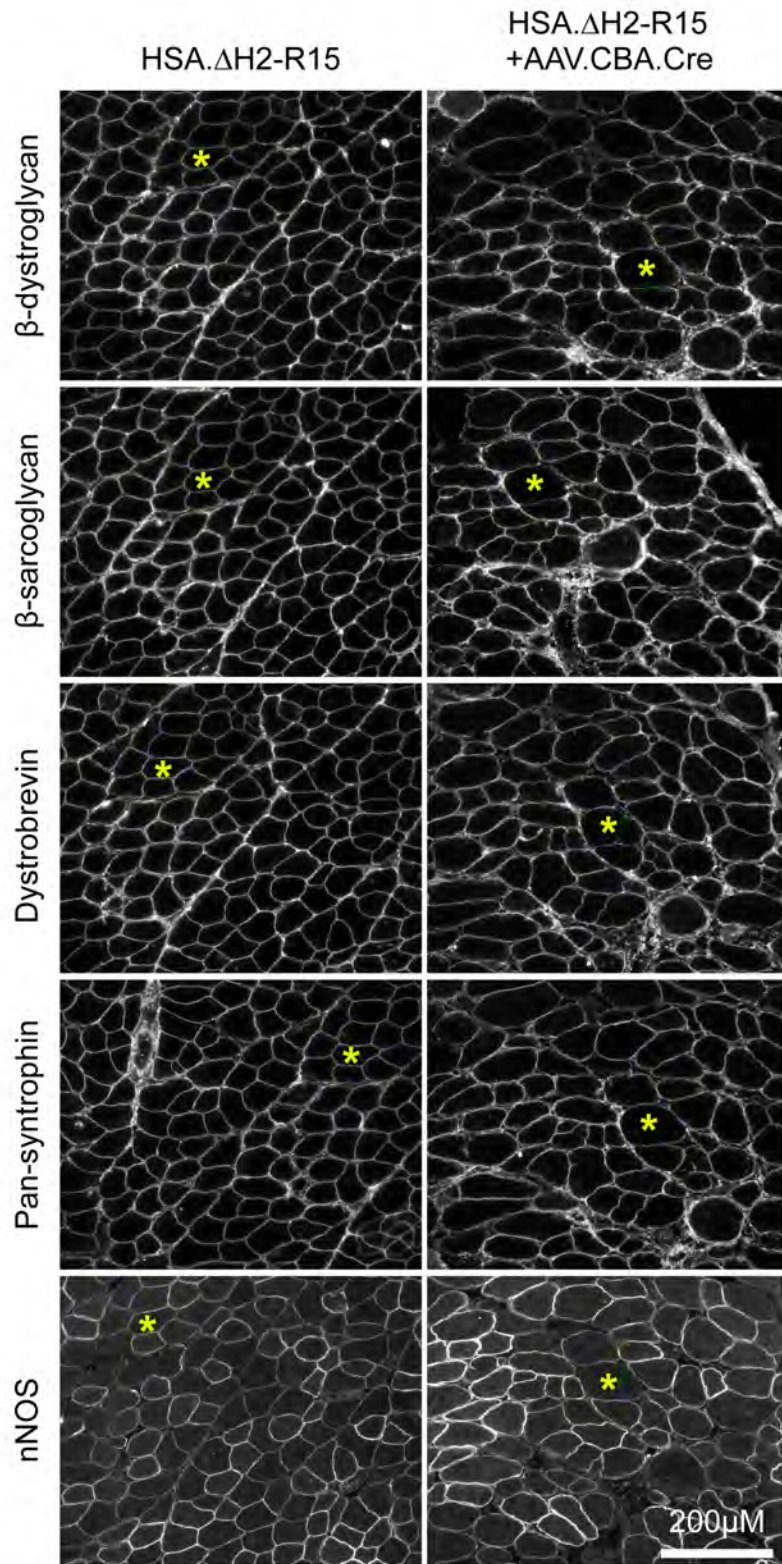
Supp Figure 3

**A**

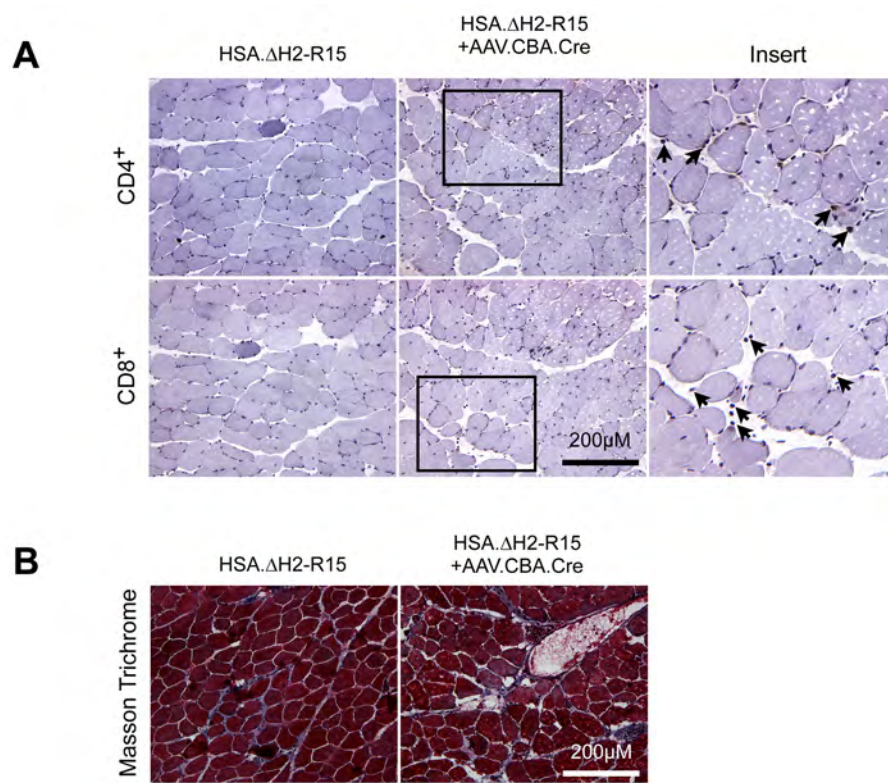


**B**

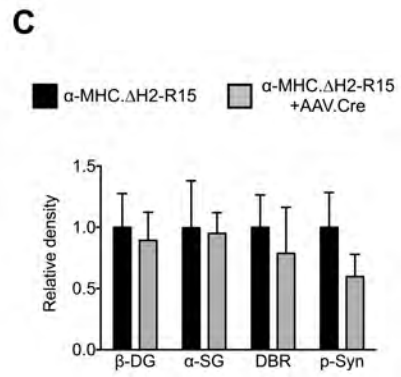
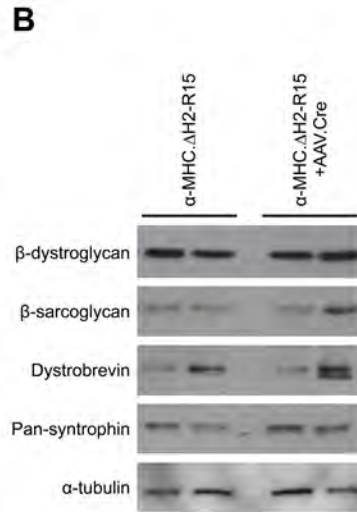
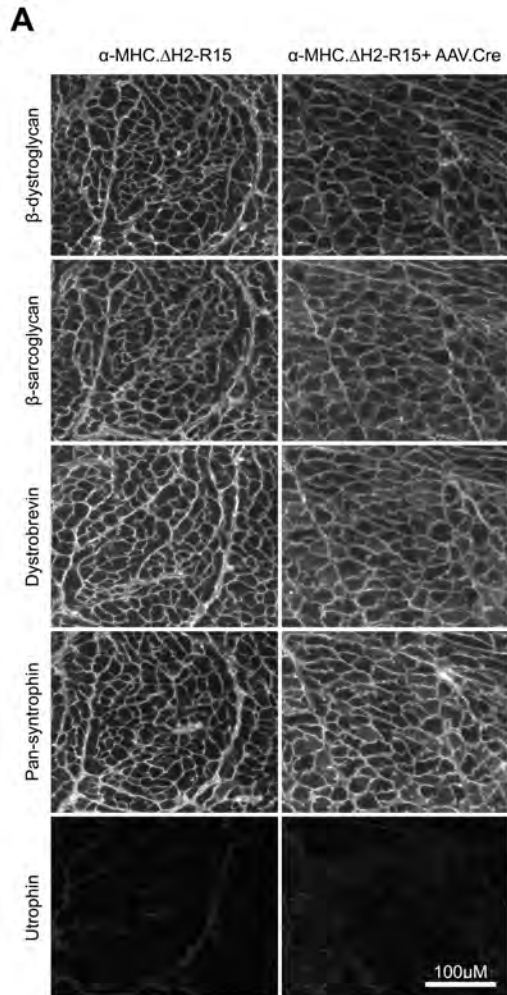




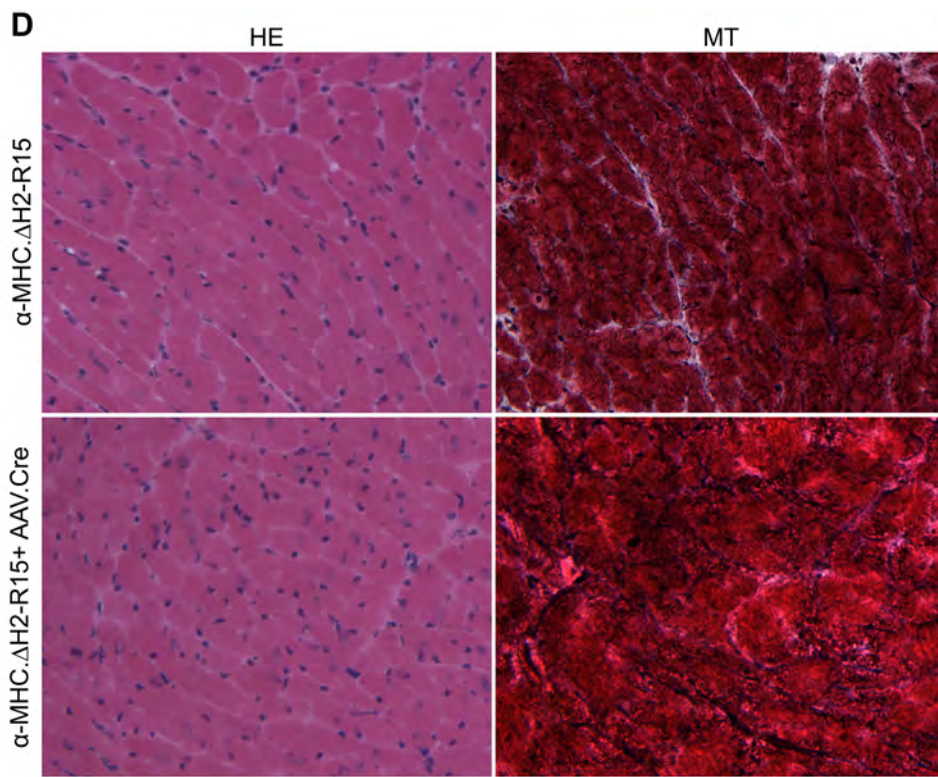
Supp Figure 5



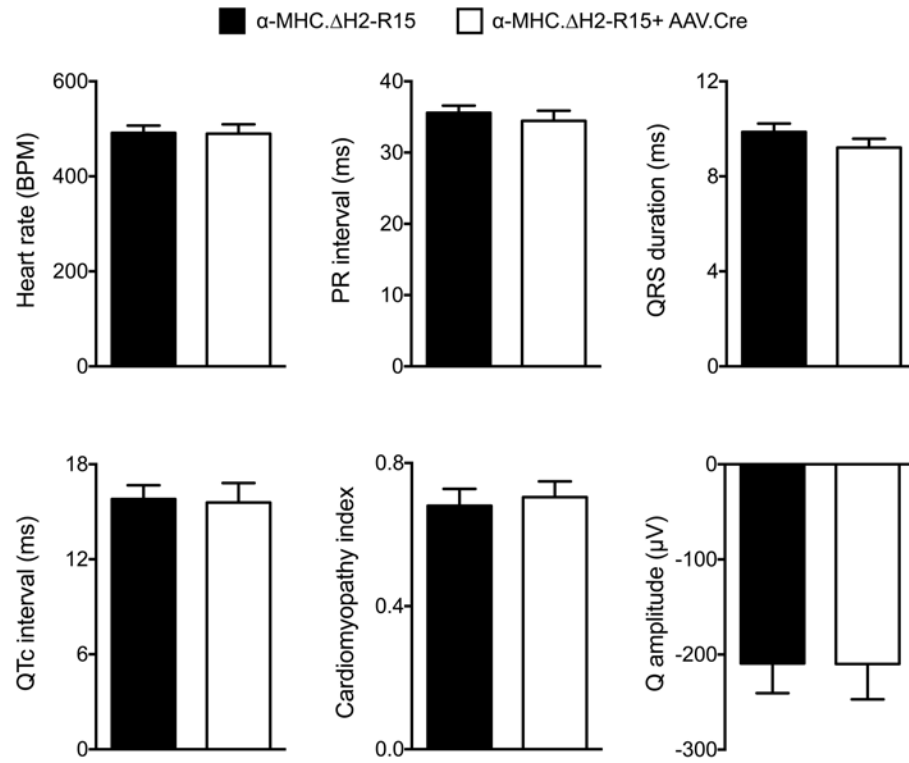
Supp Figure 6



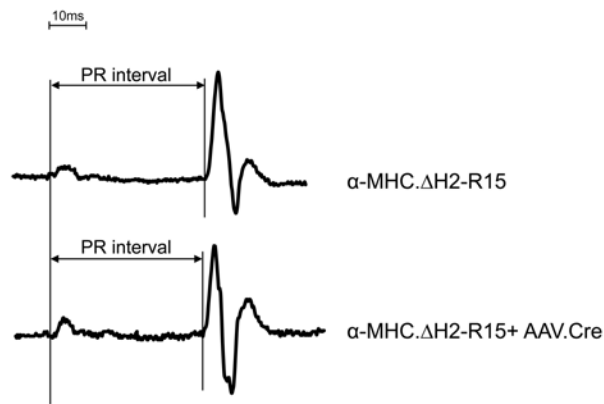
Supp Figure 6

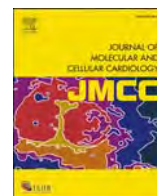


**A**



**B**





# Uniform low-level dystrophin expression in the heart partially preserved cardiac function in an aged mouse model of Duchenne cardiomyopathy



Nalinda B. Wasala<sup>a</sup>, Yongping Yue<sup>a</sup>, Jenna Vance<sup>a</sup>, Dongsheng Duan<sup>a,b,c,d,\*</sup>

<sup>a</sup> Department of Molecular Microbiology and Immunology, School of Medicine, The University of Missouri, Columbia, MO 65212, USA

<sup>b</sup> Department of Neurology, School of Medicine, The University of Missouri, Columbia, MO 65212, USA

<sup>c</sup> Department of Bioengineering, The University of Missouri, Columbia, MO 65212, USA

<sup>d</sup> Department of Biomedical Sciences, College of Veterinary Medicine, The University of Missouri, Columbia, MO 65212, USA

## ARTICLE INFO

### Article history:

Received 4 July 2016

Received in revised form 17 November 2016

Accepted 23 November 2016

Available online 29 November 2016

### Keywords:

Duchenne muscular dystrophy

DMD

Duchenne cardiomyopathy

Dystrophin

Gene therapy

Heart

Low-level expression

Dilated cardiomyopathy

Adeno-associated virus

AAV

ECG

Hemodynamics

## ABSTRACT

Dystrophin deficiency results in Duchenne cardiomyopathy, a primary cause of death in Duchenne muscular dystrophy (DMD). Gene therapy has shown great promise in ameliorating the cardiac phenotype in mouse models of DMD. However, it is not completely clear how much dystrophin is required to treat dystrophic heart disease. We and others have shown that mosaic dystrophin expression at the wild-type level, depending on the percentage of dystrophin positive cardiomyocytes, can either delay the onset of or fully prevent cardiomyopathy in dystrophin-null mdx mice. Many gene therapy strategies will unlikely restore dystrophin to the wild-type level in a cardiomyocyte. To determine whether low-level dystrophin expression can reduce the cardiac manifestations in DMD, we examined heart histology, ECG and hemodynamics in 21-m-old normal BL6 and two strains of BL6-background dystrophin-deficient mice. Mdx3cv mice show uniform low-level expression of a near full-length dystrophin protein in every myofiber while mdx4cv mice have no dystrophin expression. Immunostaining and western blot confirmed marginal level dystrophin expression in the heart of mdx3cv mice. Although low-level expression did not reduce myocardial histopathology, it significantly ameliorated QRS prolongation and normalized diastolic hemodynamic deficiencies. Our study demonstrates for the first time that low-level dystrophin can partially preserve heart function.

© 2016 Elsevier Ltd. All rights reserved.

## 1. Introduction

Deficiency of cytoskeletal protein dystrophin leads to Duchenne muscular dystrophy (DMD) [1,2]. Skeletal muscle related symptoms (such as limited ambulation and respiratory restriction) are observed early on in young DMD patients [3]. While cardiac involvement appears at the later stage of the disease, all patients eventually develop cardiac dysfunction and heart failure causes up to 40% of death [4–6]. Currently, only palliative treatments are available for symptom management. Restoration of dystrophin expression using adeno-associated virus (AAV)-mediated micro/mini-dystrophin gene transfer, exon-skipping and genome editing are promising new approaches to treat DMD [7, 8]. However, these therapies may not restore dystrophin expression to the normal level in patients. An important issue is whether low-level dystrophin expression is therapeutically relevant.

Numerous studies have investigated the amount of dystrophin required for treating skeletal muscle disease in mouse models of DMD

and in human patients. These studies suggest that homogenous dystrophin expression at 20–30% of the wild-type level in every myofiber can significantly enhance muscle function and reduce muscle pathology [9–13]. Recent studies further suggest that uniform low-level dystrophin expression at even 5% of the normal level can still improve clinical outcome in dystrophic mice [14–17]. In the case of mosaic expression, approximately 50% myofibers have to express dystrophin in order to achieve a mild phenotype in skeletal muscle [18–20].

In contrast to the abundant information on low-level dystrophin expression in skeletal muscle, little is known about the dystrophin level needed for correcting heart disease in DMD. A study in genetically modified mice suggests that expression in 3 to 5% of cardiomyocytes at the wild-type level (in every dystrophin positive cell) may delay the onset of heart disease [21]. In a different study, Wu et al. found that 5% dystrophin positive cells in the heart of adult mdx mice did not improve cardiac histology/baseline function although mice tolerated dobutamine stress better [22]. We examined female carrier mice and found that normal level dystrophin expression in half of heart cells is sufficient to completely prevent dystrophic cardiomyopathy [23,24]. While these results have provided critical insight on the percentage of dystrophin positive cells needed for treating cardiac manifestations, it should be noted

\* Corresponding author at: Department of Molecular Microbiology and Immunology, One Hospital Dr., Columbia, MO 65212, USA.

E-mail address: [duand@missouri.edu](mailto:duand@missouri.edu) (D. Duan).

that in all these studies dystrophin is expressed at the wild-type level in every positive cardiomyocyte. It remains unclear whether sub-physiological expression in a cardiomyocyte can benefit the heart.

We and others have previously shown that mdx3cv mice express marginal level dystrophin in skeletal muscle [14,15,25]. This residual level expression significantly enhanced skeletal muscle function although it did not improve histopathology [14,26]. Mdx3cv mice were generated by Chapman et al. using N-ethyl-N-nitrosourea mutagenesis [27]. A point mutation in intron 65 aborts full-length dystrophin expression. However, a slightly truncated  $\Delta 65/66$  transcript is generated

(Supplementary Fig. 1). This results in the production of a near full-length dystrophin protein at ~5% of the wild-type level [15,25].

To study the impact of low-level uniform dystrophin expression in the heart, we compared the cardiac phenotype among C57Bl/6 (BL6), mdx3cv and mdx4cv mice. All three strains are on the BL6 background. BL6 and mdx4cv mice are normal and dystrophin-null controls, respectively. The characteristic heart presentation in DMD is dilated cardiomyopathy. We have previously shown that dystrophin-deficient mice do not develop dilated cardiomyopathy until they reach 21 months of age [24,28]. For this reason, we intentionally conducted our study in aged

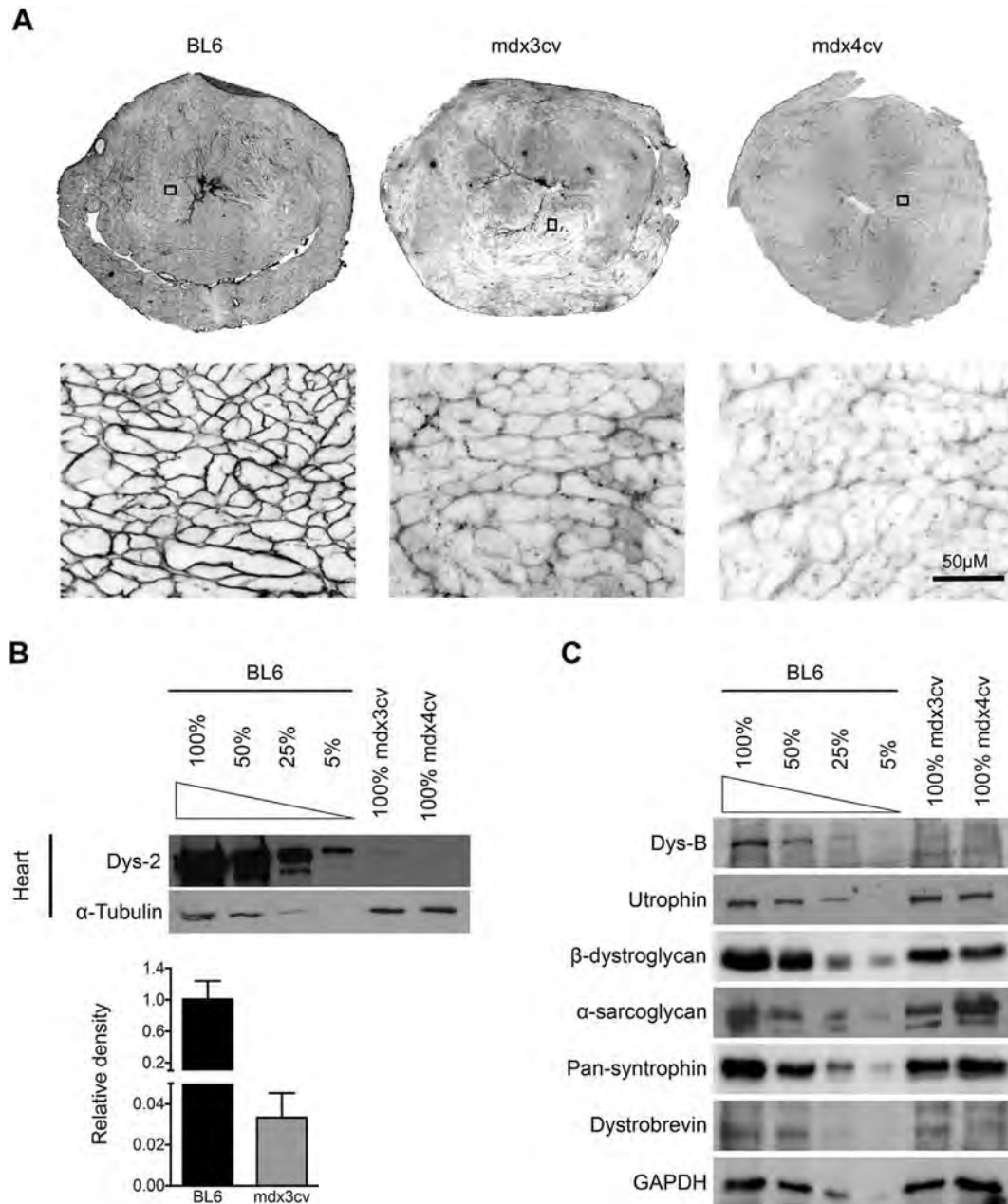


**Fig. 1.** Mdx3cv mouse heart expressed low-level dystrophin. **A**, Representative photomicrographs of dystrophin immunofluorescence staining in BL6, mdx3cv and mdx4cv heart. Upper panel shows the whole heart view and the lower panel shows a higher magnification of the corresponding boxed region in the whole heart view. **B**, Top panel, Representative heart western blot from BL6, mdx3cv and mdx4cv mice. The BL6 heart lysate was loaded at 100%, 50%, 25% and 5%. The mdx3cv and mdx4cv heart lysate was loaded at 100%; Bottom panel, Densitometry quantification of cardiac dystrophin expression ( $N = 3$  for each group). Dys-2, a monoclonal antibody against the dystrophin C-terminal domain. The heart of mdx3cv mice showed uniform dystrophin expression at approximately 3.3% of the wild-type level. **C**, Representative cardiac western blots for utrophin and selected components of dystrophin-associated glycoprotein complex ( $\beta$ -dystroglycan,  $\alpha$ -sarcoglycan, syntrophin and dystrobrevin). DysB, a monoclonal antibody against the dystrophin exons 10–12; GAPDH, glyceraldehyde 3-phosphate dehydrogenase.

mice. We detected uniform dystrophin expression at ~3.3% of the wild-type level in the heart of 21-m-old mdx3cv mice. Importantly, we observed significant improvement in some ECG and hemodynamic parameters suggesting low-level dystrophin expression can benefit the heart.

## 2. Results

### 2.1. The heart of aged mdx3cv mice expressed low-level dystrophin

We first performed dystrophin immunostaining in the heart (Fig. 1A). We observed robust, no and very low expression in the heart of BL6, mdx4cv and mdx3cv mice, respectively. To quantify dystrophin expression, we performed whole heart lysate western blot (Fig. 1B). Serially diluted BL6 heart lysate was used to show band intensity at 5, 25, 50 and 100% of the wild-type levels (Fig. 1B). As expected, no dystrophin was detected in mdx4cv. Mdx3cv showed a faint band. On quantification, it reached approximately 3.3% of the wild-type level (Fig. 1B).

### 2.2. Low dystrophin expression in the mdx3cv heart had minimal impact on the expression of utrophin and components of the dystrophin-associated glycoprotein (DGC) complex

We have previously found that the hearts of 21-m-old normal BL10 mice and BL10-background dystrophin-null mdx mice had similar levels of utrophin expression on western blot [29]. Consistently, there was not much difference in the cardiac utrophin level among aged BL6, mdx3cv and mdx4cv mice (Fig. 1C). We also compared the expression level of representative DGC components including  $\beta$ -dystroglycan,  $\alpha$ -sarcoglycan, syntrophin and dystrobrevin. Compared to that of the BL6 mouse heart, there appeared a slight reduction of the DGC components in the heart of mdx3cv and mdx4cv mice (Fig. 1C).

### 2.3. Low-level dystrophin expression did not improve cardiac histopathology

On HE staining, BL6 mouse heart showed normal morphology (Fig. 2A). Some myocardial distortion and mononuclear cell infiltration were noted in both mdx3cv and mdx4cv heart. But there was no apparent difference between these two strains (Fig. 2A). Cardiac fibrosis was examined using Masson trichrome staining (Fig. 2B). The BL6 heart had no fibrosis. The hearts of mdx3cv and mdx4cv mice showed similar patchy myocardial fibrosis (Fig. 2B). Cardiac inflammation was examined by immunohistochemical staining (Fig. 2C). Abundant macrophages and neutrophils were detected in the heart of mdx3cv and mdx4cv mice but not BL6 mice (Fig. 2C).

### 2.4. The anatomic properties of the heart were similar between mdx3cv and mdx4cv mice

The absolute heart weight (HW) and ventricular weight (VW) were similar between mdx3cv and mdx4cv mice (Table 1). Both were significantly lower than those of BL6 mice. For the tibial length (TL) and anterior tibialis muscle weight (TW) normalized heart weight and ventricular weight (HW/TL, HW/TW, VW/TL and VW/TW), we did not see a difference between mdx3cv and mdx4cv mice. These ratios were all significantly lower than those of BL6 mice (Table 1). The body weight (BW) of BL6 and mdx3cv mice was comparable. However, the BW of mdx4cv mice was significantly reduced (Table 1). Hypertrophy of anterior tibialis muscle was obvious in mdx3cv and mdx4cv mice. Interestingly, the TW of mdx3cv mice was significantly higher than that of mdx4cv mice (Table 1).

### 2.5. Mdx3cv mice showed improved QRS duration

To study cardiac electrophysiology, we performed 12-lead ECG recordings using our published protocol [30,31]. Compared with BL6,

mdx4cv showed characteristic dystrophic ECG changes such as tachycardia, PR-interval reduction, QRS duration and QT interval prolongation, and a significant increase in the cardiomyopathy index (Fig. 3) [24,28,32,33]. Surprisingly, we did not detect a significant change in the amplitude of Q wave among three strains (Fig. 3). Compared to those of mdx4cv, several ECG parameters (the heart rate, QT interval and cardiomyopathy index) showed a trend of improvement in mdx3cv mice but did not reach statistical significance. The only ECG parameter that was significantly improved in mdx3cv mice was the QRS duration. It was significantly reduced compared to that of mdx4cv mice (Fig. 3).

### 2.6. Low-level dystrophin in the heart normalized diastolic function in mdx3cv mice

We next examined the pump function of the heart using an ultra-miniature Millar ventricular catheter [30,31]. Compared with BL6, mdx4cv showed the characteristic profile of dilated cardiomyopathy (Fig. 4). Specifically, the end-systolic volume was significantly increased (Fig. 4A). The end-diastolic volume also showed an apparent increase though not statistically significant (Fig. 4B). Cardiac contractility (as reflexed by the maximum pressure, absolute values of dP/dt max and dP/dt min) was significantly reduced. The isovolumic relaxation time constant during diastole ( $\tau$ ) was prolonged (Fig. 4B). As a result, the stroke volume, ejection fraction and cardiac output were all significantly decreased in mdx4cv mice (Fig. 4C).

Low-level dystrophin expression in mdx3cv mice completely normalized diastolic parameters including the end diastolic volume,  $\tau$  and dP/dt min (Fig. 4B). The end systolic volume showed a trend of reduction (Fig. 4A). However, overall heart performance (stroke volume, ejection fraction and cardiac output) was not significantly improved in mdx3cv mice.

### 2.7. Expression of sarcoplasmic/endoplasmic reticulum calcium ATPase 2a (SERCA2a), phospholamban and calsequestrin in aged BL6, mdx3cv and mdx4cv hearts

To gain molecular insight on how low-level dystrophin controls heart function, we performed quantitative western blot on the expression of three major calcium handling proteins in the heart including SERCA2a, phospholamban and calsequestrin. No statistically significant difference was detected among BL6, mdx3cv and mdx4cv mice (Fig. 5). Unfortunately, our western blot for the phosphorylated form of phospholamban did not work.

## 3. Discussion

In this study, we tested the hypothesis that a uniform low-level dystrophin expression can benefit the heart in the mouse model of Duchenne cardiomyopathy. We found marginal level (approximately 3.3% of the wild-type level) homogenous dystrophin expression in the myocardium of aged mdx3cv mice (Fig. 1). This residual level expression did not change the anatomic properties of the heart (Table 1). Neither did it reduce histological lesions in the heart (Fig. 2). However, some aspects of heart function measures were significantly improved (Figs. 3 and 4). Specifically, the abnormally elongated QRS duration was shortened and deficiencies in diastolic hemodynamics were completely prevented (Figs. 3 and 4). Interestingly, there was no difference in the expression level of SERCA2a, phospholamban and calsequestrin (Fig. 5). Our results suggest that low-level dystrophin is far from sufficient to cure Duchenne cardiomyopathy. However, it can still offer some protection to the heart.

Recent progress in genetic engineering and molecular medicine is making gene therapy for DMD a reality [7,8]. Large scale clinical trials have been conducted to test therapeutic benefits of exon-skipping [34, 35]. Systemic AAV micro-dystrophin therapy is slated to start in the

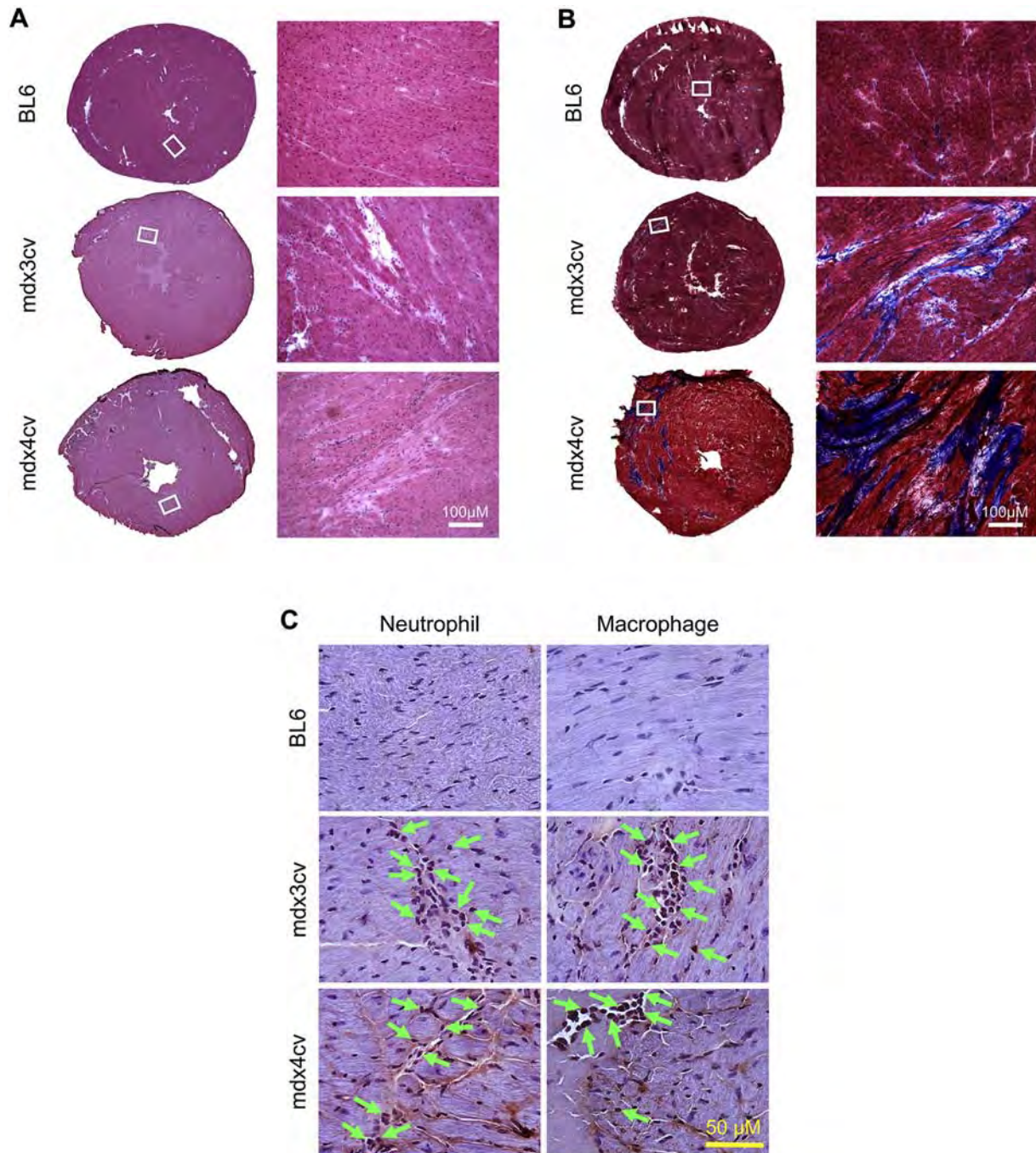


**Fig. 2.** Low-level dystrophin expression did not ameliorate myocardial inflammation and fibrosis in mdx3cv mice. **A**, Representative heart HE staining photomicrographs from BL6, mdx3cv and mdx4cv mice. Left panel, whole heart cross-sectional images; right panel, high-power images of the respective boxed areas in the whole heart view. **B**, Representative Masson trichrome staining photomicrographs of the BL6, mdx3cv and mdx4cv heart. Left panel, whole heart cross-sectional images; right panel, high-power images of the respective boxed areas in the whole heart view. The blue color in Masson trichrome staining marks myocardial fibrosis. **C**, Representative macrophage and neutrophil immunohistochemical staining photomicrographs of the BL6, mdx3cv and mdx4cv heart. Arrow, dark brown stained macrophages and neutrophils.

next couple of years [7,8]. Most recently, investigators have achieved remarkable proof-of-concept evidence in repairing the mutated dystrophin gene in mdx mice [36]. Despite these successes, it is still not completely clear whether sub-physiological level dystrophin expression can help mitigating dystrophic manifestations. A comprehensive understanding of the dystrophin expression level in striated muscle requires information on (a) the percentage of dystrophin positive myofibers and (b) the amount of dystrophin protein in these positive myofibers. The former is obtained by quantifying dystrophin immunostaining and the latter by western blot. Accordingly, for DMD gene therapy we

need to know what percentage of muscle cells should express dystrophin and what are the dystrophin levels in these cells.

Therapeutic relevance of mosaic dystrophin expression has been extensively examined [18–20,23,24]. These studies have documented remarkable disease amelioration and function preservation in both skeletal and cardiac muscles when half myofibers show positive dystrophin staining. Homogenous sub-physiological dystrophin expression has been shown to protect skeletal muscle by a number of laboratories [9–17]. However, it is not clear whether a low-level uniform dystrophin expression in the heart can reduce cardiomyopathy.

**Table 1**  
Anatomical measurements and ratios.

	BL6	mdx3cv	mdx4cv
Sample size (N)	11	28	19
Age (m)	21.67 ± 0.54	21.85 ± 0.33	20.76 ± 0.19
BW (g)	26.78 ± 0.79	27.60 ± 0.37	23.59 ± 0.91 <sup>a</sup>
HW (mg)	117.80 ± 3.42	101.99 ± 2.73 <sup>b</sup>	101.58 ± 3.22 <sup>b</sup>
VW (mg)	111.49 ± 3.25	89.91 ± 2.52 <sup>b</sup>	94.32 ± 3.10 <sup>b</sup>
TL (mm)	18.51 ± 0.09	18.42 ± 0.08	18.94 ± 0.09 <sup>a</sup>
TW (mg)	36.75 ± 1.14 <sup>a</sup>	63.14 ± 2.02 <sup>a</sup>	55.42 ± 2.32 <sup>a</sup>
HW/BW (mg/g)	4.41 ± 0.11	3.71 ± 0.11 <sup>a</sup>	4.38 ± 0.16
HW/TL (mg/mm)	6.36 ± 0.17	5.21 ± 0.10 <sup>b</sup>	5.17 ± 0.16 <sup>b</sup>
HW/TW (mg/g)	3.25 ± 0.16	1.81 ± 0.25 <sup>b</sup>	1.89 ± 0.10 <sup>b</sup>
VW/TL (mg/mm)	6.02 ± 0.16	4.81 ± 0.11 <sup>b</sup>	4.78 ± 0.15 <sup>b</sup>
VW/TW (mg/g)	3.08 ± 0.15	1.60 ± 0.23 <sup>b</sup>	1.76 ± 0.09 <sup>b</sup>

Abbreviations: BW, body weight; HW, heart weight; VW, ventricle weight; TL, tibia length; TW, anterior tibialis muscle weight.

<sup>a</sup> Significantly different from other two groups.

<sup>b</sup> Significantly different from BL6 mice.

Townsend et al. compared dystrophin expression in the heart of young adult (4-m-old) and aged (23-m-old) BL10 mice [37]. The authors observed a ubiquitous reduction of dystrophin content in every cardiomyocyte in aged mice. On average, the dystrophin level was reduced by 57% in the aged BL10 heart. Loss of dystrophin resulted in a decline of cardiac function in aged BL10 mice [37]. Our recent studies also suggest that removal of existing dystrophin from the myocardium can compromise the pump function of the heart [38]. These two studies suggest that sub-physiological level dystrophin is insufficient to maintain normal heart function. While this is an important conclusion, it does not tell us whether a heart with low-level dystrophin expression is structurally and/or functionally superior to a heart that has no dystrophin expression. Our study in aged mdx3cv mice is aimed to address this knowledge gap. Consistent with our previous studies on the

mdx3cv mouse skeletal muscle [14,15], we demonstrated a partial function preservation but not histopathology amelioration in the mdx3cv heart.

Little is known about the molecular mechanisms underlying electrophysiological defects and hemodynamic deficiencies in Duchenne cardiomyopathy. A number of hypotheses have been suggested such as myocardial necrosis and inflammation, cardiac fibrosis, vacuolar degeneration in the conduction system, perturbation of calcium homeostasis, oxidative stress, sarcolemma tearing, mitochondrial dysfunction and aberrant signaling [39–42]. We have previously demonstrated characteristic ECG changes in young adult (4-m-old) mdx mice in the absence of apparent histological lesions in the heart [43]. We have also shown significant ECG improvement but not histology amelioration in terminally aged (21 to 23-m-old) mdx mice by AAV micro-dystrophin gene therapy [32]. These data challenge a direct causal relationship between myocardial structural damage and ECG abnormality. In mdx3cv mice, residual level dystrophin expression did not reduce myocardial inflammation and fibrosis. Yet the extended QRS complex was significantly shortened. The QRS complex reflects depolarization of ventricular cells. In the absence of dystrophin, the time of ventricular depolarization was increased by 30% (Fig. 3). With merely ~3.3% dystrophin, the speed of ventricular depolarization was significantly increased. As a result, the QRS duration was reduced in mdx3cv mice compared to that of dystrophin-null mdx4cv mice (Fig. 3). Cardiomyocyte depolarization and repolarization is tightly controlled by various ion channels on the sarcolemma. Interestingly, dystrophin and some DGC components (such as syntrophin and nNOS) have been shown to regulate these ion channels [44–47]. Our results suggest that low-level dystrophin may partially restore dystrophin/DGC-mediated regulation on ion channels.

An unexpected finding of our study is the full normalization of diastolic hemodynamic parameters in mdx3cv mice. This suggests that low-level dystrophin may meet the need of myocardial relaxation during the cardiac cycle. However, a much higher level of dystrophin

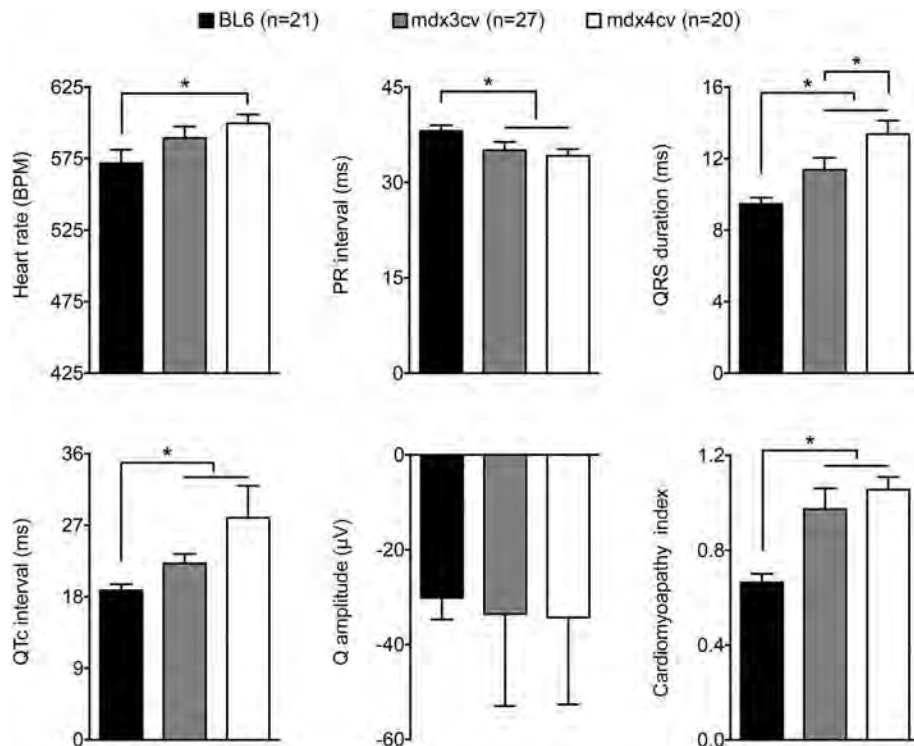


**Fig. 3.** Low-level dystrophin expression improved QRS duration but not other ECG parameters in mdx3cv mice. Quantitative evaluation of the heart rate, PR interval, QRS duration, Mitchell corrected QT interval (QTc), cardiomyopathy index and the Q wave amplitude. The QTc interval was determined by correcting the QT interval with the heart rate as described by Mitchell et al. [49]. Asterisk, statistically significant ( $p < 0.05$ ).

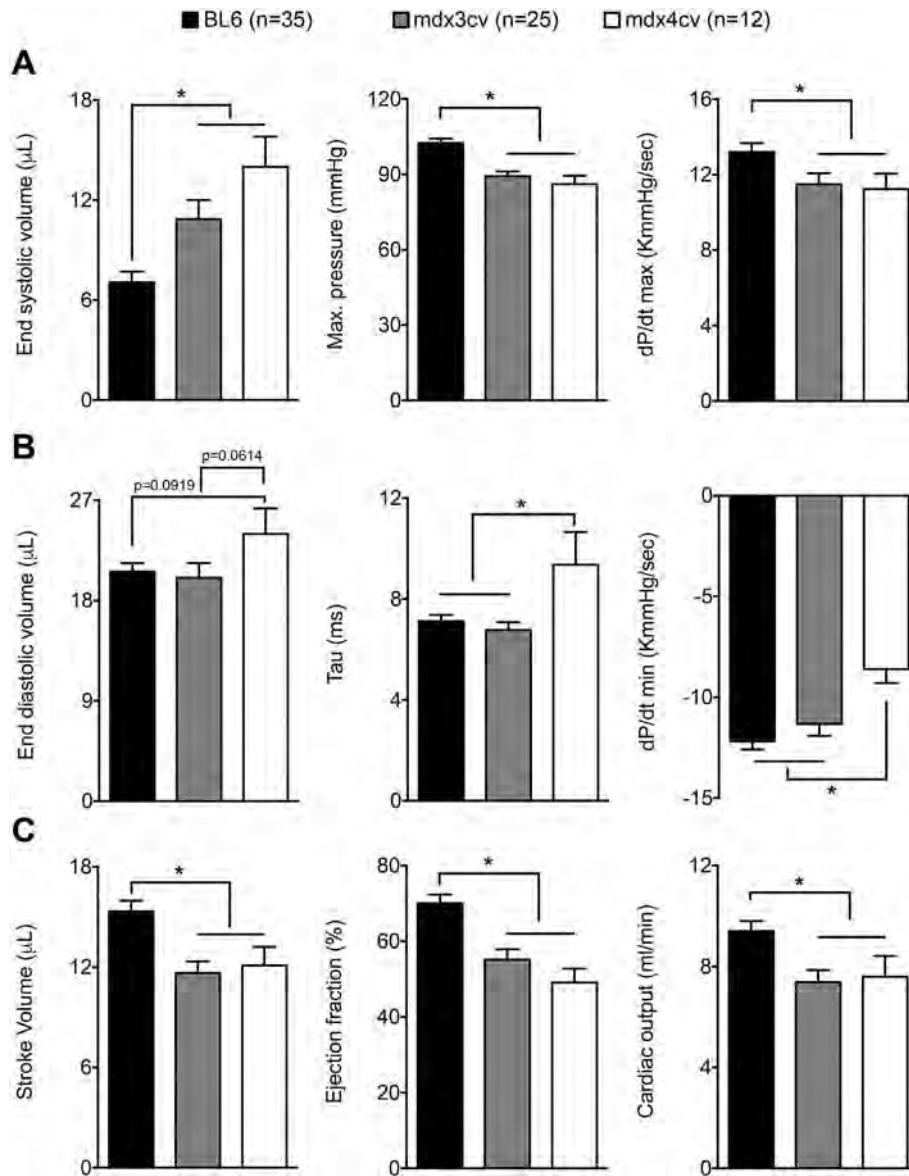


**Fig. 4.** Low-level dystrophin expression partially improved hemodynamics in mdx3cv mice. A, Quantitative evaluation of systolic hemodynamic parameters. B, Quantitative evaluation of diastolic hemodynamic parameters. End-diastolic volume, tau and dP/dt min were all normalized in mdx3cv mice. C, Quantitative evaluation of overall heart function. Asterisk, statistically significant ( $p < 0.05$ ). The heart rate at the hemodynamic assay was  $616.9 \pm 9.10$  bpm,  $619.9 \pm 25.5$  bpm and  $629.3 \pm 8.3$  bpm for BL6, mdx3cv and mdx4cv, respectively. There is no statistically significance difference.

expression is needed to enhance ventricular muscle contraction in order to improve the blood pumping function of the heart. We would like to point out that it is not unusual that different levels of dystrophin expression are needed for the correction of different aspects of disease. For example, a recent study in skeletal muscle by Godfrey et al. suggests that protection against eccentric contraction-induced injury requires homogenous dystrophin expression at the 15% of wild-type level. However, reduction of skeletal muscle histopathology requires much more dystrophin [11].

While the ultimate goal of the study is to translate our findings into human patients, it is important to remember that scaling up to a large dystrophic mammal is much more complex than we can model in mice. Whether marginal level expression can result in clinically appreciable improvement in human patients will depend on a number of factors, such as the configuration of the therapeutic dystrophin protein (full-length, moderately truncated mini-dystrophin, or highly abbreviated micro-dystrophin), treatment regime (the age at the start of the therapy, the duration of the therapy and the gene therapy vector dose etc.), and the abundance of dystrophin (percentage of dystrophin

expressing cells and dystrophin level in these cells). Our data suggest that uniform low-level dystrophin expression may have therapeutic implications for treating Duchenne cardiomyopathy. Future studies in large animal models of DMD (such as dystrophic dogs) may testify whether this observation can be translated to large mammals.

#### 4. Materials and methods

##### 4.1. Experimental animals

All animal experiments were approved by the institutional animal care and use committee and were in accordance with NIH guidelines. Experimental mice were generated in a barrier facility using founders from The Jackson Laboratory (Bar Harbor, ME). Female mice were used in the study because we have previously shown that female mice are better than male mice in modeling Duchenne cardiomyopathy seen in human patients [28]. All mice were maintained in a specific-pathogen free animal care facility on a 12-h light (25 lx):12-h dark

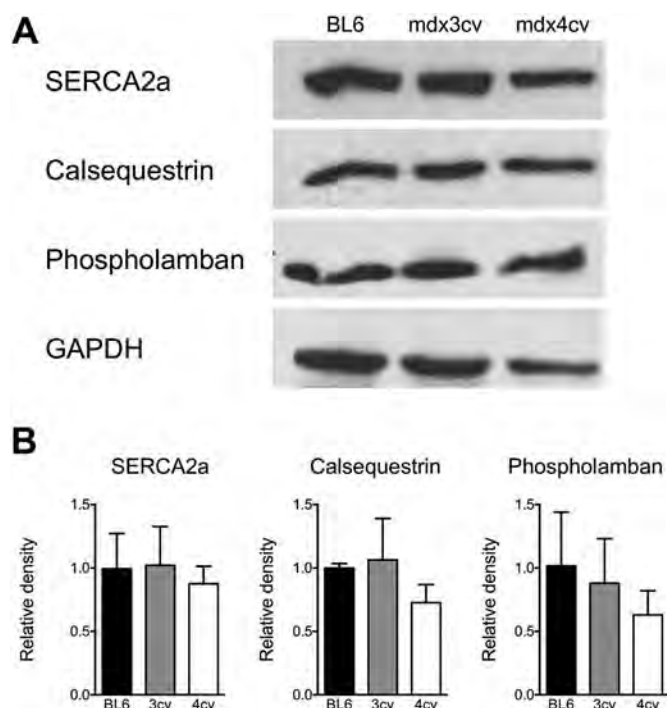


**Fig. 5.** Western blot evaluation of SERCA2a, calsequestrin and phospholamban in the heart. A, Representative western blot results from BL6, mdx3cv and mdx4cv mice. B, Densitometry quantification of calcium handling proteins shown in panel A ( $N = 3$  for each group).

cycle with access to food and water ad libitum. Mice were euthanized following functional assays for tissue collection.

#### 4.2. Morphological studies

Dystrophin expression was evaluated by immunofluorescence staining using the Dys2 monoclonal antibody (1:30; Vector Laboratories, Burlingame, CA). General histology was examined by hematoxylin and eosin (HE) staining. Fibrosis was examined by Masson trichrome staining. Inflammation was studied with immunohistochemistry staining using antibodies specific to mouse neutrophils (Ly-6G, 1:8,00, BD Pharmingen, San Diego, CA) and macrophages (F4/80, 1:200, Caltag Laboratories, Burlingame, CA) according to our published protocol [29]. Slides were viewed at the identical exposure setting using a Nikon E800 fluorescence microscope. Photomicrographs were taken with a QImage Retiga 1300 camera [31].

#### 4.3. Western blot

Whole heart lysate was prepared as we described before [48]. Briefly, the freshly isolated heart was snap frozen in liquid nitrogen. The frozen heart sample was ground to fine powder in liquid nitrogen followed by homogenization in a buffer containing 10% sodium dodecyl sulfate, 5 mM ethylenediaminetetraacetic acid, 62.5 mM Tris at pH 6.8 and the protease inhibitor cocktail (Roche, Indianapolis, IN). The crude lysate was heated at 95 °C for 3 min, chilled on ice for 2 min and then centrifuged at 14,000 rpm for 2 min (Eppendorf 5418, Hauppauge, NY). Supernatant was collected as the whole muscle lysate. Protein concentration was measured using the DC protein assay kit (Bio-Rad, Hercules, CA). For western blot, we loaded 5 to 100  $\mu$ g of protein per lane as indicated in the figures. Dystrophin was detected with Dys2 (1:100 Vector Laboratories, Burlingame, CA) and DysB (1:100, clone 34C5, IgG1; Novocastra, Newcastle, United Kingdom) antibodies. Utrophin was detected with a mouse monoclonal antibody against utrophin amino acid residues 768–874 (1:200; clone 55, IgG1; BD

Biosciences, San Diego, CA).  $\beta$ -Dystroglycan was detected with a mouse monoclonal antibody against the  $\beta$ -dystroglycan C-terminus (NCL-b-DG, 1:100; clone 43DAG1/8D5, IgG2a; Novocastra, Newcastle, United Kingdom).  $\alpha$ -Sarcoglycan was detected with a mouse monoclonal antibody against  $\alpha$ -sarcoglycan amino acid residues 217–289 (VP-A105; 1:1000; clone Ad1/20A6, IgG1; Vector Laboratories, Burlingame, CA). Syntrophin was detected with a pan-syntrophin mouse monoclonal antibody that recognizes the syntrophin PDZ domain (ab11425, 1:2000; clone 1351, IgG1; Abcam, Cambridge, MA). Dystrobrevin was detected with a mouse monoclonal antibody against dystrobrevin amino acid residues 249 to 403 (#610766, 1:1000; clone 23, IgG1; BD Biosciences, San Diego, CA). The calcium handling proteins were detected using sarcoplasmic/endoplasmic reticulum calcium ATPase 2a (SERCA2a, 1:2500 Badrilla, Leeds UK), calsequestrin (1:2500, Thermo Scientific, Grand Island NY) and phospholamban (1:2500 Badrilla, Leeds UK) antibodies. For the loading control, we used an antibody against glyceraldehyde 3-phosphate dehydrogenase (1:3000; Millipore, Billerica, MA) and the  $\alpha$ -tubulin antibody (1:3000; clone B-5-1-2; Sigma, St Louis, MO). Western blot quantification was performed using the ImageJ software (<http://rsbweb.nih.gov/ij/>) and LI-COR Image Studio Version 5.0.21 (<https://www.licor.com>) software. The intensity of the respective protein band was normalized to the corresponding loading control in the same blot. The relative band intensity in mdx3cv and mdx4cv mice was normalized to that of BL6 mice.

#### 4.4. ECG and hemodynamic assay

A 12-lead ECG assay was performed using a commercial system from AD Instruments (Colorado Springs, CO) according to our previously published protocol [30,31]. The Q wave amplitude was determined using the lead I tracing. Other ECG parameters were analyzed using the lead II tracing. The QTc interval was determined by correcting the QT interval with the heart rate as described by Mitchell et al. [49]. The cardiomyopathy index was calculated by dividing the QT interval by the PQ segment [50]. Left ventricular hemodynamics was evaluated using a Millar ultra-miniature pressure–volume (PV) catheter SPR 839. The catheter was placed in the left ventricle using a closed chest approach as we have previously described [30,31]. The resulting PV loops were analyzed with the PVAN software (Millar Instruments, Houston, TX). Detailed protocols for ECG and hemodynamic assays are available at the Parent Project Muscular Dystrophy standard operating protocol web site ([http://www.parentprojectmd.org/site/PageServer?pagename=Advance\\_researchers\\_sops](http://www.parentprojectmd.org/site/PageServer?pagename=Advance_researchers_sops)) [51].

#### 4.5. Statistical analysis

Data are presented as mean  $\pm$  stand error of mean. One-way ANOVA with Bonferroni's multiple comparison analysis was performed using the GraphPad PRISM software version 6.0 for Mac OSX (GraphPad Software, La Jolla, CA, [www.graphpad.com](http://www.graphpad.com)). A  $P < 0.05$  was considered statistically significant.

Supplementary data to this article can be found online at <http://dx.doi.org/10.1016/j.jmcc.2016.11.011>.

#### Disclosures/conflict of interests

DD is a member of the scientific advisory board for Solid GT, LLC and equity holders of Solid GT, LLC. DD and YY are inventors on patents that were licensed to Solid GT, LLC. The Duan lab has received research supports from Solid GT, LLC.

#### Acknowledgments

This work was supported by grants from the National Institutes of Health (HL-91883, NS-90634, AR-69085), Department of Defense (MD130014, MD150133), Jesse's Journey-The Foundation for Gene and Cell

Therapy. N.W. was partially supported by the life science fellowship, University of Missouri. We thank Dr. Brian Bostick for helpful discussion.

## References

- [1] L.M. Kunkel, 2004 William Allan award address. Cloning of the DMD gene, *Am. J. Hum. Genet.* 76 (2005) 205–214.
- [2] E.P. Hoffman, R.H. Brown Jr., L.M. Kunkel, Dystrophin: the protein product of the duchenne muscular dystrophy locus, *Cell* 51 (1987) 919–928.
- [3] A.E.H. Emery, F. Muntoni, *Duchenne Muscular Dystrophy*, 3rd ed. Oxford University Press, New York, 2003.
- [4] F. Muntoni, Cardiomyopathy in muscular dystrophies, *Curr. Opin. Neurol.* 16 (2003) 577–583.
- [5] J. Finsterer, C. Stollberger, The heart in human dystrophinopathies, *Cardiology* 99 (2003) 1–19.
- [6] G.F. Cox, L.M. Kunkel, Dystrophies and heart disease, *Curr. Opin. Cardiol.* 12 (1997) 329–343.
- [7] D. Duan, Dystrophin gene replacement and gene repair therapy for Duchenne muscular dystrophy in 2016, *Hum. Gene Ther. Clin. Dev.* 27 (2016) 9–18.
- [8] N.E. Bengtsson, J.T. Seto, J.K. Hall, J.S. Chamberlain, G.L. Odom, Progress and prospects of gene therapy clinical trials for the muscular dystrophies, *Hum. Mol. Genet.* 25 (R1) (2016) R9–17.
- [9] S.F. Phelps, M.A. Hauser, N.M. Cole, J.A. Rafael, R.T. Hinkle, J.A. Faulkner, et al., Expression of full-length and truncated dystrophin mini-genes in transgenic mdx mice, *Hum. Mol. Genet.* 4 (1995) 1251–1258.
- [10] D.J. Wells, K.E. Wells, E.A. Asante, G. Turner, Y. Sunada, K.P. Campbell, et al., Expression of human full-length and minidystrophin in transgenic mdx mice: implications for gene therapy of Duchenne muscular dystrophy, *Hum. Mol. Genet.* 4 (1995) 1245–1250.
- [11] C. Godfrey, S. Muses, G. McClorey, K.E. Wells, T. Coursindel, R.L. Terry, et al., How much dystrophin is enough: the physiological consequences of different levels of dystrophin in the mdx mouse, *Hum. Mol. Genet.* 24 (2015) 4225–4237.
- [12] P.S. Sharp, H. Bye-a-Jee, D.J. Wells, Physiological characterization of muscle strength with variable levels of dystrophin restoration in mdx mice following local antisense therapy, *Mol. Ther.* 19 (2011) 165–171.
- [13] M. Neri, S. Torelli, S. Brown, I. Ugo, P. Sabatelli, L. Merlini, et al., Dystrophin levels as low as 30% are sufficient to avoid muscular dystrophy in the human, *Neuromuscul. Disord.* 17 (2007) 913–918.
- [14] D. Li, Y. Yue, D. Duan, Preservation of muscle force in mdx3cv mice correlates with low-level expression of a near full-length dystrophin protein, *Am. J. Pathol.* 172 (2008) 1332–1341.
- [15] D. Li, Y. Yue, D. Duan, Marginal level dystrophin expression improves clinical outcome in a strain of dystrophin/utrophin double knockout mice, *PLoS One* 5 (2010), e15286.
- [16] M. van Putten, M. Hulsker, V.D. Nadarajah, S.H. van Heiningen, E. van Huizen, M. van Iterson, et al., The effects of low levels of dystrophin on mouse muscle function and pathology, *PLoS One* 7 (2012), e31937.
- [17] M. van Putten, M. Hulsker, C. Young, V.D. Nadarajah, H. Heemskerk, L. van der Weerd, et al., Low dystrophin levels increase survival and improve muscle pathology and function in dystrophin/utrophin double-knockout mice, *FASEB J.* 27 (2013) 2484–2495.
- [18] J.S. Chamberlain, Dystrophin levels required for correction of Duchenne muscular dystrophy, *Basic Appl. Myol.* 7 (1997) 251–255.
- [19] E.P. Hoffman, K. Arahata, C. Minetti, E. Bonilla, L.P. Rowland, Dystrophinopathy in isolated cases of myopathy in females, *Neurology* 42 (1992) 967–975.
- [20] R.W. Arpke, R. Darabi, T.L. Mader, Y. Zhang, A. Toyama, C.L. Lonetree, et al., A new immuno-, dystrophin-deficient model, the NSG-mdx4cv mouse, provides evidence for functional improvement following allogeneic satellite cell transplantation, *Stem Cells* 31 (2013) 1611–1620.
- [21] M. van Putten, E.M. van der Pijl, M. Hulsker, I.E. Verhaart, V.D. Nadarajah, L. van der Weerd, et al., Low dystrophin levels in heart can delay heart failure in mdx mice, *J. Mol. Cell. Cardiol.* 69 (2014) 17–23.
- [22] B. Wu, B. Xiao, C. Cloer, M. Shaban, A. Sali, P. Lu, et al., One-year treatment of morpholino antisense oligomer improves skeletal and cardiac muscle functions in dystrophic mdx mice, *Mol. Ther.* 19 (2011) 576–583.
- [23] Y. Yue, J.W. Skimming, M. Liu, T. Strawn, D. Duan, Full-length dystrophin expression in half of the heart cells ameliorates beta-isoproterenol-induced cardiomyopathy in mdx mice, *Hum. Mol. Genet.* 13 (2004) 1669–1675.
- [24] B. Bostick, Y. Yue, C. Long, D. Duan, Prevention of dystrophin-deficient cardiomyopathy in twenty-one-month-old carrier mice by mosaic dystrophin expression or complementary dystrophin/utrophin expression, *Circ. Res.* 102 (2008) 121–130.
- [25] G.A. Cox, S.F. Phelps, V.M. Chapman, J.S. Chamberlain, New mdx mutation disrupts expression of muscle and nonmuscle isoforms of dystrophin, *Nat. Genet.* 4 (1993) 87–93.
- [26] J.A. Rafael, Y. Nitta, J. Peters, K.E. Davies, Testing of SHIRPA, a mouse phenotypic assessment protocol, on Dmd(mdx) and Dmd(mdx3cv) dystrophin-deficient mice, *Mamm. Genome* 11 (2000) 725–728.
- [27] V.M. Chapman, D.R. Miller, D. Armstrong, C.T. Caskey, Recovery of induced mutations for X chromosome-linked muscular dystrophy in mice, *Proc. Natl. Acad. Sci.* 86 (1989) 1292–1296.
- [28] B. Bostick, Y. Yue, D. Duan, Gender influences cardiac function in the mdx model of Duchenne cardiomyopathy, *Muscle Nerve* 42 (2010) 600–603.
- [29] Y. Lai, J. Zhao, Y. Yue, N.B. Wasala, D. Duan, Partial restoration of cardiac function with  $\Delta$ PDZ nNOS in aged mdx model of Duchenne cardiomyopathy, *Hum. Mol. Genet.* 23 (2014) 3189–3199.
- [30] B. Bostick, Y. Yue, D. Duan, Phenotyping cardiac gene therapy in mice, *Methods Mol. Biol.* 709 (2011) 91–104 (Clifton, NJ).
- [31] N.B. Wasala, B. Bostick, Y. Yue, D. Duan, Exclusive skeletal muscle correction does not modulate dystrophic heart disease in the aged mdx model of Duchenne cardiomyopathy, *Hum. Mol. Genet.* 22 (2013) 2634–2641.
- [32] B. Bostick, J.H. Shin, Y. Yue, N.B. Wasala, Y. Lai, D. Duan, AAV micro-dystrophin gene therapy alleviates stress-induced cardiac death but not myocardial fibrosis in >21-month-old mdx mice, an end-stage model of Duchenne muscular dystrophy cardiomyopathy, *J. Mol. Cell. Cardiol.* 53 (2012) 217–222.
- [33] B. Bostick, J.H. Shin, Y. Yue, D. Duan, AAV-microdystrophin therapy improves cardiac performance in aged female mdx mice, *Mol. Ther.* 19 (2011) 1826–1832.
- [34] A. Aartsma-Rus, A. Ferlini, N. Goemans, A.M. Pasmooij, D.J. Wells, K. Bushby, et al., Translational and regulatory challenges for exon skipping therapies, *Hum. Gene Ther.* 25 (2014) 885–892.
- [35] T. Koo, M.J. Wood, Clinical trials using antisense oligonucleotides in Duchenne muscular dystrophy, *Hum. Gene Ther.* 24 (2013) 479–488.
- [36] C.E. Nelson, C.H. Hakim, D.G. Ousterout, P.I. Thakore, E.A. Moreb, R.M. Rivera, et al., In vivo genome editing improves muscle function in a mouse model of Duchenne muscular dystrophy, *Science* 351 (2016) 403–407.
- [37] D. Townsend, M. Daly, J.S. Chamberlain, J.M. Metzger, Age-dependent dystrophin loss and genetic reconstitution establish a molecular link between dystrophin and heart performance during aging, *Mol. Ther.* 19 (2011) 1821–1825.
- [38] N.B. Wasala, Y. Lai, J.H. Shin, J. Zhao, Y. Yue, D. Duan, Genomic removal of a therapeutic mini-dystrophin gene from adult mice elicits a Duchenne muscular dystrophy-like phenotype, *Hum. Mol. Genet.* 25 (2016) 2633–2644.
- [39] S. Guiraud, A. Aartsma-Rus, N.M. Vieira, K.E. Davies, E.J. van Ommen, L.M. Kunkel, The pathogenesis and therapy of muscular dystrophies, *Annu. Rev. Genomics Hum. Genet.* 16 (2015) 281–308.
- [40] N. Shirokova, E. Niggli, Cardiac phenotype of duchenne muscular dystrophy: insights from cellular studies, *J. Mol. Cell. Cardiol.* 58 (2013) 217–224.
- [41] F. Kamdar, D.J. Garry, Dystrophin-deficient cardiomyopathy, *J. Am. Coll. Cardiol.* 67 (2016) 2533–2546.
- [42] T.L. van Westering, C.A. Betts, M.J. Wood, Current understanding of molecular pathology and treatment of cardiomyopathy in duchenne muscular dystrophy, *Molecules* 20 (2015) 8823–8855.
- [43] B. Bostick, Y. Yue, Y. Lai, C. Long, D. Li, D. Duan, Adeno-associated virus serotype-9 microdystrophin gene therapy ameliorates electrocardiographic abnormalities in mdx mice, *Hum. Gene Ther.* 19 (2008) 851–856.
- [44] B. Gavillet, J.S. Rougier, A.A. Domenighetti, R. Behar, C. Boixel, P. Ruchat, et al., Cardiac sodium channel Nav1.5 is regulated by a multiprotein complex composed of syntrophins and dystrophin, *Circ. Res.* 99 (2006) 407–414.
- [45] B.C. Willis, D. Ponce-Balbuena, J. Jalife, Protein assemblies of sodium and inward rectifier potassium channels control cardiac excitability and arrhythmogenesis, *Am. J. Physiol. Heart Circ. Physiol.* 308 (2015) H1463–H1473.
- [46] L.A. Barouch, R.W. Harrison, M.W. Skaf, G.O. Rosas, T.P. Cappola, Z.A. Kobeissi, et al., Nitric oxide regulates the heart by spatial confinement of nitric oxide synthase isoforms, *Nature* 416 (2002) 337–339.
- [47] G.P. Ahern, S.F. Hsu, V.A. Klyachko, M.B. Jackson, Induction of persistent sodium current by exogenous and endogenous nitric oxide, *J. Biol. Chem.* 275 (2000) 28810–28815.
- [48] D. Li, Y. Yue, Y. Lai, C.H. Hakim, D. Duan, Nitrosative stress elicited by nNOS $\beta$  delocalization inhibits muscle force in dystrophin-null mice, *J. Pathol.* 223 (2011) 88–98.
- [49] G.F. Mitchell, A. Jeron, G. Koren, Measurement of heart rate and Q-T interval in the conscious mouse, *Am. J. Phys.* 274 (1998) H747–H751.
- [50] G. Nigro, L.I. Comi, L. Politano, G. Nigro, Cardiomyopathies associated with muscular dystrophies, in: A. Engel, C. Franzini-Armstrong (Eds.), *Myology: Basic and Clinical*, third ed. McGraw-Hill, Medical Pub. Division, New York 2004, pp. 1239–1256.
- [51] D. Duan, J.A. Rafael-Fortney, A. Blain, D.A. Kass, E.M. McNally, J.M. Metzger, et al., Standard operating procedures (SOPs) for evaluating the heart in preclinical studies of Duchenne muscular dystrophy, *J. Cardiovasc. Transl. Res.* 9 (2016) 85–86.

**Uniform low-level dystrophin expression in the heart partially preserved cardiac function  
in an aged mouse model of Duchenne cardiomyopathy**

Nalinda B. Wasala<sup>1</sup>, Yongping Yue<sup>1</sup>, Jenna Vance<sup>1</sup>, Dongsheng Duan<sup>1-4,\*</sup>

1, Department of Molecular Microbiology and Immunology, School of Medicine, The University of Missouri, Columbia, MO 65212, USA

2, Department of Neurology, School of Medicine, The University of Missouri, Columbia, MO 65212, USA

3, Department of Bioengineering, The University of Missouri, Columbia, MO 65212, USA

4, Department of Biomedical Sciences, College of Veterinary Medicine, The University of Missouri, Columbia, MO 65212, USA

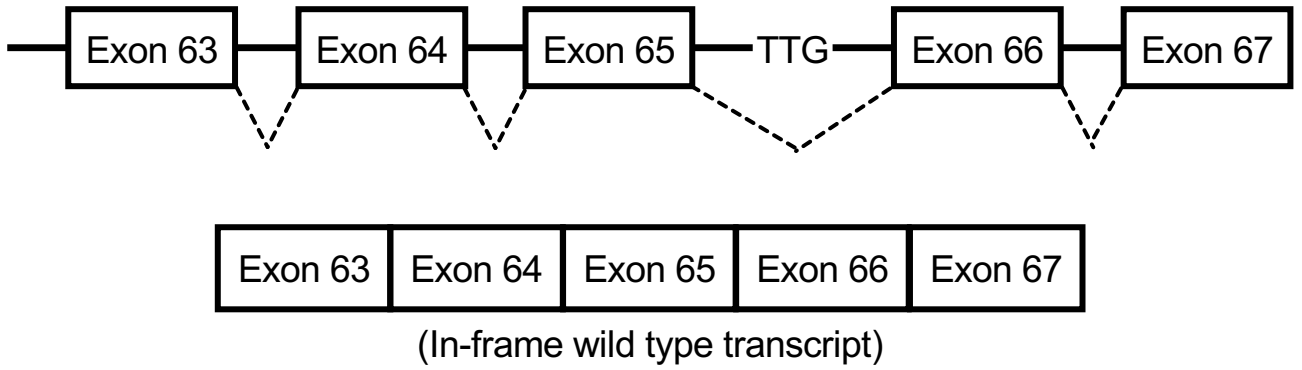
\*Corresponding Address:

Dongsheng Duan Ph.D.  
Professor  
Department of Molecular Microbiology and Immunology  
One Hospital Dr.  
Columbia, MO 65212  
Phone: 573-884-9584  
Fax: 573-882-4287  
Email: [duand@missouri.edu](mailto:duand@missouri.edu)

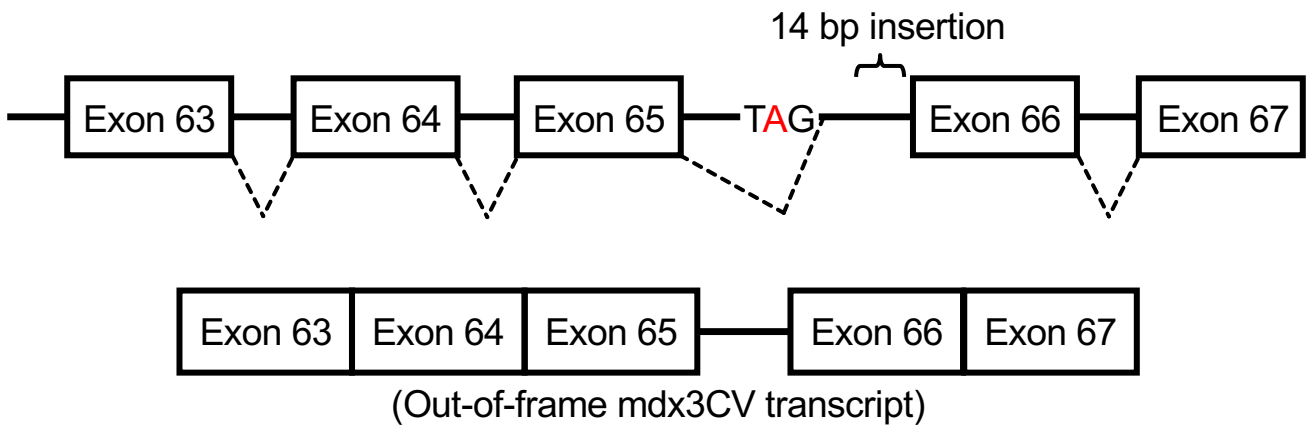
## Supplementary Figure legend

**Supplementary Figure 1. Mdx3cv mouse produces low levels of dystrophin due to an aberrant splicing event.** **A**, A cartoon showing in-frame splicing events (occurring in exon 63-67) in wildtype mice to produce full length dystrophin. **B**, In mdx3cv mice, a mutation (marked in red) results in out-of-frame transcript. **C**, The transcript generated by skipping exons 65 and 66 ( $\Delta 65/66$ ) generates an in-frame transcript that produces low levels of dystrophin in mdx3cv mice.

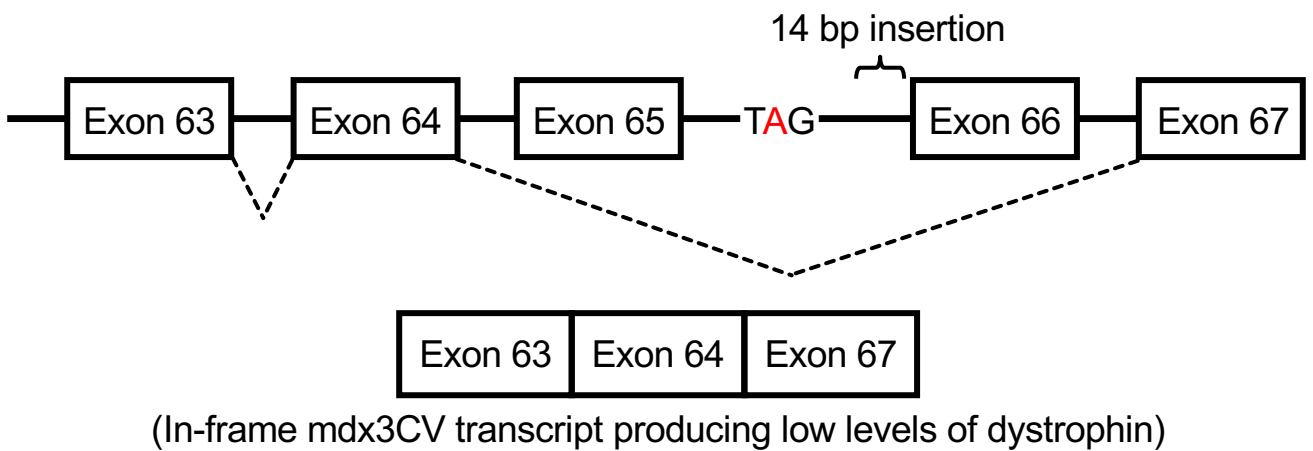
A



B



C





# Nanotherapy for Duchenne muscular dystrophy

Michael E. Nance,<sup>1</sup> Chady H. Hakim,<sup>1,2</sup> N. Nora Yang<sup>2</sup> and Dongsheng Duan<sup>1,3,4,5\*</sup>

Duchenne muscular dystrophy (DMD) is a lethal X-linked childhood muscle wasting disease caused by mutations in the dystrophin gene. Nanobiotechnology-based therapies (such as synthetic nanoparticles and naturally existing viral and nonviral nanoparticles) hold great promise to replace and repair the mutated dystrophin gene and significantly change the disease course. While a majority of DMD nanotherapies are still in early preclinical development, several [such as adeno-associated virus (AAV)-mediated systemic micro-dystrophin gene therapy] are advancing for phase I clinical trials. Recent regulatory approval of Ataluren (a nonsense mutation read-through chemical) in Europe and Exondys51 (an exon-skipping antisense oligonucleotide drug) in the United States shall offer critical insight in how to move DMD nanotherapy to human patients. Progress in novel, optimized nano-delivery systems may further improve emerging molecular therapeutic modalities for DMD. Despite these progresses, DMD nanotherapy faces a number of unique challenges. Specifically, the dystrophin gene is one of the largest genes in the genome while nanoparticles have an inherent size limitation per definition. Furthermore, muscle is the largest tissue in the body and accounts for 40% of the body mass. How to achieve efficient bodywide muscle targeting in human patients with nanomedication remains a significant translational hurdle. New creative approaches in the design of the miniature micro-dystrophin gene, engineering of muscle-specific synthetic AAV capsids, and novel nanoparticle-mediated exon-skipping are likely to result in major breakthroughs in DMD therapy. © 2017 Wiley Periodicals, Inc.

## How to cite this article:

*WIREs Nanomed Nanobiotechnol* 2017, e1472. doi: 10.1002/wnan.1472

\*Correspondence to: duand@missouri.edu

<sup>1</sup>Department of Microbiology and Immunology, University of Missouri School of Medicine, Columbia, MO, USA

<sup>2</sup>National Center for Advancing Translational Sciences, NIH, Rockville, MD, USA

<sup>3</sup>Department of Neurology, University of Missouri, Columbia, MO, USA

<sup>4</sup>Department of Bioengineering, University of Missouri, Columbia, MO, USA

<sup>5</sup>Department of Biomedical Sciences, University of Missouri, Columbia, MO, USA

Conflict of interest: The authors ME Nance, CH Hakim and NN Yang have declared no conflicts of interest for this article whereas author D Duan has the following conflict of interest. D Duan is a member of the scientific advisory board for Solid GT, LLC and an equity holder of Solid GT, LLC. D Duan is an inventor on a patent licensed to Solid GT, LLC. The Duan lab has received research supports from Solid GT, LLC.

## INTRODUCTION

Duchenne muscular dystrophy (DMD) is a progressive, eventually fatal muscle wasting disease in male children resulting from the functional loss of the dystrophin protein. The estimated disease occurrence is 1:5000 male births.<sup>1–3</sup> Affected children are typically diagnosed between the ages of 2 and 5 due to delayed motor skills, cognitive delay, and elevated creatine kinase. Without intervention, patients are unable to walk and require a wheelchair by the ages of 10–12 and have a mean survival of 19 years due to cardiopulmonary complications (<http://www.cdc.gov/ncbddd/muscardystrophy/data.html#ref>).<sup>4</sup> Microscopically, affected muscles show an absence of dystrophin at the sarcolemma by immunostaining and a variety of histological features of muscle degeneration, regeneration, inflammation, and fatty fibrosis (Figure 1). In

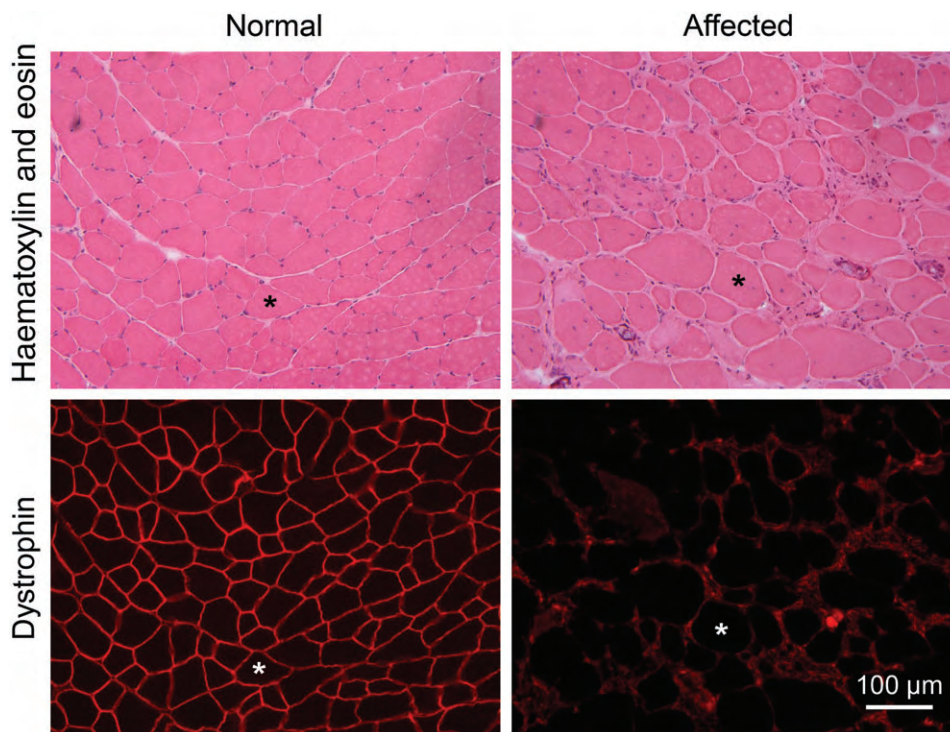


**FIGURE 1** | Histopathology and dystrophin immunostaining. Top panels show representative photomicrographs of hematoxylin–eosin (HE)-stained skeletal muscle cross-sections from a normal and an affected mouse. Bottom panels are serial sections immunostained with a monoclonal antibody that recognizes dystrophin. In normal muscle, dystrophin is localized at the muscle cell membrane. Lack of dystrophin leads to muscle degeneration/regeneration, necrosis, inflammatory cell infiltration, and replacement of deceased muscle by fat and fibrotic tissues. The presence of centrally located nuclei in dystrophic muscle fibers indicates recent fiber regeneration. Asterisks represent the same myofiber in serial muscle sections. The interstitial fluorescence signals seen in the immunostaining image of the affected mouse muscle is due to cross-reaction of the secondary antibody (Alex 594-conjugated anti-mouse antibody) to the inflamed mouse muscle.

the heart, dystrophin-deficient cardiomyocytes are vulnerable to mechanical stress resulting in cardiac injury and the development of dilated cardiomyopathy and arrhythmias (see Box 1).<sup>5,6</sup> Currently, glucocorticoids are the most widely used medication for DMD. Although it has been shown that glucocorticoids can expand the lifespan by approximately 3 years, reduce scoliosis, and delay cardiomyopathy,<sup>7–9</sup> long-term use of steroid is notoriously associated with a constellation of side effects including Cushingoid features, adverse behavioral events, hypertension, vertebral fracture, cataracts, excessive weight gain, and growth retardation.<sup>10,11</sup> These untoward reactions reduce the life quality and health span of patients. A definitive therapy for DMD will require restoration of a functional dystrophin protein to the muscle sarcolemma. This can be achieved by replacing, repairing, or bypassing the mutated dystrophin gene. The emergence of several viable options for DMD gene therapy has turned the focus to drug delivery systems. Indeed, the pharmacokinetic challenges involved in the delivery of

therapeutic molecules is one of the foremost obstacles in the gene therapy field. Selectivity is a key concern especially when considering gene supplementation, replacement, integration, or genome editing. Herein lies a great opportunity for nanomedicine and, in particular, nanometer scale drug delivery systems. In this review, we discuss the current and emerging nanomedications and nanotechnologies that can restore dystrophin expression. We divide DMD nanotherapy into nonviral and viral approaches. We begin with a historical discussion on strategies that are highly relevant but often not considered as nanotherapy. These include read-through molecules, naked plasmid DNA, and antisense oligonucleotides (AONs). Next, we discuss nonviral nanotechnology including lipid- and polymer-based nanoparticles, chemically modified nanoparticles, and exosome therapies. Finally, we consider viral approaches with a special focus on the progress with adeno-associated virus (AAV)-mediated micro-dystrophin gene therapy (Table 1).

## BOX 1

## CLINICAL AND PATHOLOGICAL ASPECTS OF DILATED CARDIOMYOPATHY IN DMD

Cardiac manifestations are present in around 25% of patients by age 6, 59% by age 10, and >90% by age 18 years or older.<sup>31</sup> Primary clinical findings include fatigue, shortness of breath, and palpitations related to a decline in the systolic ejection fraction, autonomic dysfunction, and increased occurrence of arrhythmias. On electrocardiogram, DMD patients show tachycardia and have a shortened PR interval, tall R wave, and deep Q wave in the left precordial leads.<sup>32</sup> Echocardiography typically shows decreased wall motion in the left postero-basal ventricle, ventricular wall dilation, and thinning with a reduced ejection fraction. Histologically, the progression of dystrophic cardiomyopathy is characterized by interstitial fibrosis, myocardial inflammation, and loss of cardiomyocytes.<sup>32</sup>

## A HISTORICAL PERSPECTIVE ON DMD GENE THERAPY

Great successes have been achieved over the last four decades in the development of a genetic therapy for DMD. These include reading through of nonsense mutations using chemicals, modulation of the splicing machinery to skip mutated exons using AONs, and introduction of a functional dystrophin gene. Advances in these fronts have set the stage for nanoparticle-mediated DMD gene therapy. To frame DMD nanotherapy in the right context, next we briefly review the current status of nonnanotherapies.

## Small Molecules Targeting Nonsense Mutations

About 10% of DMD cases results from nonsense mutation (a mutation that converts an amino acid coding codon into one of the three stop codons including TAG, TGA, or TAA). Premature stop codons result in various truncated, nonfunctional dystrophin proteins that are often degraded. For these mutations, small molecules targeting ribosomal recognition of stop codons may be used to continue translation through the premature stop codon. Initially, this phenomenon was appreciated with the aminoglycoside antibiotic gentamicin. However, gentamicin is poorly tolerated in humans and has a low potency.<sup>33</sup> In 2007, Welch and colleagues identified

PTC124 through high-throughput screening of over 800,000 small molecules followed by chemical modification and optimization.<sup>34</sup> PTC124, now known as Ataluren, is thought to cause translation read through; however, this mechanism has been debated. Several studies have raised questions about the assay used in the molecule's discovery.<sup>35,36</sup> Although contested, a subset of patients treated with low-dose (40 mg/kg/day) Ataluren showed improvement in the 6-min walk test (6MWT).<sup>37</sup> Interestingly, these benefits were not seen with the high dose (80 mg/kg/day). Based on the results of the clinical trials, Ataluren may be well suited for patients that meet a certain set of criteria. In July 2014, Ataluren received approval in the European Union for treatment of ambulant DMD patients who are older than 5 years and carry a nonsense mutation.<sup>38</sup> Additional high-throughput screenings are ongoing in several places. It is very likely that new compounds with better pharmacokinetic and pharmacodynamic profiles will be identified to suppress nonsense mutations in DMD.<sup>39</sup>

## Naked Plasmid DNA Delivery of the Dystrophin Gene

In the early 1990s, it was recognized that naked plasmid DNA containing the dystrophin cDNA could be delivered to muscle via direct injection.<sup>40,41</sup> Naked plasmid DNA has the advantage of delivering a full-length dystrophin coding sequence and may likely be minimally immunogenic. However, low transduction efficiency has limited its use. A number of strategies have been developed to enhance plasmid DNA delivery by electroporation, ultrasound, or pretreatment with hyaluronidase.<sup>42,43</sup> Yet, it is not clear whether these strategies can be translated to human patients. Furthermore, even with these strategies, dystrophin expression remains moderate from naked plasmid delivery. Some groups have shown that dystrophin plasmid can be delivered to dystrophic dog muscle.<sup>44</sup> A human trial by direct muscle injection showed some limited dystrophin expression with no evidence of an immune response.<sup>45</sup> Limiting factors for direct plasmid DNA delivery may include, but not limited to, promoter inactivation, plasmid loss, and inefficient trafficking to the nucleus.

## Exon-Skipping with AONs

More than 90% mutations in DMD disrupt the reading frame. AONs-mediated exon-skipping is developed to modulate the cellular splicing machinery, so that the targeted exon(s) can be deleted in the RNA transcript. Exon-skipping could, in theory, address a large percentage of frame-shift mutations by intentionally skipping one or multiple exons to restore the normal

**TABLE 1** | Overview of DMD Nanotherapy

	Comments	Reference
<i>Nonviral nanotherapy</i>		
Polymersomes	Amphiphilic block copolymers encapsidating AON, siRNA, or viral nucleic acids. Improved exon-skipping in mdx mice	Kim et al. <sup>12</sup>
Liposomes and lipid-nucleic acid complexes	Liposomes, thermoplastic nanoparticles with cationic lipids and bubble liposomes. Tested in mice	Afzal et al. <sup>13</sup> ; Negishi et al. <sup>14</sup>
Cell-penetrating peptides and peptide-nucleic acid complexes	Peptide-AONs. Very promising for improved exon-skipping; studies mainly in mice	Ezzat et al. <sup>15</sup> ; Gao et al. <sup>16</sup> ; Lehto et al. <sup>17</sup> ; Shabanpoor et al. <sup>18</sup>
PMMA nanoparticles	T1 and ZM2 nanoparticles are highly promising for bodywide muscle delivery. Greatly enhances exon-skipping in mice	Rimessi et al. <sup>19</sup> ; Ferlini et al. <sup>20</sup> ; Bassi et al. <sup>21</sup> ; Falzarano et al. <sup>22</sup>
Exosomes	A very promising new gene delivery approach not explored for DMD therapy yet	
<i>Viral nanotherapy</i>		
AAV	20–25 nm. Persists as episome. AAV micro-dystrophin has been tested in human patients. Systemic AAV microgene therapy is at the forefront for DMD therapy. AAV-mediated CRISPR genome editing also holds great promise.	Mendell et al. <sup>23</sup> ; Yue et al. <sup>24</sup> ; Nelson et al. <sup>25</sup>
Adenovirus	100 nm. Tested in animals extensively in 1990s. Unlikely to be used due to toxicity and immunogenicity	DelloRusso et al. <sup>26</sup> ; Deol et al. <sup>27</sup> ; Maggio et al. <sup>28</sup>
Lentivirus	80–120 nm. Chromosomally integrated. Lentiviral micro-dystrophin tested in mice. Transduces satellite cells	Muir et al. <sup>29</sup> ; Naldini et al. <sup>30</sup>

reading frame. This results in the production of internally truncated but likely functional dystrophin proteins. Uncharged phosphorodiamidate morpholino oligonucleotides (PMOs) are among the most commonly used AONs. PMOs have phosphorodiamidate linkages and a morpholine ring instead of ribose sugar. These modifications confer nuclease resistance, enhance binding to mRNA, and prevent RNaseH activity that would degrade the mRNA. The most widely known PMO for DMD exon-skipping is Exondys51 (also known as AVI-4658 and Eteplirsen). Exondys51 specifically targets exon 51, which could theoretically treat 13% of DMD patients. Exondys51 has been tested in several clinical trials.<sup>46</sup> These studies suggest that Exondys51 is safe and can restore dystrophin expression on immunofluorescence staining. Compared with historic data, Exondys51 appears to have improved ambulation. On September 19, 2016, the U.S. Food and Drug Administration (FDA) granted accelerated approval to Exondys51 as an injection drug for treating DMD patients who have a confirmed mutation amenable to exon 51 skipping (<http://www.fda.gov/NewsEvents/Newsroom/PressAnnouncements/ucm521263.htm>).

One of the most exciting new developments in exon-skipping is the engineering of tri-cycloDNA

AONs (tcDNA-AONs) by Goyenvalle et al.<sup>47</sup> TcDNA spontaneously forms nanoparticles ranging in size from 40 to 100 nm. Systemic administration of tcDNA-AONs resulted in phenomenal uptake in many tissues including skeletal muscle, heart, and brain. Importantly, tcDNA exon-skipping significantly attenuated dystrophic phenotypes in mdx mice and the much severer utrophin–dystrophin double knockout mice. Skeletal muscle, cardiac, respiratory, and behavior functions were all significantly improved and were not associated with overt toxicity.<sup>47</sup> In addition to tcDNA-AONs, another recently developed octa-guanidine dendrimer-conjugated AONs (called vivo-morpholinos) may also greatly enhance exon-skipping efficiency (reviewed in Ref 48). Studies from several groups suggest that vivo morpholinos are highly powerful for long-term systemic exon-skipping therapy in both rodent and canine models of DMD.<sup>49–52</sup>

## NONVIRAL-BASED NANOPARTICLES FOR DMD THERAPY

The delivery of nucleic acids can be significantly enhanced by the modification of nucleotide chemistry and/or complexing with polymers, lipids, and

peptides. In essence, these changes result in the formation of chemically and/or biologically engineered nanoparticles. Such nanoparticles can improve tissue targeting/penetration, protect nucleic acids from degradation, and help evade untoward immune reactions. A number of conjugated AONs have been tested in animal models of DMD.<sup>48</sup> Next, we discuss the current and emerging nonviral nano delivery strategies focusing on advances in AON exon skipping.

## Polymersomes

Originally described in 1995, polymersomes are biocompatible nanoparticles composed of amphiphilic block copolymers (e.g., polyethylene glycol and polylactic acid mixtures).<sup>53,54</sup> In the years following their discovery, polymersomes were shown to have enhanced physical properties in comparison to liposomes such as increased water resistance and enormous flexibility in composition.<sup>55</sup> Recent studies have further expanded our knowledge of polymer-some formulation. Polymersomes are highly variable in terms of their properties. Depending on the polymers used in formulation and methods used in production, polymersomes can be generated to display a variety of different chemical, physical, and biological features.<sup>56</sup> Polymersomes may also be functionalized by the inclusion of integral membrane proteins such as channels and tailored to specific sizes. The ideal size of polymersomes is in the range of approximately 90 to  $\leq 120$  nm. This size allows efficiently entry into the cells while at the same time not be removed from the blood by the mononuclear phagocyte system.<sup>57</sup> Importantly, polymersomes may be loaded with DNA molecules either through encapsidation during formulation or by using virus to inject DNA through integral proteins.<sup>57,58</sup> As a tool for DMD therapy, Discher's group recently developed a polycaprolactone-formulated, degradable polymersome for AON delivery. Compared to naked AON, polymersome delivery significantly enhanced exon-skipping efficiency in mdx mice.<sup>12</sup> Recent data from the Lu laboratory suggest that polyethylenimine-conjugated pluronic polycarbamates represent yet another type of chemically complexed nanoparticles very promising for enhancing dystrophin exon-skipping.<sup>59–62</sup>

## Lipid Nanoparticles

The concept of lipid enclosed drug delivery systems emerged over 40 years ago (reviewed in Ref 63). The initial observations in the early 1980s that lipid formulations could enhance the delivery of nucleic acids

opened an entire field of nanomedicines.<sup>64,65</sup> Over the years, our understanding of lipid–nucleic acid complexes has greatly increased. In addition to extending the circulation time and reducing toxicity, lipid-based nanoparticles also enhance the potency of the nucleic acid cargo by protecting it from degradation.<sup>66</sup>

Lipid nanoparticles and liposomes have been used to deliver exon-skipping AONs for DMD gene therapy. In the former, cationic lipids are used to coat chemically engineered dendrimeric AON nanoparticles such as poly-methyl methacrylate (PMMA) nanoparticles.<sup>67</sup> In the later, AONs are encapsidated inside hollow lipid nanospheres. Dendritic nanoparticles can also be incorporated into liposomes and form nanolipodendrosome for improved delivery.<sup>13</sup> Recently, investigators have begun to explore bubble liposomes for AON delivery. Bubble liposomes contain an ultrasound-responsive imaging gas such as perfluoropropane that may be triggered to burst with ultrasound cavitation.<sup>68</sup> This novel strategy has greatly improved localized exon-skipping following direct muscle injection.<sup>14</sup> Lastly, as liposomes mimic the cellular membrane, it is possible to functionalize liposomes with various cell targeting peptides.

## PMMA Nanoparticles

Dendrimeric PMMA nanoparticles are a highly promising group of drug carriers developed by the Ferlini laboratory (reviewed in Ref 67). Based on the size, PMMA nanoparticles are divided into two categories, approximately 420 nm T1 PMMA nanoparticles and approximately 130 nm ZM2 PMMA nanoparticles. T1 nanoparticles have greatly improved the pharmacokinetics of AONs delivery. In one study, T1 nanoparticles at a 50-fold lower dose ( $\sim 3$  mg/kg) yielded the similar levels of exon-skipping in comparison to that of naked AONs ( $\sim 150$  mg/kg).<sup>19</sup> The major limitation of T1 nanoparticles is the poor transduction efficiency in the heart. Furthermore, accumulation of T1 nanoparticles in circulating macrophages and endothelial cells may represent an important immunological concern. ZM2 nanoparticles are developed as an alternative to T1 nanoparticles. They consist of a PMMA core and an *N*-isopropyl-acrylamide shell. In contrast to T1 nanoparticles, ZM2 nanoparticle delivery resulted in efficient myocardial exon-skipping. Recent studies suggest that PMMA nanoparticles can greatly improve bodywide delivery of AONs and dystrophin restoration by exon-skipping in striated muscles.<sup>19–22,67</sup> Further development of this delivery strategy is warranted.

## Cell-Penetrating Peptides

Peptide conjugation significantly enhances biological activities of AON nanoparticles (reviewed in Refs 69–71). Two types of peptides are used including (1) cell-penetrating peptides which contain peptide transduction domains for efficient delivery into cells, and (2) homing peptides for targeting specific cells and/or tissues. In this regard, muscle- and heart-specific peptides are especially critical for DMD gene therapy.<sup>72</sup> Peptide can be conjugated to the cargo either covalently or indirectly via a linker. Failure to reach the heart is a major hurdle in early DMD exon-skipping studies. The development of peptide-conjugated AON nanoparticles has successfully overcome this obstacle.<sup>61,73–83</sup> Recent studies have further illustrated therapeutic potential of peptide-AON nanoparticles for DMD therapy.<sup>15–18</sup>

## Exosomes, Naturally Occurring Biological Nanoparticles for DMD Therapy

Exosomes are 30–100 nm extracellular vesicles released by many cell types throughout the body. Naturally, exosomes may be found in the blood and are known to transport mRNA, small noncoding RNAs, and proteins. Exosomes originate from endosomal-derived multivesicular bodies, which give rise to intraluminal vesicles.<sup>84</sup> Exosomes are nonimmunogenic and tend to share characteristics with the host cell from which they are derived. Exosomes have been explored to treat ischemia/reperfusion in the myocardial infarction model in animals.<sup>85,86</sup> Recent studies suggest that exosomes may also be responsible for conveying the cardioprotective effects of cardiosphere-derived cells.<sup>87</sup> Importantly, exosomes have been used to package therapeutically relevant nucleic acids (such as short-interfering silencing RNAs) for *in vivo* gene therapy in muscle.<sup>88</sup> Furthermore, cell/tissue-targeting peptides can be fused to the selected exosomal membrane proteins to achieve targeted delivery.<sup>88</sup> While direct evidence for exosome-mediated DMD nanotherapy is currently lacking, it is expected that engineered exosomes will be a highly attractive future avenue for delivering muscle/heart-specific noncoding RNAs (such as microRNAs, silencing RNAs, and long noncoding RNAs) to modulate DMD pathogenesis.<sup>89–92</sup> Perhaps, the most appealing application of exosomes is to use these nanoparticles to deliver dystrophin mRNA (either full-length or abbreviated) for DMD gene replacement therapy and/or to deliver the CRISPR-Cas9 system for DMD gene-editing therapy.

## VIRAL VECTORS AS BIOLOGICAL NANOPARTICLES

Viral particles have a long history as gene therapy tools but the utility and modularity of viral particles is only being realized in more recent years. Compared to nonviral nanoparticles, viral vectors have inherent advantages. Viruses are versatile, nano-scale biological carriers that have been evolved over millions of years to target, enter, and alter cellular behaviors through the expression of viral-coded genes. Several viruses also establish latent infection which leads to prolonged gene expression. This is highly beneficial for DMD where long-term expression is required. Furthermore, the atomic structures of many viruses have been solved and structure–function correlation studies have started to reveal critical structural domains involved in targeting, stability, and immune evasion.<sup>72</sup>

In the context of this review article, it is worth pointing out that the distinction between viral and nonviral nanoparticles is increasingly becoming blurred from the standpoint of gene delivery vehicles. On one hand, viral proteins have been incorporated in nanoparticles for effective cellular and nuclear entry (such as the Tat protein from human immunodeficiency virus). On the other hand, numerous fully striped or gutted viral vectors have emerged over the last two decades. These gutless viral vectors contain minimal viral sequences and do not express any viral replication or capsid proteins. The development of custom-designed viral capsids by forced evolution and/or educated engineering has created huge potentials in manufacturing virus-like capsids. These custom-designed capsid proteins bear nominal amino acid similarity to wild-type viral capsid proteins. In other words, such engineered virus-like particles have no naturally existing counterpart.

Due to space limitations, we only discuss vectors based on lentivirus, adenovirus, and AAV.

## Lentivirus

Lentivirus is a genus of retroviridae family virus. Lentivirus is enveloped and has a size of 80–120 nm. Lentivirus carries two copies of the positive single-stranded RNA genome. Lentivirus can infect quiescent cells and induces long-term expression by integrating into the host genome.<sup>30,93</sup> While it has been shown that lentivirus can target satellite cells *in vivo* in neonatal and young dystrophic mice,<sup>94,95</sup> most applications have focused on *ex vivo* cell therapy. In brief, stem cells (including myogenic progenitor cells, mesenchymal stem cells, and dermal fibroblasts) are

infected with a lentivirus carrying either a full-length or an abbreviated dystrophin gene. Subsequent engraftment in dystrophic muscle results in dystrophin expression in regenerated muscle.<sup>29,96–100</sup> Alternatively, stem cells can also be isolated from human patients and transplanted back to dystrophic muscle after correction with lentivirus-mediated delivery of various dystrophin repair mechanisms.<sup>99,101,102</sup>

## Adenovirus

Adenoviruses are 90–100 nm nonenveloped icosahedral double-stranded DNA viruses. Several generations of adenovirus vectors have been developed including E1/E3-deleted first-generation (can package ~8 kb), E1/E2/E3 and E4-deleted second-generation (can package ~14 kb), and the entire genome-deleted gutted adenovirus (can package ~38 kb). Adenovirus has been used to deliver the 6- to 8-kb mini-dystrophin gene, the full-length dystrophin coding sequence, the dystrophin homologue utrophin gene, and the CRISPR-Cas9 system.<sup>26–28,103–105</sup> However, because adenovirus infection induces prominent cellular immune responses and adenovirus cannot efficiently infect mature muscle, it is generally agreed that adenoviral vector is not an ideal vector system for DMD gene therapy.

## Adeno-Associated Virus

### Basic Biology of AAV

AAV is the premier gene delivery vector for DMD.<sup>106,107</sup> It belongs to the parvovirus family and is dependent on a helper virus (such as adenovirus) for productive infection.<sup>108–111</sup> The nonenveloped, icosahedral AAV capsid is approximately 20 nm.<sup>112</sup> Wild-type AAV is considered nonpathogenic. Recombinant AAV vectors are in general devoid of all viral genes. AAV can persist episomally allowing long-term gene expression.<sup>113</sup> Most importantly, AAV is the only virus that can effectively transduce all striated muscles in the body.<sup>114</sup>

Twelve AAV serotypes and several hundreds of AAV variants have been published.<sup>72,115–121</sup> While they all share significant sequence homology, the differences in regions primarily localized to the surface exposed loops yield a variety of unique tropisms and immunogenicity.<sup>122–125</sup>

### Overcoming the Packaging Size Restrain

AAV-mediated DMD gene therapy faces several unique challenges. The most obvious one is the limited packaging capacity of AAV. The wild-type AAV

genome is approximately 4.6 to 4.8 kb. The maximal size of a recombinant AAV genome is 5 kb.<sup>126</sup> The size of the dystrophin gene, mRNA, and coding sequence is 2.4 mb, 14 kb, and 11.2 kb, respectively. This creates a compatibility dilemma. Several distinctive approaches have been investigated to overcome this hurdle. These include the development of highly truncated micro-dystrophins, invention of high-capacity dual and tri-AAV vectors, and AAV-mediated exon-skipping.

The micro-dystrophin genes are less than 4 kb in size.<sup>106</sup> The first series of microgenes were published in 1998.<sup>127</sup> Unfortunately, they were minimally protective. In early 2000s, the C-terminal deleted second-generation microgenes were developed in the Xiao lab and Chamberlain lab.<sup>128,129</sup> These microgenes effectively ameliorated skeletal muscle disease, improved muscle function, and reduced Duchenne cardiomyopathy in various mouse models of DMD.<sup>128–145</sup> Recent optimization (such as codon usage optimization, removal/replacement of rigid hinge 2, and inclusion of the syntrophin/dystrobrevin-binding site) has further enhanced therapeutic potency.<sup>146–148</sup>

To validate the therapeutic effect of micro-dystrophin in a large mammal, many studies have been performed in the canine model of DMD.<sup>149,150</sup> While AAV administration induces minimal cellular immune reaction in rodents, it turns out that the T-cell response is a major hurdle for AAV gene therapy in dystrophic large mammals.<sup>23,151,152</sup> Application of transient immune suppression greatly attenuates the immune response and results in robust and persistent expression following local gene transfer in the canine model of DMD.<sup>153,154</sup> Importantly, direct injection of the AAV micro-dystrophin vector to affected dog muscle has ameliorated muscle pathology and enhanced muscle function.<sup>155</sup>

A major deficiency of these early microgenes is their failure to restore neuronal nitric oxide synthase (nNOS) to the sarcolemma. Membrane localization of nNOS is crucial for muscle physiology.<sup>156</sup> Loss of sarcolemmal nNOS leads to functional ischemia, a significant insult to muscle health and function.<sup>157,158</sup>

Delocalized nNOS causes nitrosative stress, which directly inhibits muscle contractility.<sup>159</sup> Collectively, disruption of normal nNOS homeostasis is undoubtedly an important factor of DMD pathogenesis.<sup>160–162</sup> Through a comprehensive structure–function analysis, we recently identified spectrin-like repeats 16 and 17 (R16/17) as the dystrophin nNOS-binding domain.<sup>135,163,164</sup> With this new information, we developed R16/17-based third-generation micro-dystrophins.<sup>135</sup> Inclusion of R16/17

in synthetic dystrophin genes significantly enhanced recovery in dystrophic mice.<sup>135,165</sup> As commented by Harper, 'the structural elements (R16/17) required for proper nNOS localization should be included in any DMD therapy for which dystrophin restoration is the goal.'<sup>166</sup>

An alternative to the gene shrink strategy is to expand the carrying capacity of the AAV vector. This is achieved with dual and tri-AAV vectors.<sup>167,168</sup> Basically, a large expression cassette is split into two or three parts and delivered into the cell by independent AAV vectors. Reconstitution is achieved by concatamerization between AAV-inverted terminal repeats and/or via homologous recombination. Following initial proof-of-principle studies with various reporter genes,<sup>169–175</sup> we demonstrated the feasibility of delivering a 6- to 8-kb mini-dystrophin gene with a set of dual AAV vectors.<sup>176–178</sup> Importantly, optimized mini-dystrophin dual AAV vectors resulted in a transduction efficiency comparable to that of a single AAV vector, significantly reduced muscle degeneration and inflammation, and increased muscle force.<sup>176</sup> Most recently, our group and Dickson's lab independently demonstrated feasibility of delivering the full-length dystrophin coding sequence using the tri-AAV system.<sup>179,180</sup> The transduction efficiency of the tri-AAV vectors remains low. Significant amount of work is needed before we can achieve therapeutically meaningful level of expression from tri-AAV full-length dystrophin vectors.

DMD is caused by out-of-frame mutations. Many of these mutations can be converted to an in-frame coding transcript by removing the mutated exon(s) and/or the neighboring exons using AONs.<sup>181</sup> While many exon-skipping therapeutics have focused on the chemical modification and optimization of AONs (see *Nonviral-Based Nanoparticles for DMD Therapy* section), investigators have begun to take the advantage of the powerful gene transfer capability of AAV to deliver AONs.<sup>182–184</sup> In AAV-mediated AON exon skipping, AONs are embedded in a U7 snRNA expression cassette for delivery to muscle nuclei. In the nucleus, AAV directs long-term expression of the AON and the U7 snRNA directs the AON to the complementary sequences in the dystrophin pre-mRNA. By binding to splicing enhancers/silencers and splicing donor and acceptor signals, AONs may alter the inclusion and/or exclusion of one or more exons allowing the targeted 'skipping' of out-of-frame mutations.<sup>183,184</sup> The removal of out-of-frame mutations restores the reading frame and results in the production of a functional, albeit, truncated dystrophin. As AAV directs long-term gene expression, packaging AON in AAV

allows for persistent AON expression and obviates the need for weekly or biweekly injections.<sup>185</sup> Unlike AAV-mediated dystrophin gene replacement therapy, exon-skipping has to be tailored to the specific mutations. Nevertheless, recent successes in the canine model suggest that AAV exon-skipping has reached its prime time for a clinical trial.<sup>185–188</sup>

### **Bodywide Gene Therapy**

Muscle is one of the largest tissues in the body. An effective gene therapy for DMD requires efficient delivery of the therapeutic gene to muscles all over the body including limb, respiratory, and cardiac muscles.<sup>114</sup> While there are some preclinical evidence suggesting that drug-mediated endothelial permeabilization can lead to multiple muscle transduction through a regional vessel,<sup>189</sup> bodywide treatment has been considered a mission impossible for many years. The situation changed in 2004 when several newly identified AAV serotypes were tested for intravenous delivery.<sup>190–192</sup> A flow of studies from different laboratories showed that AAV-6, -8, and -9 can effectively reach to all body muscles through the circulation.<sup>138,193–196</sup> Subsequent studies indicate that many other AAV serotypes are also capable of systemic delivery with different levels of efficiency (reviewed in Ref 114). Unprecedented results from reporter gene vectors stimulated immediate application of this novel gene delivery technology to animal models of muscular dystrophies including DMD (Figure 2).<sup>134,138,193</sup> Of particular interest are the studies performed in severely affected mouse models including utrophin/dystrophin double knockout mice and aged mdx mice.<sup>136,137,139,143</sup> These models are thought to better model dystrophic changes than young adult mdx mice. Surprisingly, severe muscle pathology, especially extensive fibrosis, did not limit AAV transduction. Systemic injection significantly improved overall condition of these mice, increased lifespan, and mitigated dystrophic cardiomyopathy.<sup>136,137,139,143</sup>

Following the success of systemic delivery of a single AAV vector, we explored systemic delivery of the dual AAV vectors.<sup>197,198</sup> Consistent with the results of the single AAV vector, we found that intravenous injection of the dual AAV vectors also results in fairly efficient transduction of skeletal muscle and the heart in normal and mdx mice.<sup>197,198</sup> Subsequent tests with therapeutic mini-dystrophin dual AAV vectors have provided unequivocal evidence that AAV therapy with a larger, 6- to 8-kb mini-dystrophin gene can offer whole body benefits in mouse models of DMD.<sup>165,199</sup>

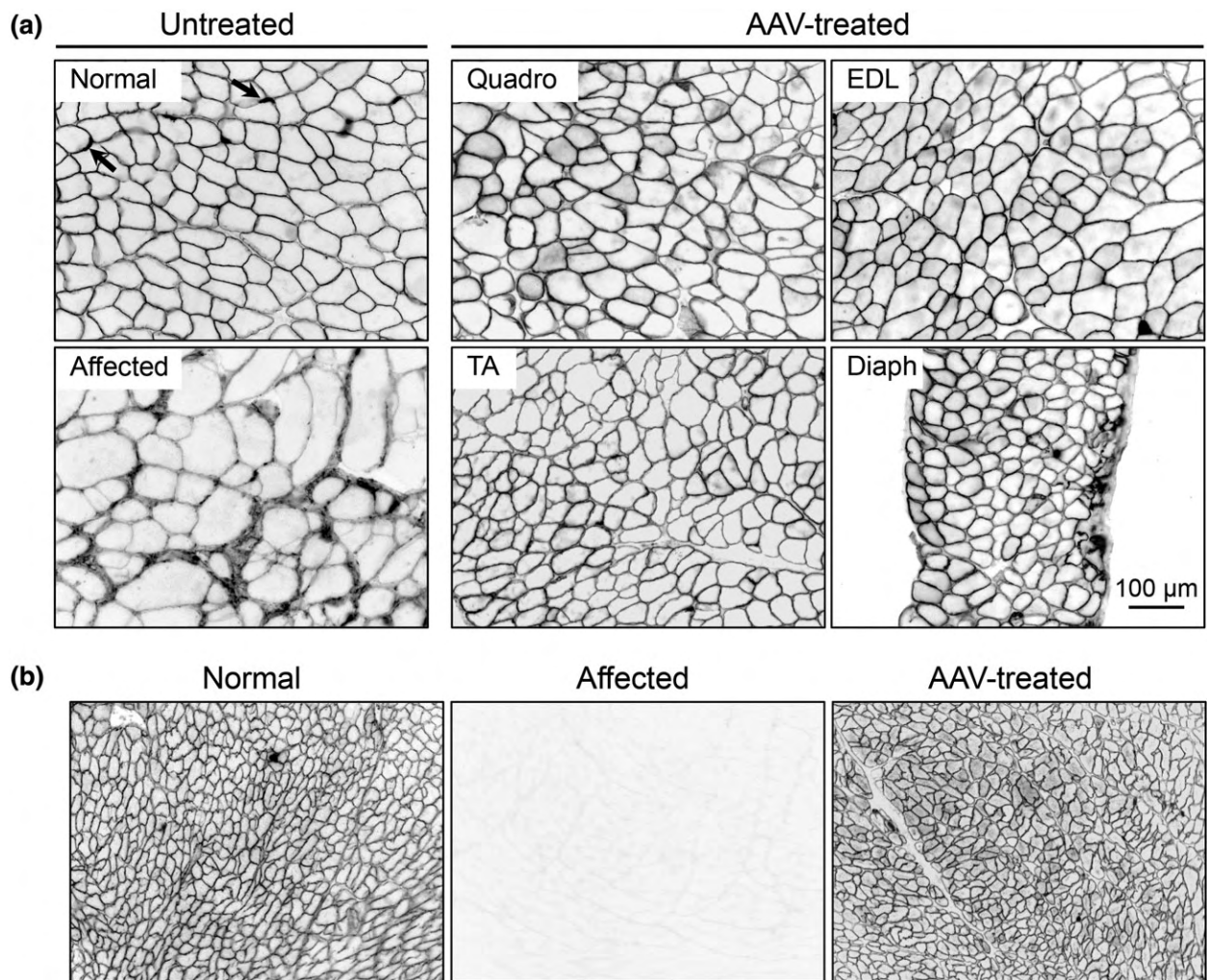


**FIGURE 2** | Systemic AAV-9 micro-dystrophin gene transfer results in bodywide dystrophin restoration in striated muscles in the mouse model of Duchenne muscular dystrophy. (a) Representative dystrophin immunostaining photomicrographs from skeletal muscles of normal, untreated, and adeno-associated virus (AAV)-treated mdx mice. Normal muscle shows sarcolemmal expression of dystrophin, which is enriched at the neuromuscular junction (arrows). Dystrophic muscle has no dystrophin expression at the sarcolemma. Cross-reaction of the immunostaining antibody with inflamed/fibrotic interstitial tissues illustrates an irregular pattern of dystrophin with extremely large and small myofibers. Systemic AAV-9 micro-dystrophin therapy restores dystrophin expression in the quadriceps (Quadro), extensor digitorum longus (EDL), tibialis anterior (TA), and diaphragm (Diaph). (b) Representative dystrophin immunostaining photomicrographs from the heart of normal, affected, and AAV micro-dystrophin-treated mice. Scale bar in panel (a) applies to all images.

The body weight of a 20-g young adult mouse is 750-fold lower than that of a 15-kg boy. To minimize the risks of scaling up from mice to humans, we have tested systemic AAV gene delivery in dogs. The body weight difference between a 20-g mouse and a 5-kg dog is 250-fold while going from a dog to a boy is only threefold. Initial studies in neonatal dogs have revealed several species-specific differences in AAV transduction biology between mice and dogs. First, cardiotropic AAV-9 fails to transduce the newborn dog heart.<sup>152,200</sup> Screening of alternative AAV serotypes identifies AAV-8 and Y445F/Y731F AAV-1 as

the preferred vectors for effective heart and skeletal muscle gene transfer in newborn puppies.<sup>201–203</sup> Second, unlike mice, dogs carry high titers of AAV-6 neutralization antibody, which blocks systemic delivery with AAV-6.<sup>201,204–206</sup> Third, intravenous delivery by AAV-8 and -9 leads to high-level expression in the liver in mice.<sup>194</sup> However, there is minimal expression in the liver of dogs (even with a ubiquitous promoter and a reporter gene) although a significant amount of the AAV genome is detected in the liver.<sup>152,201–203</sup> Finally, a study from the Xiao lab suggests that systemic injection of AAV-9 may result

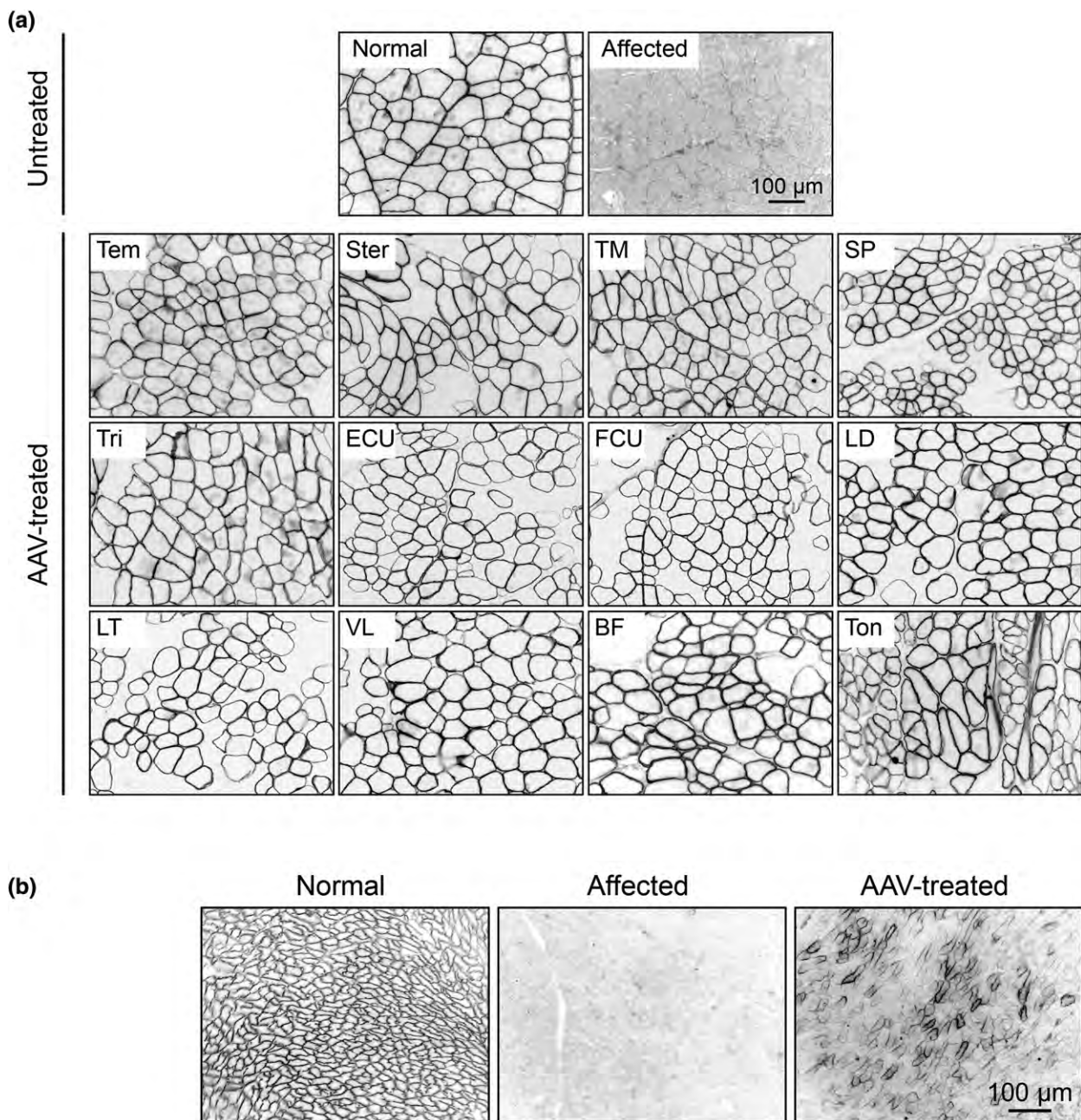


**FIGURE 3** | A single intravenous injection of the adeno-associated virus (AAV)-9 micro-dystrophin vector leads to bodywide muscle transduction in the canine model of Duchenne muscular dystrophy. (a) Top panels: representative dystrophin immunostaining photomicrographs from skeletal muscles of normal and affected dogs. Bottom panels: representative dystrophin immunostaining photomicrographs from different skeletal muscle of an AAV-treated dog. Tem, temporalis; Ster, sternohyoid; TM, teres major; SP, superficial pectoral; Tri, triceps; ECU, extensor carpi ulnaris; FCU, flexor carpi ulnaris; LD, latissimus dorsi; LT, longissimus thoracis; VL, vastus lateralis; BF, biceps femoris; Ton, tongue. (b) Representative dystrophin immunostaining photomicrographs from the heart of normal, affected, and AAV micro-dystrophin-treated dogs.

in a massive inflammatory response under certain condition (the ubiquitous promoter, human transgene, dystrophic puppy, or vector stock impurity).<sup>207</sup>

As our ultimate goal is to treat DMD boys with systemic gene therapy, we recently explored AAV-9-

mediated micro-dystrophin therapy in young adult affected dogs.<sup>24,208</sup> After a single dose injection, we observed widespread bodywide micro-dystrophin expression in skeletal muscle and the heart (Figure 3). No adverse reactions were detected.

AAV-9 micro-dystrophin therapy greatly reduced dystrophic histopathology, improved the growth, and enhanced function.<sup>24,155</sup> Our data suggest that systemic AAV micro-dystrophin therapy is safe and efficient in young adult dystrophic large mammals. A similar approach may translate to DMD boys in the near future (<https://solidbio.com/content/steps-forward-duchenne-muscular-dystrophy>).<sup>106</sup>

### ***New Developments in AAV-Mediated DMD Gene Therapy***

Dystrophin-independent DMD gene therapy has emerged as a highly promising new direction. These therapeutic candidates can be divided into two categories including (1) structure and/or functional homologues of dystrophin such as utrophin and integrin,<sup>209,210</sup> and (2) alternative targets that are involved in different aspects of disease mechanisms such as follistatin, nNOS, cytotoxic T-cell GalNAc transferase (Galgt2), sarcospan, and sarcoplasmic reticulum calcium ATPase (SERCA).<sup>211–215</sup> In these approaches, the therapeutic candidate genes are already expressed in DMD patients. Hence, they are unlikely to induce the transgene product-associated immune response.

The biological properties of AAV (such as tissue tropism and intracellular processing) are largely dependent on the viral capsids. A number of highly creative strategies have been used to engineer novel AAV capsids with superior properties for different applications. In the forced evolution approach, an AAV capsid library is subject to a variety of *in vitro* and *in vivo* selection pressures. The best-fit capsids can then be used for gene therapy.<sup>119</sup> The resolution of the high-definition AAV capsid structure and the discovery of AAV receptors and coreceptors in recent years have opened the door for educated engineering of AAV capsids to meet the needs of gene therapy applications.<sup>123–125,216</sup> It is expected that an integrated approach combining various rational design and direct evolution methods will yield one or several super-AAV capsids for DMD gene therapy in the near future.<sup>72</sup>

There is no doubt that the CRISPR technology is the most exciting advance in the entire field of biology in recent years.<sup>217,218</sup> While it is still at an early stage of development, AAV-mediated genome editing with the CRISPR technology has yielded very promising results in mdx mice.<sup>25,219,220</sup> Further improvement in this technology, especially in terms of increasing editing specificity and minimizing potential immunogenicity of bacterial derived Cas9 protein,

may one day bring this revolutionary technology to DMD patients.

### **NANOTHERAPY AGAINST PATHOGENIC MECHANISMS OF DMD**

While most of the above-described DMD nanotherapies focus on restoration of dystrophin in diseased muscle, many investigators have also begun to apply nanotechnology to address the downstream pathogenic events in DMD. For example, it has been recognized that loss of dystrophin influences muscle autophagy.<sup>221,222</sup> Hence, modulating or enhancing autophagy could theoretically improve DMD pathogenesis. Several studies show that upregulation of autophagy by rapamycin can significantly ameliorate muscle pathology.<sup>222,223</sup> However, improvement on muscle function was moderate.<sup>222</sup> By delivering rapamycin in nanoparticles, Bibee et al. showed a much better enhancement of muscle function.<sup>222</sup> These findings suggest that nanoparticle delivery may also greatly improve the therapeutic outcomes of drugs targeting dystrophic mechanisms such as fibrosis and inflammation.

### **CONCLUSION**

The small size and modular flexibility of the nanotechnology provides an excellent platform for the development of drug and gene therapies that target the etiology of DMD. Improvements in analytical chemistry, instrumentation, structural biology, protein and nucleic acid engineering, and the availability of nanomaterials have fostered an explosion in nanotechnology for DMD in the last decade. The regulatory approval of the read-through drug Ataluren and exon-skipping drug Exondys51 has set good examples on the path forward for DMD nanotherapy. Rapid advance in the nanotechnology offers an expanding repertoire of candidate therapies for DMD. Preclinical studies in small and large animals as well as early phase human trials have been instrumental in the development of nanotherapy for DMD. It is clear from these studies that some of the strategies (such as naked plasmid injection and adenovirus gene therapy) will not be appropriate for DMD therapy. However, some of the emerging new technologies (such as nanoparticle-AONs and AAV micro-dystrophin vectors) are likely going to change the landscape of DMD nanotherapy in next few years. With the extensive possibilities of nanotechnology, the future of etiology-based DMD therapies should be very exciting in the coming years.

## ACKNOWLEDGMENTS

The Duchenne muscular dystrophy gene therapy research in the Duan lab is currently supported by the National Institutes of Health (NS-90634, AR-69085, AR-67985 and AR-70517), Department of Defense (MD130014 and MD150133), Jesse's Journey-The Foundation for Gene and Cell Therapy, Jackson Freeland DMD Research Fund, Solid GT LLC and the University of Missouri.

## REFERENCES

- Mendell JR, Lloyd-Puryear M. Report of MDA muscle disease symposium on newborn screening for Duchenne muscular dystrophy. *Muscle Nerve* 2013, 48:21–26.
- Romitti PA, Zhu Y, Puzhankara S, James KA, Nabukera SK, Zamba GK, Ciafaloni E, Cunniff C, Druschel CM, Mathews KD, et al. Prevalence of Duchenne and Becker muscular dystrophies in the United States. *Pediatrics* 2015, 135:513–521. (Epub ahead of print; February 16, 2015).
- Mah JK, Korngut L, Dykeman J, Day L, Pringsheim T, Jette N. A systematic review and meta-analysis on the epidemiology of Duchenne and Becker muscular dystrophy. *Neuromuscul Disord* 2014, 24:482–491.
- Bushby K, Finkel R, Birnkrant DJ, Case LE, Clemens PR, Cripe L, Kaul A, Kinnett K, McDonald C, Pandya S, et al. Diagnosis and management of Duchenne muscular dystrophy, part 1: diagnosis, and pharmacological and psychosocial management. *Lancet Neurol* 2010, 9:77–93.
- Danielou G, Comtois AS, Dudley R, Karpati G, Vincent G, Des Rosiers C, Petrof BJ. Dystrophin-deficient cardiomyocytes are abnormally vulnerable to mechanical stress-induced contractile failure and injury. *FASEB J* 2001, 15:1655–1657.
- McNally EM, Kaltman JR, Benson DW, Canter CE, Cripe LH, Duan D, FINDER JD, Groh WJ, Hoffman EP, Judge DP, et al. Contemporary cardiac issues in Duchenne muscular dystrophy. Working Group of the National Heart, Lung, and Blood Institute in collaboration with Parent Project Muscular Dystrophy. *Circulation* 2015, 131:1590–1598.
- Bello L, Gordish-Dressman H, Morgenroth LP, Henricson EK, Duong T, Hoffman EP, Cnaan A, McDonald CM, CINRG Investigators. Prednisone/prednisolone and deflazacort regimens in the CINRG Duchenne Natural History Study. *Neurology* 2015, 85:1048–1055.
- Pane M, Fanelli L, Mazzone ES, Olivieri G, D'Amico A, Messina S, Scutifero M, Battini R, Petillo R, Frosini S, et al. Benefits of glucocorticoids in non-ambulant boys/men with Duchenne muscular dystrophy: a multicentric longitudinal study using the Performance of Upper Limb test. *Neuromuscul Disord* 2015, 25:749–753.
- Tandon A, Villa CR, Hor KN, Jefferies JL, Gao Z, Towbin JA, Wong BL, Mazur W, Fleck RJ, Sticka JJ, et al. Myocardial fibrosis burden predicts left ventricular ejection fraction and is associated with age and steroid treatment duration in Duchenne muscular dystrophy. *J Am Heart Assoc* 2015, 4:e001338.
- Ricotti V, Ridout DA, Muntoni F. Steroids in Duchenne muscular dystrophy. *Neuromuscul Disord* 2013, 23:696–697.
- Ricotti V, Ridout DA, Scott E, Quinlivan R, Robb SA, Manzur AY, Muntoni F, NorthStar CN. Long-term benefits and adverse effects of intermittent versus daily glucocorticoids in boys with Duchenne muscular dystrophy. *J Neurol Neurosurg Psychiatry* 2013, 84:698–705.
- Kim Y, Tewari M, Pajerowski JD, Cai S, Sen S, Williams JH, Sirsi SR, Lutz GJ, Discher DE. Polymer-some delivery of siRNA and antisense oligonucleotides. *J Control Release* 2009, 134:132–140.
- Afzal E, Zakeri S, Keyhanvar P, Bagheri M, Mahjoubi P, Asadian M, Omoomi N, Dehqanian M, Ghalandaraki N, Darvishmohammadi T, et al. Nanolipodendrosome-loaded glatiramer acetate and myogenic differentiation 1 as augmentation therapeutic strategy approaches in muscular dystrophy. *Int J Nanomed* 2013, 8:2943–2960.
- Negishi Y, Ishii Y, Shiono H, Akiyama S, Sekine S, Kojima T, Mayama S, Kikuchi T, Hamano N, Endo-Takahashi Y, et al. Bubble liposomes and ultrasound exposure improve localized morpholino oligomer delivery into the skeletal muscles of dystrophic mdx mice. *Mol Pharm* 2014, 11:1053–1061.
- Ezzat K, Aoki Y, Koo T, McClorey G, Benner L, Coenen-Stass A, O'Donovan L, Lehto T, Garcia-Guerra A, Nordin J, et al. Self-assembly into nanoparticles is essential for receptor mediated uptake of therapeutic antisense oligonucleotides. *Nano Lett* 2015, 15:4364–4373.
- Gao X, Shen X, Dong X, Ran N, Han G, Cao L, Gu B, Yin H. Peptide nucleic acid promotes systemic dystrophin expression and functional rescue in dystrophin-deficient mdx mice. *Mol Ther Nucleic Acids* 2015, 4:e255.

17. Lehto T, Castillo Alvarez A, Gauck S, Gait MJ, Coursindel T, Wood MJ, Lebleu B, Boisguerin P. Cellular trafficking determines the exon skipping activity of Pip6a-PMO in mdx skeletal and cardiac muscle cells. *Nucleic Acids Res* 2014, 42:3207–3217.
18. Shabanpoor F, McClorey G, Saleh AF, Jarver P, Wood MJ, Gait MJ. Bi-specific splice-switching PMO oligonucleotides conjugated via a single peptide active in a mouse model of Duchenne muscular dystrophy. *Nucleic Acids Res* 2015, 43:29–39.
19. Rimessi P, Sabatelli P, Fabris M, Braghetta P, Bassi E, Spitali P, Vattemi G, Tomelleri G, Mari L, Perrone D, et al. Cationic PMMA nanoparticles bind and deliver antisense oligoribonucleotides allowing restoration of dystrophin expression in the mdx mouse. *Mol Ther* 2009, 17:820–827.
20. Ferlini A, Sabatelli P, Fabris M, Bassi E, Falzarano S, Vattemi G, Perrone D, Gualandi F, Maraldi NM, Merlini L, et al. Dystrophin restoration in skeletal, heart and skin arrector pili smooth muscle of mdx mice by ZM2 NP-AON complexes. *Gene Ther* 2010, 17:432–438.
21. Bassi E, Falzarano S, Fabris M, Gualandi F, Merlini L, Vattemi G, Perrone D, Marchesi E, Sabatelli P, Sparnacci K, et al. Persistent dystrophin protein restoration 90 days after a course of intraperitoneally administered naked 2'OMePS AON and ZM2 NP-AON complexes in mdx mice. *J Biomed Biotechnol* 2012, 2012:897076.
22. Falzarano MS, Passarelli C, Bassi E, Fabris M, Perrone D, Sabatelli P, Maraldi NM, Dona S, Selvatici R, Bonaldo P, et al. Biodistribution and molecular studies on orally administered nanoparticle-AON complexes encapsulated with alginate aiming at inducing dystrophin rescue in mdx mice. *Biomed Res Int* 2013, 2013:527418.
23. Mendell JR, Campbell K, Rodino-Klapac L, Sahenk Z, Shilling C, Lewis S, Bowles D, Gray S, Li C, Galloway G, et al. Dystrophin immunity in Duchenne's muscular dystrophy. *N Engl J Med* 2010, 363:1429–1437.
24. Yue Y, Pan X, Hakim CH, Kodippili K, Zhang K, Shin JH, Yang HT, McDonald T, Duan D. Safe and bodywide muscle transduction in young adult Duchenne muscular dystrophy dogs with adeno-associated virus. *Hum Mol Genet* 2015, 24:5880–5890.
25. Nelson CE, Hakim CH, Ousterout DG, Thakore PI, Moreb EA, Castellanos Rivera RM, Madhavan S, Pan X, Ran FA, Yan WX, et al. In vivo genome editing improves muscle function in a mouse model of Duchenne muscular dystrophy. *Science* 2016, 351:403–407.
26. DelloRusso C, Scott JM, Hartigan-O'Connor D, Salvatori G, Barjot C, Robinson AS, Crawford RW, Brooks SV, Chamberlain JS. Functional correction of adult mdx mouse muscle using gutted adenoviral vectors expressing full-length dystrophin. *Proc Natl Acad Sci USA* 2002, 99:12979–12984.
27. Deol JR, Danialou G, Larochelle N, Bourget M, Moon JS, Liu AB, Gilbert R, Petrof BJ, Nalbantoglu J, Karpati G. Successful compensation for dystrophin deficiency by a helper-dependent adenovirus expressing full-length utrophin. *Mol Ther* 2007, 15:1767–1774.
28. Maggio I, Stefanucci L, Janssen JM, Liu J, Chen X, Mouly V, Goncalves MA. Selection-free gene repair after adenoviral vector transduction of designer nucleases: rescue of dystrophin synthesis in DMD muscle cell populations. *Nucleic Acids Res* 2016, 44:1449–1470.
29. Muir LA, Nguyen QG, Hauschka SD, Chamberlain JS. Engraftment potential of dermal fibroblasts following in vivo myogenic conversion in immunocompetent dystrophic skeletal muscle. *Mol Ther Methods Clin Dev* 2014, 1:14025.
30. Naldini L, Trono D, Verma IM. Lentiviral vectors, two decades later. *Science* 2016, 353:1101–1102.
31. Nigro G, Comi LI, Politano L, Bain RJ. The incidence and evolution of cardiomyopathy in Duchenne muscular dystrophy. *Int J Cardiol* 1990, 26:271–277.
32. Kamdar F, Garry DJ. Dystrophin-deficient cardiomyopathy. *J Am Coll Cardiol* 2016, 67:2533–2546.
33. Malik V, Rodino-Klapac LR, Viollet L, Wall C, King W, Al-Dahhak R, Lewis S, Shilling CJ, Kota J, Serrano-Munuera C, et al. Gentamicin-induced read-through of stop codons in Duchenne muscular dystrophy. *Ann Neurol* 2010, 67:771–780.
34. Welch EM, Barton ER, Zhuo J, Tomizawa Y, Friesen WJ, Trifillis P, Paushkin S, Patel M, Trotta CR, Hwang S, et al. PTC124 targets genetic disorders caused by nonsense mutations. *Nature* 2007, 447:87–91.
35. Auld DS, Thorne N, Maguire WF, Inglese J. Mechanism of PTC124 activity in cell-based luciferase assays of nonsense codon suppression. *Proc Natl Acad Sci USA* 2009, 106:3585–3590.
36. McElroy SP, Nomura T, Torrie LS, Warbrick E, Gartner U, Wood G, McLean WH. A lack of premature termination codon read-through efficacy of PTC124 (Ataluren) in a diverse array of reporter assays. *PLoS Biol* 2013, 11:e1001593.
37. Bushby K, Finkel R, Wong B, Barohn R, Campbell C, Comi GP, Connolly AM, Day JW, Flanigan KM, Goemans N, et al. Ataluren treatment of patients with nonsense mutation dystrophinopathy. *Muscle Nerve* 2014, 50:477–487.
38. Haas M, Vlcek V, Balabanov P, Salmonson T, Bakchine S, Markey G, Weise M, Schlosser-Weber G, Brohmann H, Yerro CP, et al. European Medicines Agency review of ataluren for the treatment of ambulant patients aged 5 years and older with Duchenne muscular dystrophy resulting from a nonsense

- mutation in the dystrophin gene. *Neuromuscul Disord* 2015, 25:5–13.
39. Gintjee TJ, Magh AS, Bertoni C. High throughput screening in Duchenne muscular dystrophy: from drug discovery to functional genomics. *Biology (Basel)* 2014, 3:752–780.
  40. Wolff JA, Malone RW, Williams P, Chong W, Acsadi G, Jani A, Felgner PL. Direct gene transfer into mouse muscle in vivo. *Science* 1990, 247:1465–1468.
  41. Acsadi G, Dickson G, Love DR, Jani A, Walsh FS, Gurusinghe A, Wolff JA, Davies KE. Human dystrophin expression in mdx mice after intramuscular injection of DNA constructs. *Nature* 1991, 352:815–818.
  42. Danialou G, Comtois AS, Dudley RW, Nalbantoglu J, Gilbert R, Karpati G, Jones DH, Petrof BJ. Ultrasound increases plasmid-mediated gene transfer to dystrophic muscles without collateral damage. *Mol Ther* 2002, 6:687–693.
  43. Pichavant C, Chapdelaine P, Cerri DG, Bizario JC, Tremblay JP. Electrotransfer of the full-length dog dystrophin into mouse and dystrophic dog muscles. *Hum Gene Ther* 2010, 21:1591–1601.
  44. Romero NB, Benveniste O, Payan C, Braun S, Squiban P, Herson S, Fardeau M. Current protocol of a research phase I clinical trial of full-length dystrophin plasmid DNA in Duchenne/Becker muscular dystrophies. Part II: clinical protocol. *Neuromuscul Disord* 2002, 12(suppl 1):S45–48.
  45. Duan D. Myodys, a full-length dystrophin plasmid vector for Duchenne and Becker muscular dystrophy gene therapy. *Curr Opin Mol Ther* 2008, 10:86–94.
  46. Kinali M, Arechavala-Gomez V, Feng L, Cirak S, Hunt D, Adkin C, Guglieri M, Ashton E, Abbs S, Nihoyannopoulos P, et al. Local restoration of dystrophin expression with the morpholino oligomer AVI-4658 in Duchenne muscular dystrophy: a single-blind, placebo-controlled, dose-escalation, proof-of-concept study. *Lancet Neurol* 2009, 8:918–928.
  47. Goyenville A, Griffith G, Babbs A, El Andaloussi S, Ezzat K, Avril A, Dugovic B, Chaussonot R, Ferry A, Voit T, et al. Functional correction in mouse models of muscular dystrophy using exon-skipping tricyclo-DNA oligomers. *Nat Med* 2015, 21:270–275.
  48. Moulton HM, Wu B, Jearawiriyapaisarn N, Szani P, Lu QL, Kole R. Peptide-morpholino conjugate: a promising therapeutic for Duchenne muscular dystrophy. *Ann N Y Acad Sci* 2009, 1175:55–60.
  49. Wu B, Li Y, Morcos PA, Doran TJ, Lu P, Lu QL. Octa-guanidine morpholino restores dystrophin expression in cardiac and skeletal muscles and ameliorates pathology in dystrophic mdx mice. *Mol Ther* 2009, 17:864–871.
  50. Aoki Y, Yokota T, Nagata T, Nakamura A, Tanihata J, Saito T, Duguez SM, Nagaraju K, Hoffman EP, Partridge T, et al. Bodywide skipping of exons 45–55 in dystrophic mdx52 mice by systemic antisense delivery. *Proc Natl Acad Sci USA* 2012, 109:13763–13768.
  51. Yokota T, Nakamura A, Nagata T, Saito T, Kobayashi M, Aoki Y, Echigoya Y, Partridge T, Hoffman EP, Takeda S. Extensive and prolonged restoration of dystrophin expression with vivo-morpholino-mediated multiple exon skipping in dystrophic dogs. *Nucleic Acid Ther* 2012, 22:306–315.
  52. Echigoya Y, Aoki Y, Miskew B, Panesar D, Touznik A, Nagata T, Tanihata J, Nakamura A, Nagaraju K, Yokota T. Long-term efficacy of systemic multiexon skipping targeting dystrophin exons 45–55 with a cocktail of vivo-morpholinos in mdx52 mice. *Mol Ther Nucleic Acids* 2015, 4:e225.
  53. van Hest JC, Delnoye DA, Baars MW, van Genderen MH, Meijer EW. Polystyrene-dendrimer amphiphilic block copolymers with a generation-dependent aggregation. *Science* 1995, 268:1592–1595.
  54. Zhang L, Eisenberg A. Multiple morphologies of “crew-cut” aggregates of polystyrene-b-poly(acrylic acid) block copolymers. *Science* 1995, 268:1728–1731.
  55. Discher BM, Won YY, Ege DS, Lee JC, Bates FS, Discher DE, Hammer DA. Polymersomes: tough vesicles made from diblock copolymers. *Science* 1999, 284:1143–1146.
  56. Lee JS, Feijen J. Biodegradable polymersomes as carriers and release systems for paclitaxel using Oregon Green(R) 488 labeled paclitaxel as a model compound. *J Control Release* 2012, 158:312–318.
  57. Discher DE, Eisenberg A. Polymer vesicles. *Science* 2002, 297:967–973.
  58. Graff A, Sauer M, Van Gelder P, Meier W. Virus-assisted loading of polymer nanocontainer. *Proc Natl Acad Sci USA* 2002, 99:5064–5068.
  59. Wang M, Wu B, Tucker JD, Bollinger LE, Lu P, Lu Q. Poly(ester amine) composed of polyethylenimine and pluronic enhance delivery of antisense oligonucleotides in vitro and in dystrophic mdx mice. *Mol Ther Nucleic Acids* 2016, 5:e341.
  60. Wang M, Wu B, Lu P, Tucker JD, Milazi S, Shah SN, Lu QL. Pluronic-PEI copolymers enhance exon-skipping of 2'-O-methyl phosphorothioate oligonucleotide in cell culture and dystrophic mdx mice. *Gene Ther* 2014, 21:52–59.
  61. Wang M, Tucker JD, Lu P, Wu B, Cloer C, Lu Q. Tris[2-(acryloyloxy)ethyl]isocyanurate cross-linked low-molecular-weight polyethylenimine as gene delivery carriers in cell culture and dystrophic mdx mice. *Bioconjug Chem* 2012, 23:837–845.
  62. Wang M, Wu B, Tucker JD, Lu P, Lu Q. Tris[2-(acryloyloxy)ethyl]isocyanurate cross-linked polyethylenimine enhanced exon-skipping of antisense 2'-O-

- methyl phosphorothioate oligonucleotide in vitro and in vivo. *J Nanomed Nanotechnol* 2015, 6:1000261.
63. Allen TM, Cullis PR. Liposomal drug delivery systems: from concept to clinical applications. *Adv Drug Deliv Rev* 2013, 65:36–48.
  64. Fraley R, Straubinger RM, Rule G, Springer EL, Papahadjopoulos D. Liposome-mediated delivery of deoxyribonucleic acid to cells: enhanced efficiency of delivery related to lipid composition and incubation conditions. *Biochemistry* 1981, 20:6978–6987.
  65. Fraley R, Subramani S, Berg P, Papahadjopoulos D. Introduction of liposome-encapsulated SV40 DNA into cells. *J Biol Chem* 1980, 255:10431–10435.
  66. Prakash TP, Lima WF, Murray HM, Elbashir S, Cantley W, Foster D, Jayaraman M, Chappell AE, Manoharan M, Swayze EE, et al. Lipid nanoparticles improve activity of single-stranded siRNA and gapmer antisense oligonucleotides in animals. *ACS Chem Biol* 2013, 8:1402–1406.
  67. Falzarano MS, Passarelli C, Ferlini A. Nanoparticle delivery of antisense oligonucleotides and their application in the exon skipping strategy for Duchenne muscular dystrophy. *Nucleic Acid Ther* 2014, 24:87–100.
  68. Negishi Y, Endo Y, Fukuyama T, Suzuki R, Takizawa T, Omata D, Maruyama K, Aramaki Y. Delivery of siRNA into the cytoplasm by liposomal bubbles and ultrasound. *J Control Release* 2008, 132:124–130.
  69. Jarver P, Coursindel T, Andaloussi SE, Godfrey C, Wood MJ, Gait MJ. Peptide-mediated cell and in vivo delivery of antisense oligonucleotides and siRNA. *Mol Ther Nucleic Acids* 2012, 1:e27.
  70. Betts CA, Wood MJ. Cell penetrating peptide delivery of splice directing oligonucleotides as a treatment for Duchenne muscular dystrophy. *Curr Pharm Des* 2013, 19:2948–2962.
  71. Boisguerin P, Deshayes S, Gait MJ, O'Donovan L, Godfrey C, Betts CA, Wood MJ, Lebleu B. Delivery of therapeutic oligonucleotides with cell penetrating peptides. *Adv Drug Deliv Rev* 2015, 87:52–67.
  72. Nance ME, Duan D. Perspective on adeno-associated virus capsid modification for Duchenne muscular dystrophy gene therapy. *Hum Gene Ther* 2015, 26:786–800.
  73. Wu B, Moulton HM, Iversen PL, Jiang J, Li J, Spurney CF, Sali A, Guerron AD, Nagaraju K, Doran T, et al. Effective rescue of dystrophin improves cardiac function in dystrophin-deficient mice by a modified morpholino oligomer. *Proc Natl Acad Sci USA* 2008, 105:14814–14819.
  74. Yin H, Moulton HM, Seow Y, Boyd C, Boutilier J, Iversen P, Wood MJ. Cell-penetrating peptide-conjugated antisense oligonucleotides restore systemic muscle and cardiac dystrophin expression and function. *Hum Mol Genet* 2008, 17:3909–3918.
  75. Yin H, Lu Q, Wood M. Effective exon skipping and restoration of dystrophin expression by peptide nucleic acid antisense oligonucleotides in mdx mice. *Mol Ther* 2008, 16:38–45.
  76. Jearawiriyapaisarn N, Moulton HM, Buckley B, Roberts J, Sazani P, Fucharoen S, Iversen PL, Kole R. Sustained dystrophin expression induced by peptide-conjugated morpholino oligomers in the muscles of mdx mice. *Mol Ther* 2008, 16:1624–1629.
  77. Jearawiriyapaisarn N, Moulton HM, Sazani P, Kole R, Willis MS. Long-term improvement in mdx cardiomyopathy after therapy with peptide-conjugated morpholino oligomers. *Cardiovasc Res* 2010, 85:444–453.
  78. Yin H, Moulton HM, Betts C, Seow Y, Boutilier J, Iversen PL, Wood MJ. A fusion peptide directs enhanced systemic dystrophin exon skipping and functional restoration in dystrophin-deficient mdx mice. *Hum Mol Genet* 2009, 18:4405–4414.
  79. Yin H, Betts C, Saleh AF, Ivanova GD, Lee H, Seow Y, Kim D, Gait MJ, Wood MJ. Optimization of peptide nucleic acid antisense oligonucleotides for local and systemic dystrophin splice correction in the mdx mouse. *Mol Ther* 2010, 18:819–827.
  80. Yin H, Saleh AF, Betts C, Camelliti P, Seow Y, Ashraf S, Arzumanov A, Hammond S, Merritt T, Gait MJ, et al. Pip5 transduction peptides direct high efficiency oligonucleotide-mediated dystrophin exon skipping in heart and phenotypic correction in mdx mice. *Mol Ther* 2011, 19:1295–1303.
  81. Jirka SM, Heemskerk H, Tanganyika-de Winter CL, Muilwijk D, Pang KH, de Visser PC, Janson A, Karnaoukh TG, Vermue R, t Hoen PA, et al. Peptide conjugation of 2'-O-methyl phosphorothioate antisense oligonucleotides enhances cardiac uptake and exon skipping in mdx mice. *Nucleic Acid Ther* 2014, 24:25–36.
  82. Betts C, Saleh AF, Arzumanov AA, Hammond SM, Godfrey C, Coursindel T, Gait MJ, Wood MJ. Pip6-PMO, a new generation of peptide-oligonucleotide conjugates with improved cardiac exon skipping activity for DMD treatment. *Mol Ther Nucleic Acids* 2012, 1:e38.
  83. Betts CA, Saleh AF, Carr CA, Hammond SM, Coenen-Stass AM, Godfrey C, McClorey G, Varela MA, Roberts TC, Clarke K, et al. Prevention of exercised induced cardiomyopathy following Pip-PMO treatment in dystrophic mdx mice. *Sci Rep* 2015, 5:8986.
  84. Lee Y, El Andaloussi S, Wood MJ. Exosomes and microvesicles: extracellular vesicles for genetic information transfer and gene therapy. *Hum Mol Genet* 2012, 21:R125–134.
  85. Leroyer AS, Ebrahimian TG, Cochain C, Recalde A, Blanc-Brude O, Mees B, Vilar J, Tedgui A, Levy BI, Chimini G, et al. Microparticles from ischemic muscle

- promotes postnatal vasculogenesis. *Circulation* 2009, 119:2808–2817.
86. Chen L, Wang Y, Pan Y, Zhang L, Shen C, Qin G, Ashraf M, Weintraub N, Ma G, Tang Y. Cardiac progenitor-derived exosomes protect ischemic myocardium from acute ischemia/reperfusion injury. *Biochem Biophys Res Commun* 2013, 431:566–571.
  87. Ibrahim AG, Cheng K, Marban E. Exosomes as critical agents of cardiac regeneration triggered by cell therapy. *Stem Cell Rep* 2014, 2:606–619.
  88. Alvarez-Erviti L, Seow Y, Yin H, Betts C, Lakhal S, Wood MJ. Delivery of siRNA to the mouse brain by systemic injection of targeted exosomes. *Nat Biotechnol* 2011, 29:341–345.
  89. Fiorillo AA, Heier CR, Novak JS, Tully CB, Brown KJ, Uaesoontrachoon K, Vila MC, Ngheim PP, Bello L, Kornegay JN, et al. TNF-alpha-induced microRNAs control dystrophin expression in Becker muscular dystrophy. *Cell Rep* 2015, 12:1678–1690.
  90. Alexander MS, Casar JC, Motohashi N, Vieira NM, Eisenberg I, Marshall JL, Gasperini MJ, Lek A, Myers JA, Estrella EA, et al. MicroRNA-486-dependent modulation of DOCK3/PTEN/AKT signaling pathways improves muscular dystrophy-associated symptoms. *J Clin Invest* 2014, 124:2651–2667.
  91. Liu N, Williams AH, Maxeiner JM, Bezprozvannaya S, Shelton JM, Richardson JA, Bassel-Duby R, Olson EN. microRNA-206 promotes skeletal muscle regeneration and delays progression of Duchenne muscular dystrophy in mice. *J Clin Invest* 2012, 122:2054–2065.
  92. Perry MM, Muntoni F. Noncoding RNAs and Duchenne muscular dystrophy. *Epigenomics* 2016, 8:1527–1537.
  93. Naldini L, Verma IM. Lentiviral vectors. *Adv Virus Res* 2000, 55:599–609.
  94. Kobinger GP, Louboutin JP, Barton ER, Sweeney HL, Wilson JM. Correction of the dystrophic phenotype by in vivo targeting of muscle progenitor cells. *Hum Gene Ther* 2003, 14:1441–1449.
  95. Kimura E, Li S, Gregorevic P, Fall BM, Chamberlain JS. Dystrophin delivery to muscles of mdx mice using lentiviral vectors leads to myogenic progenitor targeting and stable gene expression. *Mol Ther* 2010, 18:206–213.
  96. Li S, Kimura E, Fall BM, Reyes M, Angello JC, Welikson R, Hauschka SD, Chamberlain JS. Stable transduction of myogenic cells with lentiviral vectors expressing a minidystrophin. *Gene Ther* 2005, 12:1099–1108.
  97. Bachrach E, Li S, Perez AL, Schienda J, Liadaki K, Volinski J, Flint A, Chamberlain J, Kunkel LM. Systemic delivery of human microdystrophin to regenerating mouse dystrophic muscle by muscle progenitor cells. *Proc Natl Acad Sci USA* 2004, 101:3581–3586.
  98. Goncalves MA, de Vries AA, Holkers M, van de Watering MJ, van der Velde I, van Nierop GP, Valerio D, Knaan-Shanzer S. Human mesenchymal stem cells ectopically expressing full-length dystrophin can complement Duchenne muscular dystrophy myotubes by cell fusion. *Hum Mol Genet* 2006, 15:213–221.
  99. Quenneville SP, Chapdelaine P, Skuk D, Paradis M, Goulet M, Rousseau J, Xiao X, Garcia L, Tremblay JP. Autologous transplantation of muscle precursor cells modified with a lentivirus for muscular dystrophy: human cells and primate models. *Mol Ther* 2007, 15:431–438.
  100. Pichavant C, Chapdelaine P, Cerri DG, Dominique JC, Quenneville SP, Skuk D, Kornegay JN, Bizario JC, Xiao X, Tremblay JP. Expression of dog microdystrophin in mouse and dog muscles by gene therapy. *Mol Ther* 2010, 18:1002–1009.
  101. Benchaouir R, Meregalli M, Farini A, D'Antona G, Belicchi M, Goyenvalle A, Battistelli M, Bresolin N, Bottinelli R, Garcia L, et al. Restoration of human dystrophin following transplantation of exon-skipping-engineered DMD patient stem cells into dystrophic mice. *Cell Stem Cell* 2007, 1:646–657.
  102. Cazzella V, Martone J, Pinnaro C, Santini T, Twayana SS, Sthandier O, D'Amico A, Ricotti V, Bertini E, Muntoni F, et al. Exon 45 skipping through U1-snRNA antisense molecules recovers the Dyn-NOS pathway and muscle differentiation in human DMD myoblasts. *Mol Ther* 2012, 20:2134–2142.
  103. Ragot T, Vincent N, Chafey P, Vigne E, Gilgenkrantz H, Couton D, Cartaud J, Briand P, Kaplan JC, Perricaudet M, et al. Efficient adenovirus-mediated transfer of a human minidystrophin gene to skeletal muscle of mdx mice. *Nature* 1993, 361:647–650.
  104. Kochanek S, Clemens PR, Mitani K, Chen HH, Chan S, Caskey CT. A new adenoviral vector: replacement of all viral coding sequences with 28 kb of DNA independently expressing both full-length dystrophin and beta-galactosidase. *Proc Natl Acad Sci USA* 1996, 93:5731–5736.
  105. Xu L, Park KH, Zhao L, Xu J, El Refaey M, Gao Y, Zhu H, Ma J, Han R. CRISPR-mediated genome editing restores dystrophin expression and function in mdx mice. *Mol Ther* 2016, 24:564–569.
  106. Duan D. Dystrophin gene replacement and gene repair therapy for Duchenne muscular dystrophy in 2016. *Hum Gene Ther Clin Dev* 2016, 27:9–18.
  107. Bengtsson NE, Seto JT, Hall JK, Chamberlain JS, Odom GL. Progress and prospects of gene therapy clinical trials for the muscular dystrophies. *Hum Mol Genet* 2015, 25:R9–17. (Epub ahead of print; October 8, 2015).

108. Muzyczka N. Use of adeno-associated virus as a general transduction vector for mammalian cells. *Curr Top Microbiol Immunol* 1992, 158:97–129.
109. Carter BJ. Adeno-associated virus and the development of adeno-associated virus vectors: a historical perspective. *Mol Ther* 2004, 10:981–989.
110. Samulski RJ, Muzyczka N. AAV-mediated gene therapy for research and therapeutic purposes. *Annu Rev Virol* 2014, 1:427–451.
111. Muzyczka N, Berns KI. AAV's golden jubilee. *Mol Ther* 2015, 23:807–808.
112. Atchison RW, Casto BC, Hammon WM. Adenovirus-associated defective virus particles. *Science* 1965, 149:754–756.
113. Duan D, Sharma P, Yang J, Yue Y, Dudus L, Zhang Y, Fisher KJ, Engelhardt JF. Circular intermediates of recombinant adeno-associated virus have defined structural characteristics responsible for long term episomal persistence in muscle. *J Virol* 1998, 72:8568–8577.
114. Duan D. Systemic delivery of adeno-associated viral vectors. *Curr Opin Virol* 2016, 21:16–25.
115. Wu Z, Asokan A, Grieger JC, Govindasamy L, Agbandje-McKenna M, Samulski RJ. Single amino acid changes can influence titer, heparin binding, and tissue tropism in different adeno-associated virus serotypes. *J Virol* 2006, 80:11393–11397.
116. Gao G, Vandenberghe LH, Wilson JM. New recombinant serotypes of AAV vectors. *Curr Gene Ther* 2005, 5:285–297.
117. Vandenberghe LH, Wilson JM, Gao G. Tailoring the AAV vector capsid for gene therapy. *Gene Ther* 2009, 16:311–319.
118. Daya S, Berns KI. Gene therapy using adeno-associated virus vectors. *Clin Microbiol Rev* 2008, 21:583–593.
119. Kotterman MA, Schaffer DV. Engineering adeno-associated viruses for clinical gene therapy. *Nat Rev Genet* 2014, 15:445–451.
120. Santiago-Ortiz J, Ojala DS, Westesson O, Weinstein JR, Wong SY, Steinsapir A, Kumar S, Holmes I, Schaffer DV. AAV ancestral reconstruction library enables selection of broadly infectious viral variants. *Gene Ther* 2015, 22:934–946.
121. Zinn E, Pacouret S, Khaychuk V, Turunen HT, Carvalho LS, Andres-Mateos E, Shah S, Shelke R, Maurer AC, Plovie E, et al. In silico reconstruction of the viral evolutionary lineage yields a potent gene therapy vector. *Cell Rep* 2015, 12:1056–1068.
122. Van Vliet KM, Blouin V, Brument N, Agbandje-McKenna M, Snyder RO. The role of the adeno-associated virus capsid in gene transfer. *Methods Mol Biol* 2008, 437:51–91.
123. Drouin LM, Agbandje-McKenna M. Adeno-associated virus structural biology as a tool in vector development. *Future Virol* 2013, 8:1183–1199.
124. Agbandje-McKenna M, Kleinschmidt J. AAV capsid structure and cell interactions. *Methods Mol Biol* 2011, 807:47–92.
125. Srivastava A. In vivo tissue-tropism of adeno-associated viral vectors. *Curr Opin Virol* 2016, 21:75–80.
126. Lai Y, Yue Y, Bostick B, Duan D. Delivering large therapeutic genes for muscle gene therapy. In: Duan D, ed. *Muscle Gene Therapy*. New York: Springer Science + Business Media, LLC; 2010, 205–218.
127. Yuasa K, Miyagoe Y, Yamamoto K, Nabeshima Y, Dickson G, Takeda S. Effective restoration of dystrophin-associated proteins in vivo by adenovirus-mediated transfer of truncated dystrophin cDNAs. *FEBS Lett* 1998, 425:329–336.
128. Wang B, Li J, Xiao X. Adeno-associated virus vector carrying human minidystrophin genes effectively ameliorates muscular dystrophy in mdx mouse model. *Proc Natl Acad Sci USA* 2000, 97:13714–13719.
129. Harper SQ, Hauser MA, DelloRusso C, Duan D, Crawford RW, Phelps SF, Harper HA, Robinson AS, Engelhardt JF, Brooks SV, et al. Modular flexibility of dystrophin: implications for gene therapy of Duchenne muscular dystrophy. *Nat Med* 2002, 8:253–261.
130. Wang B, Li J, Fu FH, Xiao X. Systemic human minidystrophin gene transfer improves functions and life span of dystrophin and dystrophin/utrophin-deficient mice. *J Orthop Res* 2009, 27:421–426.
131. Yue Y, Li Z, Harper SQ, Davisson RL, Chamberlain JS, Duan D. Microdystrophin gene therapy of cardiomyopathy restores dystrophin-glycoprotein complex and improves sarcolemma integrity in the mdx mouse heart. *Circulation* 2003, 108:1626–1632.
132. Liu M, Yue Y, Harper SQ, Grange RW, Chamberlain JS, Duan D. Adeno-associated virus-mediated microdystrophin expression protects young mdx muscle from contraction-induced injury. *Mol Ther* 2005, 11:245–256.
133. Yue Y, Liu M, Duan D. C-terminal truncated microdystrophin recruits dystrobrevin and syntrophin to the dystrophin-associated glycoprotein complex and reduces muscular dystrophy in symptomatic utrophin/dystrophin double knock-out mice. *Mol Ther* 2006, 14:79–87.
134. Bostick B, Yue Y, Lai Y, Long C, Li D, Duan D. Adeno-associated virus serotype-9 microdystrophin gene therapy ameliorates electrocardiographic abnormalities in mdx mice. *Hum Gene Ther* 2008, 19:851–856.

135. Lai Y, Thomas GD, Yue Y, Yang HT, Li D, Long C, Judge L, Bostick B, Chamberlain JS, Terjung RL, et al. Dystrophins carrying spectrin-like repeats 16 and 17 anchor nNOS to the sarcolemma and enhance exercise performance in a mouse model of muscular dystrophy. *J Clin Invest* 2009, 119:624–635.
136. Bostick B, Shin J-H, Yue Y, Duan D. AAV-microdystrophin therapy improves cardiac performance in aged female mdx mice. *Mol Ther* 2011, 19:1826–1832.
137. Bostick B, Shin JH, Yue Y, Wasala NB, Lai Y, Duan D. AAV micro-dystrophin gene therapy alleviates stress-induced cardiac death but not myocardial fibrosis in >21-m-old mdx mice, an end-stage model of Duchenne muscular dystrophy cardiomyopathy. *J Mol Cell Cardiol* 2012, 53:217–222.
138. Gregorevic P, Blankinship MJ, Allen JM, Crawford RW, Meuse L, Miller DG, Russell DW, Chamberlain JS. Systemic delivery of genes to striated muscles using adeno-associated viral vectors. *Nat Med* 2004, 10:828–834.
139. Gregorevic P, Allen JM, Minami E, Blankinship MJ, Haraguchi M, Meuse L, Finn E, Adams ME, Froehner SC, Murry CE, et al. rAAV6-microdystrophin preserves muscle function and extends lifespan in severely dystrophic mice. *Nat Med* 2006, 12:787–789.
140. Percival JM, Gregorevic P, Odom GL, Banks GB, Chamberlain JS, Froehner SC. rAAV6-microdystrophin rescues aberrant Golgi complex organization in mdx skeletal muscles. *Traffic* 2007, 8:1424–1439.
141. Townsend D, Blankinship MJ, Allen JM, Gregorevic P, Chamberlain JS, Metzger JM. Systemic administration of micro-dystrophin restores cardiac geometry and prevents dobutamine-induced cardiac pump failure. *Mol Ther* 2007, 15:1086–1092.
142. Banks GB, Chamberlain JS, Froehner SC. Truncated dystrophins can influence neuromuscular synapse structure. *Mol Cell Neurosci* 2009, 40:433–441.
143. Gregorevic P, Blankinship MJ, Allen JM, Chamberlain JS. Systemic microdystrophin gene delivery improves skeletal muscle structure and function in old dystrophic mdx mice. *Mol Ther* 2008, 16:657–664.
144. Rodino-Klapac LR, Chicoine LG, Kaspar BK, Mendell JR. Gene therapy for Duchenne muscular dystrophy: expectations and challenges. *Arch Neurol* 2007, 64:1236–1241.
145. Yoshimura M, Sakamoto M, Ikemoto M, Mochizuki Y, Yuasa K, Miyagoe-Suzuki Y, Takeda S. AAV vector-mediated microdystrophin expression in a relatively small percentage of mdx myofibers improved the mdx phenotype. *Mol Ther* 2004, 10:821–828.
146. Banks GB, Judge LM, Allen JM, Chamberlain JS. The polyproline site in hinge 2 influences the functional capacity of truncated dystrophins. *PLoS Genet* 2010, 6:e1000958.
147. Foster H, Sharp PS, Athanasopoulos T, Trollet C, Graham IR, Foster K, Wells DJ, Dickson G. Codon and mRNA sequence optimization of microdystrophin transgenes improves expression and physiological outcome in dystrophic mdx mice following AAV2/8 gene transfer. *Mol Ther* 2008, 16:1825–1832.
148. Koo T, Malerba A, Athanasopoulos T, Trollet C, Boldrin L, Ferry A, Popplewell L, Foster H, Foster K, Dickson G. Delivery of AAV2/9-microdystrophin genes incorporating helix 1 of the coiled-coil motif in the C-terminal domain of dystrophin improves muscle pathology and restores the level of alpha1-syntrophin and alpha-dystrobrevin in skeletal muscles of mdx mice. *Hum Gene Ther* 2011, 22:1379–1388.
149. Duan D. Duchenne muscular dystrophy gene therapy in the canine model. *Hum Gene Ther Clin Dev* 2015, 26:57–69.
150. McGreevy JW, Hakim CH, McIntosh MA, Duan D. Animal models of Duchenne muscular dystrophy: from basic mechanisms to gene therapy. *Dis Model Mech* 2015, 8:195–213.
151. Wang Z, Allen JM, Riddell SR, Gregorevic P, Storb R, Tapscott SJ, Chamberlain JS, Kuhr CS. Immunity to adeno-associated virus-mediated gene transfer in a random-bred canine model of Duchenne muscular dystrophy. *Hum Gene Ther* 2007, 18:18–26.
152. Yue Y, Ghosh A, Long C, Bostick B, Smith BF, Kornegay JN, Duan D. A single intravenous injection of adeno-associated virus serotype-9 leads to whole body skeletal muscle transduction in dogs. *Mol Ther* 2008, 16:1944–1952.
153. Wang Z, Kuhr CS, Allen JM, Blankinship M, Gregorevic P, Chamberlain JS, Tapscott SJ, Storb R. Sustained AAV-mediated dystrophin expression in a canine model of Duchenne muscular dystrophy with a brief course of immunosuppression. *Mol Ther* 2007, 15:1160–1166.
154. Shin JH, Yue Y, Srivastava A, Smith B, Lai Y, Duan D. A simplified immune suppression scheme leads to persistent micro-dystrophin expression in Duchenne muscular dystrophy dogs. *Hum Gene Ther* 2012, 23:202–209.
155. Shin JH, Pan X, Hakim CH, Yang HT, Yue Y, Zhang K, Terjung RL, Duan D. Microdystrophin ameliorates muscular dystrophy in the canine model of Duchenne muscular dystrophy. *Mol Ther* 2013, 21:750–757.
156. Stamler JS, Meissner G. Physiology of nitric oxide in skeletal muscle. *Physiol Rev* 2001, 81:209–237.

157. Thomas GD, Victor RG. Nitric oxide mediates contraction-induced attenuation of sympathetic vasoconstriction in rat skeletal muscle. *J Physiol* 1998, 506:817–826.
158. Sander M, Chavoshan B, Harris SA, Iannaccone ST, Stull JT, Thomas GD, Victor RG. Functional muscle ischemia in neuronal nitric oxide synthase-deficient skeletal muscle of children with Duchenne muscular dystrophy. *Proc Natl Acad Sci USA* 2000, 97:13818–13823.
159. Li D, Yue Y, Lai Y, Hakim CH, Duan D. Nitrosative stress elicited by nNOSmu delocalization inhibits muscle force in dystrophin-null mice. *J Pathol* 2011, 223:88–98.
160. Thomas GD. Functional muscle ischemia in Duchenne and Becker muscular dystrophy. *Front Physiol* 2013, 4:381.
161. Rando TA. Role of nitric oxide in the pathogenesis of muscular dystrophies: a “two hit” hypothesis of the cause of muscle necrosis. *Microsc Res Tech* 2001, 55:223–235.
162. Tidball JG, Wehling-Henricks M. Nitric oxide synthase deficiency and the pathophysiology of muscular dystrophy. *J Physiol* 2014, 592:4627–4638.
163. Lai Y, Zhao J, Yue Y, Duan D. alpha2 and alpha3 helices of dystrophin R16 and R17 frame a microdomain in the alpha1 helix of dystrophin R17 for neuronal NOS binding. *Proc Natl Acad Sci USA* 2013, 110:525–530.
164. Li D, Bareja A, Judge L, Yue Y, Fairclough R, Davies KE, Chamberlain JS, Duan D. Sarcolemmal nNOS anchoring reveals a qualitative difference between dystrophin and utrophin. *J Cell Sci* 2010, 123:2008–2013.
165. Zhang Y, Yue Y, Li L, Hakim CH, Zhang K, Thomas GD, Duan D. Dual AAV therapy ameliorates exercise-induced muscle injury and functional ischemia in murine models of Duchenne muscular dystrophy. *Hum Mol Genet* 2013, 22:3720–3729.
166. Harper SQ. Molecular dissection of dystrophin identifies the docking site for nNOS. *Proc Natl Acad Sci USA* 2013, 110:387–388.
167. Duan D, Yue Y, Yan Z, Engelhardt JF. Trans-splicing vectors expand the packaging limits of adeno-associated virus for gene therapy applications. *Methods Mol Med* 2003, 76:287–307.
168. Ghosh A, Duan D. Expanding adeno-associated viral vector capacity: a tale of two vectors. *Biotechnol Gene Eng Rev* 2007, 24:165–177.
169. Duan D, Yue Y, Yan Z, Engelhardt JF. A new dual-vector approach to enhance recombinant adeno-associated virus-mediated gene expression through intermolecular cis activation. *Nat Med* 2000, 6:595–598.
170. Yan Z, Zhang Y, Duan D, Engelhardt JF. Trans-splicing vectors expand the utility of adeno-associated virus for gene therapy. *Proc Natl Acad Sci USA* 2000, 97:6716–6721.
171. Duan D, Yue Y, Engelhardt JF. Expanding AAV packaging capacity with trans-splicing or overlapping vectors: a quantitative comparison. *Mol Ther* 2001, 4:383–391.
172. Sun L, Li J, Xiao X. Overcoming adeno-associated virus vector size limitation through viral DNA heterodimerization. *Nat Med* 2000, 6:599–602.
173. Halbert CL, Allen JM, Miller AD. Efficient mouse airway transduction following recombination between AAV vectors carrying parts of a larger gene. *Nat Biotechnol* 2002, 20:697–701.
174. Hirsch ML, Wolf SJ, Samulski RJ. Delivering transgenic DNA exceeding the carrying capacity of AAV vectors. *Methods Mol Biol* 2016, 1382:21–39.
175. Yan Z, Lei-Butters DC, Zhang Y, Zak R, Engelhardt JF. Hybrid adeno-associated virus bearing nonhomologous inverted terminal repeats enhances dual-vector reconstruction of minigenes in vivo. *Hum Gene Ther* 2007, 18:81–87.
176. Lai Y, Yue Y, Liu M, Ghosh A, Engelhardt JF, Chamberlain JS, Duan D. Efficient in vivo gene expression by trans-splicing adeno-associated viral vectors. *Nat Biotechnol* 2005, 23:1435–1439.
177. Ghosh A, Yue Y, Lai Y, Duan D. A hybrid vector system expands adeno-associated viral vector packaging capacity in a transgene-independent manner. *Mol Ther* 2008, 16:124–130.
178. Zhang Y, Duan D. Novel mini-dystrophin gene dual adeno-associated virus vectors restore neuronal nitric oxide synthase expression at the sarcolemma. *Hum Gene Ther* 2012, 23:98–103.
179. Lostal W, Kodippili K, Yue Y, Duan D. Full-length dystrophin reconstitution with adeno-associated viral vectors. *Hum Gene Ther* 2014, 25:552–562.
180. Koo T, Popplewell L, Athanasopoulos T, Dickson G. Triple trans-splicing adeno-associated virus vectors capable of transferring the coding sequence for full-length dystrophin protein into dystrophic mice. *Hum Gene Ther* 2014, 25:98–108.
181. Spitali P, Aartsma-Rus A. Splice modulating therapies for human disease. *Cell* 2012, 148:1085–1088.
182. Goyenvallé A, Vulin A, Fougère F, Leturcq F, Kaplan JC, Garcia L, Danos O. Rescue of dystrophic muscle through U7 snRNA-mediated exon skipping. *Science* 2004, 306:1796–1799.
183. Goyenvallé A, Babbs A, van Ommen GJ, Garcia L, Davies KE. Enhanced exon-skipping induced by U7 snRNA carrying a splicing silencer sequence: Promising tool for DMD therapy. *Mol Ther* 2009, 17:1234–1240.

184. Goyenvalle A, Babbs A, Wright J, Wilkins V, Powell D, Garcia L, Davies KE. Rescue of severely affected dystrophin/utrophin-deficient mice through scAAV-U7snRNA-mediated exon skipping. *Hum Mol Genet* 2012, 21:2559–2571.
185. Bish LT, Sleeper MM, Forbes SC, Wang B, Reynolds C, Singletary GE, Trafny D, Morine KJ, Sanmiguel J, Cecchini S, et al. Long-term restoration of cardiac dystrophin expression in golden retriever muscular dystrophy following rAAV6-mediated exon skipping. *Mol Ther* 2012, 20:580–589.
186. Vulin A, Barthelemy I, Goyenvalle A, Thibaud JL, Beley C, Griffith G, Benchaouir R, le Hir M, Unterfinger Y, Lorain S, et al. Muscle function recovery in golden retriever muscular dystrophy after AAV1-U7 exon skipping. *Mol Ther* 2012, 20:2120–2133.
187. Barbash IM, Cecchini S, Faranesh AZ, Virag T, Li L, Yang Y, Hoyt RF, Kornegay JN, Bogan JR, Garcia L, et al. MRI roadmap-guided transendocardial delivery of exon-skipping recombinant adeno-associated virus restores dystrophin expression in a canine model of Duchenne muscular dystrophy. *Gene Ther* 2013, 20:274–282.
188. Le Guiner C, Montus M, Servais L, Cherel Y, Francois V, Thibaud JL, Wary C, Matot B, Larcher T, Guigand L, et al. Forelimb treatment in a large cohort of dystrophic dogs supports delivery of a recombinant AAV for exon skipping in Duchenne patients. *Mol Ther* 2014, 22:1923–1935.
189. Greelish JP, Su LT, Lankford EB, Burkman JM, Chen H, Konig SK, Mercier IM, Desjardins PR, Mitchell MA, Zheng XG, et al. Stable restoration of the sarcoglycan complex in dystrophic muscle perfused with histamine and a recombinant adeno-associated viral vector. *Nat Med* 1999, 5:439–443.
190. Rutledge EA, Halbert CL, Russell DW. Infectious clones and vectors derived from adeno-associated virus (AAV) serotypes other than AAV type 2. *J Virol* 1998, 72:309–319.
191. Gao GP, Alvira MR, Wang L, Calcedo R, Johnston J, Wilson JM. Novel adeno-associated viruses from rhesus monkeys as vectors for human gene therapy. *Proc Natl Acad Sci USA* 2002, 99:11854–11859.
192. Gao G, Vandenberghe LH, Alvira MR, Lu Y, Calcedo R, Zhou X, Wilson JM. Clades of Adeno-associated viruses are widely disseminated in human tissues. *J Virol* 2004, 78:6381–6388.
193. Wang Z, Zhu T, Qiao C, Zhou L, Wang B, Zhang J, Chen C, Li J, Xiao X. Adeno-associated virus serotype 8 efficiently delivers genes to muscle and heart. *Nat Biotechnol* 2005, 23:321–328.
194. Inagaki K, Fuess S, Storm TA, Gibson GA, McTiernan CF, Kay MA, Nakai H. Robust systemic transduction with AAV9 vectors in mice: efficient global cardiac gene transfer superior to that of AAV8. *Mol Ther* 2006, 14:45–53.
195. Pacak CA, Mah CS, Thattaliyath BD, Conlon TJ, Lewis MA, Cloutier DE, Zolotukhin I, Tarantal AF, Byrne BJ. Recombinant adeno-associated virus serotype 9 leads to preferential cardiac transduction in vivo. *Circ Res* 2006, 99:e3–9.
196. Bostick B, Ghosh A, Yue Y, Long C, Duan D. Systemic AAV-9 transduction in mice is influenced by animal age but not by the route of administration. *Gene Ther* 2007, 14:1605–1609.
197. Ghosh A, Yue Y, Long C, Bostick B, Duan D. Efficient whole-body transduction with trans-splicing adeno-associated viral vectors. *Mol Ther* 2007, 15:750–755.
198. Ghosh A, Yue Y, Shin JH, Duan D. Systemic trans-splicing adeno-associated viral delivery efficiently transduces the heart of adult mdx mouse, a model for Duchenne muscular dystrophy. *Hum Gene Ther* 2009, 20:1319–1328.
199. Odom GL, Gregorevic P, Allen JM, Chamberlain JS. Gene therapy of mdx mice with large truncated dystrophins generated by recombination using rAAV6. *Mol Ther* 2011, 19:36–45.
200. Yue Y, Shin JH, Duan D. Whole body skeletal muscle transduction in neonatal dogs with AAV-9. *Methods Mol Biol* 2011, 709:313–329.
201. Hakim CH, Yue Y, Shin JH, Williams RR, Zhang K, Smith BF, Duan D. Systemic gene transfer reveals distinctive muscle transduction profile of tyrosine mutant AAV-1, -6 and -9 in neonatal dogs. *Mol Ther Methods Clin Dev* 2014, 1:14002.
202. Pan X, Yue Y, Zhang K, Lostal W, Shin JH, Duan D. Long-term robust myocardial transduction of the dog heart from a peripheral vein by adeno-associated virus serotype-8. *Hum Gene Ther* 2013, 24:584–594.
203. Pan X, Yue Y, Zhang K, Hakim CH, Kodippili K, McDonald T, Duan D. AAV-8 is more efficient than AAV-9 in transducing neonatal dog heart. *Hum Gene Ther Methods* 2015, 26:54–61.
204. Shin JH, Yue Y, Smith B, Duan D. Humoral immunity to AAV-6, 8, and 9 in normal and dystrophic dogs. *Hum Gene Ther* 2012, 23:287–294.
205. Rapti K, Louis-Jeune V, Kohlbrenner E, Ishikawa K, Ladage D, Zolotukhin S, Hajjar RJ, Weber T. Neutralizing antibodies against AAV serotypes 1, 2, 6, and 9 in sera of commonly used animal models. *Mol Ther* 2011, 20:73–83.
206. Calcedo R, Franco J, Qin Q, Richardson DW, Mason JB, Boyd S, Wilson JM. Preexisting neutralizing antibodies to adeno-associated virus capsids in large animals other than monkeys may confound in vivo gene therapy studies. *Hum Gene Ther Methods* 2015, 26:103–105.

207. Kornegay JN, Li J, Bogan JR, Bogan DJ, Chen C, Zheng H, Wang B, Qiao C, Howard JF Jr, Xiao X. Widespread muscle expression of an AAV9 human mini-dystrophin vector after intravenous injection in neonatal dystrophin-deficient dogs. *Mol Ther* 2010, 18:1501–1508.
208. Hakim CH, Pan X, Kodippili K, Blessa T, Yang HT, Yao G, Leach S, Emter C, Yue Y, Zhang K, et al. Intravenous delivery of a novel micro-dystrophin vector prevented muscle deterioration in young adult canine Duchenne muscular dystrophy dogs. *Mol Ther* 2016, 24:S198–199.
209. Heller KN, Montgomery CL, Janssen PM, Clark KR, Mendell JR, Rodino-Klapac LR. AAV-mediated overexpression of human alpha7 integrin leads to histological and functional improvement in dystrophic mice. *Mol Ther* 2013, 21:520–525.
210. Odom GL, Gregorevic P, Allen JM, Finn E, Chamberlain JS. Microtrophin delivery through rAAV6 increases lifespan and improves muscle function in dystrophic dystrophin/utrophin-deficient mice. *Mol Ther* 2008, 16:1539–1545.
211. Shin JH, Bostick B, Yue Y, Hajjar R, Duan D. SERCA2a gene transfer improves electrocardiographic performance in aged mdx mice. *J Transl Med* 2011, 9:132.
212. Lai Y, Zhao J, Yue Y, Wasala NB, Duan D. Partial restoration of cardiac function with  $\Delta$ PDZ nNOS in aged mdx model of Duchenne cardiomyopathy. *Hum Mol Genet* 2014, 23:3189–3199.
213. Mendell JR, Sahenk Z, Malik V, Gomez AM, Flanigan KM, Lowes LP, Alfano LN, Berry K, Meadows E, Lewis S, et al. A phase IIIa follistatin gene therapy trial for Becker muscular dystrophy. *Mol Ther* 2015, 23:192–201.
214. Xu R, Camboni M, Martin PT. Postnatal overexpression of the CT GalNAc transferase inhibits muscular dystrophy in mdx mice without altering muscle growth or neuromuscular development: evidence for a utrophin-independent mechanism. *Neuromuscul Disord* 2007, 17:209–220.
215. Marshall JL, Crosbie-Watson RH. Sarcospan: a small protein with large potential for Duchenne muscular dystrophy. *Skelet Muscle* 2013, 3:1.
216. Huang LY, Halder S, Agbandje-McKenna M. Parvovirus glycan interactions. *Curr Opin Virol* 2014, 7:108–118.
217. Hsu PD, Lander ES, Zhang F. Development and applications of CRISPR-Cas9 for genome engineering. *Cell* 2014, 157:1262–1278.
218. Barrangou R, Doudna JA. Applications of CRISPR technologies in research and beyond. *Nat Biotechnol* 2016, 34:933–941.
219. Long C, Amoasii L, Mireault AA, McAnally JR, Li H, Sanchez-Ortiz E, Bhattacharyya S, Shelton JM, Bassel-Duby R, Olson EN. Postnatal genome editing partially restores dystrophin expression in a mouse model of muscular dystrophy. *Science* 2016, 351:400–403.
220. Tabebordbar M, Zhu K, Cheng JK, Chew WL, Widrick JJ, Yan WX, Maesner C, Wu EY, Xiao R, Ran FA, et al. In vivo gene editing in dystrophic mouse muscle and muscle stem cells. *Science* 2016, 351:407–411.
221. Dogra C, Changotra H, Wergedal JE, Kumar A. Regulation of phosphatidylinositol 3-kinase (PI3K)/Akt and nuclear factor-kappa B signaling pathways in dystrophin-deficient skeletal muscle in response to mechanical stretch. *J Cell Physiol* 2006, 208:575–585.
222. Bibee KP, Cheng YJ, Ching JK, Marsh JN, Li AJ, Keeling RM, Connolly AM, Golumbek PT, Myerson JW, Hu G, et al. Rapamycin nanoparticles target defective autophagy in muscular dystrophy to enhance both strength and cardiac function. *FASEB J* 2014, 28:2047–2061.
223. Pauly M, Daussin F, Burelle Y, Li T, Godin R, Fauconnier J, Koechlin-Ramonatxo C, Hugon G, Lacampagne A, Coisy-Quivy M, et al. AMPK activation stimulates autophagy and ameliorates muscular dystrophy in the mdx mouse diaphragm. *Am J Pathol* 2012, 181:583–592.

RESEARCH ARTICLE

Dystrophin-deficient dogs are by far the best available large animal models for Duchenne muscular dystrophy (DMD), the most common lethal childhood muscle degenerative disease. The use of the canine DMD model in basic disease mechanism research and translational studies will be greatly enhanced with the development of reliable outcome measures. Electrical impedance myography (EIM) is a non-invasive painless procedure that provides quantitative data relating to muscle composition and histology. EIM has been extensively used in neuromuscular disease research in both human patients and rodent models. Recent studies suggest that EIM may represent a highly reliable and convenient outcome measure in DMD patients and the mdx mouse model of DMD. To determine whether EIM can be used as a biomarker of disease severity in the canine model, we performed the assay in fourteen young (~6.6-m-old; 6 normal and 8 affected) and ten mature (~16.9-m-old; 4 normal and 6 affected) dogs of mixed background breeds. EIM was well tolerated with good inter-rater reliability. Affected dogs showed higher resistance, lower reactance and phase. The difference became more straightforward in mature dogs. Importantly, we observed a statistically significant correlation between the EIM data and muscle fibrosis. Our results suggest that EIM is a valuable objective measurement in the canine DMD model.

Chady H. Hakim<sup>1‡</sup>, Alex Mijailovic<sup>2</sup>, Thais B. Lessa<sup>1</sup>, Joan R. Coates<sup>3</sup>, Carmen Shin<sup>2</sup>, Seward B. Rutkove<sup>2\*</sup>, Dongsheng Duan<sup>1,4,5,6\*</sup>

**1** Department of Molecular Microbiology and Immunology, School of Medicine, The University of Missouri, Columbia, MO, United States of America, **2** Department of Neurology, Beth Israel Deaconess Medical Center, Boston, MA, United States of America, **3** Department of Veterinary Medicine and Surgery, College of Veterinary Medicine, University of Missouri, Columbia, MO, United States of America, **4** Department of Biomedical Sciences, College of Veterinary Medicine, University of Missouri, Columbia, MO, United States of America, **5** Department of Neurology, School of Medicine, University of Missouri, Columbia, MO, United States of America, **6** Department of Bioengineering, University of Missouri, Columbia, MO, United States of America

‡ Current address: National Center for Advancing Translational Sciences (NCATS) Bethesda, MD, United States of America

\* [srutkove@bidmc.harvard.edu](mailto:srutkove@bidmc.harvard.edu) (SBR); [duand@missouri.edu](mailto:duand@missouri.edu) (DD)



OPEN ACCESS

**Abstract**  
 Duchenne muscular dystrophy (DMD) is a devastating degenerative muscle disease affecting 1 in every 5,000 male births [1±3]. DMD is caused by the loss of dystrophin, an essential muscle protein that links the cytoskeleton to the cell membrane and extracellular matrix. The loss of dystrophin leads to muscle fiber damage and replacement by fibrous tissue. The use of the canine DMD model in basic disease mechanism research and translational studies will be greatly enhanced with the development of reliable outcome measures. Electrical impedance myography (EIM) is a non-invasive painless procedure that provides quantitative data relating to muscle composition and histology. EIM has been extensively used in neuromuscular disease research in both human patients and rodent models. Recent studies suggest that EIM may represent a highly reliable and convenient outcome measure in DMD patients and the mdx mouse model of DMD. To determine whether EIM can be used as a biomarker of disease severity in the canine model, we performed the assay in fourteen young (~6.6-m-old; 6 normal and 8 affected) and ten mature (~16.9-m-old; 4 normal and 6 affected) dogs of mixed background breeds. EIM was well tolerated with good inter-rater reliability. Affected dogs showed higher resistance, lower reactance and phase. The difference became more straightforward in mature dogs. Importantly, we observed a statistically significant correlation between the EIM data and muscle fibrosis. Our results suggest that EIM is a valuable objective measurement in the canine DMD model.

**Introduction**  
 Duchenne muscular dystrophy (DMD) is a devastating degenerative muscle disease affecting 1 in every 5,000 male births [1±3]. DMD is caused by the loss of dystrophin, an essential muscle protein that links the cytoskeleton to the cell membrane and extracellular matrix. The loss of dystrophin leads to muscle fiber damage and replacement by fibrous tissue. The use of the canine DMD model in basic disease mechanism research and translational studies will be greatly enhanced with the development of reliable outcome measures. Electrical impedance myography (EIM) is a non-invasive painless procedure that provides quantitative data relating to muscle composition and histology. EIM has been extensively used in neuromuscular disease research in both human patients and rodent models. Recent studies suggest that EIM may represent a highly reliable and convenient outcome measure in DMD patients and the mdx mouse model of DMD. To determine whether EIM can be used as a biomarker of disease severity in the canine model, we performed the assay in fourteen young (~6.6-m-old; 6 normal and 8 affected) and ten mature (~16.9-m-old; 4 normal and 6 affected) dogs of mixed background breeds. EIM was well tolerated with good inter-rater reliability. Affected dogs showed higher resistance, lower reactance and phase. The difference became more straightforward in mature dogs. Importantly, we observed a statistically significant correlation between the EIM data and muscle fibrosis. Our results suggest that EIM is a valuable objective measurement in the canine DMD model.

Introduction

Duchenne muscular dystrophy (DMD) is a devastating degenerative muscle disease affecting 1 in every 5,000 male births [1±3]. DMD is caused by the loss of dystrophin, an essential muscle

1. Introduction  
 2. Materials and Methods  
 3. Results  
 4. Discussion  
 5. Conclusion  
 6. Acknowledgments  
 7. Author Contributions  
 8. Funding  
 9. References  
 10. Supporting Information

structure protein. Absence of dystrophin renders muscle susceptible to contraction-induced damage and eventually muscle death and fibrosis. Over the last three decades, tremendous information has been generated regarding disease mechanisms and experimental therapeutics using inbred mouse models, in particular the mdx mouse [4]. Unfortunately, translation of the mdx data to human patients has been modest due to the limitation of the model [5±7]. Standard C57BL/10-background mdx mice do not develop clinical disease as seen in DMD patients [4]. Dystrophin-deficient dogs, on the other hand, show characteristic symptoms of muscular dystrophy and they also have a body size closer to that of humans [4]. Clearly, results obtained from dystrophic dogs will better inform the design of future clinical studies [8, 9].

Despite the general appreciation of the dog model, our understanding of dystrophic dogs remains limited [4, 10, 11]. A particular challenge is the lack of reliable, easy to use and non-invasive assays to monitor disease progression and response to therapy. Muscle biopsy, magnetic resonance imaging (MRI) and force measurement require putting affected dogs under general anesthesia which poses a significant risk of sudden cardiac death, malignant hyperthermia and rhabdomyolysis [12±16]. Gait analysis and activity monitoring are good non-invasive whole body assays, but they cannot provide disease status of individual muscle [17, 18].

Electrical impedance myography (EIM) is a painless, non-invasive, portable and easy to use technique to assess intrinsic muscle electric properties [19]. In EIM, a weak, high frequency electrical current is passed between two outer electrodes and the resulting voltages are measured from two inner electrodes. The electric impedance signals are determined by muscle composition, texture and architecture (such as myofiber size, edema, fatty infiltration and fibrosis). The EIM data allow investigators to quantitatively analyze muscle composition and structure. EIM has been extensively used as a painless and reliable outcome measurement to study various neuromuscular diseases including amyotrophic lateral sclerosis (ALS) [20±27], spinal muscular atrophy [28], facioscapulohumeral muscular dystrophy [29], congenital muscular dystrophy [30], inflammatory myopathy [31], inclusion-body myositis [19, 32], radiculopathy [33], and disuse atrophy [34]. Of relevance to our study, EIM has been successfully used in DMD patients and mdx mice [35±42]. These studies have revealed excellent reliability and validity of EIM as a powerful noninvasive biomarker for both pre-clinical and clinical studies.

Here we evaluated for the first time whether EIM can be used to distinguish muscle status in normal and affected dogs at ~ 6.6-m-old (young) and ~ 16.9-m-old (mature). We found EIM is a highly reliable and easy to use assay to study skeletal muscle in conscious dogs. Clear differences were detected between normal and affected dogs in multiple EIM parameters. Further, EIM changes correlated with the amount of fibrotic tissue in dog muscle.

## Materials and methods

### Animals

All animal experiments were approved by the Animal Care and Use Committee of the University of Missouri and were performed in accordance with NIH guidelines. A total of 24 dogs were used in the study including 10 normal male dogs and 14 affected dogs of both sexes (Table 1). Of the normal dogs, five were at the ages between 5.7 and 7-month-old (young normal dogs) and four were at the ages between 16.1 and 19.1-month-old (mature normal dogs). Of the affected dogs, eight were at the ages between 5.7 and 8.6-month-old (young affected dogs) and six were at the ages between 16.1 and 16.7-month-old (mature affected dogs). All experimental dogs were on a mixed genetic background and generated in house by artificial insemination. Affected dogs carry various mutations in the dystrophin gene that abort dystrophin expression. The genotype was determined by polymerase chain reaction according to published protocols [43±45]. The diagnosis was confirmed by the significantly elevated serum

**Table 1. Demographic information of experimental dogs.**

Dog ID	Age (m)	Type*	Sex	BW (kg)	Biopsy
E06	5.7	N	M	19.2	No
E21	5.7	N	M	20.0	Yes
E09	5.7	N	M	15.9	Yes**
E15	5.7	N	M	19.2	No
E11	7.0	N	M	19.5	Yes
E14	7.0	N	M	20.5	Yes
E01	5.7	A	F	10.2	No
E02	5.7	A	F	8.2	No
E13	7.0	A	F	18.6	Yes
E18	7.0	A	F	9.8	No
E04	7.1	A	M	16.2	No
E07	7.4	A	M	16.6	Yes
E10	7.4	A	F	10.4	No
E08	8.6	A	F	13.1	Yes
E03	16.1	N	M	19.0	No
E12	16.1	N	M	21.2	Yes
E24	19.1	N	M	17.2	No
E23	19.1	N	M	18.1	Yes
E20	16.1	A	M	19.0	No
E22	16.1	A	M	21.7	No
E17	16.1	A	M	15.1	Yes
E16	16.6	A	F	20.2	No
E19	16.6	A	F	17.1	No
E05	16.7	A	M	20.4	Yes

\*, Type refers to the genotype of the dog. N stands for a normal dog and A stands for an affected dog.  
 \*\*, Hydroxyproline assay was not performed due to insufficient amount of tissue obtained from biopsy.

<https://doi.org/10.1371/journal.pone.0173557.t001>

creatinase (CK) level in affected dogs. In a subset of dogs, diagnosis was also confirmed by muscle biopsy. All experimental dogs were housed in a specific-pathogen free animal care facility and kept under a 12-hour light/12-hour dark cycle. Affected dogs were housed in a raised platform kennel while normal dogs were housed in regular floor kennel. Depending on the age and size, two or more dogs are housed together to promote socialization. Normal dogs were fed dry Purina Lab Diet 5006 while affected dogs were fed wet Purina Proplan Puppy food. Dogs were given *ad libitum* access to clean drinking water. Toys were allowed in the kennel with dogs for enrichment. Dogs were monitored daily by the caregiver for overall health condition and activity. A full physical examination was performed by the veterinarian from the Office of Animal Research at the University of Missouri for any unusual changes (such as behavior, activity, food and water consumption, and clinical symptoms). The body weight of the dogs was measured every two weeks to monitor growth. Blood biochemistry was evaluated every 3 months in the first year and every six months thereafter. None of the experimental subjects were euthanized at the end of this study. However, a protocol was in place for euthanasia of animals at humane endpoints according to the 2013 AVMA Guidelines for the Euthanasia of Animals. Clinical signs for early euthanasia may include inability to obtain feed or water, pain unresponsive to analgesic therapy, paralysis of one or more extremities, and other signs of severe organ system dysfunction non-responsive to treatment or with a poor prognosis as determined by the veterinarian.

## EIM measurements

The handheld EIM 1103 device (Skulpt, Inc., San Francisco, CA) was used in the assay to collect multi-frequency impedance data (Fig 1). This device measures amplified signals directly using high-speed analog-to-digital converters. The EIM 1103 has a disposable multi-electrode array held in place via magnets. The electrode array used in this study was originally designed for use in young children and consists of three groups of electrodes, two nested sets for assessing current flow parallel to the major muscle fiber direction and one set for transverse measurement. The nested electrode design provides different depths of current penetration.

We chose to study the biceps femoris muscle because (1) it was sufficiently large to accommodate the EIM electrode array, which was developed for use in pediatric patients, (2) it was one of the most convenient muscles to perform the assay, and (3) it is the muscle most commonly used in biopsy.

The dog was awake throughout the assay and gently restrained in lateral recumbency (Fig 1). The muscle was identified according to anatomic markings. The fur on the skin was carefully removed with a fine shaving razor to ensure the skin was smooth for good contact with the electrode. The skin was cleaned and moistened with physiological saline. The electrode surface of the EIM device was positioned over the center of the bulk of the muscle on the skin as described in detail elsewhere [46]. Three consecutive multi-frequency impedance measurements were made on each muscle. Each measurement was performed at 40 discrete frequencies between 1 kHz to 1 MHz. The surface voltage patterns were recorded by the EIM device. The skin was remoistened with saline between each individual measurement. For each measurement, we collected data from three different electrode array configurations including the short longitudinal array, short transverse array and long longitudinal array. The real and imaginary components of the impedance (resistance and reactance) were calculated from the



**Fig 1. EIM assessment in dogs.** The photomicrograph illustrates the placement of the EIM device on the biceps femoris muscle of an experimental subject. Asterisk, the EIM device used in the assay.

<https://doi.org/10.1371/journal.pone.0173557.g001>

recorded voltages [19]. The phase was derived from the ratio of reactance and resistance. Specifically, phase (in radians) =  $\arctan(\text{reactance/resistance})$ . The resulting value in radians is then converted to degrees by multiplying the conversion constant 57.296. The assay was performed on both the left and right side in each dog.

Two investigators performed the EIM recording (CHH and SBR) (Fig 2). SBR had many years of experience in performing the EIM assay. CHH had never done the assay before and he was trained on site on how to perform the assay. The training included preparation of the dog skin, placement of the EIM probe, and evaluation of the data on a display to distinguish good signals versus poor signals that were caused by technical errors. No ongoing oversight was provided outside of this basic training. A similar training approach had been used previously in the clinical setting and revealed good reproducibility [38, 47].

### Histopathology

A muscle biopsy was obtained from the central portion of the biceps femoris in a subset of normal and affected dogs after the EIM measurement (Table 1). Haematoxylin and eosin (HE) staining was used to study the general histopathology. Slides were viewed using a Nikon E800 fluorescence microscope. Photomicrographs were taken with a QImage Retiga 1300 camera. Central nucleation and the myofiber diameter were determined from  $\geq 5$  random microscopic fields of an HE stained muscle section. The myofiber diameter was determined by the Feret minimum diameter method using Image J (<https://imagej.nih.gov/ij/docs/guide/146-30.html>).

### Hydroxyproline assay

Muscle fibrosis was measured by quantifying the hydroxyproline content according to a previously published protocol [48]. Briefly, the muscle sample was hydrolyzed in 1 ml 6 N HCl for 3 h at 115°C. After neutralization with 10 N NaOH (to the final pH of 7.5), the muscle lysate was oxidized with chlormatine-T. The hydroxyproline content was quantified by measuring the color absorbance at 558 nm. The hydroxyproline concentration was determined from a standard curve calculated from a linear dilution of L-hydroxyproline (Sigma-Aldrich, Saint Louis,

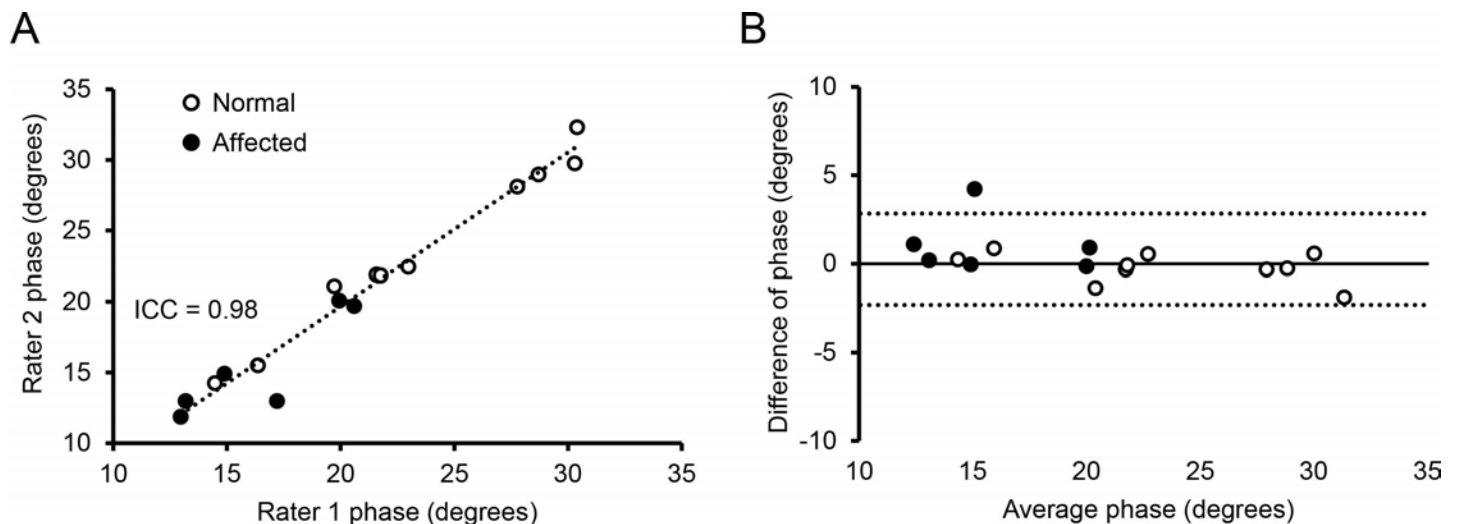


**Fig 2. Inter-rater reliability of the EIM assay in normal and affected dogs.** (A) The intra-class correlation plot of the two evaluators for phase at 150 kHz. (B) The Bland±Altman inter-rater plot. The solid line indicates the mean difference. Dashed lines mark standard deviations. Open circle, normal dogs; closed circle, affected dogs. Each circle represents one independent subject.

<https://doi.org/10.1371/journal.pone.0173557.g002>

MO). Due to insufficient amount of muscle tissue obtained from biopsy, the hydroxyproline content in one of the study dogs (Dog ID: E09) was not measured (Table 1).

## EIM data analysis

The dog identification was coded and the data analyzed blindly. A large set of multi-frequency EIM data was collected from each subject. Data from the triplicate measurements were averaged at each frequency prior to analysis. Data from the left and right side of the same subject were similar and were averaged as a single entry in data analysis. All three electrode-array configurations yielded similar results. For the purpose of presentation, figures were drawn with the data from the long longitudinal array in this manuscript. Multi-frequency analyses were performed to show the entire spectral view of EIM values in normal and affected dogs. Selected single frequencies were further analyzed to illustrate the differences between groups (young dogs versus mature dogs and normal dogs versus affected dogs). Such frequency variation is important to assess since the myofiber size is inversely related to the peak of the reactance and phase curves. Given that dogs have not been studied with EIM to date, the frequency that is most sensitive to dystrophic alteration cannot be known a priori.

## Statistical analysis

The bar graph data were presented as mean  $\pm$  standard error of mean. The multi-frequency data were presented as the population average. The myofiber diameter distribution data were presented as the percentage of the whole population. The correlation data were presented for individual subject. Statistical analysis was performed with the Matlab software (Mathworks, Natick MA). Statistical significance among multiple groups was determined by two-way ANOVA. If significance was established, post-hoc Mann-Whitney tests were performed to determine statistical significance between two groups. The relationship between the EIM data and the hydroxyproline content/myofiber diameter was established by Spearman correlation analysis using the EIM data from the subjects that had undergone biopsy. Significance was established at  $p < 0.05$ .

## Results

### Overview of the study and reliability of the assay

An important goal of our study is to determine whether the EIM assay can be reliably conducted by different investigators. We compared phase data obtained by an expert evaluator and a beginner (Fig 2). The intra-class correlation coefficient (ICC) is a commonly used index for quantifying the reliability of measurements between different raters [49]. The ICC was 0.98 in our study (Fig 2A). The Bland $\pm$ Altman plot illustrates dispersion of agreement by showing the magnitudes of differences in ratings in relation to the standard deviation of differences [50]. In our study, all differences were within the range of  $\pm 2$  ohms on the Bland $\pm$ Altman plot irrespective of the health condition of the dogs (normal or affected) (Fig 2B). There is no indication for systematic over- or under-rating.

### Qualitative assessment of EIM multifrequency data in dystrophic and healthy dogs

After establishing the robustness of the assay, we examined the overall EIM profile between normal and affected dogs cross the entire spectrum of the current frequencies from 1 kHz to 1 MHz. Similar to humans and mice, the resistance showed an exponential decline with increasing frequency in both normal and affected dogs (Fig 3A). Dystrophic and normal muscle had

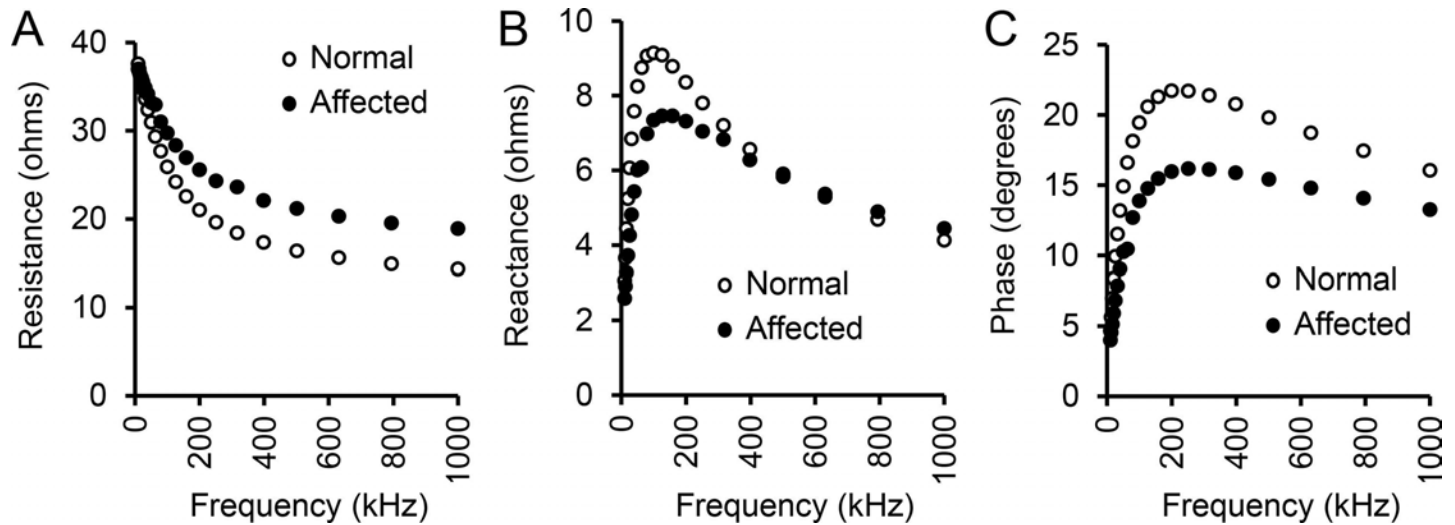


**Fig 3. Multifrequency EIM signature in normal and affected dogs.** (A) Relationship between resistance and frequency. (B) Relationship between reactance and frequency. (C) Relationship between phase and frequency. Open circle, normal dogs (n = 10); Closed circle, affected dogs (n = 14). Points represent average values across the population studied.

doi:10.1371/journal.pone.0173557.g003

similar resistance at the frequency of  $\leq 25$  kHz. Affected dog muscle showed consistently higher resistance thereafter. With the increase in the assay frequency, the difference in resistance between dystrophic and normal muscle became more apparent and it reached a plateau of  $\sim 5$  ohms at the frequency of  $\geq 200$  kHz (Fig 3A).

The overall average reactance and phase pattern showed trends similar to that observed in humans and mice (Fig 3B and 3C). The multi-frequency reactance pattern was interesting (Fig 3B). When the frequency was  $< 500$  kHz, normal muscle had a higher reactance value. The difference reached the peak at 40 to 70 kHz where the reactance of normal muscle was  $\sim 2.5$  ohms higher than that of dystrophic muscle. At the frequency of 500 kHz, normal and affected dogs yielded a similar reactance of  $\sim 6$  ohms. When the frequency was  $> 500$  kHz, the trend appeared to have reversed. The reactance of dystrophic muscle became slightly higher than that of normal muscle (Fig 3B).

The phase value of normal muscle was higher than that of dystrophic muscle in all frequencies tested (Fig 3C). The maximal difference was seen at 100 to 200 kHz where the difference was  $\sim 6$  degrees.

### Detailed analysis reveals statistically significant differences between normal and affected mature dogs in phase values

Given that most of our previous EIM studies have focused on analysis of phase values [20±28, 31±42], we specifically focused on this parameter here as well. The maximal phase was obtained at  $\sim 250$  kHz for both normal and dystrophic dogs (Fig 3C), a value considerably higher than typically seen in humans. Thus, in order to identify which frequency most effectively distinguished all four groups, we compared the phase values at 250 kHz as well as two lower frequencies (50 kHz and 150 kHz) and one higher frequency (400 kHz) in all four experimental groups (Fig 4). In young dogs, the phase values of affected dogs were reduced compared to those of normal dogs at these frequencies. However, the difference did not reach statistical significance. In mature dogs, the phase values of normal dogs were significantly higher than the corresponding values of affected dogs at all four frequencies. No difference

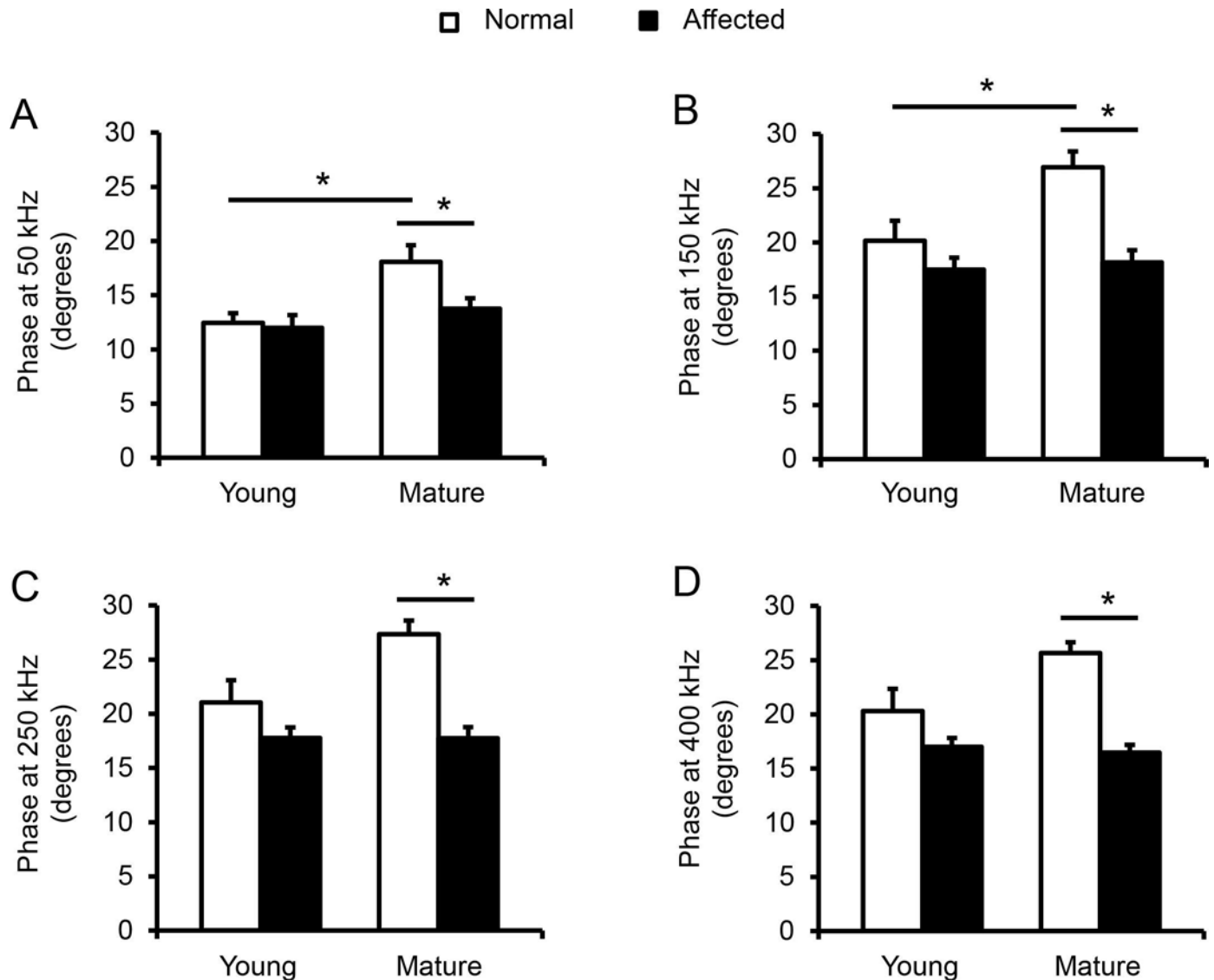


**Fig 4. Multi-group comparison of phase.** (A) Phase at 50 kHz. There was statistically significant difference between young and mature normal dogs, and between mature normal and affected dogs. (B) Phase at 150 kHz. There was a significant difference between immature young adult and mature adult normal dogs and between mature normal and affected dogs. (C) Phase at 250 kHz. There was a significant difference between mature normal and affected dogs. (D) Phase at 400 kHz. There was a significant difference between mature normal and affected dogs. Open bar, normal dogs; filled bar, affected dogs. The sample size for young normal, young affected, mature normal and mature affected dogs are 6, 8, 4 and 6, respectively. Asterisk, significantly different.

was detected between young affected dogs and mature affected dogs. At all four frequencies, the phase values of young normal dogs were lower than those of mature normal dogs. The difference was statistically significant at 50 and 150 kHz but not at 250 and 400 kHz.

### Biopsy reveals disease and age-related changes in muscle histology and fibrosis

To correlate the EIM results with muscle disease, we biopsied the biceps femoris muscle after the EIM assay in 11 dogs including 4 young normal dogs, 3 young affected dogs, 2 mature normal dogs and 2 mature affected dogs (Table 1). On HE staining, muscle samples from normal

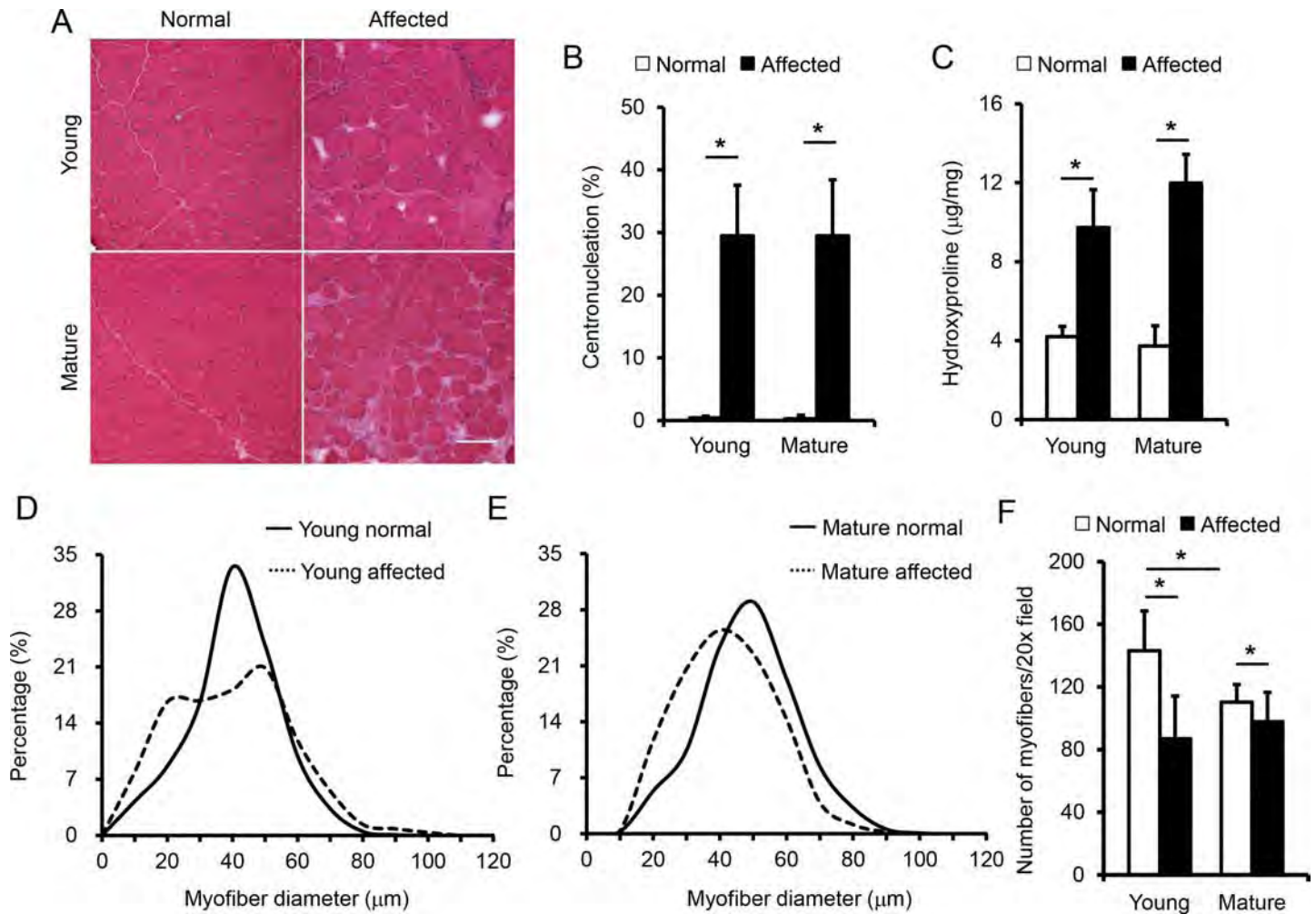


**Fig 5. Quantitative evaluation of muscle histology and fibrosis.** (A) Representative photomicrographs of the biceps femoris muscle of young normal, young affected, mature normal and mature affected dogs. Scale bar, 100 µm. Enlarged image is presented in S1 Fig. (B) Quantification of myofibers that contain centrally localized nuclei. The sample size for young normal, young affected, mature normal and mature affected groups are 4, 3, 2 and 3 dogs, respectively. There was a significant difference between normal and affected dogs in the mature age groups. (C) Quantification of muscle fibrosis by the hydroxyproline assay. The sample size for young normal, young affected, mature normal and mature affected groups are 3, 3, 2 and 3 dogs, respectively. There was a significant difference between normal and affected dogs in both age groups, but no significant difference between young and mature affected dogs. (D) Distribution of the minimum Feret diameter in young normal (n = 1,441 myofibers) and young affected (n = 1,104 myofibers) dogs. (E) Distribution of the minimum Feret diameter in mature normal (n = 1,045 myofibers) and mature affected (n = 1,225 myofibers) dogs. (F) Quantification of myofiber density per 20x field. The numbers of 20x field counted in young normal, young affected, mature normal and mature affected dogs were 37, 30, 24 and 20, respectively. There was a significant difference between young and mature normal dogs and between normal and affected dogs. Open bar, normal dogs; filled bar, affected dogs. Asterisk, significantly different.

doi:10.1371/journal.pone.0173557.g005

dogs showed expected histology such as a homogenous myofiber size, peripheral localization of myonuclei, and lack of inflammatory cell infiltration and interstitial fibrosis (Fig 5A, S1 Fig). The muscle from affected dogs showed characteristic features of dystrophic pathology. Specifically, extremely large and small myofibers co-existed next to each other. In a substantial portion of myofibers, myonuclei were present at the center. There were also abundant inflammatory cells and a clear increase of interstitial tissue between muscle cells indicating muscle fibrosis (Fig 5A, S1 Fig). Nevertheless, there was no substantial difference between affected dogs at the two different ages (Fig 5A, S1 Fig).

To more accurately document muscle pathology, we quantified the percent of centrally nucleated myofibers (Fig 5B), the hydroxyproline content (Fig 5C), myofiber size distribution (Fig 5D and 5E), and muscle cell density (Fig 5F). On morphometric quantification, affected dogs showed a centronucleation of ~30% while normal dogs had < 0.5% in both age groups (Fig 5B). The hydroxyproline quantification is one of the most reliable assays to evaluate muscle fibrosis. In normal dogs, it was ~ 4 µg/mg but in affected dogs it reached ≥ 10 µg/mg (Fig 5C). Adult affected dogs had a slightly higher hydroxyproline content than young adult affected dogs but the difference was not statistically significant (Fig 5C). On fiber diameter quantification, young adult normal dogs showed a sharp bell curve indicating most of the myofibers are of a similar size (Fig 5D). Young affected dogs showed an interesting broad dual peak curve. They also had more very small and very large myofibers (Fig 5D). In adult normal dogs, the upstroke of the curve shifted toward left suggesting an absence of extremely small myofibers (Fig 5E). This correlated well with the dog growth during maturation. This was also consistent with the myofiber density quantification which showed a significant reduction of the myofiber number per 20x field in mature normal dogs compared to that of young normal dogs (Fig 5F). Compared with mature normal dogs, mature affected dogs had a broader myofiber size distribution curve and also more small myofibers (Fig 5E). It is worth pointing out that in both age groups, there were significantly more myofibers per 20x field in normal dogs compared to that of affected dogs (Fig 5F). This is consistent with our HE staining and hydroxyproline quantification suggesting there was more interstitial fibrosis in affected dogs.

### EIM changes correlates with muscle fibrosis

With quantitative data from the EIM assay and muscle pathology evaluation, we examined whether there was a correlation between these two different outcome measurements. For the purpose of analysis, we used data from phase at 150 kHz since it showed the greatest differences across groups (Fig 4). On Spearman correlation analysis, we detected a statistically significant inverse correlation between the EIM data and the hydroxyproline content (Rho = -0.82 and p = 0.006) (Fig 6A). Specifically, when the level of fibrosis was low, the phase value

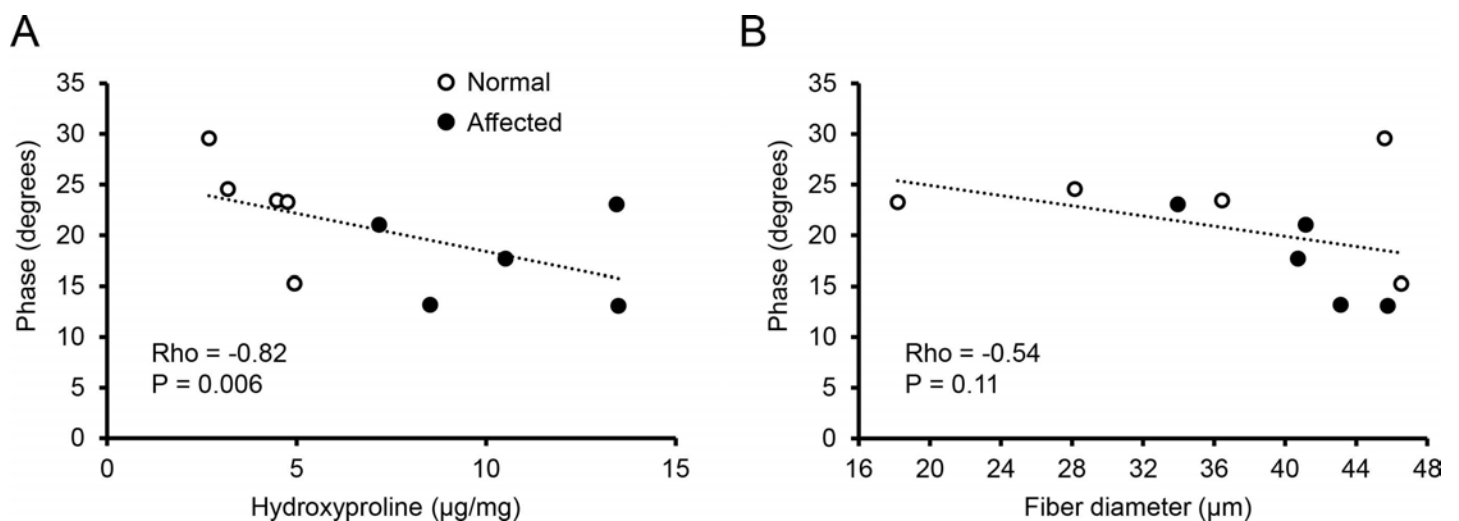


**Fig 6. Spearman analysis of correlation between the EIM data and disease status.** (A) Correlation between phase at 150 kHz and the hydroxyproline content. (B) Correlation between phase at 150 kHz and the myofiber diameter. Rho and p values are marked for each correlation analysis. Open circle, normal dogs; closed circle, affected dogs. Each circle represents one independent subject.

<https://doi.org/10.1371/journal.pone.0173557.g006>

was high (Fig 6A). Correlation analysis between the phase and the myofiber size showed a modest relationship, which was not statistically significant ( $Rho = -0.54$  and  $p = 0.11$ ) (Fig 6B).

## Discussion

EIM has been extensively used to study neuromuscular pathologies in humans and rodents. Some studies also explored EIM in bovine muscle in vitro [51]. However, EIM has never been used in dogs. Here we present the first study applying EIM to the canine model of a neuromuscular disease. Our goals were to determine (1) whether it is easy to conduct the EIM assay in dogs and whether reproducible data can be generated, (2) whether EIM can discriminate normal and dystrophic dog muscle, (3) whether age maturation (from immature young adult to mature adult) influences the EIM results, and (4) whether the EIM data correlate with disease status determined by classical histological quantification and biochemical assays.

Consistent with our previous studies in human patients and rodent models, we found EIM measurement was easy to perform on the surface muscle of a dog limb (Fig 1). Training was straightforward. There was excellent inter-evaluator reliability between an experienced assay performer and a trainee (Fig 2) [35, 42, 52±54].

In early studies, a single 50 kHz frequency device was used to measure muscle electric impedance. Recent studies suggest that multi-frequency EIM is a better option in diagnosing normal from diseased muscle and even in distinguishing different neuromuscular diseases [26, 32, 37, 55]. By profiling three impedance parameters (resistance, reactance and phase), we obtained distinctive patterns between normal and affected dogs, suggesting EIM is a sensitive measure in the canine model of DMD (Fig 3). Comparing with our published data in amyotrophic lateral sclerosis (ALS) and inclusion-body myositis patients [19, 32], we noticed that the values of resistance were always increased but the values of phase were always reduced in diseased muscles across a spectrum of frequencies (Fig 3) [19, 32]. However, there were unique disease-specific features. For example, at low frequencies, the difference in resistance was lost between normal and affected dogs in our study but the difference persisted between normal people and patients with inclusion-body myositis throughout the entire range of frequencies (Fig 3A) [19]. Importantly, these multifrequency variations in measured phase values are mirrored in boys with DMD that have taken part in the longitudinal QED study [SBR, unpublished results] (<https://clinicaltrials.gov/ct2/show/NCT01491555>).

Previous studies suggested that the age influences EIM results [41, 56, 57]. Specifically, EIM parameters display an age-associated decline in phase and reactance in older individuals [56, 57] but an increase in phase and reactance in children with growth [28]. A direct comparison of EIM results of 2-m-old and 18-m-old normal mice also suggests that phase and reactance were significantly increased from 2 to 18 months [41]. Similarly, in our study, phase at 50 and 150 kHz was also significantly increased in mature adult dogs (Fig 4A and 4B). A similar trend was observed at 250 and 400 kHz though it did not reach statistical significance (Fig 4C and 4D). We suspect that the increase of the phase values in mature adult dogs of our study is likely due to muscle growth. The subjects in our young and mature normal dogs were at ~7 and ~17-m-old, respectively (Table 1). During this period, dogs are reaching their sexual maturity and still growing. In support, mature normal dogs had fewer small-size myofibers (Fig 5D and 5E) and fewer myofibers per unit area (Fig 5F), suggesting they indeed had larger myofibers.

Interestingly, we did not see much difference between young and mature affected dogs in phase (Fig 4). EIM measures muscle composition and structure. Hence, EIM results are subject to changes of many factors (such as the myofiber size, amount of fat and fibrotic tissue, and inflammation and edema). Although some differences in the pattern of myofiber size distribution were observed between young and mature affected dogs (Fig 5D and 5E), we did not see

noticeable progress of muscle disease from ~7 to ~17 months by quantitative analyses of muscle pathology (centronucleation, myofiber number per unit area and hydroxyproline content). Clinically, no major differences in disease presentations were noticed between young and mature affected dogs used in this study. There was no significant difference in the body weight (Table 1). Dogs in both age groups showed similar activity. Although hypersalivation was seen in some mature affected dogs, immobilization was not observed in any affected dog in our study. Collectively, it appears that muscle disease was relatively stable from ~7 to ~17 months in affected dogs evaluated in this study. Although large-scale population studies are needed to validate this intriguing finding, our observations in affected dogs seems to mirror the so-called "honeymoon phase" in DMD patients [4, 58±61]. Hence, the lack of difference in the EIM assay agreed well with the relatively stationary disease course. To more accurately quantify the relationship between the EIM data and muscle status, we performed a Spearman correlation analysis using the reactance value at 150 kHz (Fig 6). Although there was no clear correlation between the reactance and the myofiber diameter, a statistically definitive correlation was found between the EIM data and the level of muscle fibrosis (Fig 6A). Collectively, the EIM findings appear to have reliably reflected muscle health in the context of the canine DMD model.

As a proof-of-principle study, we have demonstrated that the EIM assay is a promising technique for studying neuromuscular diseases in large animal models. However, validity studies are needed to fully establish EIM as a biomarker. Specifically, (1) we have collected a vast amount of impedance data in this study. Additional in-depth data mining is needed to identify the most sensitive parameters, including evaluation of a variety of multifrequency measures, such as multi-frequency ratios and arithmetically derived composite scores [36, 37]; (2) in this study, we only had male normal dogs. Since sex may influence EIM [57], we need to expand our study to include both male and female normal dogs; (3) for the convenience, we have only studied one dog muscle (biceps femoris) in the current study. With the further development of the technique (for example, the custom-designed EIM apparatus), we may evaluate a variety of different surface muscles to gain a more global evaluation of the disease in the dog model; (4) in this study, we have focused on correlating the pathological findings with the EIM data, there is a need to determine whether the EIM data relate well with the results of physiological assays such as muscle force measurement, gait analysis and activity monitoring in dogs [12, 17, 18]; results in mdx mice (Seward B. Rutkove, unpublished results) and ALS mice suggest a relationship between muscle force measurement and impedance values [26]. Similarly, it will be worthwhile to compare EIM with muscle ultrasound and MRI [38, 40]; (5) as a cross-sectional study, we only selected two age groups. To establish a robust natural history profile for the entire population of normal and affected dogs, we are obligated to conduct longitudinal follow-up studies on a large cohort of dogs; (6) as our ultimate goal is to develop an effective therapy for DMD, it will be necessary to implement the EIM assay in preclinical therapy studies to help quantify the efficacy of novel experimental interventions.

## Supporting information

**S1 Fig. This is an enlarged image of Fig 5A.**  
(TIF)

## Acknowledgments

This study was supported by the National Institutes of Health (NS-90634 and AR-70517 to DD; NS-055099 to SBR), Department of Defense (MD130014 to DD), Jesse's Journey-The

Foundation for Gene and Cell Therapy (to DD) and Hope for Javier (to DD). The funders had no role in study design, data collection and analysis, decision to publish, or preparation of the manuscript. We would like to thank Keqing Zhang, Yongping Yue, Austin Peters, Dr. Scott W. Korte, Dr. Dietrich H. Volkman, and Dr. Dawna Voelkl for their technical help.

## Author Contributions

**Conceptualization:** DD SBR.

**Data curation:** AM CHH CS DD SBR.

**Formal analysis:** AM CHH CS DD JRC SBR.

**Funding acquisition:** DD SBR.

**Investigation:** AM CHH CS DD JRC SBR TBL.

**Methodology:** AM CHH CS DD JRC SBR TBL.

**Project administration:** DD SBR.

**Resources:** DD SBR.

**Software:** AM CS SBR.

**Supervision:** DD SBR.

**Validation:** CHH SBR.

**Visualization:** AM CHH CS DD SBR.

**Writing ± original draft:** CHH DD SBR.

**Writing ± review & editing:** AM CHH CS DD JRC SBR TBL.

## References

1. Mendell JR, Lloyd-Puryear M. Report of MDA muscle disease symposium on newborn screening for Duchenne muscular dystrophy. *Muscle Nerve*. 2013; 48(1):21±6. <https://doi.org/10.1002/mus.23810> PMID: 23716304
2. Romitti PA, Zhu Y, Puzhankara S, James KA, Nabukera SK, Zamba GK, et al. Prevalence of Duchenne and Becker muscular dystrophies in the United States. *Pediatrics*. 2015:Online publication ahead of print on Feb 16, 2015.
3. Mah JK, Korngut L, Dykeman J, Day L, Pringsheim T, Jette N. A systematic review and meta-analysis on the epidemiology of Duchenne and Becker muscular dystrophy. *Neuromuscul Disord*. 2014; 24(6):482±91. <https://doi.org/10.1016/j.nmd.2014.03.008> PMID: 24780148
4. McGreevy JW, Hakim CH, McIntosh MA, Duan D. Animal models of Duchenne muscular dystrophy: from basic mechanisms to gene therapy. *Dis Model Mech*. 2015; 8(3):195±213. <https://doi.org/10.1242/dmm.018424> PMID: 25740330
5. Mendell JR, Kissel JT, Amato AA, King W, Signore L, Prior TW, et al. Myoblast transfer in the treatment of Duchenne's muscular dystrophy. *N Engl J Med*. 1995; 333(13):832±8. <https://doi.org/10.1056/NEJM199509283331303> PMID: 7651473
6. Wagner KR, Fleckenstein JL, Amato AA, Barohn RJ, Bushby K, Escolar DM, et al. A phase I/II trial of MYO-029 in adult subjects with muscular dystrophy. *Ann Neurol*. 2008; 63(5):561±71. Epub 2008/03/13. <https://doi.org/10.1002/ana.21338> PMID: 18335515
7. Birmingham K. Controversial muscular dystrophy therapy goes to court. *Nature medicine*. 1997; 3(10):1058. PMID: 9334704
8. Duan D. Duchenne muscular dystrophy gene therapy: lost in translation? *Res Rep Biol*. 2011; 2:31±42.
9. Duan D. Duchenne muscular dystrophy gene therapy in the canine model. *Hum Gene Ther Clin Dev*. 2015; 26(1):57±69. <https://doi.org/10.1089/humc.2015.006> PMID: 25710459

10. Valentine BA, Winand NJ, Pradhan D, Moise NS, de Lahunta A, Kornegay JN, et al. Canine X-linked muscular dystrophy as an animal model of Duchenne muscular dystrophy: a review. *American journal of medical genetics*. 1992; 42(3):352±6. <https://doi.org/10.1002/ajmg.1320420320> PMID: 1536178
11. Kornegay JN, Bogan JR, Bogan DJ, Childers MK, Li J, Nghiem P, et al. Canine models of Duchenne muscular dystrophy and their use in therapeutic strategies. *Mammalian genome official journal of the International Mammalian Genome Society*. 2012; 23(1±2):85±108. PubMed Central PMCID: PMC3911884. <https://doi.org/10.1007/s00335-011-9382-y> PMID: 22218699
12. Yang HT, Shin JH, Hakim CH, Pan X, Terjung RL, Duan D. Dystrophin deficiency compromises force production of the extensor carpi ulnaris muscle in the canine model of Duchenne muscular dystrophy. *PLoS ONE*. 2012; 7(9):e44438. <https://doi.org/10.1371/journal.pone.0044438> PMID: 22973449
13. Yue Y, Pan X, Hakim CH, Kodippili K, Zhang K, Shin JH, et al. Safe and bodywide muscle transduction in young adult Duchenne muscular dystrophy dogs with adeno-associated virus. *Hum Mol Genet*. 2015; 24(20):5880±90. <https://doi.org/10.1093/hmg/ddv310> PMID: 26264580
14. Yue Y, Shin JH, Duan D. Whole body skeletal muscle transduction in neonatal dogs with AAV-9. *Methods Mol Biol*. 2011; 709:313±29. PubMed Central PMCID: PMC3118043. [https://doi.org/10.1007/978-1-61737-982-6\\_21](https://doi.org/10.1007/978-1-61737-982-6_21) PMID: 21194038
15. Hayes J, Veyckemans F, Bissonnette B. Duchenne muscular dystrophy: an old anesthesia problem revisited. *Paediatric anaesthesia*. 2008; 18(2):100±6. Epub 2008/01/11. <https://doi.org/10.1111/j.1460-9592.2007.02302.x> PMID: 18184239
16. Segura LG, Lorenz JD, Weingarten TN, Scavonetto F, Bojanic K, Selcen D, et al. Anesthesia and Duchenne or Becker muscular dystrophy: review of 117 anesthetic exposures. *Paediatric anaesthesia*. 2013; 23(9):855±64. <https://doi.org/10.1111/pan.12248> PMID: 23919455
17. Shin JH, Greer B, Hakim CH, Zhou Z, Chung YC, Duan Y, et al. Quantitative phenotyping of Duchenne muscular dystrophy dogs by comprehensive gait analysis and overnight activity monitoring. *PLoS One*. 2013; 8(3):e59875. <https://doi.org/10.1371/journal.pone.0059875> PMID: 23544107
18. Hakim CH, Peters AA, Feng F, Yao G, Duan D. Night activity reduction is a signature physiological biomarker for Duchenne muscular dystrophy dogs. *Journal of neuromuscular diseases*. 2015; 2(4):397±407. <https://doi.org/10.3233/JND-150114> PMID: 27812508
19. Rutkove SB. Electrical impedance myography: Background, current state, and future directions. *Muscle Nerve*. 2009; 40(6):936±46. PubMed Central PMCID: PMC2824130. <https://doi.org/10.1002/mus.21362> PMID: 19768754
20. Li J, Staats WL, Spieker A, Sung M, Rutkove SB. A technique for performing electrical impedance myography in the mouse hind limb: data in normal and ALS SOD1 G93A animals. *PLoS One*. 2012; 7(9):e45004. PubMed Central PMCID: PMC3460964. <https://doi.org/10.1371/journal.pone.0045004> PMID: 23028733
21. Rutkove S. Electrical impedance myography as a biomarker for ALS. *Lancet Neurol*. 2009; 8(3):226; author reply 7. PubMed Central PMCID: PMC2719292. [https://doi.org/10.1016/S1474-4422\(09\)70030-4](https://doi.org/10.1016/S1474-4422(09)70030-4) PMID: 19233030
22. Rutkove SB, Caress JB, Cartwright MS, Burns TM, Warder J, David WS, et al. Electrical impedance myography as a biomarker to assess ALS progression. *Amyotrophic lateral sclerosis official publication of the World Federation of Neurology Research Group on Motor Neuron Diseases*. 2012; 13(5):439±45. PubMed Central PMCID: PMC3422377.
23. Rutkove SB, Zhang H, Schoenfeld DA, Raynor EM, Shefner JM, Cudkowicz ME, et al. Electrical impedance myography to assess outcome in amyotrophic lateral sclerosis clinical trials. *Clinical neurophysiology official journal of the International Federation of Clinical Neurophysiology*. 2007; 118(11):2413±8. PubMed Central PMCID: PMC2080665. <https://doi.org/10.1016/j.clinph.2007.08.004> PMID: 17897874
24. Li J, Sung M, Rutkove SB. Electrophysiologic biomarkers for assessing disease progression and the effect of riluzole in SOD1 G93A ALS mice. *PLoS One*. 2013; 8(6):e65976. PubMed Central PMCID: PMC3675066. <https://doi.org/10.1371/journal.pone.0065976> PMID: 23762454
25. Rutkove SB, Caress JB, Cartwright MS, Burns TM, Warder J, David WS, et al. Electrical impedance myography correlates with standard measures of ALS severity. *Muscle Nerve*. 2014; 49(3):441±3. <https://doi.org/10.1002/mus.24128> PMID: 24273034
26. Li J, Pacheck A, Sanchez B, Rutkove SB. Single and modeled multifrequency electrical impedance myography parameters and their relationship to force production in the ALS SOD1G93A mouse. *Amyotrophic lateral sclerosis & frontotemporal degeneration*. 2016; 17(5±6):397±403. PubMed Central PMCID: PMC5004347.
27. McIluff CE, Yim SJ, Pacheck AK, Rutkove SB. Optimizing electrical impedance myography of the tongue in ALS. *Muscle Nerve*. 2016.

28. Rutkove SB, Gregas MC, Darras BT. Electrical impedance myography in spinal muscular atrophy: a longitudinal study. *Muscle Nerve*. 2012; 45(5):642±7. <https://doi.org/10.1002/mus.23233> PMID: [22499089](https://pubmed.ncbi.nlm.nih.gov/22499089/)
29. Statland JM, Heatwole C, Eichinger K, Dilek N, Martens WB, Tawil R. Electrical impedance myography in facioscapulohumeral muscular dystrophy. *Muscle Nerve*. 2016; 54(4):696±701. PubMed Central PMCID: PMC4972708. <https://doi.org/10.1002/mus.25065> PMID: [26840230](https://pubmed.ncbi.nlm.nih.gov/26840230/)
30. Schwartz DP, Dastgir J, Salman A, Lear B, Bonnemann CG, Lehky TJ. Electrical impedance myography discriminates congenital muscular dystrophy from controls. *Muscle Nerve*. 2016; 53(3):402±6. <https://doi.org/10.1002/mus.24770> PMID: [26179210](https://pubmed.ncbi.nlm.nih.gov/26179210/)
31. Tarulli A, Esper GJ, Lee KS, Aaron R, Shiffman CA, Rutkove SB. Electrical impedance myography in the bedside assessment of inflammatory myopathy. *Neurology*. 2005; 65(3):451±2. <https://doi.org/10.1212/01.wnl.0000172338.95064.cb> PMID: [16087913](https://pubmed.ncbi.nlm.nih.gov/16087913/)
32. Esper GJ, Shiffman CA, Aaron R, Lee KS, Rutkove SB. Assessing neuromuscular disease with multifrequency electrical impedance myography. *Muscle Nerve*. 2006; 34(5):595±602. <https://doi.org/10.1002/mus.20626> PMID: [16881067](https://pubmed.ncbi.nlm.nih.gov/16881067/)
33. Rutkove SB, Esper GJ, Lee KS, Aaron R, Shiffman CA. Electrical impedance myography in the detection of radiculopathy. *Muscle Nerve*. 2005; 32(3):335±41. <https://doi.org/10.1002/mus.20377> PMID: [15948202](https://pubmed.ncbi.nlm.nih.gov/15948202/)
34. Tarulli AW, Duggal N, Esper GJ, Garmirian LP, Fogerson PM, Lin CH, et al. Electrical impedance myography in the assessment of disuse atrophy. *Archives of physical medicine and rehabilitation*. 2009; 90(10):1806±10. Central PMCID: PMC2829834. <https://doi.org/10.1016/j.apmr.2009.04.007> PMID: [19801075](https://pubmed.ncbi.nlm.nih.gov/19801075/)
35. Zaidman CM, Wang LL, Connolly AM, Florence J, Wong BL, Parsons JA, et al. Electrical impedance myography in Duchenne muscular dystrophy and healthy controls: A multicenter study of reliability and validity. *Muscle Nerve*. 2015; 52(4):592±7. <https://doi.org/10.1002/mus.24611> PMID: [25702806](https://pubmed.ncbi.nlm.nih.gov/25702806/)
36. Shklyar I, Pasternak A, Kapur K, Darras BT, Rutkove SB. Composite biomarkers for assessing Duchenne muscular dystrophy: an initial assessment. *Pediatric neurology*. 2015; 52(2):202±5. PubMed Central PMCID: PMC4336219. <https://doi.org/10.1016/j.pediatrneurol.2014.09.014> PMID: [25447928](https://pubmed.ncbi.nlm.nih.gov/25447928/)
37. Schwartz S, Geisbush TR, Mijailovic A, Pasternak A, Darras BT, Rutkove SB. Optimizing electrical impedance myography measurements by using a multifrequency ratio: a study in Duchenne muscular dystrophy. *Clinical neurophysiology official journal of the International Federation of Clinical Neurophysiology*. 2015; 126(1):202±8. PubMed Central PMCID: PMC4234696. <https://doi.org/10.1016/j.clinph.2014.05.007> PMID: [24929900](https://pubmed.ncbi.nlm.nih.gov/24929900/)
38. Rutkove SB, Geisbush TR, Mijailovic A, Shklyar I, Pasternak A, Visyak N, et al. Cross-sectional evaluation of electrical impedance myography and quantitative ultrasound for the assessment of Duchenne muscular dystrophy in a clinical trial setting. *Pediatric neurology*. 2014; 51(1):88±92. PubMed Central PMCID: PMC4063877. <https://doi.org/10.1016/j.pediatrneurol.2014.02.015> PMID: [24814059](https://pubmed.ncbi.nlm.nih.gov/24814059/)
39. Li J, Yim S, Pacheck A, Sanchez B, Rutkove SB. Electrical impedance myography to detect the effects of electrical muscle stimulation in wild type and mdx mice. *PLoS One*. 2016; 11(3):e0151415. PubMed Central PMCID: PMC4795734. <https://doi.org/10.1371/journal.pone.0151415> PMID: [26986564](https://pubmed.ncbi.nlm.nih.gov/26986564/)
40. Wu JS, Li J, Greenman RL, Bennett D, Geisbush T, Rutkove SB. Assessment of aged mdx mice by electrical impedance myography and magnetic resonance imaging. *Muscle Nerve*. 2015; 52(4):598±604. <https://doi.org/10.1002/mus.24573> PMID: [25597760](https://pubmed.ncbi.nlm.nih.gov/25597760/)
41. Li J, Geisbush TR, Rosen GD, Lachey J, Mulivor A, Rutkove SB. Electrical impedance myography for the in vivo and ex vivo assessment of muscular dystrophy (mdx) mouse muscle. *Muscle Nerve*. 2014; 49(6):829±35. <https://doi.org/10.1002/mus.24086> PMID: [24752469](https://pubmed.ncbi.nlm.nih.gov/24752469/)
42. Geisbush TR, Visyak N, Madabusi L, Rutkove SB, Darras BT. Inter-session reliability of electrical impedance myography in children in a clinical trial setting. *Clinical neurophysiology official journal of the International Federation of Clinical Neurophysiology*. 2015; 126(9):1790±6. PubMed Central PMCID: PMC4447621. <https://doi.org/10.1016/j.clinph.2014.11.017> PMID: [25533276](https://pubmed.ncbi.nlm.nih.gov/25533276/)
43. Smith BF, Yue Y, Woods PR, Kornegay JN, Shin JH, Williams RR, et al. An intronic LINE-1 element insertion in the dystrophin gene aborts dystrophin expression and results in Duchenne-like muscular dystrophy in the corgi breed. *Lab Invest*. 2011; 91(2):216±31. PubMed Central PMCID: PMC2999660. <https://doi.org/10.1038/labinvest.2010.146> PMID: [20714321](https://pubmed.ncbi.nlm.nih.gov/20714321/)
44. Fine DM, Shin JH, Yue Y, Volkmann D, Leach SB, Smith BF, et al. Age-matched comparison reveals early electrocardiography and echocardiography changes in dystrophin-deficient dogs. *Neuromuscul Disord*. 2011; 21(7):453±61. Epub 2011/05/17. <https://doi.org/10.1016/j.nmd.2011.03.010> PMID: [21570848](https://pubmed.ncbi.nlm.nih.gov/21570848/)

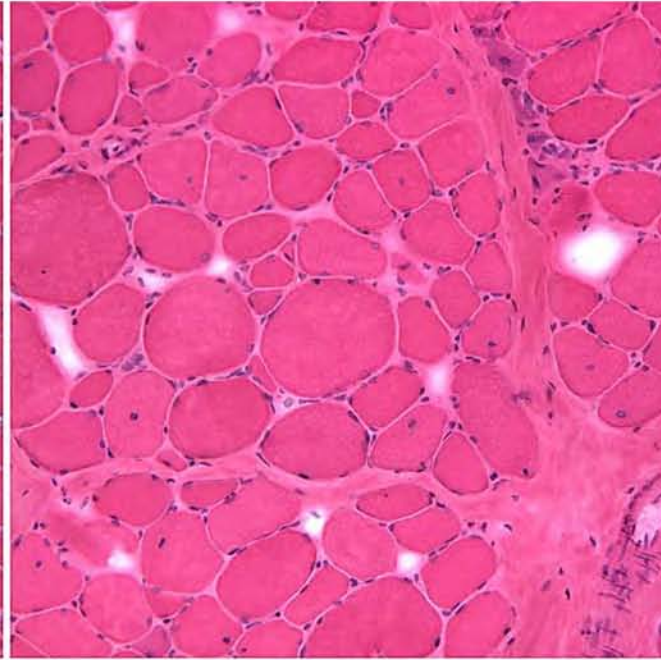
45. Sharp NJ, Kornegay JN, Van Camp SD, Herbstreith MH, Secore SL, Kettle S, et al. An error in dystrophin mRNA processing in golden retriever muscular dystrophy, an animal homologue of Duchenne muscular dystrophy. *Genomics*. 1992; 13(1):115±21. PMID: [1577476](#)
46. Sanchez B, Pacheck A, Rutkove SB. Guidelines to electrode positioning for human and animal electrical impedance myography research. *Scientific reports*. 2016; 6:32615. PubMed Central PMCID: PMC5009322. <https://doi.org/10.1038/srep32615> PMID: [27585740](#)
47. Narayanaswami P, Spieker AJ, Mongioli P, Keel JC, Muzin SC, Rutkove SB. Utilizing a handheld electrode array for localized muscle impedance measurements. *Muscle Nerve*. 2012; 46(2):257±63. PubMed Central PMCID: PMC3400114. <https://doi.org/10.1002/mus.23307> PMID: [22806375](#)
48. Hakim CH, Grange RW, Duan D. The passive mechanical properties of the extensor digitorum longus muscle are compromised in 2 to 20-month-old mdx mice. *J Appl Physiol*. 2011; 110(6):1656±63. Epub 2011/03/19. <https://doi.org/10.1152/jappphysiol.01425.2010> PMID: [21415170](#)
49. Shrout PE, Fleiss JL. Intraclass correlations: uses in assessing rater reliability. *Psychological bulletin*. 1979; 86(2):420±8. PMID: [18839484](#)
50. Bland JM, Altman DG. Statistical methods for assessing agreement between two methods of clinical measurement. *Lancet*. 1986; 1(8476):307±10. PMID: [2868172](#)
51. Tarulli AW, Chin AB, Partida RA, Rutkove SB. Electrical impedance in bovine skeletal muscle as a model for the study of neuromuscular disease. *Physiological measurement*. 2006; 27(12):1269±79. <https://doi.org/10.1088/0967-3334/27/12/002> PMID: [17135699](#)
52. Ahad MA, Rutkove SB. Electrical impedance myography at 50kHz in the rat: technique, reproducibility, and the effects of sciatic injury and recovery. *Clinical neurophysiology official journal of the International Federation of Clinical Neurophysiology*. 2009; 120(8):1534±8. PubMed Central PMCID: PMC2762741. <https://doi.org/10.1016/j.clinph.2009.05.017> PMID: [19570710](#)
53. Rutkove SB, Lee KS, Shiffman CA, Aaron R. Test-retest reproducibility of 50 kHz linear-electrical impedance myography. *Clinical neurophysiology official journal of the International Federation of Clinical Neurophysiology*. 2006; 117(6):1244±8. <https://doi.org/10.1016/j.clinph.2005.12.029> PMID: [16644269](#)
54. Shiffman CA, Rutkove SB. Circuit modeling of the electrical impedance: II. Normal subjects and system reproducibility. *Physiological measurement*. 2013; 34(2):223±35. PubMed Central PMCID: PMC3593107. <https://doi.org/10.1088/0967-3334/34/2/223> PMID: [23354000](#)
55. Shiffman CA, Rutkove SB. Circuit modeling of the electrical impedance: I. Neuromuscular disease. *Physiological measurement*. 2013; 34(2):203±21. PubMed Central PMCID: PMC3593043. <https://doi.org/10.1088/0967-3334/34/2/203> PMID: [23353926](#)
56. Aaron R, Esper GJ, Shiffman CA, Bradonjic K, Lee KS, Rutkove SB. Effects of age on muscle as measured by electrical impedance myography. *Physiological measurement*. 2006; 27(10):953±9. <https://doi.org/10.1088/0967-3334/27/10/002> PMID: [16951455](#)
57. Kortman HG, Wilder SC, Geisbush TR, Narayanaswami P, Rutkove SB. Age- and gender-associated differences in electrical impedance values of skeletal muscle. *Physiological measurement*. 2013; 34(12):1611±22. PubMed Central PMCID: PMC3895401. <https://doi.org/10.1088/0967-3334/34/12/1611> PMID: [24165434](#)
58. Brooke MH, Fenichel GM, Griggs RC, Mendell JR, Moxley R, Miller JP, et al. Clinical investigation in Duchenne dystrophy: 2. Determination of the "power" of therapeutic trials based on the natural history. *Muscle Nerve*. 1983; 6(2):91±103. <https://doi.org/10.1002/mus.880060204> PMID: [6343858](#)
59. Mendell JR, Province MA, Moxley RT 3rd, Griggs RC, Brooke MH, Fenichel GM, et al. Clinical investigation of Duchenne muscular dystrophy. A methodology for therapeutic trials based on natural history controls. *Arch Neurol*. 1987; 44(8):808±11. PMID: [3115236](#)
60. McDonald CM, Henricson EK, Abresch RT, Han JJ, Escolar DM, Florence JM, et al. The cooperative international neuromuscular research group Duchenne natural history study: a longitudinal investigation in the era of glucocorticoid therapy: design of protocol and the methods used. *Muscle Nerve*. 2013; 48(1):32±54. <https://doi.org/10.1002/mus.23807> PMID: [23677550](#)
61. Merlini L, Sabatelli P. Improving clinical trial design for Duchenne muscular dystrophy. *BMC neurology*. 2015; 15:153. PubMed Central PMCID: PMC4549867. <https://doi.org/10.1186/s12883-015-0408-z> PMID: [26306629](#)

Normal

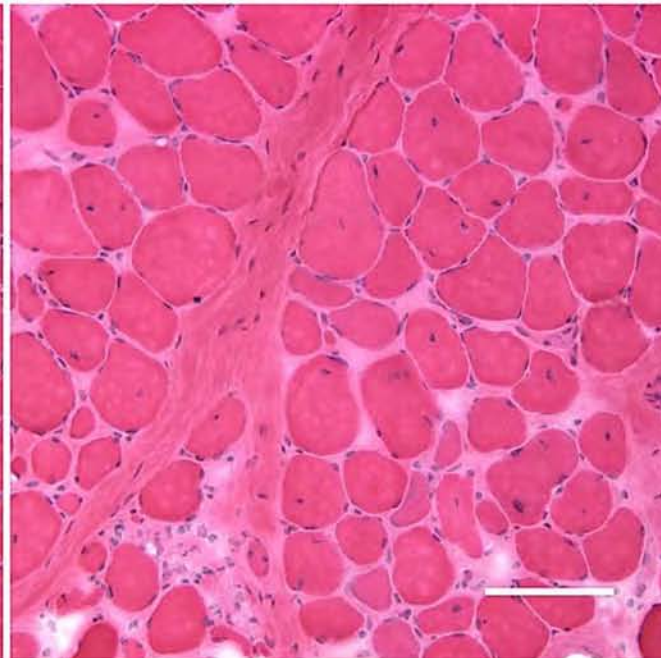
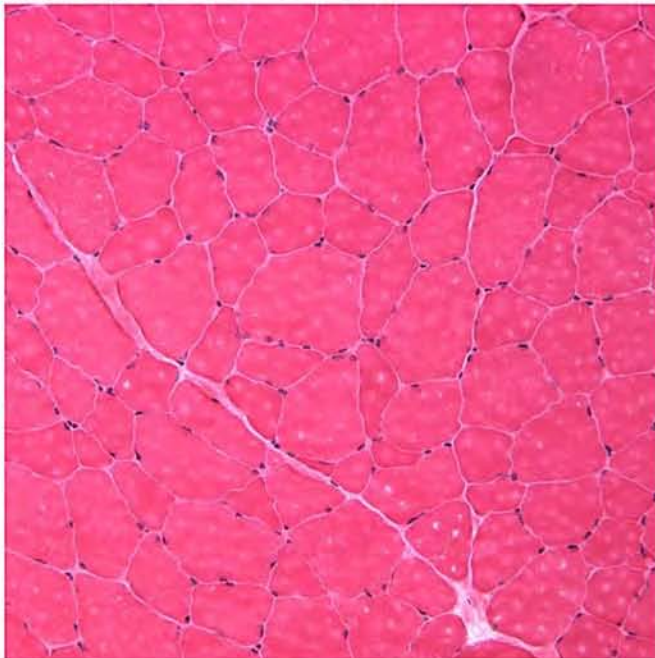
Affected

Hakim et al 2017  
Supp. Figure 1

Young



Mature



# A Five-Repeat Micro-Dystrophin Gene Ameliorated Dystrophic Phenotype in the Severe DBA/2J-mdx Model of Duchenne Muscular Dystrophy

Chady H. Hakim,<sup>1,2</sup> Nalinda B. Wasala,<sup>1</sup> Xiufang Pan,<sup>1</sup> Kasun Kodippili,<sup>1</sup> Yongping Yue,<sup>1</sup> Keqing Zhang,<sup>1</sup> Gang Yao,<sup>3</sup> Brittney Haffner,<sup>1</sup> Sean X. Duan,<sup>1</sup> Julian Ramos,<sup>4</sup> Joel S. Schneider,<sup>5</sup> N. Nora Yang,<sup>2</sup> Jeffrey S. Chamberlain,<sup>4</sup> and Dongsheng Duan<sup>1,3,6,7</sup>

<sup>1</sup>Department of Molecular Microbiology and Immunology, School of Medicine, University of Missouri, Columbia, MO 65212, USA; <sup>2</sup>National Center for Advancing Translational Sciences (NCATS), Bethesda, MD 20892, USA; <sup>3</sup>Department of Bioengineering, University of Missouri, Columbia, MO 65212, USA; <sup>4</sup>Department of Neurology, Wellstone Muscular Dystrophy Research Center, University of Washington, Seattle, WA 98105, USA; <sup>5</sup>Solid Biosciences, LLC, Cambridge, MA 02142, USA; <sup>6</sup>Department of Neurology, School of Medicine, University of Missouri, Columbia, MO 65212, USA; <sup>7</sup>Department of Biomedical Sciences, College of Veterinary Medicine, University of Missouri, Columbia, MO 65212, USA

**Micro-dystrophins are highly promising candidates for treating Duchenne muscular dystrophy, a lethal muscle disease caused by dystrophin deficiency. Here, we report robust disease rescue in the severe DBA/2J-mdx model with a neuronal nitric oxide synthase (nNOS)-binding micro-dystrophin vector.  $2 \times 10^{13}$  vector genome particles/mouse of the vector were delivered intravenously to 10-week-old mice and were evaluated at 6 months of age. Saturated micro-dystrophin expression was detected in all skeletal muscles and the heart and restored the dystrophin-associated glycoprotein complex and nNOS. In skeletal muscle, therapy substantially reduced fibrosis and calcification and significantly attenuated inflammation. Centronucleation was significantly decreased in the tibialis anterior (TA) and extensor digitorum longus (EDL) muscles but not in the quadriceps. Muscle function was normalized in the TA and significantly improved in the EDL muscle. Heart histology and function were also evaluated. Consistent with the literature, DBA/2J-mdx mice showed myocardial calcification and fibrosis and cardiac hemodynamics was compromised. Surprisingly, similar myocardial pathology and hemodynamic defects were detected in control DBA/2J mice. As a result, interpretation of the cardiac data proved difficult due to the confounding phenotype in control DBA/2J mice. Our results support further development of this microgene vector for clinical translation. Further, DBA/2J-mdx mice are not good models for Duchenne cardiomyopathy.**

## INTRODUCTION

Dystrophin is a large subsarcolemmal protein essential for muscle health. Out-of-frame mutations in the dystrophin gene abort dystrophin expression. The absence of dystrophin leads to Duchenne muscular dystrophy (DMD), an X-linked lethal debilitating muscle disease. Restoration of dystrophin expression in muscle cells by gene therapy will address the fundamental problem of dystrophin deficiency in DMD. A number of highly promising strategies are

currently under development to replace or repair the mutated dystrophin gene or message RNA.<sup>1–3</sup> Adeno-associated virus (AAV)-mediated micro-dystrophin gene therapy stands out as an extremely attractive approach due to the AAV vector's unique capability for bodywide muscle transduction.<sup>4</sup> Encouragingly, AAV gene therapy has resulted in unequivocal clinical successes in treating other inherited diseases such as Leber congenital amaurosis, hemophilia, and spinal muscular atrophy.<sup>5,6</sup>

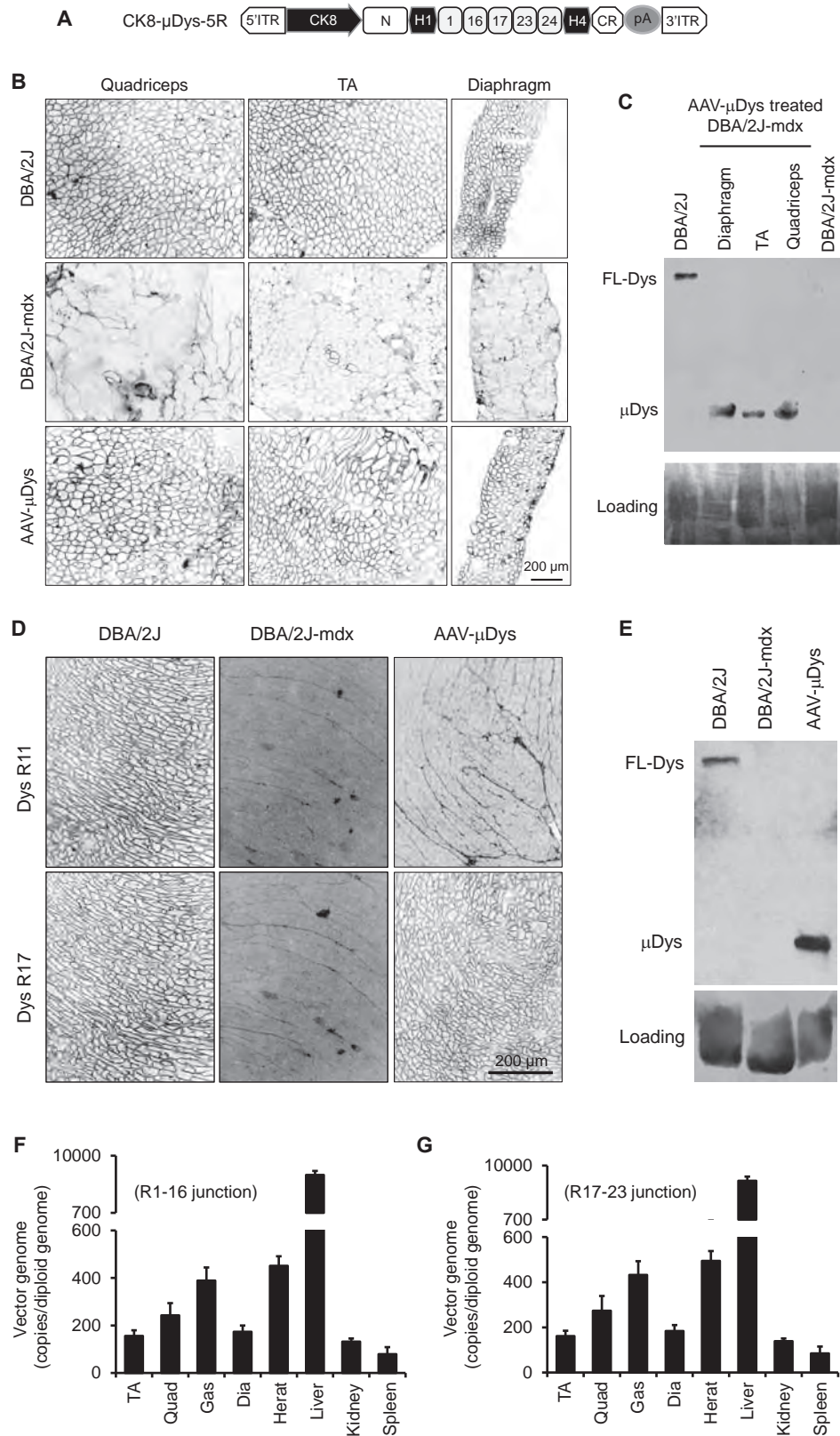
AAV is a single-stranded DNA virus with a packaging capacity of ~5 kb.<sup>7</sup> This creates a challenge for dystrophin gene delivery because the dystrophin coding sequence exceeds 11 kb. Full-length dystrophin contains four major structural domains, including the amino-terminal, rod, cysteine-rich, and C-terminal domains. The rod domain can be further divided into 24 spectrin-like repeats and four hinges. Some portions of these domains encode motifs for dystrophin to interact with the sarcolemma, extracellular matrix (via dystroglycan), cytoskeleton (actin microfilament, intermediate filament, and microtubule), and neuronal nitric oxide synthase (nNOS).

In the early 1990s, England et al.<sup>8</sup> found that some naturally occurring rod domain-truncated dystrophins are highly functional, suggesting that not all internal segments of dystrophin are essential. A subsequent study by Crawford et al.<sup>9</sup> showed that removal of the C-terminal domain has minimal impact on mouse muscle function. Based on these findings, investigators have generated rod domain-abbreviated and C-terminal domain-deleted micro-dystrophins that are about one-third the size of the full-length protein.<sup>10,11</sup> Importantly,

Received 3 April 2017; accepted 24 June 2017;  
<http://dx.doi.org/10.1016/j.omtm.2017.06.006>.

**Correspondence:** Dongsheng Duan, PhD, Department of Molecular Microbiology and Immunology, School of Medicine, University of Missouri, One Hospital Dr., Columbia, MO 65212, USA.

**E-mail:** [duand@missouri.edu](mailto:duand@missouri.edu)



(legend on next page)

microgenes are less than 4 kb and can fit into an AAV particle. Local or systemic delivery of these micro-dystrophin AAV vectors greatly ameliorates muscle disease in mouse models of DMD.<sup>10–14</sup>

Despite these encouraging reports, the early versions of micro-dystrophin could not anchor nNOS to the sarcolemma.<sup>15</sup> The loss of sarcolemmal nNOS has been recognized as a critical pathogenic factor in DMD.<sup>16,17</sup> A microgene capable of normalizing nNOS localization would be highly preferable for DMD gene therapy. We recently discovered that dystrophin spectrin-like repeats 16 and 17 (R16/17) are the long-sought-after nNOS-binding domain.<sup>18,19</sup> We engineered several 6- to 8-kb R16/17-containing mini-dystrophin genes and demonstrated their therapeutic efficacy in mildly affected mdx and mdx4cv mice.<sup>18,20,21</sup> As an initial step toward the development of nNOS-binding micro-dystrophin gene therapy, we expressed a four-repeat R16/17-containing microgene from the ubiquitous cytomegalovirus (CMV) promoter in mdx mice via AAV-mediated gene transfer.<sup>22</sup> We obtained the expected sarcolemmal nNOS restoration, amelioration of pathology, and muscle function improvement.<sup>22</sup> While the results were encouraging, the vector was not ideal for human use (e.g., the use of the CMV promoter). To further establish the therapeutic utility of AAV-mediated nNOS-binding microgene therapy and in preparation for future clinical trials, we engineered a new vector. In this vector, a five-repeat R16/17-containing microgene was expressed from a muscle-specific CK8 promoter.<sup>1,23</sup> The construct was packaged in AAV serotype-9 (AAV-9) and delivered via the tail vein to 10-week-old DBA/2J-mdx mice, a recently developed severe mouse model for DMD.<sup>24,25</sup> At 15 weeks after AAV injection, we examined micro-dystrophin expression, dystrophin-associated/related proteins, histology, and skeletal muscle and heart function. Saturated skeletal muscle and heart transduction was observed in every treated animal. Micro-dystrophin greatly ameliorated skeletal muscle pathology and enhanced skeletal muscle function. Unexpectedly, we observed significant cardiomyopathy in control DBA/2J mice, limiting our ability to thoroughly evaluate heart rescue in treated animals.

## RESULTS

### Systemic AAV-9 Delivery Resulted in Robust Bodywide Micro-Dystrophin Expression in Muscles of DBA/2J-mdx Mice

The microgene construct used in this study has several unique features. Expression is driven by the muscle-specific CK8 promoter.

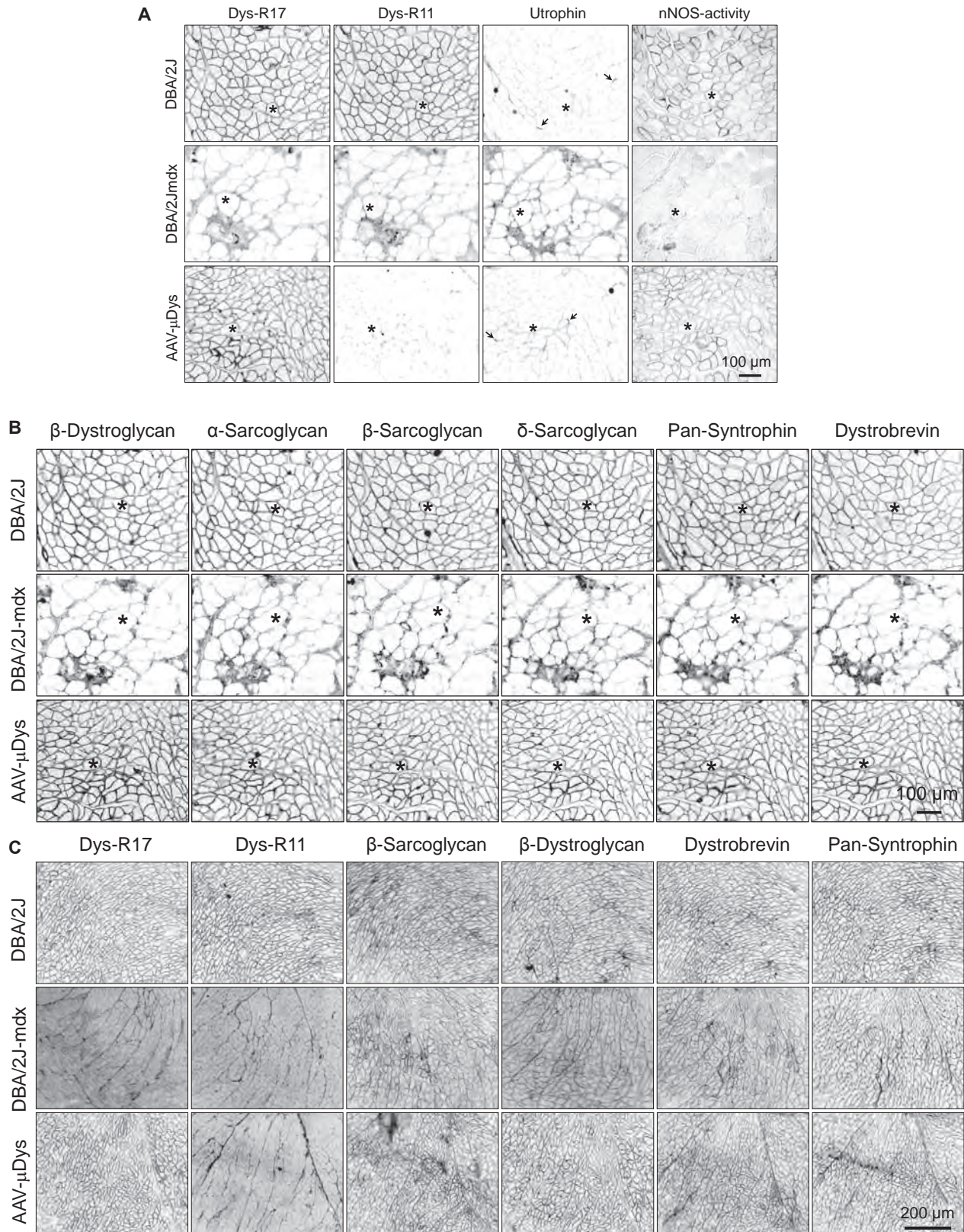
The rod domain of micro-dystrophin contains five repeats (R1, R16, R17, R23, and R24) and two hinges (H1 and H4) (Figure 1A). The AAV-9 micro-dystrophin vector was delivered intravenously to five 10-week-old male and five 10-week-old female DBA/2J-mdx mice at the dose of  $2 \times 10^{13}$  vector genome (vg) particles/mouse. At 15 weeks after AAV injection, we examined micro-dystrophin expression and AAV genome distribution. On immunofluorescence staining, we observed saturated micro-dystrophin expression in all skeletal muscles in every treated mouse (Figure 1B; see also Figure S1A). The heart was also completely transduced (Figure 1D; see also Figure S1B). Western blot analysis confirmed high-level micro-dystrophin expression in both the skeletal muscle and the heart (Figures 1C and 1E). Quantification of the AAV genome copy number revealed accumulation of most of the vg in the liver, as expected from intravenous delivery. Nevertheless, approximately 150–500 copies/diploid genome of the vg were detected in the skeletal muscle and the heart (Figures 1F and 1G; see also Figure S1C).

### Micro-Dystrophin Normalized nNOS Localization and Enhanced Recruitment of Other Components of the Dystrophin-Associated Glycoprotein Complex to the Sarcolemma

Dystrophin recruits a number of transmembrane (e.g., dystroglycans and sarcoglycans) and cytosolic (e.g., syntrophin and dystrobrevin) proteins into the dystrophin-associated glycoprotein complex (DGC). Dystrophin anchors nNOS to the sarcolemma in skeletal muscle.<sup>18,19</sup> We evaluated DGC restoration and nNOS expression by immunostaining on serial muscle sections (Figure 2). Epitope-specific dystrophin monoclonal antibodies confirmed the presence of R17 and absence of R11 in the skeletal muscle (Figure 2A) and heart (Figures 1D and 2C) of the AAV-injected DBA/2J-mdx mouse. In situ nNOS activity staining revealed successful sarcolemmal localization of enzymatically active nNOS in skeletal muscle following AAV micro-dystrophin therapy (Figure 2A). All components of the DGC were greatly diminished at the sarcolemma of untreated DBA/2J-mdx skeletal muscle (Figure 2B). Their expression was restored following AAV micro-dystrophin therapy (Figure 2B). DGC components in the heart of untreated DBA/2J-mdx mice were also reduced but appeared to be to a lesser extent compared to that of skeletal muscle (Figure 2C). After AAV micro-dystrophin therapy, the immunostaining intensity of the DGC was greatly enhanced in the heart (Figure 2C).

### Figure 1. Systemic AAV-9 Injection Leads to Robust Expression of a Five-Repeat Micro-Dystrophin Gene in the Skeletal Muscle and Heart of DBA/2J-mdx Mice

(A) Schematic illustration of the AAV microgene vector. Micro-dystrophin consists of the N-terminal domain, two hinges (H1 and H4), five spectrin-like repeats (R1, R16, R17, R23, and R24), and the cysteine-rich (CR) domain. Micro-dystrophin expression is regulated by the muscle-specific CK8 promoter. (B) Representative dystrophin immunostaining photomicrographs demonstrating widespread microgene expression in the quadriceps, TA muscle, and diaphragm in treated DBA/2J-mdx mice. (C) A representative dystrophin western blot showing micro-dystrophin ( $\mu$ Dys) at the expected size in AAV-treated muscles. (D) Representative immunostaining photomicrographs demonstrating robust myocardial micro-dystrophin expression in treated DBA/2J-mdx mice. Full-length dystrophin in the control DBA/2J heart reacted with both R11- and R17-specific antibodies. Therapeutic micro-dystrophin was recognized by the R17-specific but not the R11-specific antibody. (E) A representative dystrophin western blot showing abundant  $\mu$ Dys at the expected size in the heart of treated DBA/2J-mdx mice. (F) Quantitative evaluation of AAV genome distribution in muscle and internal organs using in AAV microgene-injected female DBA/2J-mdx mice ( $n = 5$ ). TaqMan qPCR detects the junction of R1-R16. Error bars are mean  $\pm$  SEM. (G) Quantitative evaluation of AAV genome distribution in muscle and internal organs using in AAV microgene-injected female DBA/2J-mdx mice ( $n = 5$ ). Error bars are mean  $\pm$  SEM. TaqMan qPCR detects the junction of R17-R23. Dia, diaphragm; FL-Dys, full-length dystrophin; Gas, gastrocnemius; ITR, inverted terminal repeat; Quad, quadriceps; TA, tibialis anterior.



(legend on next page)

Utrophin is a dystrophin-related protein. In DBA mice, utrophin was mainly concentrated at the neuromuscular junctions (Figure 2A). Utrophin expression was moderately upregulated at the sarcolemma of untreated DBA/2J-mdx mice (Figure 2A). Micro-dystrophin appeared to have reduced sarcolemmal utrophin expression in DBA/2J-mdx mice (Figure 2A). Utrophin expression at the neuromuscular junction was not altered following micro-dystrophin therapy (Figure 2A).

#### Micro-Dystrophin Ameliorated Skeletal Muscle Pathology

On H&E staining, untreated DBA/2J-mdx mouse muscle showed characteristic dystrophic pathology, such as centrally localized nuclei, a large variety in myofiber size, and infiltration of mononuclear cells (Figures 3A; see also Figure S2). These pathologic lesions were clearly reduced following AAV micro-dystrophin therapy (Figure 3A; see also Figure S2). Masson trichrome staining and alizarin red staining revealed extensive interstitial fibrosis (blue color) and frequent appearance of calcified myofibers (dark red color), respectively, in untreated DBA/2J-mdx mouse muscle (Figure 3A). Fibrosis and calcification were all mitigated in AAV micro-dystrophin-treated muscle (Figure 3A).

To characterize inflammation, we performed immunohistochemistry staining using antibodies specific for macrophages and neutrophils. Patches of dark-brown stained macrophages and neutrophils were present throughout the muscle section in untreated DBA/2J-mdx mice but were barely visible in muscle of AAV micro-dystrophin-treated DBA/2J-mdx mice (Figure 3B). On quantification, macrophage and neutrophil numbers were significantly elevated in untreated DBA/2J-mdx muscle (Figure 3B). AAV treatment resulted in a significant reduction of these inflammatory cells.

To better appreciate the protective effect of micro-dystrophin, we performed morphometric quantification on the distribution of the myofiber size and the percentage of myofibers with centrally localized myonuclei in three representative limb muscles, including the quadriceps, tibialis anterior (TA), and extensor digitorum longus (EDL) muscle (Figures 3C and 3D). Compared to that of DBA/2J mice, the distribution of the myofiber size in untreated DBA/2J-mdx mice showed a marked leftward shift, indicating the presence of high numbers of small-size myofibers in dystrophic limb muscles (Figure 3C). The right end tail of the fiber size curve was elevated and spread farther in untreated DBA/2J-mdx mice, suggesting that they also have more large-size myofibers (Figure 3C). AAV micro-dystrophin therapy corrected the abnormal fiber size distribution to different extents in different muscles. It was nearly normalized in the EDL muscle but only partially improved in the quadriceps and

TA muscle (Figure 3C). Central nucleation is a hallmark of muscle degeneration/regeneration. In untreated DBA/2J-mdx mice, ~40% of myofibers contained centrally localized nuclei (Figure 3D). AAV micro-dystrophin treatment significantly reduced centronucleation to approximately 30% in the TA and EDL muscle. Interestingly, there was no difference in the number of centrally nucleated myofibers in the quadriceps between treated and untreated DBA/2J-mdx mice (Figure 3D).

#### Micro-Dystrophin Normalized Skeletal Muscle Function

To thoroughly evaluate physiological consequences of micro-dystrophin therapy, we evaluated skeletal muscle force using two different approaches, including the ex vivo assay of the freshly dissected EDL muscle and the in situ assay of the TA muscle in live mice. On immunostaining, we observed saturated micro-dystrophin expression in both EDL and TA muscles (Figures 1B, S1, and S3). The EDL muscle of untreated DBA/2J-mdx mice showed significant atrophy, as demonstrated by the reduced muscle weight and cross-sectional area (CSA) (Table 1). Absolute twitch and tetanic forces of the untreated DBA/2J-mdx EDL muscle were significantly lower than those of the control DBA/2J EDL muscle (Figure S4). These deficiencies were almost completely corrected in AAV-treated mice (Figure S4). Specific twitch and tetanic forces of the EDL muscle in untreated DBA/2J-mdx mice were reduced by ~50% compared to those of control DBA/2J mice. Micro-dystrophin therapy fully normalized specific forces in the EDL muscle (Figure 4A). Force reduction following consecutive cycles of eccentric contraction is a highly sensitive index for studying dystrophic muscle function.<sup>12,26,27</sup> The control DBA/2J mouse EDL muscle was able to maintain ~80% of the force following 10 cycles of eccentric contraction stress (Figure 4A). Muscle force dropped dramatically during the first five cycles of eccentric contraction in the EDL muscle of untreated DBA/2J-mdx mice. Interestingly, force reduction became less apparent thereafter (Figure 4A). Micro-dystrophin-treated DBA/2J-mdx mice showed an eccentric contraction profile essentially identical to that of control DBA/2J mice (Figure 4A).

In situ examination of the TA muscle function yielded similar but slightly different results. The muscle weight and CSA of untreated DBA/2J-mdx mice were reduced compared to those of control DBA/2J mice but to a lesser extent compared to what was observed in the EDL muscle (Table 1). Absolute and specific forces of untreated DBA/2J-mdx mice were significantly lower than those of control DBA/2J mice (Figure 4B; see also Figure S4). Micro-dystrophin therapy normalized absolute and specific twitch forces in DBA/2J-mdx mice (Figure 4B; see also Figure S4). Absolute and specific tetanic forces were significantly improved but did not reach those

#### Figure 2. Five-Repeat Micro-Dystrophin Improves Sarcolemmal Localization of Dystrophin-Associated Glycoprotein Complex and Restores Membrane-Associated nNOS Activity

(A) Representative photomicrographs of dystrophin R17 and R11 immunostaining, utrophin immunostaining, and nNOS activity staining. Asterisks indicate the same myofiber in serial skeletal muscle sections. Arrows indicate the neuromuscular junction. (B) Representative photomicrographs of  $\beta$ -dystroglycan,  $\alpha$ -sarcoglycan,  $\beta$ -sarcoglycan,  $\delta$ -sarcoglycan, pan-syntrophin, and dystrobrevin from the same serial muscle sections shown in (A). (C) Representative photomicrographs of dystrophin R17 and R11,  $\beta$ -dystroglycan,  $\beta$ -sarcoglycan, pan-syntrophin, and dystrobrevin in the heart.

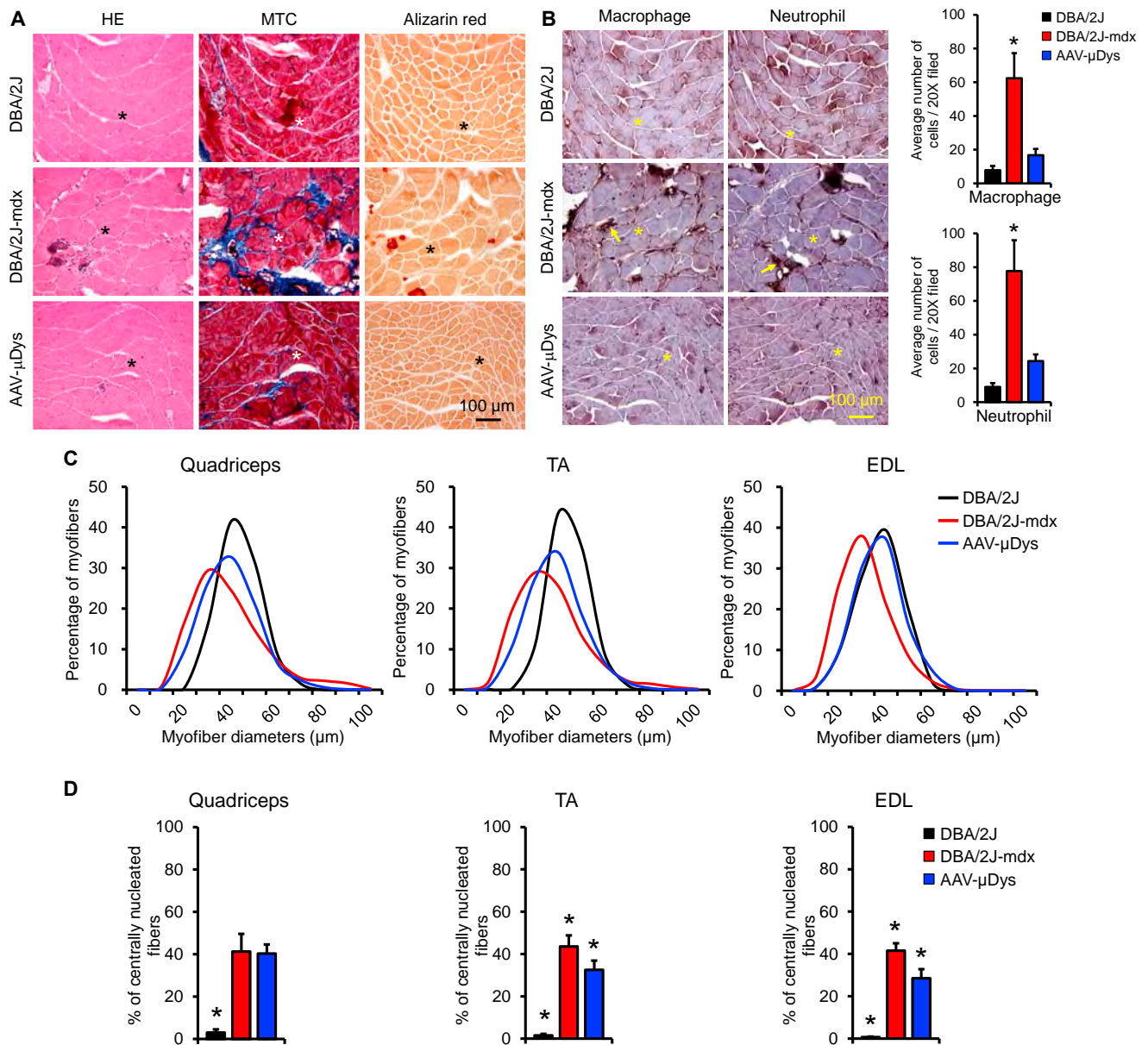


**Figure 3. Five-Repeat Micro-Dystrophin Ameliorates Dystrophic Pathology in Skeletal Muscle of DBA/2J-mdx Mice**

(A) Representative photomicrographs of H&E (HE), Masson trichrome (MTC), and alizarin red staining. The blue color in MTC staining indicates fibrosis. The dark red color in alizarin red staining marks calcification. (B) Representative photomicrographs of macrophage and neutrophil immunohistochemical staining from the same serial sections shown in (A). Arrows mark inflammatory cells. Bar graphs show macrophage and neutrophil quantification. Error bars are mean  $\pm$  SEM. (C) Myofiber size distribution in the quadriceps, tibialis anterior muscle (TA), and extensor digitorum longus muscle (EDL). (D) Quantification of the proportion of centrally nucleated myofibers. Error bars are mean  $\pm$  SEM. Asterisks in photomicrographs indicate the same myofiber in serial sections. Asterisks in bar graphs indicate significantly different from other groups.

of control DBA/2J mice (Figure 4B; see also Figure S4). In the eccentric contraction assay, we detected minimal force reduction in AAV micro-dystrophin-treated DBA/2J-mdx mice. In sharp contrast, there was a large force reduction in untreated DBA/2J-mdx mice (Figure 4B).

**Absence of Dystrophin Did Not Cause Appreciable Alterations in the Heart Pathology of DBA/2J Mice**

A recent study reported an absence of heart pathology in 7- to 52-week-old DBA/2J mice.<sup>24</sup> However, others have demonstrated myocardial calcification and inflammation as early as 4 weeks of

**Table 1. Anatomic Properties of the Experimental Muscles**

Muscle	Strain	n	Body Weight (g)	Muscle Weight (mg)	Lo (mm)	CSA (mm <sup>2</sup> )
EDL	DBA/2J	10	28.22 ± 0.48 <sup>a</sup>	10.36 ± 0.32 <sup>a</sup>	13.08 ± 0.08 <sup>a</sup>	1.71 ± 0.05 <sup>a</sup>
	DBA/2J-mdx	8	24.50 ± 0.58	7.31 ± 0.25 <sup>b</sup>	13.70 ± 0.15	1.15 ± 0.04 <sup>b</sup>
	DBA/2J-mdx treated	5	25.00 ± 0.76	8.80 ± 0.24	13.98 ± 0.07	1.35 ± 0.03
TA	DBA/2J	5	27.28 ± 1.11	40.22 ± 1.16	14.67 ± 0.05	4.33 ± 0.12
	DBA/2J-mdx	8	24.41 ± 0.52	37.38 ± 1.43	14.78 ± 0.17 <sup>b</sup>	3.99 ± 0.13
	DBA/2J-mdx treated	5	25.00 ± 0.76	38.12 ± 1.00	14.14 ± 0.07	4.25 ± 0.11

Data are presented as means ± SEM. CSA, cross-sectional area; EDL, extensor digitorum longus; Lo, optimal muscle length; TA, tibialis anterior.

<sup>a</sup>Significantly different from both untreated and AAV-treated DBA/2J-mdx mice.

<sup>b</sup>Significantly different from DBA/2J and AAV-treated DBA/2J-mdx.

age in DBA/2 mice.<sup>28–30</sup> We observed readily visible calcification and/or fibrosis on the surface of the DBA/2J but not C57Bl/10 mouse heart (Figure S5A). Consistent with previous publications,<sup>28–30</sup> epicardial calcified/fibrotic lesions in DBA/2J mice were primarily located on the surface of the right ventricle (Figure 5A; see also Figure S5A). Sporadic lesions of myocardial fibrosis and calcification were also observed in the septum and left ventricle (Figure 5; see also Figure S5B). Cardiac lesions were found not only in DBA/2J mice generated from in-house breeding but also in mice directly ordered from The Jackson Laboratory. Similar pathological changes were detected in the heart of untreated and AAV micro-dystrophin-treated DBA/2J-mdx mice (Figure 5; see also Figure S5B).

#### Impact of AAV Micro-Dystrophin Gene Therapy on Cardiac Function in DBA/2J-mdx Mice

We previously showed that dystrophin-deficient female mice can better model Duchenne cardiomyopathy seen in human patients.<sup>31</sup> Hence, we evaluated anatomic properties, electrophysiology, and cardiac hemodynamics in female mice. The body weight (BW), TA muscle weight (TW), heart weight (HW), and ventricle weight (VW) of untreated DBA/2J-mdx mice were significantly lower than those of control DBA/2J mice (Table 2). Micro-dystrophin-treated mice showed a significant increase in these weights (Table 2). DBA/2J-mdx mice had a significantly higher HW/BW ratio and VW/BW ratio than control DBA/2J mice. Micro-dystrophin therapy did not change these ratios (Table 2). The HW/TW and VW/TW ratios of DBA/2J-mdx mice were significantly higher than those of control DBA/2J mice. There was a trend of reduction in these two ratios in micro-dystrophin-treated DBA/2J-mdx mice, although it did not reach statistical significance (Table 2). The tibia length (TL) was not affected by muscle disease. Hence, the TL normalized heart weight ratio (HW/TL) and ventricle weight ratio (VW/TL) were considered better indicators of heart disease in the case of muscular dystrophy.<sup>32</sup> Interestingly, the HW/TL and VW/TL ratios were significantly reduced in DBA/2J-mdx mice. These ratios were significantly increased per the Mann-Whitney test in AAV-treated DBA/2J-mdx mice (Table 2).

Untreated DBA/2J-mdx mice displayed several electrocardiographic (ECG) features often seen in dystrophin-deficient mammals such as a significant reduction in the PR interval, significant prolongation of the QRS duration and QTc interval, and an increase in the cardiomyopathy index (Figures 6A and S6A).<sup>33,34</sup> Interestingly, DBA/2J-mdx mice did not show statistically significant tachycardia. Their heart rate was only slightly increased over that of DBA/2J mice (Figure 6A). Unexpectedly, the Q wave of DBA/2J mice was significantly deeper than that of DBA/2J-mdx mice (Figure 6A). AAV micro-dystrophin therapy did not lead to statistically significant improvement, although a trend of improvement was detected in several parameters, including the QRS duration, QTc interval, and cardiomyopathy index (Figure 6A).

On the cardiac catheter assay, there were no statistically significant differences in systolic parameters (end systolic volume, maximum pressure, and rate of rise of left ventricular pressure during heart contraction [dP/dt] max) and two diastolic parameters (end-diastolic volume and relaxation constant tau) among three experimental groups (Figure 6B; see also Figure S6B). The only statistically significant difference was dP/dt min. The absolute value of dP/dt min in DBA/2J mice was significantly larger than that of two other groups (Figure 6B; see also Figure S6B). Importantly, we did not see a statistically significant difference in indices for overall heart pump function (stroke volume, ejection fraction, and cardiac output) among three experimental groups (Figure 6B; see also Figure S6B).

#### DISCUSSION

To generate potentially supportive preclinical data for a new DMD clinical gene therapy program,<sup>1,2</sup> here we evaluated systemic AAV-9 micro-dystrophin therapy using a novel expression construct in severely affected DBA/2J-mdx mice. We observed highly efficient whole-body gene transfer and restoration of the DGC (including nNOS) by micro-dystrophin. In skeletal muscle, our treatment significantly reduced histological lesions and enhanced contractility. A recent study suggests that the DBA/2J-mdx mouse is a good model for DMD heart disease.<sup>24</sup> Surprisingly, we noticed clear cardiac

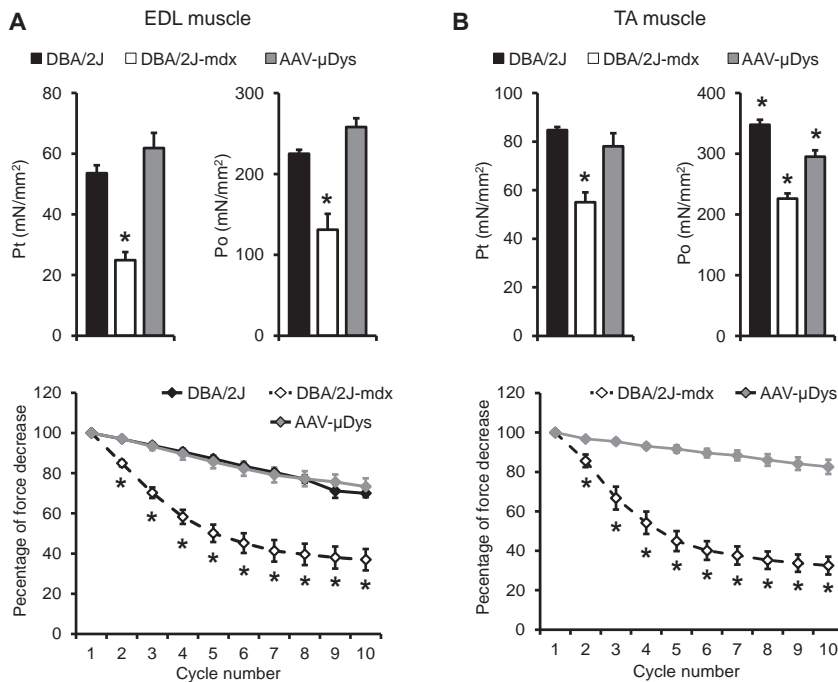


**Figure 4. Five-Repeat Micro-Dystrophin Enhances Skeletal Muscle Function of DBA/2J-mdx Mice**

(A) Quantitative evaluation of muscle contractility in the extensor digitorum longus (EDL) muscle. (Top Panel) Specific twitch (Pt) and tetanic (Po) forces. (Bottom Panel) Eccentric contraction profile. Error bars are mean  $\pm$  SEM. (B) Quantitative evaluation of muscle contractility in the tibialis anterior (TA) muscle. (Top Panel) Specific twitch and tetanic forces. (Bottom Panel) Eccentric contraction profile. Error bars are mean  $\pm$  SEM. Asterisks indicate significantly different from other group(s).

lesions in control DBA/2J mice and a lack of differences in heart pump function between DBA/2J and DBA/2J-mdx mice. Thus, despite supra-physiological expression of micro-dystrophin in the heart of treated DBA/2J-mdx mice, we were unable to reach a conclusion on cardiac rescue.

The large size of the dystrophin cDNA has been a major hurdle for AAV-mediated DMD gene replacement therapy. Despite the invention of dual and tri-vector systems for delivering the half-size and full-length dystrophin cDNA, these technologies are still in the early development stage and are not ready for clinical translation.<sup>20,21,35–39</sup> On the other side, a phase I trial has been conducted to deliver a highly shrunk micro-dystrophin gene by direct muscle injection.<sup>40</sup> To develop single AAV gene therapy for DMD, researchers have invented synthetic microgenes that carry only one-third of the dystrophin coding sequence.<sup>10,11,18</sup> These microgenes contain one to five spectrin-like repeats and many can effectively reduce muscle pathology and improve muscle function in dystrophic mice when delivered by AAV.<sup>10–12,14,41</sup> Importantly, our recent studies suggest that AAV microgene therapy protects muscle in large mammals afflicted by DMD.<sup>22,42</sup> In support of our results, Baroncelli et al.<sup>43</sup> found that naturally existing micro-dystrophin is associated with the mild Becker form of muscular dystrophy. Collectively, existing evidence justifies further development of AAV microgene therapy to treat human patients. With this backdrop, we initiated this study.

Several factors were considered in the design of this study. First, we designed a new expression cassette distinctive from the existing constructs. We used a novel muscle-specific CK8 promoter to drive strong expression in both skeletal muscle and cardiac muscle.<sup>1,23</sup>

More than 30 different micro-dystrophin genes have been tested. The major difference in these microgenes is in the rod domain. In this regard, we opted to pursue a novel microgene that contains the R16/17 nNOS-binding domain. As homeostasis of nNOS is disrupted in DMD and in light of the critical role that nNOS plays in muscle regeneration, metabolism, mitochondria biogenesis, blood flow, and contraction,<sup>44–47</sup> it is critical to normalize nNOS homeostasis. Validation of the mouse data in affected dogs sets the foundation for treating dystrophic large mammals, including human patients. Species-related immune rejection has been a major confounding factor in gene therapy performed in the canine model.<sup>48</sup> In preparation for the subsequent dog study, and as an early readout for transgene efficacy, we have opted to use the canine microgene in our study. This canine construct had identical composition to a human construct ( $\mu$ Dys5) currently in preclinical development (J.R. and J.C., unpublished data).

Second, we performed systemic delivery with AAV-9. In DMD, all body muscles are affected. An effective gene therapy for DMD will have to depend on efficient whole-body muscle transduction. A number of newly developed AAV serotypes are capable of bodywide systemic gene delivery following intravascular injection.<sup>4</sup> Among these, AAV-9 stands out as an extremely attractive candidate for systemic DMD gene therapy. AAV-9 was originally isolated from human tissues.<sup>49</sup> Subsequent studies have revealed efficient whole-body muscle transduction in rodents and dogs.<sup>50–52</sup> Furthermore, AAV-9-mediated systemic gene therapy significantly ameliorates disease phenotype in murine and canine models of DMD.<sup>42,53,54</sup> Importantly, an ongoing clinical trial on spinal muscular atrophy suggests that systemic AAV-9 gene therapy can be used to treat severely affected human patients without causing major adverse reactions.<sup>6</sup>

Third, we evaluated therapeutic efficacy in DBA/2J-mdx mice, a newly developed model that is thought to better phenocopy DMD than the commonly used mdx mice.<sup>24,25</sup> Although DMD mainly affects boys, dystrophin-deficient animals of both genders can be created by breeding. Interestingly, male mdx mice show more severe skeletal muscle disease, while cardiomyopathy is more accurately

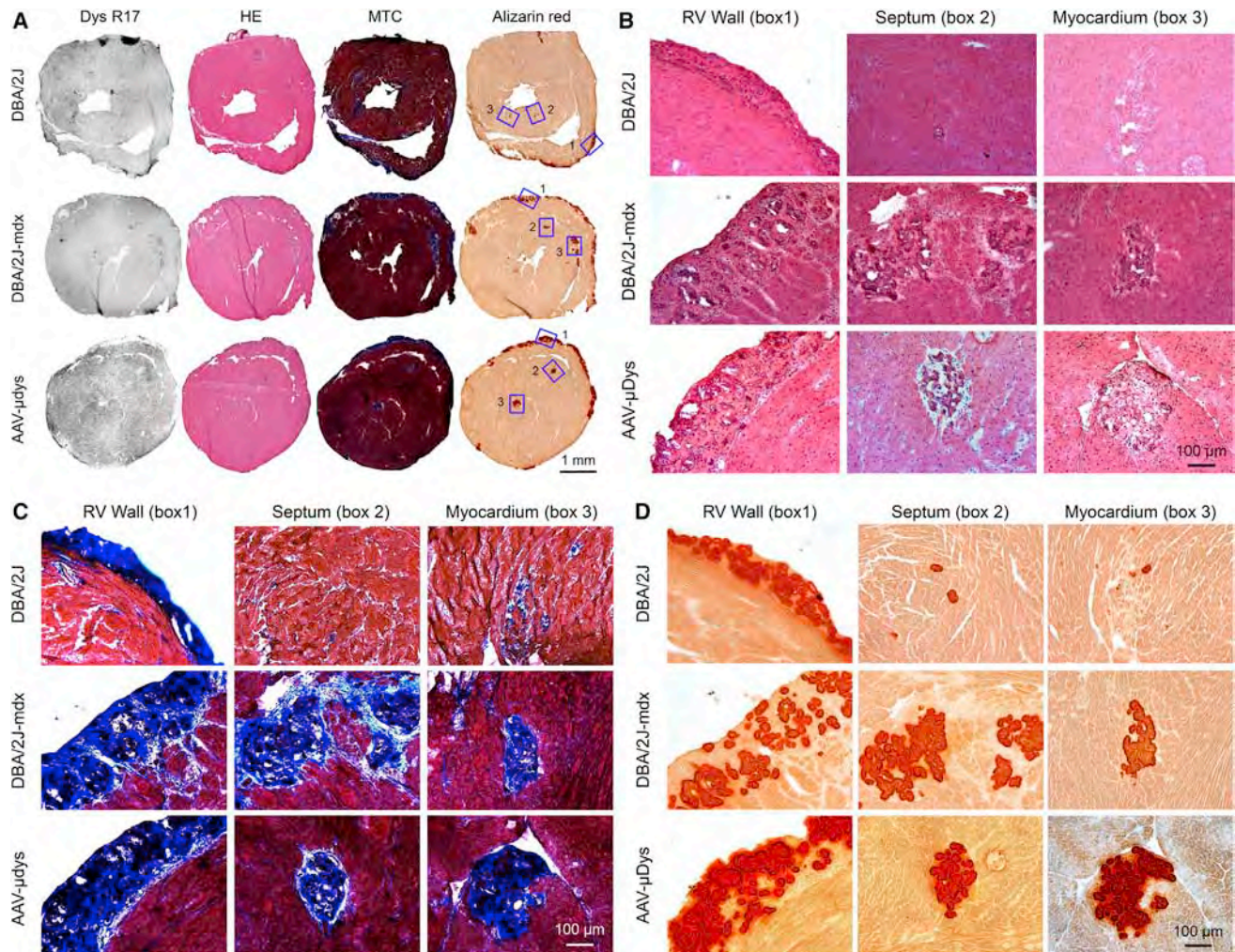


**Figure 5. Abnormal Heart Histology in DBA/2J Mice Reveals the Limitation of DBA/2J-mdx Mice as a Model for Studying DMD Heart Disease**

(A) Representative full-view photomicrographs of H&E (HE), Masson trichrome (MTC), and alizarin red staining and dystrophin R17 immunostaining of the heart of DBA/2J, untreated, and AAV-treated DBA/2J-mdx mice. Selected areas of interest are numbered with 1, 2, and 3 to represent the right ventricular (RV) wall, septum, and myocardium, respectively. (B) A close view of H&E-stained images of boxed areas 1, 2, and 3 in (A). (C) A close view of Masson trichrome-stained images of boxed areas 1, 2, and 3 in (A). (D) A close view of alizarin red-stained images of boxed areas 1, 2, and 3 in (A).

modeled in female mdx mice.<sup>31,55</sup> Since DBA/2J-mdx mice were suggested to display early-onset heart disease, we included both male and female mice in the study (for the skeletal muscle function assay and cardiac function assay, respectively). We confirmed the severe skeletal muscle phenotype reported in the literature (e.g., fibrosis, calcification, inflammation, relatively poor regeneration, and reduction in muscle force) (Figures 3 and 4; see also Figures S2 and S4).<sup>24,25</sup> AAV micro-dystrophin therapy greatly attenuated (on some occasions, completely normalized) skeletal muscle pathology and restored muscle strength (Figures 3 and 4; see also Figures S2 and S4). Surprisingly, on cardiac evaluation, we were not able to reproduce the published data on the cardiac manifestations of DBA/2J-mdx mice.<sup>24</sup> We observed salient pathological changes in the heart of control DBA/2J mice (both male and female) (Figure 5; see also Figure S5).<sup>24</sup> Cardiac

lesions have been observed in DBA/2J mice by several laboratories.<sup>28–30</sup> The existing pathology in control mice rendered it difficult to distinguish additional changes caused by dystrophin deficiency. In fact, we did not detect apparent differences between DBA/2J and DBA/2J-mdx hearts on histological examination (Figure 5; see also Figure S5). Coley et al.<sup>24</sup> found that the maximal cardiac function difference between DBA/2J and DBA/2J-mdx mice occurred at ~6 months of age on echocardiography. The ejection fraction of DBA/2J and DBA/2J-mdx was ~60% and 48%, respectively, at this time point.<sup>24</sup> After which, the heart function of DBA/2J-mdx mice appeared partially recovered although still statistically different from that of DBA/2J mice (the ejection fraction of DBA/2J and DBA/2J-mdx was ~61 and 55, respectively, at 52 weeks of age).<sup>24</sup> We performed our hemodynamic assay at ~6 months of age using the

**Table 2. Weights and Weight Ratios**

	DBA/2J	DBA/2J-mdx	DBA/2J-mdx Treated
Sample size (n)	10	10	5
Age (months)	6.22 ± 0.15	6.10 ± 0.15	6.12 ± 0.24
BW (g)	25.89 ± 1.25 <sup>a</sup>	20.78 ± 0.51	22.48 ± 0.76
TW (mg)	36.68 ± 1.02	30.20 ± 0.72 <sup>b</sup>	36.68 ± 0.64
TL (mm)	17.83 ± 0.09	17.84 ± 0.16	17.76 ± 0.08
HW (mg)	110.78 ± 4.32 <sup>a</sup>	99.29 ± 2.18	108.74 ± 2.85 <sup>c</sup>
VW (mg)	105.41 ± 3.98 <sup>a</sup>	94.81 ± 2.09	103.92 ± 2.85 <sup>c</sup>
HW/BW (mg/g)	4.30 ± 0.09 <sup>b</sup>	4.79 ± 0.07	4.85 ± 0.13
VW/BW (mg/g)	4.10 ± 0.08 <sup>b</sup>	4.57 ± 0.07	4.63 ± 0.12
HW/TW (mg/g)	3.02 ± 0.06 <sup>a</sup>	3.30 ± 0.09	3.11 ± 0.05
VW/TW (mg/g)	2.87 ± 0.06 <sup>a</sup>	3.15 ± 0.08	2.97 ± 0.05
HW/TL (mg/mm)	6.20 ± 0.22 <sup>a</sup>	5.56 ± 0.11	6.12 ± 0.14 <sup>c</sup>
VW/TL (mg/mm)	5.90 ± 0.20 <sup>a</sup>	5.31 ± 0.10	5.85 ± 0.14 <sup>c</sup>

Data are presented as means ± SEM.

<sup>a</sup>Significantly different from DBA/2J-mdx.

<sup>b</sup>Significantly different from other two groups.

<sup>c</sup>Significantly different from DBA/2J-mdx on the Mann-Whitney test but not by ANOVA.

cardiac catheter assay (Table 2). Unexpectedly, we did not detect a statistically significant difference in any of the systolic parameters or in most of diastolic parameters between DBA/2J and DBA/2J-mdx mice (Figure 6B). No difference was seen in overall heart function parameters either (e.g., the ejection fraction of DBA/2J and DBA/2J-mdx was  $74 \pm 4$  and  $69 \pm 4$ , respectively) (Figure 6B). DMD patients and dystrophic animals display characteristic ECG changes such as tachycardia, reduction in the PR interval, prolongation of the QRS duration and QT interval, a deep Q wave, and an increase in the cardiomyopathy index.<sup>32,34,56–62</sup> However, to our knowledge, ECG has not been examined in DBA/2J-mdx mice. To better understand the heart disease in this model, we compared ECG in DBA/2J, DBA/2J-mdx, and AAV micro-dystrophin treated DBA/2J-mdx mice (Figure 6A; see also Figure S6A). Compared to control DBA/2J mice, untreated DBA/2J-mdx mice showed several features consistent with dystrophin deficiency. Specifically, we detected a statistically significant increase in the QRS duration, QT interval, and cardiomyopathy index. The heart rate was increased but did not reach statistical significance. Intriguingly, a deep Q wave was found in control DBA/2J mice but not in DBA/2J-mdx mice (Figure 6A). In our previous studies, we demonstrated beneficial ECG changes following systemic AAV-9 therapy with a four-repeat micro-dystrophin gene in young and aged mdx mice.<sup>34,53,54</sup> Here, we observed a clear trend of improvement in several ECG parameters but none of them reached statistical significance (Figure 6A). This may be due to the genetic background of the model or the sample size. However, we believe it is not due to a lack of gene transfer, because immunostaining showed saturated expression and western blot analysis suggested a dystrophin level much higher than that of control DBA/2J mice (Figures 1D, 1E, and 5; see also Figure S1B).

In summary, we have provided strong compelling preclinical data in a symptomatic mouse model to support the further development of nNOS-binding five-repeat micro-dystrophin gene therapy for DMD with systemic AAV-9 delivery. The unexpected findings in the heart of control DBA/2J mice reveal the potential limitations of the DBA/2J-mdx model for cardiac studies.

## MATERIALS AND METHODS

### Animal Studies

All animal experiments were approved by the animal care and use committee of the University of Missouri and were performed in accordance with NIH guidelines. Congenic D2.B10-Dmd<sup>mdx</sup>/J (stock number 013141; referred to as DBA/2J-mdx in this article) and control DBA/2J (stock number 000671) mice were purchased from The Jackson Laboratory. Experimental mice were generated in house in a barrier facility using founders from The Jackson Laboratory. Both male and female mice were used in the study. Specifically, male mice were used to evaluate skeletal muscle function and female mice were used to study heart function. All mice were maintained in a specific-pathogen free animal care facility on a 12-hr light (25 lux)/12-hr dark cycle with access to food and water ad libitum.

### Micro-Dystrophin Construct

The codon-optimized canine microgene  $\Delta R2-15/\Delta R18-22/\Delta C$  was based on the human micro-dystrophin cDNA  $\mu$ Dys5 (J.R. and J.C., unpublished data) and was synthesized by GenScript. It contains the N-terminal domain, hinges 1 and 4, five spectrin-like repeats (R1, R16, R17, R23, and R24), and the cysteine-rich domain (Figure 1A). The expression cassette was under transcriptional regulation of the muscle-specific CK8 promoter and a 49-bp synthetic pA signal.<sup>1,23,63</sup> The *cis*-AAV packaging plasmid is called pXP42.

### AAV Delivery

Recombinant AAV-9 stock was generated at the University of Pennsylvania Vector Core (<https://www.med.upenn.edu/gtp/vectorcore>) by transient transfection according to the standard protocol of the core. AAV was delivered to 10-week-old DBA/2J-mdx mice through the tail vein in a volume of 500  $\mu$ L/mouse at the dose of  $2 \times 10^{13}$  vg particles/mouse over a period of 60 s.

### AAV Genome Copy Number Quantification

Freshly dissected muscles were snap frozen in liquid nitrogen-cooled isopentane in optimal cutting temperature compound (OCT) (Sakura Finetek). Genomic DNA was extracted from OCT-embedded tissue samples. DNA concentration was quantified with the Qubit dsDNA HS assay kit (Thermo Fisher Scientific). Quantitative TaqMan PCR assays were performed using TaqMan Universal PCR master mix (Thermo Fisher Scientific) to detect either the R1-R16 or R17-R23 junction in the vg. For the R1-R16 junction PCR reaction, the forward primer is 5' GAGTCGCTCTATGGAAAAGCA, the reverse primer is 5' GGTCAGATAAGTACTTGGCAGGTAA, and the probe is 5' ATCTCTTTGTGCAGATTAC. For the R17-R23 junction PCR reaction, the forward primer is 5' GCCGAACGCAAGAAAAGACT, the reverse primer is 5' CAGATGGAGCCGCTTCCA, and the probe

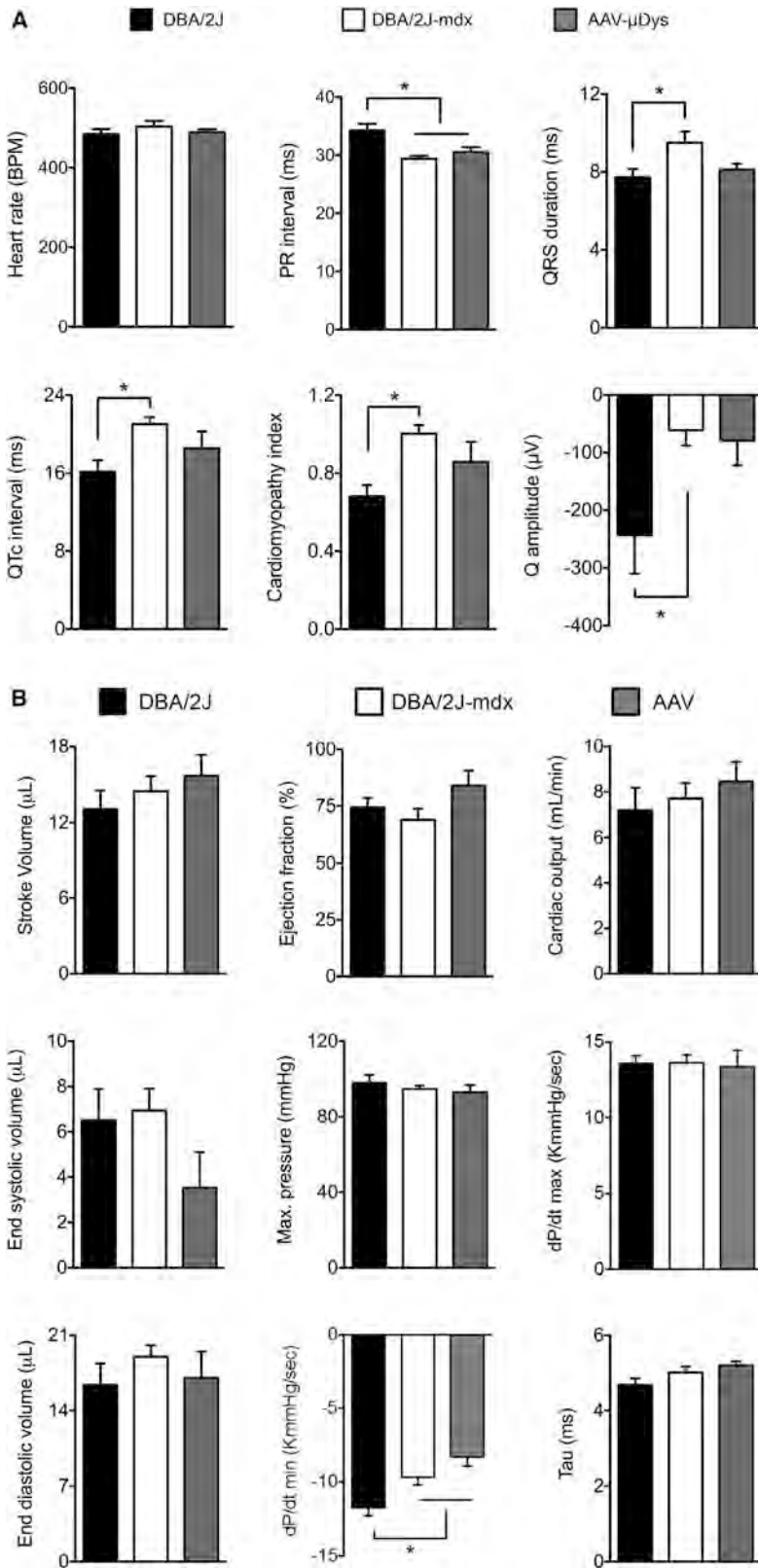


**Figure 6. Evaluation of the Cardiac Impact of AAV Micro-Dystrophin Therapy in DBA/2J-mdx Mice**

(A) Quantitative evaluation of ECG in DBA/2J (n = 10), untreated (n = 10), and AAV-treated (n = 5) DBA/2J-mdx mice. Error bars are mean  $\pm$  SEM. Asterisks indicate significant differences from the indicated group(s). (B) Quantitative analysis of systolic function (top panels), diastolic function (middle panels), and overall heart performance (bottom panels). Error bars are mean  $\pm$  SEM. Asterisks indicate that the result of DBA/2J mice is significantly different from that of AAV-treated DBA/2J-mdx mice.

is 5' CTGGTCGGAGCTTTCCT. The threshold cycle (Ct) value of each reaction was converted to the vg copy number by measuring against the copy number standard curve of known amount of the pXP42 plasmid. The data are reported as the vg copy number per diploid genome.

### Morphological Analysis

Cryosections (10  $\mu\text{m}$  in thickness) were sectioned from OCT-embedded tissue samples and used for staining. General muscle histopathology was revealed with H&E staining. Masson trichrome staining and alizarin red staining were used to reveal muscle fibrosis and myofiber calcification according to our published protocols.<sup>64</sup> Dystrophin expression was evaluated by immunofluorescence staining using two monoclonal antibodies including Mandys-8 (1:200; Sigma) and Manex44A (1:300; a gift from Dr. Glenn Morris, The Robert Jones and Agnes Hunt Orthopaedic Hospital).<sup>65</sup> Mandys-8 recognizes an epitope in dystrophin spectrin-like repeat 11 (R11), which is absent in our micro-dystrophin. Manex44A recognizes an epitope in dystrophin spectrin-like 17 repeat (R17) that is presented in micro-dystrophin. Utrophin was examined with a mouse monoclonal antibody against the utrophin N-terminal domain (VP-U579, 1:20; clone DRP3/20C5, IgG1; Vector Laboratories).  $\beta$ -dystroglycan was revealed with a mouse monoclonal antibody against the C terminus (NCL-b-DG, 1:50; clone 43DAG1/8D5, IgG2a; Novocastra).  $\beta$ -sarcoglycan was revealed with a mouse monoclonal antibody (NCL-b-SARC, 1:50; clone 5B1, IgG1; Novocastra/Leica Biosystems). Dystrobrevin was revealed with a mouse monoclonal antibody (no. 610766, 1:200; clone 23, IgG1; BD Biosciences). Syntrophin was revealed with a pan-syntrophin mouse monoclonal antibody (ab11425, 1:200; clone 1351, IgG1; Abcam). In situ nNOS activity staining was performed according to a published protocol.<sup>18</sup> Macrophages and neutrophils were detected by immunohistochemical staining with the rat anti-mouse F4/80 antibody (1:200; Caltag Laboratories) and the rat anti-mouse Ly-6G antibody (1:800; BD Biosciences Pharmingen), respectively. Slides were viewed at the identical exposure setting using a Nikon E800 fluorescence microscope. Photomicrographs were taken with a QImage Retiga 1300 camera (QImaging).

Central nucleation and the myofiber size were determined from digitalized H&E-stained images using Fiji imaging software (<https://fiji.sc>).<sup>66</sup> The myofiber size was determined using Feret's minimum diameter method.

### Western Blot Analysis

Freshly dissected muscle tissues were snap frozen in liquid nitrogen. Muscle was then homogenized using a liquid nitrogen-cooled mortar and pestle in a homogenization buffer containing 10% SDS, 5 mM ethylenediaminetetraacetic acid, 62.5 mM Tris-HCl (pH 6.8), and 2% protease inhibitor (Roche). Homogenate was spun at 14,000 rpm for 2 min (Eppendorf centrifuge, model 5417C; Eppendorf-Netheler-Hinz). The supernatant was used for western blot analysis. Protein concentration was determined using the Bio-Rad DC protein assay kit (Bio-Rad). 100–150  $\mu\text{g}$  protein was loaded on a 3% stacking/6% separating SDS-polyacrylamide gel and run for

3.5 hr at 100 V. Following electrophoresis, protein was transferred to a polyvinylidene fluoride (PVDF) membrane. The PVDF membrane was blocked with 5% milk in Tris-buffered saline (TBS)-Tween 20 (TBST) solution (containing  $1\times$  TBS and 0.1% Tween 20) for 1 hr at room temperature. The PVDF membrane was subsequently incubated with a dystrophin monoclonal antibody MANHINGE1A (1:100 dilution; a gift from Dr. Glenn Morris) in 5% milk/TBST overnight at 4°C. The membrane was washed in TBST three times for 10 min each and then incubated with the horseradish peroxidase-conjugated goat anti-mouse IgG secondary antibody (1:2,000 dilution in TBST; Santa Cruz) for 1 hr at room temperature. After another round of TBST wash (three times, 10-min each), signals were detected using the enhanced chemiluminescence (ECL) system (GE Healthcare Biosciences). Protein loading was confirmed with Ponceau S staining.

### Skeletal Muscle Function Assay

Function of the EDL muscle and the TA muscle was evaluated *ex vivo* and *in situ*, respectively, according to our published protocols.<sup>67,68</sup> Specifically, the twitch force, tetanic force, and eccentric contraction profile were measured. Experimental mice were anesthetized via intraperitoneal injection of a cocktail containing 25 mg/mL ketamine, 2.5 mg/mL xylazine, and 0.5 mg/mL acepromazine at 2.5  $\mu\text{L/g}$  body weight. For the *ex vivo* EDL muscle function assay, the muscle was gently dissected and mounted to a muscle test system (Aurora Scientific). Muscle force was evaluated with a 305B dual-mode servomotor transducer (Aurora Scientific). For the *in situ* TA muscle function assay, the TA muscle and the sciatic nerve were exposed. The mouse was then transferred to a custom-designed thermo-controlled footplate platform.<sup>67</sup> Subsequently, forces were measured *in situ* with a 305C-LR dual-mode servomotor transducer (Aurora Scientific). Data acquisition and analysis was performed with Dynamic Muscle Control and Analysis software (Aurora Scientific). The specific muscle force was calculated by dividing the absolute muscle force by the muscle cross-sectional area. Muscle CSA was calculated according to the following equation:  $\text{CSA} = (\text{muscle mass, in g}) / [(\text{muscle density, in g/cm}^3) \times (\text{length ratio}) \times (\text{optimal muscle length, in cm})]$ ; 1.06 g/cm<sup>3</sup> was used for muscle density.<sup>69</sup> The length ratio refers to the ratio of the optimal fiber length to the optimal muscle length. The length ratios for the EDL and TA muscles were 0.44 and 0.6, respectively.<sup>70,71</sup>

### Heart Function Assay

A 12-lead ECG assay was performed using a commercial system from AD Instruments according to our previously published protocol.<sup>72,73</sup> The Q wave amplitude was determined using the lead I tracing. Other ECG parameters were analyzed using the lead II tracing. The QTc interval was determined by correcting the QT interval with the heart rate, as described by Mitchell et al.<sup>74</sup> The cardiomyopathy index was calculated by dividing the QT interval by the PQ segment.<sup>75</sup> Left ventricular hemodynamics was evaluated using a Millar ultra-miniature pressure-volume (PV) catheter SPR 839. The catheter was placed in the left ventricle using a closed chest approach as we previously described.<sup>72,73</sup> The resulting PV loops were analyzed with PVAN software (Millar Instruments). The relaxation constant of the left ventricle was determined using the method of Weiss

et al.<sup>76</sup> Detailed protocols for ECG and hemodynamic assays are available at the Parent Project Muscular Dystrophy standard operating protocol website ([http://www.parentprojectmd.org/site/PageServer?pagename=Advance\\_researchers\\_sops](http://www.parentprojectmd.org/site/PageServer?pagename=Advance_researchers_sops)).<sup>77</sup>

### Statistical Analysis

Data are presented as means  $\pm$  SEM. Statistical significance was determined with one-way ANOVA followed by Tukey multiple comparison analysis or Bonferroni post hoc analysis using GraphPad Prism software (version 7.0) or SPSS statistical software (IBM). For data that did not fit into the Gaussian distribution, the nonparametric Mann-Whitney test was used to evaluate the statistical significance in two-group comparisons. The difference was considered significant when  $p < 0.05$ .

### SUPPLEMENTAL INFORMATION

Supplemental Information includes six figures and can be found with this article online at <http://dx.doi.org/10.1016/j.omtm.2017.06.006>.

### AUTHOR CONTRIBUTIONS

Conceived and designed experiments: C.H.H., N.B.W., J.S.S., J.S.C., and D.D. Performed the experiments: C.H.H., N.B.W., X.P., K.K., Y.Y., K.Z., G.Y., B.H., S.X.D., and J.R. Analyzed the data: C.H.H., N.B.W., J.S.S., N.N.Y., J.S.C., and D.D. Wrote the paper: C.H.H., N.B.W., and D.D. All authors edited the paper and approved the submission.

### CONFLICTS OF INTEREST

D.D. and J.S.C. are members of the scientific advisory board and are equity holders of Solid Biosciences, LLC. D.D., J.R., J.S.C., and Y.Y. are inventors on patents that were licensed to Solid Biosciences, LLC. The Duan laboratory and the Chamberlain laboratory have received research support from Solid Biosciences, LLC. J.S.S. is an employee of Solid Biosciences, LLC.

### ACKNOWLEDGMENTS

This work was supported in part by Solid Biosciences, LLC and by grants from the NIH (NS-90634 to D.D. and HL-122332 to J.S.C.), the Department of Defense (MD130014 to D.D.), Jesse's Journey—The Foundation for Gene and Cell Therapy (to D.D.), and the Jackson Freeland DMD Research Fund (to D.D.). We thank Dr. Patrick Gonzalez for the critical reading of the manuscript. We thank Dr. Stephen Hauschka for providing the CK8 promoter.

### REFERENCES

- Bengtsson, N.E., Seto, J.T., Hall, J.K., Chamberlain, J.S., and Odom, G.L. (2016). Progress and prospects of gene therapy clinical trials for the muscular dystrophies. *Hum. Mol. Genet.* 25, R9–R17.
- Duan, D. (2016). Dystrophin gene replacement and gene repair therapy for Duchenne muscular dystrophy in 2016. *Hum. Gene Ther. Clin. Dev.* 27, 9–18.
- Al-Zaidy, S., Rodino-Klapac, L., and Mendell, J.R. (2014). Gene therapy for muscular dystrophy: moving the field forward. *Pediatr. Neurol.* 51, 607–618.
- Duan, D. (2016). Systemic delivery of adeno-associated viral vectors. *Curr. Opin. Virol.* 21, 16–25.
- Mingozzi, F., and High, K.A. (2011). Therapeutic in vivo gene transfer for genetic disease using AAV: progress and challenges. *Nat. Rev. Genet.* 12, 341–355.
- Mendell, J.R., Al-Zaidy, S., Shell, R., Arnold, W.D., Rodino-Klapac, L., Kissel, J.T., Prior, T.W., Miranda, C., Lowes, L., Alfano, L., and Berry, K. (2016). Gene therapy for spinal muscular atrophy type 1 shows potential to improve survival and motor functional outcomes. *Mol. Ther.* 24, S190.
- Carter, B.J. (2004). Adeno-associated virus and the development of adeno-associated virus vectors: a historical perspective. *Mol. Ther.* 10, 981–989.
- England, S.B., Nicholson, L.V., Johnson, M.A., Forrest, S.M., Love, D.R., Zubrzycka-Gaarn, E.E., Bulman, D.E., Harris, J.B., and Davies, K.E. (1990). Very mild muscular dystrophy associated with the deletion of 46% of dystrophin. *Nature* 343, 180–182.
- Crawford, G.E., Faulkner, J.A., Crosbie, R.H., Campbell, K.P., Froehner, S.C., and Chamberlain, J.S. (2000). Assembly of the dystrophin-associated protein complex does not require the dystrophin COOH-terminal domain. *J. Cell Biol.* 150, 1399–1410.
- Wang, B., Li, J., and Xiao, X. (2000). Adeno-associated virus vector carrying human minidystrophin genes effectively ameliorates muscular dystrophy in mdx mouse model. *Proc. Natl. Acad. Sci. USA* 97, 13714–13719.
- Harper, S.Q., Hauser, M.A., DelloRusso, C., Duan, D., Crawford, R.W., Phelps, S.F., Harper, H.A., Robinson, A.S., Engelhardt, J.F., Brooks, S.V., and Chamberlain, J.S. (2002). Modular flexibility of dystrophin: implications for gene therapy of Duchenne muscular dystrophy. *Nat. Med.* 8, 253–261.
- Liu, M., Yue, Y., Harper, S.Q., Grange, R.W., Chamberlain, J.S., and Duan, D. (2005). Adeno-associated virus-mediated microdystrophin expression protects young mdx muscle from contraction-induced injury. *Mol. Ther.* 11, 245–256.
- Gregorevic, P., Allen, J.M., Minami, E., Blankinship, M.J., Haraguchi, M., Meuse, L., Finn, E., Adams, M.E., Froehner, S.C., Murry, C.E., and Chamberlain, J.S. (2006). rAAV6-microdystrophin preserves muscle function and extends lifespan in severely dystrophic mice. *Nat. Med.* 12, 787–789.
- Wang, B., Li, J., Fu, F.H., and Xiao, X. (2009). Systemic human minidystrophin gene transfer improves functions and life span of dystrophin and dystrophin/utrophin-deficient mice. *J. Orthop. Res.* 27, 421–426.
- Yue, Y., Liu, M., and Duan, D. (2006). C-terminal-truncated microdystrophin recruits dystrobrevin and syntrophin to the dystrophin-associated glycoprotein complex and reduces muscular dystrophy in symptomatic utrophin/dystrophin double-knockout mice. *Mol. Ther.* 14, 79–87.
- Brennan, J.E., Chao, D.S., Xia, H., Aldape, K., and Bredt, D.S. (1995). Nitric oxide synthase complexed with dystrophin and absent from skeletal muscle sarcolemma in Duchenne muscular dystrophy. *Cell* 82, 743–752.
- Li, D., Yue, Y., Lai, Y., Hakim, C.H., and Duan, D. (2011). Nitrosative stress elicited by nNOS $\mu$  delocalization inhibits muscle force in dystrophin-null mice. *J. Pathol.* 223, 88–98.
- Lai, Y., Thomas, G.D., Yue, Y., Yang, H.T., Li, D., Long, C., Judge, L., Bostick, B., Chamberlain, J.S., Terjung, R.L., and Duan, D. (2009). Dystrophins carrying spectrin-like repeats 16 and 17 anchor nNOS to the sarcolemma and enhance exercise performance in a mouse model of muscular dystrophy. *J. Clin. Invest.* 119, 624–635.
- Lai, Y., Zhao, J., Yue, Y., and Duan, D. (2013).  $\alpha 2$  and  $\alpha 3$  helices of dystrophin R16 and R17 frame a microdomain in the  $\alpha 1$  helix of dystrophin R17 for neuronal NOS binding. *Proc. Natl. Acad. Sci. USA* 110, 525–530.
- Zhang, Y., and Duan, D. (2012). Novel mini-dystrophin gene dual adeno-associated virus vectors restore neuronal nitric oxide synthase expression at the sarcolemma. *Hum. Gene Ther.* 23, 98–103.
- Zhang, Y., Yue, Y., Li, L., Hakim, C.H., Zhang, K., Thomas, G.D., and Duan, D. (2013). Dual AAV therapy ameliorates exercise-induced muscle injury and functional ischemia in murine models of Duchenne muscular dystrophy. *Hum. Mol. Genet.* 22, 3720–3729.
- Shin, J.H., Pan, X., Hakim, C.H., Yang, H.T., Yue, Y., Zhang, K., Terjung, R.L., and Duan, D. (2013). Microdystrophin ameliorates muscular dystrophy in the canine model of duchenne muscular dystrophy. *Mol. Ther.* 21, 750–757.
- Himeda, C.L., Chen, X., and Hauschka, S.D. (2011). Design and testing of regulatory cassettes for optimal activity in skeletal and cardiac muscles. *Methods Mol. Biol.* 709, 3–19.

24. Coley, W.D., Bogdanik, L., Vila, M.C., Yu, Q., Van Der Meulen, J.H., Rayavarapu, S., Novak, J.S., Nearing, M., Quinn, J.L., Saunders, A., et al. (2016). Effect of genetic background on the dystrophic phenotype in mdx mice. *Hum. Mol. Genet.* 25, 130–145.
25. Fukada, S., Morikawa, D., Yamamoto, Y., Yoshida, T., Sumie, N., Yamaguchi, M., Ito, T., Miyagoe-Suzuki, Y., Takeda, S., Tsujikawa, K., and Yamamoto, H. (2010). Genetic background affects properties of satellite cells and mdx phenotypes. *Am. J. Pathol.* 176, 2414–2424.
26. Wasala, N.B., Zhang, K., Wasala, L.P., Hakim, C.H., and Duan, D. (2015). The FVB background does not dramatically alter the dystrophic phenotype of mdx mice. *PLoS Curr.*, Published online February 10, 2015. <http://dx.doi.org/10.1371/currents.md.28266819ca0ec5fefcac767ea9a3461c>.
27. Li, D., Yue, Y., and Duan, D. (2008). Preservation of muscle force in Mdx3cv mice correlates with low-level expression of a near full-length dystrophin protein. *Am. J. Pathol.* 172, 1332–1341.
28. Maeda, N., Doi, K., and Mitsuoka, T. (1986). Development of heart and aortic lesions in DBA/2Ncrj mice. *Lab. Anim.* 20, 5–8.
29. Brownstein, D.G. (1983). Genetics of dystrophic epicardial mineralization in DBA/2 mice. *Lab. Anim. Sci.* 33, 247–248.
30. Nabors, C.E., and Ball, C.R. (1969). Spontaneous calcification in hearts of DBA mice. *Anat. Rec.* 164, 153–161.
31. Bostick, B., Yue, Y., and Duan, D. (2010). Gender influences cardiac function in the mdx model of Duchenne cardiomyopathy. *Muscle Nerve* 42, 600–603.
32. Bostick, B., Yue, Y., Long, C., and Duan, D. (2008). Prevention of dystrophin-deficient cardiomyopathy in twenty-one-month-old carrier mice by mosaic dystrophin expression or complementary dystrophin/utrophin expression. *Circ. Res.* 102, 121–130.
33. Yue, Y., Wasala, N.B., Bostick, B., and Duan, D. (2016). 100-fold but not 50-fold dystrophin overexpression aggravates electrocardiographic defects in the mdx model of Duchenne muscular dystrophy. *Mol. Ther. Methods Clin. Dev.* 3, 16045.
34. Bostick, B., Yue, Y., Lai, Y., Long, C., Li, D., and Duan, D. (2008). Adeno-associated virus serotype-9 microdystrophin gene therapy ameliorates electrocardiographic abnormalities in mdx mice. *Hum. Gene Ther.* 19, 851–856.
35. Lai, Y., Yue, Y., Liu, M., Ghosh, A., Engelhardt, J.F., Chamberlain, J.S., and Duan, D. (2005). Efficient in vivo gene expression by trans-splicing adeno-associated viral vectors. *Nat. Biotechnol.* 23, 1435–1439.
36. Ghosh, A., Yue, Y., Lai, Y., and Duan, D. (2008). A hybrid vector system expands adeno-associated viral vector packaging capacity in a transgene-independent manner. *Mol. Ther.* 16, 124–130.
37. Lostal, W., Kodippili, K., Yue, Y., and Duan, D. (2014). Full-length dystrophin reconstitution with adeno-associated viral vectors. *Hum. Gene Ther.* 25, 552–562.
38. Odom, G.L., Gregorevic, P., Allen, J.M., and Chamberlain, J.S. (2011). Gene therapy of mdx mice with large truncated dystrophins generated by recombination using rAAV6. *Mol. Ther.* 19, 36–45.
39. Koo, T., Popplewell, L., Athanasopoulos, T., and Dickson, G. (2014). Triple trans-splicing adeno-associated virus vectors capable of transferring the coding sequence for full-length dystrophin protein into dystrophic mice. *Hum. Gene Ther.* 25, 98–108.
40. Mendell, J.R., Campbell, K., Rodino-Klapac, L., Sahenk, Z., Shilling, C., Lewis, S., Bowles, D., Gray, S., Li, C., Galloway, G., et al. (2010). Dystrophin immunity in Duchenne's muscular dystrophy. *N. Engl. J. Med.* 363, 1429–1437.
41. Gregorevic, P., Blankinship, M.J., Allen, J.M., Crawford, R.W., Meuse, L., Miller, D.G., Russell, D.W., and Chamberlain, J.S. (2004). Systemic delivery of genes to striated muscles using adeno-associated viral vectors. *Nat. Med.* 10, 828–834.
42. Yue, Y., Pan, X., Hakim, C.H., Kodippili, K., Zhang, K., Shin, J.H., Yang, H.T., McDonald, T., and Duan, D. (2015). Safe and bodywide muscle transduction in young adult Duchenne muscular dystrophy dogs with adeno-associated virus. *Hum. Mol. Genet.* 24, 5880–5890.
43. Baroncelli, A.B., Abellonio, F., Pagano, T.B., Esposito, I., Peirone, B., Papparella, S., and Paciello, O. (2014). Muscular dystrophy in a dog resembling human Becker muscular dystrophy. *J. Comp. Pathol.* 150, 429–433.
44. Stamler, J.S., and Meissner, G. (2001). Physiology of nitric oxide in skeletal muscle. *Physiol. Rev.* 81, 209–237.
45. De Palma, C., and Clementi, E. (2012). Nitric oxide in myogenesis and therapeutic muscle repair. *Mol. Neurobiol.* 46, 682–692.
46. Thomas, G.D. (2013). Functional muscle ischemia in Duchenne and Becker muscular dystrophy. *Front. Physiol.* 4, 381.
47. Tidball, J.G., and Wehling-Henricks, M. (2014). Nitric oxide synthase deficiency and the pathophysiology of muscular dystrophy. *J. Physiol.* 592, 4627–4638.
48. Wang, Z., Kuhr, C.S., Allen, J.M., Blankinship, M., Gregorevic, P., Chamberlain, J.S., Tapscott, S.J., and Storb, R. (2007). Sustained AAV-mediated dystrophin expression in a canine model of Duchenne muscular dystrophy with a brief course of immunosuppression. *Mol. Ther.* 15, 1160–1166.
49. Gao, G., Vandenberghe, L.H., Alvira, M.R., Lu, Y., Calcedo, R., Zhou, X., and Wilson, J.M. (2004). Clades of Adeno-associated viruses are widely disseminated in human tissues. *J. Virol.* 78, 6381–6388.
50. Bostick, B., Ghosh, A., Yue, Y., Long, C., and Duan, D. (2007). Systemic AAV-9 transduction in mice is influenced by animal age but not by the route of administration. *Gene Ther.* 14, 1605–1609.
51. Yue, Y., Ghosh, A., Long, C., Bostick, B., Smith, B.F., Kornegay, J.N., and Duan, D. (2008). A single intravenous injection of adeno-associated virus serotype-9 leads to whole body skeletal muscle transduction in dogs. *Mol. Ther.* 16, 1944–1952.
52. Yue, Y., Shin, J.H., and Duan, D. (2011). Whole body skeletal muscle transduction in neonatal dogs with AAV-9. *Methods Mol. Biol.* 709, 313–329.
53. Bostick, B., Shin, J.-H., Yue, Y., and Duan, D. (2011). AAV-microdystrophin therapy improves cardiac performance in aged female mdx mice. *Mol. Ther.* 19, 1826–1832.
54. Bostick, B., Shin, J.H., Yue, Y., Wasala, N.B., Lai, Y., and Duan, D. (2012). AAV micro-dystrophin gene therapy alleviates stress-induced cardiac death but not myocardial fibrosis in >21-m-old mdx mice, an end-stage model of Duchenne muscular dystrophy cardiomyopathy. *J. Mol. Cell. Cardiol.* 53, 217–222.
55. Hakim, C.H., and Duan, D. (2012). Gender differences in contractile and passive properties of mdx extensor digitorum longus muscle. *Muscle Nerve* 45, 250–256.
56. Shin, J.H., Bostick, B., Yue, Y., Hajjar, R., and Duan, D. (2011). SERCA2a gene transfer improves electrocardiographic performance in aged mdx mice. *J. Transl. Med.* 9, 132.
57. Fine, D.M., Shin, J.H., Yue, Y., Volkman, D., Leach, S.B., Smith, B.F., McIntosh, M., and Duan, D. (2011). Age-matched comparison reveals early electrocardiography and echocardiography changes in dystrophin-deficient dogs. *Neuromuscul. Disord.* 21, 453–461.
58. Perloff, J.K., Roberts, W.C., de Leon, A.C., Jr., and O'Doherty, D. (1967). The distinctive electrocardiogram of Duchenne's progressive muscular dystrophy. An electrocardiographic-pathologic correlative study. *Am. J. Med.* 42, 179–188.
59. Perloff, J.K. (1984). Cardiac rhythm and conduction in Duchenne's muscular dystrophy: a prospective study of 20 patients. *J. Am. Coll. Cardiol.* 3, 1263–1268.
60. Fayssoil, A. (2008). Holter electrocardiogram should be systematic in Duchenne muscular dystrophy. *Int. J. Cardiol.* 128, 442–443.
61. Takami, Y., Takeshima, Y., Awano, H., Okizuka, Y., Yagi, M., and Matsuo, M. (2008). High incidence of electrocardiogram abnormalities in young patients with Duchenne muscular dystrophy. *Pediatr. Neurol.* 39, 399–403.
62. Thrush, P.T., Allen, H.D., Viollet, L., and Mendell, J.R. (2009). Re-examination of the electrocardiogram in boys with Duchenne muscular dystrophy and correlation with its dilated cardiomyopathy. *Am. J. Cardiol.* 103, 262–265.
63. Levitt, N., Briggs, D., Gil, A., and Proudfoot, N.J. (1989). Definition of an efficient synthetic poly(A) site. *Genes Dev.* 3, 1019–1025.
64. Smith, B.F., Yue, Y., Woods, P.R., Kornegay, J.N., Shin, J.H., Williams, R.R., and Duan, D. (2011). An intronic LINE-1 element insertion in the dystrophin gene aborts dystrophin expression and results in Duchenne-like muscular dystrophy in the corgi breed. *Lab. Invest.* 91, 216–231.
65. Kodippili, K., Vince, L., Shin, J.H., Yue, Y., Morris, G.E., McIntosh, M.A., and Duan, D. (2014). Characterization of 65 epitope-specific dystrophin monoclonal antibodies in canine and murine models of duchenne muscular dystrophy by immunostaining and western blot. *PLoS ONE* 9, e88280.

66. Schindelin, J., Arganda-Carreras, I., Frise, E., Kaynig, V., Longair, M., Pietzsch, T., Preibisch, S., Rueden, C., Saalfeld, S., Schmid, B., et al. (2012). Fiji: an open-source platform for biological-image analysis. *Nat. Methods* 9, 676–682.
67. Hakim, C.H., Wasala, N.B., and Duan, D. (2013). Evaluation of muscle function of the extensor digitorum longus muscle ex vivo and tibialis anterior muscle in situ in mice. *J. Vis. Exp.* 72, 50183.
68. Hakim, C.H., Li, D., and Duan, D. (2011). Monitoring murine skeletal muscle function for muscle gene therapy. *Methods Mol. Biol.* 709, 75–89.
69. Mendez, J., and Keys, A. (1960). Density and composition of mammalian muscle. *Metabolism* 9, 184–188.
70. Burkholder, T.J., Fingado, B., Baron, S., and Lieber, R.L. (1994). Relationship between muscle fiber types and sizes and muscle architectural properties in the mouse hindlimb. *J. Morphol.* 221, 177–190.
71. Brooks, S.V., and Faulkner, J.A. (1988). Contractile properties of skeletal muscles from young, adult and aged mice. *J. Physiol.* 404, 71–82.
72. Bostick, B., Yue, Y., and Duan, D. (2011). Phenotyping cardiac gene therapy in mice. *Methods Mol. Biol.* 709, 91–104.
73. Wasala, N.B., Bostick, B., Yue, Y., and Duan, D. (2013). Exclusive skeletal muscle correction does not modulate dystrophic heart disease in the aged mdx model of Duchenne cardiomyopathy. *Hum. Mol. Genet.* 22, 2634–2641.
74. Mitchell, G.F., Jeron, A., and Koren, G. (1998). Measurement of heart rate and Q-T interval in the conscious mouse. *Am. J. Physiol.* 274, H747–H751.
75. Nigro, G., Comi, L.I., Politano, L., and Nigro, G. (2004). Cardiomyopathies associated with muscular dystrophies. In *Myology: Basic and Clinical, Third Edition, Volume 2*, A. Engel and C. Franzini-Armstrong, eds. (McGraw-Hill, Medical Publishing Division), pp. 1239–1256.
76. Weiss, J.L., Frederiksen, J.W., and Weisfeldt, M.L. (1976). Hemodynamic determinants of the time-course of fall in canine left ventricular pressure. *J. Clin. Invest.* 58, 751–760.
77. Duan, D., Rafael-Fortney, J.A., Blain, A., Kass, D.A., McNally, E.M., Metzger, J.M., Spurney, C.F., and Kinnett, K. (2016). Standard operating procedures (SOPs) for evaluating the heart in preclinical studies of Duchenne muscular dystrophy. *J. Cardiovasc. Transl. Res.* 9, 85–86.

OMTM, Volume ■ ■ ■

## **Supplemental Information**

### **A Five-Repeat Micro-Dystrophin Gene**

### **Ameliorated Dystrophic Phenotype in the Severe**

### **DBA/2J-mdx Model of Duchenne Muscular Dystrophy**

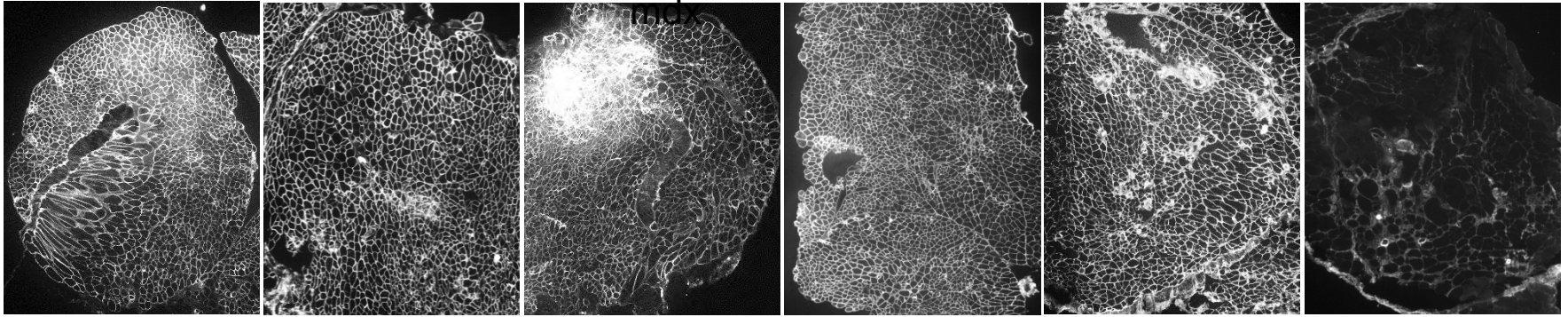
**Chady H. Hakim, Nalinda B. Wasala, Xiufang Pan, Kasun Kodippili, Yongping Yue, Keqing Zhang, Gang Yao, Brittney Haffner, Sean X. Duan, Julian Ramos, Joel S. Schneider, Nora N. Yang, Jeffrey Chamberlain, and Dongsheng Duan**

A

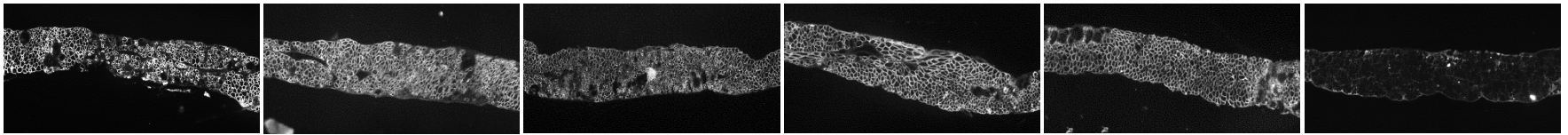
AAV- $\mu$ Dys treated DBA/2J-

Untreated  
DBA/2J-mdx

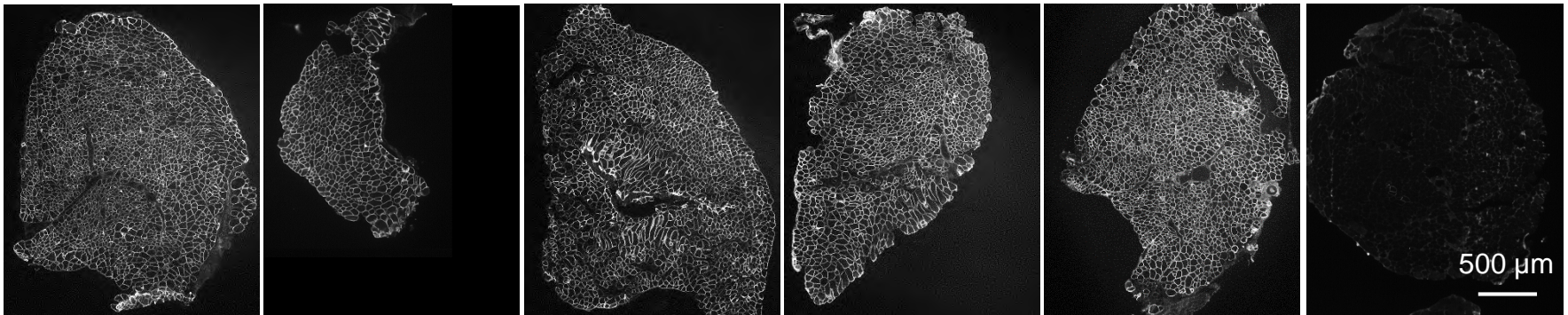
Quadriceps



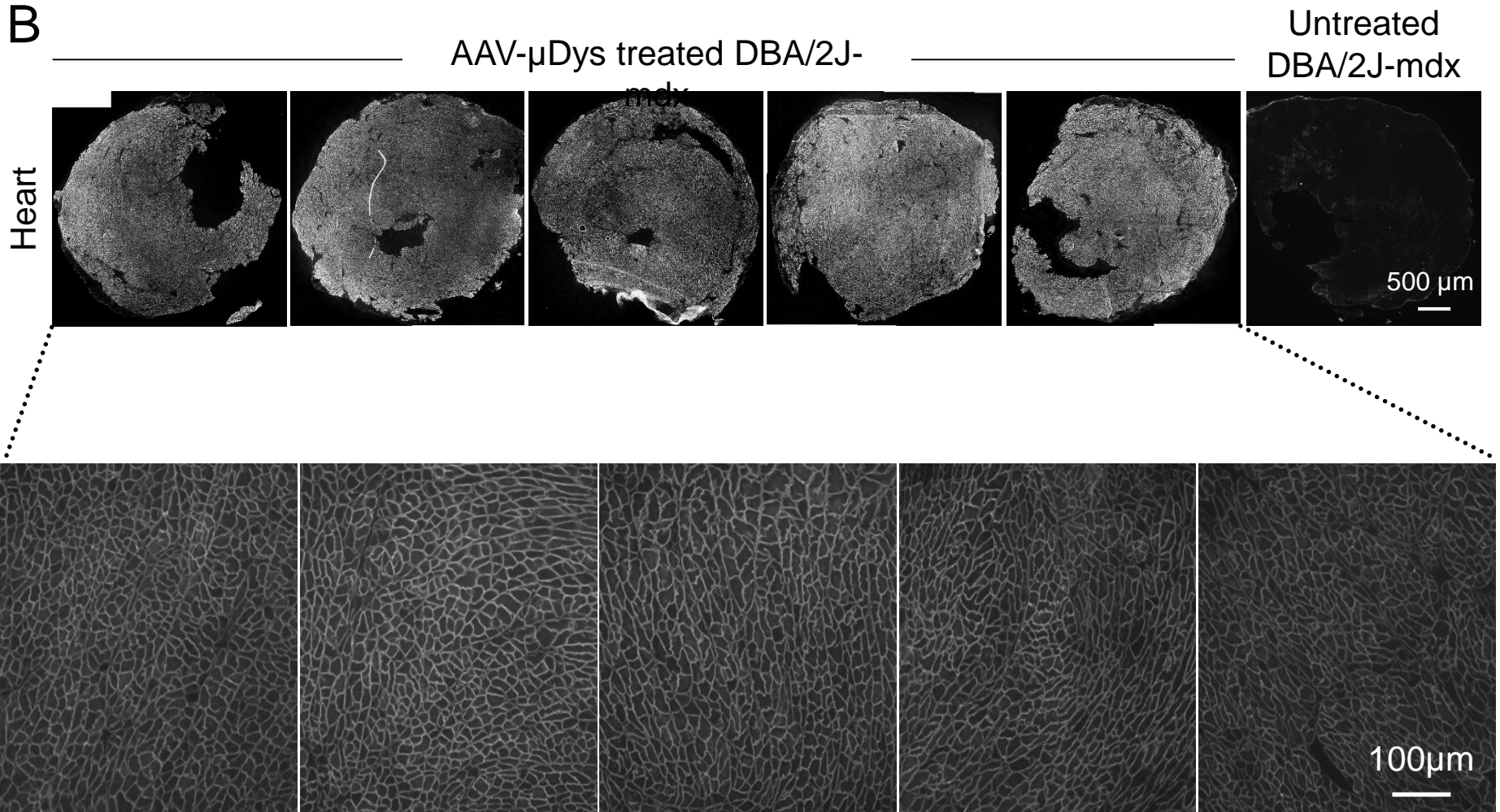
Diaphragm

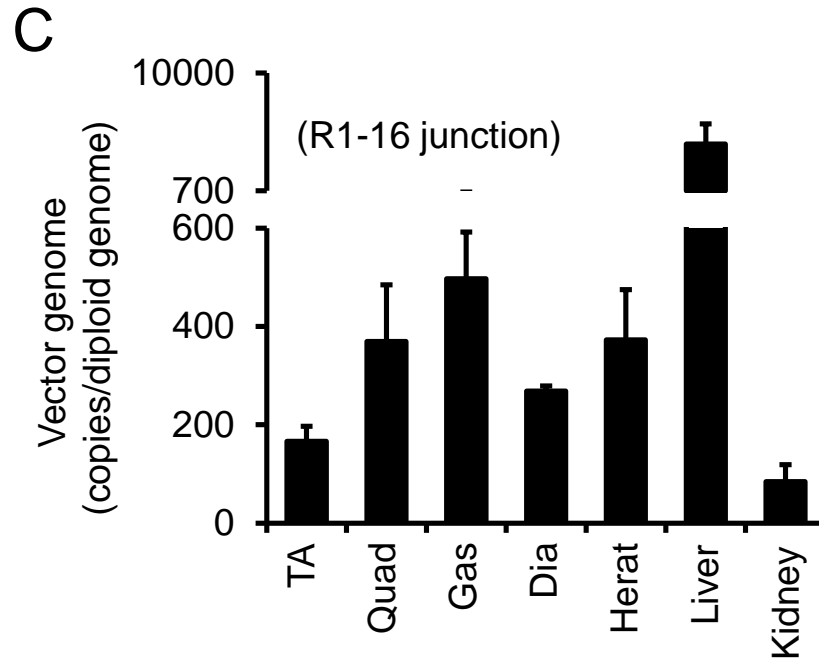


TA



**B**





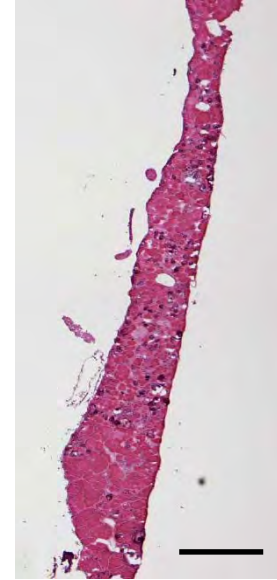
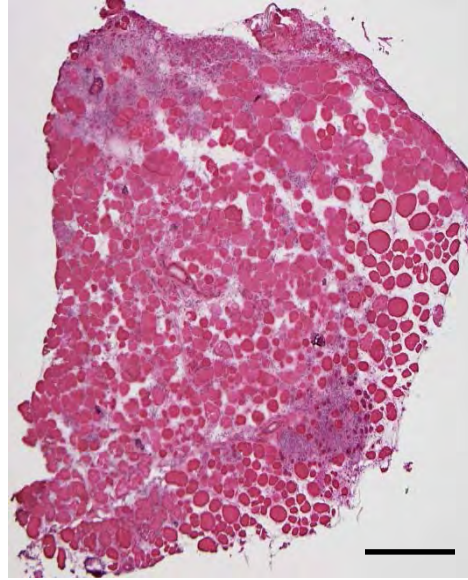
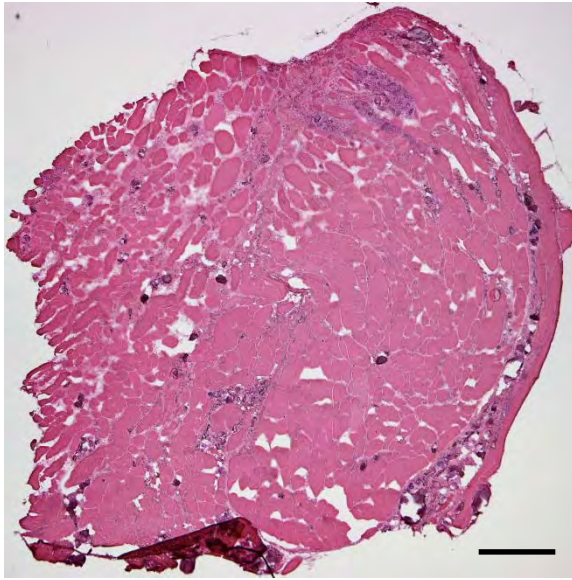
A

Quadriceps

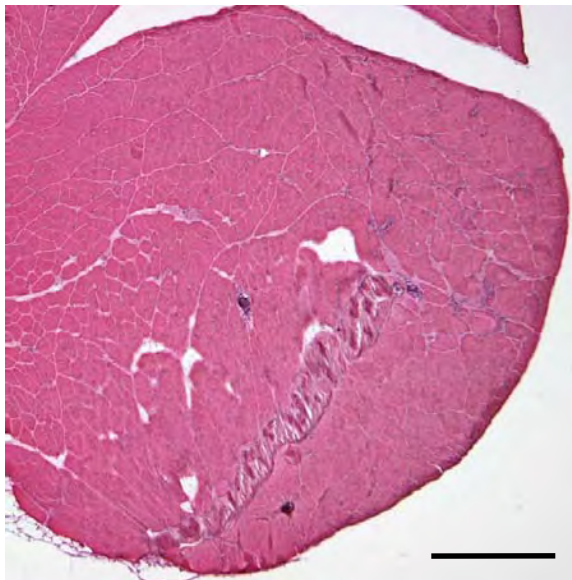
TA

Diaphragm

DBA/2J-mdx



AAV- $\mu$ Dys



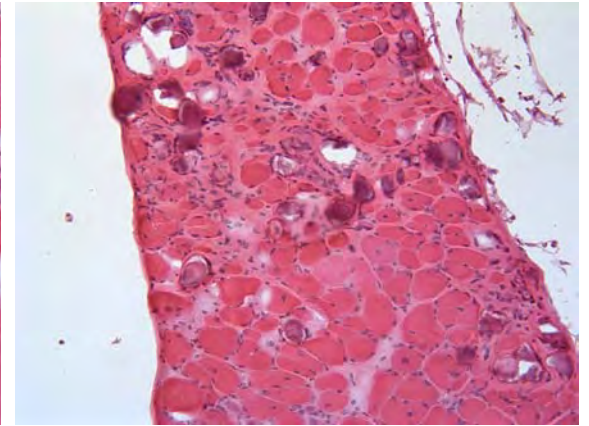
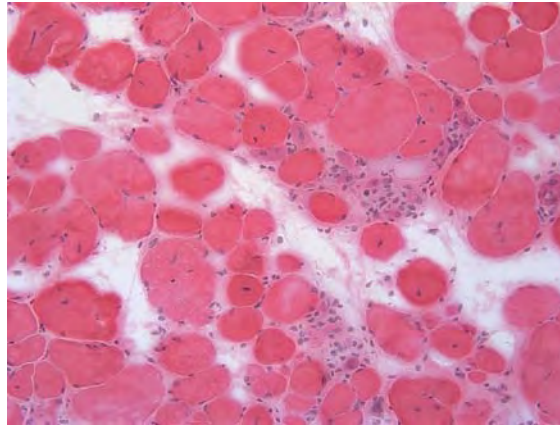
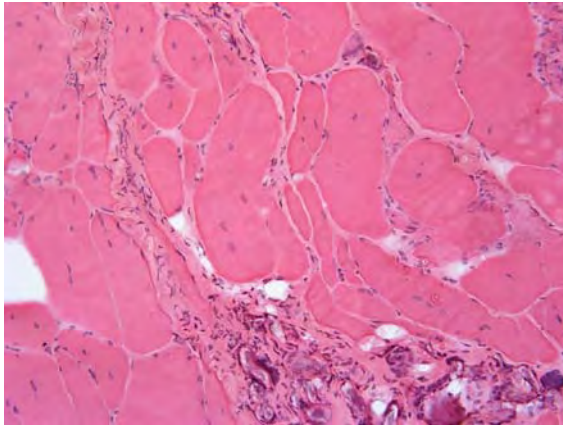
**B**

Quadriceps

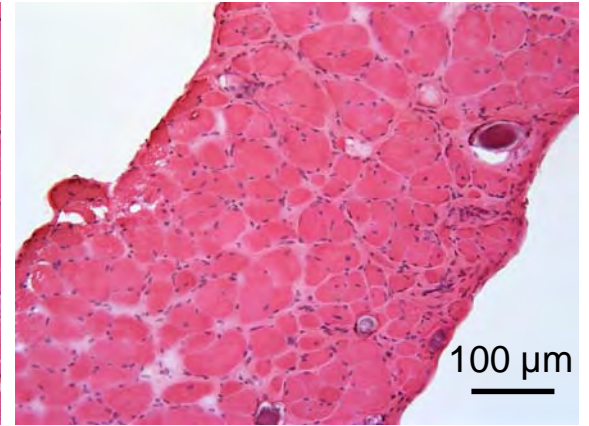
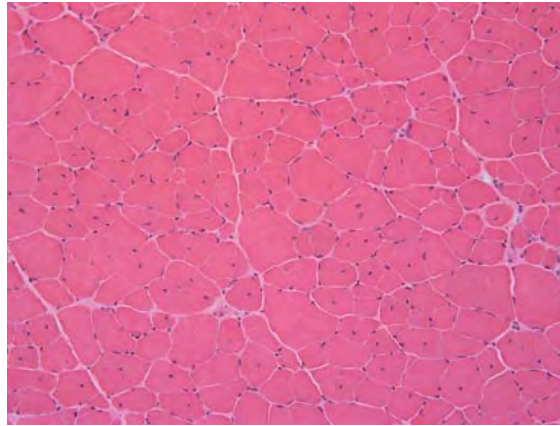
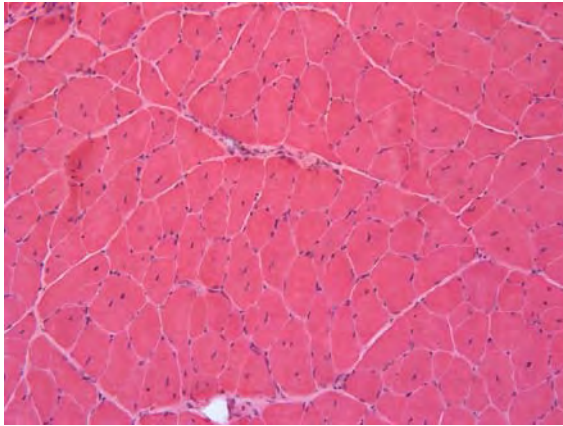
TA

Diaphragm

DBA/2J-mdx

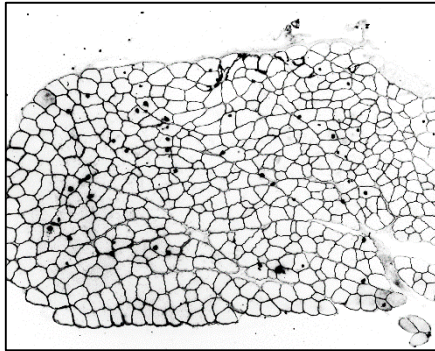


AAV- $\mu$ Dys

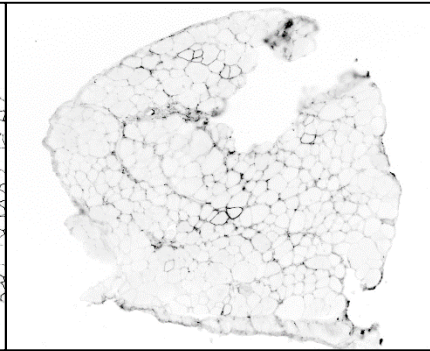


100  $\mu$ m

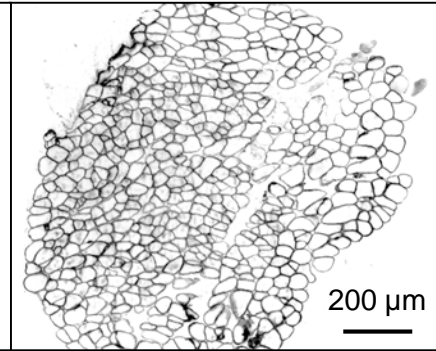
DBA/2J

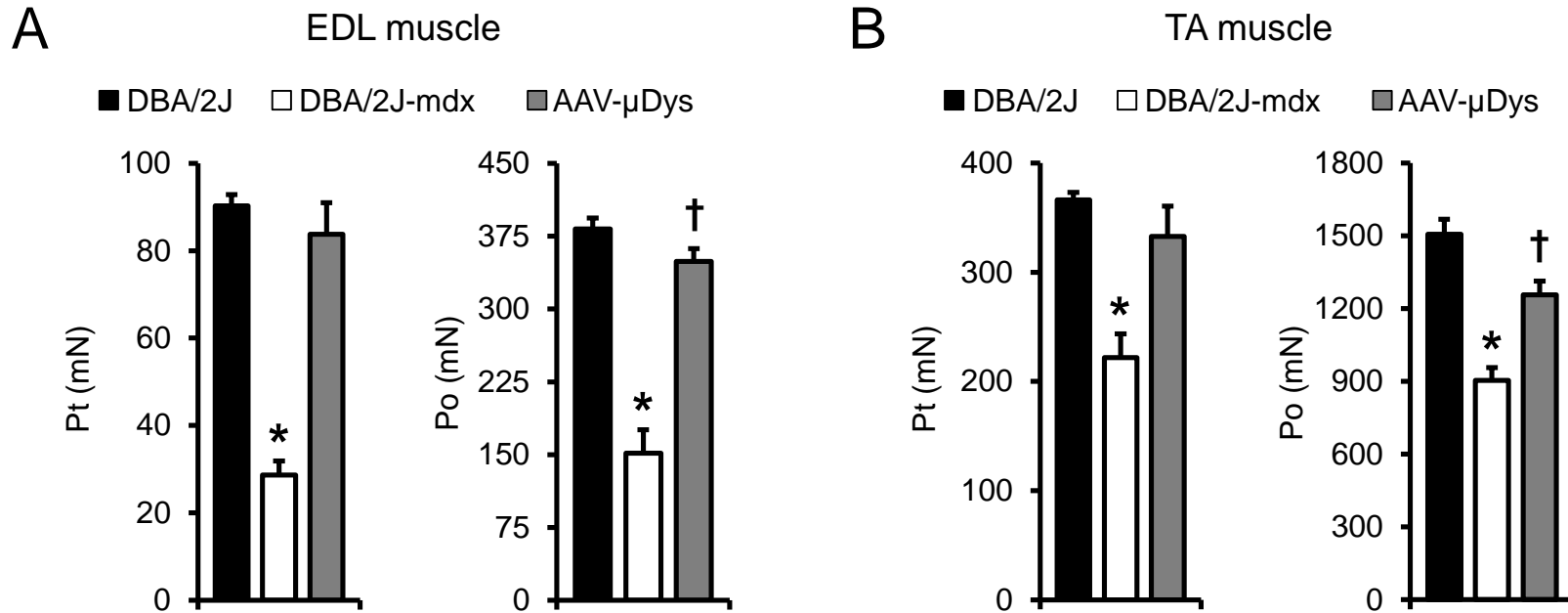


DBA/2J-  
mdx

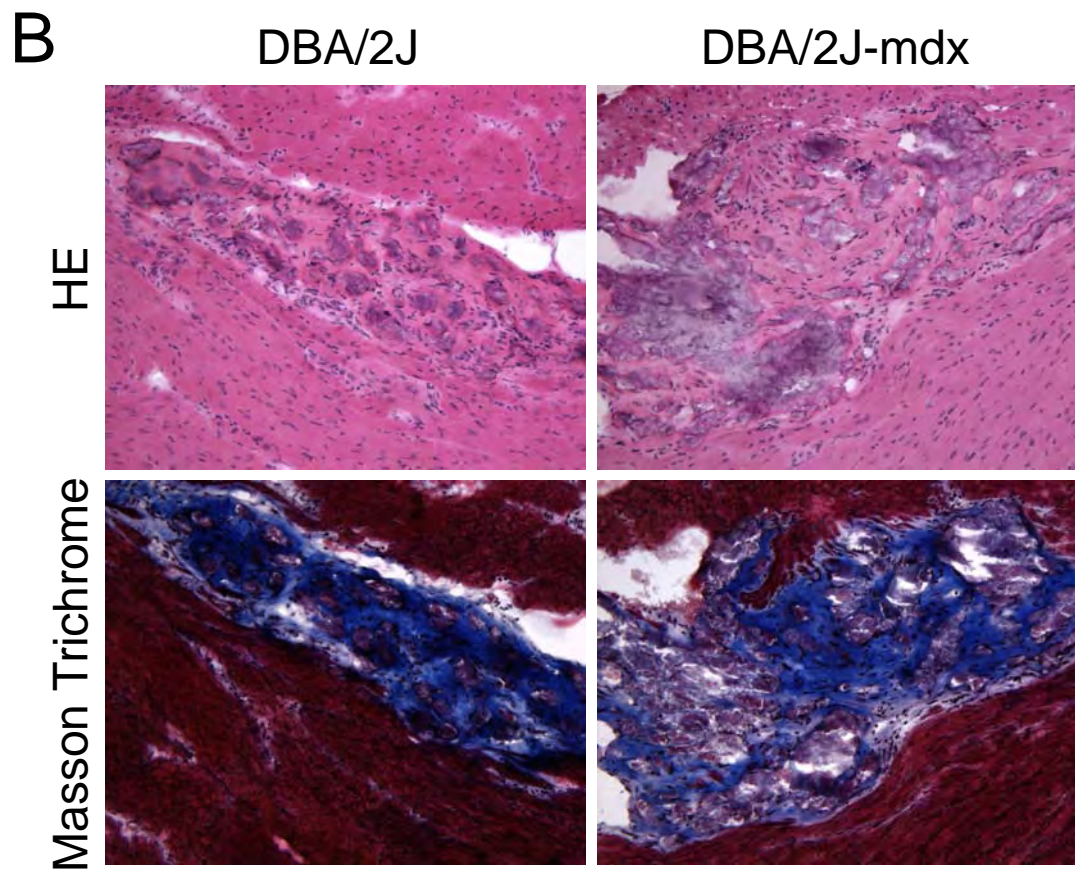
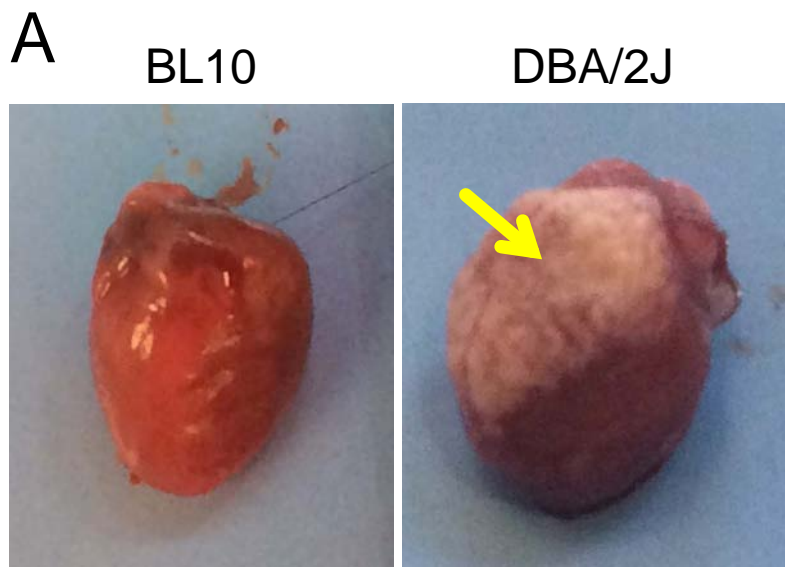


AAV- $\mu$ Dys treated  
DBA/2J-mdx

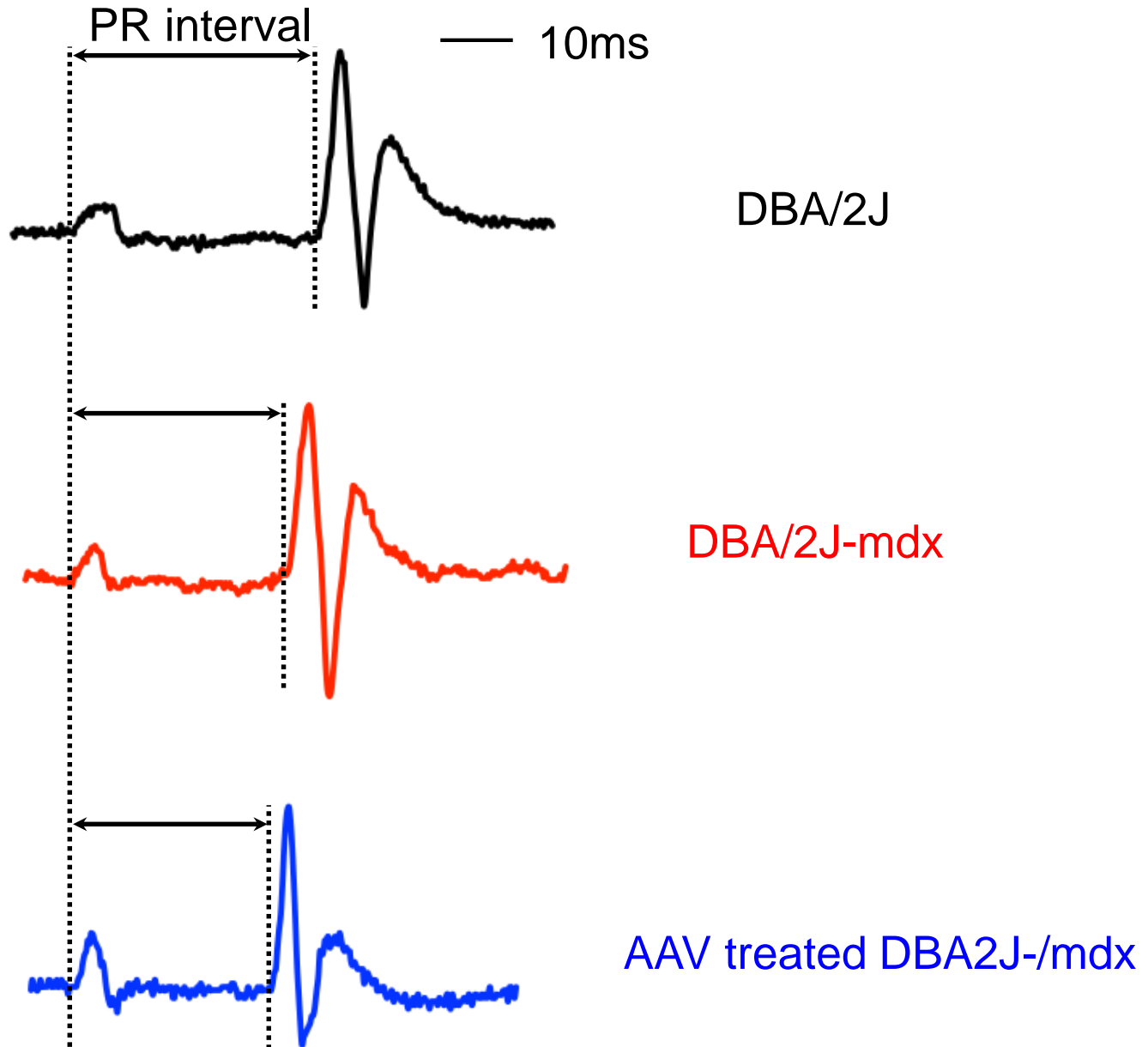


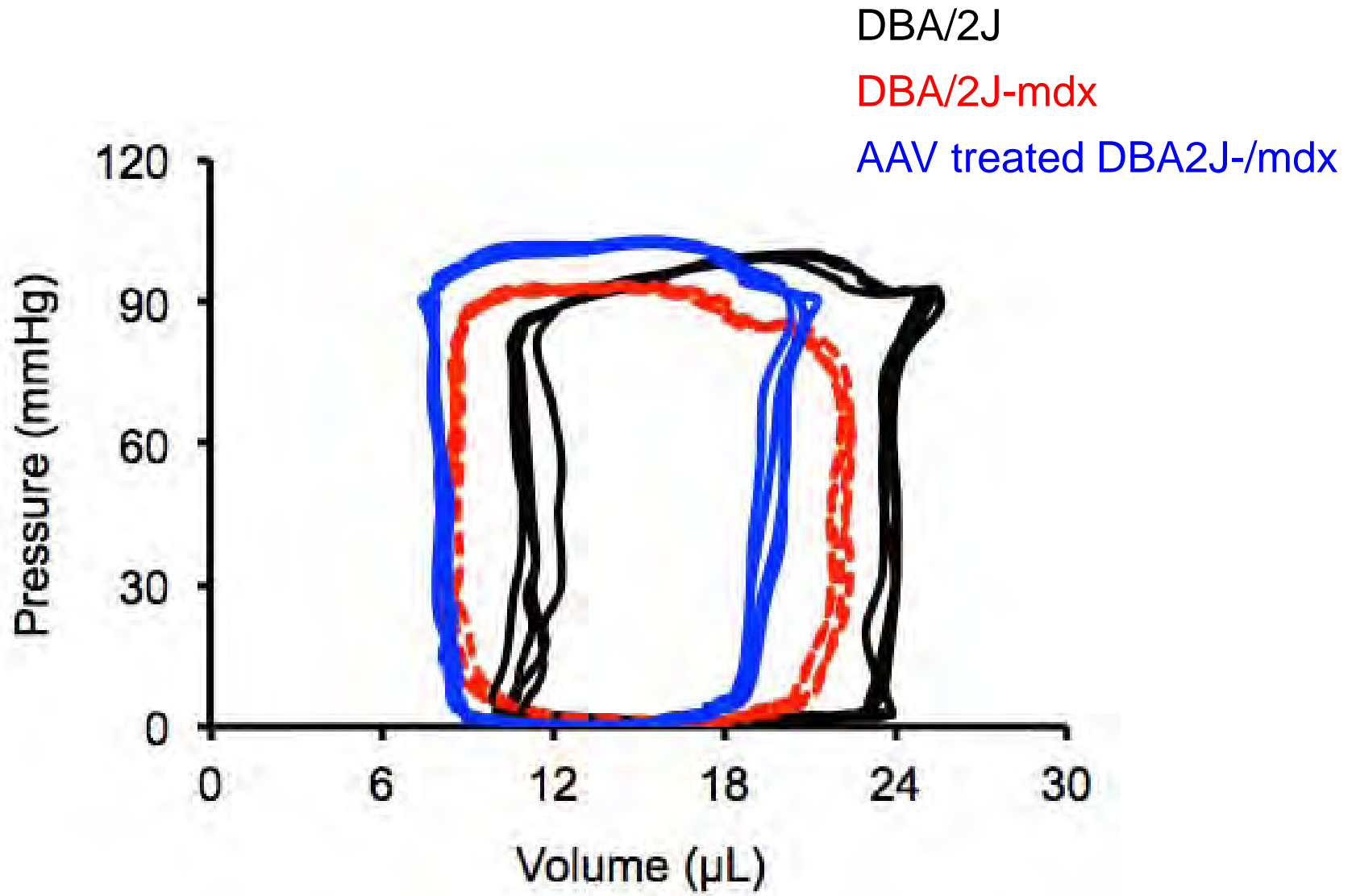


\*, DBA/mdx is significant different from DBA and AAV treated  
 †, DBA is significant different from treated AAV treated



A





## Supplemental Figure Legends

**Figure S1. Widespread micro-dystrophin expression in skeletal muscle and the heart of AAV-9 treated DBA/2J-mdx mice.** **A**, Representative photomicrographs of dystrophin immunostaining of the tibialis anterior muscle (TA), quadriceps and diaphragm from five AAV injected mice and an untreated DBA/2J-mdx mouse. **B**, Representative photomicrographs of dystrophin immunostaining of the heart (Top panel, full-view images; Bottom panel, high-power images) from five AAV injected mice and an untreated DBA/2J-mdx mouse. **C**, Quantitative evaluation of AAV genome distribution in muscle and internal organs using in AAV microgene injected male DBA/2J-mdx mice (N=5). TaqMan quantitative PCR detects the junction of R1-R16. Dia, diaphragm; Gas, gastrocnemius; Quad, quadriceps; TA, tibialis anterior.

**Figure S2. Micro-dystrophin expression reduces skeletal muscle disease in DBA/2J-mdx mice.** **A**, Representative full-view photomicrographs of the HE stained quadriceps, tibialis anterior muscle (TA) and diaphragm from untreated and AAV injected DBA/2J-mdx mice. Scale bar, 500  $\mu$ m. **B**, Representative high-magnification photomicrographs of the HE stained quadriceps, TA and diaphragm from untreated and AAV injected DBA/2J-mdx mice.

**Figure S3. Intravenous AAV-9 delivery results in saturated micro-dystrophin expression in the extensor digitorum longus muscle in DBA/2J-mdx mice.** Representative full-view photomicrographs of dystrophin immunostaining from DBA/2J. DBA/2J-mdx and treated DBA/2J-mdx mice.

**Figure S4. AAV micro-dystrophin therapy improves absolute muscle force of DBA/2J-mdx mice.** **A**, Quantitative evaluation of the absolute twitch force and absolute maximal tetanic force in the extensor digitorum longus muscle (EDL). **B**, Quantitative evaluation of the absolute twitch force and absolute maximal tetanic force in the tibialis anterior (TA) muscle. Asterisk, untreated DBA/2J-mdx mice is significant different from that of DBA/2J and AAV treated DBA/2J-mdx mice. Cross, DBA/2J is significant different from that of AAV treated DBA/2J-mdx mice.

**Figure S5. DBA/2J mice show spontaneous muscle pathology.** **A**, Representative photomicrographs of freshly dissected BL10 and DBA/2J mouse hearts. Arrow indicates epicardial calcification and/or fibrosis on the surface of the right ventricle in the DBA/2J mouse. **B**, Representative high-magnification photomicrographs of HE and Masson trichrome-stained heart sections from DBA/2J and DBA/2J-mdx mice.

**Figure S6. Representative ECG and the pressure-volume loop tracing from experimental mice.** **A**, ECG reveals the shortened PR interval in a DBA/2J-mdx mouse. Micro-dystrophin therapy did not increase the PR interval. **B**, The pressure-volume loop shows a similar hemodynamic profile in DBA/2J and DBA/2J-mdx mice.

HUM-2018-012 Revision 1

## **Micro-dystrophin gene therapy goes systemic in Duchenne muscular dystrophy patients**

Dongsheng Duan, Ph.D.

Department of Molecular Microbiology and Immunology, School of Medicine, University of Missouri, Columbia, MO 65212, USA

Department of Biomedical Sciences, College of Veterinary Medicine, University of Missouri, Columbia, MO 65211, USA

Department of Neurology, School of Medicine, University of Missouri, Columbia, MO 65212, USA

Department of Bioengineering, University of Missouri, Columbia, MO 65212, USA

Corresponding Address: Dongsheng Duan Ph.D.  
Professor  
Department of Molecular Microbiology and Immunology  
One Hospital Dr.  
Columbia, MO 65212  
Phone: 573-884-9584  
Fax: 573-882-4287  
Email: [duand@missouri.edu](mailto:duand@missouri.edu)

## Abstract

Whole body systemic gene therapy is likely the most effective way to greatly reduce the disease burden of Duchenne muscular dystrophy (DMD), an X-linked inherited muscle disease that leads to premature death in early adulthood. Genetically, DMD is due to null mutation of the dystrophin gene, one of the largest genes in the genome. Recent studies have shown highly promising improvements in animal models with intravascular delivery of the engineered micro-dystrophin gene by adeno-associated virus (AAV). Several human trials are now started to advance AAV micro-dystrophin therapy to DMD patients. This is a historical moment for the entire field. Results from these trials will shape the future of neuromuscular disease gene therapy.

**Key words:** Duchenne muscular dystrophy, dystrophin, micro-dystrophin, microgene, adeno-associated virus, systemic delivery, AAV, DMD, gene therapy, clinical trial

Many diseases affect tissues distributed throughout the body. These diseases present a great challenge for gene therapy due to the need for bodywide delivery of a large quantity of a viral vector. A major breakthrough published in December 2017 has now provided the proof-of-principle for systemic gene therapy in human patients <sup>1</sup>. Mendell and colleagues treated infants with spinal muscular atrophy type 1 (SMA1) using a single intravenous injection of a therapeutic adeno-associated virus serotype-9 (AAV-9) vector at doses up to  $2 \times 10^{14}$  viral genome (vg) particles/kg. Treatment resulted in spectacular improvement in morbidity and mortality. Following this success, three independent systemic AAV gene therapy trials have been started in USA to treat Duchenne muscular dystrophy (DMD), the most common lethal muscle disease in boys. These include Solid Biosciences (NCT03368742), Nationwide Children's Hospital (NCT03375164), and Pfizer (NCT03362502). A fourth trial has also been planned in Europe by Genethon and Sarepta Therapeutics <sup>2</sup>. DMD is caused by null mutations in the dystrophin gene <sup>3</sup>. Patients become wheelchair bound in their early teenage years and die from diaphragm muscle and/or cardiac muscle failure.

Systemic AAV gene therapy for DMD faces a unique hurdle. Unlike the SMA1 trial in which the therapeutic gene can fit into an AAV particle <sup>1</sup>, the size of the dystrophin coding sequence (~11.5 kb) greatly exceeds the 5 kb AAV packaging capacity <sup>4</sup>. A hint for the solution surfaces from studying Becker muscular dystrophy (BMD). BMD is a mild form caused by in-frame deletions in the dystrophin gene. It was found that BMD patients who lost nearly half of the gene still lived a quite healthy life, suggesting half-size dystrophin is protective in human patients <sup>5</sup>. Subsequent studies in animal models confirmed that the 6~8 kb mini-dystrophin genes indeed provided excellent protection. However, the minigene still exceeds the packaging limit of the AAV vector. The problem was finally solved with the development of micro-dystrophin genes smaller than 4 kb. More than 30 different microgenes have been tested since 1997. While not all microgenes reduce muscle disease, many have resulted in good protection in various mouse models. Recent studies in young adult affected dogs further suggest that administration of a high dose AAV micro-dystrophin vector through the circulation can result in safe and bodywide

transduction in a diseased large mammal<sup>6,7</sup>. Collectively, these preclinical results set the foundation to test systemic AAV microgene therapy in human patients.

Several important questions are to be answered in ongoing trials. The first and most important is safety. In the SMA1 trial all patients tolerated high dose intravenous AAV-9 injection. In young adult affected dogs, systemic AAV-8 or AAV-9 micro-dystrophin injection showed good safety profiles<sup>6,7</sup>. Acute toxicity was not observed in the first patient in the trial conducted by Nationwide Children's Hospital ( $2 \times 10^{14}$  vg/kg)<sup>8</sup>. In a trial on X-Linked myotubular myopathy (NCT 03199469), four patients (0.8 to 4.1-year-old) received intravenous injection of an AAV-8 vector expressing the human myotubularin 1 gene at the dose of  ~~$2 \times 10^{14}$  vg/kg~~<sup>9</sup>. According to the interim report from Audentes Therapeutics, the sponsor of the trial, treatment resulted in neuromuscular and respiratory function improvement. No death was reported. Some adverse events were found but all manageable<sup>9</sup>. Collectively, there seems a good chance that DMD patients may tolerate systemic AAV micro-dystrophin gene therapy.

$1 \times 10^{14}$  vg/kg

With this backdrop, a newly published study should also be mentioned because it raises potential toxicity of high dose systemic AAV administration in large mammals<sup>10</sup>. Specifically, Hinderer et al injected an AAV-9 variant (AAV-hu68) expressing the human survival of motor neuron gene to three 14-month-old nonhuman primates (NHPs) and three 3 to 30-day-old piglets at the dose of  $2 \times 10^{14}$  vg/kg. All NHPs developed liver toxicity and one had to be euthanized at day 4 after injection due to liver failure. No hepatic toxicity was noticed in piglets but all of them developed neuronal toxicity within 14 days after injection and had to be euthanized<sup>10</sup>. In light of the new report, extreme caution should be taken and toxicity carefully monitored when moving forward with ongoing trials.

In the SMA1 trial, all patients received AAV administration before the age of 8 months. Only one DMD trial accepted patients in this age range. Infants have unique immunological advantages due to the relatively immature nature of their immune system. Ongoing trials in DMD patients will show whether older children can tolerate high quantity intravenous AAV delivery.

The next question is whether the highly shortened microgene can ameliorate muscle disease in boys with DMD. The half-size minigene is originated from human patients but there is no human precedent for the microgene. The micro-size dystrophin proteins have been detected (even at high abundance) in patients that carry very large in-frame deletions<sup>11</sup>. But clinical manifestations of these patients' symptoms are not alleviated. It is believed that the rationally designed synthetic microgene should outperform the naturally existing ones that are found in patients. However the vast majority of the efficacy data of the synthetic microgene are from mice. Limited functional study in the canine model suggests that micro-dystrophin may improve muscle force in affected dogs, but certainly not to the levels seen in the murine model<sup>12</sup>. The primary outcome of the ongoing DMD phase 1 trials is not to determine muscle histology and motor function improvement. Hence, these trials will not yield a conclusive answer on whether microgene can attenuate muscular dystrophy in human patients. However, the results from these trials should give some clues on the performance of micro-dystrophin in the muscle of DMD patients such as the expression level of micro-dystrophin, restoration of dystrophin-associated protein complex and amelioration of some aspects of histological lesions. Motor function assay has been included in the protocol in at least one trial. The data from the functional assay, while limited due to the small sample size, will still shed important light.

Simultaneous initiation of three independent trials in USA and one additional trial planned in Europe presents a unique opportunity to address several puzzling issues in the field. One is dystrophin immunity. An early local injection trial suggests that the T cell immune response to dystrophin may constitute a barrier in patients<sup>13</sup>. In this case, patients will have to be carefully selected based on the configuration of the microgene to minimize cellular immune reaction. This is very difficult to investigate in animal models due their inherent limitations. A conclusion may likely come out from the ongoing trials since different inclusion criteria are used in regard to mutation. One trial only treats patients that carry specific mutations. The other two trials, however, are open to patients with any mutation.

The full-length dystrophin protein contains a N-terminal (NT) domain, 24 spectrin-like repeats, 4 hinges, a cysteine-rich (CR) domain and a C-terminal domain. Among four hinges, hinges 1 and 4 are positioned before and after 24 repeats, respectively. Hinges 2 and 3 are dispersed in the middle of 24 repeats. Animal studies have shown muscle protection with microgenes that carry either four or five repeats, with or without a centrally located hinge. However, it is unclear which configuration offers better protection due to the lack of side-by-side comparisons. Interestingly, a four-repeat microgene is used in one trial and two different five-repeat microgenes are used in the other two trials. Furthermore, the microgene used in one trial does not have a central hinge but a central hinge is included in the microgenes used in the other two trials. Hopefully, the results from these ongoing trials will help to clarify our understanding.

All the existing microgenes carry the NT and CR domains. The major difference is in the formulation of the repeats and hinges. The inclusion/exclusion of a particular repeat/hinge should be experimentally determined. However, only few comprehensive studies have been reported so far. The Chamberlain lab studied the consequences of including hinge 2 in micro-dystrophin<sup>14</sup>. The authors found that a polyproline site in hinge 2 negatively impacted the myotendinous junction and neuromuscular junction in some muscles. Further, they found that the presence of hinge 2 (i) compromised the capacity of micro-dystrophin to prevent muscle degeneration and (ii) resulted in the formation of abnormal ring fibers in the gastrocnemius muscle. Replacing hinge 2 with hinge 3 or deleting the polyproline site from hinge 2 prevented these negative effects<sup>14</sup>.

Neuronal nitric oxide synthase (nNOS) plays a crucial role in many muscle activities<sup>15</sup>. nNOS is tied to the sarcolemma by dystrophin in normal muscle. My laboratory discovered R16/17 as the dystrophin nNOS-binding domain for anchoring nNOS to the muscle cell membrane<sup>16, 17</sup>. Loss of sarcolemmal nNOS leads to functional ischemia which contributes to the initiation and progression of muscle disease in DMD<sup>18, 19</sup>. Delocalization of nNOS to the cytosol reduces muscle force generation<sup>20</sup>. Inclusion of R16/17 in synthetic dystrophin genes restored membrane nNOS localization, significantly prevented functional ischemia and ischemic damage, and significantly enhanced exercise capacity<sup>16, 21</sup>.

It should be noted that aforementioned studies on hinge 2 and R16/17 were conducted in the mouse model. It remains unclear whether the same is true in large mammals. Although current clinical trials are not designed to test therapeutic advantages/disadvantages of hinge 2 and R16/17, the differences in the microgene design of ongoing trials have now made it possible to get a clue about these important details. In particular, an R16/17-containing microgene is used in one trial. Of two trials using a central hinge-containing microgene, one has hinge 2 and the other has hinge 3. Muscle biopsy from the trial patients should be carefully examined for the integrity of the structure of myotendinous and neuromuscular junctions, as well as sarcolemmal localization of nNOS.

Besides new knowledge on micro-dystrophin biology, it is expected that the ongoing trials should also provide important first-hand information on the use of different AAV serotypes and different muscle-specific promoters in DMD patients. For the ongoing trials in USA, two AAV serotypes (AAV-9 and AAV-rh74) and three different muscle promoters are used. The detailed information on AAV serotype and the muscle promoter for the planned trial in Europe is not announced. It is possible that they may be different from those used in the ongoing USA trials. AAV-9 was isolated from human tissues<sup>22</sup>. AAV-rh74 was isolated from rhesus macaque monkeys and it shares 93% homology with AAV-8<sup>23</sup>. Because tissues are not available, it is usually not possible to perform bodywide bio-distribution study or to check expression in every muscle in human patients. In this regards, preclinical studies have revealed a satisfactory transduction profile for the AAV serotypes used in the ongoing trials. Systemic delivery of AAV-8, AAV-rh74 and AAV-9 has resulted in robust muscle transduction in mice though AAV-8 and AAV-rh74 also showed liver preference and AAV-9 displayed cardiac tropism<sup>24-26</sup>. High dose systemic AAV-8 and AAV-9 delivery has been tested in several studies in normal and affected dogs. Bodywide muscle transduction was obtained in these studies. Bio-distribution studies showed the presence of the AAV genome in all muscles in the body but the liver had the highest abundance<sup>6, 27-29</sup>. Surprisingly, AAV-9 which is cardiotropic in mice was much less efficient in transducing the heart in canines<sup>30</sup>.

Systemic DMD gene therapy has come a long way. Progresses in the fields of virology, immunology, dystrophin biology, animal models, and large-scale clinical grade

AAV manufacture have shaped the design of current trials. However, we still do not have a crystal clear picture on the function of every portion of the dystrophin protein. Improved understanding on dystrophin biology, as illustrated in the recent discovery of multiple new dystrophin membrane-binding domains, will teach us how to engineer more potent microgenes<sup>31</sup>. On the other side, application of state-of-the-art forced in vivo evolution strategies in relevant models is expected to yield novel AAV capsids that can better meet the needs of DMD patients<sup>32</sup>.

The ongoing systemic AAV microgene therapy trials mark an important milestone in the development of DMD gene therapy. It is the fruit of accumulated knowledge spanning more than 30 years' research from many laboratories. These trials will start the process for the eventual approval of an effective genetic treatment for DMD by regulatory agencies.

### **Acknowledgement**

AAV micro-dystrophin gene therapy research in the Duan lab is currently supported by the National Institute of Neurological Disorders and Stroke (NS-90634), the Department of Defense (MD130014), Solid Biosciences, Jesse's Journey: The Foundation for Gene and Cell Therapy, and the Jackson Freel DMD Research Fund. The author thanks the Cocklin family for the unconditional support of DMD research in the Duan lab.

### **Disclosure**

The author is a member of the scientific advisory board for Solid Biosciences and an equity holder of Solid Biosciences. The Duan lab has received research support from Solid Biosciences.

## References

1. Mendell JR, Al-Zaidy S, Shell R et al. Single-dose gene-replacement therapy for spinal muscular atrophy. *N Engl J Med* 2017;377:1713-1722.
2. Sarepta Therapeutics --. Sarepta Therapeutics and Genethon Announce a Gene Therapy Research Collaboration for the Treatment of Duchenne Muscular Dystrophy (<http://investorrelations.sarepta.com/news-releases/news-release-details/sarepta-therapeutics-and-genethon-announce-gene-therapy-research>). Jun 21, 2017. Last accessed on Feb 8, 2018.
3. Kunkel LM. 2004 William Allan award address. cloning of the DMD gene. *Am J Hum Genet* 2005;76:205-214.
4. Koenig M, Hoffman EP, Bertelson CJ et al. Complete cloning of the Duchenne muscular dystrophy (DMD) cDNA and preliminary genomic organization of the DMD gene in normal and affected individuals. *Cell* 1987;50:509-517.
5. England SB, Nicholson LV, Johnson MA et al. Very mild muscular dystrophy associated with the deletion of 46% of dystrophin. *Nature* 1990;343:180-182.
6. Yue Y, Pan X, Hakim CH et al. Safe and bodywide muscle transduction in young adult Duchenne muscular dystrophy dogs with adeno-associated virus. *Hum Mol Genet* 2015;24:5880-5890.
7. Le Guiner C, Servais L, Montus M et al. Long-term microdystrophin gene therapy is effective in a canine model of Duchenne muscular dystrophy. *Nat Commun* 2017;8:16105.
8. Parent Project Muscular Dystrophy --. First Duchenne Patient Dosed in Microdystrophin Gene Therapy! (<http://community.parentprojectmd.org/profiles/blogs/first-duchenne-patient-dosed-in-microdystrophin-gene-therapy>). Jan 10, 2018. Last accessed on Feb 8, 2018.
9. Audentes Therapeutics --. Audentes Announces Positive Interim Data from First Dose Cohort of ASPIRO, a Phase 1/2 Clinical Trial of AT132 in Patients With X-Linked

Myotubular Myopathy ([http://investors.audentestx.com/phoenix.zhtml?c=254280&p=irol-newsArticle\\_print&ID=2324833](http://investors.audentestx.com/phoenix.zhtml?c=254280&p=irol-newsArticle_print&ID=2324833)). Jan 4, 2018. Last accessed on Feb 8, 2018.

10. Hinderer C, Katz N, Buza EL et al. Severe toxicity in nonhuman primates and piglets following high-dose intravenous administration of an AAV vector expressing human SMN. *Hum Gene Ther* 2018.

11. Fanin M, Freda MP, Vitiello L et al. Duchenne phenotype with in-frame deletion removing major portion of dystrophin rod: threshold effect for deletion size? *Muscle Nerve* 1996;19:1154-1160.

12. Shin J-H, Pan X, Hakim CH et al. Microdystrophin ameliorates muscular dystrophy in the canine model of Duchenne muscular dystrophy. *Mol Ther* 2013;21:750-757.

13. Mendell JR, Campbell K, Rodino-Klapac L et al. Dystrophin immunity in Duchenne's muscular dystrophy. *N Engl J Med* 2010;363:1429-1437.

14. Banks GB, Judge LM, Allen JM et al. The polyproline site in hinge 2 influences the functional capacity of truncated dystrophins. *PLoS genetics* 2010;6:e1000958.

15. Stamler JS, Meissner G. Physiology of nitric oxide in skeletal muscle. *Physiological reviews* 2001;81:209-237.

16. Lai Y, Thomas GD, Yue Y et al. Dystrophins carrying spectrin-like repeats 16 and 17 anchor nNOS to the sarcolemma and enhance exercise performance in a mouse model of muscular dystrophy. *J Clin Invest* 2009;119:624-635.

17. Lai Y, Zhao J, Yue Y et al. alpha2 and alpha3 helices of dystrophin R16 and R17 frame a microdomain in the alpha1 helix of dystrophin R17 for neuronal NOS binding. *Proc Natl Acad Sci U S A* 2013;110:525-530.

18. Mendell JR, Engel WK, Derrer EC. Duchenne muscular dystrophy: functional ischemia reproduces its characteristic lesions. *Science* 1971;172:1143-1145.

19. Thomas GD. Functional muscle ischemia in Duchenne and Becker muscular dystrophy. *Frontiers in physiology* 2013;4:381.

20. Li D, Yue Y, Lai Y et al. Nitrosative stress elicited by nNOS $\mu$  delocalization inhibits muscle force in dystrophin-null mice. *The Journal of pathology* 2011;223:88-98.
21. Zhang Y, Yue Y, Li L et al. Dual AAV therapy ameliorates exercise-induced muscle injury and functional ischemia in murine models of Duchenne muscular dystrophy. *Hum Mol Genet* 2013;22:3720-3729.
22. Gao G, Vandenberghe LH, Alvira MR et al. Clades of adeno-associated viruses are widely disseminated in human tissues. *J Virol* 2004;78:6381-6388.
23. Rodino-Klapac LR, Montgomery CL, Bremer WG et al. Persistent expression of FLAG-tagged micro dystrophin in nonhuman primates following intramuscular and vascular delivery. *Mol Ther* 2010;18:109-117.
24. Pozsgai ER, Griffin DA, Heller KN et al. Systemic AAV-Mediated beta-Sarcoglycan Delivery Targeting Cardiac and Skeletal Muscle Ameliorates Histological and Functional Deficits in LGMD2E Mice. *Mol Ther* 2017;25:855-869.
25. Zincarelli C, Soltys S, Rengo G et al. Analysis of AAV serotypes 1-9 mediated gene expression and tropism in mice after systemic injection. *Mol Ther* 2008;16:1073-1080.
26. Duan D. Systemic delivery of adeno-associated viral vectors. *Current opinion in virology* 2016;21:16-25.
27. Mack DL, Poulard K, Goddard MA et al. Systemic AAV8-Mediated Gene Therapy Drives Whole-Body Correction of Myotubular Myopathy in Dogs. *Mol Ther* 2017;25:839-854.
28. Pan X, Yue Y, Zhang K et al. Long-term robust myocardial transduction of the dog heart from a peripheral vein by adeno-associated virus serotype-8. *Hum Gene Ther* 2013;24:584-594.
29. Yue Y, Ghosh A, Long C et al. A single intravenous injection of adeno-associated virus serotype-9 leads to whole body skeletal muscle transduction in dogs. *Mol Ther* 2008;16:1944-1952.

30. Pan X, Yue Y, Zhang K et al. AAV-8 is more efficient than AAV-9 in transducing neonatal dog heart. *Human gene therapy methods* 2015;26:54-61.
31. Zhao J, Kodippili K, Yue Y et al. Dystrophin contains multiple independent membrane-binding domains. *Hum Mol Genet* 2016;25:3647-3653.
32. Nance ME, Duan D. Perspective on adeno-associated virus (AAV) capsid modification for Duchenne muscular dystrophy gene therapy. *Hum Gene Ther* 2015;26:786-800.